Luminescent Conjugated Polyelectrolytes for DNA Biosensing

Wayne Nicholson George

Department of Chemistry, Imperial College London

– December 2006 –

Imperial College London

Supervisors:
Dr Joachim H. G. Steinke
Dr John C. de Mello

A DISSERTATION SUBMITTED IN PART FULFILMENT FOR THE DEGREE OF DOCTOR OF PHILOSOPHY

Dedicated to Mum and Dad.

Luminescent Conjugated Polyelectrolytes for DNA Biosensing

The ability to identify DNA or RNA strands with minimal treatment represents a challenge that has generated significant scientific interest. Rapid techniques for the detection of small amounts of DNA/RNA are important for a variety of applications and as a result, new techniques that can identify target analytes in a highly sensitive and selective manner are eagerly sought-after.

The use of conjugated polymers (CPs) is rapidly emerging as an innovative approach for the development of highly sensitive biosensors. Here, we describe the synthesis and analysis of novel water-soluble CPs based on a poly(phenylene ethynylene) (PPE) backbone, as sensitive probes for DNA detection.

PPEs containing anionic, cationic and hydrogen bonding side chains were first synthesised and compared to small model analogues in luminescence quenching experiments. Initially, a cationic CP was investigated as a possible DNA sensor, and its performance analysed. Armed with this knowledge, second generation polymers were then synthesised and these included structures with isothiouronium and guanidinium recognition units that are potentially able to discern oxoanion groups specifically.

The ability of these second-generation materials to interact with a range of emission quenchers as well as single-stranded DNA fragments was investigated. The impact of surfactants on the emission of these materials was also studied.

In other work we sought to monitor the activity of an enzyme, using the fluorescence emission from a CP and phosphate-based small molecule quencher. Enzymes represent an attractive target for monitoring due to the sheer variety of processes that they impact. In order to conduct the assays in biologically relevant media, we investigated the factors that affected the emission intensity of the second generation polymers.

In the final part of this thesis we present preliminary results from quenching experiments conducted using a prototype solid state sensor.

Acknowledgments

First and foremost, I must thank my supervisors Dr Joachim H. G. Steinke and Dr John C. de Mello. They were kind and brave enough to offer me a chance to work in their groups and provided unlimited enthusiasm, support and guidance. The working environment made learning a pleasure. I hope I have repaid the faith they placed in me. I am also indebted to Merck Chemicals Ltd. and in particular Dr Mark Giles and Dr Iain McCulloch for providing support and ideas. I am also grateful for the generous funding that was secured on my behalf.

Lab work is communal affair and thanks to the members of both Steinke and de Mello groups the experience was rich and rewarding. I would like to thank the early members who provided much input and advice. I am grateful to Dr Jo Wilson and Dr Mattijs Koeberg for their patience in helping me acquire lifetime and QE measurements and for chaperoning me through the early photophysical experiments. I am indebted to Dr Jenny Rickerby and Dr Tim Morley for providing useful synthetic tips and guidance when new in the lab. Also special thanks to Barny Greenland for his enthusiasm and for looking out for me on those weekend lab ventures and Siva Krishnadasan for the random IT and physics queries that I would sporadically bother him with. I am grateful to Dr David Mann for his kind donation of buffer solutions, enzymes and DNA material and his invaluable advice on the handling of all. Thank you to Dr Emma Child for her help with gel electrophoresis. I am grateful to Dr Takashi Sagawa for his useful insight on electron transfer processes.

The working environment has been complemented by the presence of the following lab faithful, past and present – thanks to, in order to appearance; Dr Shuyuan Liu, Dr Simon Gretton-Watson, Dr Carolina Galmes, Dr Phillipe Massiot, Dr Eva Gonzalez, Dr Pilar Formetin, Dr Peter Jepson, Chris Drake, Federica Paina, Gavin Fitzgerald, Manuel Ellerman, Dr Christian Nielsen, Michelle Lewis, Dr Magda Milewska, Dr Natasha Shirshova, Eduardo Galiana Daniel, Jonathan Martinelli, Karin Nordgren, Sally Ewen and members of the Armstrong and Welton groups.

I would like to acknowledge members of the NMR service (Dick Sheppard, Pete Haycock) and MS service (John Barton). Stephen Boyer (Elemental Analysis service), Steve Holding (GPC analysis at Rapra Technology Ltd.), James Pullen (400 MHz NMR) and Simon Turner (Technician, Briscoe Lab.) also deserve thanks.

Finally, I must thank my family for their unstinting support throughout all my studies.

Table of Contents

Abbreviations

Ac	Acetyl
AcOH	Acetic acid
aq.	Aqueous
AQS	9,10-Anthraquinone-2,6-disulfonic acid disodium salt
Ar	Aromatic
BOC	Butoxycarbonyl
br	Broad
Bu	Butyl
cat.	Catalyst
CB[6]	Cucurbit[6]uril
$CDCl_3$	Deuterochloroform
C.I	Chemical ionisation
^{13}C NMR	Carbon nuclear magnetic resonance
CNT	carbon nanotube
CP	Conjugated polymer
CPE	Conjugated polyelectrolyte
CV	Cyclic voltammetry
d	Doublet
DBU	1,8-Diazabicyclo[5.4.0]undec-7-ene
dd	Doublet of doublets
d_6-DMSO	Hexadeuterodimethyl sulphoxide
DHP	Disodium hydrogen phosphate
DIPA	Diisopropylamine
DMAc	*N,N*-Dimethylacetamide
d_4-MeOD	Tetradeuteromethanol
DMF	*N,N*-Dimethylformamide
DMSO	Dimethyl sulphoxide
DNA	Deoxyribonucleic acid
DP	Degree of polymerisation
DPP	Diphenyl phosphate
DPy	4,4′-Dipyridyl hydrate
DSC	Differential scanning calorimetry
EDAC	1-(3-Dimethylaminopropyl)-3-ethylcarbodiimide hydrochloride

E.I	Electron ionisation
eq. / Eq.	Equivalents
ET	Energy transfer
Et	Ethyl
Et_2O	Diethyl ether
EtOH	Ethanol
FRET	Fluorescence resonance energy transfer
FTIR	Fourier transform infrared spectroscopy
GPC	Gel permeation chromatography
h	Hours
^1H NMR	Proton nuclear magnetic resonance
HOMO	Highest occupied molecular orbital
HRMS	High resolution mass spectrometry
Hz	Hertz
i-	Iso
IP	Ionisation potential
I.R.	Infra-red spectroscopy
J	Coupling constant
KOH	Potassium hydroxide
LUMO	Lowest unoccupied molecular orbital
$[M]^+$	Molecular ion
M	Molar
m	Multiplet
m	Meta
MALDI-tof	Matrix assisted laser desorption ionisation, time-of-flight
Me	Methyl
MeOH	Methanol
min(s)	Minute(s)
M_n	Number average molecular weight
mol%	Molar %
m.p	Melting point
MS	Mass spectroscopy
MV^{2+}	1,1′-Dimethyl-4,4′-bipyridinium dichloride hydrate
M_w	Weight average molecular weight

m/z	mass/charge
n-	Normal
NHS	*N*-Hydroxysuccinimide
NMR	Nuclear magnetic resonance
4-NP	4-Nitrophenol
NPP	4-Nitrophenyl phosphate, bis(cyclohexylammonium) salt hydrate
o	Ortho
p	Para
PDI	Polydispersity index
PDT	Photo dynamic therapy
PEG	Polyethylene glycol
PET	Photoinduced electron transfer
Ph	Phenyl
PL	Photoluminescence
PPE	Poly(phenylene ethynylene)
ppm	Parts per million
Pr	Propyl
q	Quartet
QD	Quantum dot
QE	Quantum efficiency
RET	Resonance energy transfer
R_f	Retention factor
r. t.	Room temperature
s	Singlet
SNP	single nucleotide polymorphism
str.	Stretch
t	Triplet
TBAF	Tetrabutylammonium fluoride
TEA	Triethylamine
THF	Tetrahydrofuran
TLC	Thin layer chromatography
TMS	Trimethyl silyl / tetramethyl silane
TRIS	Tris(hydroxymethyl) aminomethane
UV	Ultraviolet spectroscopy

List of Figures

List of Schemes

List of Tables

1 Semiconducting Polymers – An Overview

Semiconducting organic polymers, also referred to as conjugated polymers (CPs), have excitation energies that typically lie in the visible to near UV range (1.4 – 4.0 eV).[1] Recently, the study of these polymers has formed a nascent research area in modern materials chemistry, with interest driven by the potential to fabricate devices for commercial and scientific applications.

A search through the chemical literature provides many examples of conjugated polymers being used in a range of optoelectronic devices from polymer LEDs,[2] plastic lasers,[3] chemical sensors,[4] nonlinear optics,[5,6] FETs[7] and solar cells[8] to molecular machines.[9] The ability to fabricate such devices, at the single-molecule level, has led to these developments being keenly followed in the wider field of nanotechnology, as researchers seek to miniaturise existing technologies.

In 1977, Heeger, MacDiarmid, Shirakawa and co-workers reported their work on the selective doping of polyacetylene $(CH)_x$ to produce the first conducting polymer, in a key discovery that led to the 'fourth generation' of polymeric materials.[10,11] In their work on *trans*-poly(acetylene), in its as formed state a black powdery polymer, they noted a 'conductivity increase' upon exposure to either chlorine, bromine or iodine vapour. This original conducting polymer, the forerunner of today's variants, underpins a multi-million dollar industry, and the importance of this work was soon recognised with Shirakawa, MacDiarmid and Heeger being jointly awarded the Nobel Prize for Chemistry in 2000.[11,12]

This work challenged the traditional thinking, of polymers being used as insulators in electronic devices, and inspired chemists and physicists over the next thirty years to explore the conducting properties of such materials.

Due to the insolubility of un-substituted poly(acetylene) in all organic solvents and its instability upon exposure to oxygen and water, attention soon turned to other more processable conjugated polymers. Substituted versions of poly(arylene vinylene)s gained prominence as they exhibit electronic properties that are comparable with poly(acetylene), and display good solubility in common organic solvents thereby allowing easier processing for the production of commercial devices.[13]

Most of the commercial interest in conducting polymers centres on the process of electroluminescence (EL), whereby the emission of light from conjugated polymers can be stimulated by an electric current.[14] Electroluminescence in organic materials was first noted in

1963 with a resurgent interest triggered in the 1980s with work on organic fluorescent dyes.[2] In Cambridge in the early 1990s, Burroughes *et al.* observed, for the first time, electroluminescent conjugated polymers.[14,15] The key advance in this work centred on the avoidance of expensive vapour deposition methods, by using soluble derivatives of the polymers that were amenable to dip-coating, spin-coating and reel-to-reel techniques.[14]

Two of the most common types of polymer in this class are poly(2,5-phenylene vinylene) (PPV) and poly(1,4-thienylene vinylene) (PTV), shown in Table 1.1. However, as is also shown in this table, there are numerous different CPs used for a variety of applications. The attention focused on PPV and its derivatives in the early days, stems from the demonstration of electroluminescence that Burroughes *et al.* reported back in 1990.[14] Other advantages for using PPV in electronic devices include their relative ease of synthesis, which makes their fabrication inexpensive.

Table 1.1 Examples of the structures of some of the common conjugated luminescent polymers.[16]

Entry / Structure number	Polymer structure	Full name	Abbreviation
1 / **1**	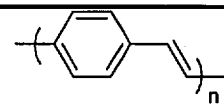	poly(2,5-phenylene vinylene)	PPV
2 / **2**	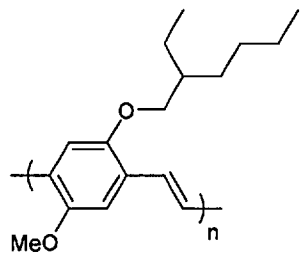	poly(2-methoxy-5-(2'ethyl-hexoxy)-1,4-phenylene vinylene)	MEH-PPV
3 / **3**	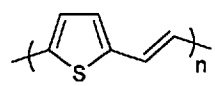	poly(2,5-thienylene vinylene)	PTV
4 / **4**	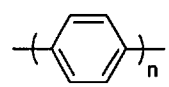	poly(p-phenylene)	PPP
5 / **5**	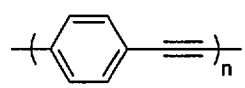	poly(phenylene ethynylene)	PPE
6 / **6**	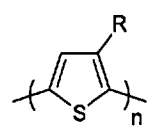	poly(3-alkylthiophene)	P3AT or PT
7 / **7**	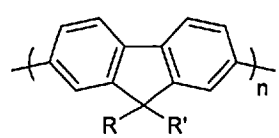	poly(9,9-dialkylfluorene)	PDAF or PF

1.1 Conjugated polymer applications

In the following sections, a brief overview of some of the main applications of conjugated polymers as used in modern materials chemistry along with some of the more recent breakthroughs will be described.

1.1.1 Polymer Light-Emitting Diodes (PLEDs)

This is perhaps the most well documented use for conjugated polymers and as a result the best known. Since the phenomenon of electroluminescence was first noted[14] (*vide supra*) there have been numerous reviews[17] detailing advances in materials synthesis and device fabrication. In this section, a brief summary of some landmark discoveries will be covered along with recent solutions

to potential drawbacks that in the early days dogged OLED technologies. Additionally, methods used to increase the efficiency of devices, including adding additional layers and multilayered devices will be discussed.

Work on fluorescent polymer light-emitting diodes began in earnest after the discovery by Friend *et al.* of electroluminescence in polymer **1** (Table 1.1).[14]

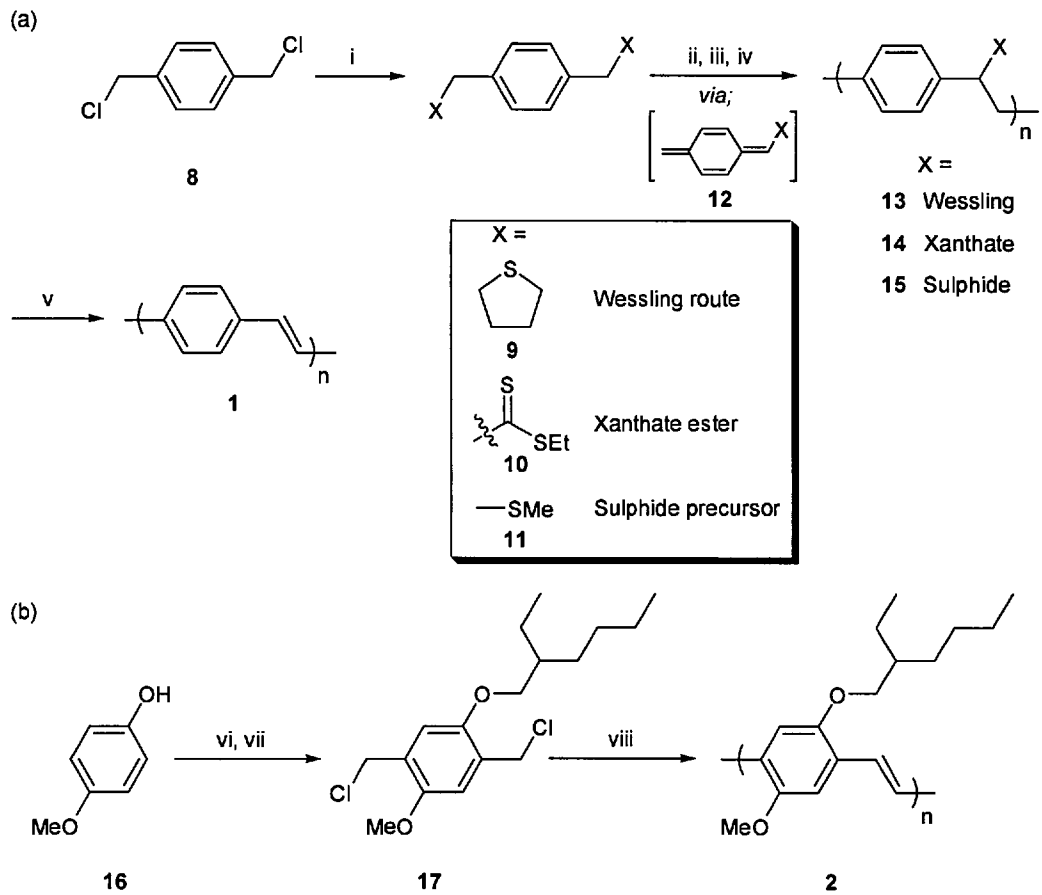

Scheme 1.1 General synthetic routes to PPVs. (a) Synthesis of an un-substituted PPV. Conditions: (i) (*for the sulphonium precursor*) Tetrahydrothiophene, MeOH, 65 °C; (ii) NaOH, MeOH/H_2O, 0 °C; (iii) neutralisation (HCl); (iv) dialysis (H_2O); (v) 180 – 300 °C, vacuum, 12 h. (b) Synthesis of MEH-PPV. Conditions: (vi) 3-(Bromomethyl)heptane, KOH, EtOH, reflux, 16 h; (vii) HCHO (37%), HCl, dioxane, 20 °C, 18 h, reflux, 4 h; (viii) KO^tBu, THF, 20 °C, 24 h.

The synthetic route to PPV **1** is shown in Scheme 1.1 and involves a precursor polymer that can be easily converted in solution or the solid state to give the fully conjugated polymer. This is advantageous as it allows for easy processing of films, especially over wide areas. Additionally this method yields high conjugation lengths and *trans* C=C bond ratios, which is important for

packing.[2] In early syntheses, 'X' was commonly a sulphonium ion in which case the corresponding synthesis is known as the Wessling precursor route.

Alternative routes to **1** can involve a xanthate ester, which can lead to improved PPV film quality and device efficiencies.[18] Sulphide and sulphonyl intermediates have also been used in similar precursor polymer routes, although such methods sometimes result in undesirable side reactions.[2] The intractable nature of **1** meant that soluble, and therefore more easily processable, derivatives of such PPVs were sought. Chief amongst these are dialkoxy PPV polymers that contain branching side chains, off the main polymer backbone, that allow for good solubility in common organic solvents, by allowing increased solvent interaction and by increasing the interchain distance, thereby preventing π-stacking. In this regard, MEH-PPV, **2**, (Scheme 1.1) has received much attention as an example of this class of polymer and, for example, benefits from having good solubility in many organic solvents. In addition, the synthesis leading to **2**, known as the Gilch route (Scheme 1.1b), is shorter than the Wessling route and gives rise to a polymer with a distinctly red-shifted emission (λ_{max} = 590 nm). However, this route often results in materials that contain significant defects that arise from unwanted head-to-head or tail-to-tail coupling.[19] ^{13}C NMR studies have confirmed the presence of a tolane-bisbenzyl structural unit as the main defect.[20] The impact on devices can be appreciable; in a recent comparative study, the power conversion efficiency (η_c) for two organic bulk heterojunction solar cells (see section 1.1.2) based on a PPV and C_{60} derivative were measured, with the only difference being in the synthetic route used to synthesise the PPV. For the Gilch polymer η_c was ~ 2.5% as compared with 3% measured for the sulphinyl derived polymer.[21] The difference was attributed to changes in the polymer microstructure which in turn depend on the fidelity of the polymeric route followed.[21,22]

OLED device fabrication from CPs involves a multi-layered process (Figure 1.1a and Figure 1.1b); the anode is typically made from ITO (indium tin oxide; a transparent conductor that allows the generated light to exit the device) and one or more layers of the polymer is deposited onto the anode by spin-coating.[2] The top layer cathode is chosen such that electron injection is facile and typically calcium or aluminium are chosen as they have low work-functions.[2] When the system is forward biased, electrons and holes are injected into the device and neutral excited states known as excitons are formed that can undergo radiative decay giving rise to light emission. Importantly, unlike for photoexcited CPs, where only singlet excitons are generated, the formation of excitons by the combination of electrically injected electrons and holes results in the generation of excitons in both the singlet and triplet states, with as many as 75% of the charges in the three-fold degenerate triplet state.[23] As the spin-allowed radiative emission (fluorescence) in organic conjugated polymers originates from singlet states only, this imparts a statistical imbalance that

potentially limits the efficiency of such devices to 25%, though more recent investigations have shown deviations from the theoretical limit.[24]

To circumvent such issues, recent efforts have focused on incorporating transition metals into the polymeric backbone. These high-atomic number elements induce the necessary spin-orbit coupling that then allow emission to also occur from the triplet excited state. Alternative phosphors that display significant spin-orbit coupling are organometallic complexes, particularly those derived from iridium where phosphorescent efficiencies of 87% have been reported.[25]

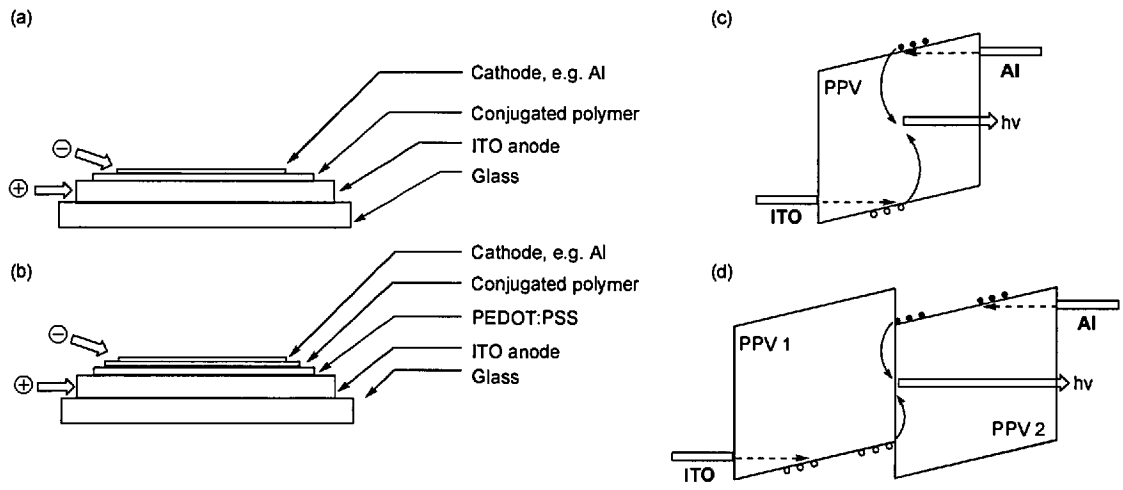

Figure 1.1 Representation of (a) a single layer device and (b) a single layer device with a hole-injection layer. (c) Band scheme for the description of the HOMO-LUMO levels in a single layer device and (d) a double layer device.

It is important to balance the injection rates and mobilities for both holes and electrons in the device to maximise the probability of exciton formation by electron/hole recombination. Efforts to improve the efficiency of OLED have looked at the deposition methods and the electrode interfaces. The nature of the ITO anode was also considered and in a bid to improve the hole-injection properties researchers have included hole-transporting layers, like poly(3,4-ethylenedioxythiophene) (PEDOT) doped with poly(styrene sulphonate) (PSS), into the typical OLED device structure (Figure 1.1b) which is also advantageous as such additional layers cover the roughness of the ITO surface.[1] Such changes have led to notable improvements in the performance of such diodes with efficiencies of 16 lmW^{-1} (lumens per watt) reported for PPV-based systems.[23,26]

A common problem for OLEDs is related to the good hole mobility in conjugated polymers and poor electron transport due to electron traps such as molecular oxygen. This gives rise to

recombination near the metal-cathode interface, which reduces the efficiency of the device. A strategy often used to avoid this involves the incorporation of an electron conducting hole blocking (ECHB) layer between the cathode and the polymer layer, which serves to move the recombination site closer to the centre of the polymer layer.[2] This is desirable because efficient emission only occurs away from the electrodes. The area in the vicinity of the electrodes displays low radiative efficiencies due to quenching by surface plasmons[2] and confining electrons and holes to the narrow recombination zone in the middle of the device is therefore advantageous.[27] Other changes to the standard device setup, involve multilayered structures where a potential barrier is created in the middle of the device (Figure 1.1d) in which both electrons and holes are accumulated prior to recombination and subsequent emission, allowing for an even current balance as they are much more likely to recombine there.[28]

1.1.2 Solar cells

Another important use for conjugated polymers is as an active layer in organic solar cells. Such devices consist of at least one heterojunction, between a donor material and an acceptor material. They operate by enabling photogenerated excitons (formed by the absorbance of solar light) to dissociate at the donor/acceptor junction, a process which is dependent on the nature of the excited state (exciton). Optimal materials for photovoltaics have to harvest the excitons efficiently to ensure that as many as possible are dissociated at the interface, and that this interface is at a distance that is ideally within the range of the displacement of the exciton during its lifetime (the exciton diffusion length).[8]

Some of the latest advances in organic solar cells include designs based on a blend of soluble C_{60}-derivatives (that are electron accepting) and conjugated polymers, an example of which is given in Figure 1.2. C_{60} molecules have often been used as the electron acceptor since it was shown that they can participate in rapid photoinduced electron transfer (PET) with conjugated polymers.[29]

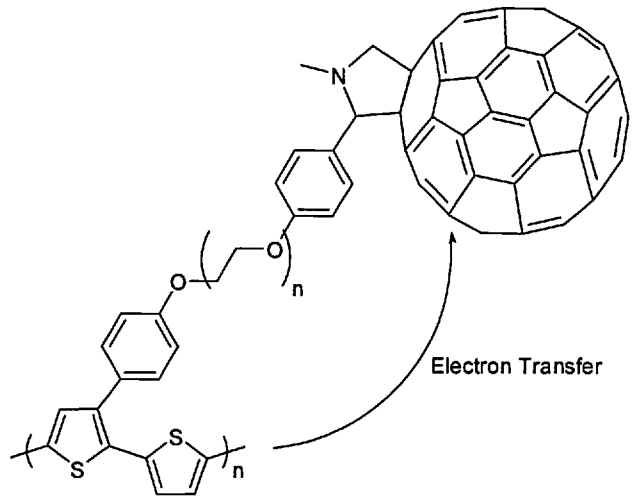

18

Figure 1.2 A C_{60}-derivitised poly(thiophene) for use in photovoltaics.[30]

Poly(alkylthiophenes) (PATs) are perhaps the most widely used polymers in such applications as they have high hole mobilities and a small band gap compared to other CP derivatives, providing an improved match to the theoretical optimal bandgap of 1.4 eV.[8] The synthesis of **18** (Figure 1.2) can be accomplished by electropolymerisation and proceeds in good yield. Polymer **18** is typical of the types of PAT materials investigated for photovoltaics.[31] Other examples of fullerene-containing CPs based on organic bulk heterojunctions include a C_{60}-derivitised PPV[32] that displays an open-circuit voltage of 0.83 V, which it is claimed is the highest for a *single-component* system.[8] Despite these steps forward, the overall efficiencies for such solar cells are currently limited to around 5% compared with, for example, ~ 24% for single crystal silicon.[33]

Early work on solar cells focused on improving efficiencies by vastly increasing the interface area of heterojunctions in inorganic-organic dye-sensitised solar cells.[13] In a recent development in this field Haque *et al.* described how they have increased the lifetime of the charge-separated state in such a material (Figure 1.3).[34]

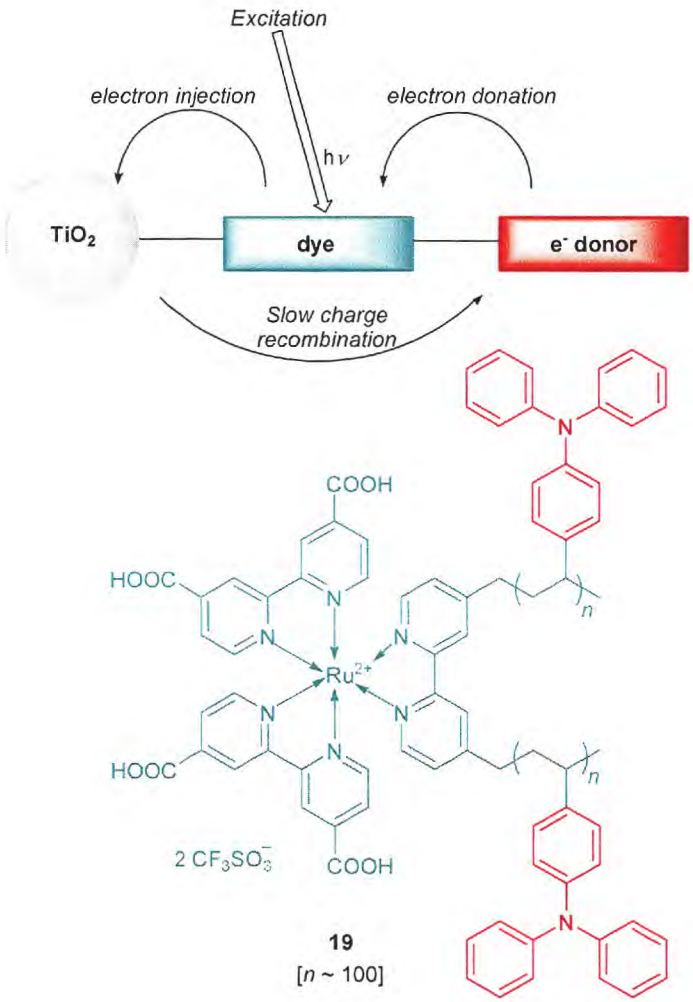

Figure 1.3 An explanation of the charge transfer processes along with the structure of one of the dyes used in the solar cells designed by Haque *et al.*; incorporation of this dye led to a charged-separated state with a lifetime of 4 s.[34]

Upon photoexcitation, such solar cells eject an electron which is then delocalised in the semiconducting TiO_2 layer.[35] For the different dyes tested the delays varied between 350 μs and 4 s which is, according to Haque *et al.*, the longest lifetime recorded for a dye-sensitised metal-oxide film.[34,36] By modulating the distance between the dye and the TiO_2 surface, they were able to slow the charge-recombination kinetics, with the origin of this long-lived excited state being the multi-step relaxation process that has to occur before the molecular ensemble reaches the ground state.[34]

1.1.3 Towards molecular machines and insulated wires

The building blocks used for the construction of semiconducting polymers are increasingly finding uses in other fields. Molecular machines and devices – miniaturised constructions that have the

ability to do work or exhibit controlled motion – are increasingly being explored as potential components for use in a variety of applications. To this end molecular electronics is ripe for investigation as many of the properties of semiconducting polymers are well suited for use in such machines. There are numerous examples of switches,[37] rectifiers,[38] rotors,[9] gearboxes,[39] DNA damage detectors[40] and transistors based on organic semiconducting units.[41] In a recent addition to this list, Tour *et al.* described their work on the synthesis and testing of a thermally driven 'nanocar' based on semiconducting phenylene ethnylene subunits for the chassis and axels and C_{60} fullerene units for the wheels.[42] An important requisite for any molecular machine device is directionality of motion[6] and, for the nanocar, the wheels (C_{60} units) have the potential to rotate along the axis of the C-C single bonds (the cars axel) to which they were attached, meaning that they could rotate independently and restrict coherent motion. Indeed as the thermal gradient was applied, the ability of the C_{60} units to rotate freely led to 2D motion as opposed to 1D motion that the researchers expected. Tour *et al.* observed direction-controlled motion when an STM tip was placed in front of the car enabling them to pull the vehicle in a given direction. Since this initial disclosure, Tour *et al.* have reported more details on their surface-rolling molecules, including the synthesis of a 'nanotruck' containing a planar chassis perpendicular to the C_{60} wheels.[43] However, as yet no progress has been made in demonstrating useful functions for such molecular entities.[44]

Actuators[45] (specifically microactuators) based on conjugated polymers were reported by Baughman in the early 1990s. An actuator has the ability to convert one type of energy into mechanical energy (motion) and such devices are finding a myriad of uses in biomedical applications. In particular, conjugated polymers are well-suited to applications at the biological interface as they are insensitive to the high ionic strength conditions. These materials are approaching the standard required for use in biomedical devices as actuation strains of up to 26% have been reported together with an improvement, compared with earlier designs, in the voltage levels required for actuation.[46,47]

The mechanism for actuation relies on the electrolytic solution which the polymer comes into contact with. Ions from solution act as a dopant for the polymer and the flow of ions into and out of the polymer controls the conformation.[46] This allows for changes in the dimension of the polymer to be achieved electrochemically. For example, the reconnection of severed blood vessels is a time-consuming and difficult procedure, but the development of a microfabricated polypyrrole bilayer, which works in a similar sense to a stent, could ease the problem. In essence, the polymer in its coiled-up conformation (achieved by applying a reducing potential), is placed between the two ends of the vessel and following the removal of the potential difference, returns to its elongated form, still holding the two ends of tissue while they knit together.[46] This system has several advantages as it doesn't block the blood vessel while it heals and can be fitted quickly, thus

avoiding extensive trauma. This use of CP actuators highlights one of the many advantages for such systems, namely that they can operate in highly polar environments such as body fluids.[45] Most work on actuators to date has focused on polyaniline, poly(thiophene) and poly(pyrrole) (PPy), which are also biocompatible and have been used in tissue engineering and such electroactive polymers have been used to trigger controlled cell growth.[46]

As will be described later (section 1.4.2) the aggregation of conjugated polymer chains in solution is a common phenomenon. The effect stems from π-π interactions between neighbouring chains and is of central importance in allowing photoexcitations to travel across a vast polymer network, which has implications for sensing (see Chapter Three) and charge mobility in polymer FETs.[48] However, such strong interchain interactions can be to the detriment of OLED design as the emission can be red-shifted and partially quenched. To avoid such issues, Anderson and Cacialli *et al.* prepared insulated molecular wires based on conjugated polyrotaxanes (**24** in Scheme 1.2).[49]

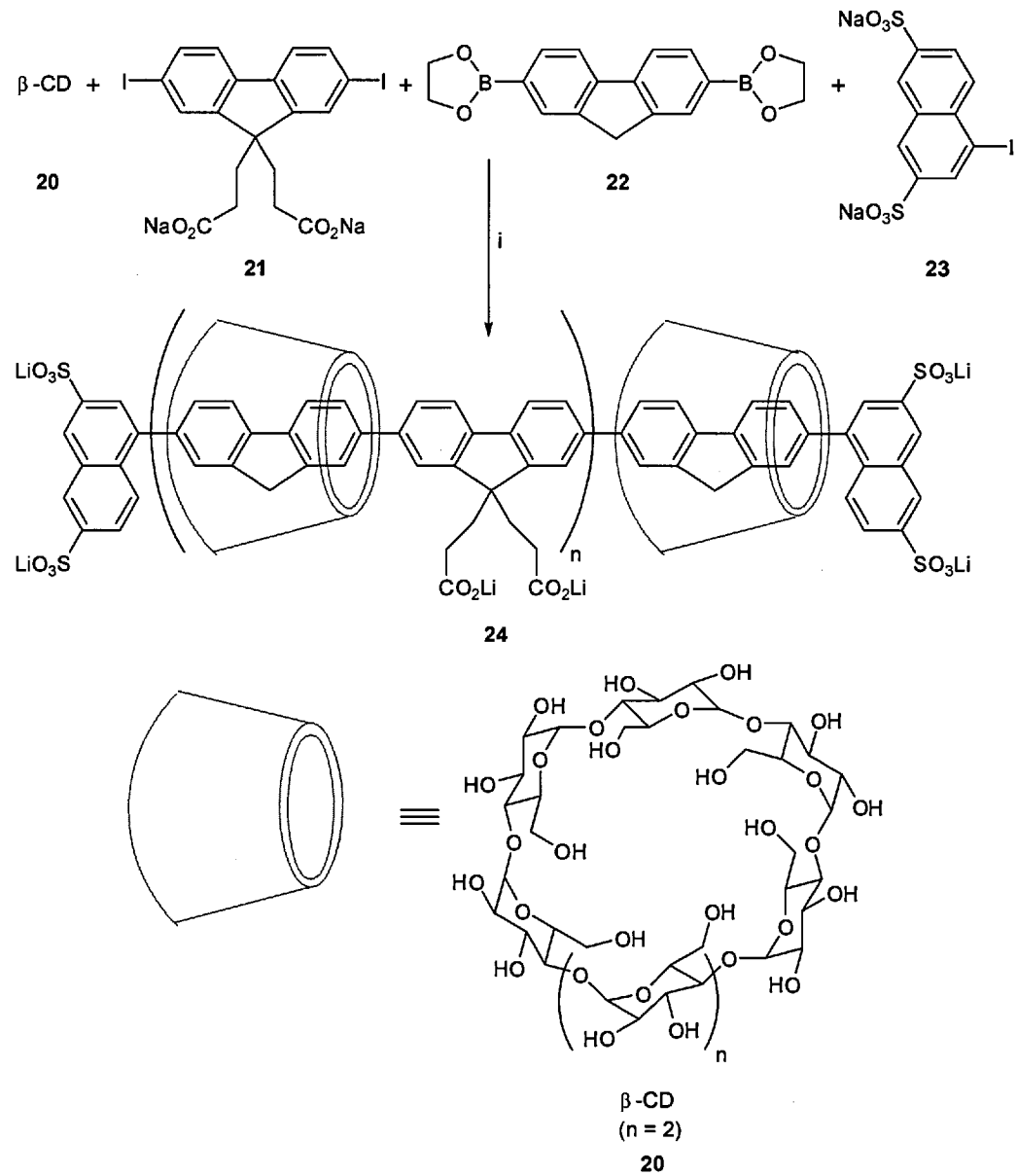

Scheme 1.2 Synthesis of an insulated molecular wire in the form of a rotaxinated conjugated polymer. Conditions: (i) $Pd(OAc)_2$, Li_2CO_3, r. t., 18 h, 86%.[49,50]

The synthesis of the polyrotaxanes was achieved by aqueous Suzuki cross-coupling in the presence of the enscapsulating agent β-cyclodextrin (**20**), with threading of the macrocycle driven by the hydrophobic effect. This A + B step-growth polycondensation was used to produce PPP and PF conjugated polymers and gave materials with moderate degrees of polymerisation (~ 20 repeat units) as confirmed by ^{1}H NMR (*via* integration of stopper end-groups), MALDI-tof (for the PPP polymers) and analytical ultracentrifugation (AUC).[49,50] Analysis of the luminescent properties of the rotaxinated polymers showed that their absorption and emission maximum were blue-shifted (typically by 10-30 nm) and PL efficiencies increased (6%) relative to the non-insulated material.[49]

The threaded materials were also used to fabricate LEDs which displayed luminance levels of 'several candela per square metre'.[49] SFM of thin films showed the PPP rotaxanes as individual rods.[49] Taken together, all this evidence confirms the vastly reduced aggregation tendency of the insulated material and the associated benefits that this brings.

1.2 What is a biosensor?

Examples of common optoelectronic devices based on conjugated polymers have been described in the previous section. The use of these materials in sensory technologies represents a new avenue of research. CP based sensors have been used to detect small molecules as well as biomolecules.[51] Such systems exploit the semiconducting properties of the polymers with transduction based on changes in electrical conductivity, chemical potential or optical properties. Some examples of these different techniques will be discussed in the following sections (1.2.2 to 1.2.6).

The ability to detect DNA hybridisation, in a highly sensitive and selective manner, has always been a central objective in the development of modern biosensing techniques. In recent times the demand for such technologies has been even more pressing as threats from biohazards, like the current Avian Flu epidemic,[52] and advances in genetics, such as the mapping of the human genome, demand more robust and rapid diagnostic techniques.[53]

A chemical sensor can be described as a device that selectively and continuously recognises the presence or concentration of a given analyte and converts this information into an electrical or optical signal. As biosensors fall into a specific subset of chemical sensors, they can be defined as follows; *a biosensor is a chemical sensor in which the sensing element is able to respond to the biological analyte of choice, with the system able to undergo a chemical or physical change that is observable on a macroscopic level.*[54]

In such devices, the biological sensing (recognition) element is coupled to a transducer that is able to report the recognition event, that occurs on the sub-microscopic scale, into a useful and easily observable macroscopic signal such as an optical, electrical or electrochemical output (Figure 1.4).[53]

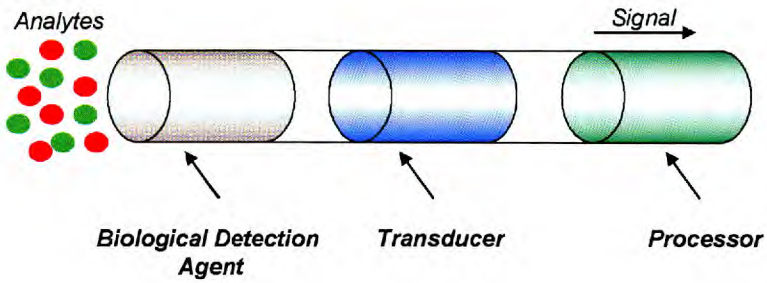

Figure 1.4 A simple schematic of a biosensor.

For CP biosensors based on changes in optical responses, the biological detection agent and transducer (Figure 1.4) are commonly incorporated in the polymer backbone.

1.2.1 Current applications of detection technology - techniques for the selective detection of DNA

In the past decade, several examples of DNA sensing using a variety of techniques have been outlined in the literature. As was alluded to in the previous section, the interest in such techniques has been strongly driven by the need for analytical devices for the detection and monitoring of biological entities (for example in the completion of the human genome project) and the need to diagnose genetic diseases in a timely fashion. These devices, once perfected, would find use in a variety of medical applications and research. For example semiconducting polymers could supplant currently used methods for the identification of biological molecules, like the ELISA (enzyme-linked immunosorbant assay) technique, which has certain drawbacks such as being time-consuming and labour intensive.[55] Methods for the detection and discrimination of DNA biopolymers have sparked fervent interest among many research groups for many reasons:

(i) Novel ways are required to track gene delivery, for example *via* fluorescence monitoring; and

(ii) Specific genomic techniques could be explored, which would provide a useful tool for, amongst other things, genetic fingerprinting (as an aid in crime prevention) and systems biology input.

Clearly unlocking a sequence specific technique to DNA biosensing would have far reaching ramifications and the potential for commercial exploitation is high.[56] In the following sections, some generic and state-of-the-art DNA detection techniques will be considered and comparisons drawn between them and our proposed detection platform.

1.2.2 Electrochemical biosensors

Electrochemical biosensors rely on a change in the electrochemical response upon hybridisation and numerous examples are documented in the literature.[57] DNA sensing using surface techniques has many potential advantages including ease of access of the target genetic material to the surface and the ability to obtain rapid, sequence-specific detection without significant pre-treatment of the target material.[53]

A recent example of such a device is provided by Korri-Youssoufi *et al.* and involves an oligonucleotide-functionalised electroactive polypyrrole conjugated polymer (Figure 1.5).[58]

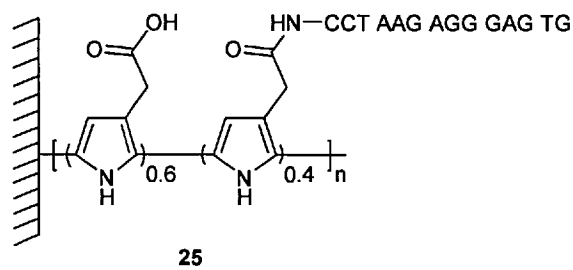

25

Figure 1.5 Structure of the functionalised polypyrrole electrode poly[(3-acetic acid pyrrole-*co*-3-ODN acetamido pyrrole)] electrode, as employed by Koumi-Youssououfi *et al.* in an electrochemical DNA sensor.[58]

In this example, the hybridisation of non-complementary strands with the probe oligonucleotide (ODN) appended onto the polypyrrole backbone (**25**), led to an unchanged electrochemical response. Exposure to the exact complementary strand (by incubation in a buffered aqueous solution for two hours) had the effect of decreasing the current level, which led to a concomitant increase in oxidation potential.[58]

The use of electrochemical-based DNA sensors has also been explored by Barton *et al.* to determine base-pair mismatches and points of damage (lesions) along oligonucleotide strands, which can result from contact with carcinogens.[59] Surface techniques often involve thiol-terminated probes that are used in conjunction with gold surfaces – thus exploiting the auriophilic nature of sulphur[13] – and Barton *et al.* used this principle to construct an assembly involving (thiol-terminated) probe oligonucleotides on a gold surface. In their scheme, single base-pair mismatches can be monitored electrochemically (as the reduction of a carefully chosen intercalator can occur *via* DNA-mediated charge transfer only if complete base-pair matching is present along the DNA fragment up to that point) and perturbations along the chain affect the efficiency of the reduction process. The detection limits for this technique are at the micromolar level, and are limited to the concentration of the intercalator (methylene blue, MB, at 2 μM).[59]

The versatility of such methods was demonstrated by Anzai *et al.* who were the first to use a redox polymer for the electrochemical sensing of DNA.[60] In an idea similar to that used by Barton *et al.*,[59] a thiol probe sequence was appended to a gold surface and then exposed to the target sequence, after initially being cleaned (by running a scanning potential in a solution of sulphuric acid) to remove excess DNA fragments that remained during the surface treatment process. Specific hybridisation could be detected by deposition of the redox-active polymer to the surface and performing differential pulse voltametry in (tris(hydroxymethyl) aminomethane) TRIS buffered solutions, thereby allowing for the detection of double-stranded DNA at the picomolar concentration level.[60]

1.2.3 Detection of DNA by chip-based methods

The growing field of chip-based sensor technology involves the integration of the initial detection and subsequent processing and output signal all on a single device. One of the most attractive features of lab-on-a-chip schemes is the inherent miniaturisation of the analysis system which reduces the amount of sample required to perform the detection, along with the time required for analysis.[61] Some disadvantages of early planar chip-based sensors, including the necessity for amplification of genetic material, have since been overcome.[62]

McDevitt *et al.* have described a second-generation sensor array where they sought to avoid problems of low sensitivity.[62] Here, agarose polymer microbeads were stationed in an embossed multiple-well silicon wafer grid (Figure 1.6). Columns of the microbeads, containing three different DNA capture strands, were previously arranged on the silicon wafer. Each well, filled with the avidin coated microbead, was then treated with biotinylated DNA capture probes, with the resulting wafer able to accommodate fluid flow into the bead chamber whilst allowing optical analyses, which were recorded using a CCD camera. The target materials were functionalised with three different fluorophores which allowed the hybridisation events to be monitored in real-time.[62]

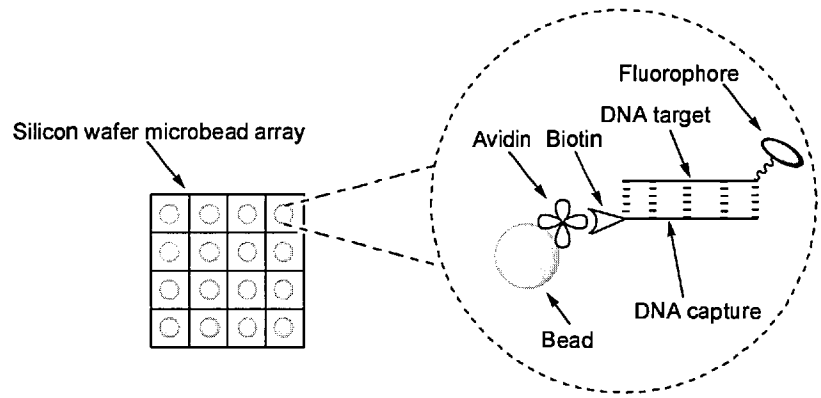

Figure 1.6 The experimental setup for the chip-based microbead array, used for detecting single base-pair mismatches in DNA.[62]

The system can be used to detect other targets by a simple 'flush' procedure which allows for the beads to be regenerated by addition of a buffered formamide solution, which can wash through the chip *via* microdrains. Despite boasting detection limits of ~ 10^{-13} M, with all assays completed within an hour, the modification of the DNA material prior to analysis (pre-treatment by addition of a fluorophore group) is still a hurdle to be overcome, as this would restrict the use of such a system in the field.

1.2.4 Carbon nanotubes for DNA detection

Increasing interest in the use of carbon nanotubes (CNTs) in the area of biotechnology has driven researchers to find out how these materials can be used as ion-channel blockers, biocatalysts and as sensors.[63] In these systems, CNTs are often used as the sensing device and when coupled to a sensitive transduction technique, form a reliable way of reporting the recognition process. A carbon nanotube electrode, combined with an electrochemical system, has been shown to form the basis for a sensitive DNA detection system.[64] In such a system, amine-terminated probe DNA strands (in the first instance with 10 base-pairs) were coupled to a CNT based nanoelectrode to form an array, using the traditional coupling agents (water-soluble variants) EDAC and NHS (Figure 1.7).

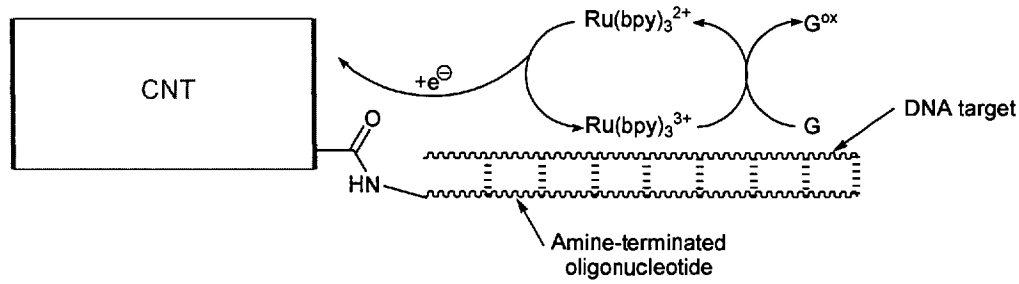

Figure 1.7 A primary amine-functionalised CNT and the associated mechanism of $Ru(bpy)_3^{2+}$ mediated guanine oxidation.[64]

The hybridisation process was monitored using cyclic voltammetry (CV) with the oxidation current of a particular base (guanine) used as an indicator. However, this technique proved difficult to implement due to high 'noise' signals, and a mediator, in the form of the complex $Ru(bpy)_3^{2+}$, was used instead. This allowed for a detection limit of 'a few attomoles'.[64] One shortcoming for this technique is related to the amount of probe preparation and modification required. As CV signals from guanine bases were used, a polyG sequence had to be attached to the target strand and the G-bases in the probe were exchanged, to ensure the current contribution was entirely due to the presence of the target. This combined with the relatively intricate fabrication techniques required to make and attach the CNTs to the silica surface somewhat limits the general appeal of such techniques.

1.2.5 Optical methods for DNA detection

Their ease of use combined with high selectivities, have propelled FRET-based (fluorescence resonance energy transfer) DNA detection schemes to the fore in recent years. In examples to be described later (section 1.5) light-harvesting conjugated polymers were combined with dye-tethered probes in a CP-FRET-based detection scheme for oligonucleotides. One drawback of such methods comes from strong background emission from the polymer or dye (due to unintentional excitation) which hinders observation of the hybridisation event. To combat this, Wang *et al.* have recently described a single-quantum-dot-based nanosensor (Figure 1.8) that uses CdSe-ZnS core-shell quantum dots (QDs) combined with biotinylated capture probes and a dye-tethered reporter probe.[65] Key to minimising the unwanted background fluorescence (stray emission) is the use of QDs, which due to their broad absorption allow for excitation at a wavelength which is well away from that of the dye, thus minimising direct excitation of the dye. In the system, a streptavidin-coated QD associates with the biotinylated capture probe, the reported probe and the target DNA to form an assembly in which the local concentration of the target material is enhanced.

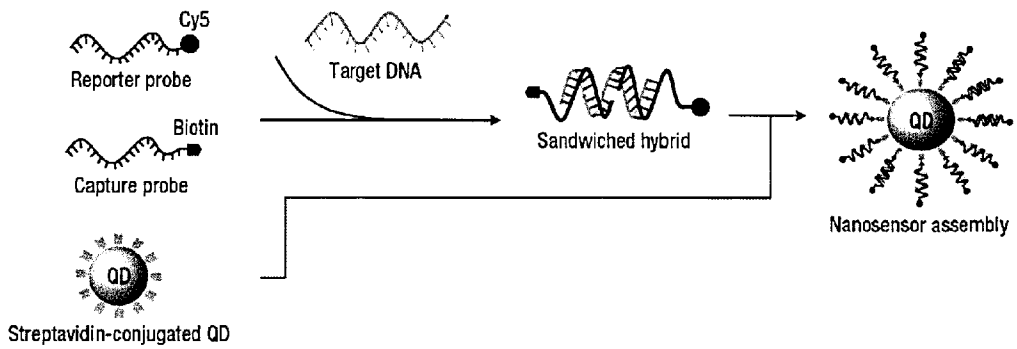

Figure 1.8 Schematic showing a DNA nanosensor assembly, formed from the quantum dot (QD), capture and reporter probes (reproduced from Zhang *et al.*).[65]

For the completed nanosensor assembly, illumination of the quantum dot gives rise to a FRET process which results in fluorescence from the dye located on the reporter probe. The system was validated by testing it against clinical samples of oligonucleotides, where it was able to successfully discriminate single base-pair mismatches. The benefits of this technique over other fluorescence-based methods were also noted; compared with the hairpin approach (see section 1.2.6, below) where background fluorescence is a major issue, the limit of detection could be extended to 10^{-15} M, which is comparable with the best conjugated polymer systems. Other advantages for Wang *et al.*'s system include the absence of pre-treatment steps for the target material and that no washing stages are required *en route* to the formation of the nano-ensemble.

1.2.6 DNA detection by hairpin molecular beacons

A common approach used to monitor DNA hybridisation involves a molecular hairpin; the principle is summarised in Figure 1.9. In this system the emission from a donor fluorophore can be modulated by changes in the conformation of the sensor. Hairpin molecular beacons (principle illustrated in Figure 1.9) represent a more recent development in this area, where a single-strand of DNA is modified at either end by addition of a donor and quencher species, which are typically incorporated into the structure of oligonucleotides using a DNA synthesiser and standard phosphoramidite chemistry.[66,67]

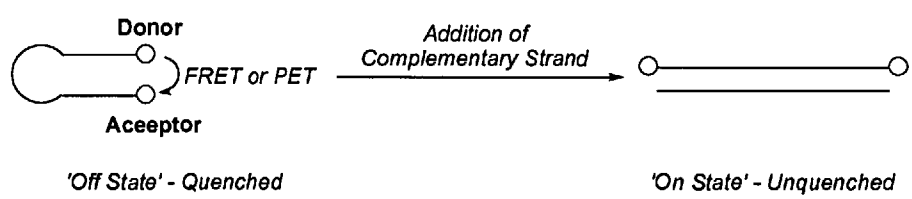

Figure 1.9 Structure and working principle behind the operation of a molecular beacon.

In the absence of target DNA material the beacons are non-fluorescent due to emission quenching by resonance energy transfer (RET) or photoinduced electron transfer (PET) from the donor to the acceptor. Quenching occurs due to the conformation of the native state of the beacon. The favourable π-π interactions ensure that the hairpin is closed – this forces the donor and quencher to be spatially close allowing energy or electron transfer. Upon annealing with target oligonucleotides the distance between the donor and quencher is vastly increased such that the no quenching occurs allowing the hairpin system to recover its fluorescence. In a new development, Kim *et al.* have detailed a molecular beacon probe that is quencher free;[67] emission from a fluorophore (fluorene) appended to the probe was shown to be quenched by C, T and G bases (by PET) but not the A (adenosine) base. This system allows one to discriminate the A base along a strand but it is worth noting that extensive preparation of the beacons is required prior to use.[67]

1.3 Reversible fluorescence quenching: sensitive chemical and biological sensors

Fluorescence quenching can be defined as an event in which an excited state molecule or polymer has its fluorescence reduced or eliminated.[66] After excitation, the electron can relax rapidly from the higher vibrational states to the lowest vibrational state, of the electronic excited state. Several mechanisms can result in decay to the ground state.[66] These include; excited-state reactions, molecular conformational rearrangements, energy transfer, electron transfer, dynamic (collisional) quenching, static (ground-state complex formation) quenching, solvent or quencher induced aggregation, non-radiative processes (internal conversion – heat) as well as a variety of trivial mechanisms.[66] For the sake of brevity this discussion will be limited to two important classes, namely the interactions between fluorophores and quencher molecules as depicted in the modified Jablonski diagram (Figure 1.10).

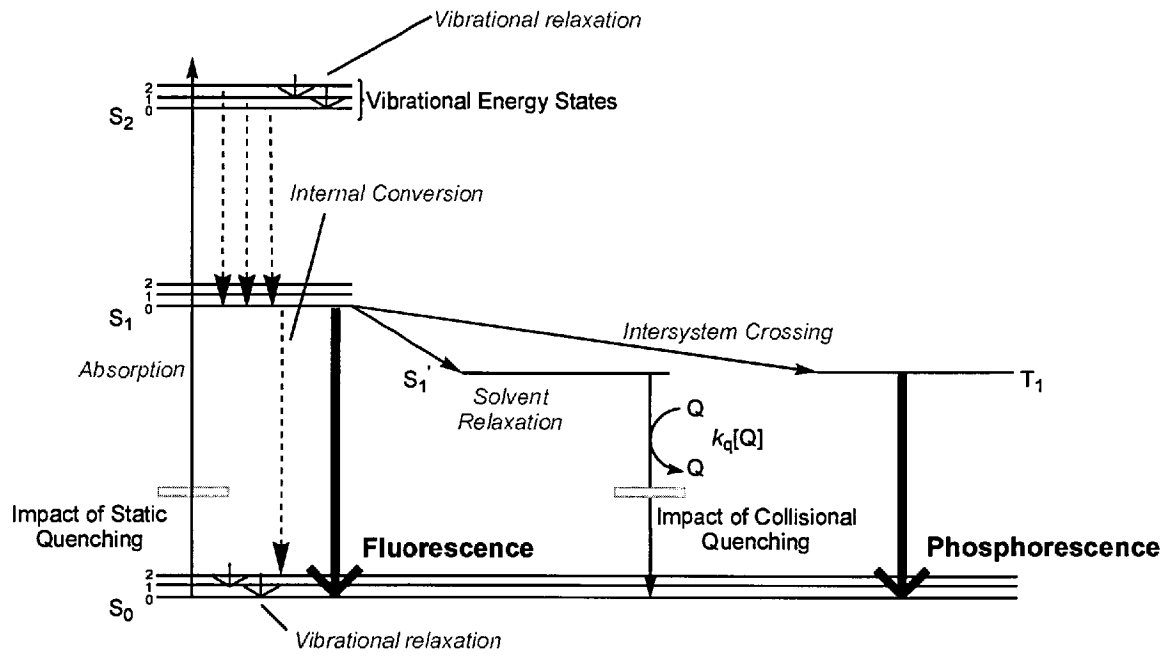

Figure 1.10 A modified Jablonski diagram, highlighting the differences between static and collisional quenching and the point at which they impact the quenching process.

The reduction in the resulting emission from the fluorophore is proportional to the concentration of the quenching species present and is defined by the Stern-Volmer equation[68] (derived below) which relates the fluorescence intensity I to the quencher concentration $[Q]$.

The Stern-Volmer equation is derived by considering the emission intensities in the presence and absence of a quencher.[66] The emission intensity is dependent on the concentration of the excited state species and under continuous optical excitation a constant population of the excited state species is established. Under these conditions, the rate of change ($d[F^*] / dt$) of the concentration of excited state molecules, $[F^*]$, is zero. Differential equations describing the variation of F^* (excited state molecules) can be defined; in the absence of the quencher, this is represented by:

$$\frac{d[F^*]}{dt} = f(t) - \lambda[F^*]_0 = 0$$

Equation 1

where $f(t)$ is the constant excitation function, λ (the decay rate) defines the radiative lifetime ($\lambda = \tau_0^{-1}$) in the absence of the quencher and $[F^*]_0$ is the concentration of excited state molecules in the

absence the quencher molecules. In this case λ includes both the radiative and non-radiative decay constants. In the presence of the quencher, this is modified as shown:

$$\frac{d[F^*]}{dt} = f(t) - (\lambda + k_q[Q])[F^*] = 0$$

Equation 2

where $k_q[Q]$ is the additional decay constant due to the quencher. The two differential equations can be simplified because under continuous laser excitation, the population of fluorophores in the excited state remains constant. Therefore, combining Equations 1 and 2:

$$1 = \frac{\lambda[F^*]_0}{(\lambda + k_q[Q])[F^*]}$$

Equation 3

which can be rearranged to give the Stern-Volmer equation, which is commonly written in terms of the emission intensities:[66]

$$I = \frac{I_0}{1 + k_{SV}[Q]}$$

Equation 4

where I_0 is the emission intensity in the absence of the quencher, I represents the emission intensity in the presence of the quencher and k_{SV} the Stern-Volmer constant, which is also equal to the product of the bimolecular quenching constant (k_q) and the emission lifetime, τ_0, in the absence of the quencher (this discussion only applies to dynamic quenching). Using this non-linear equation (Equation 4), a Stern-Volmer plot of I versus $[Q]$ allows one to extract k_{SV}.

The different modes for fluorescence quenching impact the relaxation pathways at different points. The collisional deactivation of a fluorophore results from interaction of an excited-state fluorophore with quencher molecules, and for solution studies is significant. For static quenching, a ground state non-emissive complex is formed, which, when excited, returns to the ground state immediately without the emission of a photon.[66] In this case the value of k_{SV} represents the effective binding constant for the formed complex. Experimentally this type of quenching is easily

distinguished from dynamic quenching by considering the relative changes in the emission lifetime during the quenching process; for static quenching, the ratio τ_0/τ, remains constant (= 1) as the emission observed emanates from the non-complexed fraction, which is unaffected upon addition of the quencher.[66] Additionally, if the Stern-Volmer constant obtained from intensity quenching is greater than that recorded using lifetime quenching measurements, static quenching is dominant.[69] If the polymer excited state has higher energy than the LUMO level of the quencher, the resulting electron transfer would be energetically favourable (high rates of electron transfer, with large negative free energies).[70]

The energy transfer (ET) mechanism of emission quenching involves the absorbance of a photon emitted from the donor, by the acceptor. For this process to occur efficiently, good spectral overlap is required between the emission spectrum of the donor species and the absorption spectrum of the acceptor. Also important in the process is the distance between the absorbing and emitting molecules, with the amount of energy transfer having an inverse relationship with increasing distance between the two (ET $\propto r^{-6}$).[55] Other factors affecting the rate of energy transfer include the shape and directionality of transition dipoles for the donor and acceptor and the fluorescence quantum yield of the donor.[66]

In solution, as a quencher diffuses towards a fluorophore, the resulting collision between the two can lead to quenching. This dynamic (collisional) quenching mechanism, like ET and static quenching can be described by the Stern-Volmer equation. Dynamic quenching can be differentiated from static quenching by consideration of the gradient of the Stern-Volmer plot which increases with temperature due to higher rates of diffusion which increases the rate constant (k_q) for collisional quenching. The Stern-Volmer constant allows one to gain an insight into the efficiency of the overall quenching process as values for k_q can be obtained, providing knowledge of the radiative lifetime is known.[66]

Solvent or quencher-induced aggregation can lead to emission quenching and is often observed for PPE polymers. Some examples are illustrated in later sections in this chapter. In these cases, it has been suggested that the quencher serves as template to promote aggregation of polymer chains.[71] Crucially, this increases the number of fluorophores that are within close proximity to the quencher, thus extending its quenching radius.[72] The characteristic signature for this mode of quenching is a narrowing and red-shifting of the position of the absorption band and a broadening of the fluorescence.

Other mechanisms to dissipate the absorbed photon energy and that may be important for quenching include non-radiative energy transfer (internal conversion – heat), for example, induced

by an external heavy-atom effect. Alternatively, a non-radiative decrease in fluorescence intensity may be attributed to exciton-exciton annihilation, which could be probed by observing the effect on the emission intensity upon varying the excitation intensity.[73]

Enhanced or amplified quenching is an extremely efficient emission quenching process that has been thoroughly investigated in conjugated polymers by Chen *et al.*[74] and others.[75] This work formed the basis for such materials to be touted as potentially new biosensors. However, for this to be realised, the amplified quenching effect had to be observed in aqueous milieu and this was duly proved by several groups soon after, where a range of different CPEs were investigated with complementary charged quenchers.[76,77] Amplified fluorescence quenching, like conventional emission quenching, is approximately described by the Stern-Volmer equation, which allows for quantification of the sensitivity of the quenching process. Importantly, for conjugated polyelectrolytes the two dominant mechanisms for quenching, energy transfer and electron transfer through complex formation (static quenching), are both described by Equation 4. The significance of the amplification process is best emphasised by consideration of the two systems (**26** and **27**) in Figure 1.11.

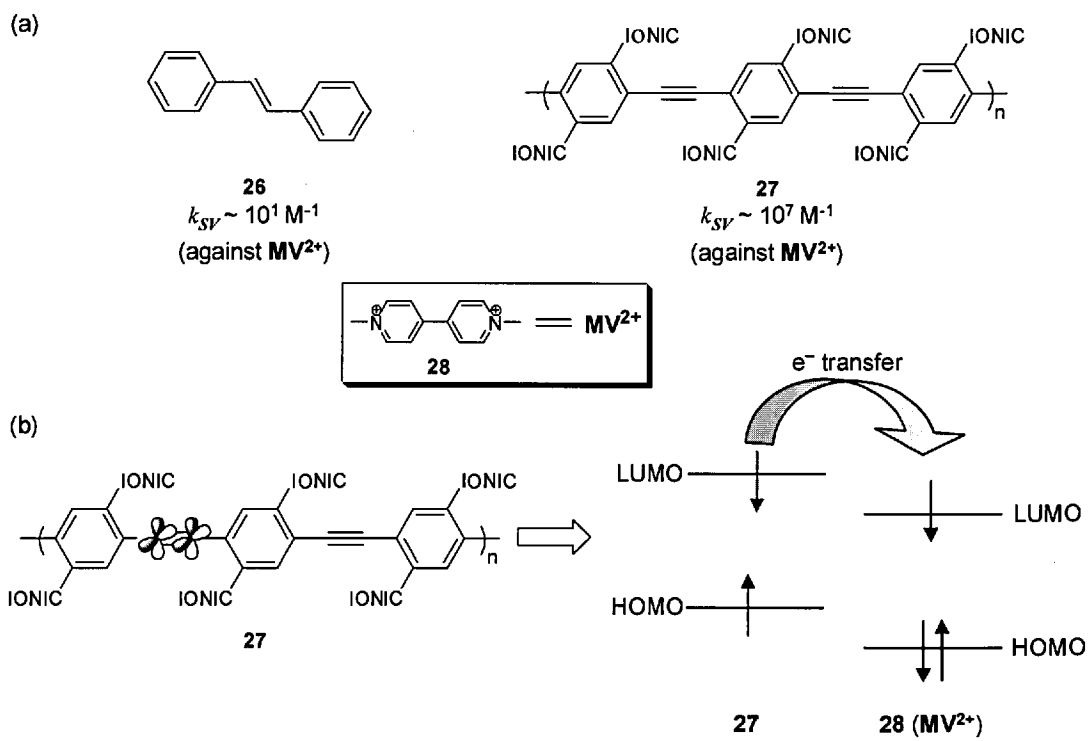

Figure 1.11 (a) Comparison of Stern-Volmer coefficients for the quenching of *trans*-stilbene and an ionic CPE by MV^{2+} (b) the photoinduced electron transfer process that occurs between CPEs and an emission quencher such as MV^{2+}.

Typically, values observed for the quenching of CPEs by common electron acceptors such as methyl viologen ($\mathbf{MV^{2+}}$), **AQS** and metal complexes range from $k_{SV} = 10^6 - 10^8$ M^{-1}.[71,78] The equivalent quenching of *trans*-stilbene by $\mathbf{MV^{2+}}$ yields a Stern-Volmer constant of 15 M^{-1}.[79] Schanze has attributed the high quenching efficiency to two effects;[77] the first, ion-pairing, results from charge complementarity between the quencher and polymer. This effectively increases the concentration of the quencher that is within close proximity to the polymer. The second effect, centres on the nature of the excited state exciton which is extensively delocalised along the polymer backbone. Importantly, it can move rapidly between polymer chains due to interchain interactions (that result from aggregation). The combination of these effects allows the quencher to impact distant polymer chains, thus significantly increasing its 'quenching radius'. Indeed extensive investigations by Swager *et al.*,[76] Schanze *et al.*,[71] and Whitten *et al.*[80] has led to essentially all of the latest work on CPE biosensors being concentrated on a specific class of polyelectrolyte, namely poly(phenylene ethynylene)s (PPEs). This material is preferred because the singlet exciton is highly delocalised and able diffuse rapidly along and between polymer chains.[66,71] Additionally, PPEs display high quantum yields.

Photoexcitation of these conjugated polymers results in an excited state consisting of electrons and holes. The formed electron-hole pairs are called excitons (which act like particles in their own right with an associated binding energy).[13] Fundamental studies have shown[76,77,81] that the excitons in PPEs are highly mobile and can easily traverse the polymer chain. It is this ability of excitons to sample many sites during their lifetime which leads to such aggressive emission quenching, as the binding of the quencher at any point along the polymer backbone allows for excitons to be split (with an electron transferred to the quencher, leading to oxidation of the polymer). The fluorophore is shunted to the ground state when the electron is transferred back. The potency of this effect is often elegantly demonstrated by comparison of the size of the Stern-Volmer coefficients recovered from polymer emission quenching and model compound emission quenching. Often the model compound will be a small molecule analogue of the polymer, typically 2-3 repeat units in lengths. The differences are stark and commonly a 100-10000-fold increase in sensitivity can be observed for the polymeric derivative compared to the small model analogue, showing the central importance of the conjugation length (though appreciable polymer aggregation is vital in enabling the photoexcitations to delocalise between polymer chains) and exciton diffusion in quenching.

1.4 Conjugated polymers for DNA sensing

From the arguments discussed so far, the relevance of DNA-detection methods that can analyse small quantities of genetic material in a timely fashion are obvious as is the pressing need to widen

the scope of such technologies. Of the methods outlined, homogeneous assays (as opposed to heterogeneous assays) still remain the most attractive sensing techniques due to the remarkable sensitivities that can be achieved. Development of homogeneous assays based on fluorescent conjugated polymers is a relatively new field investigated by few researchers so far. However, the results detailed by these groups are very encouraging, especially with respect to the ease of use of the systems. Moreover, detection limits are rapidly approaching those reported for the best DNA sensing techniques.[82] There are important hurdles to overcome, for example, with respect to gaining a better understanding of the effect on emission properties of various biological media (which is the subject of Chapter Three), and such issues are being actively investigated by many groups including our own. In the following sections, examples of CPEs used to detect DNA strands will be considered along with the merits of each technique.

1.4.1 Synthetic routes to conjugated polymers

In order to develop generic biosensing technologies based on conjugated polymers, water-soluble derivatives are needed. Since the initial findings by Wudl[83] and Novak[84] in the 1990s, the following decade saw many reports detailing syntheses to a variety of water-soluble CPs with various backbones. CPs can be rendered water-soluble by attachment of ionic side-chains along the central polymer backbone. The newly formed polymers, known as conjugated polyelectrolytes, (CPEs), are commonly employed in various biosensing schemes. However, there is some interest in neutral water-soluble polymers as it is thought that such polymers would minimise non-specific interactions when used for biosensing (see sections 1.4.2 and 1.4.6).

In this section, typical syntheses of the main classes of CPs will be considered, with a particular focus on water-soluble materials. In preceding sections various CPEs with different architectures have been shown and, thanks to recent breakthroughs in cross-coupling chemistries, most can be accessed, under mild conditions, from transition-metal-based catalysis.[85]

Water-solubilising functional groups commonly employed include carboxylic, sulphonate, phosphate, ammonium and imidazolium moieties.[86] It is thought that such side-chains form a sheath around the hydrophobic conjugated polymer backbone, thereby insulating it from the neighbouring aqueous environment.[77] However an additional benefit involves the impact of these side-chains on the emission properties of the polymers, a point investigated by Schanze *et al.*, who showed that by careful control of the solution pH, the aggregation of a phosphate-based PPE polymer could be reduced, limiting the overall impact on the quantum yield for the material as interchain interactions are minimised (described in Scheme 1.5).[71]

The synthesis of this category of macromolecules is varied and the description given here represents a brief overview of some of the more commonly used routes to polymers used for such applications. Most synthetic schemes involve C-C bond forming reactions promoted by organometallic catalysts. The main types of conjugated polymer made *via* this procedure are listed in Table 1.2.

Table 1.2 Polymer categories and their typical synthetic routes.

Polymer type	Abbreviation	Synthetic route
Poly(*para*-phenylene)	PPP	Suzuki, Stille, Yamamoto couplings[87]
Poly(phenylene vinylene)	PPV	Wittig-Horner, Heck reactions, Gilch/Wessling routes[88]
Poly(phenylene ethynylene)	PPE	Sonogashira and alkyne metathesis reactions[85,89]
Poly(fluorene)	PF	Suzuki cross-coupling[90]
Poly(thiophene)	PT	oxidative polymerisation (e.g. $FeCl_3$ as oxidising agent)[91]

Typically these reactions benefit from mild reaction conditions, tolerance of a wide selection of functionalities (various ionic groups, such as carboxylates and phosphates are used)[86] and solvents (water and DMF are commonly employed for polymerisations).[86] Other important factors include the ability to obtain high molecular weights and the ease of synthesis of the monomers.

1.4.2 Water-soluble poly(phenylene ethynylene)s (PPEs)

The usual method used to prepare PPEs involves the Sonogashira coupling (a copolymerisation) of a dihalosubstituted aromatic molecule and a diethynyl-substituted aromatic molecule. Though other routes to PPEs exist, Sonogashira coupling is very widely applicable and has been shown to furnish many types of PPEs with widely varying substituents.[86] The diethynyl-substituted monomers are generally prepared by Sonogashira coupling of TMSA (trimethylsilyl acetylene) and a dihalosubstituted aromatic molecule followed by deprotection of the TMS groups. Polymerisation is catalysed by $Pd(PPh_3)_4$ (Pd(0) is the active complex) or $Pd(PPh_3)_2Cl_2$ which generates Pd(0) *in situ*.[92] PPEs from Sonogashira coupling (detailed in Scheme 1.4) are light yellow/green in colour and are strongly fluorescent materials. The first PPE material was prepared by Li *et al.* and involved coupling acetylene and the benzoic acid derivative **29** (Scheme 1.3).[93,94]

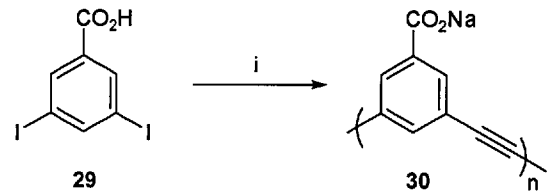

Scheme 1.3 Synthesis of a water-soluble PPE derivative. Conditions: (i) Acetylene, Pd(0), $NaOH/NEt_3/H_2O$, r. t., 72 h.[93,94]

The mechanism for the cross-coupling reaction (described in Scheme 1.4) is similar to that observed for many palladium catalysed cross-coupling reactions. The metal-catalysed cross-coupling reaction between an sp^2-carbon halide and a terminal acetylene was first reported by Heck, Cassar and Sonogashira in 1975.[95,96] Since then, the specific coupling of an unsaturated organic halide with a terminal acetylene has come to be known as a Sonogashira-Hagihara coupling[92] and has been used to great effect to synthesise a variety of different CPs.[86]

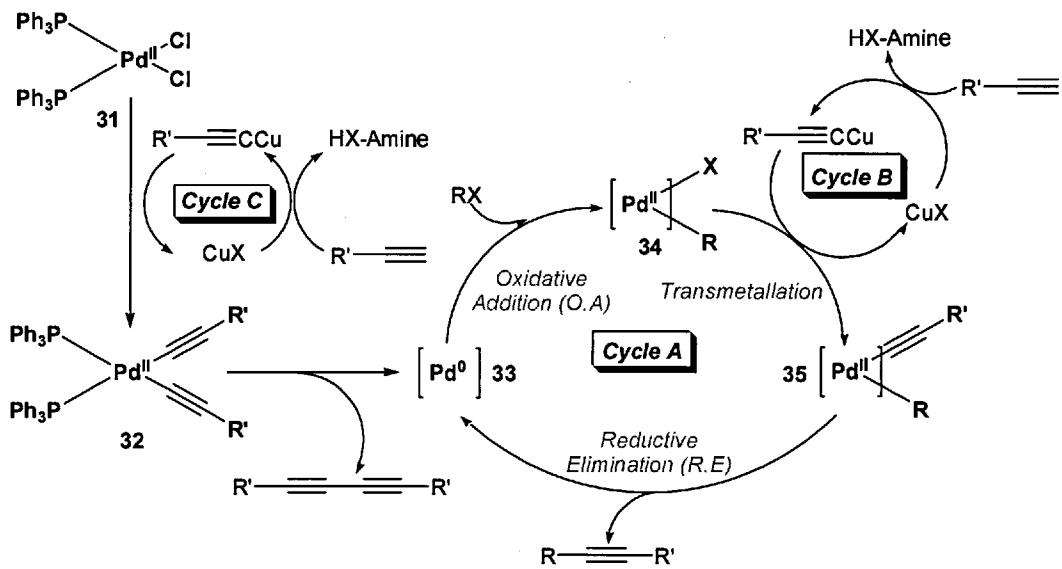

Scheme 1.4 The Sonogashira mechanism; mechanistic steps involved in the palladium-catalysed cross-coupling reaction used to make some PPE polymers.[95]

The exact mechanism for the reaction remains unclear though steps common to other palladium catalysed cross-coupling reactions, namely oxidative addition and reductive elimination, are involved.[85] The cycle described in Scheme 1.4, detailed by Sonogashira, involves three separate cycles. Cycle C is important when the source of palladium is the pre-catalyst $PdCl_2$, and leads to palladium (0) species **33**, which undergoes oxidative addition with the aryl iodide to yield **34**. The next stage, transmetallation, possibly occurs *via* a copper acetylide moiety, giving species **35**. Reductive elimination then gives the cross-coupled product, whilst simultaneously re-generating

the neutral palladium (0) species. Examples of the types of PPE structures that have been synthesised using this chemistry are illustrated in Figure 1.12.

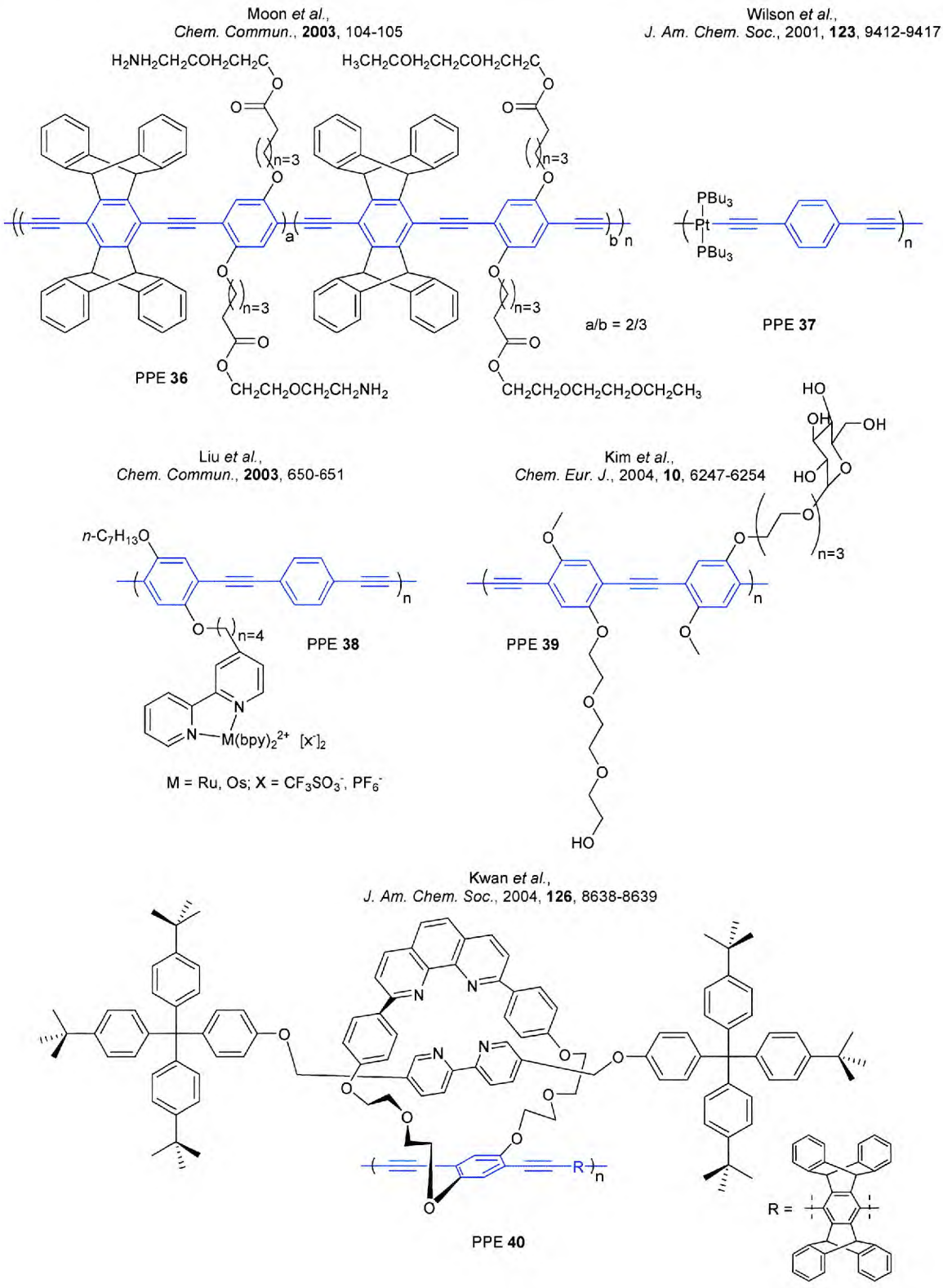

Figure 1.12 Examples of some of the complex structures that can be accessed using the versatile Sonogashira cross-coupling reaction.

The structural diversity shown by these examples highlights the wide applicability of this type of cross-coupling chemistry, which is also a common feature of many similar metal-catalysed cross-coupling reactions. The formed polymers were employed in a variety of applications; Moon *et al.* used the pentiptycene derived PPE **36** in an oligonucleotide solid state sensor, with the incorporation of the bulky groups serving to limit self-quenching.[97] Wilson *et al.* managed to incorporate the group 10 metal platinum into the polymer backbone (**37**).[98] This allows for the observation of phosphorescence from a CP, which is not generally observed for such polymers. Introduction of the heavy metal allows spin-orbit coupling which partially alleviates the spin-selection rules, thereby allowing transition of the triplet excited state to the ground state (singlet), which is normally forbidden (see section 1.1.1). This allowed them to study the Energy Gap law for a series of phosphorescent CPs.[98] Jiang *et al.* were also interested in phosphorescent conjugated polymers and synthesised examples where a metal complex was included as a pendent unit (PPE **38** in Figure 1.12).[99] Emission quenching experiments with these materials led to Stern-Volmer constants of 10^6 M^{-1} being recovered for the polymers, some 2-orders of magnitude higher than those observed for structurally similar small model analogues. Kim *et al.* synthesised the sugar-derivitised PPE **39** which was used for the sensing of Hg^{2+} and Pb^{2+} ions with moderate success; Stern-Volmer values of 10^4 M^{-1} were recorded.[100] Finally, Kwan *et al.* made rotaxinated PPE **40**, where the PPE backbone lies below the 'axel' of the rotaxane. This interesting structure with hydrogen bond acceptors, allowed for the detection of the H-bond donor phenol, which led to efficient emission quenching, attributable entirely to the interactions of the rotaxane groups, as confirmed by control experiments.[101]

The work described so far has emanated from some of the principal researchers, all based in the United States, who have conducted extensive work in the area of PPE synthesis and analysis. The groups of Swager,[76] Schanze,[86] Whitten[74] and Bunz[85] have all produced high molecular weight polymers for their anticipated use in sensor devices. Their syntheses generally involve the use of mild Sonogashira coupling conditions in water/DMF mixtures (to aid the solubility of the monomers and organic starting materials) with the resulting polymers isolated by precipitation into a large excess of organic solvent. The next section details some examples of the types of structures that have been typically used in such studies. In Table 1.3, examples of some PPEs employed in sensing studies are described along with polymer characterisation and sensing analysis.

Table 1.3 Examples of some of the PPE structures used in the latest sensor designs, along with polymer properties.

Entry / Structure number	Polymer structure	Molecular weight	Abs. / Em., λ (nm)	Sensing experiment / k_{SV} / M^{-1}
1 / **41**[77]	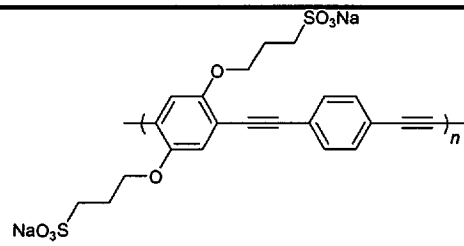	M_n = 100 kDa (by centrifug-ation)	425/447 (MeOH)	10^6-10^7 (H_2O)
2 / **42**[71]	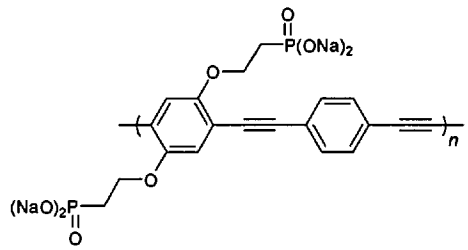	M_n = 55 kDa (THF, PS standards)	412/437 (in H_2O pH = 11)	10^7, (H_2O)
3 / **43**[102]	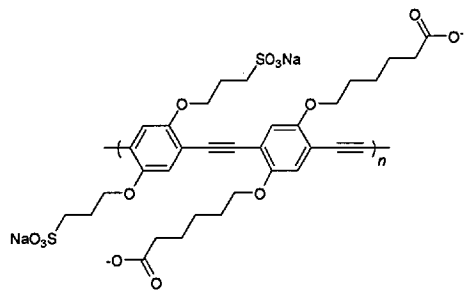	-	-	Enzyme assay

For most examples where the polymeric materials are used in direct sensing experiments, quantification of the amplified quenching effect is achieved by synthesis of a small molecule/model analogue which contains the same functionality. For PPEs, molecules such as **44** (Figure 1.13) are commonly used (effectively a 1.5 PPE repeat unit).

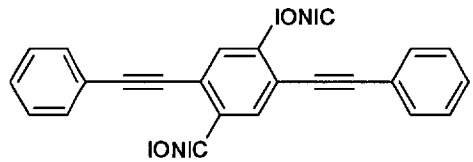

44

Figure 1.13 Structure of a typical small model analogue (phenylene ethynylene, PE) widely used to quantify the quenching enhancement observed with PPEs.

By repetition of the quenching experiments with the small model analogue one can easily observe the increased sensitivity imparted to the polymer, due to its extended conjugation length and associated increase in exciton diffusion range.

Difficulties associated with acquiring satisfactory GPC data for rigid-rod polyelectrolytes are well documented and are generally attributed to unfavourable interactions of the polymer with the column packing material.[103] For PPE materials the problem is further exacerbated by the rigid-rod nature of the polymer backbone which leads to an inherent overestimate of molecular weights.[85] These problems have inspired some inventive methods for determining the molecular weights of PPE polyelectrolytes; these include pulsed-field gradient NMR,[104] membrane osmometry,[105] ultrafiltration,[77] end-group analysis[77] and agarose gel electrophoresis analysis with *ds*-DNA as standard.[93] Some of these issues are discussed further in Chapter Two.

In more recent examples, researchers have been trying to avoid the direct synthesis of water-soluble polymers by making precursor polymers that have good solubility in organic solvents, and which can be converted to water-soluble derivatives by facile post-polymerisation reactions (Scheme 1.5a and Scheme 1.5c). The precursor polymers are soluble in organic solvents allowing for the complete characterisation of the materials. Also shown in Scheme 1.5b, is the effect on the conformational order of PPE **42** upon decreasing the solution pH. Aggregation is triggered at low pH values as increasing numbers of the phosphonate groups become protonated. This results in reduced electrostatic repulsion between neighbouring polymer chains, which leads to increased π-π stacking and subsequent self-quenching.[71]

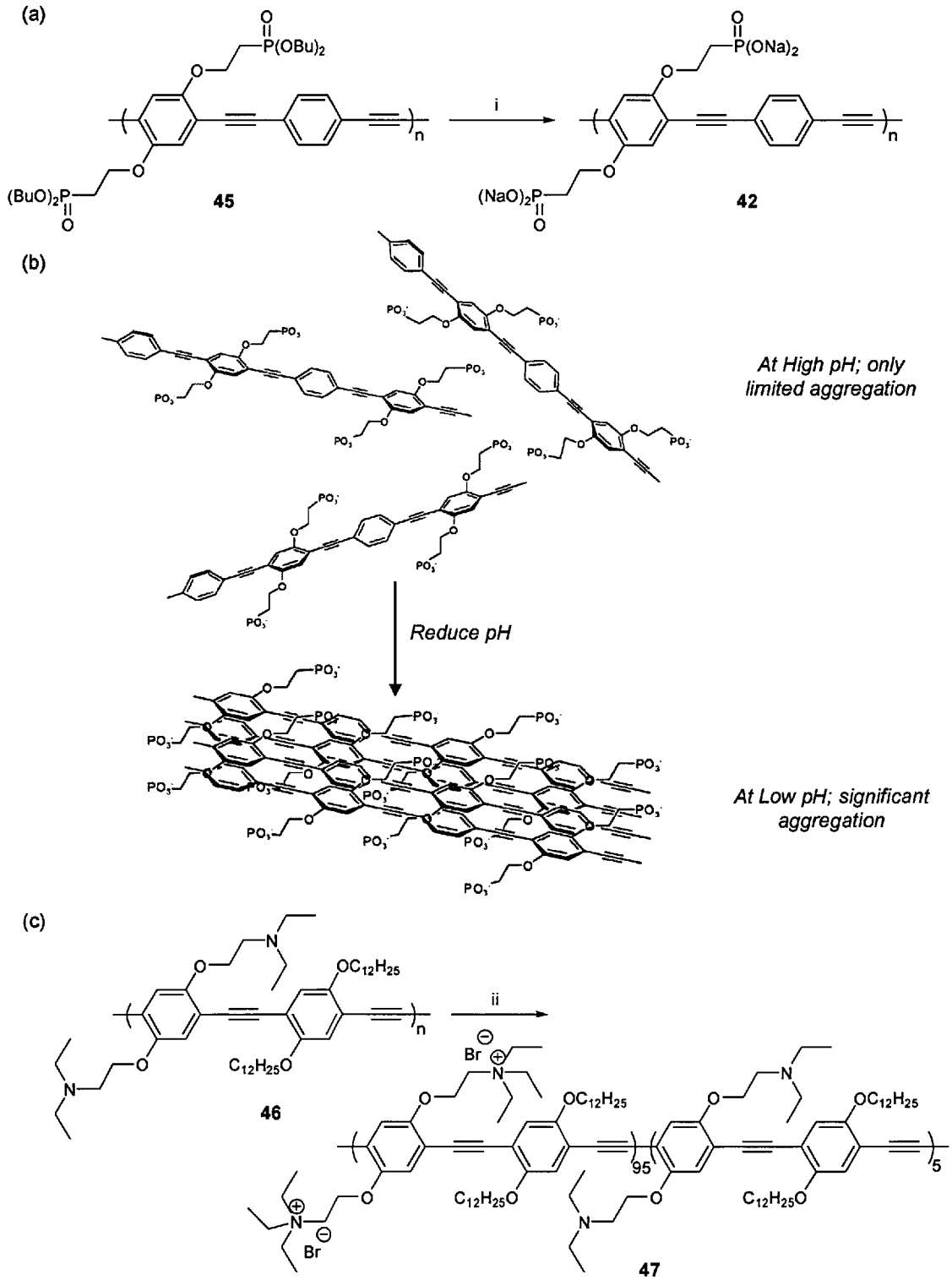

Scheme 1.5 Examples of post-polymerisation reactions conducted on PPE derivatives. (a) Removal of phosphate groups as demonstrated by Schanze *et al.*,[71] (b) impact of pH on the conformational order of PPE **42** (reproduced from Schanze *et al.*)[71] and (c) quaternisation to form an ammonium derivitised PPE.[106] Conditions: (i) Me_3SiBr, 2,6-lutidine, 1,2-dichlorobenzene, r. t., 6 h, followed by $NaOH/H_2O/MeOH$, 52%; (ii) C_2H_5Br, THF/DMSO (4:1), 50 °C, 5 d.

As will be discussed later (Chapter Two), the nature of the polymer backbone leads to overestimates of M_n and this has provided the focus of numerous studies. Recently, Bunz *et al.* calculated a correction factor that could be applied to values of M_n to help estimate a more accurate value (thereby accounting for the overestimate) of the number-average molecular weight of such materials (for PPEs, they found that the value of M_n is on average 1.42 times larger than its true value).[107] Using the Mark-Houwink-Sakurada equation (Equation 5), the value of α would be expected to approach 2, the theoretical maximum for a true rigid-rod polymer.[85]

$$[\eta] = KM^{\alpha}$$

Equation 5

where $[\eta]$ = intrinsic viscosity, K = constant, M = molar mass and α is a constant that depends upon the polymer, the dielectric constant of the solvent and the temperature.[108]

In order to avoid problems with non-specific interactions when applied to biological systems as well as issues surrounding molecular weight characterisation, there has been interest in the synthesis of non-ionic water-soluble PPE derivatives (Figure 1.14). One common feature is the size of the water-solubilising groups required (e.g. the dendritic nature of the pendent group in PPE **48**). This could be seen as a drawback when considering the anticipated mechanism for quenching, namely *via* electron transfer through complex formation, but polymers containing such branched units could prevent aggregation, as was achieved in the second example by Hecht *et al.*[109]

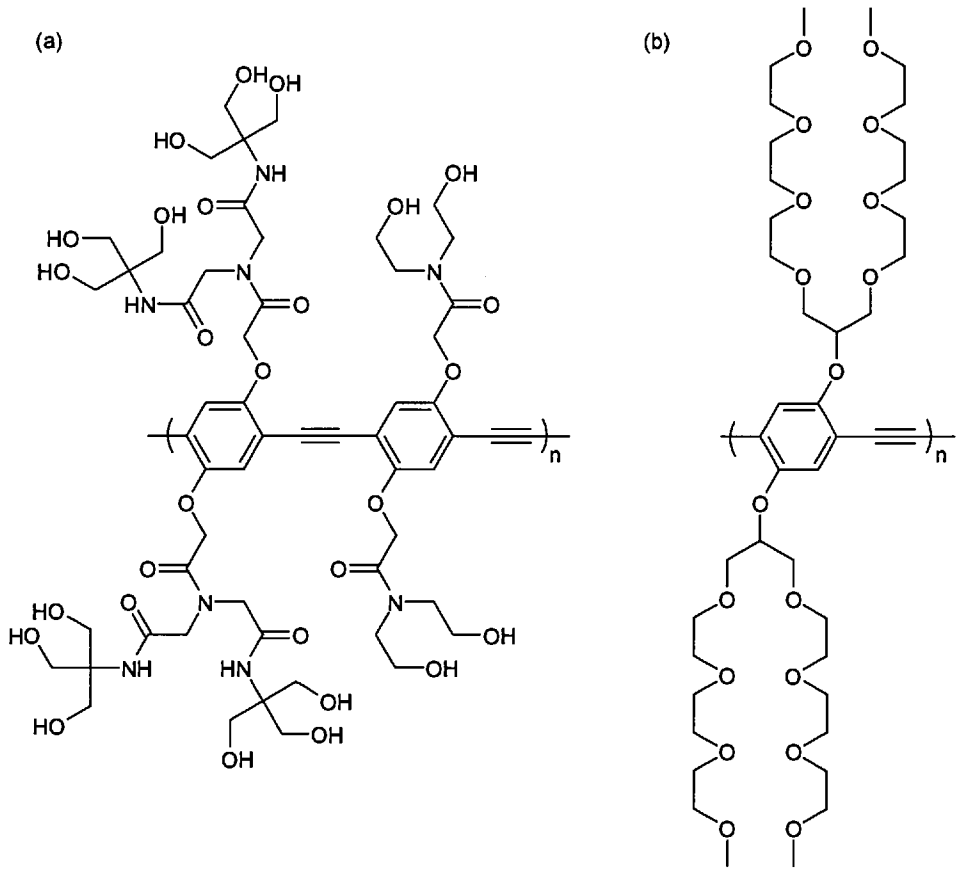

Figure 1.14 Examples of non-ionic water-soluble PPEs by (a) Swager *et al.*[110] and (b) Hecht *et al.*[109]

The example by Hecht *et al.* (PPE **49**) is especially promising from a sensory point of view as the non-ionic and non-protic design shows good water-solubility and results in a material that displays a high quantum yield (0.43 in water). The synthesis was backed-up by facile full characterisation of the polymer, which included GPC analysis indicating an X_n value of approximately 30.[109]

1.4.3 Water-soluble poly(*para*-phenylene)s (PPPs)

This class of polymer has high thermal and chemical stability and therefore reactions are carried out on the preformed polymer without degradation of the main chain. An example is the first sulphonated PPP derivative (**53**), accessed through Suzuki coupling (Scheme 1.6).[111]

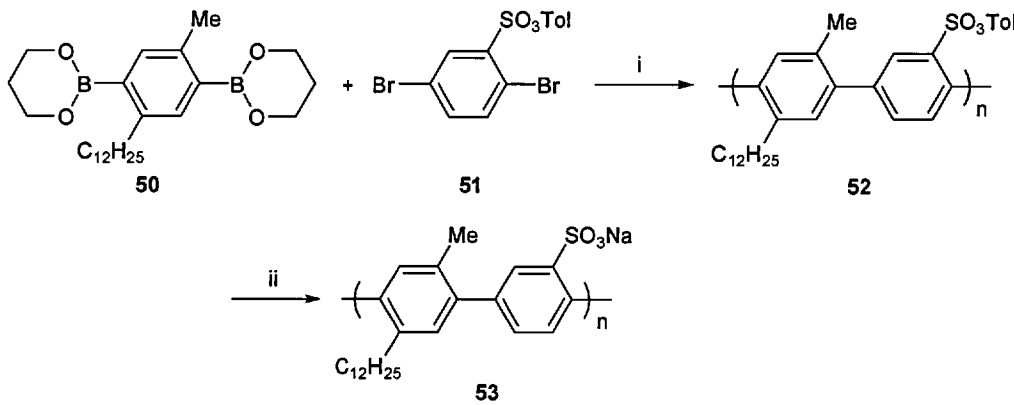

Scheme 1.6 Synthesis of the first sulphonated PPP. Conditions: (i) $Pd(PPh_3)_4$, Na_2CO_3, H_2O, THF, toluene, reflux; (ii) *n*-BuOH, *n*-BuONa.[111]

The mechanism for the Suzuki reaction is related to other palladium-catalysed coupling reactions (like the Sonogashira mechanism shown in Scheme 1.4) and involves the three distinct stages of oxidative addition, transmetallation, and reductive elimination.

1.4.4 Water-soluble poly(phenylene vinylene)s (PPVs)

Syntheses of PPVs are typically accomplished using the well-established Wessling[83] (Scheme 1.7) or Gilch[112] (Scheme 1.8) routes.

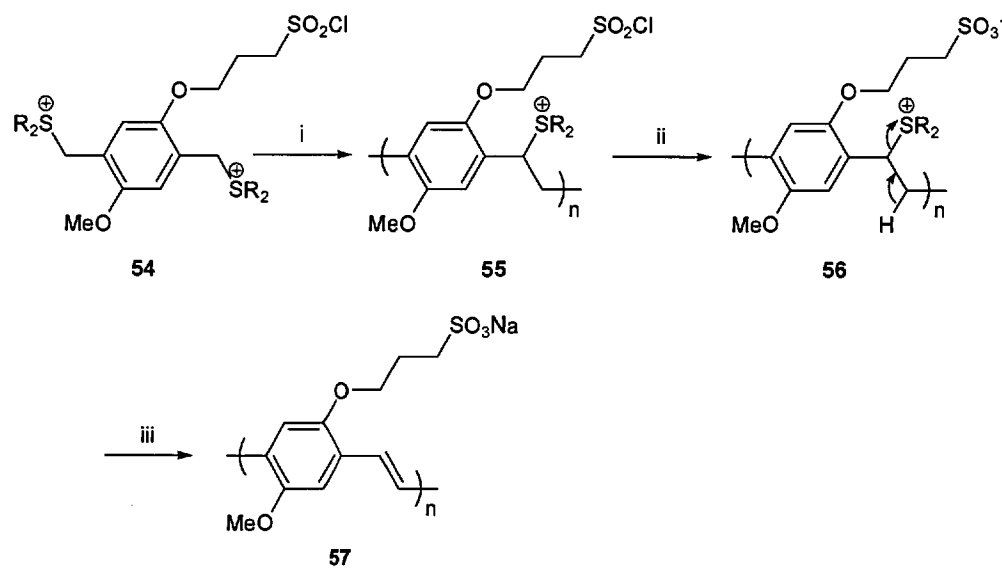

Scheme 1.7 Generic synthesis of a PPV derivative *via* a sulphonium ion intermediate (Wessling route). Conditions: (i) Base; (ii) H_2O/DMF; (iii) acid or base.[83]

The synthesis of **57** was achieved by Shi and Wudl[83] in 10 steps (overall yield: < 5%) and optimisation of the polymerisation of **54** enabled a molecular weight (M_n) of ≈ 100 kDa (PDI = 16) to be obtained. The synthesis of the water-soluble polymer **59** represents another rapid synthesis of a PPV derivative. Of interest is the neutral monomer **58**, which is hydrolysed during the polymerisation under basic conditions.

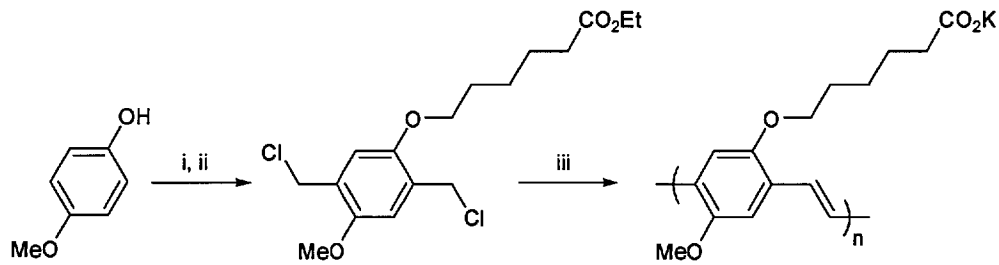

16 **58** **59**

Scheme 1.8 Synthesis of a PPV derivative *via* the Gilch route. Conditions: (i) $Br(CH_2)_5CO_2Et$, base; (ii) HCl (aq.), HCHO; (iii) *t*-BuOK, *t*-BuOH/xylene.[112]

The mechanism for these polymerisations is still the subject of ongoing research (with both anionic and radical routes having been suggested).[113]

1.4.5 Water-soluble poly(fluorene)s (PFs)

Poly(fluorene)s have been used as promising materials in light-emitting diodes due to their high PL QEs and stabilities, though electron transport in such materials is less good (lower mobilities).[114] In addition to these uses, water-soluble poly(fluorene)s have been used as fluorophore units in biosensing methods based on energy cascade processes, as will be discussed.[115] The general route to these polymers involves Suzuki cross-coupling of suitable monomers to produce either alternating or random copolymers, as shown in the examples in Scheme 1.9. In part (a) Jenekhe *et al.* synthesised poly(fluorene) **63**, which is a copolymer containing poly(fluorene) and quinoxaline units, which were incorporated into the polymer design in a bid to improve the electron transport properties in the PFs.[116]

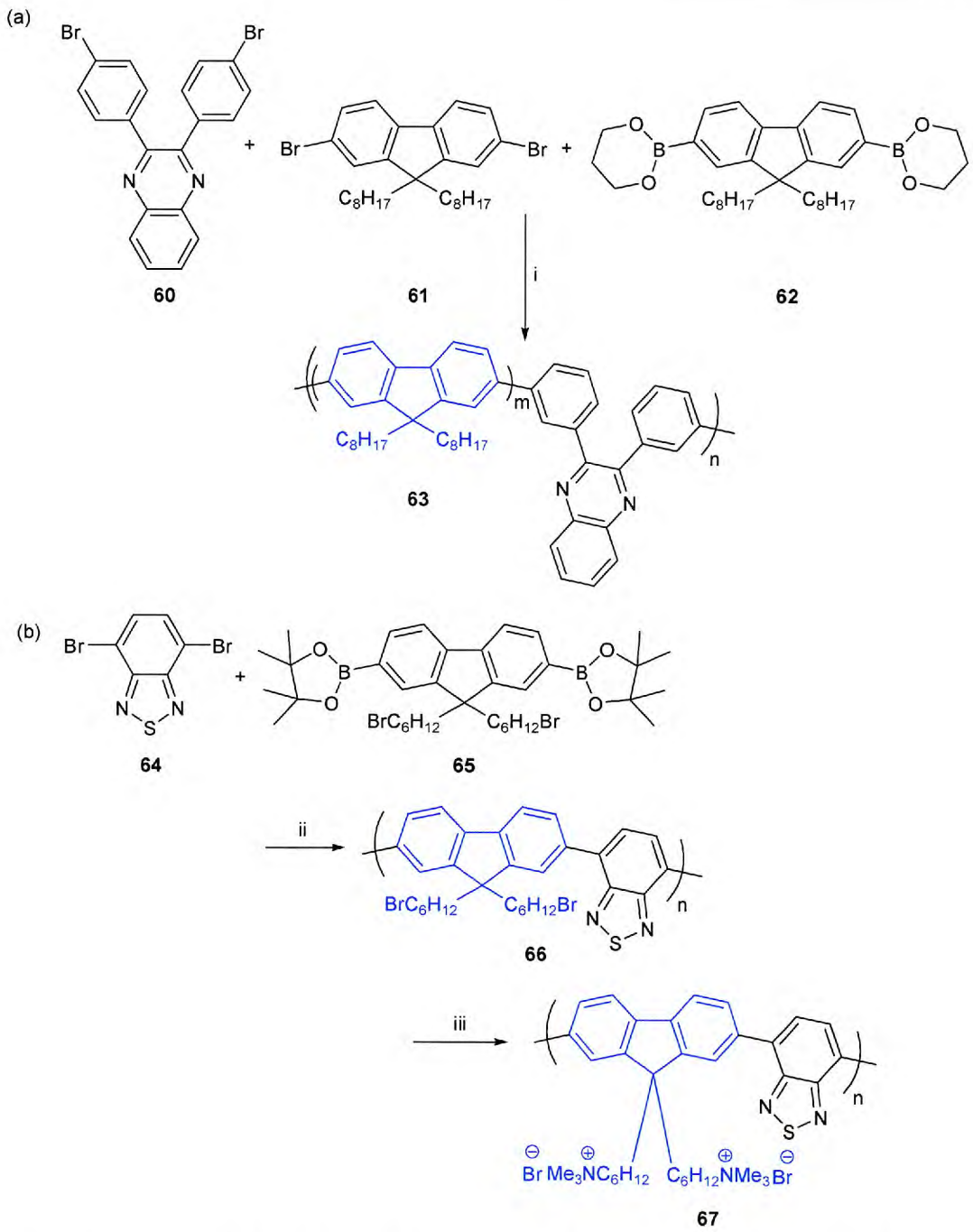

Scheme 1.9 Synthesis of poly(fluorene) derivatives. (a) An organic-soluble PF for blue light-emitting applications[116] and (b) a water-soluble variant for use in DNA biosensing.[117] Conditions: (i) $Pd(PPh_3)_4$, toluene/2M Na_2CO_3, reflux; (ii) $Pd(PPh_3)_4$, toluene/2M K_2CO_3; (iii) NMe_3, THF/H_2O.

Water-soluble derivatives are made in a similar manner to that described above, through a palladium-catalysed Suzuki cross-coupling copolymerisation. An example is shown in Scheme 1.9b and in common with other palladium-catalysed reactions the polymer synthesis involves stirring the monomers, a diboronic ester and diarylhalide, in an inert atmosphere at slightly

elevated temperatures for typically 24 hours. Polymer **67**, which will be discussed in more depth in section 1.5, was synthesised in good yield (65%) and is another example of a poly(fluorene) copolymer this time containing a benzothiadiazole moiety. This structural motif enabled the researchers to excite at a much lower energy (488 nm) and gave the polymer improved solid state emission properties.[117]

1.4.6 Water-soluble poly(thiophene)s (PTs)

Poly(thiophene)s have been used in a wide variety of applications from solar cells[31] to highly sensitive biosensors for the detection of single nucleotide polymorphisms in DNA.[118] The poly(thiothene) (**72**) used for DNA sensing by the Leclerc group was synthesised by oxidative polymerisation in chloroform, which has the advantage of yielding polymers with narrow PDIs (polydispersity index; typically 1.2 – 1.9), and good molecular weights (6 – 10 kDa).[119,120]

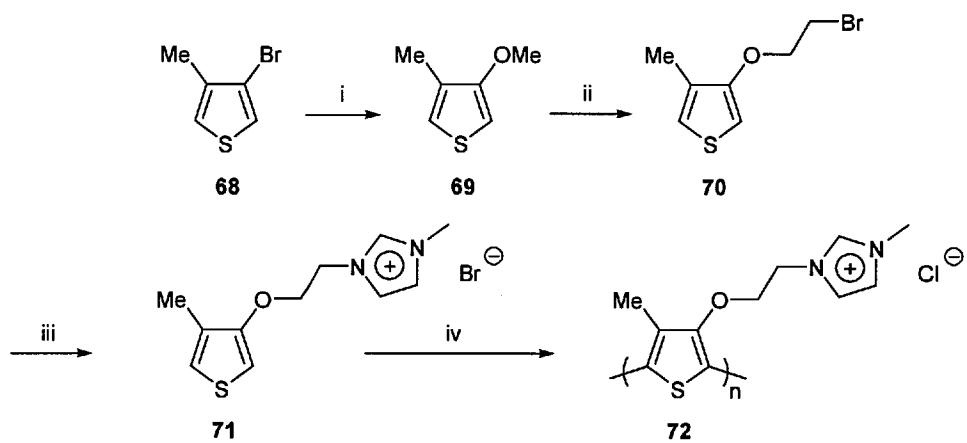

Scheme 1.10 Synthesis of a cationic poly(thiophene) by Leclerc *et al.*.[91,121] Conditions: (i) NaOMe, CuBr; (ii) $NaHSO_4$, $HO\text{-}CH_2CH_2\text{-}Br$; (iii) methylimidazole; (iv) $FeCl_3$, Bu_4NCl.

This method for the synthesis of such materials is fairly typical and was recently exploited by Meijer *et al.* who prepared a water-soluble non-ionic poly(thiophene) (**76**, Scheme 1.11).[122]

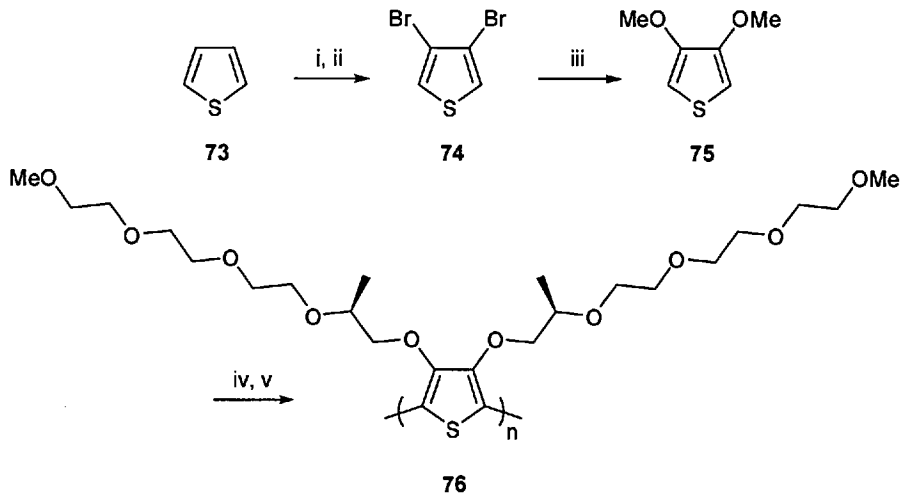

Scheme 1.11 A non-ionic water-soluble poly(thiophene), as synthesised recently by Meijer *et al.*.[122] Conditions: (i) Br_2, $CHCl_3$, 50 °C, 4 h; (ii) BuLi, then H_2O; (iii) NaOMe, MeOH, reflux, 24 h; (iv) TsOH, ROH as solvent, 90 °C, 3 d; (v) $FeCl_3$, $CHCl_3$, r. t., 24 h.

This material is of interest in the field of organic electronics as is alluded in the paper by Meijer *et al.*, as one of the common challenges in conjugated polymer applications surrounds the formation of polymer aggregates which can limit quantum yields and hinder polymer characterisation. For example, Leclerc *et al.* described how their attempts to determine the molecular weight of the polymer by SEC were unsuccessful, presumable due to strong interaction of the polymers with the column packing material.[91] By contrast, the neutral polymer **76** synthesised by the Meijer group was *purified* by size exclusion chromatography and exhibits vastly reduced aggregation, (attributed to the presence of the non-ionic side-chains) an advantage confirmed by detailed UV measurements. The number average molecular weight for this polymer was 7.9 kDa with a PDI of 4.1 (GPC analysis conducted in water).

1.5 Hybrid conjugated systems for metal-ion and fluoride sensing

So far the CPs shown have consisted of a single type of conjugated repeat unit, but there is increasing interest in developing systems where selective receptor units are appended through a small saturated tether to the main CP backbone.[123] By keeping the recognition unit in direct communication with the CP, sensitivity is enhanced. Such polymers have been used as potential heavy metal sensors and many reports have been published on these as well as related metallopolymers.[123,124] The favourable optical properties of many of the polymers described above have led to them being conjugated with receptor units *in the main chain*, which results in enhanced sensitivity. This results from the increased electronic communication when the ligands are linked

directly to the polymer. In a good example of this, a hybrid polymer (**77**, Figure 1.15a) with a repeat unit consisting of phenylene ethynylene and thiophene ethynylene subunits, showed increased sensitivity for Ni^{2+} ions, over polymer **78**, which contained a methylene tether that served to disrupt the conjugation.[125]

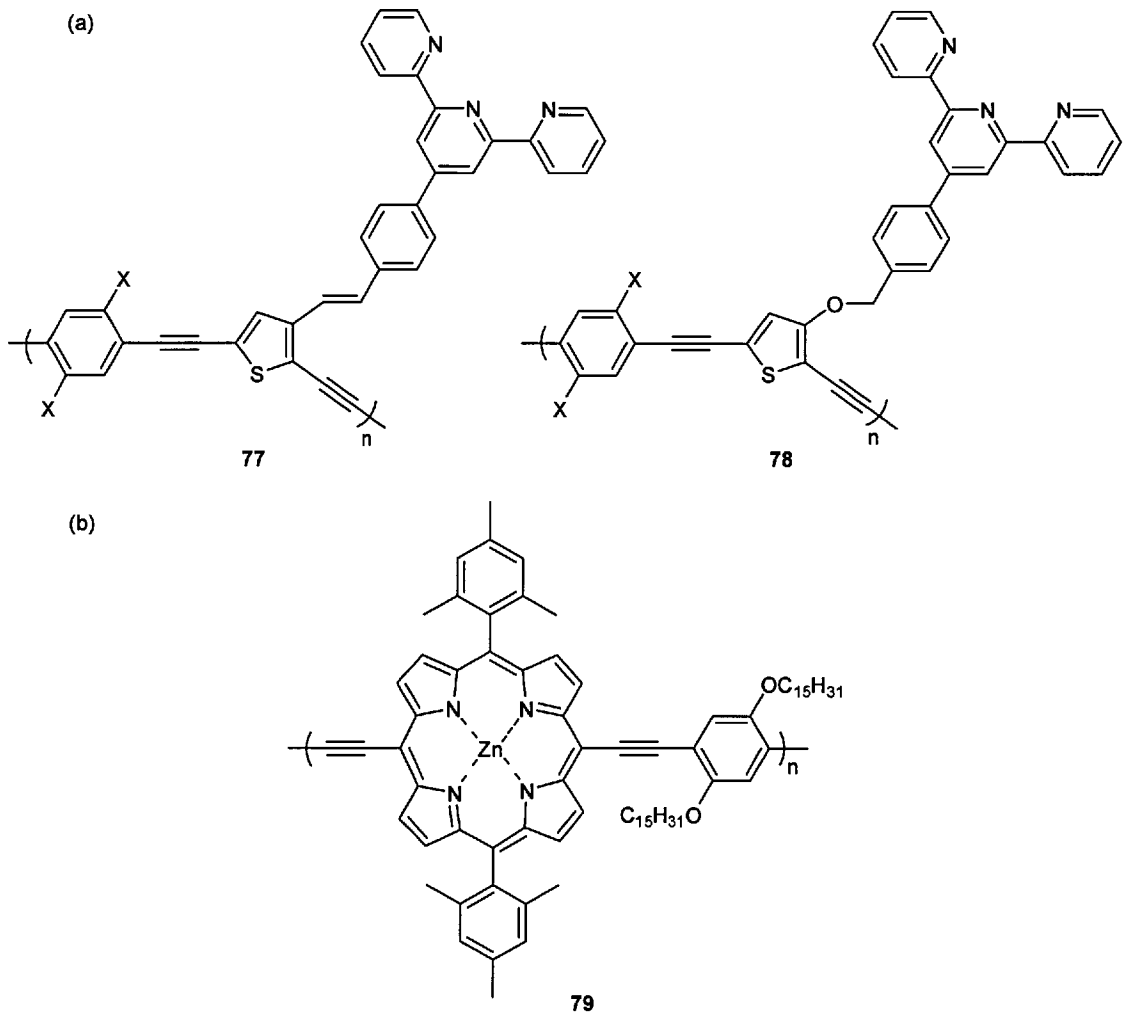

Figure 1.15 (a) Hybrid CPs used for metal ion detection. The increased electron communication between the polymer and the ligand in **77** led to this polymer having increased sensitivity compared to polymer **78** (it was 2.6-fold more efficient).[125] (b) A zinc-porphyrin PPE that exhibits emission changes upon changing solvent environment.[126]

The binding of metal ions to the conjugated backbone can lead *inter alia*, to changes in the planarity of the backbone, which influences the degree of conjugation. Such complexation can also cause interesting solvent effects. The hybrid porphyrin-containing PPE **79** displayed variable emission on solvent changes, with electron-donating solvents leading to red-shifts in the polymer emission (Figure 1.15b). The large red-shifts are attributed to changes in the electron density of the

porphyrin, which dominates the emission spectra.[126] In addition to the sensing of potentially toxic metals ions, the fluoride ion has also been a common target due to its importance in understanding plant and animal metabolism and as a by-product in the manufacturing process leading to certain chemical weapons.[127] An elegant ion sensor was recently synthesised by Swager *et al.* who used PPE **80** (Figure 1.16) to detect fluoride ions.[127]

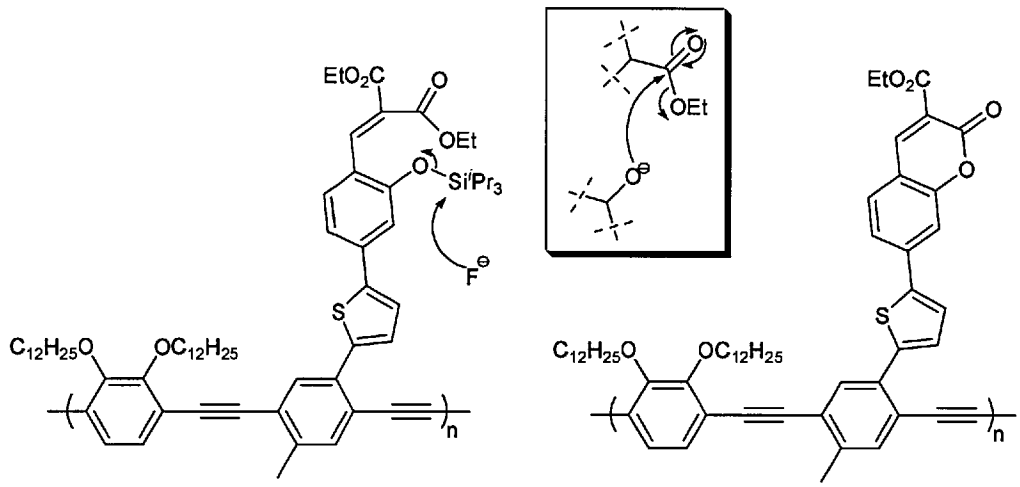

PPE **80** PPE **81**

Figure 1.16 A fluoride-ion sensitive PPE.[127]

Exposure of PPE **80** to F^- ions (by addition of TBAF) leads to deprotection of the silyl group revealing a phenolate which is then perfectly set up to undergo cyclisation to yield PPE **81**, which contains the coumarin dye in direct conjugation with the PPE backbone. Though in principle the high affinity of fluorine for silicon should render any silicon-containing protecting group suitable, the polymerisation conditions demanded the use of the more thermally robust TIPS group. The choice of dye was crucial to ensure efficient energy transfer from the polymer could take place (*via* the Dexter mechanism). Swager *et al.* used the thiophene unit to link the dye to the polymer as such moieties are known to be efficient at delocalising π-electron density.[127] Addition of TBAF to a solution of PPE **80** led to a reduction in polymer emission and an increase in the emission from the newly formed dye. The fluorescence transformation triggered by the dye attached to the polymer is 100-times more sensitive than for the small molecule equivalent. This is a desirable sensor format as it is preferable to detect a new emission signal than it is to look for a small modulation of an existing one.[127] The authors made no mention of whether the sensor can be recycled.

1.6 Biosensing using non-PPE derived conjugated polymers

The sequence-specific detection of DNA is of widespread importance in a variety of applications from medical diagnostics and general research applications to therapeutic programmes like monitoring gene delivery.[128]

As with any biosensing platform, efficient coupling of the transduction element with the sensing probe is often the biggest challenge. This is because information regarding the recognition event can be lost or altered whilst being transferred to the transducer. Conjugated polymers are an attractive proposition for DNA sensing as they combine efficient transduction with the potential to interact directly with DNA strands.

A major breakthrough in this area was described by Chen *et al.*[74] in 1999 when they described how the luminescence from a conjugated polymer could be quenched efficiently upon exposure to minute quantities of an electron acceptor (quenching agent).[74] In this case the polymer used was a water-soluble PPV derivative (**57**), synthesised as shown in Scheme 1.12.[129]

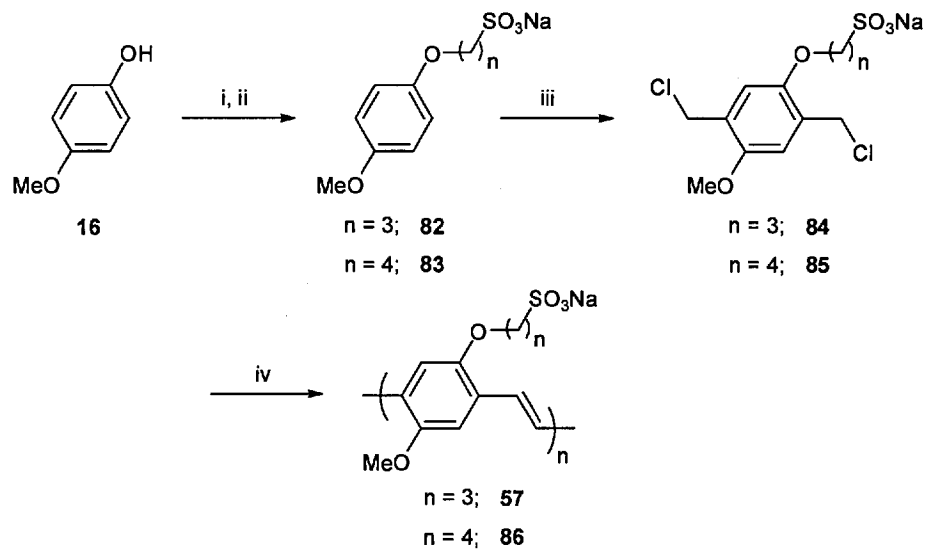

Scheme 1.12 Synthesis of anionic PPVs. Conditions: (i) NaOMe/MeOH; (ii) 1,3-propanesultone or 1,4-butane sultone, reflux; (iii) HCHO (37%), HCl, dioxane; (iv) *t*-BuOK, DMF, THF.[129]

The significance of this work did not lie in the realisation that the emission from a luminescent species could be quenched by an electron deficient species (it was known that the emission from a stilbene dimer could be quenched by such compounds, *vide supra*), but in the efficiency of the process.[74,129] When quantified, the quenching process was *seven* orders of magnitude more sensitive compared to the *trans*-stilbene case. This finding led to extensive research being

conducted into how similar conjugated polymers could be used as sensing devices and the factors that affect their limits of detection.

The potential to implement the ideas presented by Chen *et al.* in a broader sense, is an exciting prospect especially as current technologies in the field of medical diagnostics suffer from many potential drawbacks. In one such example, the selective targeting of bioanalytes is commonly accomplished by the ELISA technique (enzyme-linked immunosorbant assay), which though accurate, is time-consuming and expensive.

An important contribution to the field of CP DNA sensors was made by Leclerc *et al.* who in 1997 published work detailing the synthesis of a highly conducting water-soluble poly(thiophene) CP (**72**).[128,130] In subsequent communications they explored the use of this poly(thiophene) in affinitychromic (where optical changes are triggered by target interaction) diagnostic schemes.[131] The cationic polymer **72**, shown in Scheme 1.10, exhibits changes in its absorption and emission properties upon interacting with single-stranded DNA, which can be attributed to conformational alterations.[91,120,132]

An oxidative polymerisation with $FeCl_3$ was used to access **72**, which was estimated to have a number-average molecular weight of 6 – 10 kDa (PDI = 1.2 – 2.9).[91] As will be discussed in Chapter Two, performing GPC analysis on polyelectrolytes is notoriously difficult due to adsorption on to the column packing material.[103]

The polymer allows the detection of single-base pair mismatches with a detection limit in the zeptomolar (10^{-21} M) range, thus highlighting the powerful ability of fluorescence-based sensors.[121] The system works as follows; in the first stage the polymer is essentially primed for sensing when a probe oligonucleotide strand is added to **72** (in a 1:1 ratio, based on polymer repeat units; Figure 1.17). This addition is easily observed as there is corresponding colour change in the solution (from yellow, the random coil configuration, to red) and the emission band of the polymer is significantly quenched and red-shifted, due to increased aggregation of the polymer chains in this state. When in this duplex form (**87a**, Figure 1.17), the polymer backbone is effectively 'straightened out' thereby extending the conjugation length which directly impacts the emission maximum.

Addition of the target DNA material leads to further changes in the emission spectrum, ascribed to changes in the conformational structure of the polymer; the colour of the solution changes (back to yellow) and the emission intensity increases (five-fold increase reported) which is also accompanied by a blue-shift in the peak maximum. Leclerc *et al.* explained this second colour

change by suggesting that in the presence of the target material, the hybridisation results in a triplex ensemble (**87b**, Figure 1.17) where the polymer remains associated with the hybridised strands and adopts a helical shape.[121] Circular dichroism (CD) measurements lend weight to this argument as they showed a signal indicating the formation of a right-hand helical conformation for the polymer. The formation of the triplex structure can also be tracked by emission measurements, as the helical triplex arrangement leads to a breakdown in the extent of conjugation, due to kinks developing along the polymer backbone, which leads to a relative blue-shift in the emission spectrum for the polymer.

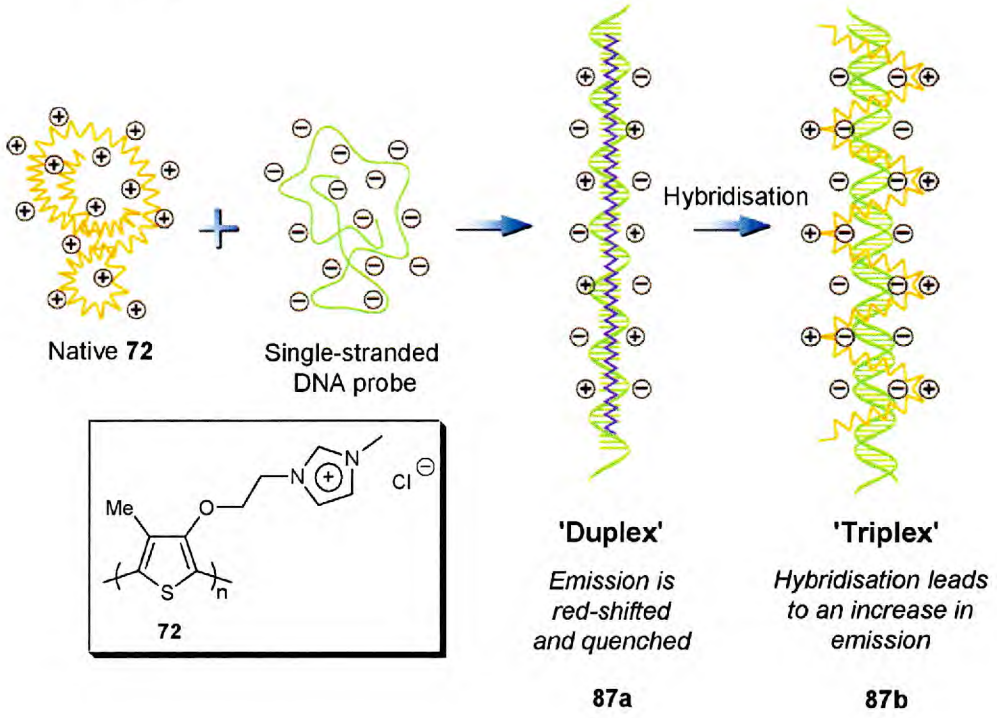

Figure 1.17 Structure of the poly(thiophene) used together with the perceived structure of the duplex and upon hybridisation, the triplex (adapted from Leclerc *et al.*).[121]

To determine the limits of this system, Leclerc *et al.* investigated whether the primed state (duplex formation) could identify single and double base-pair mismatches along a DNA strand. Indeed, it was possible to discriminate such polymorphisms under kinetic monitoring and the whole sensing procedure was completed with concentrations in the zeptomolar range and volumes totalling no more than 150 μL.[121] Interestingly, it was discovered that the addition of the non-ionic surfactant Triton X-100 (0.3 mM) improved the limit of detection by an order of magnitude, which was attributed to the surfactant allowing the formation of more extended polymer chains in the aqueous environment of the experiment.[121]

A possible minor drawback for the Leclerc method is the length of time required to obtain results regarding DNA detection. The discrimination of single base-pair mismatches is achieved by noting the increase in emission signal intensity with time, through the hybridisation kinetics. This can take up to an hour, which given the power and ease of the technique is still impressive, but a quicker response time would be desirable.

The many advantages identified in sensing for water-soluble poly(thiophene)s, combined with their efficiency and sensitivity prompted the Leclerc group to consider them for other detection schemes, such as the sensing of proteins.

The water-soluble poly(thiophene) **72**, described above, was also used to report the binding of an aptamer to its target (Figure 1.18). An aptamer is an artificial nucleic acid ligand which has the ability to bind a wide variety of analytes including metal ions, amino acids and proteins.[119]

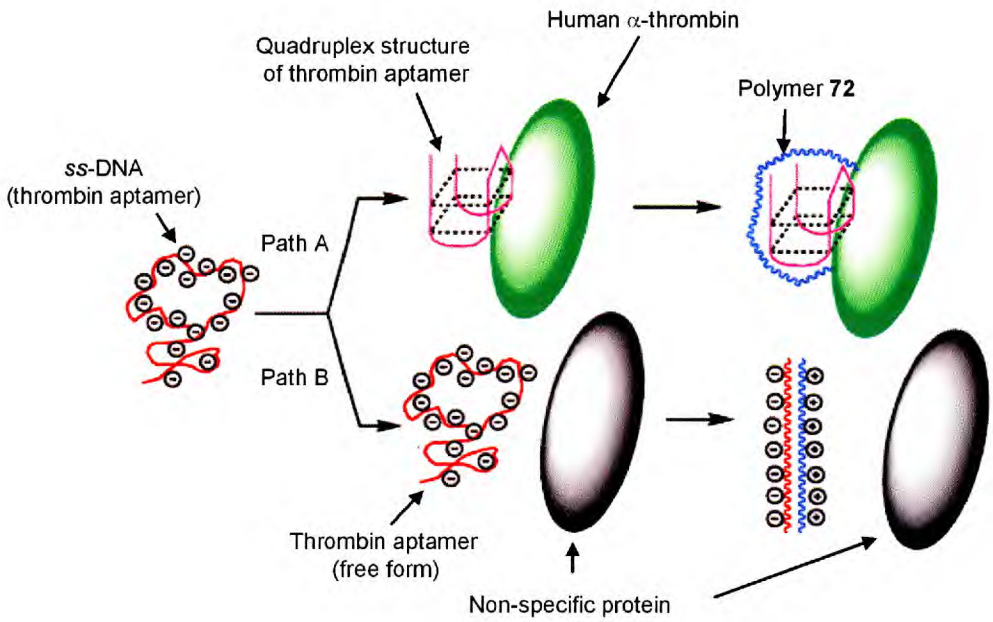

Figure 1.18 The incorporation of polymer **72** in the specific detection of a human α-thrombin (Path A) and the alternative conformational structure of **72** in the presence of a non-specific protein (Path B); reproduced from Leclerc *et al.*.[119]

As shown in Figure 1.18, the aptamer for the protein human α-thrombin was used in conjunction with poly(thiophene) **72** to sense the target (in green). The 1:1:1 complex of the target, cationic polymer and aptamer (path A) gave rise to orange polymer emission, which is distinct from the red-shifted emission (expected at λ = 527 nm) expected from the polymer when the polymer has a more rigid conformation, and hence a greater effective conjugation length. Path B represents a

control experiment where a non-binding protein was selected; as expected, the red-shift in the emission from the polymer indicated that no complex formation had occurred and therefore there was no specific binding of the target.[119]

Similar arguments to those described previously can be used to explain the associated colour changes in this scheme. The red-shifted quenched state of the polymer persists in the case where there is interaction with the non-specific thrombin aptamer, which arises due to aggregation effects. When exposed to the right combination, namely the human α-thrombin target and its corresponding aptamer, the cationic poly(thiophene) is again luminescent and the emission blue-shifted, relative to the quenched state. The sensitivity of this detection scheme was not as high as for the DNA system, though a limit of detection of approximately 10^{-15} M was established for this very practicable assay.[119,128] The authors suggested that the sensor could be tailored to detect various protein targets by changing the *ss*-DNA (aptamer) to a specific binding sequence for the target protein.

In a conceptually different approach, Bazan *et al.* have also been actively pursuing DNA detection schemes using poly(fluorene) conjugated polymers (polymer **88** in Figure 1.19).[133] This group have concentrated their efforts on systems that involve a transduction process based on FRET. The FRET process is a through-space energy transfer and its efficiency or rate is inversely proportional to the distance (r^{-6}) between the donor and acceptor.[66]

(a)

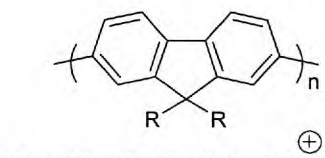

R = $CH_2CH_2CH_2CH_2CH_2CH_2\overset{\oplus}{N}Me_3\ \overset{\ominus}{I}$

88

(b)

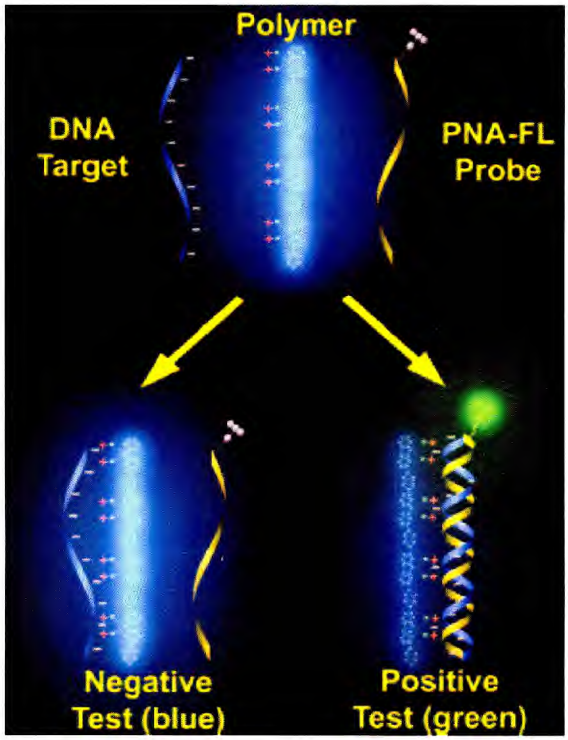

Figure 1.19 (a) structure of the conjugated polymer used by Bazan *et al.* and (b) a diagram (by Bazan *et al.*)[133] detailing the overall process of FRET in the three-component system.[133]

In the positive test, the Förster energy transfer condition is met and subsequent excitation of the polymer results in emission from the dye fluorophore (fluorescein was used as its absorption profile overlaps with the emission profile of the polymer). In the negative test, when the 'incorrect' (i.e. non-binding) target is present, complexation with the polymer exists, but efficient FRET cannot occur (due to an increased distance between the polymer and dye), and there is no emission from fluorescein.[133]

In a recent contribution Bazan *et al.* detailed RNA-protein detection, using a three-component system; a cationic CP (conjugated polymer), a protein probe and the complementary charged target RNA.[133] In many respects the overall system is similar to that described by Whitten *et al.* (section 1.6); binding of the correct (target) RNA sequence to the protein probe (with a tethered fluorophore molecule), allows efficient energy transfer (FRET) from the polymer to the fluorophore which

signals the detection of the analyte. If the RNA sequence is not bound by the probe protein, the FRET process cannot occur and there is no emission from the fluorophore. Typically, the probe used is a PNA (peptide nucleic acid) strand which is favoured over DNA probes as the absence of negatively charged phosphate groups affords tighter binding of the target with the probe as detrimental Coulombic repulsions in the formed duplex are eliminated. This allows for the formation of complexes of greater stability.[134] Additionally, the resulting duplex suffers greater destabilisation when mismatches are incorporated into the structure, thereby accentuating the detection of such defects.[135] PNA, a neutral analogue of DNA, differs in two ways from DNA; as well as an absence of phosphate groups (replaced by polyamide backbone), the nucleobases are incorporated *via* a methylenecarbonyl linkage.[136] The bases are the same distances apart as in standard DNA. The overall detail of the sensor operation is shown in Figure 1.19 alongside the polymer used.

In a logical extension to this work, this group also designed a simple DNA sensor based on the shuttling energy transfer process. Bazan *et al.* describe a sensor which is able to detect *ss*-DNA through a cascading energy transfer process illustrated in Figure 1.20.[137]

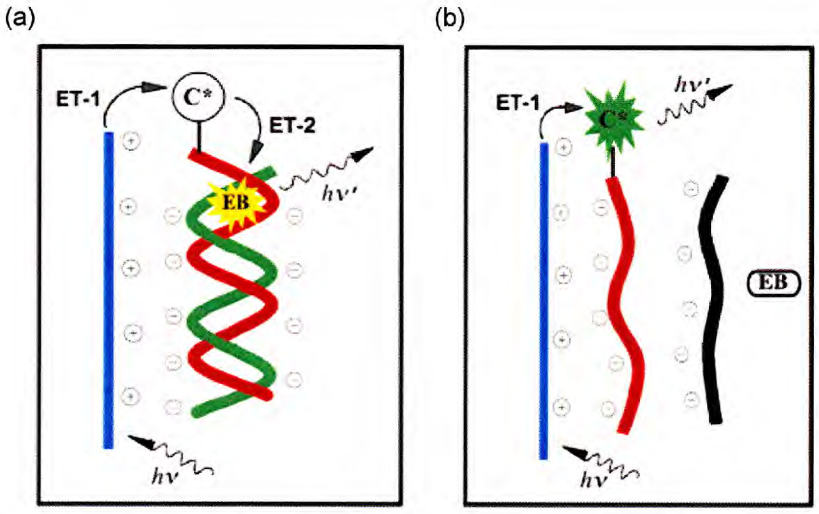

Figure 1.20 The cascading energy transfer processes involved in *ss*-DNA detection using Bazan's poly(fluorene)-based system (reproduced from Bazan *et al.*).[137] (a) In the presence of the complementary strand, two energy transfers occur leading to emission from the intercalator and (b) with the non-complementary target, only transfer to the appended fluorophore occurs.

Exciting the conjugated polymer (the same poly(fluorene) derivative used previously, **88**, shown schematically in blue in Figure 1.20) led to an initial energy transfer to a fluorophore appended to the probe *ss*-DNA, which then induced energy transfer to an intercalator, ethidium bromide (EB),

which was located within the formed *ds*-DNA strand (Figure 1.20a). In the second case (Figure 1.20b), the presence of a non-complementary strand (in black) precluded such complex formation and no emission from EB was observed.

Bazan *et al.* further exploited their poly(fluorene) CPs by introducing a mixture of meta and para linkages into the polymer backbone and performing energy transfer experiments as detailed above. They noted an improvement in the efficiency of the FRET process upon incorporating increasing meta linkages into the polymer backbone.[138] They attributed this trend to improved binding of the synthetic polymer to the secondary structure of DNA, which results in increased FRET efficiencies (consistent with shorter distances between the polymer and dye-labelled DNA).[138] In a further refinement of the process, a more recent report[139] details a process where these polymers can be used to emit three specific colours based on whether there is complementary, non-complementary or a complete absence of any DNA material in solution. The polymer used for this technique, a poly(fluorene) copolymer derivative containing benzothiadiazole units (polymer **67**), has its emission controlled by the concentration of the polymer in solution. By introducing small quantities of different monomers during the polymerisation, the usual blue (poly(fluorene)) emission from the polymer is disrupted. At higher concentrations, emission is dominated by these new green units (emission from the benzothiadiazole). Upon addition of different DNA material, aggregation effects determine the colour of the emission observed, with the perfectly complementary strands leading to efficient FRET processes.[115,139]

These researchers also showed that this polymer could be used for strand-specific DNA detection by using the excellent solid state emission properties of the benzothiadiazole units. In a recent report,[117] polymer **67** was used in the solid state to detect complementary strands through sensitised emission to a dye-labelled probe strand. The unique optical properties of the polymer allowed for excitation at long wavelengths (488 nm) which allowed this traditionally 'blue' poly(fluorene) to emit at wavelengths that were compatible with the dye probe, a condition essential for efficient FRET. Additionally, it was found that hybridisation of the polymer with the target strand and the PNA probe on a glass or silica surface could be achieved without the need to label the probe strand. By monitoring the emission intensity from the polymer, Bazan *et al.* noticed that the emission from **67**, in the case of complementary binding, was approximately five-times more intense as compared with the binding of non-complementary strands. This potentially allows for further simplification of the FRET-based system favoured by this group.[117]

In addition, the DNA-induced aggregation of polymer **67** has recently been used to determine the concentration of *ss*-DNA and *ds*-DNA.[140]

1.6.1 Biosensing using PPE derived polymers

There are presently many examples of conjugated polyelectrolytes based on a PPE backbone being used in biosensing schemes. Amongst the many groups working on PPE biosensors, those led by Schanze, Swager, Whitten and Bunz have been at the forefront of many of the developments in this area of research.[76,85,86,141]

A recent example of a PPE derivative used for the detection of DNA was demonstrated by Hancock *et al.* in 2003.[97] Particles of PPE **36** (Figure 1.12) were dispersed in aqueous solution by phase inversion techniques. These particles have the advantage of allowing for increased three-dimensional exciton migration, which leads to increased sensitivity and enhanced quenching, reducing the detrimental impact of reduced emission through different forms of aggregation. Titration of a modified (cyanine-labelled oligonucleotide, with 16 bases) DNA strand, which is able to quench the emission from the polymer by continually shunting excitons to the ground state, led to a k_{SV} of 8.8×10^7 M^{-1}. As was stated by the authors, such sensitivity combined with the ease of fabrication of the solid state device could lay the foundations for an automated DNA sensing platform with these polymers, though no indication of the selectivity for such a system was described.[97]

Prior to the disclosure by Hancock *et al.*, Whitten *et al.* were also looking at methods for the fabrication of PPE-based DNA sensors that could be used in a solid state format.[141] They opted for polymer-coated beads and used biotinylated PPEs coated onto streptavidin-derivitised polystyrene microspheres. Their method utilised a biotinylated-capture probe, which binds to a microsphere and serves to capture a quencher-modified target strand. Inevitably, this led to dimming of the CPEs emission upon hybridisation and by doing several assays to establish a relationship between the quenching ratio and the quantity of target strands, they constructed a calibration curve that allowed unknown amounts of oligonucleotide target material to be measured.[123,141] In later results, this group optimised their detection system by using PNA detection strands (as probe sequences) as many studies have shown that they form stronger duplexes with target sequences due to the absence of phosphate groups along their backbone.[123,142]

Schanze *et al.* demonstrated selective protease sensing using a water-soluble PPE derivative, similar to those synthesised in this work (see Chapter Two).[143] Their technique demonstrates the broad applicability of conjugated polymers for the detection of biomolecules and in their most recent work they show how the polymer, which serves as the transduction element, can be used in two differing methods dubbed, the 'turn-on' and 'turn-off' approaches (Figure 1.21).[143]

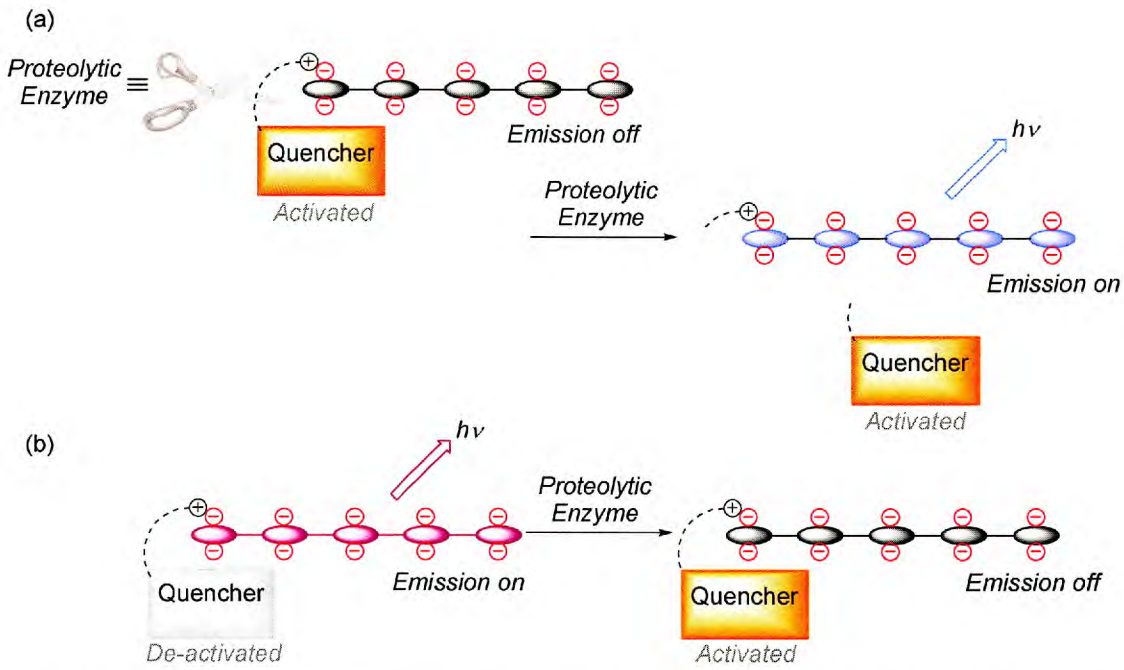

Figure 1.21 Schematic representation of the quenching processes as defined by Schanze *et al.*;[143] (a) with PPE **41**, the 'turn-on' approach,[144] (b) the 'turn-off' approach (for PPE **89**).

The two approaches can be summarised thus; in the former (Figure 1.22a), a cationic peptide labelled with a strong quencher (**90**), ion-pairs with the polyelectrolyte which serves to suppress the luminescence from the polymer. When the polymer/quencher mixture is exposed to a proteolytic enzyme, the emission quenching unit (**90**) is hydrolysed and when separated from the peptide, is prevented from ion-pairing with the polymer; luminescence from the polymer is therefore recovered.

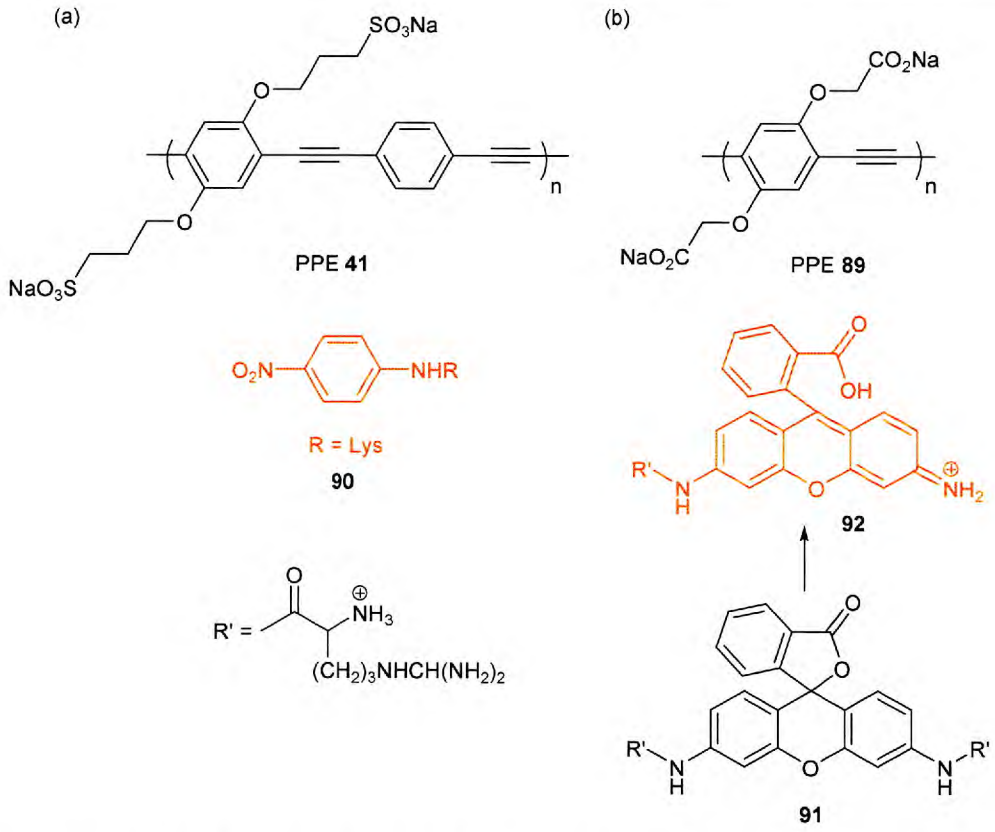

Figure 1.22 Polymers and quenchers used in (a) the 'turn-on' approach and (b) the 'turn-off' approach.[143]

The latter approach (Figure 1.21b & Figure 1.22b) involves a different polyelectrolyte (PPE **89**); luminescence from this polymer is suppressed upon exposure to a protease.[143] A solution containing the polymer and a 'masked variant' of the quencher (**91**) are prepared and in this state the luminescence properties of the polymer are unaffected. Upon exposure to a specific protease, amide hydrolysis is induced which activates the quencher (forming **92**). In the nanomolar range, this quencher efficiently decreases the luminescence from the polymer. Interestingly, this second quencher also has a different mechanism for luminescence quenching, whereby good spectral overlap of its absorption profile in the emission region of the polymer allows efficient resonance energy transfer (FRET).[66] By monitoring the emission intensity from PPE **89** a gradual decrease (over 30 minutes) was observed, after addition and incubation of the proteolytic enzyme papain. Stern-Volmer constants for the quenching observed between **90** and PPE **41** were found to be in the range of 10^6 – 10^7 M^{-1} comparable with those obtained from their previous work and they found that increasing the strength of the buffer solution diminished the quenching efficiency, an expected result given that the main mechanism for emission suppression is ion-pairing (static quenching) which is based on Coulombic interactions.

Independently, the Whitten group also used CPEs to track the activity of an enzyme and showed that the modulated emission from polymers like PPE **41** could be used to monitor phosphatase or kinase activity.[102] The system is comprised of several parts; for studying phosphatase enzymes, PPE **43** was absorbed onto positively charged microspheres which have the ability to complex with Ga^{3+} ions. This ensemble can then associate selectively to phosphorylated peptides and proteins. The key to this approach is the ability of the polymer/microsphere/Ga^{3+} ensemble to retain its emission properties. The system is summarised in Figure 1.23.[102]

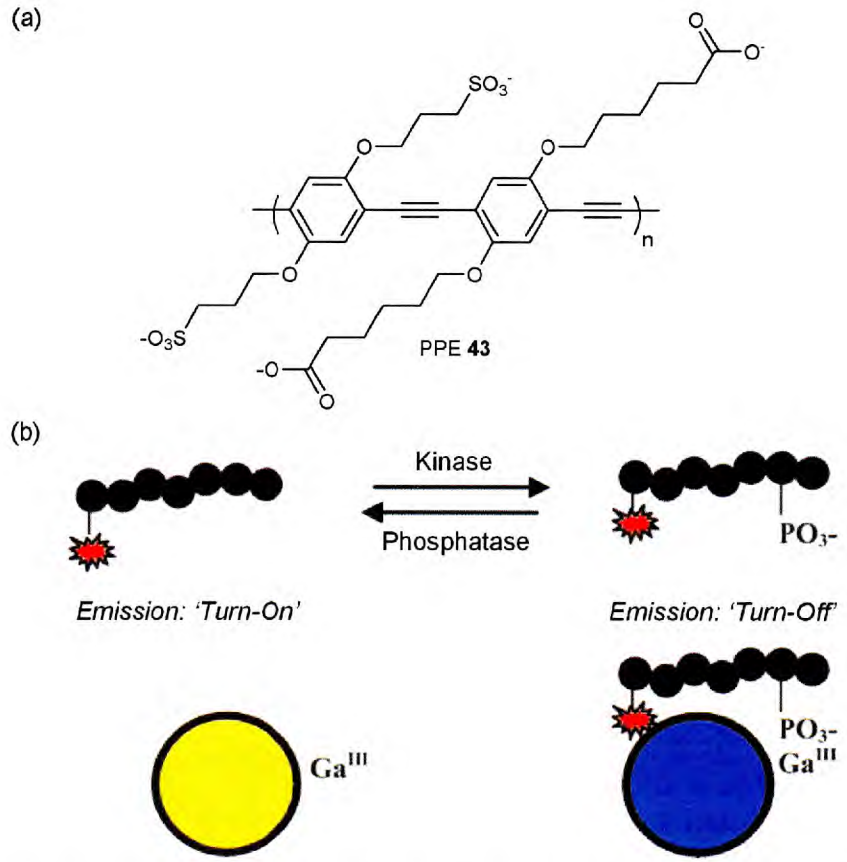

Figure 1.23 Description of Whitten's enzyme assay technique; (a) the PPE employed in this sensor, (b) mode of operation of the system (reproduced from Whitten *et al.*).[102]

Whitten *et al.* modified the peptide they used such that it contained a rhodamine dye, which can effectively quench the emission from the polymer with a Stern-Volmer constant of 10^7 M^{-1}. Importantly, this quenching only occurred when PPE **43** was used thus proving that the Ga^{3+} ions were bound to the polymer by the carboxylic acid groups (confirmed by control experiments involving PPEs that did not contain the carboxylic acid groups). The assay developed here allowed for the observation of kinase activity as the presence of the enzyme led to phosphorylation of peptide substrates that were then bound selectively by the polymer-microsphere assembly, leading

to emission quenching (i.e. the detection was monitored as a 'turn-off' effect).[102] These researchers showed that their system could be used to monitor a wide range of kinase assays and the sensitivity of the system, as judged by IC_{50} values (concentration of the inhibitor that is required for 50% enzyme inhibition), was comparable with other literature values.[102] The versatility of the assay system was increased by enabling any unmodified peptide to be used, with a corresponding 'turn-on' effect being observed.

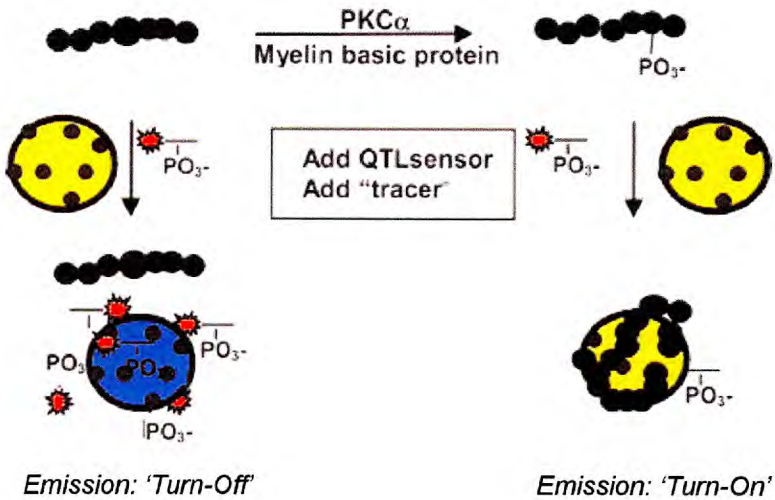

Figure 1.24 Extension of the original Whitten enzyme assay system; application for the detection of unmodified proteins and peptides (reproduced from Whitten *et al.*).[102] PKC = protein kinase C, myelin basic protein (MBP) is a small (18.4 kDa) protein.

The idea for this kind of assay is described in Figure 1.24; the phosphorylation action of the kinase enzyme leads to a product that can preferentially bind to the polymer-coated microspheres therefore blocking the quenching action of the modified tracer peptides.[102] The principle was tested for a small protein substrate and found to be effective albeit slightly less efficiently than the previously described assay, which was explained by inefficient blocking. The overall advantages for the assays developed by this group are quite clear; the direct approach employed means that any sample pre-treatment is avoided, which increases the simplicity of the PPE method and as was indicated, the overall performance of the assay is very similar to that seen for commercial systems (in terms of sensitivity).

In related work, Whitten *et al.* also detailed an alternative sensor format (Figure 1.25) that allowed the detection of proteolytic enzymes, this time by incorporating a reactive peptide sequence into a tether linking the quencher to biotin (in green).[80] This allowed Whitten *et al.* to use the reliable and well-documented biotin-avidin interactions to draw the biotin-quencher unit towards the avidin-

containing polymer, triggering strong quenching. The sensor system can then work in two ways; in the absence of association or an interaction with a target enzyme, the emission from the polymer is quenched, due to the proximity of the quencher to the polymer. Alternatively, a positive interaction of the target with the polymer-tether system, leads to cleavage of the tether which is then accompanied by a concomitant increase in the emission from the polymer.[80]

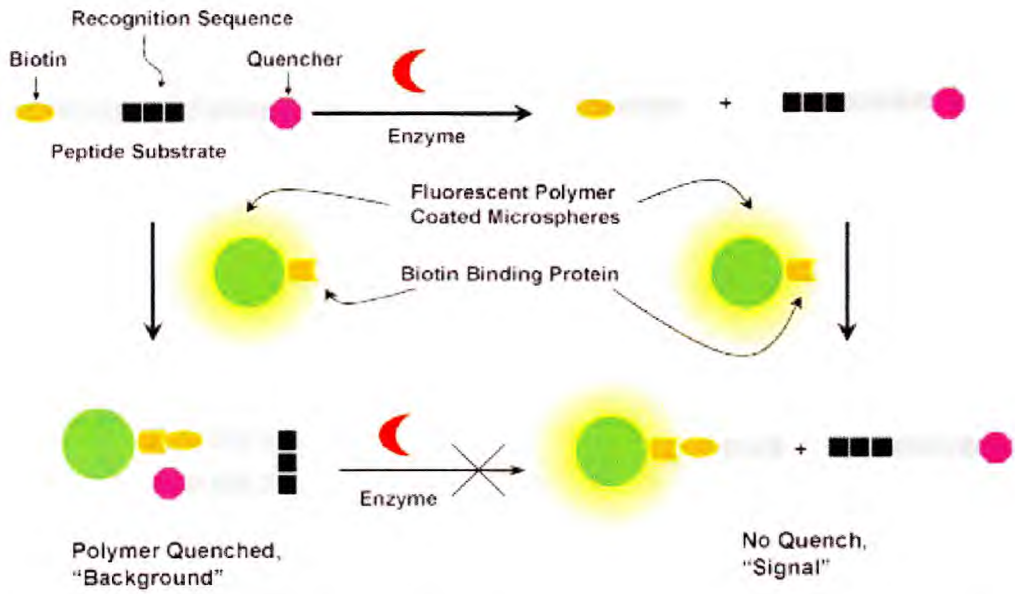

Figure 1.25 A method developed by Whitten *et al.* and based on biotin-avidin interactions, to detect proteolytic enzymes (reproduced from Whitten *et al.*).[80]

For this sensory scheme Whitten *et al.* employed biotin-functionalised PPE derivatives and in the experiments described, Stern-Volmer constants of the order 7.7 x 10^7 M^{-1} were reported (typical values for these systems are $10^6 - 10^8$ M^{-1}).[80,145]

Bunz *et al.* have also made use of the strong binding constant associated with biotin-avidin interactions and produced a biotin-substituted PPE (**95** in Figure 1.26) derivative that allowed them to study the interactions of such polymers with bacteria.[146] In their model system they used a streptavidin-coated polystyrene bead to mimic a cell surface/bacterium with the subsequent polymer-bead interaction then representing the cell-wall recognition process.

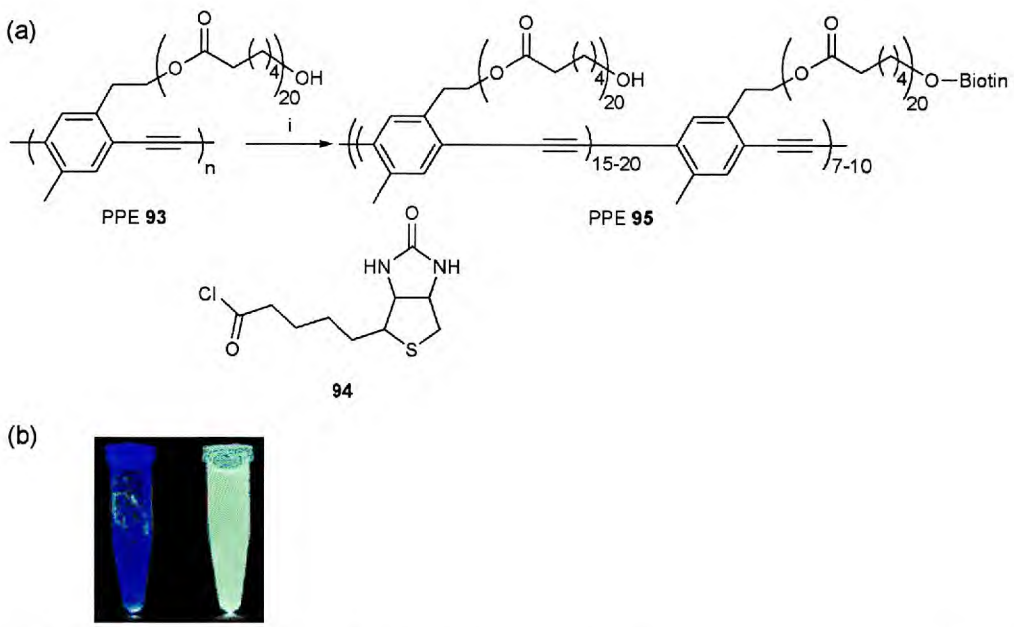

Figure 1.26 (a) A PPE derivative used by Bunz *et al.* in an quenching experiment mimicking cell-surface interaction; (b) the photograph (from Bunz *et al.*)[146] illustrates the aggregated polymer/microsphere moiety (left-hand side vial) and the emission observed from the unbound polymer (right-hand side vial).[146] Conditions: (i) **94**, THF, 0 °C.

Upon addition of the streptavidin-coated polystyrene beads to a solution of PPE **95**, a polymer precipitate was isolated from the solution which was attributed to the biotin-streptavidin binding.[146] In similar work the same group were able to synthesise the mannose-decorated PPE **96** in 95% yield (Figure 1.27) and were able to acquire GPC data in DMF (M_n = 22 kDa, by ^{1}H NMR, M_n = 62 kDa, by GPC, PDI = 1.5).[147] Such sugar-coated materials are of interest in a variety of areas of research, such as heavy metal sensing,[148] as they can potentially impact cellular activity through cell-surface interactions.[149] Bunz *et al.* made a concanavalin A (ConA) detector based on PPE **96** and assessed its ability to sense ConA *via* emission quenching experiments (a Stern-Volmer constant of 5.6 x 10^6 M^{-1} was recovered).[147] In control experiments, no quenching of PPE **96** was observed upon addition of bovine serum albumin or jacalin (a galactose-binding lectin) confirming good specificity.[147]

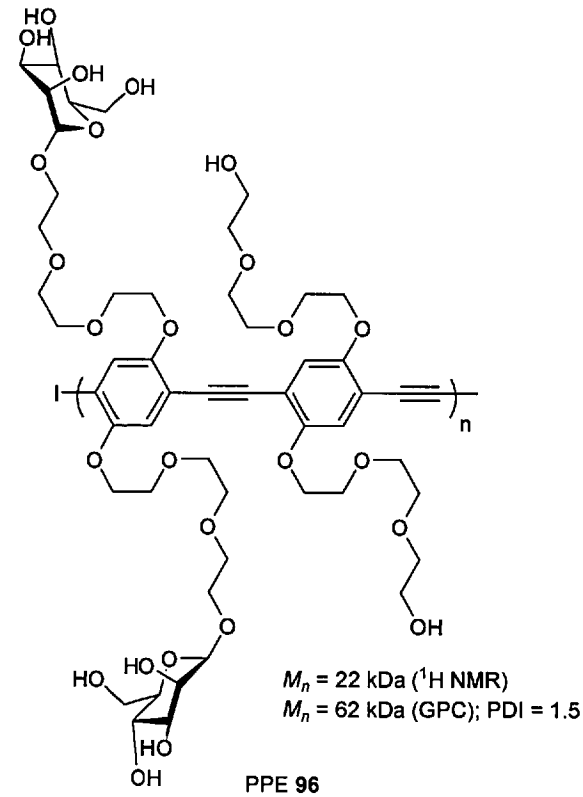

Figure 1.27 Mannose-substituted PPE used by Bunz *et al.* to detect the lectin ConA.[147]

PPEs **95** and **96** indicate the subtle synthetic variations that can be important for building polymers for biosensing. Bunz notes that the synthetic route to PPE **96** is advantageous as it avoids post-polymerisation functionalisation steps (no need for cleavage of the acetate groups that were used to protect the alcohols as these were removed under the basic conditions of the polymerisation process) which can give rise to incomplete reactions and introductions of defects along the chain.[147]

However, post-polymerisation reactions are sometimes desirable since they allow a parent polymer to be adapted to detect different analytes through the attachment of different receptor units. Swager *et al.* used conjugated polymer PPE **98** (Scheme 1.13) to monitor the performance of an enzyme in solution and looked at the effects of surfactant and pH on its emission properties.[103] The polymer was synthesised using Sonogashira chemistry with the peptide portion synthesised by solid-phase techniques and subsequently coupled to the polymer using the coupling agent EDAC and *N*-hydroxysuccinimde.[103]

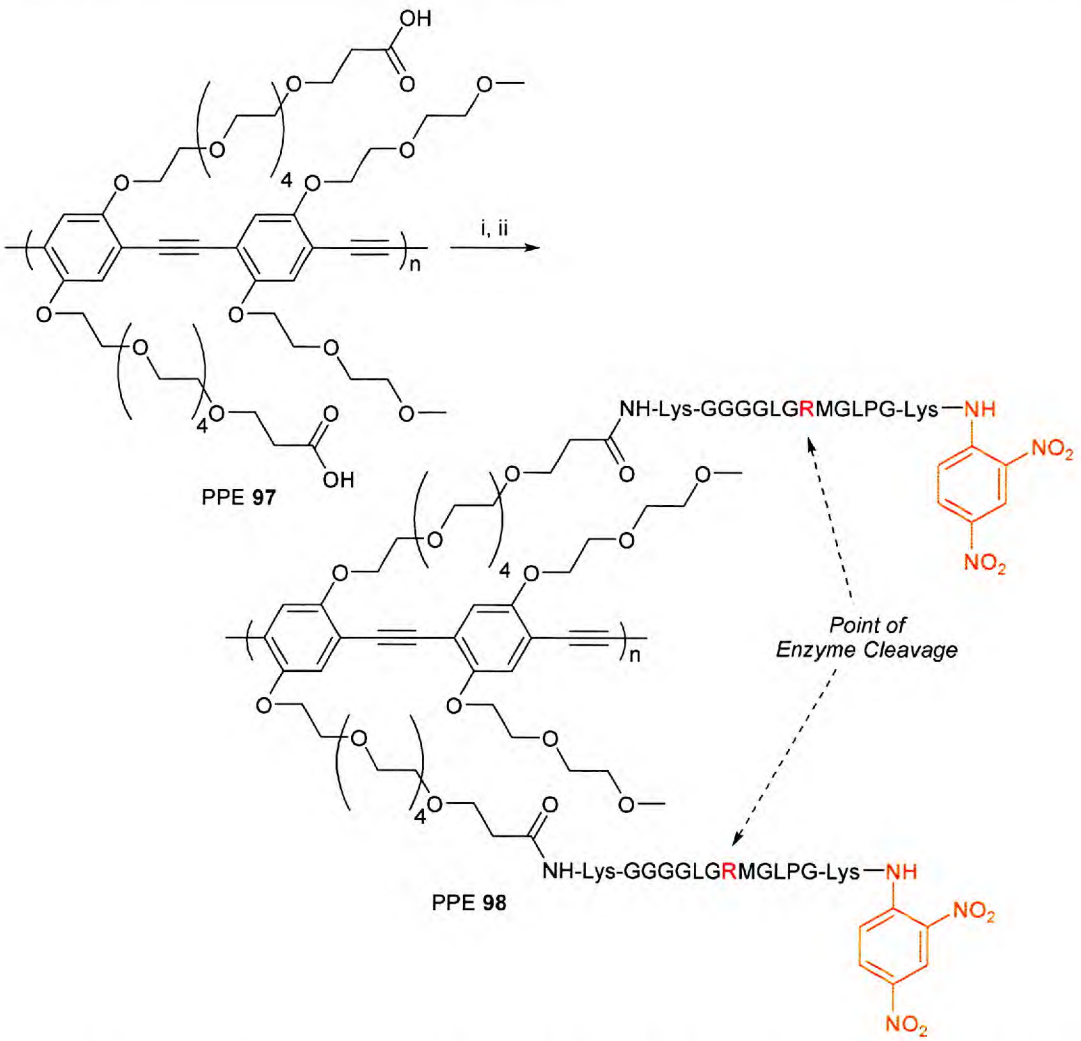

Scheme 1.13 Swager's post-polymerisation reaction to obtain a 'turned-off' peptide-substituted PPE.[103] Conditions: (i) EDAC/NHS, (ii) AcHN-Lys(DNP)-GPLGMRGLGGGGLys-OH.

Importantly, the presence of the PEG side chains renders PPEs **97** and **98** water-soluble. As mentioned previously, for biological applications this feature can be useful, as non-specific interactions can be avoided.[103] Prior to attaching the peptide chain to PPE **98**, the ability of the quencher (dinitrophenyl moiety) to strongly suppress the emission from the polymer was investigated and subsequent Stern-Volmer analysis indicated that modest quenching occurred with k_{SV} = 5.8 x 10^4 M^{-1} in un-buffered water.[103] Addition of salt-containing buffered solutions or surfactants led to a decrease in the efficiency of the quenching process. The protease assay that was proposed by Swager *et al.* can be summarised as shown in Scheme 1.13. The addition of the enzyme trypsin (which specifically hydrolyses peptide bonds at the carboxyl side of lysine and arginine residues) leads to scissoring of the peptide bond in the arginine residue (R) indicated in Scheme 1.13, which results in fluorescence recovery as the dinitrophenyl quenching moiety is removed from the vicinity of the polymer backbone. In practice this result was indeed observed,

with an increase in the fluorescence of one order of magnitude being recorded after the addition of the enzyme.[103]

In a conceptually different application for water-soluble PPEs, Whitten *et al.* reported the use of a cationic PPE as a white-light triggerable biocide.[150] In this system, PPE **99** (Figure 1.28) was coated onto an anionic microsphere, in order to have the polymer on a supported format. The mechanism for bacterial destruction was thought to be an entirely photoinitiated process, and was found to be specific for white-light excitation; excitation with yellow light for example was found to have no effect (presumably due to reduced absorption).[150] The researchers looked at the relative effect on bacterial survival rates with polymer concentration. It was found that increasing the polymer concentration beyond 30 μM, led to a 66% reduction in the ability of the polymer to act as a biocide, compared to the effectiveness at sub-micro molar concentrations where a 38% reduction in bacteria colonies was recorded. The reason for the concentration-dependent activity was related to the polymer possibly being able to undergo significant self-absorption, thereby insulating the bacteria from the absorbed light.

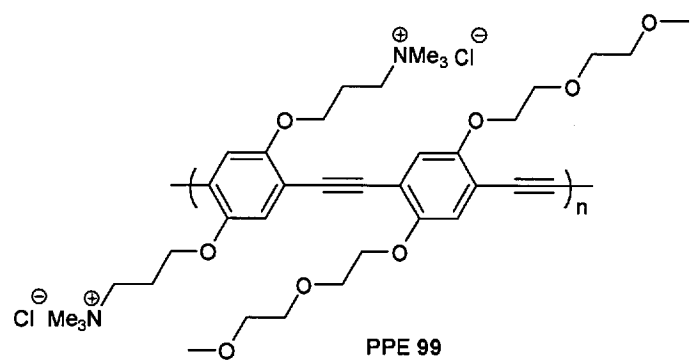

Figure 1.28 The cationic PPE used by the Whitten group as a biocide.[150]

To test this theory and identify possible mechanisms for the light-induced biocidal activity, Whitten and co-workers looked at the effect and behaviour of two dye molecules, methylene blue (MB) and rose bengal lactone (RBL), when used for the same application. They found that under white-light illumination, the dyes had a similar biocidal effect at concentrations of 10 μM and attributed the mode of destruction of bacteria to an established effect whereby the dyes and polymers were considered to act as singlet oxygen sensitisers. This very reactive form of oxygen is known to be lethal to cells.[151] The mechanism of action is therefore similar to that observed in photo dynamic therapy (PDT) where, for example, porphyrins are used as sensitisers for the generation of singlet oxygen, which is the active species in PDT.[152]

One of the goals of our research program was to develop a CPE that could selectively detect DNA and identify single nucleotide polymorphisms (SNPs). This could be achieved in a manner similar to that described by Leclerc (*vide supra*) or by adapting the polymer structure in a way that directly incorporated the recognition elements in the polymer architecture. An example of the latter approach was reported by Tan *et al.* at the beginning of 2005 where a PPE derivative (based on PPE **41**) was attached to a single-stranded oligonucleotide by effectively end-capping the polymer with a 5I-dU base (see Figure 1.29).[153] To aid separation of the DNA-polymer conjugate, the oligonucleotide was attached to a solid support (controlled pore glass, CPG) and the Sonogashira polymerisation carried out in the same way as for the solution state reaction, using typical reaction conditions (stirred under an argon atmosphere, at room temperature for 24 hours).

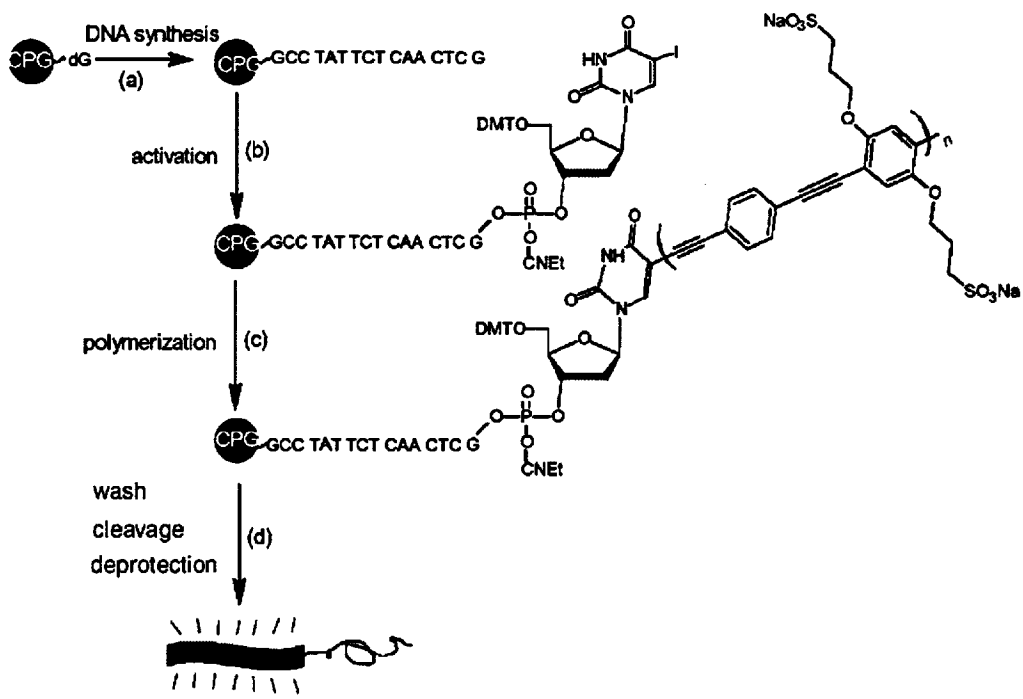

Figure 1.29 The process to end-cap a growing PPE chain with a DNA sequence; the final product is anchored to a solid support thus allowing for easy separation of the polymer post-reaction (reproduced from Schanze *et al.*).[153]

Evidence for the successful formation of the polymer-DNA construct included emission experiments (the emission maximum was at 455 nm in methanol). A control experiment in which the key 5I-dU base was omitted and the polymerisation carried out in the same way, led to no fluorescence being observed. Further evidence included mass spectrometry and gel electrophoresis (using 0.5% agarose gel) that showed migration of the DNA-PPE structure with the new bands being assigned to the DNA-PPE structure and free DNA. The functionalised polymer was used as a

biosensor in the form of a molecular beacon; the basic mode of operation of the system is shown in Figure 1.30.

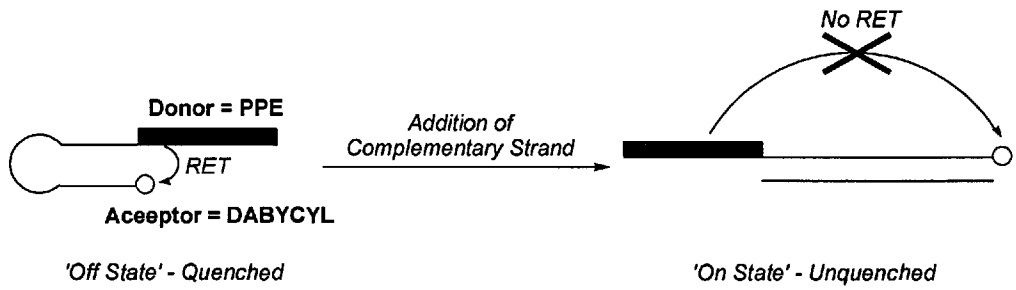

Figure 1.30 Principle of operation behind the polymer molecular beacon designed by Tan *et al.*[153]

Tan *et al.* believed that the major advantage for this system would centre on the enhanced emission quenching of the polymer. The energy acceptor DABCYL was used as the emission quencher and incorporated into the polymer synthesis in-place of the CPG unit. The ability of this quencher to suppress the emission from the polymer was measured in free solution and a Stern-Volmer constant of 4×10^6 M^{-1} was obtained, a value typically recorded for the superquenching effect for these polymers. The result ensured that the formed molecular beacon performed well when exposed to the target sequence, with the hybridisation of the target evidenced by a relative increase in emission of $10^4 - 10^5$ (for a five-fold excess of the target). More dilute solutions of the target led to slower reaction profiles. Overall, this sensory scheme has several salient features; there is a clear change in the emission profile upon addition of the target material and importantly no need for target pre-treatment. Additionally, it should be possible to detect SNPs with the beacon, though this was not probed by the investigators. One aspect that would require analysis is whether the presence of the anionic sulphonate groups on the polymer backbone, would lead to non-specific interactions with other non-target materials in solution, a problem that could be overcome by using a non-ionic PPE.

The successes for PPE-based polymers described in this section clearly demonstrate the huge potential that such polymers possess for biosensing in general. However one crucial point that has yet to be addressed concerns the potential for non-specific interactions between the polymers and biomolecules which could lead to significant quenching or other optical changes, and result in a confused output for the observer seeking to target one particular type of molecule in a solution composed of many differing types. This important potential pitfall for polymer-based biosensors was recently given thorough consideration by Bunz *et al.* who noted that the anionic sugar-derivitised water-soluble PPE **102** exhibited interactions with a wide range of proteins which led to strong fluorescence quenching (Scheme 1.14).[154]

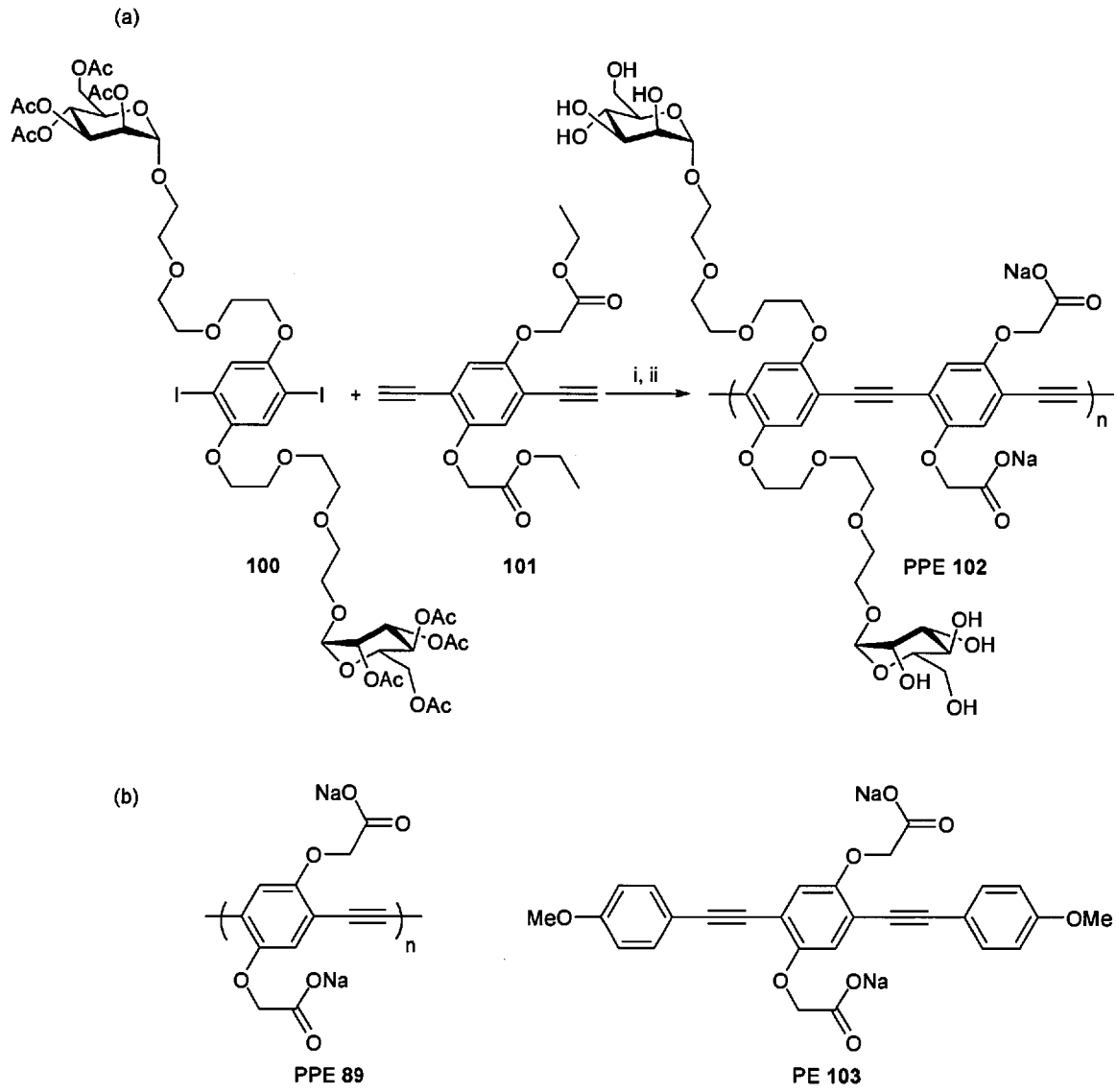

Scheme 1.14 (a) Synthesis of an anionic sugar-substituted PPE for use in a protein detection study and (b) an anionic PPE polymer and small model analogue (phenylene ethynylene, PE) used by Bunz *et al.* in the same analysis.[154] Conditions: (i) $Pd(PPh_3)_2Cl_2$/CuI, NEt_3, CH_2Cl_2; (ii) NaOH/MeOH.

For the commercially available proteins investigated by Bunz *et al.*, it was found that Stern-Volmer constants were in the 10^3 - 10^7 M^{-1} range, which represents moderate to strong quenching. This lack of selectivity highlights a potential problem that CPEs may encounter when attempts are made to implement them in biosensory schemes, as real biological mixtures may contain one or more of these elements which would make the use of such materials difficult. In addition, it was found that the protein BSA (bovine serum albumin) had a similar effect on the emission of PPEs **89** and **102**, to that of a surfactant, i.e. its addition led to an increase in the emission intensity from the polymer. Bunz *et al.* attributed this to the surfactant-like properties that this protein is known to possess.[154]

The result reveals an added complication that could be encountered with real biological mixtures, which would have to be carefully considered when implementing CPEs as biosensors. During their investigation, this group used small model analogue PE **103** in order to quantify the beneficial quenching effects expected to be observed by the polymer. The large (up to 1000-fold increase) quenching enhancement recorded was ascribed to multivalency effects for the binding of the polymer to the proteins.[100,154]

1.7 Important criterion in selecting conjugated polymers for biosensing

To date, the main classes of polymers used for DNA detection are the poly(thiophene)s and poly(fluorene)s and there is a considerable body of work, some of which has been detailed here, dedicated to the findings of DNA sensing experiments in this area.[115,128] To vigorously interrogate biological systems, synthetic polymer sensors have to function in the complex aqueous milieu that such materials are found in and this provides the first challenge when deciding upon the overall polymer structure best suited for the task.

In the first instance, water-solubility is one of the main criteria for selecting a suitable polymer for sensing of analytes, along with high fluorescence quantum yields and low detection limits, as approximated by the Stern-Volmer constant.

In addition to this, careful inspection of the emission spectra from such polymers can allow one to discern differences upon interaction with biological substrates as was demonstrated by the Leclerc group (section 1.5). Other important factors include the nature of the synthesis and whether it is amenable to optimisation in order to obtain high molecular weights. This might be of critical importance as a long persistence length, can impact the potential diffusion range for the exciton, which is directly related to sensitivity. For example, PPEs have a persistence length of 15 nm (20 PE repeating units)[85] but migration of excitations between polymer chains (intermolecular motion) is now known to be just as important as migration along a single polymer chain.[140] As a result, it may be possible to tune sensitivity of a CP by varying the solvent conditions as to facilitate exciton motion, by enabling neighbouring chains to electronically communicate with each other.

The chosen polymer would also have to emit in a region of the spectrum that is easily observed, to simplify the analysis and characterisation. In this case the preference was for a polymer that would emit in the yellow/green region of the spectrum ($\approx 450 - 600$ nm).

As was recently noted by Swager, one of the main proponents in the field of conjugated polymer sensors, 'sensitivity without specificity is nothing'.[155] In order to distinguish different types of biomolecules in solution, probe (receptor) strands are necessary and in most of the recent examples of CP sensors for DNA, these have tended to be complementary strands of DNA. This allows for optimal interaction with the target intended for detection, which minimises instances of 'false positives' when detecting target material from a broth of various analytes.

In order to select a suitable polymer backbone for the fabrication of a highly sensitive emission sensor, we focused on two main points; the ease of synthesis and the resulting fluorescence quantum yields and Stern-Volmer constants. In this regard PPEs were the most promising class of polymer to be considered as there was considerable evidence in the literature of their high sensitivities when used in emission quenching, as has been documented by Schanze,[86] Swager[51,81] and Bunz[85] amongst others. The highly delocalised nature of the singlet exciton directly impacts the Stern-Volmer coefficient (that are usually in excess of 10^6 M^{-1}) as is illustrated by their comparatively high values. The materials can be accessed *via* robust palladium cross-coupling chemistry and give polymers of moderately high molecular weight (M_n = 20 – 100 kDa).[77,106]

Having carefully selected the class of polymer for applications in biosensing, the next important issue concerned the synthetic route to the polymer and whether it could be broadened to allow for more structurally demanding motifs to be included. The Sonogashira copolymerisation that we sought to use to construct these materials is tolerant to a wide range of functional groups (e.g. ionic functional groups; sulphonate, carboxylate, phosphonate, ammonium),[86] which is important as one the longer term aims of the project involves the introduction of more selective side chains along the polymer backbone. This idea is summarised in Figure 1.31.

Generic PPE Structure

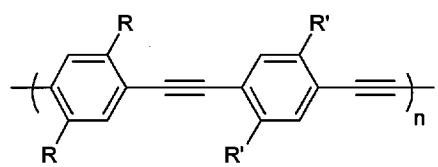

R and R' = connection *via* an alkoxy or alkyl linkage.
Appended functional groups could then include; $-SO_3^-$, $-CO_2^-$, $-PO_3^{2-}$, $-NMe_3^+$, and/or alkyl chains.

Figure 1.31 Structure of the target PPE polymer sought.

In theory, the pendent side-chains of the polymer backbone should allow for elaboration on the monomer units. This would permit the use of more complex monomers to be employed in the copolymerisation to furnish various PPE architectures.

In our intended detection scheme, we wanted to optimise the direct interaction between the synthetic polymer and DNA; we aimed to minimise or eliminate the need for probe modification, by using a functionalised polymer that can selectively bind to the diphosphate ester groups along the DNA backbone. The probe can then be another DNA strand thus allowing for interchangeable DNA probe strands and hence wide applicability and selectivity. Ultimately the intention is to identify SNPs with this optical-based sensing system, driven by proof-of-concept studies detailing the high sensitivity of these polyelectrolytes for potential use in such applications.

This approach differs from previously described strategies for DNA sensing, as we intend to tailor and optimise the design of the polymer specifically for DNA sensing. In the DNA detection technique used by Bazan *et al.* (section 1.6),[133] the emphasis was on maximising the efficiency of the ET process between the polymer and the dye-labelled probe sequence. The poly(fluorene) used had a simple purpose; to draw together, *via* electrostatic interactions, the probe strand to a distance small enough to allow efficient FRET to occur. Similarly, Leclerc's use of poly(thiophene)s for detecting SNPs hinged on the direct interaction of an un-optimised polymer.[121] By using the known and highly sensitive PPE polymers and engaging in structure optimisation, we hoped to develop a more sophisticated, purpose-built sensor.

In this Chapter, an outline of the myriad of uses for CPs in a variety of applications has been discussed. In addition to the early uses for such materials, in for example LEDs and solar cells, newer technologies centred on biosensor advances have received particular attention. The use of such polymers in various biosensor devices has also been reviewed and the salient features fluorescence-based sensors highlighted. The various synthetic routes to CPEs were illustrated and the versatility of the reactions used to derive such structures confirmed the potential to elaborate on a given polymer design (for example see Figure 1.12). Examples of biosensing schemes for the detection of enzymatic activity, untreated DNA, proteins as well as biocidal activity revealed the vast array of potential uses for these materials.

Chapter Two describes the synthesis and analysis of first generation CPEs including optimisation of the Sonogashira polymerisation using neutral PPE derivatives. The properties of second generation polyelectrolytes are illustrated in Chapter Three, where the impact of surfactants on the emission quenching properties and QEs of the polymers are considered. Presented in Chapter Four, are results on the sensing properties of novel guanidinium-containing PPEs and PEs. The response

of these materials was shown to be much more sensitive to oppositely-charged quencher molecules than traditional alkoxy-derived PPEs and PEs. This effect was attributed to the distance separating the conjugated backbone and the recognition unit. Finally, in Chapter Five, the initial findings on the use of PPEs and PEs for single-stranded DNA detection are described.

The research programme sought to identify suitable PPE structures that could be used for the sensitive and selective biosensing of DNA oligonucleotides, which could be synthesised from commercially available starting materials in relatively few steps. It was hoped that the resulting polymers could also be used in other biosensing schemes, for example monitoring enzyme activity and that selectivity through the judicious attachment of discriminating side chains/groups would allow for the further enhancement of the biorecognition process. Reported herein are the findings of our investigations.

1.8 Notes and References

1. A. Ciferri, *Supramolecular Polymers*, Taylor & Francis, Boca Raton, Florida, 2005.
2. A. Kraft, A. C. Grimsdale and A. B. Holmes, *Angew. Chem., Int. Ed.*, 1998, **37**, 403-428.
3. (a) D. Bradley, *Nature*, 1996, **382**, 671; (b) F. Hide, M. A. Diaz-Garcia, B. J. Schwartz and A. J. Heeger, *Acc. Chem. Res.*, 1997, **30**, 430-436; (c) N. Tessler, G. J. Denton and R. H. Friend, *Nature*, 1996, **382**, 695-697; (d) F. Hide, B. J. Schwartz, M. A. Diaz-Garcia and A. J. Heeger, *Synth. Met.*, 1997, **91**, 35-40; (e) M. A. Diaz-Garcia, F. Hide, B. J. Schwartz, M. R. Andersson, Q. Pei and A. J. Heeger, *Synth. Met.*, 1997, **84**, 455-462.
4. B. Wang, W. Yang and H. Fang, *Chem. Commun.*, **2003**, 792-793.
5. (a) H. L. Anderson, *Chem. Commun.*, **1999**, 2323-2330; (b) J. Wang, M. Lu, Y. Pan and Z. Peng, *J. Org. Chem.*, 2002, **67**, 7781-7786; (c) P. N. Taylor, J. Huuskonen, R. T. Aplin, H. L. Anderson, G. Rumbles and E. Williams, *Chem. Commun.*, **1998**, 909-910.
6. J. W. Steed and J. L. Atwood, *Supramolecular Chemistry*, John Wiley & Sons, West Sussex, United Kingdom, 2000.
7. A. Facchetti, M.-H. Yoon and T. J. Marks, *Adv. Mater.*, 2005, **17**, 1705-1725.
8. J. Roncali, *Chem. Soc. Rev.*, 2005, **34**, 483-495.
9. X. Zheng, M. E. Mulcahy, D. Horinek, F. Galeotti, T. Magnera and J. Michl, *J. Am. Chem. Soc.*, 2004, **126**, 4540-4542.
10. H. Shirakawa, E. J. Louis, A. G. MacDiarmid, C. K. Chiang and A. J. Heeger, *J. Chem. Soc., Chem. Commun.*, **1977**, 578-580.
11. A. J. Heeger, *Angew. Chem., Int. Ed.*, 2001, **40**, 2591-2611.

12. (a) H. Shirakawa, *Angew. Chem., Int. Ed.*, 2001, **40**, 2574-2580; (b) A. G. MacDiarmid, *Angew. Chem., Int. Ed.*, 2001, **40**, 2581-2590; (c) H. Shirakawa, A. G. MacDiarmid and A. J. Heeger, *Nobel Lecture,* www.nobel.se (accessed: December 2005).
13. A. Ciferri, *Supramolecular Polymers*, Taylor & Francis, Boca Raton, Florida, 2005.
14. J. H. Burroughes, D. D. C. Bradley, A. R. Brown, R. N. Marks, K. Mackay, R. H. Friend, P. L. Burns and A. B. Holmes, *Nature*, 1990, **347**, 539-541.
15. (a) M. Pope, H. P. Kallmann and P. Magnante, *J. Chem. Phys.*, 1963, **38**, 2042-2043; (b) W. Helfrich and W. G. Schneider, *Phys. Rev. Lett.*, 1965, **14**, 229-231; (c) U. Mitschke and P. Bauerle, *J. Mater. Chem.*, 2000, **10**, 1471-1507.
16. G. Hadziioannou and P. F. van Hutten, *Semiconducting Polymers*, Wiley-VCH, Weinheim, Germany, 2000.
17. A recent comprehensive review is given by Kraft *et al.*: A. Kraft, A. C. Grimsdale and A. B. Holmes, *Angew. Chem., Int. Ed.*, 1998, **37**, 403-428; and references herein.
18. S. Son, A. J. Lovinger and M. E. Galvin, *Polym. Mater. Sci. Eng.*, 1995, **72**, 567-568.
19. P. Anuragudom, S. S. Newaz, S. Phanichphant and T. R. Lee, *Macromolecules*, 2006, **39**, 3494-3499.
20. H. Roex, P. Adriaensens, D. Vanderzande and J. Gelan, *Macromolecules*, 2003, **36**, 5613-5622.
21. T. Munters, T. Martens, L. Goris, V. Vrindts, J. Manca, L. Lutsen, W. De Ceuninck, D. Vanderzande, L. De Schepper, J. Gelan, N. S. Sariciftci and C. Brabec, *Thin Solid Films*, 2002, **403-404**, 247-251.
22. H. Becker, H. Spreitzer, K. Ibrom and W. Kreuder, *Macromolecules*, 1999, **32**, 4925-4932.
23. R. H. Friend, R. W. Gymer, A. B. Holmes, J. H. Burroughes, R. N. Marks, C. Taliani, D. D. C. Bradley, D. A. dos Santos, J. L. Bredas, M. Logdlund and W. R. Salaneck, *Nature*, 1999, **397**, 121-128.
24. (a) Y. Cao, I. D. Parker, G. Yu, C. Zhang and A. J. Heeger, *Nature*, 1999, **397**, 414-417; (b) P. K. H. Ho, J.-S. Kim, J. H. Burroughes, H. Becker, F. Y. L. Sam, T. M. Brown, F. Cacialli and R. H. Friend, *Nature*, 2000, **404**, 481-484; (c) A. S. Dhoot, D. S. Ginger, D. Beljonne, Z. Shuai and N. C. Greenham, *Chem. Phys. Lett.*, 2002, **360**, 195-201.
25. (a) A. Kohler, J. S. Wilson and R. H. Friend, *Adv. Eng. Mater.*, 2002, **4**, 453-459; (b) C. Adachi, M. A. Baldo, M. E. Thompson and S. R. Forrest, *J. Appl. Phys.*, 2001, **90**, 5048-5051.
26. H. Spreitzer, H. Becker, E. Kluge, W. Kreuder, H. Schenk, R. Demandt and H. Schoo, *Adv. Mater.*, 1998, **10**, 1340-1343.
27. W. Shi, S. Fan, F. Huang, R. Liu and Y. Cao, *J. Mater. Chem.*, 2006, **16**, 2387-2394.
28. M. Strukelj, F. Papadimitrakopoulos, T. M. Miller and L. J. Rothberg, *Science*, 1995, **267**, 1969-1972.

29. N. S. Sariciftci, L. Smilowitz and A. J. Heeger, *Science*, 1992, **258**, 1474-1476.

30. A. Cravino, G. Zerza, H. Neugebauer, M. Maggini, S. Bucella, E. Menna, M. Svensson, M. R. Andersson, C. J. Brabec and N. S. Sariciftci *J. Phys. Chem. B*, 2002, **106**, 70-76.

31. M. Reyes-Reyes, K. Kim, J. Dewald, R. Lopez-Sandoval, A. Avadhanula, S. Curran and D. L. Carroll, *Org. Lett.*, 2005, **7**, 5749-5752.

32. A. M. Ramos, M. T. Rispens, J. K. J. van Duren, J. C. Hummelen and R. A. J. Janssen, *J. Am. Chem. Soc.*, 2001, **123**, 6714-6715.

33. C. J. Brabec, N. S. Sariciftci and J. C. Hummelen, *Adv. Funct. Mater.*, 2001, **11**, 15-26.

34. S. A. Haque, S. Handa, K. Peter, E. Palomares, M. Thelakkat and J. R. Durrant, *Angew. Chem., Int. Ed.*, 2005, **44**, 5740-5744.

35. J.-E. Moser, *Nature Mater.*, 2005, **4**, 723-724.

36. S. A. Haque, E. Palomares, B. M. Cho, A. N. M. Green, N. Hirata, D. R. Klug and J. R. Durrant, *J. Am. Chem. Soc.*, 2005, **127**, 3456-3462.

37. A. H. Flood, A. J. Peters, S. A. Vignon, D. W. Steuerman, H.-R. Tseng, S. Kang, J. R. Heath and J. F. Stoddart, *Chem. Eur. J.*, 2004, **10**, 6558-6564.

38. V. Balzani, A. Credi and M. Venturi, *Molecular Devices and Machines: A Journey into the Nano World*, Wiley-VCH, Weinheim, Germany, 2004.

39. M. K. J. ter Wiel, R. A. van Delden, A. Meetsma and B. L. Feringa, *Org. Biomol. Chem.*, 2005, **3**, 4071-4076.

40. V. V. Didenko, C. L. Minchew, S. Shuman and D. S. Baskin, *Nano Lett.*, 2004, **4**, 2461-2466.

41. A. H. Flood, J. F. Stoddart, D. W. Steuerman and J. R. Heath, *Science*, 2004, **306**, 2055-2056.

42. Y. Shirai, A. J. Osgood, Y. Zhao, K. F. Kelly and J. M. Tour, *Nano Lett.*, 2005, **5**, 2330-2334.

43. Y. Shirai, A. J. Osgood, Y. Zhao, Y. Yao, L. Saudan, H. Yang, C. Yu-Hung, L. B. Alemany, T. Sasaki, J.-F. Morin, J. M. Guerrero, K. F. Kelly and J. M. Tour, *J. Am. Chem. Soc.*, 2006, **128**, 4854-4864.

44. J. Evans, *Chemistry World*, 2006, **3**, 19.

45. E. W. H. Jager, E. Smela and O. Inganas, *Science*, 2000, **290**, 1540-1545.

46. E. Smela, *Adv. Mater.*, 2003, **15**, 481-494.

47. R. H. Baughman, *Science*, 2005, **308**, 63-65.

48. H. Sirringhaus, P. J. Brown, R. H. Friend, M. M. Nielsen, K. Bechgaard, B. M. W. Langeveld-Voss, A. J. H. Spiering, R. A. J. Janssen, E. W. Meijer, P. Herwig and D. M. De Leeuw, *Nature*, 1999, **401**, 685-688.

49. F. Cacialli, J. S. Wilson, J. J. Michels, C. Daniel, C. Silva, R. H. Friend, N. Severin, P. Samori, J. P. Rabe, M. J. O'Connell, P. N. Taylor and H. L. Anderson, *Nature Mater.*, 2002, **1**, 160-164.
50. J. J. Michels, M. J. O'Connell, P. N. Taylor, J. S. Wilson, F. Cacialli and H. L. Anderson, *Chem. Eur. J.*, 2003, **9**, 6167-6176.
51. D. T. McQuade, A. E. Pullen and T. M. Swager, *Chem. Rev.*, 2000, **100**, 2537-2574.
52. (a) D. Normile, *Science*, 2005, **310**, 417; (b) N. M. Ferguson, C. Fraser, C. A. Donnelly, A. C. Ghani and R. M. Anderson, *Science*, 2004, **304**, 968-969.
53. J. Wang, *Nucleic Acids Res.*, 2000, **28**, 3011-3016.
54. A. J. deMello, *Lecture Course 'Sensors and Detectors', (Lecture 6, 'Chemical Sensors'), 2001.*
55. D. L. Wang, X. Gong, P. S. Heeger, F. Rininsland, G. C. Bazan and A. J. Heeger, *Proc. Natl. Acad. Sci. U. S. A.*, 2002, **99**, 49-53.
56. J. H. Wosnick and T. M. Swager, *Curr. Opin. Chem. Biol.*, 2000, **4**, 715-720.
57. (a) J. Wang, *Anal. Chim. Acta.*, 2002, **469**, 63; (b) E. Palecek, *Talanta*, 2002, **56**, 809-819.
58. H. Korri-Youssoufi, F. Garnier, P. Srivastava, P. Godillot and A. Yassar, *J. Am. Chem. Soc.*, 1997, **119**, 7388-7389.
59. A. K. Boal and J. K. Barton, *Bioconjugate Chem.*, 2005, **16**, 312-321.
60. J.-i. Anzai and A. Liu, *Mater. Sci. Eng.*, 2004, **C 24**, 503-505.
61. R. F. Service, *Science*, 1998, **282**, 396-401.
62. M. F. Ali, R. Kirby, A. P. Goodey, M. D. Rodriguez, A. D. Ellington, D. P. Neikirk and J. T. McDevitt, *Anal. Chem.*, 2003, **75**, 4732-4739.
63. A. Bianco, K. Kostarelos, C. D. Partidos and M. Prato, *Chem. Commun.*, **2005**, 571-577.
64. J. Li, H. T. Ng, A. Cassell, W. Fan, H. Chen, Q. Ye, J. Koehne, J. Han and M. Mayyappan, *Nano Lett.*, 2003, **3**, 597-602.
65. C.-Y. Zhang, H.-C. Yeh, M. T. Kuroki and T.-H. Wang, *Nature Mater.*, 2005, **4**, 826-831.
66. J. R. Lakowicz, *Principles of Fluorescence Spectroscopy*, Plenum Press, New York, 1983.
67. Y. J. Seo, J. H. Ryu and B. H. Kim, *Org. Lett.*, 2005, **7**, 4931-4933.
68. O. Stern and M. Volmer, *Phys. Z.*, **1919**, 183-188.
69. C. Y. Tan, E. Atas, J. G. Muller, M. R. Pinto, V. D. Kleiman and K. S. Schanze, *J. Am. Chem. Soc.*, 2004, **126**, 13685-13694.
70. M. R. Wasielewski, *Chem. Rev.*, 1992, **92**, 435-461.
71. M. R. Pinto, B. M. Kristal and K. S. Schanze, *Langmuir*, 2003, **19**, 6523-6533.
72. J. G. Muller, E. Atas, C. Tan, K. S. Schanze and V. Kleiman, *J. Am. Chem. Soc.*, 2006, **128**, 4007-4016.
73. F. Wu, J. W. Lewis, D. S. Kliger and J. Z. Zhang, *J. Chem. Phys.*, 2003, **118**, 12-16.

74. L. Chen, D. W. McBranch, H.-L. Wang, R. Helgeson, F. Wudl and D. G. Whitten, *Proc. Natl. Acad. Sci. U. S. A.*, 1999, **96**, 12287-12292.

75. For a comprehensive review, see: D. T. McQuade, A. E. Pullen and T. M. Swager, *Chem. Rev.*, 2000, **100**, 2537-2574.

76. Q. Zhou and T. M. Swager, *J. Am. Chem. Soc.*, 1995, **117**, 12593-12602.

77. C. Y. Tan, M. R. Pinto and K. S. Schanze, *Chem. Commun.*, **2002**, 446-447.

78. B. S. Harrison, M. B. Ramey, J. R. Reynolds and K. S. Schanze, *J. Am. Chem. Soc.*, 2000, **122**, 8561-8562.

79. L. Chen, D. W. McBranch, H.-L. Wang, R. Helgeson, F. Wudl and D. G. Whitten, *Proc. Natl. Acad. Sci. USA*, 1999, **96**, 12287-12292.

80. S. Kumaraswamy, T. Bergstedt, X. Shi, F. Rininsland, S. Kushon, W. Xia, K. Ley, K. Achyuthan, D. McBranch and D. Whitten, *Proc. Natl. Acad. Sci. U. S. A.*, 2004, **101**, 7511-7515.

81. T. M. Swager, *Acc. Chem. Res.*, 1998, **31**, 201-207.

82. For comparison, consider the example by Leclerc *et al.* (*J. Am. Chem. Soc.*, 2004, **126**, 4240-4244: one of the best CP-based DNA detection systems) and Li *et al.* (*Nano Lett.*, 2003, **3**, 597-602: an example of an ultrasensitive CNT detection system).

83. S. Shi and F. Wudl, *Macromolecules*, 1990, **23**, 2119-2124.

84. T. I. Wallow and B. M. Novak, *J. Am. Chem. Soc.*, 1991, **113**, 7411-7412.

85. U. H. F. Bunz, *Chem. Rev.*, 2000, **100**, 1605-1644.

86. M. R. Pinto and K. S. Schanze, *Synthesis*, **2002**, 1293-1309.

87. T. A. Skotheim, R. L. Elsenbaumer and J. R. Reynolds, eds., *Handbook of Conducting Polymers*, Marcel Dekker, New York, 1998.

88. D. L. Wise, G. E. Wnek, D. J. Trantolo, T. M. Cooper and J. D. Gresser, eds., *Photonic Polymer Systems: Fundamentals, Methods and Applications*, Marcel Dekker, New York, 1998.

89. U. H. F. Bunz, *Science*, 2005, **308**, 216-217.

90. F. He, Y. Tang, M. Yu, F. Feng, L. An, H. Sun, S. Wang, Y. Li, D. Zhu and G. C. Bazan, *J. Am. Chem. Soc.*, 2006, **128**, 6764-6765.

91. H.-A. Ho, M. Boissinot, M. G. Bergeron, G. Corbeil, K. Dore, D. Boudreau and M. Leclerc, *Angew. Chem., Int. Ed.*, 2002, **41**, 1548-1551.

92. K. Sonogashira, *J. Organomet. Chem.*, 2002, **653**, 46-49.

93. C. J. Li, W. T. Slaven, V. T. John and S. Banerjee, *Chem. Commun.*, **1997**, 1569-1570.

94. C. J. Li, W. T. Slaven, Y.-P. Chen, V. T. John and S. H. J. Rachakonda, *Mater. Sci. Pure Appl. Chem.*, 1999, **A36(7 & 8)**, 971-980.

95. S. Takahashi, Y. Kuroyama, K. Sonogashira and N. Hagihara, *Synthesis*, **1980**, 627-630.

96. (a) L. Cassar, *J. Organomet. Chem.*, 1975, **93**, 253-257; (b) H. A. Dieck and F. R. Heck, *J. Organomet. Chem.*, 1975, **93**, 259-263; (c) K. Sonogashira, Y. Tohda and N. Hagihara, *Tetrahedron Lett.*, 1975, **50**, 4467-4470.

97. J. H. Moon, R. Deans, E. Krueger and L. F. Hancock, *Chem. Commun.*, **2003**, 104-105.

98. J. S. Wilson, N. Chawdhury, M. R. A. Al-Mandhary, M. Younus, M. S. Khan, P. R. Raithby, A. Koehler and R. H. Friend, *J. Am. Chem. Soc.*, 2001, **123**, 9412-9417.

99. Y. Liu, S. J. Jiang and K. S. Schanze, *Chem. Commun.*, **2003**, 650-651.

100. I.-B. Kim, B. Erdogan, J. N. Wilson and U. H. F. Bunz, *Chem. Eur. J.*, 2004, **10**, 6247-6254.

101. P. H. Kwan, M. J. MacLachlan and T. M. Swager, *J. Am. Chem. Soc.*, 2004, **126**, 8638-8639.

102. F. Rininsland, W. Xia, S. Wittenburg, X. Shi, C. Stankewicz, K. Achyuthan, D. McBranch and D. Whitten, *Proc. Natl. Acad. Sci. U. S. A.*, 2004, **101**, 15295-15300.

103. J. H. Wosnick, C. M. Mello and T. M. Swager, *J. Am. Chem. Soc.*, 2005, **127**, 3400-3405.

104. (a) C. Y. Tan, M. R. Pinto, M. E. Kose, I. Ghiviriga and K. S. Schanze, *Adv. Mater.*, 2004, **16**, 1208-1212; (b) T. Zhao, H. W. Beckham, H. L. Ricks and U. H. F. Bunz, *Polymer*, 2005, **46**, 4839-4844.

105. I. U. Rau and M. Rehahn, *Polymer*, 1993, **34**, 2889-2893.

106. Q.-L. Fan, Y. Zhou, X.-M. Lu, X.-Y. Hou and W. Huang, *Macromolecules*, 2005, **38**, 2927-2936.

107. H. L. Ricks, U. H. Choudry, A. R. Marshall and U. H. F. Bunz, *Macromolecules*, 2003, **36**, 1424-1425.

108. M. P. Stevens, *Polymer Chemistry*, 3rd edn., OUP, Oxford, 1999.

109. A. Khan, S. Muller and S. Hecht, *Chem. Commun.*, **2005**, 584-586.

110. K. Kuroda and T. M. Swager, *Chem. Commun.*, **2003**, 26-27.

111. R. Rulkens, M. Schulze and G. Wenger, *Macromol. Rapid. Commun.*, 1994, **15**, 669-676.

112. (a) A. Fujii, T. Sonoda, K. Yoshino, *Jpn. J. Appl. Phys*, 2000, **39(3A/B)**, L249-L252; (b) A. Fujii, T. Sonoda, R. Ootake and K. Yoshino, *Synth. Met.*, 2001, **119**, 189-190.

113. L. Hontis, V. Vrindts, D. Vanderzande and L. Lusten, *Macromolecules*, 2003, **36**, 3035-3044.

114. (a) M. Redecker, D. D. C. Bradley, M. Inbasekaran and E. P. Woo, *Appl. Phys. Lett.*, 1998, **73**, 1565-1567; (b) A. Babel and S. A. Jenekhe, *Macromolecules*, 2003, **36**, 7759-7764.

115. B. Liu and G. C. Bazan, *Chem. Mat.*, 2004, **16**, 4467-4476.

116. A. P. Kulkarni, Y. Zhu and S. A. Jenekhe, *Macromolecules*, 2005, **38**, 1553-1563.

117. B. Liu and G. C. Bazan, *Proc. Natl. Acad. Sci. U. S. A.*, 2005, **102**, 589-593.

118. K. Dore, S. Dubus, H.-A. Ho, I. Levesque, M. Brunette, G. Corbeil, M. Boissinot, G. Boivin, M. G. Bergeron, D. Boudreau and M. Leclerc, *J. Am. Chem. Soc.*, 2004, **126**, 4240-4244.
119. H.-A. Ho and M. Leclerc, *J. Am. Chem. Soc.*, 2004, **126**, 1384-1387.
120. H.-A. Ho, M. Boissinot, M. G. Bergeron, G. Corbeil, K. Dore, D. Boudreau and M. Leclerc, *ACS Symp. Ser.*, 2005, **888**, 359-367.
121. K. Dore, S. Dubus, H.-A. Ho, I. Levesque, M. Brunette, G. Corbeil, M. Bossinot, G. Boivin, M. G. Bergeron, D. Boudreau and M. K. Leclerc, *J. Am. Chem. Soc.*, 2004, **126**, 4240-4244.
122. J. R. Matthews, F. Goldoni, A. P. H. J. Schenning and E. W. Meijer, *Chem. Commun.*, **2005**, 5503-5505.
123. J. Zheng and T. M. Swager, *Adv. Polym. Sci.* , 2005, **177**, 151-179.
124. B. J. Holliday and M. Swager Timothy, *Chem. Commun.*, **2005**, 23-36.
125. Y. Zhang, C. B. Murphy and W. E. Jones Jr., *Macromolecules*, 2002, **35**, 630-636.
126. B. Jiang, S.-W. Yang, D. C. Barbini and W. E. Jones Jr., *Chem. Commun.*, **1998**, 213-214.
127. T. H. Kim and T. M. Swager, *Angew. Chem., Int. Ed.*, 2003, **42**, 4803-4806.
128. H.-A. Ho, M. Bera-Aberem and M. Leclerc, *Chem. Eur. J.*, 2005, **11**, 1718-1724.
129. J. Dalvi-Malhotra and L. Chen, *J. Phys. Chem. B*, 2005, **109**, 3873-3878.
130. K. Dore, S. Dubus, H.-A. Ho, I. Levesque, M. Brunette, G. Corbeil, M. Boissinot, G. Boivin, M. G. Bergeron, D. Boudreau and M. Leclerc, *J. Am. Chem. Soc.*, 2004, **126**, 4240-4244.
131. M. Leclerc and H.-A. Ho, *Synlett*, 2004, 380-387.
132. H. A. Ho, K. Dore, M. Boissinot, M. G. Bergeron, R. M. Tanguay, D. Boudreau and M. Leclerc, *J. Am. Chem. Soc.*, 2005, **127**, 12673-12676.
133. B. Wang and G. C. Bazan, *Adv. Mater.*, 2003, **15**, 1425-1428.
134. B. S. Gaylord, A. J. Heeger and G. C. Bazan, *Proc. Natl. Acad. Sci. USA*, 2002, **99**, 10954-10957.
135. B. S. Gaylord, M. R. Massie, S. C. Feinstein and G. C. Bazan, *Proc. Natl. Acad. Sci. USA*, 2005, **102**, 34-39.
136. P. E. Nielsen, *Peptide Nucleic Acids: Protocols and Applications*, Garland Science, 2004.
137. S. Wang, B. S. Gaylord and G. C. Bazan, *J. Am. Chem. Soc.*, 2004, **126**, 5446-5451.
138. B. Liu, B. Wang, G. C. Bazan and A. Mikhailovsky, *J. Am. Chem. Soc.*, 2003, **125**, 13306-13307.
139. B. Liu and G. C. Bazan, *J. Am. Chem. Soc.*, 2004, **126**, 1942-1943.
140. J. W. Hong, W. L. Hemme, G. E. Keller, M. T. Rinke and G. C. Bazan, *Adv. Mater.*, 2006, **18**, 878-882.

141. S. A. Kushon, K. D. Ley, K. Bradford, R. M. Jones, D. McBranch and D. Whitten, *Langmuir*, 2002, **18**, 7245-7249.

142. S. A. Kushon, K. Bradford, V. Marin, C. Suhrada, B. A. Armitage, D. McBranch and D. Whitten, *Langmuir*, 2003, **19**, 6456-6464.

143. M. R. Pinto and K. S. Schanze, *Proc. Natl. Acad. Sci. USA*, 2004, **101**, 7505-7510.

144. Scissor graphic courtesy of: http://www.fotosearch.com/clip-art/scissors.html (accessed: July 2006)

145. J. Zheng and T. M. Swager, *Adv. Polym. Sci.*, 2005, **177**, 151-179.

146. J. N. Wilson, Y. Q. Wang, J. J. Lavigne and U. H. F. Bunz, *Chem. Commun.*, **2003**, 1626-1627.

147. I.-B. Kim, J. N. Wilson and U. H. F. Bunz, *Chem. Commun.*, **2005**, 1273-1275.

148. See: I.-B. Kim, B. Erdogan, J. N. Wilson and U. H. F. Bunz, *Chem. Eur. J.*, 2004, **10**, 6247-6254.

149. (a) H. Lis and N. Sharon, *Chem. Rev.*, 1998, **98**, 637-674; (b) M. Mammen, S. K. Choi and G. M. Whitesides, *Angew. Chem., Int. Ed.*, 1998, **37**, 2755-2794; (c) B. G. Davis, *J. Chem. Soc., Perkin Trans. 1*, **1999**, 2137-2160.

150. L. Lu, F. H. Rininsland, S. K. Wittenburg, K. E. Achyuthan, D. W. McBranch and D. G. Whitten, *Langmuir*, 2005, **21**, 10154-10159.

151. (a) J. P. Pooler and D. P. Valenzeno, *Med. Phys.*, 1981, **8**, 614-628; (b) *US Pat.*, WO 2003078557, 2003.

152. A. Gorman, J. Killoran, C. O'Shea, T. Kenna, W. M. Gallagher and D. F. O'Shea, *J. Am. Chem. Soc.*, 2004, **126**, 10619-10631.

153. C. J. Yang, M. R. Pinto, K. S. Schanze and W. Tan, *Angew. Chem., Int. Ed.*, 2005, **44**, 2-5.

154. I.-B. Kim, A. Dunkhorst and U. H. F. Bunz, *Langmuir*, 2005, **21**, 7985-7989.

155. G. Mancino, *Chemistry World*, 2005, **2**, 50-53.

2 First Generation Polyelectrolytes and Polymers: Synthesis and Sensing Assessments

2.1 Introduction

The literature survey presented in Chapter One illustrated several useful strategies that have been employed to construct sensors using conjugated materials. The favourable properties of water-soluble CPs have driven considerable interest in the use of these materials as sensors for monitoring biological processes including hybridisation events and enzymatic activity in challenging biological media such as blood, urine and saliva.[1,2] A variety of techniques to interrogate analyte-receptor responses using such sensors based on changes in conductivity, absorption, chemical potential and more recently emission have been described with varying levels of success.

CPs, and in particular water-soluble ionic CPs, have been successfully applied as chemical sensors in a number of studies. For instance: Leclerc *et al.* have described the use of a conjugated poly(thiophene) derivative for the ultra sensitive detection of unmodified DNA, achieving detection limits in the zeptomole (10^{-21} M) range;[3] Bazan *et al.* have successfully functionalised poly(fluorene)s that were then employed as optical reporters for hybridisation events;[4] Whitten *et al.* have demonstrated the use of poly(phenylene ethynylene) (PPE) polymer-coated microspheres for the detection of oligomeric DNA strands in a 'turn-on' assay;[5] and Schanze *et al.* have tracked the activity of enzymes[1] and detected glucose derivatives using anionic PPE derivatives.[2]

On the basis of these and other studies, PPEs have emerged as the pre-eminent class of CP biosensors. This is primarily because they undergo exceptionally strong fluorescence quenching in the presence of electron deficient species, with k_{SV} values commonly in the range 10^5-10^8 M^{-1},[6,7] with some reports detailing Stern-Volmer constants as high as 10^{10} M^{-1} for the quenching of cationic poly(fluorene)s by gold nanoparticles.[8]

The emission from PPEs can be quenched by the addition of a variety of complementary-charged acceptor molecules,[9,10] with static quenching considered to be the dominant quenching mechanism due to the large size of the observed Stern-Volmer constants and the short, concentration-independent lifetimes of the excited states.[11,12] The strong quenching observed in PPEs has been attributed to the extensive diffusion range of photoexcited excitons, which have a high probability of undergoing deactivation at a bound quencher site as they migrate along the polymer backbone. In the case of PPEs, the de-excitation mechanism is thought to involve electron transfer from the singlet excited state (LUMO) of the polymer to the LUMO level of the electron acceptor.[6,9] Other advantages for PPEs, in addition to their relative ease of synthesis, include their high

photoluminescence (PL) efficiencies in solution and their strong response to a wide range of quenchers.[12,13] The quenchers directly associate with the polymer chains and this combined with the high mobility of the excitons, allows these excited states to quickly diffuse along or between polymer chains to the quencher molecule. These characteristics make them ideally suited for use as optical reporters in recognition events.

In this work, we aimed to develop new material systems and strategies that would allow high Stern-Volmer constants, and hence high sensitivity detection, to be achieved even in high ionic strength buffered media.

Detailed herein, are our findings on the emission techniques we believed would be best suited to achieve the aims discussed previously along with a general critique of the challenges that were encountered.

2.1.1 First generation polyelectrolytes: synthesis and sensing assessments

The poly(phenylene ethynylene)s (PPEs) were selected as the class of conjugated polymer best suited to meet the needs of a sensitive, robust biosensor (see Chapter One). They benefit from high quantum yields and sensitivities, as ascertained through measurement of Stern-Volmer constants. The polymers are accessed through known, reliable protocols, giving polymers of moderate molecular weight (usually 20 – 100 kDa),[9,10] though at the time of starting the project, the number of reported water-soluble derivatives was limited. The first task was to identify an efficient synthetic route to the polymers and a reliable emission quenching protocol. To achieve this we embarked on the synthesis of a recently reported anionic CPE (PPE **41**). The retrosynthetic analysis for PPE polymers, described in Figure 2.1, shows how the most suitable disconnections lead to forward reactions involving cross-coupling chemistry, though two choices exist. The disconnections described in Figure 2.1a lead to monomers **105** and **106**. This represents a better choice than that shown in Figure 2.1b, where the disconnections can lead to a monomer that is commercially available (**109**), but the unbalanced nature of this route (revealing monomer **112**, which is heavily functionalised) is less satisfactory.

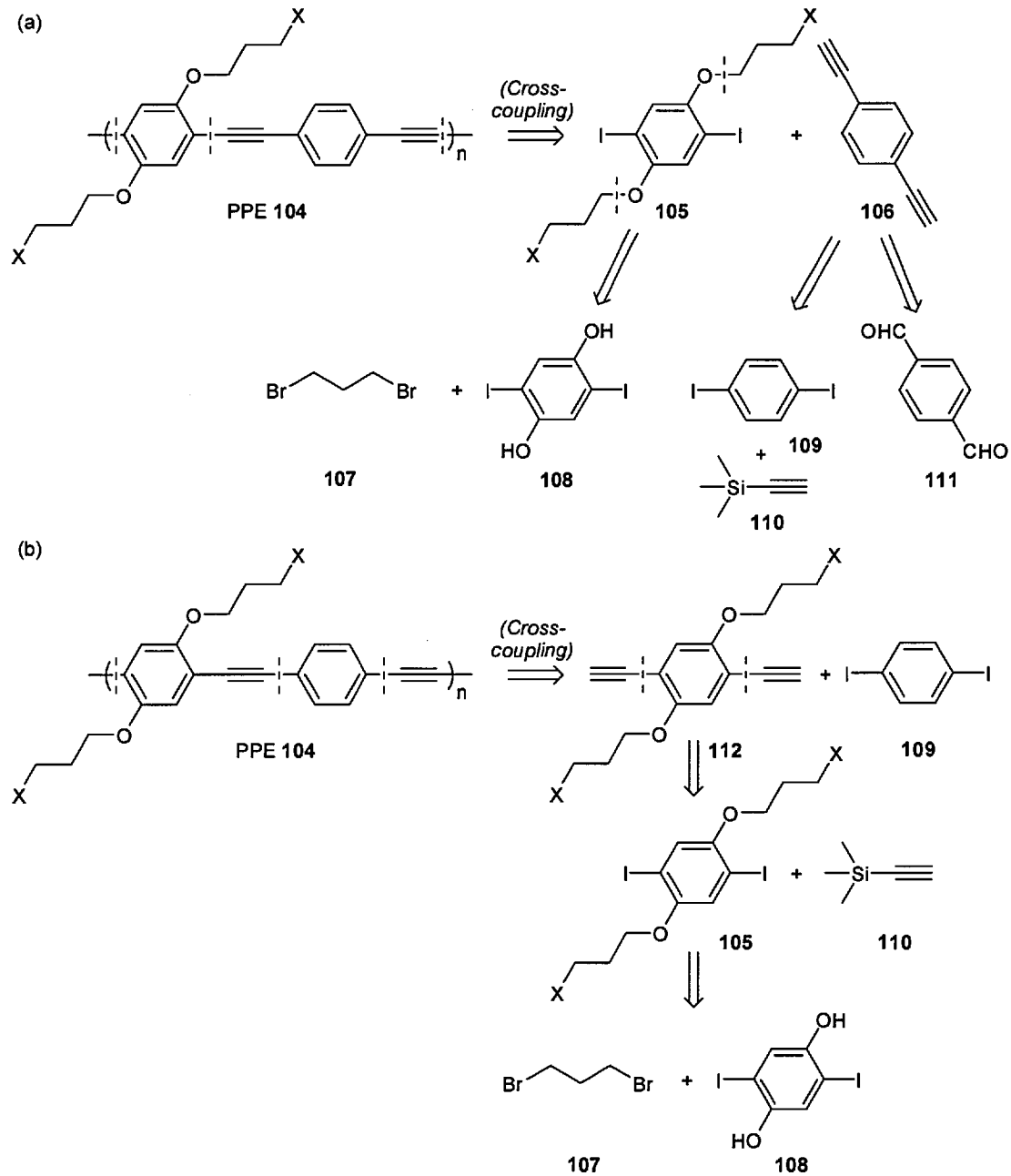

Figure 2.1 The structure of the target polymer (PPE **104**) and retrosynthetic analysis showing options for synthesis of the polymer and monomers. (a) Disconnections leading to two evenly functionalised monomers and (b) an unbalanced disconnection to give heavily functionalised monomer **112**.

This method represents a general strategy to such materials and gained prominence as many reported protocols have shown that high molecular weight polymers could be easily obtained under mild reaction conditions, with wide functional-group compatibility.[14] In many cases (as shown in Chapter One) highly functionalised polar monomers (e.g. acetyl-protected mannose[15] and β-glucopyranose units[16]), including some with ionic groups (e.g. sulphonate, carboxylate,

phosphonate, ammonium),[14] could be carried through the polymerisation, with no protecting group chemistry required.

From Carothers' theory, we know that the number-average degree of polymerisation (X_n) is defined as shown below (Equation 6);[17]

$$X_n = \frac{1}{1-p}$$

Equation 6

where p is the extent of reaction. To obtain high molecular weights, long reaction times are required to ensure complete consumption of the monomers (and therefore high values of p). In order to synthesise polymers like PPE **104**, two bifunctional monomers (which can be denoted A-A and B-B) are required. In such step-growth polymerisations the degree of polymerisation is dependent on the extent of reaction as well as the ratio of the two monomers. This is better expressed in the more general Carothers equation (Equation 7):[17]

$$X_n = \frac{1+r}{1+r-2rp}$$

Equation 7

where $r = N_A/N_B$ (N_A = moles of monomer A and N_B = moles of monomer B). The relation between the two equations is clear; Equation 6 corresponds to the case where r = 1. Crucially, a small stoichiometric imbalance between the two bifunctional monomers can lead to drastic reductions in X_n (when r is significantly less than 1). Therefore, much care is needed to ensure that accurate quantities of monomers are used and that the monomers are of high purity.

To enable the detection of analytes in aqueous solution a conjugated polymer must be rendered water-soluble which is usually achieved by introduction of ionic or highly polar functionality in the side chains of the monomers involved in the polymerisation. PPEs are usually synthesised by a Sonogashira-Hagihara palladium-catalysed cross-coupling polycondensation and as with many palladium-catalysed reactions are synthetically compatible with a wide range of functional groups.[18] The reaction was first reported in 1975 and is formally known as the Heck-Cassar-Sonogashira-Hagihara reaction,[19] but is commonly referred to as Sonogashira coupling or Sonogashira-Hagihara coupling and is the method of choice for coupling sp and sp^2-hydbridised centres.[20]

Using this method, ionic monomers can be directly polymerised in DMF-water mixtures furnishing water-soluble polymers. More recently, monomers with dendritic[21] and neutral linear polyether[22] side chains, which serve to shield the hydrophobic conjugated backbone from the local aqueous environment, have been used as water-solubilising approaches for PPEs. The side chains prevent neighbouring polymer chains from coming into close contact thereby reducing aggregation effects[23] which ordinarily lead to self-quenching and non-specific interactions.[21] However, a moderate degree of aggregation is desirable for achieving high Stern-Volmer coefficients since it allows a single quencher to communicate with multiple chains,[24] and the use of neutral side chains was therefore avoided in this work. As an alternative, post-polymerisation reactions have been used to gain water-soluble PPE derivatives, but such methods can suffer from an inability to convert the pre-polymer to the final product.[10,11]

2.1.2 Synthesis of an anionic PPE derivative

The first task involved identifying existing literature precedent for the synthesis of ionic PPE derivatives. At the time, one of the most promising studies was reported by Schanze *et al.* who detailed the short synthesis and characterisation of anionic PPE **41**.[9] Although our ultimate aims towards the fabrication of a DNA sensor would involve the synthesis of a cationic polyelectrolyte, we were keen in the first instance to pursue the synthesis of PPE **41** in order to learn more about this class of polymeric material. To this end, we opted to follow the synthetic route described by Schanze *et al.* (Scheme 2.1) which involves the three-step synthesis of the anionic monomer **115** followed by a Sonogashira-Hagihara polycondensation.

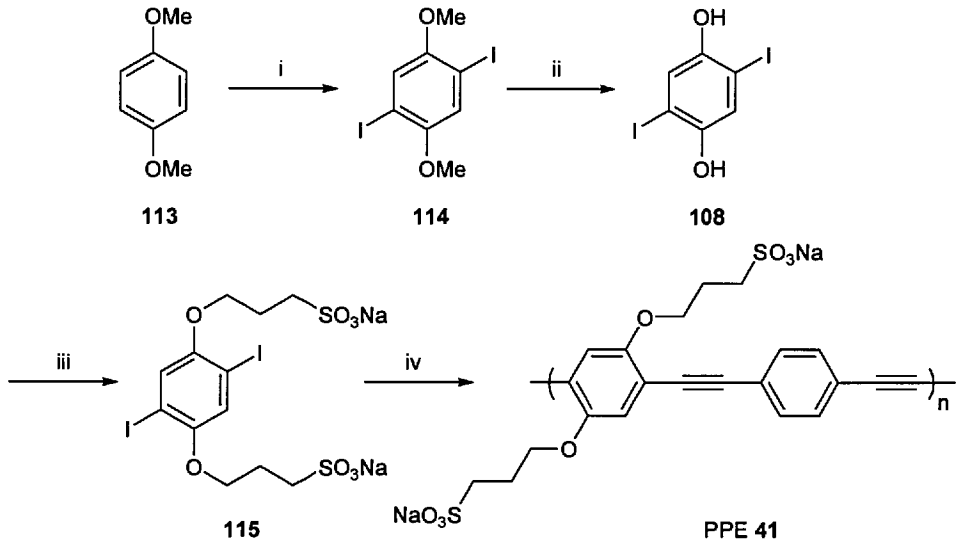

Scheme 2.1 Synthesis of PPE **141**. Conditions:* i) I_2, KIO_3, H_2SO_4, AcOH (100%), reflux, 6 h, 52% (85%); ii) BBr_3, CH_2Cl_2, 20 °C, 72 h, 77% (84%); iii) 1,3-propanesultone, NaOH, 20 °C, 50 h, 37% (70%); iv) 1,4-diethynylbenzene (**106**), $Pd(PPh_3)_4$, CuI, $^iPr_2NH$, DMF/H_2O, 50-55 °C, 18 h, 85% (69%).
*Numbers in parentheses correspond to literature yields.

The first step involves the iodination of 1,4-dimethoxybenzene (**113**) using iodine with potassium iodate in refluxing glacial acetic acid. Deprotection to reveal the hydroquinone and subsequent formation of the anionic monomer **115** are carried out under milder conditions (typically at room temperature).

The slight reduction in the yield of diiodide **114** is attributed to the repeated recrystallisation steps that were required in order to produce the product in high purity. This procedure was necessary to remove trace amounts of residual iodine (used in the iodination), which were present upon isolating the product. A modified literature procedure was used to deprotect **114** to reveal the diol (**108**).[25] We found that by increasing the reaction time (at least 70 hours was required) and by isolating the product by precipitation into water, a yield of 77% could be obtained. This optimisation resulted in a 17% increase in the yields compared to those we obtained using the unmodified literature method.[25] Similarly for **115**, by increasing the reaction time a 12% increase was realised, though the yield for this latter reaction was still lower than that reported in the literature.[25]

Many factors are important in the palladium-catalysed coupling of terminal alkynes and aromatic iodides particularly the choice of halide, substituents on the haloarene, the choice of catalyst and the purity of the monomers.[19] Aromatic iodides are known to react at room temperature and under generally mild conditions.[26] The substituents on **115** impact the rate of oxidative addition, with

electron withdrawing substituents generally being favoured. Such groups increase the rate of oxidative addition to the palladium centre (which is electron rich), though in our case this is of reduced importance as the substituents on the aromatic ring are used as solubilising groups. The amount of catalyst used is less important, though 0.1 mol% is generally considered the minimum.[19]

As has been previously described by Bunz *et al.*, the successful start of the reaction causes a steady increase in the viscosity and turbidity of the solution due to the formation of ammonium salts.[19] The generally accepted mechanism for the polymerisation is detailed in Chapter One.[19] In most examples[19] for the application of palladium catalysts to polymer synthesis, the commercially available catalyst $(Ph_3P)_2PdCl_2$ is used as it has similar activity to $Pd(PPh_3)_4$ but is air-stable.

Using $Pd(PPh_3)_4$ avoided the need to compensate for the loss of alkyne that is usually seen when the palladium source is Pd^{2+} (activation consumes some of the present alkyne).[27,28] Swager[25] confirms this observation and similarly recommends the use of excess bisalkyne in such polymerisations which together with the $Pd(PPh_3)_4$ catalyst is reported to yield high molecular weight products and reduce the possibility of butadiyne defects that reduce the molecular weight and degree of polymerisation.[29] The exclusion of oxygen from the reaction mixture is still important however and rigorously anaerobic conditions were achieved by successive vacuum-argon cycling.[30] The amount of the co-catalyst used generally matches the amount of catalyst but there are examples in the literature where there is a deliberate imbalance.[19]

PPE **41**, prepared by this Sonogashira coupling reaction, was characterised by NMR and its molecular weight was determined by GPC (running with DMAc as the eluant against polystyrene standards) which indicated M_n = 2.5 kDa (± 500 Da), with a degree of polymerisation, (DP), of 5 that corresponds to 10 phenyl rings. In the reported synthesis, Schanze *et al.* used iodine end-group analysis and ultrafiltration properties of the polymer (PPE **41**) to estimate the molecular weight (M_n ≈ 100 kDa),[9] though these measurements may have led to an overestimate of M_n as values of 100 kDa are not commonly observed for such polymerisations.[19] Alternative methods that have been used to estimate the molecular weight of similar rigid-rod polymers include pulsed-field gradient NMR (which provides the number-averaged molecular weight) and viscometry (which corresponds to the weight-averaged molecular weight).[31]

The polymer we made is therefore much shorter than many of the literature examples, but the molecular weight result provided by GPC should be considered in the context of the solubility of the polymer. At the concentration levels required to record the molecular weight by GPC, much of the polymer remained undissolved and the solution injected into the instrument represents merely the dissolved fraction. To overcome this unsatisfactory situation, attempts to improve the solubility

of the polymer were made; these included (i) gently heating the solutions, (ii) sonicating the samples for 30 minutes and (iii) leaving the solutions to dissolve over extended periods (1-3 days). Unfortunately these changes failed to improve the solubility of the polymer in the solutions used. It is possible that the polymer is of low molecular weight, perhaps owing to the catalyst used for the polymerisation being of low purity. No effort was made to investigate these issues or to optimise the reaction at this stage.

Determination of the molecular weight by GPC is problematic for PPEs due to the inherent rigidity of the polymer backbone, their anisotropic nature (PPEs displaying anisotropic absorption and emission are known)[19,32] and the difficulty of finding adequate chromatographic conditions that rule out aggregation effects. These issues invariably lead to an overestimate in the molecular weight.[19,33,34] To combat these problems, Bunz *et al.* were able to recalibrate the GPC readings by determining the molecular weights of a series of rigid-rod PPEs, by converting them to their more flexible congeners using catalytic reduction.[35] This allowed a relationship to be extrapolated from the data that indicated on average, the molecular weights of PPEs, as determined by GPC, are exaggerated by a factor of 1.42.

The molecular weight for PPE **41** can be estimated from its ^{1}H NMR data by considering the ratio of the key groups of distinct protons in the polymer in the following way: for a PPE of infinite length, one would be able assume that the ratio of the integrated areas due to the aromatic protons to that of any set of alkyl protons was 6:4. Using the ratio of the integrated aromatic signal versus the isolated aliphatic resonances, it was possible to deduce a pattern that allowed determination of the molecular weight. This is summarised by considering the trends shown in Figure 2.2.

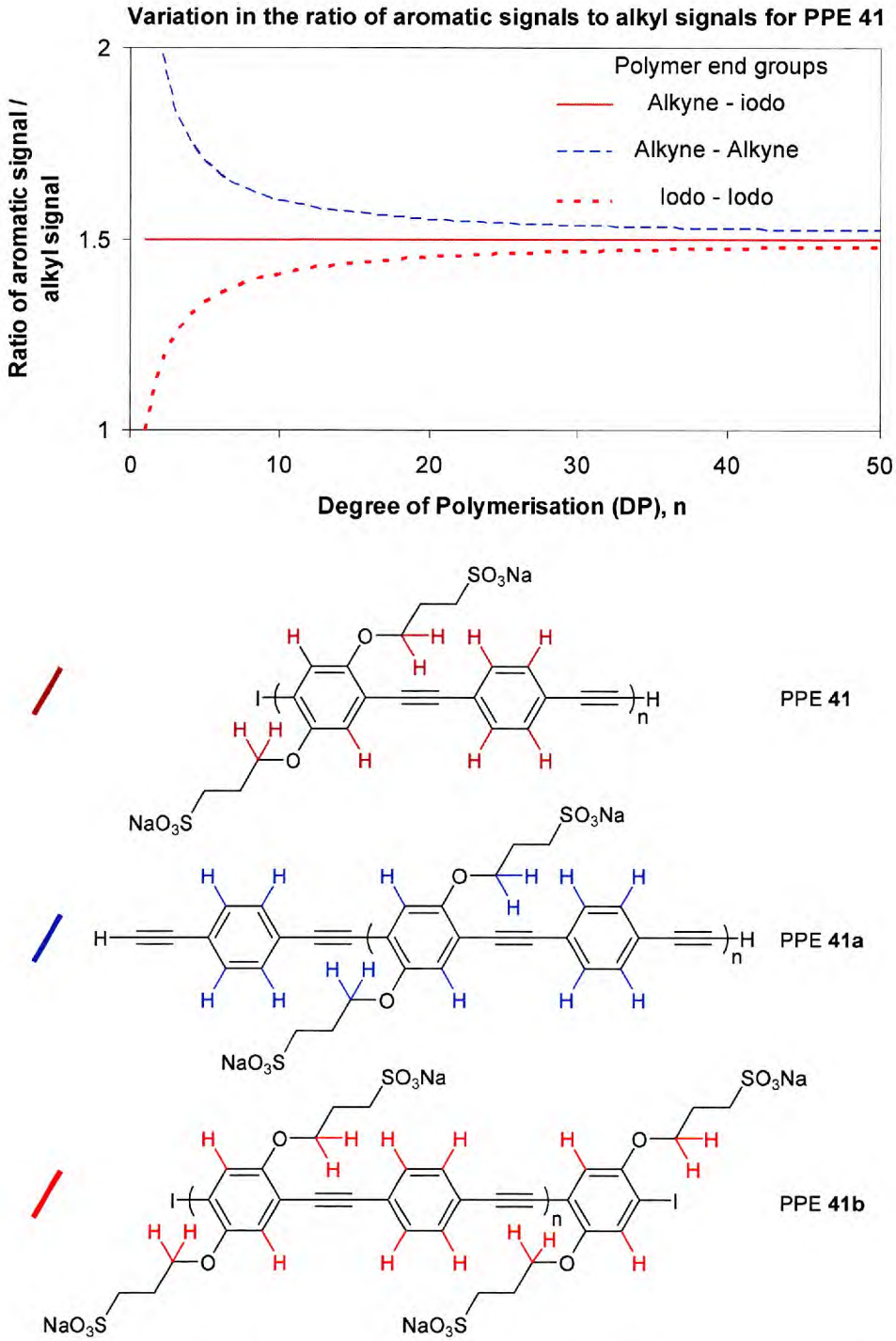

Figure 2.2 Calculation of the degree of polymerisation for PPE **41** using the ratio method.

The method is based on the observation that as the polymer grows the ratio of the aromatic protons to the specific methylene units (indicated in Figure 2.2) tends to 1.50. In Figure 2.2, it is observed that this pattern is independent of the type of end groups present on the polymeric species and therefore provides a good handle for the estimation of molecular weight by NMR. In order for this

to be true, the sample would have to be free from defects and devoid of solvent or other impurities. This enables the ratio of these two types of proton in the molecule to be calculated and in this case gives a ratio of 6:4.8.

From this, it was estimated that there were about 5 units of the aromatic ring containing the ionic side chain to every 4 containing solely the bisalkyne unit, as the area giving rise to the alkyl protons was larger than four (relative intensity). To increase the reliability of the method, the ^{1}H NMR was recorded after several precipitations and with as much solvent removed from the polymer sample as was possible.

Here, ^{1}H NMR does not provide a definite answer for the degree of polymerisation as in this example no end-capping groups were used that would have allowed an accurate determination, but the relative ratios obtained *via* ^{1}H NMR (Figure 2.3) support the GPC data insomuch that the small value for M_n was evidenced by an uneven distribution of the monomers (determined by integration) as seen by ^{1}H NMR.[36]

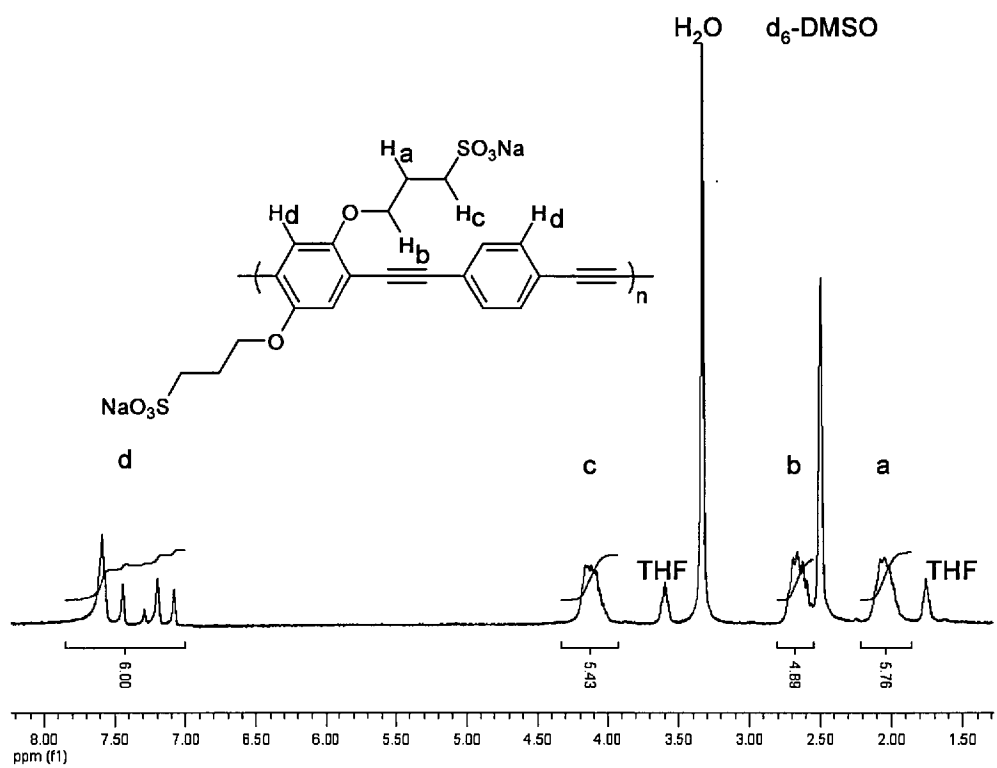

Figure 2.3 ^{1}H NMR of PPE **41** in d_6-DMSO.

The ^{1}H NMR spectrum also confirms that PPE **41** was produced in high purity, with no trace of starting materials being detected. The vigorous post-polymerisation purification procedure is one of the reasons for this, with several precipitations having been conducted, in order to eliminate the

presence of lower molecular weight species. The room temperature ^{1}H NMR for PPE **41** compares favourably with that reported by Schanze *et al.*, however at elevated temperatures (≈ 100 °C, Figure 2.4) it was expected that there would be a change in the overall resolution of the spectrum with the aromatic region (7.0 – 7.7 ppm) consisting of two resonances and the signals due to H_a and H_c resolving to multiplets with some triplet character, consistent with the findings reported by Schanze *et al.*.[9]

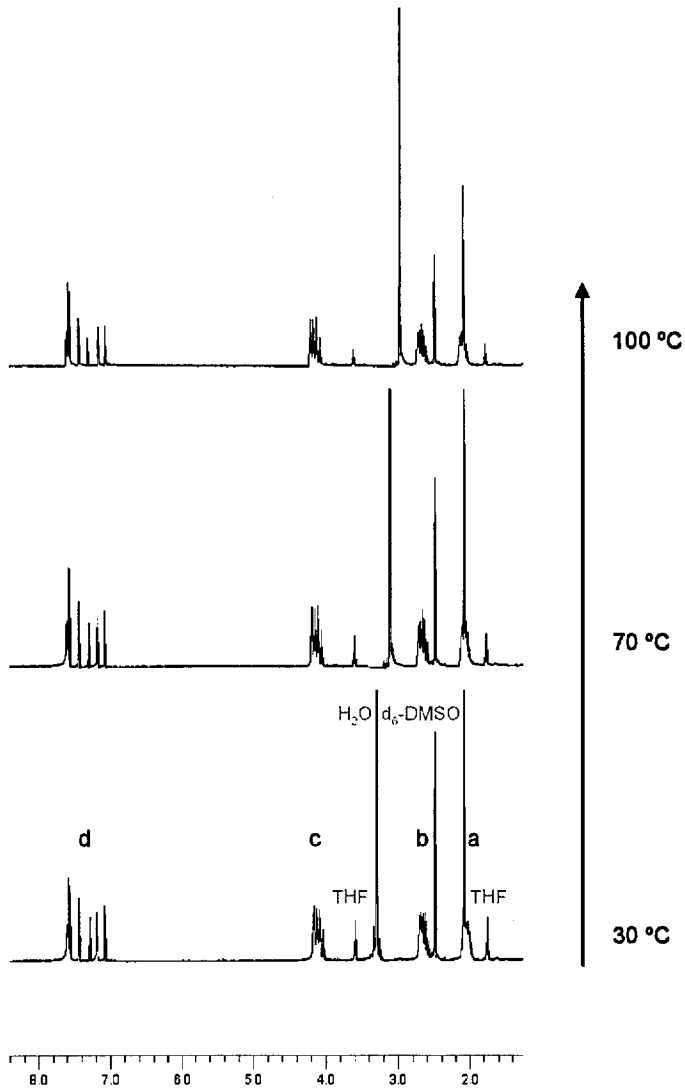

Figure 2.4 Variable temperature ^{1}H NMR (500 MHz) of PPE **41** in d_6-DMSO.

Identification of the individual signals in the aromatic region was not possible but the 'extra' resonances (at 100 °C, two resonances were expected in this region) in the observed pattern could be due to end groups. Although PPE **41** was shorter than similar polymers reported by Schanze *et al.*,[9] we were keen to measure the quenching efficiency of this material as conjugated oligomers have been previously shown to exhibit Stern-Volmer constants in excess of 10^5 M^{-1}.[37]

Characterisation by ^{1}H NMR of an oligomeric fraction of PPE **41** (named PPE **41-o**), which was isolated during dialysis of the main polymer solution, confirmed its lower molecular weight. A comparison of the ratio of the integrated values for the aromatic and alkyl regions of the spectrum, gave a value of 0.7 (suggesting that it has a molecular weight that is approximately half that of the main fraction), confirming the presence of the low molecular weight species.

2.1.3 Photophysical analysis of anionic PPE 41

To further characterise the polymer, absorption and emission spectra of PPE **41** were acquired in methanolic solutions of varying concentrations. The polymer exhibited an intense absorption band in the blue region, due to the π-π* electron transition which leads to fluorescence in the blue-green region of the spectrum. The respective absorption and emission peaks are 370 nm and 436 nm (in methanol).

Both the absorption and emission data (Table 2.1) are broadly in line with the results found by Schanze *et al.*, with slight differences being attributed to the difference in molecular weight of our sample. The absorption spectrum for PPE **41** was measured in methanol at varying polymer concentrations and only a small change was observed in the position of absorption maxima (λ_{max} = 370 – 374 nm). The lower molecular weight material would be expected to have a much larger HOMO-LUMO gap (as this is dependent on the chain-length) and as a result this change would be expected to manifest itself as a shift to shorter wavelengths for the absorption maximum. In general, both the polymer and oligomers feature a strong absorption band in the blue region which is attributed to a long-axis polarised π-π* transition.[38]

The fluorescence spectra showed no pronounced changes upon variation of the polymer concentration and contain a 61-72 nm Stokes shift from the absorption bands which were blue-shifted. Again, this was attributed to the length of the chains produced. The slight changes in the fluorescence maxima are due to the varying length polymer chains and the inherent polydispersity associated with such samples. Our findings and those published by Schanze *et al.* are summarised and compared in Table 2.1.

Table 2.1 Absorption and emission data for PPE **41** (excitation wavelength = 373 nm).

[PPE **41**] / μM	**Solvent**	λ_{max}^{1} **(absorption) / nm**	λ_{max}^{2} **(emission) / nm**
1.9	MeOH	370	436
10	MeOH	374	435
100	MeOH	374	439
1000	MeOH	-	442

[1]Reported: λ_{max}(absorption) = 425 nm. [2]Reported: λ_{max}(emission) = 447 nm

The fluorescence spectra confirm that the polymer exists in a relatively non-aggregated state (i.e. monomeric, with reduced π-π stacking) in methanolic solutions, as the bands are relatively sharp and structured and the fluorescence relatively short-lived (details on lifetimes in provided in section 2.1.4). Broad and featureless emission bands are generally indicative of emission emanating from an aggregated state, where there is an increased incidence of emission from interchain species derived from π-π stacking. This type of emission is typically seen in small molecule photochemistry when excimers are formed in solution (e.g. in the luminescence from pyrene excimers).[39] Some recent reports have indicated that excimer emission can also be generated in PPE conjugated polymers where there are intermolecular interactions mediated through rigid bicyclic [2.2.2] structures.[40]

2.1.4 Measurements of fluorescence quantum yields and lifetimes for PPE 41

To fully analyse PPE **41**, further characterisation was gathered in the form of fluorescence lifetimes and quantum yields. The measurement of quantum efficiencies for polymer solutions can be conducted *via* two different methods; the first involves the use of an integrating sphere as described by de Mello *et al.*[41] The second method involves the use of a reference solution of a dilute laser dye with a known quantum yield (ϕ). This is a standard technique for acquiring quantum efficiency data and is sufficiently accurate for most preliminary studies. The laser dye quinine bisulphate (**116**) was selected ($\phi = 0.55$)[42] as it has comparable absorption and emission wavelengths with the PPE polymers and was suitable for the dilute solutions (μM concentration) that were used.[42]

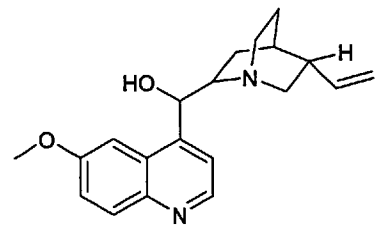

116

Figure 2.5 Quinine bisulphate (ϕ_f = 0.546 in 1N H_2SO_4)[43] was used for all quantum yield measurements as it has similar absorption and emission characteristics to the polymer samples analysed.

With the standard reference in hand, the absorption and emission spectrum of the polymer sample was recorded along with the same measurements for the reference material. Using Equation 8, (where A is the absorbance at the excitation wavelength, F the integrated emission area and ϕ the quantum yield) and after application of corrections for the refractive indices (n) for the polymer (u, unknown) and the laser dye (s, standard) solutions, values for the unknown polymer solution were calculated. Such corrections are necessary for two principle reasons;[43] firstly, as the monochromatic excitation radiation passes from the solution into the air the refraction induces intensity changes. Secondly, internal reflection within a cell can occur that can lead to significant errors for different solvents.[43]

$$\phi_u = \phi_s \left(\frac{A_s F_u n^2}{A_u F_s n_0^2} \right)$$

Equation 8

The radiative lifetimes were measured using two polymer solutions at two different concentrations. This allowed us to determine the optimal concentration at which to acquire measurements in order to minimise the extent of self-absorption, though with PPEs, some self-absorption was always inevitable as the absorption maximum was at a longer wavelength than the excitation source we used.

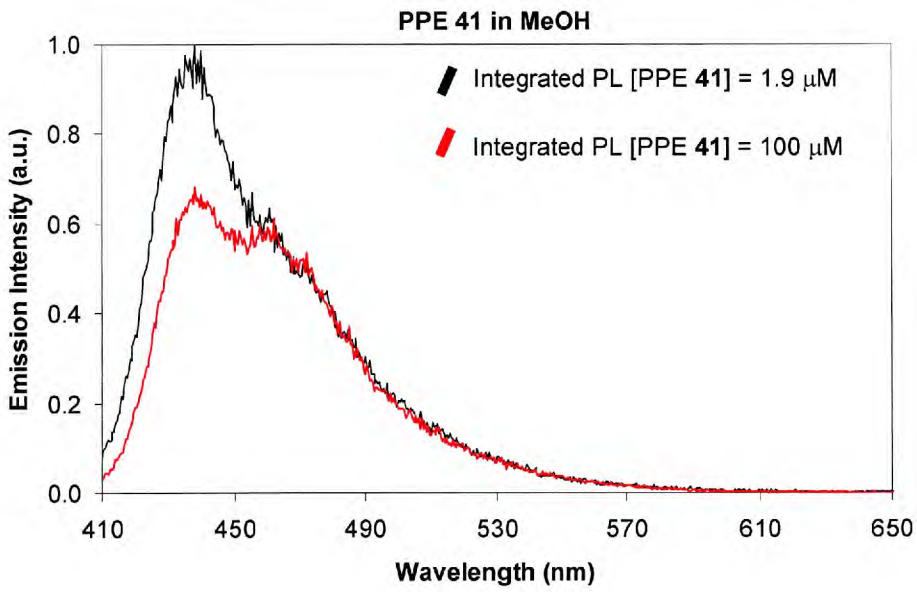

Figure 2.6 Comparison of time-integrated PL spectra for PPE **41** at different concentrations (excitation wavelength = 373 nm).

By considering the plots of the time-integrated PL spectra (Figure 2.6), it was clear that the lifetime measurement recorded using the more dilute polymer solution is more accurate, since substantially less self-absorption occurs at short wavelengths.[44] This effect is negated using a dilute polymer solution which surprisingly also had the added benefit of a marginally higher overall intensity (Figure 2.6). The PL decay intensity as a function of time was recorded and for PPE **41**, the mono-exponential decay was fitted to an exponential plot (Equation 9), where y_0 (background emission intensity) and A_0 were constants.

$$y = y_0 + A_0 \exp\left(\frac{t}{\tau_0}\right)$$

Equation 9

Further analysis of the material was conducted in non-degassed conditions. It was of interest to observe whether the good emission properties of PPE **41** would be maintained in the challenging environments that real biosensors operate in.

The information derived from the studies of the fluorescence quantum yields and lifetimes (summarised in Table 2.2) show that PPE **41** features a reasonably high ϕ_f value of 28% and a mono-exponential lifetime of 580 ps in methanol. These properties differ slightly with those

reported by Schanze *et al.* (ϕ_f = 78% and τ_{em} = 420 ps, in methanol) and the differences could be due to a number of reasons associated with the way the sample was measured (we used non-degassed conditions as this is more comparable to real environments), post-polymerisation treatment of the polymer sample and general degradation (attack by molecular oxygen),[44] all of which would serve to reduce the quantum yield. Due to the non-degassed environment in which the measurements were recorded, extrinsic effects cannot be ruled out as a source of error. As was reported recently, a possible explanation for the reduced fluorescence quantum yield may stem from an extent of excited state quenching arising from mild interchain interactions that split the highly delocalised singlet exciton.[11]

Table 2.2 Photophysical properties for polymeric PPE **41** in MeOH.[a]

[PPE **41**]	**Absorption** λ_{max} / **nm**	**Emission** λ_{max} / **nm**	τ_{em} / **ps at 409 nm**[b]	ϕ_f / %[c]
1.9 μM	372	435	580	28
100 μM	374	439	590	d

[a]All work was conducted in an aerobic environment in MeOH. [b]Results from lifetime measurements were fitted using a monoexponential; error ± 10 ps. [c]Fluorescence quantum yields measured relative to quinine bisulphate in 1N H_2SO_4 (ϕ_f = 0.546); error ± 3%. [d]Sample concentration too high to allow accurate quantum yield determination. Excitation wavelength = 373 nm.

PPE **41** exhibited mono-exponential, wavelength-dependent emission decays (Figure 2.7). Of particular interest, is the observation that the PL lifetime increases as a function of the excitation wavelength, which is characteristic for these polymers.[9] The increase can be ascribed to the diffusion of energy to long wavelength (lower energy) sites on the polymer chain resulting in an increase in the time delay for the emission to reach the detector, from the low energy sites. An additional reason for the wavelength-dependent nature of the emission lifetimes is provided by Schanze *et al.*.[9] They reported that the fluorescence decay in water, which was found to be strongly wavelength-dependent, could be attributed to the emission from an excimer-like aggregated state.[9]

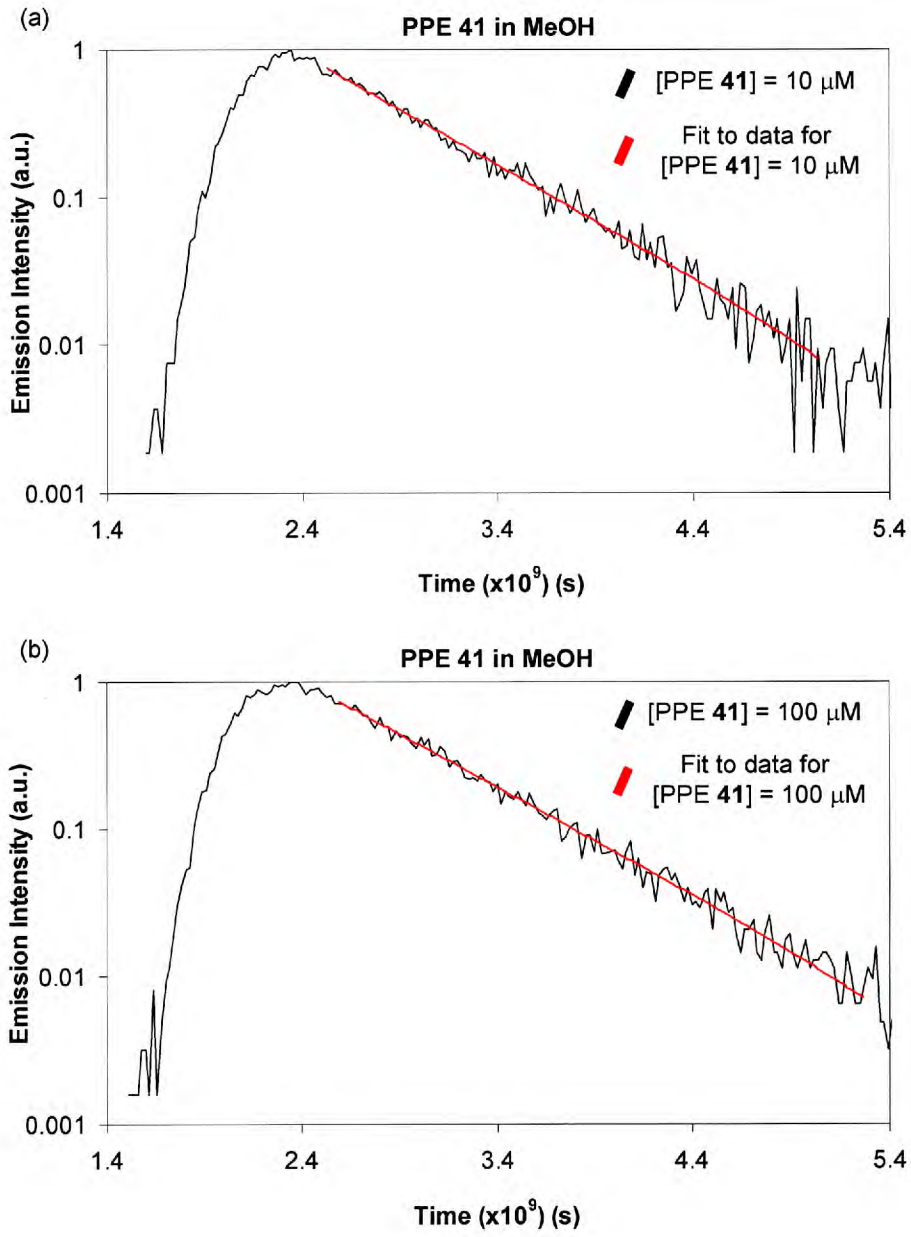

Figure 2.7 The decaying intensity of emission signals from solutions of PPE **41** at 298 K in MeOH. The fitting curves used to determine the lifetimes are shown as thick solid lines. (a) [PPE **41**] = 10 μM, τ_{em} = 580 ps, (b) [PPE **41**] = 100 μM, τ_{em} = 590 ps. Excitation wavelength = 373 nm, Emission wavelength = 430 nm.

The estimated values for the lifetime as outlined in Table 2.2 are comparable, given the lower molecular weight of our sample, with those reported by Schanze *et al.* (420 ps). These observations are only true at short wavelengths (up to ~ 500 nm). At longer wavelengths, large errors are associated with the lifetimes. This also reflects the increasing difficulty in finding an accurate fit to the data, though this is not an issue for the measurements displayed in Table 2.2 as the PL

wavelengths selected were in the region where the lifetime measurements were approximately constant (i.e. measurements conducted at excitation wavelengths < 500 nm).

2.1.5 Spectroscopic investigation of fluorescence quenching for PPE 41

In this section the emission quenching experiments involving PPE **41** and the quencher Methyl Viologen (1,1'-dimethyl-4,4'-bipyridinium dichloride, paraquat dichloride, $\mathbf{MV^{2+}}$) are reviewed and the results compared with those reported for PPE **41** by Schanze *et al.*. This information allows us to gauge the sensitivity of the materials towards quencher molecules through measurement of the Stern-Volmer constant.

Amongst other things, the differences in the quantity of the quencher required to effect quenching can be attributed to the shorter chain length of the polymer produced as compared with the PPE reported in the literature (analysed in non-degassed conditions). This reduction in chain length would lead to a substantially reduced exciton diffusion range and as a result the opportunity for the exciton to encounter many trap (quencher) sites would be reduced, which would impact on the amount of quencher required to reduce the emission.[45] In addition, the non-degassed nature of the solution would lead to a lower PL intensity in the absence of the quencher.

The efficiency of the quenching process, as measured by the Stern-Volmer constant, gave a value of 2.2×10^7 M^{-1}, in good agreement with that observed in the literature. Indeed the Stern-Volmer constant that we measured was 14-times greater than that reported (Table 2.3) despite the limited conjugation length of our polymer. Though the accuracy of these measurements is further improved in a protocol described later (Chapter Three, section 3.6) these initial results are promising and suggest that very long polymers may not be critical in the biosensor design. However, these results do confirm the importance of the conjugation length as the efficiency of quenching is seen to be extremely sensitive to the effective conjugation length. This is consistent with previous reports that have proposed that the high sensitivity associated with such materials is linked to, amongst other things, the facile and efficient delocalisation of the singlet exciton within the polymer backbone.[46] That our material exhibited higher sensitivity as compared with the literature report indicates that one of two factors may be important in influencing the results. Either, the molecular weight of the polymer prepared by Schanze *et al.*[9] was grossly overestimated (which is a realistic possibility as molecular weights in the region of 100 kDa are rare for such polymerisations)[19] or that the shorter polymer chains produced during this study are better at forming aggregates that allow efficient migration of photoexcitations between neighbouring chains.

Table 2.3 Summary of reported and measured data for the quenching of emission from PPE **41** by MV^{2+}.

	Solvent	[PPE **41**] / μM	k_{SV} / M^{-1}	M_n / kDa
Reported[9]	MeOH	10	1.6×10^6	100
Measured	MeOH	10	2.2×10^7	≈ 2.5

The impact of the quencher on the conformation of the polymer chain could also be critical and it has been previously noted that quenchers with multiple charges may trigger aggregation due to ion-paring, as revealed by changes in the emission spectra.[9,13] Such effects may be beneficial for sensing.

As described in Chapter One (section 1.3), there are two mechanisms for emission quenching; static quenching involves the formation of a complex (pre-association) between the fluorophore and quencher that is immediately returned to the ground state upon excitation. In dynamic quenching, collisional interactions between the fluorophore and the quencher are important.[44] The very low quencher and polymer concentration ranges that were used in these studies are known to produce Stern-Volmer plots that are linear but it has been previously demonstrated that at higher quencher concentrations upwards curvature in such plots are observed.[7] This deviation from linearity is indicative of multiple quenching mechanisms and has previously been investigated by Wang *et al.*.[13,47] In their work they considered the emission quenching of an anionic PPV (**117**, Figure 2.8) derivative by a series of viologen derivatives (where the mechanism for quenching is expected to be electron transfer from the polymer to the quencher).

(a)

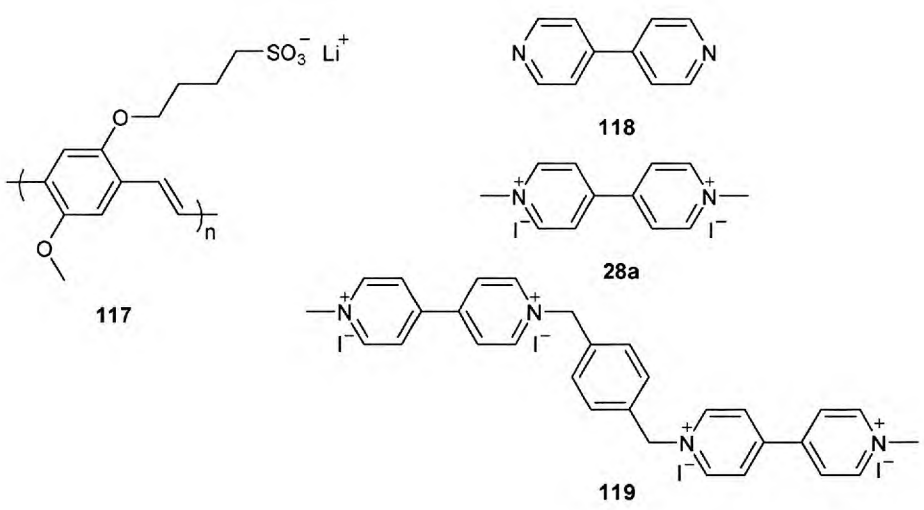

(b)

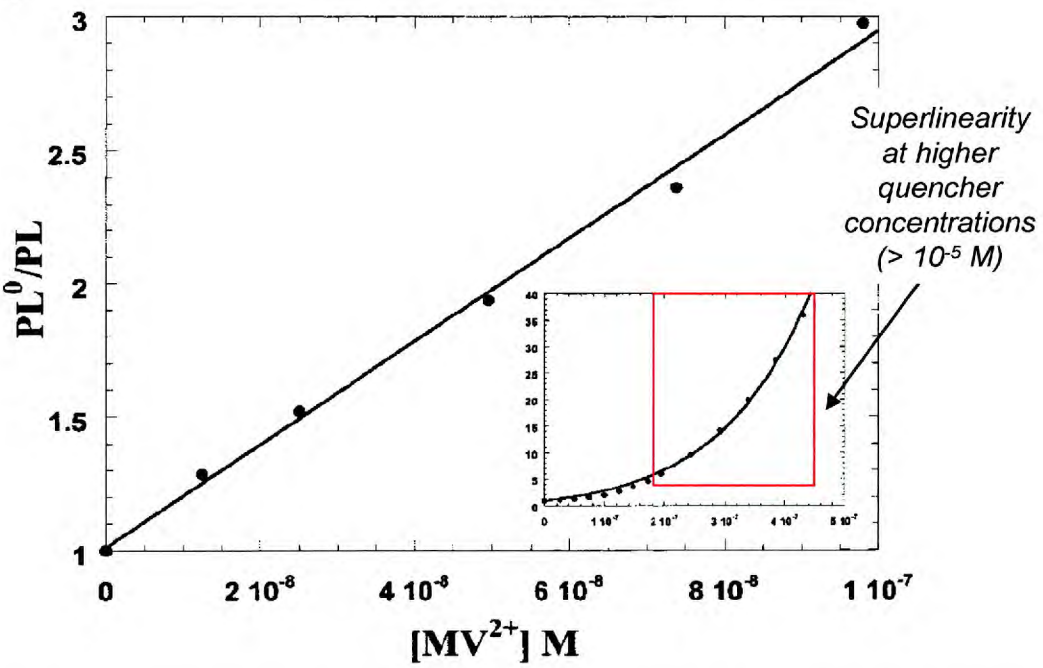

Figure 2.8 Superlinearity and the Stern-Volmer equation; (a) the anionic PPV and some representative quenchers used in the study by Wang *et al.*,[13,47] and (b) (reproduced from Wang *et al.*)[47] the Stern-Volmer plot obtained for the quenching of **117** by **28**. The inset describes the superlinear region where quenching occurs *via* a sphere-of-action mechanism.

They called the deviation from linearity at high quencher concentrations 'superlinearity' and attributed it to a sphere-of-action model, an idea first proposed by Frank and Vavilov.[47,48] This model assumes that at high quencher concentrations (~ 10^{-5} M in the example described by Wang *et al.*)[47] the mean distance between the quencher molecules is such that on average the CP is always within close proximity to the quencher, which allows efficient charge transfer to occur. To

describe the combination of these quenching mechanisms Wang *et al.*[47] defined a modified Stern-Volmer relation (Equation 10).

$$\frac{I^0}{I} = (1 + k_{SV}^S[Q])e^{\alpha V[Q]}$$

Equation 10

Where I^0 and I are the intensity of the emission in the absence and presence of the quencher respectively, k_{SV}^S is the association constant for the complex formation, V is the volume constant and α describes the enhancement of the local quencher concentration, due to the charge associated with the quencher. The importance of α is illustrated by noting that its value is larger for quencher **28** than **118**. This modified equation allowed them to estimate the radius of the sphere-of-action (~ 40 nm) for the polyelectrolyte studied, with the value comparing favourably with the average separation of the quencher molecules (~ 80 nm), thereby confirming the proximity of the macromolecule to the quencher.[13,47]

In our experiments, the Stern-Volmer plots were obtained by fitting the data to a non-linear equation as linearisation of the data, as is typically used in the literature, yields biased estimates of the Stern-Volmer constant (Equation 5).[49] A full treatment of the method used to determine all Stern-Volmer coefficients reported in this dissertation is detailed in Chapter Seven.

The oligomeric version of PPE **41** (named PPE **41-o**) was also analysed (in water) and the Stern-Volmer constant found to be over 4.3-times smaller than that observed of the polymeric version PPE **41** (determined in methanol). This result is consistent with the arguments put forward emphasising the importance of conjugation length to the sensitivity of the polymer. At the time of conducting these early studies, our focus was on increasing the conjugation lengths of the PPE materials as we believed that this was the most important factor in obtaining high k_{SV} values. However, our understanding of these materials has since improved and the size of the Stern-Volmer constant measured for PPE **41-o** provides evidence that aggregation is more important than chain length (described further in Chapter Three). The different solvents used to conduct the measurements (because of practical limitations) could have affected the magnitude of the difference between the values, as the conformational order of the conjugated materials is dependent on the solvent used (aggregation, i.e. π-π stacking, is more significant in water than methanol).[9]

Schanze noted that there was a change in the Stern-Volmer constant upon switching from methanol to water.[9] This increase (3.6-fold) has been attributed to the possibility that there is exciton

migration occurring in the aggregates of the polymer (PPE **41** is fully aggregated in water) which further amplify the quenching response. Recently, Kleiman and Schanze have investigated the role of exciton 'hopping' in quenching the emission from CPEs.[50] They used simulations to calculate the density of complexes formed between a CPE and quencher molecule. From this they suggested that only in 'dense' aggregates (formed in polar solutions) would a suitable environment persist to enable the rapid migration of excitations. Here, 'dense' refers to the size of the interchain distance, which should be short to allow π-π stacking to occur. These effects are given more consideration in Chapter Three (section 3.6).

2.2 Synthesis of a novel cationic PPE derivative (PPE 124)

The syntheses of a variety of conjugated cationic polyelectrolytes are documented in the literature, as described in the introduction. Swager *et al.* reported the synthesis of PPE **120** in 2000 and examples of cationic polymers based on other polymeric backbones, like PPPs and poly(thiophene)s are also known, with such materials often pursued as potential DNA sensors.[51] Interestingly, most of the cationic polyelectrolytes synthesised to date contain a trialkylammonium group as the ionic moiety, presumably due to the ease of which it can be incorporated into the structure.

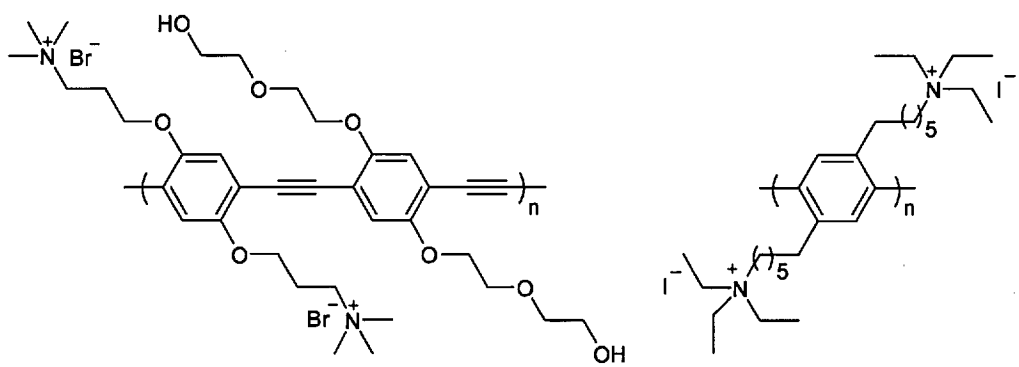

PPE **120** **121**

Figure 2.9 Examples of previously synthesised cationic polyelectrolytes, by McQuade *et al.* (PPE **120**)[52] and Brodowski *et al.* (**121**).[53]

Our interest in cationic polyelectrolytes led us to pursue the synthesis of the novel cationic PPE **124**. We reasoned that this polymer would have all of the characteristics associated with similar water-soluble PPEs (e.g. high Stern-Volmer coefficients coupled with respectable quantum yields) and allow us to use it for the detection of oppositely charged oligonucleotides. Additionally, only one of the monomers required appreciable functionalisation and simple disconnections (see Figure 2.1) led back to readily available starting materials. We also envisioned that the presence of two

side chains per repeat unit would provide the necessary polarity to enable good solubility in polar solvents (most importantly water) whilst allowing the unhindered approach of quenchers to the conjugated backbone. It was our intention to modify the literature procedure described by Swager *et al.* for the synthesis of the polymer (Scheme 2.2).[25] Literature precedents were available up to the synthesis of the dicationic monomer **123** though the actual polymerisation was hitherto unknown.

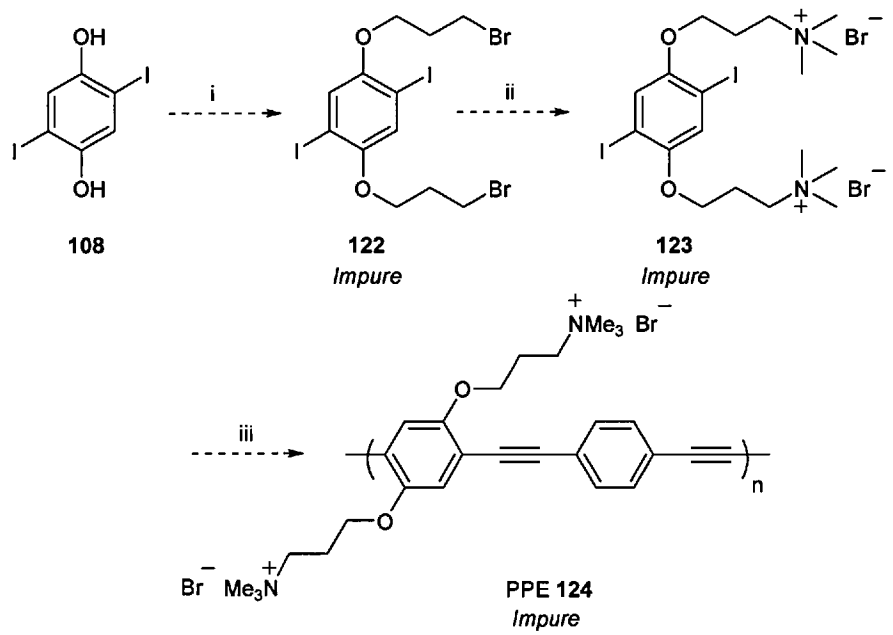

Scheme 2.2 Synthesis of PPE **124**. Conditions: i) 1,3-Dibromopropane, K_2CO_3, acetone, 70 °C, 24 h, 69%; ii) 45% NMe_3 in H_2O, EtOH, acetone, reflux, 18 h, 79%; iii) $Pd(PPh_3)_4$, CuI, DMF, $^iPr_2NH$, H_2O, 50 – 55 °C, 48 h, 45%.

A key intermediate in this strategy involved the synthesis of **122**, which we envisaged to be a synthetically flexible moiety, as nucleophilic displacement of bromine on the side chains would allow a wide array of different functional groups to be attached to the monomer.

Repetition of the etherification conditions reported by Swager *et al.* gave the required dibromo-intermediate in 60% yield though upon closer inspection of the ^1H NMR spectrum small signals (~ 1% of the total intensity) were detected at ≈ 4.1 ppm (triplet) and ≈ 7.2 ppm (singlet). Attempted purification of the main product by several recrystallisations resulted in no improvement in the purity of **122**, with the impurity remaining unidentified. Effective purification by column chromatography was not possible as suitable solvent conditions could not be identified. Various other changes (detailed in Table 2.4) were made to the reaction conditions in order to eradicate the contaminant present in **122**, all to no avail.

Table 2.4 Techniques employed to purify monomers **122** and **123.**

Entry	Monomer	Purification method[a]	Conditions	Impurities[b]	Comments
1	**122**	R – $CHCl_3$/ EtOH	Reflux, acetone 48 h	7.19 (s) 4.19 (t) 3.54 (t)	Starting material was recrystallised
2	**122**	C (CH_2Cl_2), (Un-sublimed material)	Reflux, acetone 96 h	7.22 (s) 4.19 (t) 3.80 (t)	Addition of starting material was carried out drop-wise over 96 hours 2 Spots by TLC
3	**122**	C (CH_2Cl_2) + S	Reflux, acetone 96 h	3.80 (t) 7.17 (s)	Addition of starting materials was carried out over 4 days 2 Spots by TLC
4	**122**	R – $CHCl_3$/EtOH	Reflux, acetone 24 h	7.22 (s) 4.19 (t) alkene	Reaction worked-up using literature precedent.
5	**122**	R - MeCN	Reflux, acetone 48 h	7.22 (s) 4.19 (t) 3.80 (t)	-
6	**122**	R – $CHCl_3$/EtOH	Reflux, acetone 24 h	Several	Iodination carried out in second step (Scheme 2.4); decomposition likely.
7	**123**	R – EtOH/Et_2O	Reflux, 130 °C, 18 h	7.32 (s) 4.12 (t)	2 Spots by TLC, R_f = 0.8 + 0.1 (product); MS inconclusive.
8	**123**	-	Reflux, 125 °C, 6 h	Several	Iodination carried out in second step (Scheme 2.4); decomposition likely.

[a]Purification abbreviations; R – recrystalisation, C – column, S – sublimation. [b]Impurity as observed by ^{1}H NMR, s – singlet, t – triplet.

In the literature procedure followed, a syringe pump was used for the slow addition of **108** (dissolved in acetone) to a mixture of 1,3-dibromopropane and potassium hydroxide (also dissolved in acetone). The addition has to be performed slowly in order to avoid unwanted

dimerisation of **108**. As we did not have a syringe pump available to use at the time, we manually added 2,5-diiodo-1,4-hydroquinone (**108**) to the reaction mixture over a period of 4 days. Alternative methods to furnish similar dibromo- intermediates were sought but in the best example a similar yield (69%) for **122** was obtained (*via* Route 1, Scheme 2.4), with the impurity still present.

At this stage, attempts were made to identify the unknown product that was generated together with **122**. The ^{1}H NMR signals due to the impurity differed to those of monomer **122** by ~ 0.1 ppm, which suggests a close similarity in structure. It is known that E2 elimination can occur to give the terminal alkene **125**, which can then undergo rearrangement as shown in Scheme 2.3.[54]

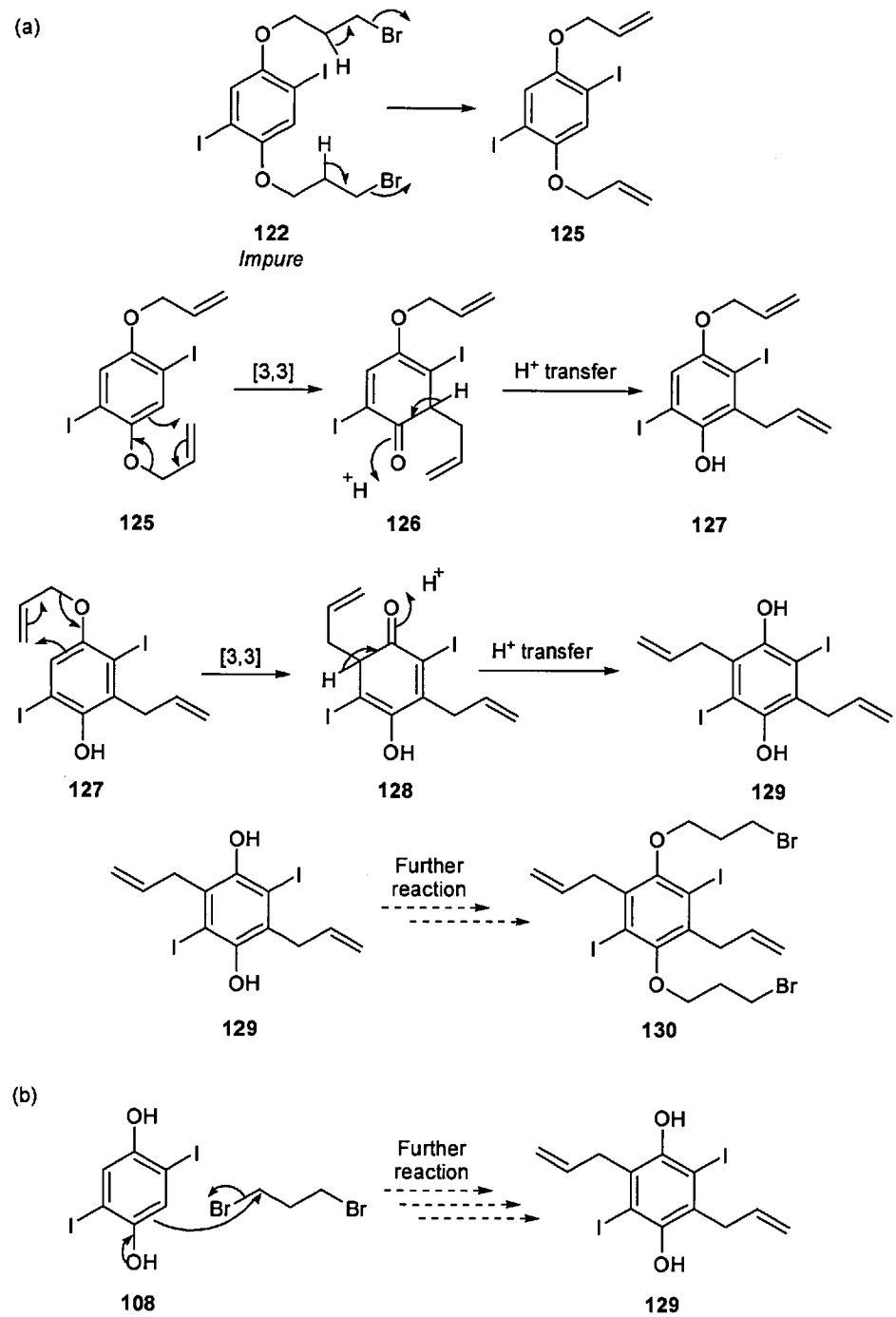

Scheme 2.3 (a) A possible Claisen rearrangement leading to the contaminant(s) isolated with monomer **122** and (b) formation of **129** by direction reaction of **108** with 1,3-dibromopropane.

The method used to form monomer **122** involves prolonged heating and under these conditions it is possible that sequential [3,3]-sigmatropic rearrangements could occur (Scheme 2.3), followed by proton transfers, to yield **129**.[54] Further reaction of monomer **129** with 1,3-dibromopropane would lead to monomer **130** that could give rise to the observed ^{1}H NMR signals, detailed in Table 2.4,

which were attributed to the impurity. Due to time constraints, these issues were not further investigated.

Despite the problems described above, the synthesis of monomer **123** was attempted with the intention of separating the impurity from the new product (Scheme 2.2). Unfortunately similar problems were encountered (see entries 7 and 8 in Table 2.4), with purification perhaps hindered by the polarity of the monomer, though the amount of the unidentified impurity in the sample was approximately the same (about 15% of the sample, as determined by ^{1}H NMR). After obtaining the monomer, as cleanly as was possible, it was employed in the polymerisation without further modification. In an attempt to overcome the difficulties associated with isolating **122** pure, the alternative route of subjecting the alkylated materials **132** and **134** to iodination were also attempted (Scheme 2.4).

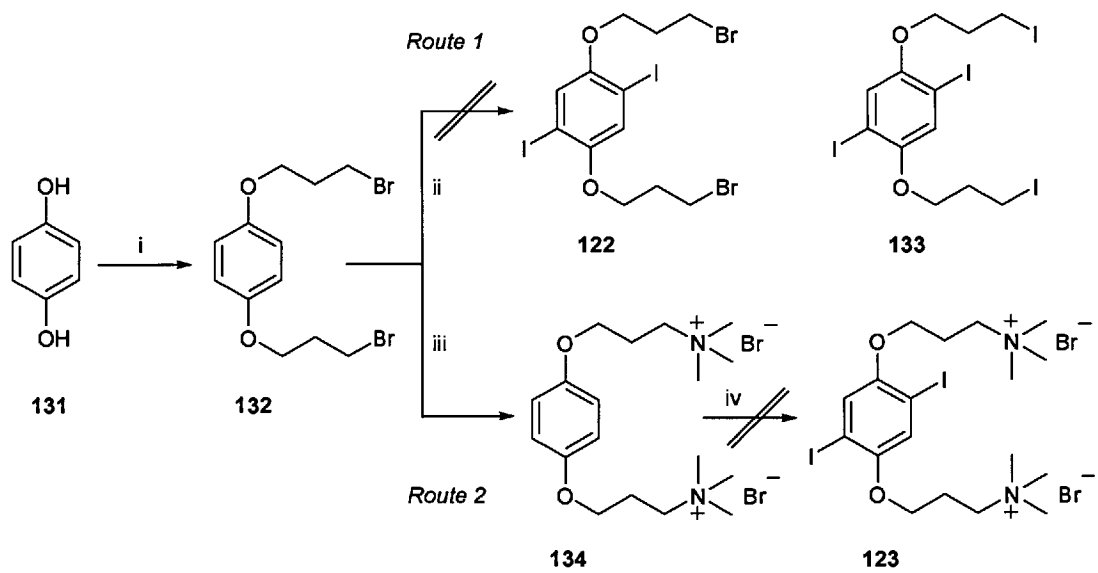

Scheme 2.4 Attempted synthetic routes to **122** and **123**. Conditions: i) 1,3-Dibromopropane, K_2CO_3, acetone, 70 °C, 24 h, 21%; ii) I_2, KIO_3, H_2SO_4, AcOH (100%), 6 h; iii) 45% NMe_3 in H_2O, EtOH, acetone, 18 h, 76%; iv) I_2, KIO_3, H_2SO_4, AcOH (100%), 6 h.

However this led to suspected decomposition of the starting materials. There was also an attempt to form the tetraiodinated monomer **133** using 1,3-diiodopropane, as it was believed that the singlet that appeared at ~ 7.2 ppm may be due to halogen exchange between the bromine and iodine atoms on the aromatic ring. Unfortunately, this reaction also produced a similar irremovable impurity. However, this theory is not supported by the chemical shift due to the other impurity signal (that appeared at 4.1 ppm) as exchange of the bromine atom for an iodine atom would cause an upfield shift.

The synthesis of the second monomer, bisalkyne **106**, was less problematic, though finding a high yielding route was troublesome. At first we attempted to convert dialdehyde **111** to the bisalkyne using a phosphonium bromide intermediate (**136**), as both starting materials are cheap and readily available (Scheme 2.5). However the hygroscopic nature of salts like **136** made their isolation difficult.[55,56] Indeed, we were unable to isolate any of the carbon tetrabromide complex **136** cleanly. As has been noted by Wang *et al.*, these materials are of limited use, due to their toxicity and exothermicity.[55] Therefore, we resorted to a method described by Aggarwal *et al.*[57] that avoids the use of phosphorus reagents/intermediates. Aggarwal *et al.* demonstrated that the base-promoted addition of chloroform to aldehydes, to yield trihalocarbinols, could be coupled with tosylation to yield intermediates like **137** that would provide access to acetylenes.[57]

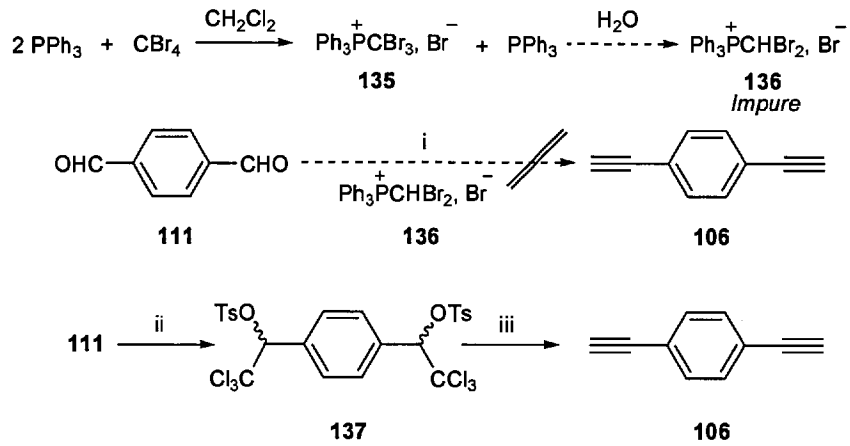

Scheme 2.5 Attempted synthesis of bisalkyne **106**. Conditions: i) **136**, *t*-BuOK, THF, 30 mins; ii) 1. DBU/$CHCl_3$; 2. TsCl / NEt_3, $CHCl_3$, 15 h, 45%; iii) MeLi, THF, -10 °C → 0 °C, 1 h, 5%.

In our hands the formation of the intermediate **137** proceeded in reasonable yield, however the deprotection and subsequent purification gave the bisalkyne in high purity (as determined by ^1H NMR), but in only 5% yield, for reasons that were not investigated. Due to the low yield of the conversion of **137** to **106**, this two-step route to acetylenes, starting from the aldehyde, though conducted under mild conditions, was not suitable for scale-up and so another procedure was sought. The proliferation of synthetic routes to a variety of PPEs for 'molecular-wire' uses has demanded efficient ways to make functionalised terminal alkynes on a multi-gram scale. Commonly, methods like the Corey-Fuchs,[58] Wittig/Horner-Emmons[59] and Gilbert-Seyferth,[60] which provide useful ways to convert aldehydes to acetylenes, involve the use of phosphorus reagents, with their associated drawbacks (*vide supra*). Recently, the method of choice for effecting this transformation involves the use of palladium cross-coupling chemistry, which is ultimately more reliable.[61]

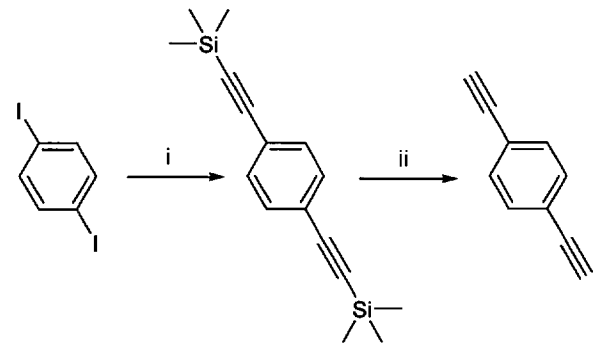

Scheme 2.6 Synthesis of bisalkyne **106**. Conditions: i) TMSA, $Pd(PPh_3)_4$, CuI, $^iPr_2NH$, toluene, 50 °C, 1.5 h, 73%; ii) K_2CO_3, MeOH, CH_2Cl_2, 20 °C, 3.5 h, 96%.

Reaction of 1,4-diiodobenzene (**109**) with trimethylsilylacetylene (TMSA, **110**) to give silyl-protected alkyne **138** occurred in good yield (71%) and the successful deprotection using potassium carbonate in methanol gave bisalkyne **106** (96%) as shown in Scheme 2.6.

The chemistry is also amenable to adaptation – the catalytic reaction allows for the presence of a variety of polar functional groups (*vide supra*) – which is important as it allows further functionalisation of the aromatic ring. Decorating monomers with such additional moieties could, for example, give the final polymer material improved sensing functions or increased solubility. The only drawback for this reaction is the quantity of the palladium catalyst required (typically 10 - 15 mol%).[62]

The ^1H NMR spectrum for PPE **124** is shown in Figure 2.10. Unlike PPE **41** the aromatic region (~ 7.1 – 7.6 ppm) consists of predominately two main resonances (due to the two different types of such protons in each repeating unit), which is consistent with that reported for structurally similar CPEs.[9] This increased symmetry in this part of the spectrum and the inability to distinguish aromatic signals due to the end-groups, suggests that the material is of higher molecular weight than PPE **41** (further evidence is provided by the emission spectrum; section 2.2.1).[11]

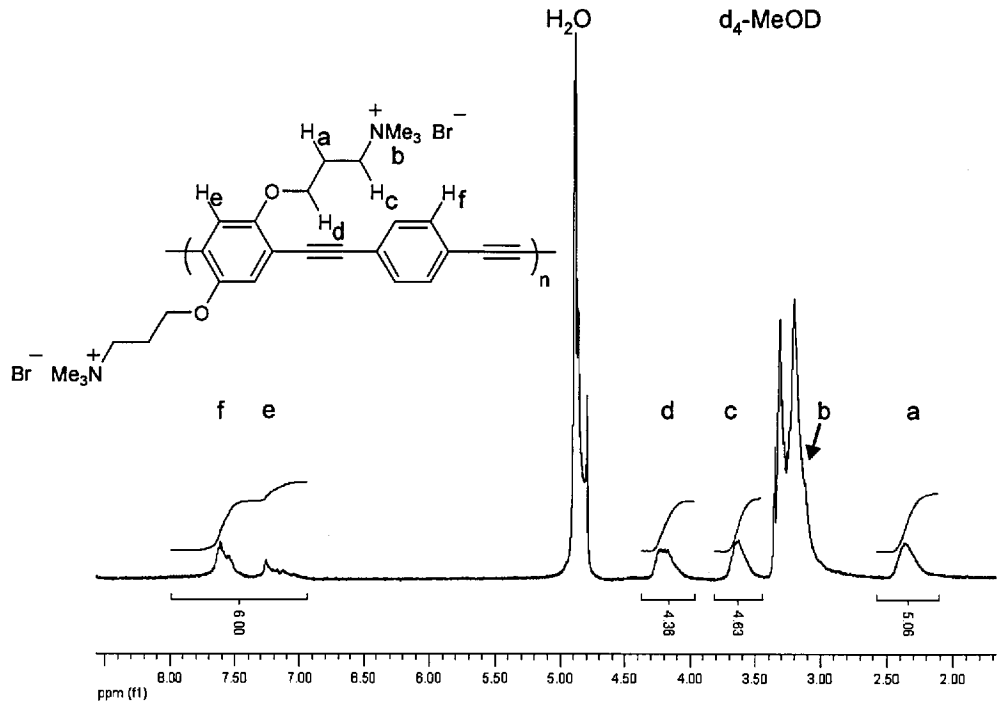

Figure 2.10 ^{1}H NMR spectrum of PPE **124** in d_4-MeOD.

From the ^{1}H NMR spectrum the relative ratio of the protons of the aromatic region and those of the due to the alkyl chains was measured and compared to PPE **41**. Using the trends noted in Figure 2.2, a ratio of 6:4.38 (= 1.37) indicates that PPE **124** is of increased molecular weight as the value is closer to the idealised case where an infinitely long polymer chain would yield a ratio of 1.5.

The spectrum is consistent with the expected structure of the polymer as there is a good correlation between the positions of the aromatic and alkyl resonances and those of the monomer **123**. That the resonances are relatively broad and unresolved is typical for polymers and is due to reduced molecular tumbling in solution. The signals (at ~ 4.1 and 7.3 ppm) attributed to the impurity that was present in monomer **123** were not observed in the ^{1}H NMR spectrum of the polymer. We were unable to establish if this was because it was eliminated during the purification procedure or if the broad polymer signals were obscuring their presence.

The analysis of the molecular weight of the polymer by GPC was hindered by the poor solubility of the material in the solvent (water) used for analysis. Some of the polymer sample remained undissolved in methanol/water (1:4) even after gentle heating and sonication.

The ^{13}C NMR spectrum of PPE **124** in d_6-DMSO and d_4-MeOD had a low signal to noise ratio and in order to get a satisfactory spectrum the polymer sample was dissolved in D_2O and heated to 363

K. This improved the quality of the spectrum and enabled a near-complete assignment of the polymer. No diyne defects were detected (discussed in section 2.3.2) with only the expected triple-bond resonances observed between 91 and 98 ppm. There were also small unidentified resonances present (166.5 ppm and 174.2 ppm) possibly attributed to aforementioned impurities.

2.2.1 Spectroscopic investigation of fluorescence quenching of PPE 124

For comparison purposes, the absorption and emission spectra for PPE **124** were recorded in an unbuffered aqueous solution and are shown in Figure 2.11. The respective absorption and emission maxima are 400 nm and 468 nm.

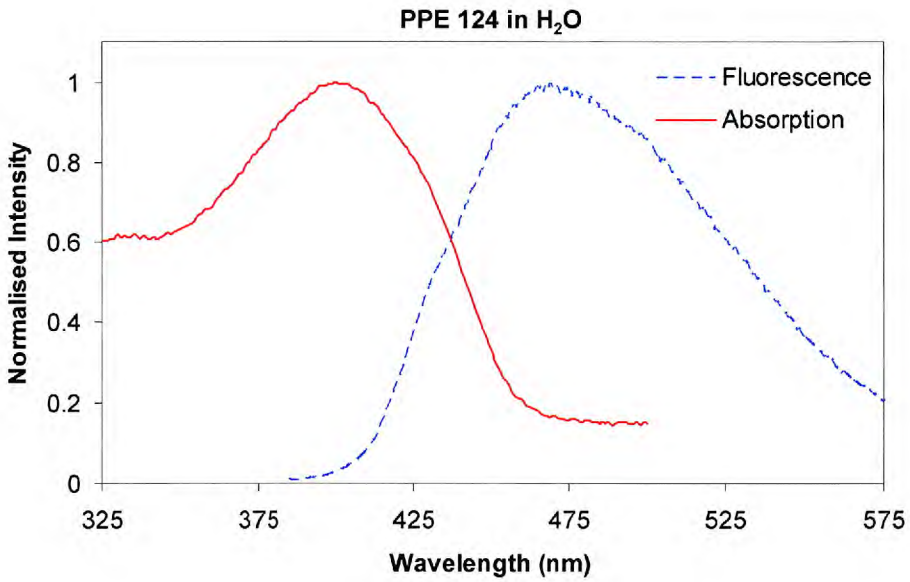

Figure 2.11 Absorption and emission spectrum for PPE **124**.

The quantum yield (determined at different concentrations) for PPE **124** was lower than that measured for PPE **41** (results summarised in Table 2.5). The difference can be explained by the different solvents used to conduct the measurements, with water being preferred for analysing PPE **124** due to its increased solubility in this solvent (the opposite behaviour to PPE **41**). The effect of the different solvents on the solution state conformations of these polymers can be quite pronounced. Schanze *et al.* reported that the quantum yield of PPE **41** *in water* was approximately a tenth of that recorded in methanol.[9] As there are increased interchain interactions in water, it may be that the increased π-π stacking in this medium, increases the amount of self-quenching which serves to reduce the quantum yield. The results detailed in Table 2.5 are within 2.9 – 6.6% of the

reported value for PPE **41** (10% in water) and suggest that for this cationic polymer similar conformational changes are important.[9]

Despite operating at low polymer concentrations (μM), a general, but unexpected trend of lower QEs at dilute polymer concentrations is evident. This result is surprising as increasing the concentration of the fluorophore usually leads a decrease in the quantum yield, a finding explained by self-absorption effects when operating in a high concentration regime (mM).

Table 2.5 Photophysical properties for PPE **124**.[a]

Entry	[PPE **124**] / μM	Excitation wavelength / nm	ϕ_f / %[d]
1	1	373	3.4
2	1	380	3.1
3	6	373	7.1
4	6	380	6.8

[a]All work was conducted in an aerobic environment, in salt-free water. [d]Fluorescence quantum yields measured relative to quinine bisulphate in 1N H_2SO_4 (ϕ_f = 0.546).

In order to measure the response of this polymer towards oppositely-charged quencher molecules, emission quenching experiments were conducted. The emission spectrum of a 10 μM aqueous solution of PPE **124** is shown in Figure 2.12 at increasing concentrations of the anionic quencher **AQS** (9,10-anthraquinone-2,6-disulphonic acid disodium salt; see Figure 2.13). As is typically observed for such polyelectrolytes,[63] the profile for PPE **124** is broad and featureless at the quencher concentrations considered, which is attributed to aggregation of the polymer chains in water, possibly induced by the presence of the quencher.[9] The Stern-Volmer plot is shown as an inset to the main diagram, with the markers denoting the experimental data points and the solid-line indicating the optimal fit to the Stern-Volmer relation.

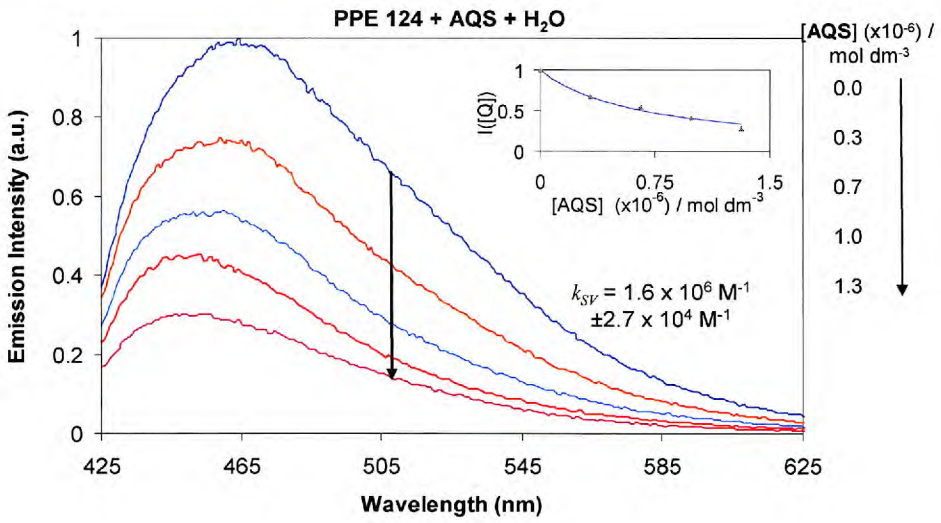

Figure 2.12 The emission spectra in salt-free water of PPE **124** at increasing concentrations of the quencher **AQS** (0 – 2.9 μM). Shown inset, is the Stern-Volmer plot acquired using data extracted from the main figure. The intensities in the Stern-Volmer plot are determined from the area beneath the corresponding curves in Figure 2.12, and are normalised with respect to the measured emission intensity in the absence of **AQS**. The markers denote experimental data lines and the solid-lines indicate the optimal fit to the Stern-Volmer relation as outlined in the Experimental section.

The Stern-Volmer coefficient (1.5×10^6 M^{-1}) is comparable with that reported for similar ionic PPEs and was ~ 15 times smaller than that measured for anionic PPE **41**. The smaller value is unexpected as the higher molecular weight PPE **124** was expected to lead to a higher k_{SV}. There are two mitigating effects that could explain this result. Firstly the measurements were conducted in different solvents (water and methanol) which are known to affect the amount of interchain interaction, which directly influences k_{SV}. Secondly, different quenchers were used (for PPE **41**, $\mathbf{MV^{2+}}$ was used; for PPE **124**, the quencher was **AQS**) which would have slightly different reduction potentials. It is clear from earlier measurements that aggregation is much more important than chain length and from the results described above it may be reasoned that PPE **41** is better at forming aggregates that PPE **124**.

It is important to note that the values of the Stern-Volmer constants quoted in this chapter suffer from the following shortcoming; no attempts were made to ensure that the concentration of the luminescent polymer remained constant throughout the measurement. However, this is important as deviations in the polymer concentrations – specifically, a steady dilution of the polymer upon addition of the quencher – would lead to errors in k_{SV}; an overestimate of the sensing efficiency would result. These issues were eventually resolved and the remedies are fully described in

Chapter Three, where an accurate and robust method for determining the Stern-Volmer constants was established.

Despite this inaccuracy in the measurement, the dilution of the polymer solution was kept to a minimum level, with an estimated error in k_{SV} of 20%. This is still not ideal, as the number of polymer chains 'visible' to the quencher, would decrease with each new addition of the quencher, but does allow for a reasonable estimate of k_{SV} using only the low quencher concentration region, where polymer dilution is minimal.

That strong emission quenching was observed between the cationic PPE **124** and anionic **AQS** is consistent, given previously published results with similar systems.[63] For example, an anionic PPV (similar to polymer **57**, detailed in Chapter One, but containing a Li^+ counter-ion) mixed with a modified cationic cyanine dye appended to poly-L-lysine, gives a complex where energy transfer from the polymer to the dye is followed by efficient quenching of the ensemble upon exposure to the electron acceptor **AQS**.[64] Additionally, Anderson *et al.* reported the quenching of emission, by **AQS**, from a cationic conjugated [3]rotaxane and dumbbell.[65] The efficient quenching yielded Stern-Volmer constants of 2.0 x 10^3 M^{-1} and 4.3 x 10^3 M^{-1} for the [3]rotaxane and dumbbell respectively.[65] To confirm the importance of charge complementarity in the emission quenching process, we investigated what emission changes, if any, would result between quenchers with varying charges upon titration against PPE **124**. The alternative quenchers (Figure 2.13) were selected as they have similar reduction potentials to **AQS** (**139**) and so make for a fair comparison. The quencher **DPy** (4,4′–dipyridyl) is a neutral version of $\mathbf{MV^{2+}}$ and all three are commercially available.

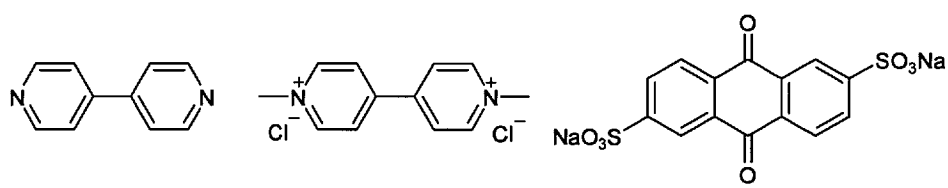

Abbreviation:	DPy	MV^{2+} (Paraquat)	AQS
	118	**28b**	**139**
Reduction potential (as electron acceptor) / V	-	-0.45	-0.5*

Figure 2.13 *Possible alternative emission quenchers for PPE **124**. For benzoquinone (potential vs. SCE in MeCN)).[66]

As expected very little quenching was observed between PPE **124** and either quencher (**DPy** and $\mathbf{MV^{2+}}$), presumably due to the lack of 'ion-pair' complex formation, which is necessary to facilitate quenching through electron or energy transfer. The modest quenching recorded (an example of typical quenching curves are displayed in Figure 2.14 for the quenching of PPE **124** by **DPy**) is a reflection of the mild sphere-of-action quenching which has been shown to dominate for the emission quenching of polyelectrolytes by neutral quenchers.[13] The modest Stern-Volmer constant of 345 M^{-1} is therefore a reflection of this subtle quenching effect, with high (mM) levels of the quencher **DPy** needed in order to achieve just 25% reduction in emission. Where pure static quenching is important, quencher levels in the μM range are sufficient to reduce the emission from these polymers by up to > 90%. The quenching effect observed in Figure 2.14 was not expected to be due to dilution of the polymer solution as control experiments confirmed that this effect could only account for a decrease in the emission of approximately 1-3%.

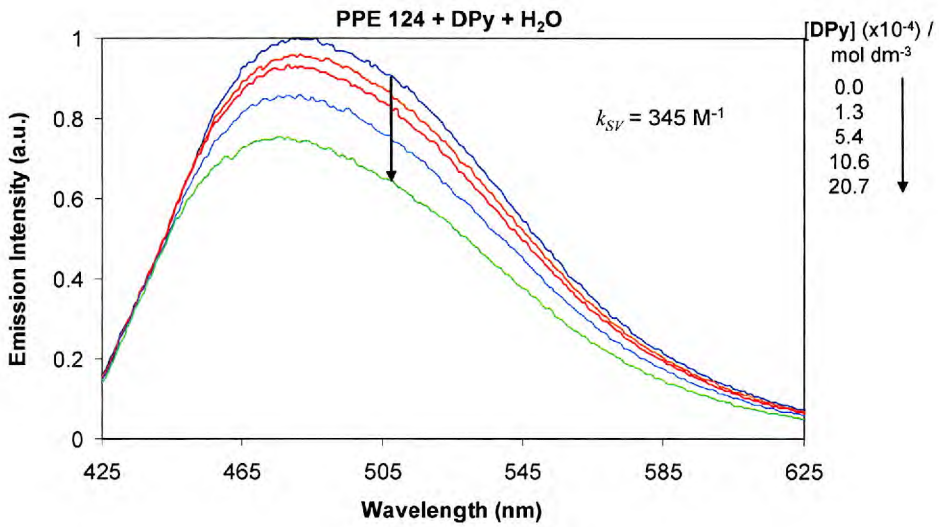

Figure 2.14 The emission spectra in salt-free water of PPE **124** at various concentrations of the quencher **DPy**. Excitation wavelength = 380 nm.

2.3 Optimisation of PPE syntheses

The efficiency of emission quenching is dependent on the diffusion range of the exciton within the CPE. The large distances covered by the exciton during its lifetime, and its ability to hop between chains in an aggregate, give rise to an amplified sensory response relative to shorter derivatives, thereby allowing for several excitations to be quenched by a single bound quencher. For this reason, the Sonogashira-Hagihara polymerisation reaction that was employed to make the polyelectrolytes was investigated in order to determine optimal reaction conditions to allow access to high molecular weight material. Our earlier results suggested that aggregate formation was

relevant in enabling high sensitivity, though at the time we believed that the length of the polymer chains was more important.

In order to achieve a high degree of polymerisation (DP) we turned our attention to the easier to characterise, but structurally similar, neutral alkoxy-substituted PPE derivatives as a model system to optimise reaction variables. The neutral materials had several advantages; partly due to the extended alkyl chain, they had increased solubility in organic solvents and a reduced tendency to aggregate (though some interdigitation effects can not be ruled out) which made them amenable to characterisation by GPC, in organic solvents, and high resolution NMR.

2.3.1 Synthesis of neutral PPE derivatives

It was anticipated that full characterisation of these neutral polymers would allow us to define optimal reaction conditions that could then be applied to the polyelectrolyte synthesis. In order to achieve this, careful selection of the diiodo monomer was required as ideally, one would like a monomer with structural features that allowed for easy analysis of the formed polymer by ^{1}H NMR. The diiodo monomers considered for this purpose are shown in Figure 2.15.

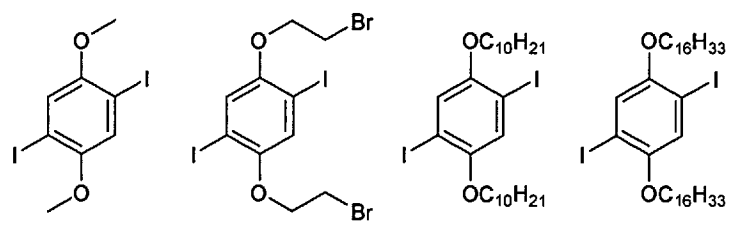

114 **140** **141** *synthesis unsuccessful* **142**

Figure 2.15 Neutral monomers for use in the Sonogashira-Hagihara copolymerisation.

We were slightly concerned that the extended alkyl chains could act as an impediment during the polymerisation, as the steric bulk of this side chain could potentially hinder the approach to the palladium centre during the cross-coupling reactions. However, as shown in Chapter One, there are numerous examples where long/bulky side chains had been included on monomers that were successfully polymerised.

In order to use ^{1}H NMR for end-group analysis to calculate the molecular weight of the neutral PPE polymers, we considered monomers that contained resonances that appeared in vacant regions (spectral window) of the NMR spectrum. Alkoxy derivatives that were used in the synthesis of the

ionic PPEs described earlier were considered, as the methylene protons appearing between 3.5 – 4.2 ppm, could be used as a handle to determine M_n.

In addition, it was envisaged that the presence of the methyl groups at the end of decorative side chains would allow for a quantitative determination of the degree of polymerisation. In the simplest example of this, the methyl groups present in monomer **114** were thought to be ideal as the sharp methyl resonance at ~ 3.8 ppm (in $CDCl_3$), would remain distinct and clearly visible in the polymer structure. However, all attempts to synthesise PPE **143** proved unsuccessful, under the usual polymerisation conditions (Scheme 2.7). ^{1}H NMR analysis revealed that appreciable deprotection of the methyl ether protecting groups occurred, possibly triggered by the presence of the metal (this was evidenced by the appearance of broad phenolic resonances in the ^{1}H NMR). These problems forced us to target different neutral polymers where this was not observed.

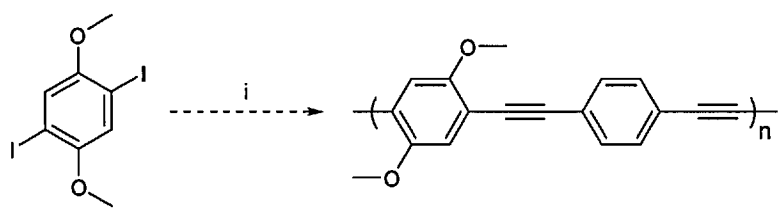

114 **PPE 143**
Impure

Scheme 2.7 Synthesis of a neutral PPE derivative. Conditions: i) 1,4-Diethynylbenzene (**106**), $Pd(PPh_3)_4$, CuI, $^iPr_2NH$, DMF, 50 °C, 24 h.

The neutral PPE **144** was targeted as a versatile precursor polymer that could be functionalised in a variety of ways. We reasoned that nucleophilic displacement of the bromide leaving groups would allow for the (post-polymerisation) introduction of a variety of functional groups along the polymer backbone. The synthesis of monomer **140** from the commercially available corresponding diol was reported by Schanze *et al.*,[11] and using their protocol we isolated it in an overall yield of 84% (more details on this monomer are given in Chapter Three).

Polymerisation of **140** with 1,4-diethynylbenzene (**106**) gave rise to the bromo-derivitised PPE **144**, isolated as a fine yellow powder, the expected colour for such materials (Scheme 2.8). However, ^{1}H NMR showed the presence of an impurity that led to a significant broadening of the signal due to the methylene unit adjacent to the oxygen atom. This would suggest that there was some substitution of the bromine atom during the polymerisation, possibly by the amine (*N,N'*-diisopropylamine), though this was not supported by the ^{1}H NMR. There is also the possibility that under the reaction conditions used, (reaction was conducted at elevated temperatures, ~ 60 °C)

some elimination leading to alkene formation may have occurred though again there was no conclusive evidence in the ^{1}H NMR for this.

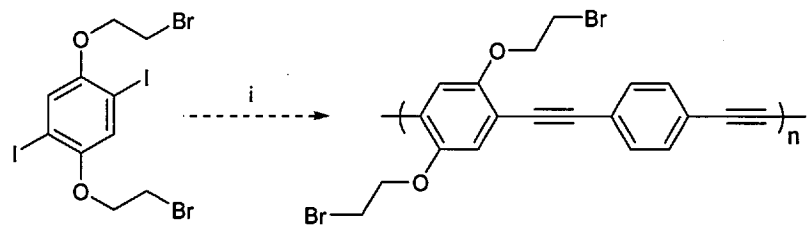

140 PPE **144** *Impure*

Scheme 2.8 Synthesis of a neutral PPE derivative. Conditions: i) 1,4-Diethynylbenzene (**106**), $Pd(PPh_3)_4$, CuI, $^iPr_2NH$, DMF, 60 °C, 24 h.

2.3.2 Evaluation of optimised polymerisation conditions – end-group analysis and emission properties of neutral 2,5-bis(cetyloxy)-substituted PPE derivatives

Alternative structures were needed to avoid the synthetic issues that hindered the synthesis and purification of the PPEs **143** and **144**. Monomers such as **141** and **142** have been used previously to make highly soluble PPE derivatives and long alkyl chains are known to lead to improved solubility characteristics for poly(phenylene vinylene) and poly(thiophene) materials for use in thin film transistor devices.[67] For our purposes, such monomers had an additional benefit: by ^{1}H NMR, the oxy-methylene group appeared as a well-resolved triplet and was far away from any other resonances (the isolated sharp triplet at approximately 4.0 ppm is shown in Figure 2.16). Though our chosen iodination conditions failed to generate **141** cleanly, the synthesis of **142** proceeded smoothly under identical conditions (Scheme 2.9).

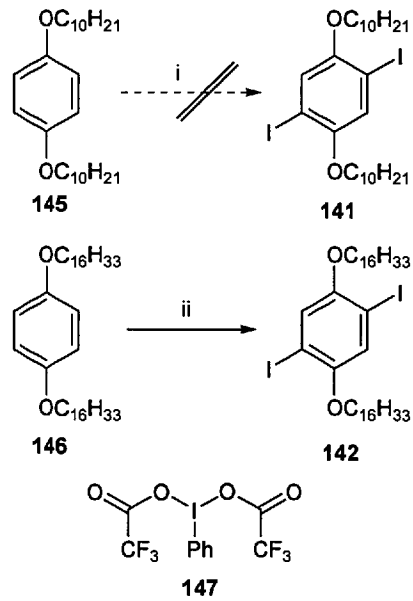

Scheme 2.9 Synthesis of a neutral 2,5-bis(cetyloxy) monomer (**142**). Conditions: i) $PhI(CF_3CO_2)_2$ (**147**), I_2, CH_2Cl_2, 20 °C, 6 h; ii) $PhI(CF_3CO_2)_2$ (**147**), I_2, CH_2Cl_2, 20 °C, 24 h, 44%.

The reasons for the failed iodination attempt (formation of monomer **141**) were not investigated (due to time constraints). However, Tour *et al.* have recently shown that iodination of **145** can be accomplished (in 83% yield) using mercury acetate and iodine in CH_2Cl_2.[68] These unusual conditions may indicate that they too encountered difficulties using more traditional iodinating methods, such as those used to synthesise **142**.

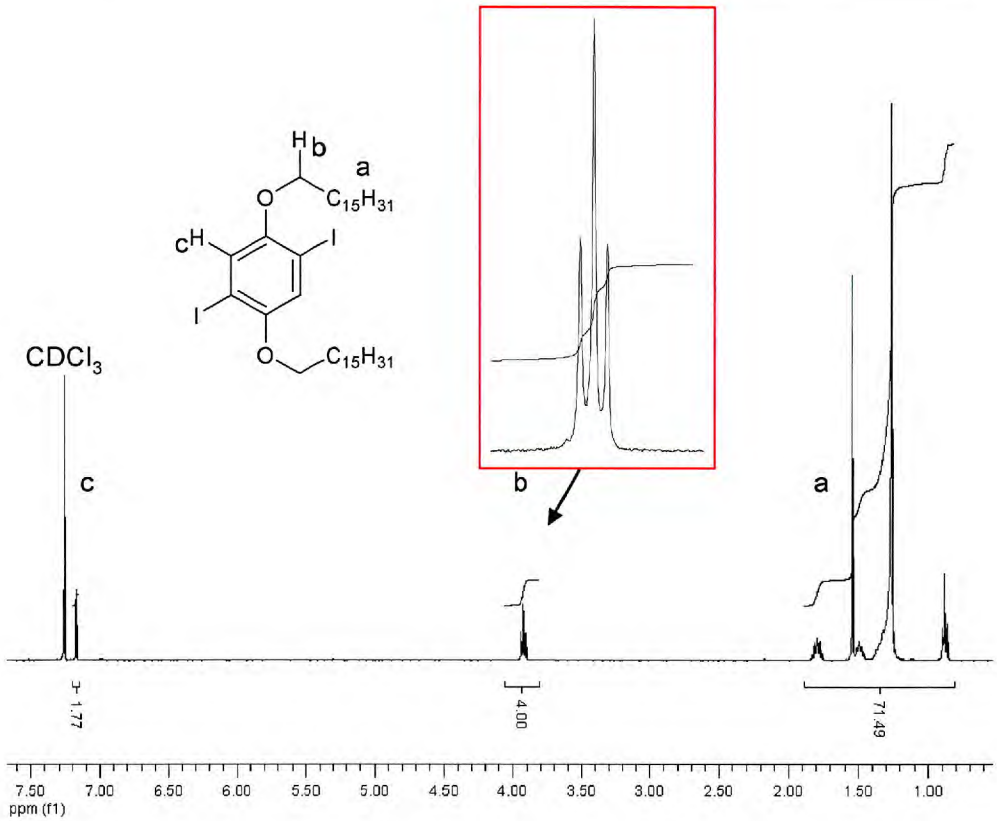

Figure 2.16 ^{1}H NMR of monomer **142** in $CDCl_3$.

The position of the sharp isolated triplet, centred at 3.92 ppm, was used as a handle to accurately calculate the degree of polymerisation (DP) for the long-chained neutral PPE derivatives. Use of the end-capping agent 4-iodotoluene (**149**, see Scheme 2.10) resulted in a sharp singlet at ≈ 2.4 ppm (methyl signal) and integration of this signal against the polymer main chain signals allowed an accurate determination of DP. The accuracy of this method depends on the sample being free from defects something that is ensured using the Pd(0) source $Pd(PPh_3)_4$ (see Chapter One).[19] For this polymerisation such assumptions are suitable as the reaction is known to produce high molecular weight polymers that are free from defects (*vide infra*; for a fuller treatment see Chapter Three).[19] The results for the neutral polymerisations that were performed are detailed in Scheme 2.10 and Table 2.6. GPC data are included where available. For the polymers that were not end-capped, molecular weights were estimated using the ratio technique, as described earlier (2.1.2).

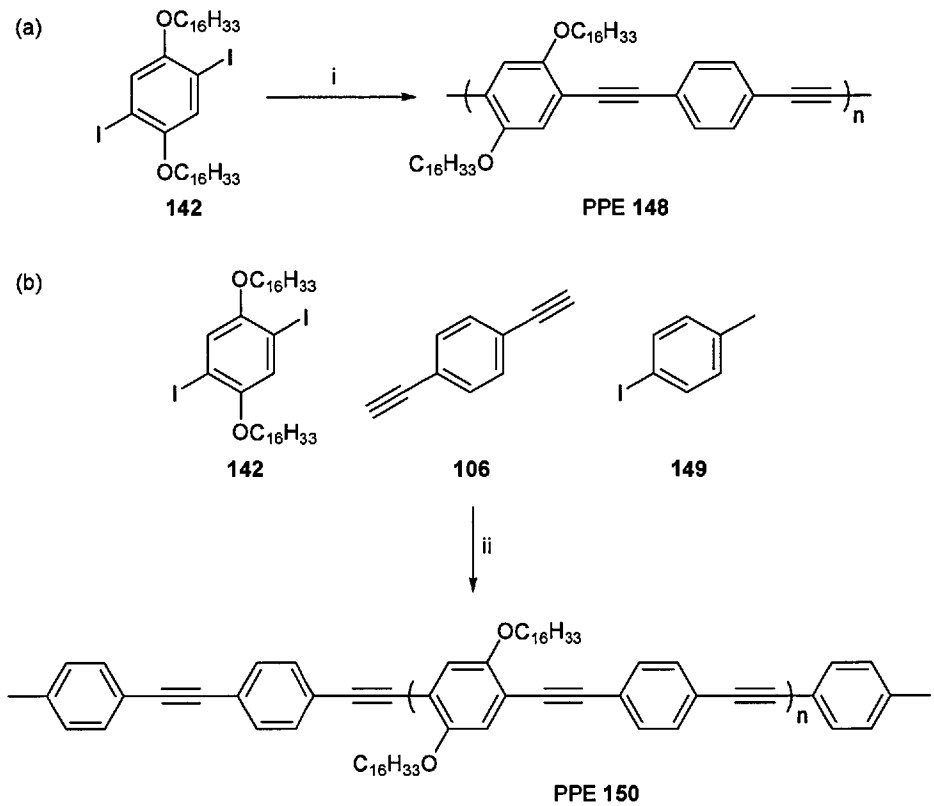

Scheme 2.10 Synthesis of 2,5-bis(cetyloxy) PPEs **148** (a) and **150** (b). Conditions; i) **106**, $Pd(PPh_3)_4$, CuI, $^iPr_2NH$, DMF or toluene, 40 – 55 °C, 24 – 140 h, 62 – ~ 90%; ii) $Pd(PPh_3)_4$, CuI, $^iPr_2NH$, toluene, 55 °C, 70 h, ~ 90%.

Table 2.6 Summary of results for the formation of neutral polymers PPE **148** and PPE **150**.

Entry	Polymer	Conditions / changes [a]	DP, by ^{1}H NMR[b]	M_n, by GPC, Da [c]	Yield (%)
1	**148**	24 h, 40 °C; $Pd(PPh_3)_4$	8	7300 (5100)	72
2	**148**	24 h, 40 °C / 5% excess of diiodo monomer added; $Pd(PPh_3)_4$	5	8000 (5600)	62
3	**148**	87.5 h, 50 °C; $Pd(PPh_3)_4$	15	8400 (5900)	-[d]
4	**148**	67.5 h, 50 °C; $Pd(PPh_3)_4$	9	11300 (8000)	-[d]
5	**148**	43 h, 50 °C; $Pd(PPh_3)_4$ Two portions of the catalysts were added. Initially the solution was sonicated for 10 minutes	20	-	-[d]
6	**150**	138 h, 55 °C; $Pd(PPh_3)_4$ Toluene used as solvent	> 20	-	~ 90[d]
7	**150**	140 h, 50 °C; $Pd(PPh_3)_4$ Two portions of the catalysts were added	11	-	~ 90[d]
8	**150**	70 h, 55 °C; $Pd(PPh_3)_4$ DMF used as solvent	15	-	-[d]
9	**150**	70 h, 55 °C; $Pd(PPh_3)_4$ Toluene used as solvent	30	-	-[d]
10	**148**	38 h, 50 °C; $Pd(PPh_3)_2Cl_2$	10	7400 (5200)	90
11	**148**	117 h, 50 °C; $Pd(PPh_3)_2Cl_2$	< 5	3500 (2500)	-[d]

[a] Conducted using a method described by Tew *et al.*:[69] this involved adding all starting materials to the Schlenk flask prior to starting, as opposed to the previous method (Schanze *et al.*)[9] where solutions of the monomers and the catalysts were prepared separately before being combined and degassed after combination; a 5% excess of the alkyne monomer was used (see main text for details). All solvents were degassed prior to use.

[b] Molecular weight determined by one of two methods: for PPE **148**, the ratio method was used and for PPE **150** end-group analysis.

[c] by light scattering (running in THF as the eluant) and stated here with the correction factor of 1.42 being applied (in parentheses).[19]

[d] Yield not determined as the polymers were stored as solutions in, $CHCl_3$, THF or toluene; ^{1}H NMR was used to analyse the polymer.

All polymerisation reactions involving the neutral monomers were performed following typical coupling procedures. In particular, the similar methods detailed by either Tew *et al.*[69] or West *et al.*,[70] who synthesised structurally similar PPE derivatives that were decorated with smaller alkoxy chains, were found to be the most useful. In general, both monomers and catalysts were placed in a Schlenk flask before the organic base and degassed solvent were added. All reactions were conducted in an argon atmosphere. The isolated polymers were fine, bright yellow powders.

In the initial reactions (Table 2.6, entries 1 – 5) variations on monomer composition, reaction times and catalyst addition were made, with a slight excess of the alkyne monomer yielding the best result. This is consistent with published findings[19] where it was found that an excess (1.03 equivalents) of the bisalkyne monomer was required to circumvent an unavoidable, but minor (1-10%),[19] competing side reaction that resulted in the formation of a small number of diacetylene linkages.[25] This reaction occurs through oxidative coupling of the alkyne units and necessarily reduces the maximum possible molecular weight of the polymer. If the unwanted consumption of this monomer is not compensated for, the ensuing stoichiometric imbalance between the two monomers limits X_n (as described in Chapter One), as is always important in polycondensation reactions. For these entries the reaction mixtures were stirred for extended periods (24 – 47 hours) and there was only a single addition of the catalyst and co-catalyst.

Gentle heating of the reaction mixture, was required to start the reaction, but increasing the temperature (> 65 °C) was observed to have a detrimental effect, with dark orange insoluble impurities isolated. This is consistent with the formation of a cross-linked material, as has been previously reported.[19] Where possible the polymers were analysed by GPC (in $CHCl_3$, against polystyrene standards) with the usual caveat that such data carries an inherent overestimation, as discussed earlier. The correction factor reported by Bunz *et al.*,[33] has been applied to the molecular weight data presented in Table 2.6, with the adjusted values in parentheses.

The results from the first 4 entries led to the conclusion that, though the polymerisation started efficiently, as observed by the rapid colour change of the reaction mixture, from brown to bright yellow, the low molecular weights isolated suggested that the catalyst was possibly being deactivated during the reaction, which affected its performance. In order to counter this, the following improvements were made:

- The solvents were degassed for about 30 minutes (with argon) prior to use
- The catalyst and co-catalyst (Cu(I)I) were added under an argon atmosphere

- Crucially, additional quantities of the catalyst materials were added to the reaction vessel after the first 24-hour period, to account for the anticipated loss in activity of the original catalyst.

Entry 5 details the findings. The slight improvement in molecular weight is instructive as it suggests that the reaction is highly dependent on maintaining the activity of the catalyst. For all subsequent reactions, fresh portions of the Pd(0) catalyst were used (the catalyst is most active when freshly made and should be a bright yellow crystalline material)[19] with samples that were slightly darker discarded. Fresh catalyst materials were rapidly employed in all polymerisation reactions.

For entries 3 – 9 the major change in the reaction conditions centred on the increased reaction times, to ensure the complete consumption of the monomers. Additionally, the freeze-pump-thaw technique was used to ensure that the reaction flask was an anaerobic environment. This led to further improvements in the molecular weights of the materials isolated, as determined by ^{1}H NMR. For entries 5 and 6, a change in solvent led to good results for the degree of polymerisation, as calculated by end-group analysis (entry 5: 20 repeat units, entry 6: > 20 repeat units). These improvements could be attributed to the increased solubility of the diiodo monomer in this solvent. Our initial reluctance to use toluene as a solvent for the polymerisation stemmed from potential problems regarding its removal from the reaction mixture after the polymerisation and that any additional signals that could remain in the sample would populate the aromatic region of the ^{1}H NMR spectrum, thus rendering the ratio method of molecular weight determination redundant.

For these latter entries, the samples were stored as solvent solutions, due to solubility problems when the polymers were dried. We noticed that upon recovering the polymer from a good solvent (usually toluene) and drying under vacuum, the ability to redissolve the material was much reduced. This observation was also noted by Schanze *et al.*,[71] who reported that the complete drying of polymer films (they synthesised neutral terthiophene end-capped PPEs) resulted in a similar problem. This is presumably due to the strength of inter-polymer interactions, which can not be overcome by solvation as solvent access to individual polymer chains is limited. As a result, subsequent polymer samples prepared by us were stored as stock solutions in chloroform or THF that were kept in the dark, after purification by re-precipitation. To obtain NMR spectra, the polymer was recovered by precipitating small quantities of the stock solution in an acetone/hexane mixture (both of which are non-solvents for the polymer). The solid is then collected by centrifugation.

In other results, (entries 10 and 11, Table 2.6) an alternative palladium catalyst was used ($Pd(PPh_3)_2Cl_2$ – which has the advantage of being less air-sensitive) but the switch from the traditional Sonogashira catalyst to an air-stable variant, resulted in no improvement in the degree of polymerisation (in these cases $X_n \leq 10$).

The three entries 7 – 9, show the results from the final modifications to the original polymerisation reactions. The degree of polymerisation for entry 9 (Table 2.6) was estimated to be 30 (21.4 kDa), 50% larger than the next best. Moreover, the method used to determine the degree of polymerisation was improved further as the ratio method, which was used earlier with moderate success to gauge the degree of polymerisation, was of limited value when using samples that contain trace amounts of toluene (*vide supra*). A better technique involves using an end-capping group that does not alter the luminescence properties of the polymer and has resonances in the NMR spectrum that fall in a vacant region and which can be used as a handle to determine the molecular weight. To this end, phenylacetylene was used initially, though the aromatic signals from this end-cap could not be accurately differentiated from other signals in this region. Therefore, the use of 4-iodotoluene (**149**) as an end-capping group, proved useful as the resonance from the methyl group (which appears at 2.4 ppm, a vacant region of the spectrum in this case) was readily visible and allowed easy determination of the molecular weight, *via* integration of this signal. In Figure 2.17 the ^1H NMR spectrum of the end-capped PPE **150** is shown along with the calculation of DP.

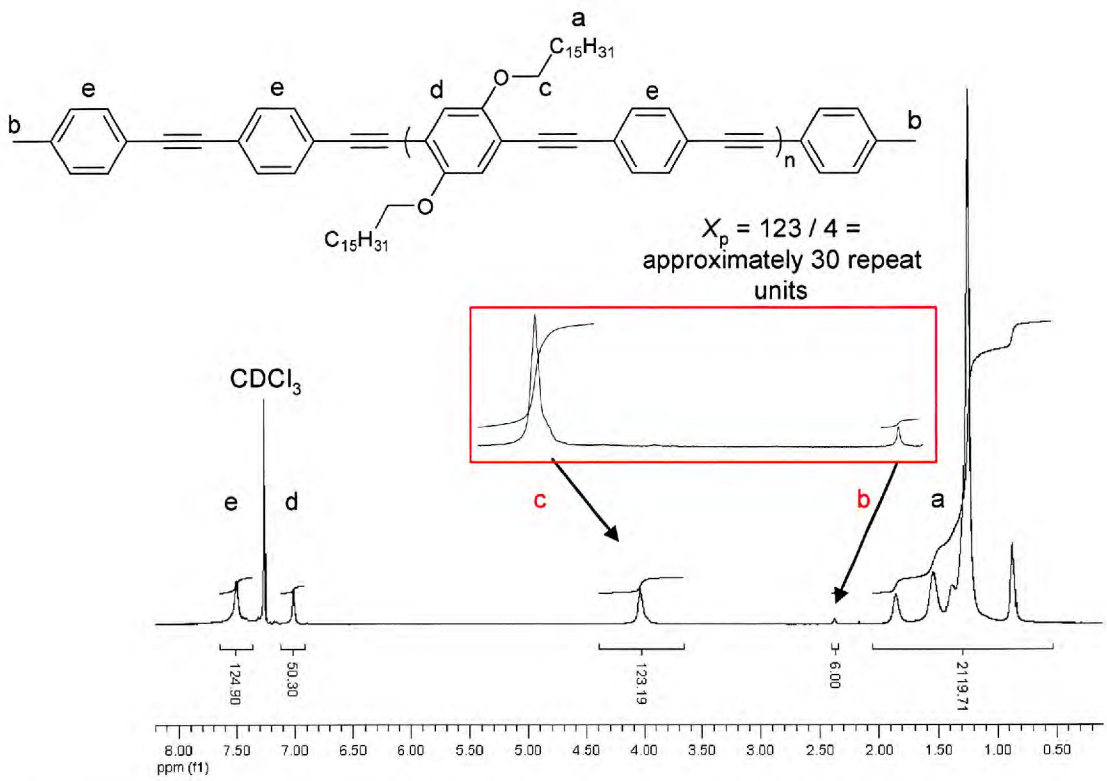

Figure 2.17 ^{1}H NMR of PPE **150**. *Inset:* Integration of areas corresponding to protons **b** and **c** allow for determination of DP (entry 9, in Table 2.6).

This result is striking, as it implies that the choice of solvent is critical in attaining high molecular weights. The method used in the most successful polymerisation was far removed from the initial procedure. Reactions corresponding to entries 8 and 9 were conducted under similar conditions with the only change being the solvent. In dry toluene (entry 9) the degree of polymerisation was estimated to be double that observed in DMF. Where appropriate, these optimised conditions were then applied to all subsequent polyelectrolyte syntheses, paying particularly attention to solvent choice.

Diacetylene defects, caused by the reaction of the palladium catalyst with ethynylides, can be a major drawback in the synthesis of PPEs, with repeated inclusion of such defects leading to reduced solubility of the formed polymer and lower molecular weights.[19] The problem is most acute when a Pd^{2+} catalyst is employed, as a small quantity of the alkyne species is then required to reduce the Pd^{2+} species to its active zero-valent form. Clearly, the problem is much reduced when Pd^0 sources of the catalyst are used though several reports remark that under such conditions diyne defects still occur.[19] Swager noted that the use of a small excess (~ 3%) of the alkyne monomer, combined with Pd^0 catalysts leads to high molecular weight PPEs.[25] Other methods employed to reduce the incidence of diyne defects include the use of a bis-TMS protected alkyne monomer,

which undergoes deprotection *in situ* (under the basic reaction conditions). This idea was first reported by Heitz *et al.*[27] and then elaborated on by Hecht *et al.*[72] and benefits from reducing the concentration of free terminal alkynes in the reaction mixture. The authors claim that this serves to reduce competing side reactions (i.e. diyne formation) and seemingly confirm the success of the method by noting that no such defects are observed by ^{13}C NMR.[22,72]

Indeed, for PPE structures such as PPE **150**, diyne defects are observed in the ^{13}C NMR as signals that arise at approximately 75 ppm and 80 ppm. The ^{13}C NMR spectra, for a variety of the neutral PPEs discussed here, were analysed for the presence of diyne defects. Due to the anisotropic nature of such polymers and their minimal solubility at concentrations required for NMR analysis, such spectra were generally 'noisy' and few resonances were observed even after a high number of scans. As a result it was not possible to observe all the expected resonances for these polymers by NMR, though no signals could be detected in the range where diyne signals would be expected.

Some typical GPC traces for the 2,5-bis(cetyloxy) PPEs (like PPEs **148** and **150**) are shown in Figure 2.18. The values for M_n and M_w ranged between 4600 Da and 45000 Da respectively, with PDIs in the range of 1.4 to 4.7, which are similar to reported values for such polycondensation processes and confirmed by the broad molecular weight distributions. Attempted acquisition of molecular weights data through MALDI-tof analysis failed as an adequate matrix material could not be identified. Various matrices were used (with and without the cationisation agent silver trifluoroacetate, AgTFA) including α-cyano-4-hydroxycinnamic acid, 2,5-dihydroxybenzoic acid, dithranol and *trans*-3-indoleacrylic acid. Samples were prepared using the dried-droplet technique, whereby a solution of the matrix is mixed with the sample (sample:matrix, ~ 1:4, w/w) and then spotted onto the target, with the solvent then allowed to evaporate. However in all cases no spectra could be produced. Both positive and negative ion modes were used on the spectrometer with various different laser intensities. If MALDI spectra could have been acquired they could be used to check for the presence of diyne defects.[19] In a report published in 2005, Ellison *et al.* described a new method for acquiring MALDI spectra of neutral ethylene glycol substituted PPEs using the evaporation-grinding (E-G) method.[73] The authors claim that this new technique is ideal for preparing and analysing polymers that have low solubility, as is the case with some PPEs. They mixed a 25:1:1 (matrix:PPE:salt) molar ratio with 60 μL of THF with a pestle and mortar to evaporate the solvent and then continued mixing to obtain a fine powder.[73] About 5 mg was then pressed into a sample well, on the MALDI sample plate. This method provided satisfactory spectra and gave high signal-to-noise ratios.[73]

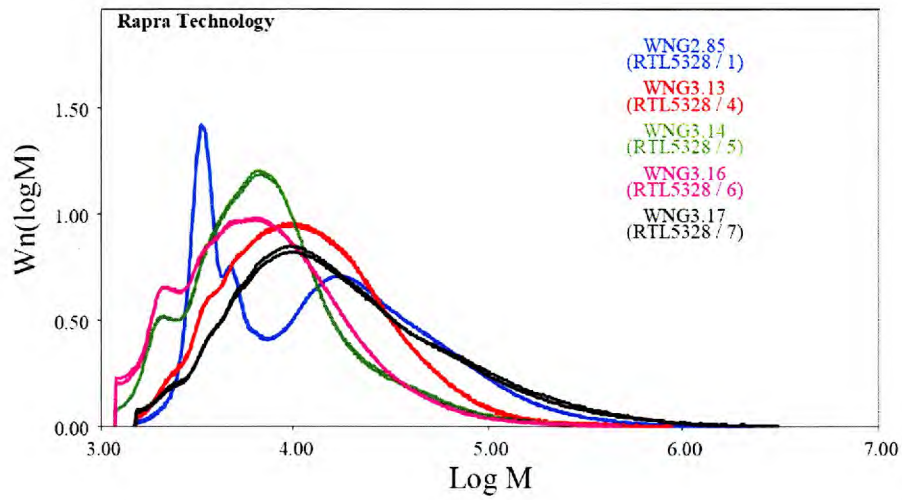

Figure 2.18 Typical calculated GPC molecular weight distribution curves for the neutral 2,5-bis(cetyloxy) PPE **150**, ($CHCl_3$ at 30 °C, 1.0 mL/min, RI detector); molecular weights are relative to PS standards; courtesy of Rapra Ltd.

As part of the full characterisation of the neutral 2,5-bis(cetyloxy) PPEs, the absorption and emission spectra for the representative polymer PPE **150** were recorded (Figure 2.19).

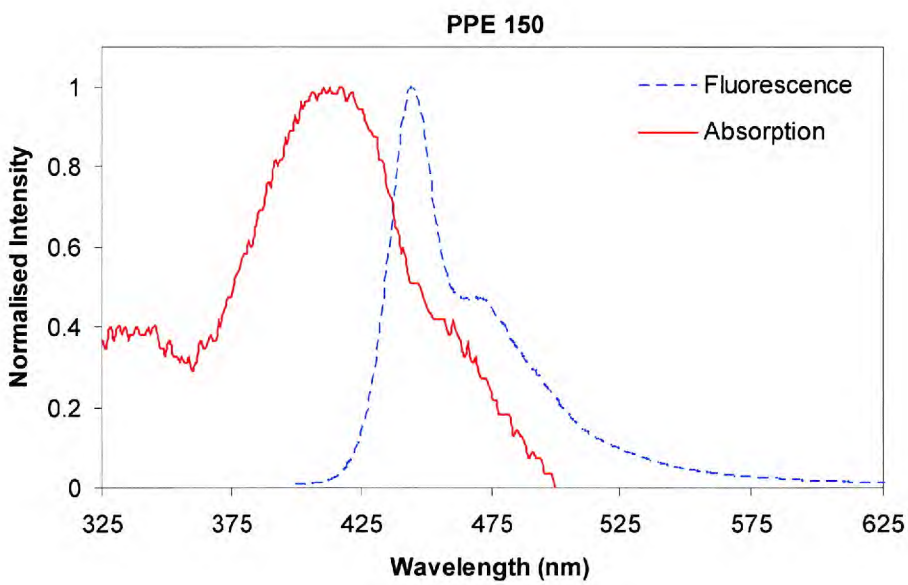

Figure 2.19 The normalised absorption and emission spectrum in THF for PPE **150** ([PPE **150**] ~ 25 μM; excitation wavelength = 375 nm).

In common with other similar neutral PPE derivatives, the polymer was highly soluble in THF, $CHCl_3$, and DMF, and emits between 400 – 500 nm. The respective absorption (418 nm) and emission peaks (445 nm) are consistent with those arising from a high molecular weight PPE polymer in a good solvent,[71] and further confirm the high degree of polymerisation. The relatively narrow emission spectrum also confirms that PPE **150** exists in a non-aggregated state in THF in contrast to typical PPE polyelectrolytes that usually exhibit broad emission, due to the formation of aggregates.[9]

2.4 Notes and references

1. M. R. Pinto and K. S. Schanze, *Proc. Natl. Acad. Sci. USA*, 2004, **101**, 7505-7510.
2. N. DiCesare, M. R. Pinto, K. S. Schanze and J. R. Lakowicz, *Langmuir*, 2002, **18**, 7785-7787.
3. K. Dore, S. Dubus, H.-A. Ho, I. Levesque, M. Brunette, G. Corbeil, M. Boissinot, G. Boivin, M. G. Bergeron, D. Boudreau and M. Leclerc, *J. Am. Chem. Soc.*, 2004, **126**, 4240-4244.
4. B. S. Gaylord, M. R. Massie, S. C. Feinstein and G. C. Bazan, *Proc. Natl. Acad. Sci. USA*, 2005, **102**, 34-39.
5. S. A. Kushon, K. Bradford, V. Marin, C. Suhrada, B. A. Armitage, D. W. McBranch and D. G. Whitten, *Langmuir*, 2003, **19**, 6456-6464.
6. L. Chen, D. W. McBranch, H.-L. Wang, R. Helgeson, F. Wudl and D. G. Whitten, *Proc. Natl. Acad. Sci. USA*, 1999, **96**, 12287-12292.
7. B. S. Harrison, M. B. Ramey, J. R. Reynolds and K. S. Schanze, *J. Am. Chem. Soc.*, 2000, **122**, 8561-8562.
8. C. H. Fan, S. Wang, J. W. Hong, G. C. Bazan, K. W. Plaxco and A. J. Heeger, *Proc. Natl. Acad. Sci. U. S. A.*, 2003, **100**, 6297-6301.
9. C. Y. Tan, M. R. Pinto and K. S. Schanze, *Chem. Commun.*, **2002**, 446-447.
10. Q.-L. Fan, Y. Zhou, X.-M. Lu, X.-Y. Hou and W. Huang, *Macromolecules*, 2005, **38**, 2927-2936.
11. M. R. Pinto, B. M. Kristal and K. S. Schanze, *Langmuir*, 2003, **19**, 6523-6533.
12. C. Y. Tan, E. Atas, J. G. Muller, M. R. Pinto, V. D. Kleiman and K. S. Schanze, *J. Am. Chem. Soc.*, 2004, **126**, 13685-13694.
13. D. L. Wang, D. Wang, D. Moses, G. C. Bazan and A. J. Heeger, *Langmuir*, 2001, **17**, 1262-1266.
14. M. R. Pinto and K. S. Schanze, *Synthesis*, **2002**, 1293-1309.

15. I.-B. Kim, J. N. Wilson and U. H. F. Bunz, *Chem. Commun.*, **2005**, 1273-1275.
16. I.-B. Kim, B. Erdogan, J. N. Wilson and U. H. F. Bunz, *Chem. Eur. J.*, 2004, **10**, 6247-6254.
17. R. J. Young and P. A. Lovell, *Introduction to Polymers*, 2nd edn., Nelson Thornes Ltd, Cheltenham, 1991.
18. K. Sonogashira, *J. Organomet. Chem.*, 2002, **653**, 46-49.
19. U. H. F. Bunz, *Chem. Rev.*, 2000, **100**, 1605-1644.
20. (a) L. Cassar, *J. Organomet. Chem.*, 1975, **93**, 253-257; (b) H. A. Dieck and F. R. Heck, *J. Organomet. Chem.*, 1975, **93**, 259-263; (c) K. Sonogashira, Y. Tohda and N. Hagihara, *Tetrahedron Lett.*, 1975, **50**, 4467-4470.
21. K. Kuroda and T. M. Swager, *Chem. Commun.*, **2003**, 26-27.
22. A. Khan, S. Muller and S. Hecht, *Chem. Commun.*, **2005**, 584-586.
23. B. C. Englert, M. D. Smith, K. I. Hardcastle and U. H. F. Bunz, *Macromolecules*, 2004, **37**, 8212-8221.
24. C. L. McCormick and G. L. Smith, *Langmuir*, 2001, **17**, 1719-1725.
25. Q. Zhou and T. M. Swager, *J. Am. Chem. Soc.*, 1995, **117**, 12593-12602.
26. J. M. Tour, A. M. Rawlett, M. Kozaki, Y. Yao, R. C. Jagessar, S. M. Dirk, D. W. Price, M. A. Reed, C.-W. Zhou, J. Chen, W. Wang and I. Campbell, *Chem. Eur. J.*, 2001, **7**, 5118-5134.
27. H. Hager and W. Heitz, *Macromol. Chem. Phys.*, 1998, **199**, 1821-1826.
28. T. M. Swager, M. S. Wrighton and D. Ofer, *Chem. Mat.*, 1995, **7**, 418-425.
29. D. Steiger, P. Smith and C. Weder, *Macromol. Rapid. Commun.*, 1997, **18**, 643-649.
30. L. M. Harwood, C. J. Moody and J. Percy, *Experimental Organic Chemistry, 2nd edition*, Oxford, 1998.
31. C. Y. Tan, M. R. Pinto, M. E. Kose, I. Ghiviriga and K. S. Schanze, *Adv. Mater.*, 2004, **16**, 1208-1212.
32. C. Weder, C. Sarwa, A. Montali, C. Bastiaansen and P. Smith, *Science*, 1998, **279**, 835-837.
33. H. L. Ricks, U. H. Choudry, A. R. Marshall and U. H. F. Bunz, *Macromolecules*, 2003, **36**, 1424-1425.
34. (a) S. L. Huang and J. M. Tour, *J. Am. Chem. Soc.*, 1999, **121**, 4908 - 4909; (b) L. R. Jones, J. S. Schumm and J. M. Tour, *J. Org. Chem.*, 1997, **62**, 1388-1410.
35. (a) U. H. F. Bunz, A. R. Marshall, H. L. Ricks and U. H. Choudry, *Macromolecules*, 2003, **36**, 1424-1425; (b) J. R. Reynolds and A. D. Child, *Macromolecules*, 1994, **27**, 1975-1977.
36. T. M. Swager, C. J. Gil and M. S. Wrighton, *J. Phys. Chem. A*, 1995, **99**, 4886-4893.
37. B. S. Gaylord, S. J. Wang, A. J. Heeger and G. C. Bazan, *J. Am. Chem. Soc.*, 2001, **123**, 6417-6418.

38. M. P. Stevens, *Polymer Chemistry*, 3rd edn., OUP, Oxford, 1999.
39. R. P. Wayne and C. E. Wayne, *Photochemistry*, OCP, 1996.
40. Y. Kim, J. Bouffard, S. E. Kooi and T. M. Swager, *J. Am. Chem. Soc.*, 2005, **127**, 13726-13731.
41. J. C. deMello, H. F. Whitmann, R. H. Friend, *Adv. Mater.*, 1997, **9**, 230-232.
42. N. C. Greenham, I. D. W. Samuel, G. R. Hayes, R. T. Phillips, Y. A. R. R. Kessener, S. C. Moratti, A. B. Holmes and R. H. Friend, *Chem. Phys. Lett.*, 1995, **241**, 89-96.
43. D. F. Eaton, *Pure & Appl. Chem.*, 1988, **60**, 1107-1114.
44. J. R. Lakowicz, *Principles of Fluorescence Spectroscopy*, Plenum Press, New York, 1983.
45. C. Fan, K. W. Plaxco and A. J. Heeger, *J. Am. Chem. Soc.*, 2002, **124**, 5642-5643.
46. H. Jiang, D. Zhao and K. S. Schanze, *Langmuir*, 2006, **22**, 5541-5543.
47. J. Wang, D. L. Wang, E. K. Miller, D. Moses, G. C. Bazan and A. J. Heeger, *Macromolecules*, 2000, **33**, 5153-5158.
48. J. M. Frank and S. I. Vavilov, *Z. Phys. Chem. (Munich)*, 1931, **69**, 100-110.
49. T. Obsil, *Protein Fluorescence,* http://members.tripod.com/obsil/fluor.htm (accessed in 2002).
50. J. G. Muller, E. Atas, C. Tan, K. S. Schanze and V. Kleiman, *J. Am. Chem. Soc.*, 2006, **128**, 4007-4016.
51. T. M. Swager, *Abstr. Pap. Am. Chem. Soc.*, 2000, **220**, 305-ORGN.
52. D. T. McQuade, A. H. Hegedus and T. M. Swager, *J. Am. Chem. Soc.*, 2000, **122**, 12389-12390.
53. G. Brodowski, A. Horvath, M. Ballauff and M. Rehahn, *Macromolecules*, 1996, **29**, 6962-6965.
54. J. Clayden, N. Greeves, S. Warren and P. Wothers, *Organic Chemistry*, OUP, Oxford, 2001.
55. Z. Wang, S. Campagna, K. Yang, G. Xu, M. E. Pierce, J. M. Fortunak, P. N. Confalone, *J. Org. Chem.*, 2000, **65**, 1889-1891.
56. H. Hagiwara, K. Morohashi, H. Sakai, T. Suzuki, M. Ando, *Tetrahedron*, 1998, **54**, 5845-5852.
57. V. K. Aggarwal, A. Mereu, *J. Org. Chem.*, 2000, **65**, 7211-7212.
58. E. J. Corey and P. L. Fuchs, *Tetrahedron Lett.*, 1972, **13**, 3769-3772.
59. (a) F. Ramirez, N. B. Desai and N. McKelvie, *J. Am. Chem. Soc.*, 1962, **84**, 1745-1747; (b) B. E. Maryanoff and A. B. Reitz, *Chem. Rev.*, 1989, **89**, 863-927.
60. (a) D. Seyferth, R. S. Marmor and P. Hilbert, *J. Org. Chem.*, 1971, **36**, 1379-1386; (b) J. C. Gilbert and U. Weerasooriya, *J. Org. Chem.*, 1982, **47**, 1837-1845.
61. G. J. Bodwell, D. O. Miller, R. J. Vermeij, *Org. Lett.*, 2001, **3**, 2093-2096.
62. T. P. Bubner and G. T. Crisp, *Tetrahedron*, 1997, **53**, 11899-11912.

63. D. T. McQuade, A. E. Pullen and T. M. Swager, *Chem. Rev.*, 2000, **100**, 2537-2574.

64. R. M. Jones, T. S. Bergstedt, D. W. McBranch and D. G. Whitten, *J. Am. Chem. Soc.*, 2001, **123**, 6726-6727.

65. P. N. Taylor, A. J. Hagan and H. L. Anderson, *Org. Biomol. Chem.*, 2003, **1**, 3851-3856.

66. G. J. Kavarnos, *Fundamentals of Photoinduced Electron Transfer*, Maruzen Co., Ltd., with Wiley-VCH, John Wiley & Sons, Inc., Tokyo, 1997.

67. J. Roncali, *Chem. Soc. Rev.*, 2005, **34**, 483-495.

68. Y. Shirai, Y. Zhao, L. Cheng and J. M. Tour, *Org. Lett.*, 2004, **6**, 2129-2132.

69. R. B. Breitenkamp and G. N. Tew, *Macromolecules*, 2004, **37**, 1163-1165.

70. H. Li, D. R. Powell, R. K. Hayashi and R. West, *Macromolecules*, 1998, **1998**, 52-58.

71. A. M. Funston, E. E. Silverman, J. R. Miller and K. S. Schanze, *J. Phys. Chem. B*, 2004, **108**, 1544-1555.

72. A. Khan and S. Hecht, *Chem. Commun.*, **2004**, 300-301.

73. S. T. Ellison, A. P. Gies and W. K. Nonidez, *Int. J. Polym. Anal. Charact*, 2005, **10**, 245-258.

3 Second Generation Polyelectrolytes: Synthesis and Sensing Assessments

3.1 Synthesis of a second generation cationic PPE and its small model analogue

In the proceeding chapter, through the synthesis of ionic (water-soluble) and neutral (non water-soluble) PPE polymers, a greater understanding of factors affecting the synthesis of such materials has been gained. The optimisation of a neutral PPE synthesis proved to be particularly instructive since long reaction times and high-purity starting materials enabled consistently pure materials to be isolated, with moderate molecular weights. Additionally, some typical photophysical and quenching properties of CPEs were reported. This information allowed us to consider key features that are desirable in a PPE sensor and how, by careful design of the PPE architecture, these can be achieved.

In order to design a synthetic polymer that could interact with the oppositely-charged biopolymer DNA, a facile route to a cationic PPE derivative was required. As detailed in the previous chapter during the synthesis of the cationic PPE **124**, we encountered difficulties when attempting to purify the ionic monomers synthesised by functionalising hydroquinone derivatives. We needed an alternative route to cationic monomers that would ideally allow for a versatile synthesis to functionalised PPEs to be achieved. The first task was to decide upon the type of PPE structure that would allow for the strongest interaction (ideally, this interaction should occur close to the conjugated backbone) with target analytes and then enable this interaction to be reported with high efficiency.

An important factor is the rigidity of PPEs which is central to the high mobility of excitons in such structures. The nature of the recognition units (i.e. whether they are charged or not), and their distance from the polymer backbone (Figure 3.1), is also crucial (as will be discussed in Chapter Four).

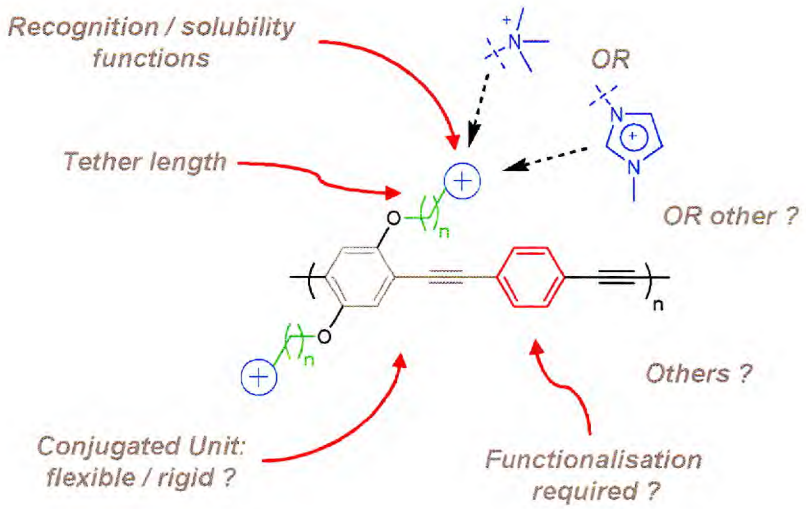

Figure 3.1 Important considerations in designing PPE architectures.

It was envisioned that by keeping the distance from the backbone to a minimum, efficient energy or electron transfer to quencher molecules would be realised. We opted to polymerise a cationic monomer which allowed rapid entry to the corresponding water-soluble PPE **155** (Scheme 3.1), without the need for polymer-analogous transformations. The cationic charges associated with the trimethylammonium groups and the polymer backbone are separated by a distance of only four bond lengths, so we reasoned the polymer should exhibit efficient electron transfer from the conjugated backbone to an electron-deficient quencher.

Importantly for the current purposes, the selected polymer system, in addition to being compatible with DNA sensing, is sufficiently flexible to allow the potential targeting of multiple enzymes depending on the choice of quencher molecule, as will be described in later sections (Chapter Five).

The design meant that water solubility could be achieved with the minimum number of functional groups present on the monomers: only one monomer required extensive functonalisation, allowing the final polymer and a related shorter analogue molecule, PE **154**, to be obtained in just four steps overall without any post-polymerisation reactions, as outlined in Scheme 3.1. In the first instance, the second aromatic ring in the repeat unit (in red, Figure 3.1) was not functionalised so as to minimise the number of steps required to synthesise the polymer. An ammonium group was selected to endow the polymer with cationic charges due to the ease with which it could be incorporated into the structure. The performance of the polymer was assessed against that of the smaller analogue molecule PE **154**.

The synthetic route to the second generation PPE **155** and its corresponding smaller model analogue PE **154** (Scheme 3.1) were based partly on a synthesis by Schanze *et al.*, published at around the same time, which described an anionic PPE derivative. In this paper, commercially available 1,4-bis(2-hydroxyethoxy)benzene (**151**) was converted to 1,4-bis(2-bromoethoxy)benzene (**152**) which was successfully iodinated with the hypervalent iodine species bistrifluoroacetate iodobenzene (**147**), under mild conditions, to yield 2,5-diiodo-1,4-bis(2-bromoethoxy)benzene (**140**). Schanze *et al.* then used monomer **140** to gain entry to a phosphate derivative, which they used to synthesise PPE **42** (see Chapter One). For our purposes, it was clear that monomer **140** could be modified using many different functional groups and this represented a better alternative to (monomer **122**) 2,5-diiodo-1,4-bis(2-bromo*propoxy*)benzene.

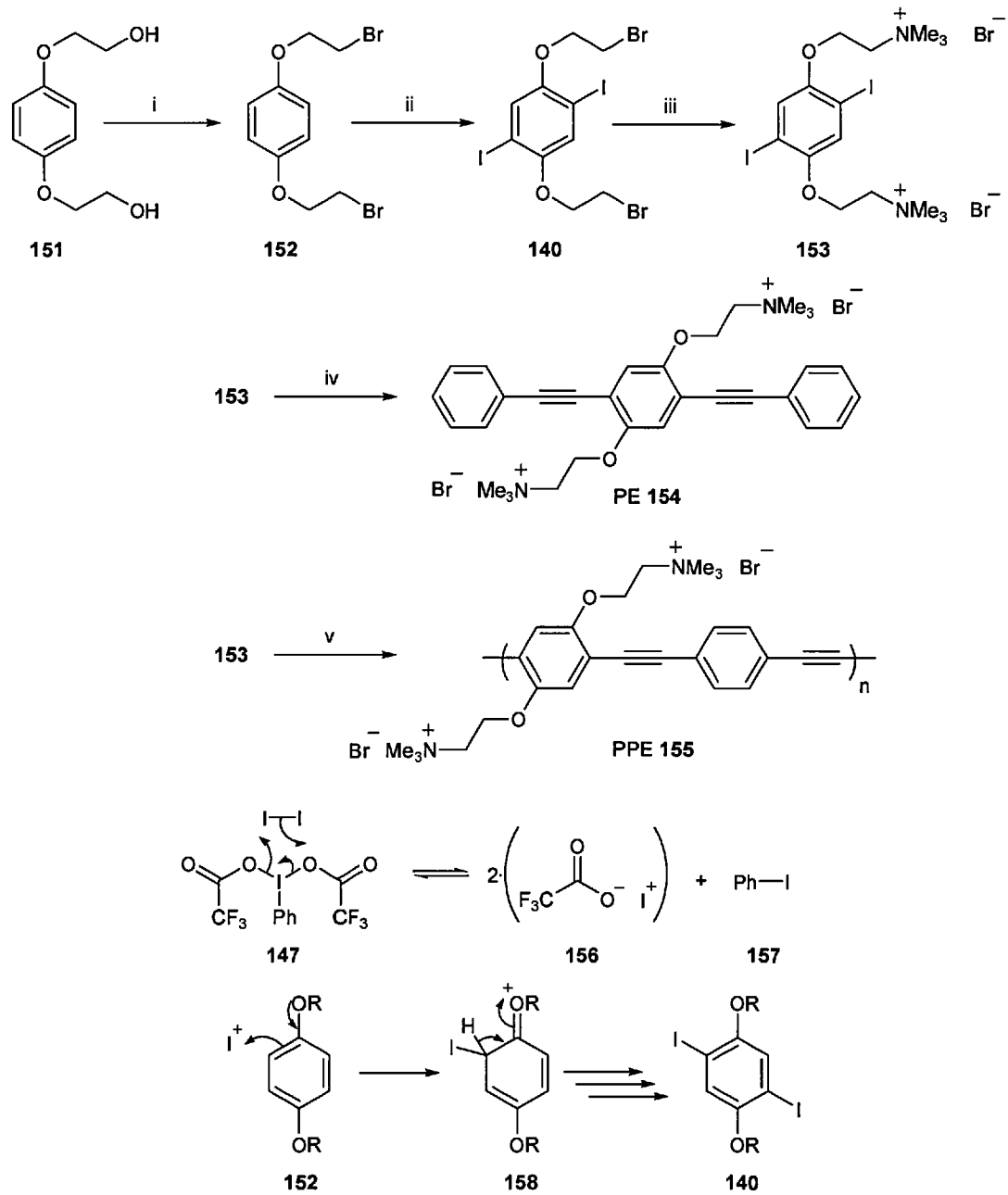

Scheme 3.1 Synthetic route to small model analogue PE **154** and polymer PPE **155**. Conditions: i) Br_2, PPh_3, MeCN, 20 °C, 4 **h**, 89%; ii) $PhI(CF_3CO_2)_2$ (**147**), I_2, CH_2Cl_2, 20 °C, 6 h, 84%; iii) 45% NMe_3 in H_2O, EtOH, acetone, reflux, 18 h, 64%; iv) phenylacetylene, $Pd(PPh_3)_4$, CuI, $^iPr_2NH$, $MeOH/H_2O$, reflux, 20 **h**, 75%; v) 1,4-diethynylbenzene (**106**), $Pd(PPh_3)_4$, CuI, $^iPr_2NH$, DMF, 50 °C, 24 h, 71%.

The basic structure of the starting material **151** is such that the side chains (1,4-bis(2-hydroxyethoxy)) are already in place and, after initial functionalisation of this diol to create convenient leaving groups (formation of 1,4-bis(2-bromoethoxy) groups), a series of subsequent nucleophilic substitution reactions provided quick access to the cationic monomer. The synthesis of

the cationic monomer **153** was completed by adapting the method of Schanze *et al.*[1] Bromination of the commercially available diol **151** proceeded smoothly and in 89% yield, 4% higher than the published result.

Iodination of **152** was accomplished using bis(trifluoroacetoxy)iodobenzene (**147**) in CH_2Cl_2 at room temperature (84% yield; a 21% increase on the reported yield). This convenient iodination method is useful in the synthesis of heterocyclic derivatives.[2] Iodine is unreactive in aromatic substitution reactions and requires the presence of an oxidising agent to generate a better electrophile (such as 'I^+').[3] Merkushev *et al.* postulated that the reaction between **147** and iodine generates trifluoroacetylhypoiodide (**156**).[4] A mechanism for this is suggested in Scheme 3.1. The driving force for the reaction is the favourable formation of iodobenzene. The iodination then proceeds in the usual manner for electrophilic aromatic substitution (Scheme 3.1).

The purity of both **152** and **140** was confirmed by TLC, where both molecules were observed as single spots, and ^{13}C NMR where all resonances could be assigned to the carbon atoms in the molecules. The other spectroscopy data matched that reported.[1] Treatment of **140** with an aqueous solution of trimethylamine gave the novel cationic monomer **153** as a white crystalline solid in 64% yield. The purity of the monomer was confirmed by TLC (one spot) which had to be run on neutral alumina plates due to the polarity of the monomer. The expected resonances in the ^{13}C NMR were all assigned with no impurities observed and the elemental analysis provided further evidence of the purity, with the carbon, hydrogen and nitrogen analyses being within 0.09% of their expected values.

The Sonogashira-Hagihara polycondensation of monomer **153** with 1,4-diethynylbenzene (**106**, synthesised as described in Chapter Two) was conducted in the presence of $Pd(PPh_3)_4$ and copper(I) iodide as co-catalyst. As previously reported by Swager *et al.*,[5] we also observed a more efficient polymerisation process when a small excess (5%) of the bisalkyne monomer was used (as described in Chapter Two). The optimised conditions described in the previous chapter were employed for this polymerisation. After rigorous deoxygenation using three freeze-pump-thaw cycles, the monomers and diisopropylamine were heated to 50 °C in a DMF/water mixture under an argon atmosphere for 24 hours. The resulting novel polymer was isolated by precipitation into cold methanol to furnish PPE **155** in 71% yield as a bright yellow solid. The yields for similar polymerisations are in the range 49 – 69%.[1,6] Other characterisation data for the polymer (*vide infra*) was consistent with the material being isolated cleanly.

The small model analogue PE **154** was prepared by a similar cross-coupling procedure involving monomer **153** and phenylacetylene, which resulted in a 75% yield after recrystallisation (the

typical range for similar reactions is 61 – 75%). The purity of the small model analogue was confirmed by TLC (one spot) and ^{13}C NMR where the spectrum contained all expected resonances. Exact NMR assignments were made using 2D NMR and by comparison to the small model analogue PE **133** (see section 3.3). Despite drying the monomer in a vacuum oven for several days, the elemental analysis indicated that water (3 water molecules per ammonium unit) was still present in the sample, which is indicative of the hygroscopic nature of the material.

The limited solubility of PPE **155** (at the mM concentration level required for NMR) resulted in a noisy ^{13}C NMR spectrum being recorded, which did not allow for complete structure assignment, but the ^{1}H NMR was consistent with the structure of the polymer shown in Scheme 3.1. It is important to emphasise that at the concentration level at which sensing experiments are conducted (≤ 10 μM) these materials display excellent solubility in both methanol and water. As previously described (Chapter Two), the ^{13}C NMR spectrum was checked for the presence of diyne defects (Figure 3.2). In the region of interest, only one triple-bond resonance can be observed, which suggests that the use of the Pd(0) catalyst prevented the formation of structural defects.

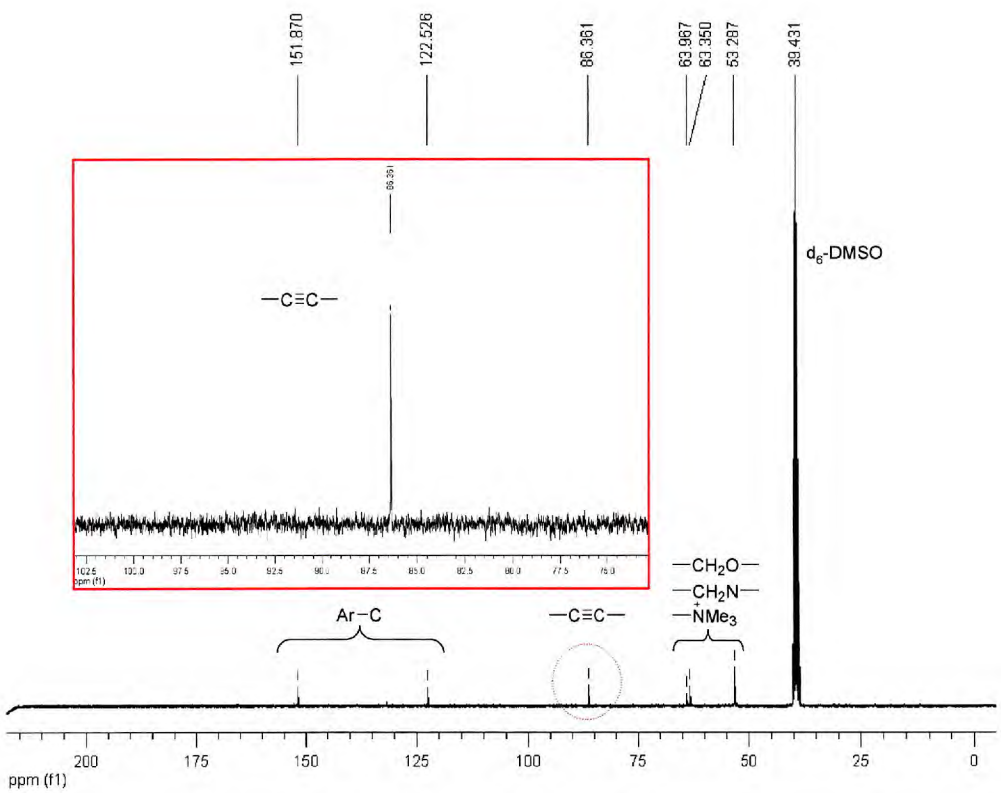

Figure 3.2 ^{13}C NMR spectrum of PPE **155** (100.6 MHz, d_6-DMSO, 298 K). The inset shows the region of potential diyne defects – in this case the only resonance present is assigned to the expected alkyne motif.

Determination of the molecular weight by GPC is problematic for PPEs due to the inherent rigidity of the polymer backbone and the difficulty of finding adequate chromatographic conditions that rule out aggregation effects, which invariably lead to an overestimate in the molecular weight.[7,8] GPC analysis of PPE **155** in DMF was not possible due to limited solubility at the concentration level (mM) required for chromatography but exchange of the bromide counter-ions for hexafluorophosphate anions slightly improved the solubility of the polymer in this solvent. This was evidenced in the ease with which the sample could be filtered and on standing for 24 hours, a reduced amount (not weighed) of the polymer precipitated out of the solution as compared with the unmodified material. This change allowed a molecular weight estimate of 7.5 kDa to be made relative to polystyrene standards. This implies an approximate degree of polymerisation of 13 repeat units, though this falls to 9 when a correction factor described by Bunz *et al.* is applied.[7,8] Other attempts at acquiring GPC data for PPE **155** are detailed in Table 3.1. In general unsatisfactory chromatograms were obtained with unmodified PPE **155**, with the polymer undetected as it passed through the column and before the detectors. The addition of 10 mM LiCl to an eluant system is known to reduce intermolecular interactions in polar solvents, by screening charges.[9] However, in our case the addition of this salt had no beneficial effect. The flow rate changes detailed in Table 3.1 reflect alterations in the solvent flow through the instrument and had no affect on the ability to detect the polymer.

Table 3.1 Details for attempts at GPC analysis of PPE **155**.

Entry	Solvent	Conditions	Result[a]
1	H_2O	1% NaN_3	polymer undetected
		flow rate of 0.5 mL min^{-1} at 50 °C	
2	DMF	no salt added	polymer undetected
		flow rate of 1.0 mL min^{-1} at 40 °C	
3	DMF	10 mM LiCl	polymer undetected
		flow rate of 1.0 mL min^{-1} at 40 °C	
4[b]	DMF	flow rate of 0.5 mL min^{-1} at 40 °C	weak polymer peak detected

[a]Using the RI detector, which was the only detection technique available; [b]modification of the polymer by ion exchange (see text for details).

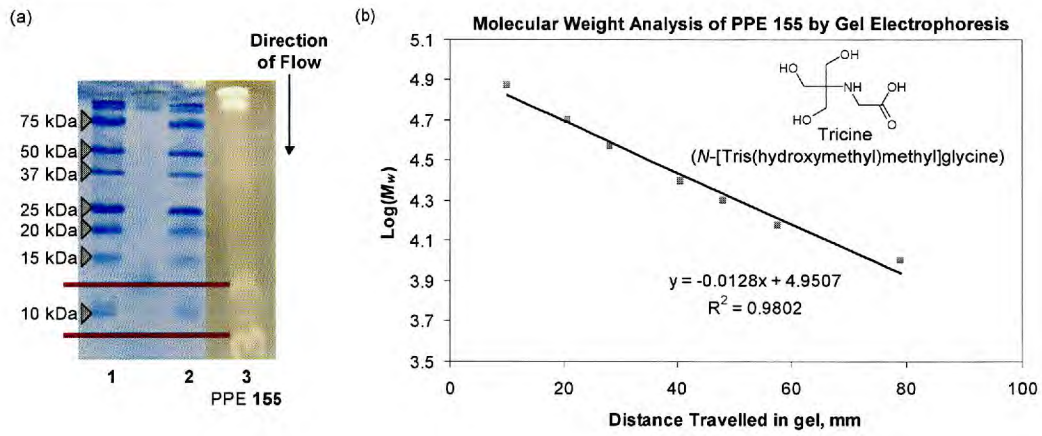

Figure 3.3 Determination of the molecular weight of PPE **155** by SDS gel electrophoresis, relative to denatured protein markers. (a) Lanes 1 and 2 show the protein standards used and lane 3 displays the progress of PPE **155**, through the gel, after coomassie staining (for details, see the Experimental section). Though the entire polymer sample did not enter the gel, a sufficient amount did penetrate allowing distributions to be distinguished. (b) The calibration curve constructed by considering the migration distance of the standards in the gel. *Inset*; structure of the gel used.

Attempts were also made to determine the molecular weight for PPE **155** *via* gel electrophoresis (Figure 3.3).[10] This technique separates charged macromolecules in a supporting medium, such as agarose or polyacrylamide gel. In this case the most suitable gel was tricine and the protein standards used were presumed to be fully denatured under the experimental conditions (the buffer contained sodium dodecyl sulphate, SDS) and so in this state can be considered as rigid-rods. This allows for a more accurate estimate of the molecular weight for the synthetic polymer, which is similarly considered as a rigid-rod polyelectrolyte. The results from this analysis revealed that two main molecular weight distributions were present, at 7100 Da and 12200 Da. The former is consistent with the result obtained from GPC analysis, but the second distribution was not detected using this technique, thus showing the benefit of the electrophoresis method.

The thermal decomposition of PPE **155** was monitored by thermal gravimetric analysis (TGA) which revealed a distinct two-step weight loss (Figure 3.4). Between ~ 275 – 480 °C, a 69% weight loss is observed which is then followed by a more gradual loss (34%) between ~ 480 – 700 °C.

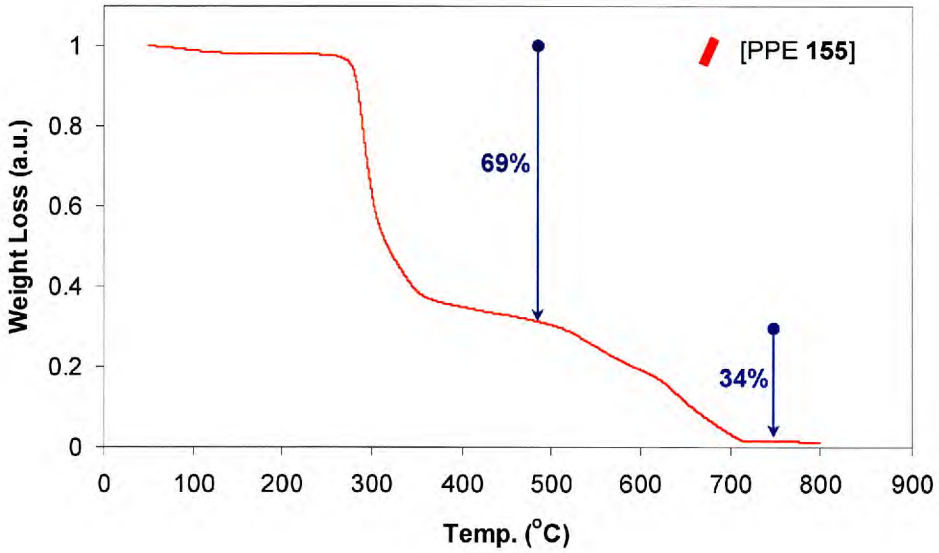

Figure 3.4 Thermogravimetric analysis (TGA) of PPE **155** (heating rate of 10 °C/min, under N_2).

The 69% weight loss could be attributed to the loss of NMe_3, HBr and water from PPE **155**. This correlates with the elemental analyses data for PPE **155**, which indicated the presence of approximately 23 water molecules associated with the polymer. In a recent report, Lu *et al.* analysed a phenylene ethynylene benzothiadiazole alternating copolymer by TGA and demonstrated that it had high thermostability.[11] A weight loss of only ~ 5% was noted up to a temperature of 321 °C. Bailey and Swager also considered the thermal decomposition of a dialkoxy PPE which contained a pentitycene motif and recorded a weight loss of 5% at a temperature > 200 °C.[12] These results are in close agreement with those measured for PPE **155**, where a 5% weight loss was observed at a temperature of 278 °C. DSC analysis of PPE **155** indicated decomposition.

3.2 Towards phosphate selectivity – synthesis of an isothiouronium small model analogue

The ultimate aim of the work was to develop a polymer-based sensor that, in the first instance, could be used to selectively detect either *ss*/*ds*-DNA or -RNA in solution and then go on to discriminate between these strands, allowing identification of single base-pair mismatches. In order to build this kind of selectivity into conjugated polymers, the reacting monomers have to be functionalised with carefully selected groups that have innate phosphate group recognition abilities.

In this regard, the reporting of the recognition process by the polymeric material could be envisaged to occur in one of two ways; the interaction of the CP with the target material could

trigger a quenching response, which could be used to determine the extent/nature of the binding process. Alternatively, if the CP was appropriately functionalised, contact with target analytes could be designed to lead to a rise in emission from the polymer. The ideas are presented in Figure 3.5.

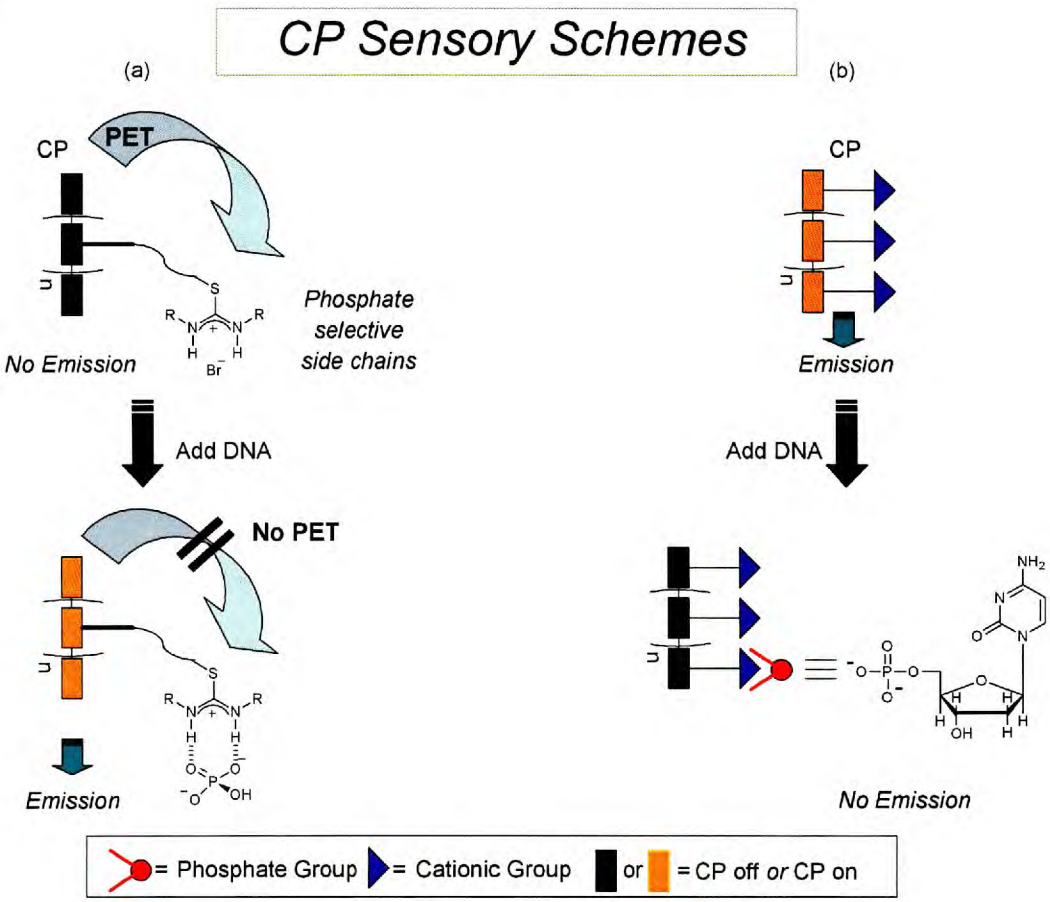

Figure 3.5 Summary of strategies for ion selectivity; (a) the 'turn-on' and (b) the 'turn-off' approaches.

Literature precedent for the latter idea exists and stems from the chemistry of anion recognition, which has long been an important aspect of supramolecular chemistry. Phosphate-selective receptors have been extensively studied in this regard, due to their potential use in biological applications.[13] To obtain selective binding, several recognition motifs have been studied including amides, ureas, thioureas, imidazoliums, and guanidiniums.[14] All these moieties bind to the target anion through hydrogen bonding and electrostatic interactions.[15] Recently there has been an additional receptor added to this group which has shown very selective binding affinities for phosphates anions. The isothiouronium group (which is effectively a sulphur analogue of the guanidinium group) was first shown as a promising candidate in this area by Yeo *et al.*,[16] who reasoned that the large dipole moment and the increased acidity of the NH groups due to *S*-alkylation would lead to a stronger binder. Since this disclosure, several groups have demonstrated

that this moiety has superior affinity for oxoanions including phosphate groups.[17] Recently, Teramae *et al.*[14,18,19] have reported an interesting use of this receptor, in combination with a fluorophore, to generate a chemosensing device. The sensor uses an isothiouronium-based receptor tethered to a naphthalene/anthracene fluorophore as a signalling device; upon exposure of the chemosensor to phosphate salts, an approximate 10-fold increase in the emission intensity resulted. The authors attributed this increase in emission to suppression of the PET effect, induced by the isothiouronium group, upon addition of the phosphate ions. This system acts effectively as an electron donor (naphthalene unit) and acceptor (isothiouronium) pair. They also identified the optimal separation needed between the isothiouronium and naphthalene units. An ethylene spacer provided the best balance between efficient PET (and therefore fluorescence signalling) and stability.[19] This result, and similar findings, (e.g. the detection of alkali metal ions, by fluorescence enhancement)[20] persuaded us to pursue a strategy whereby the incorporation of isothiouronium binding units along the PPE backbone, would lead to a similar enhanced response.

The observation of no emission (or severely quenched emission) in the absence of phosphate ions followed by an increase in emission upon addition of such anions is a desirable effect. This is because it is easier to detect increases in emission intensity as they are less likely to be due to artefacts, unlike emission quenching, which can be triggered by a variety of effects including changes in the ionic strength of the solution. The noteworthy result described by Teramae *et al.*, if applied to the highly sensitive CPE systems, would provide an alternative to the traditional 'turn-off' PPE sensors.

The first step in obtaining an isothiouronium derivitised polymer was to functionalise the monomers accordingly. The versatile monomer intermediate **140** was the ideal candidate for grafting on a binding group and the isothiouronium moiety **159** was synthesised in 79% yield (Scheme 3.2). The structure of this novel monomer was confirmed by ^{1}H and ^{13}C NMR which also indicated that the molecule was produced cleanly as confirmed by elemental analysis evidence (the measured carbon percentage was within 0.01% of the expected calculated value).

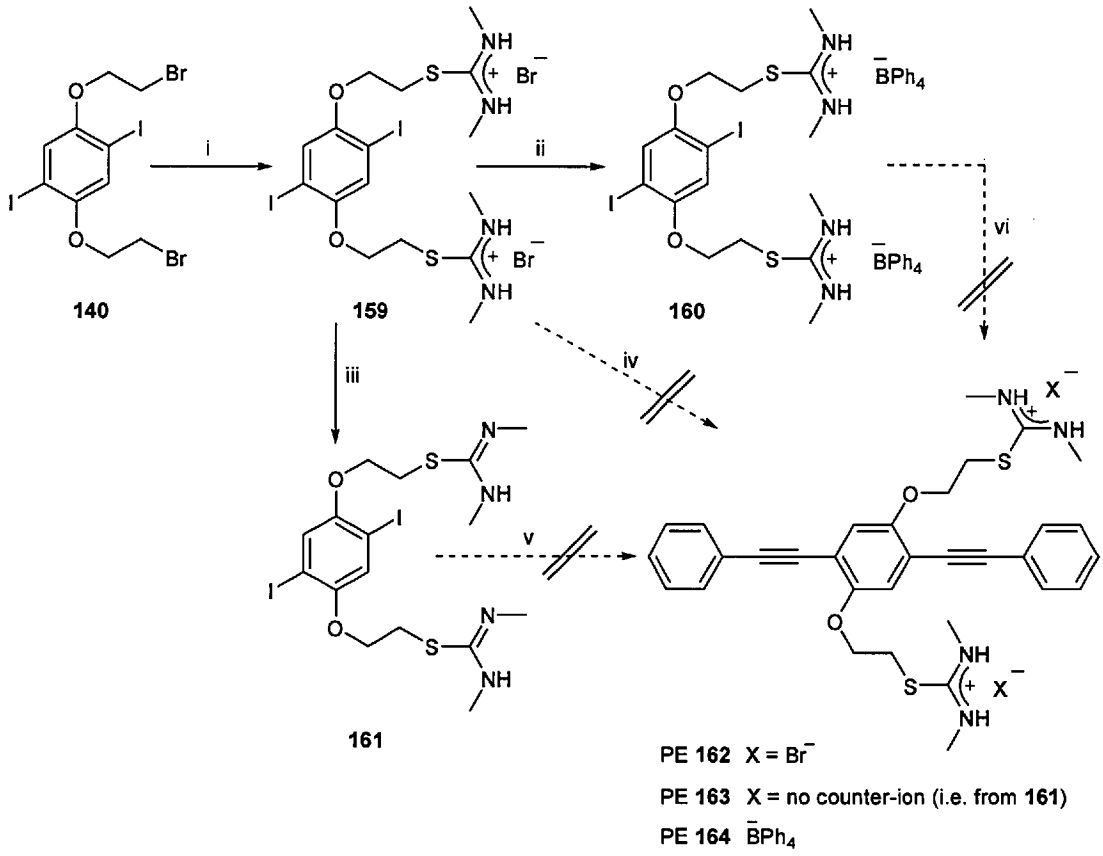

Scheme 3.2 Synthesis of isothiouronium monomers and attempted synthesis of isothiouronium-containing small model analogue. Conditions: i) 1,3-Dimethylthiourea (**122**), MeOH/MeCN, 80 °C, 24 h, 79%; ii) MeOH (80 °C), $NaBPh_4$, 5-10 mins, 62%; iii) 2.0 M NaOH, H_2O (95 °C), 5-10 mins, 71%; iv) phenylacetylene, $Pd(PPh_3)_4$, CuI, $^iPr_2NH$, MeOH/H_2O, reflux, 20 h; v) phenylacetylene, $Pd(PPh_3)_4$, CuI, $^iPr_2NH$, MeOH, reflux, 20 h; vi) phenylacetylene, $Pd(PPh_3)_4$, CuI, $^iPr_2NH$, MeOH, reflux, 20 h.

Attempts to make the model isothiouronum sensor PE **162** directly from **159** resulted in a dark oily residue, presumably from catalyst decomposition during the cross-coupling reaction. Various solvents and reaction conditions were tried without success. A variant of the thiouronium moiety was also synthesised, by addition of concentrated sodium hydroxide solution to a hot aqueous solution of **159** (Scheme 3.2). However, this neutral derivative (**161**) also failed to give the desired cross-coupled product (PE **163**), yielding similar results. ^1H NMR analysis indicated that in both cases, the starting materials were still present at the end of the reaction along with resonances in the aromatic region which could not be identified.

In a further attempt to obtain an isothiouronium-containing small model analogue, monomer **160** was synthesised by addition of excess sodium tetraphenyl borate to a methanolic solution of **159**. However, the ion-exchanged product proved no better at undergoing the cross-coupling reaction (to yield PE **164**), with similar dark, oily residues isolated. ^1H NMR suggested that the starting

material had been consumed but indicated no product formation and the presence of an unidentifiable material.

Due to time constraints, no attempts were made to identify the unwanted residues that were isolated. However, we reasoned that the interaction of the thiouronium groups (specifically the sulphur atom) with the metal catalyst, could lead to either decomposition or complete deactivation of the metal catalyst. This is reinforced by examples of reduced efficiency for similar reactions in the presence of sulphur. During the synthesis of tetrathiafulvene cruciform structure PE **167**, the yield was improved by employing modified cross-coupling conditions (extensive reaction optimisation, resulting in a different palladium catalyst being employed: $PdCl_2(PhCN)_2$)[21,22] along with ultrasonication, which is known to enhance catalyst turnover in Sonogashira couplings (Scheme 3.3).[23] Despite these efforts, only a small increase in the yield was observed, from 26% to a modest 56%, which is low compared with most Sonogashira coupling reactions.[21]

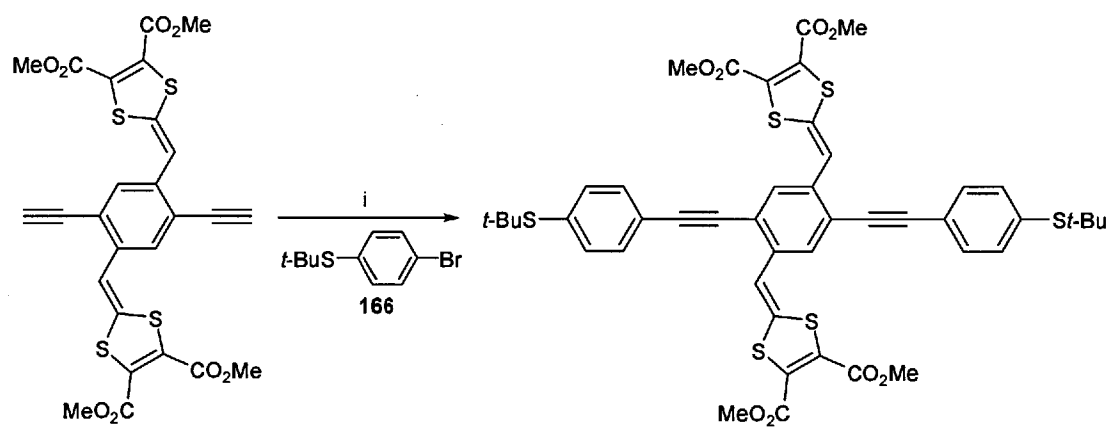

Scheme 3.3 Nielsen *et al.*'s synthesis of a tetrathiafulavene cruciform.[21] Conditions: i) **166**, $[PdCl_2(PhCN)_2]$, CuI, $P(^tBu)_3$, $^iPr_2NH$, NaOMe, THF, toluene, ultrasound, 56%.

In light of the findings by Nielsen *et al.*[21] and in an effort to avoid the cross-coupling problems encountered with monomers **159** – **161**, we opted to protect the isothiouronium motif in these molecules. Nielsen *et al.* noted that protection of the terminal sulphur atoms with *t*-Butyl groups improved their resistance to strongly acidic or basic conditions.[21] In our case, the sulphur atom in monomers **159** – **161** is part of an isothiouronium motif and so is not analogous to the Nielsen example, but their work suggested that given the basic Sonogashira conditions, some protection of the recognition group may be necessary.

To examine this idea the protected thiourea **168** was isolated by BOC protection of monomer **161** (Scheme 3.4). Unfortunately, the new monomer was not obtained cleanly as evidenced by TLC

(two spots) and ^{1}H NMR where the impurity gave rise to a resonance in the aromatic region (7.18 ppm) and as a shoulder on the resonance centred at 4.15 ppm (-OCH_2 resonance of **168**). Several attempts to purify the monomer were made. The material appeared to dissolve in hot ethanol and precipitate from the same solvent when the solution was cooled. Recrystallisation of this monomer from ethanol appeared to proceed smoothly, but when analysed by ^{1}H NMR the same impurities remained. Though the isolated material was visible as two spots, separation by column chromatography proved difficult as the products ran closely (separated by less than $R_f = 0.1$) in the most suitable solvent ($CHCl_3$). The different fractions displayed narrow separation when travelling down the column (visualised using a short-wavelength, 254 nm UV lamp) but gradually coalesced as they neared the middle of the column. ^{1}H NMR of the resulting fraction indicated that the separation had not been successful.

It was hoped that the cross-coupling reaction with phenylacetylene, to give the protected PE **169**, could proceed smoothly as the propensity for interaction of the isothiouronium groups with the palladium catalyst would be reduced (Scheme 3.4). We intended to separate the impurity from PE **169** at the end of the reaction. The small model analogue PE **169**, obtained as a fluorescent material in poor yield, could not be isolated cleanly. Attempts to perform column chromatography (in acetone) failed to separate the product from the other materials present (TLC indicated the presence of two other materials, possibly resulting from partial or full deprotection of the molecule).

Column chromatography seemed appropriate for purifying PE **169** as it allowed us to exploit the apparent higher polarity of the product which had an R_f value of ~ 0 in hexane. The impurities were then washed through the column, as they ran well above the product, and then the product was washed through with acetone. Despite this, the compound still contained trace amounts of impurities as judged by ^{1}H NMR, with the resonances appearing in the same position as for monomer **168**. Attempts to purify the product by recrystallisation from hexane also failed to affect the necessary purification with the unwanted materials still being present (and yielding the same results by ^{1}H NMR).

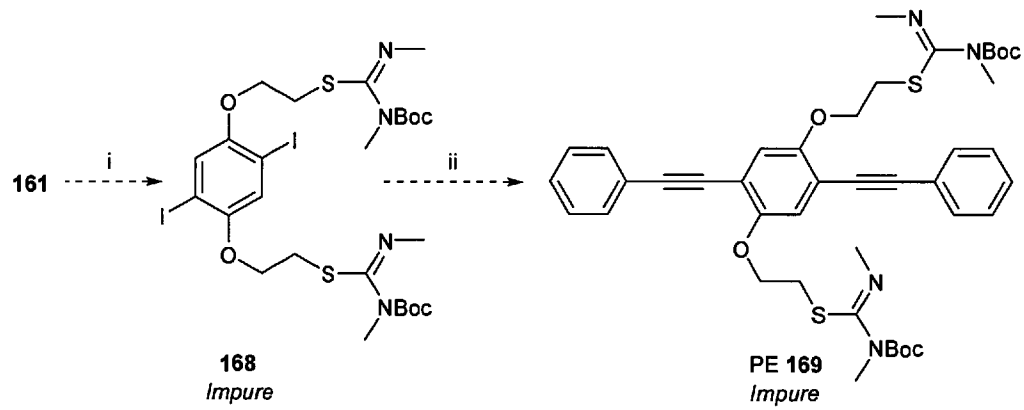

Scheme 3.4 Attempted synthesis of a protected small model analogue PE **169**. Conditions: i) $(Boc)_2O$, NaH, 20 °C, 19 h; ii) phenylacetylene, $Pd(PPh_3)_4$, CuI, $^iPr_2NH$, MeOH, reflux, 20 h.

An alternative route to the protected small model analogues was devised (Scheme 3.5). It was anticipated that protecting the thiourea prior to grafting onto monomer **140**, would avoid problems associated with the purification of moieties like PE **169**. The bis BOC protected **171** was isolated in 72% yield after column chromatography; however the attempt to isolate the tetra BOC protected isothiouronium monomer **172** by treating monomer intermediate **140** with **171** resulted in complete recovery of the starting materials even after prolonged heating at elevated temperatures (> 100 °C). It was anticipated that the nucleophilicity of the thiourea was diminished as the BOC groups 'tied-up' the lone-pair of electrons on the nitrogen atoms of the thiourea moiety. The expectation was vindicated when the same reaction was repeated with the commercially available demethylated thiourea **173**.

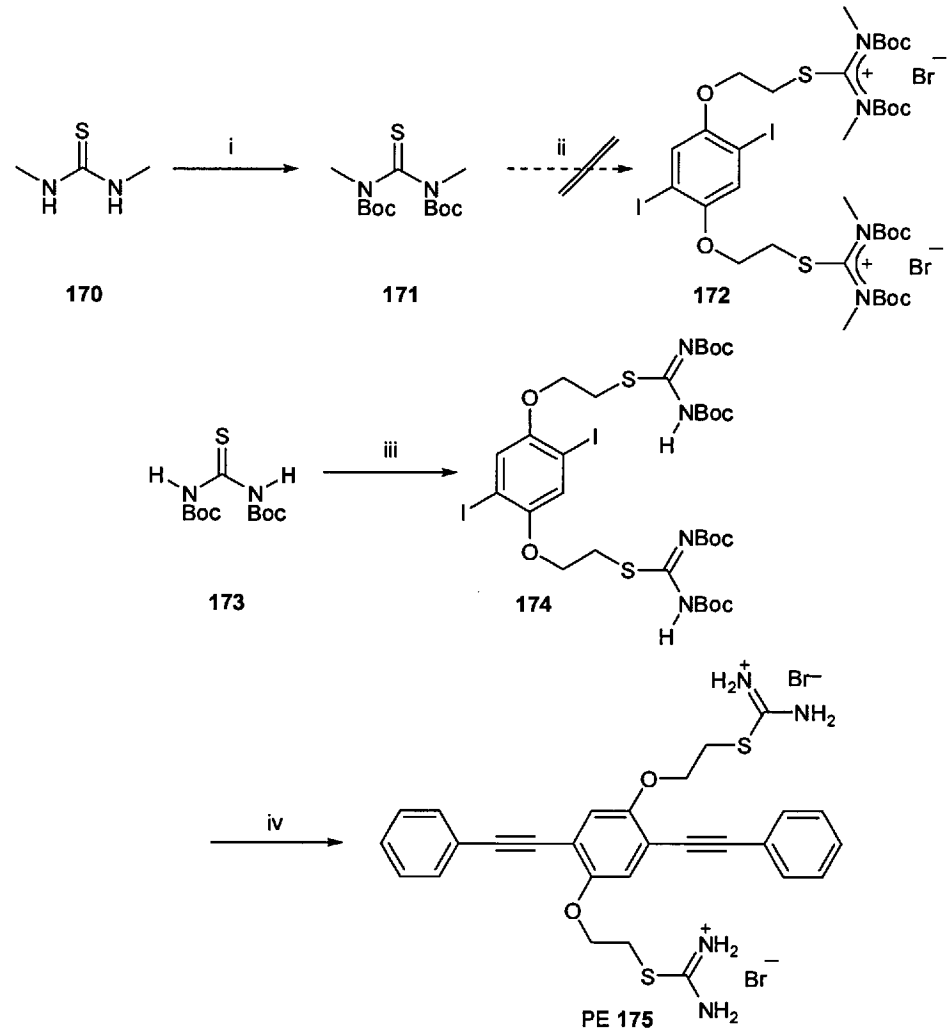

Scheme 3.5 Synthesis of protected isothiouronium monomers and a corresponding small model analogue PE **175**. Conditions: i) $(Boc)_2O$, NaH, THF, 20 °C, 19 h, 72%; ii) **140**, MeCN, 85 °C, 48 h; iii) **140**, NaH, THF, 20 °C, 19 h, 96%; iv) phenylacetylene, $Pd(PPh_3)_4$, CuI, $^iPr_2NH$, toluene, 20 °C, 20 h, 69%.

Presumably the un-substituted thiourea **173** possesses a more nucleophilic thiocarbonyl group compared to **171** (Scheme 3.5) and as a result went on to react with **140** efficiently to give the tetra BOC protected monomer **174**. The same palladium cross-coupling conditions as employed in the synthesis of PE **154** (Scheme 3.1) were used to couple **174** with phenylacetylene, which furnished the small model analogue PE **175**. Complete deprotection occurred during the reaction, presumably due to the presence of the metal which could serve as a Lewis acid. This was confirmed by NMR, where there was no evidence of the ^1H resonances that appeared at ~ 1.5 ppm due to the *t*-butyl groups of the BOC moiety.

The cleavage of acetate groups during a similar Sonogashira cross-coupling reaction has been witnessed previously.[24] As in this case, it is presumed that the metal can serve as a Lewis acid, allowing facile cleavage of the protecting group.

Having encountered potential compatibility problems between the cross-coupling chemistry of the Sonogashira reaction in the presence of isothiouronium groups, we sought to explore other potential anion receptors. A common alternative includes the guanidine unit which was identified as a suitable target as there are numerous reports in the literature regarding the use of this moiety as a phosphate receptor and as an interesting structural motif in various natural products (e.g. it is present in the amino acid arginine).[15]

Additionally, the chemistry of guanidines is well established and many reports detail how fully protected guanidines can be incorporated into natural products[25] and other biologically relevant compounds.[26] The importance of protecting guanidines is clear; the native gaunidinium ion is protonated at physiological pH and remains protonated over a large pH range (pk_a = 13.5).[15] Less basic (and therefore less polar) derivatives are sought which are amenable to easy purification by, for example, column chromatography.[26]

Several studies have been published describing ways of incorporating this structural moiety into various targets, usually *via* electrophilic amidine species.[26] Our aim was to combine the chemistry of guanidines with our existing methods for functionalising monomer intermediates. It was envisaged that the monomer intermediate **140** could be used as a starting point for a receptor molecule that contained a guanidine unit. The synthesis of the novel tetra BOC protected guanidinium derived monomer **177** was based on a preparation described by Feichtinger *et al.*[27] and was accomplished in 93% yield, as detailed in Scheme 3.6. ^{1}H NMR data was consistent with the expected structure. Subsequent coupling of this molecule with phenylacetylene, using the same cross-coupling conditions as employed in the synthesis of PE **154**, resulted in an impure sample of PE **178** being recovered. Multiple resonances could be attributed to this impurity; a resonance at 3.48 ppm (multiplet) along with shoulders on the resonances at 4.37 ppm 7.04 ppm could be observed. A similar result occurred for the polymerisation (leading to PPE **179**), where unwanted broad resonances were visible at 4.19 ppm and 4.33 ppm as well as another broad resonance at ~ 1.05 ppm. Additionally, it appeared that some deprotection had occurred, though quantifying this was complicated by the BOC resonance being overlapped by the water resonance.

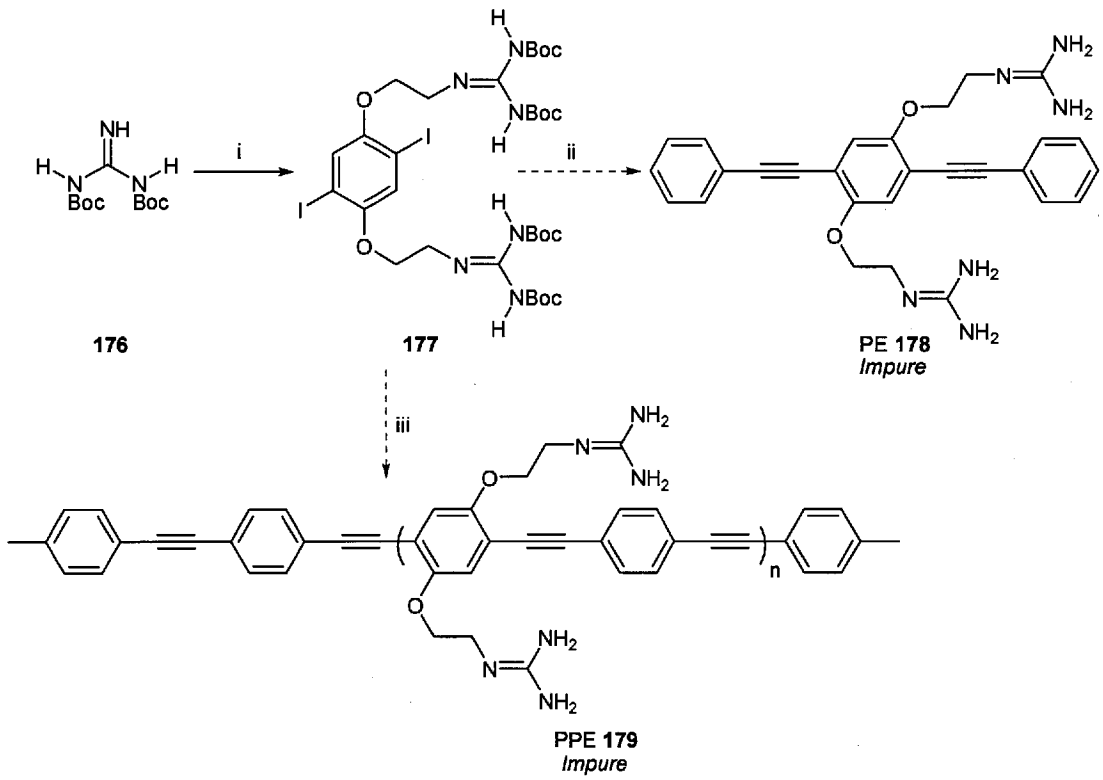

Scheme 3.6 Attempted synthesis of a guanidinium-containing PE and PPE. Conditions: i) **140**, NaH, THF, 20 °C, 18 h, 93%; ii) phenylacetylene, $Pd(PPh_3)_4$, CuI, $^iPr_2NH$, DMF, 20 °C, 20 h; iii) 1,4-diethynylbenzene (**106**), 4-iodotoluene (**149**), $Pd(PPh_3)_4$, CuI, $^iPr_2NH$, DMF, 50 °C, 90 h.

For both the small model analogue PE **178** and the polymer PPE **179** it is possible that some of the 'extra' resonances observed in the ^1H NMR spectra could be attributed to the different structures that would result from partial deprotection. There was insufficient time to pursue further purification protocols and as both materials along with PE **175** were un-optimised (from an ion-detection standpoint) we decided to analyse PE **175**, which was isolated cleanly, to learn about how its emission responds upon exposure to phosphate ions. The findings are detailed in section 3.4.

3.3 Synthesis and characterisation of a neutral water-soluble PPE and its corresponding small model analogue

As discussed in Chapter One, neutral water-soluble CPs could serve as useful alternatives to ionic versions for biosensing applications, as non-specific interactions may be minimised. As a result, different examples of this class of polymer have been published, based on poly(thiophene) and poly(phenylene ethynylene) backbones (detailed in Chapter One). In order to gain a better understanding of the molecular weight profile of the second generation PPEs produced and to accurately characterise these new materials by NMR, a novel neutral water-soluble PPE and its

corresponding small model analogue PE **181** were synthesised (also novel and shown in Scheme 3.7) using the optimised polymerisation conditions detailed in Chapter Two (section 2.3.2). The polymer, PPE **182**, had increased solubility in water, DMF and THF which allowed for easy characterisation by NMR and GPC, unlike the previously synthesised PPEs.

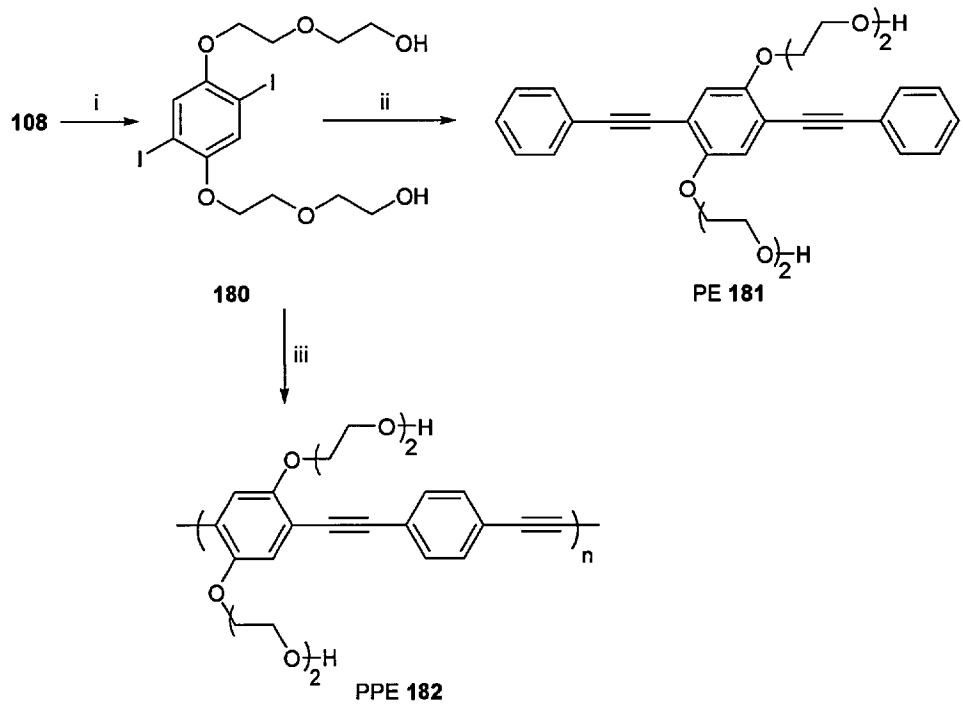

Scheme 3.7 Synthesis of a neutral water-soluble PE and PPE. Conditions: i) 2-(2-Chloroethoxy)ethanol, K_2CO_3, DMF, 75 °C, 6 d, 60%; ii) phenylacetylene, $Pd(PPh_3)_4$, CuI, $^iPr_2NH$, DMF, 20 °C, 44 h, 83%; iii) 1,4-diethynylbenzene (**106**), $Pd(PPh_3)_4$, CuI, $^iPr_2NH$, DMF, 45 °C, 32 h, 87%.

Despite the improved solubility of PPE **182** in organic solvents, compared to the previously described PPEs, the ^{13}C NMR displayed a high level of noise. The alkyne region contained very weak signals due to the expected triple-bond resonances, but the nature of the spectrum did not allow for complete assignment and it was not possible to check for diyne defects. The unsatisfactory ^{13}C NMR spectrum suggested that the rate of molecular tumbling of the polymer had been reduced possibly by aggregation effects.

The increased solubility of PPE **182** in DMF and THF allowed for determination of the molecular weight by GPC (Figure 3.6a and Figure 3.6b).

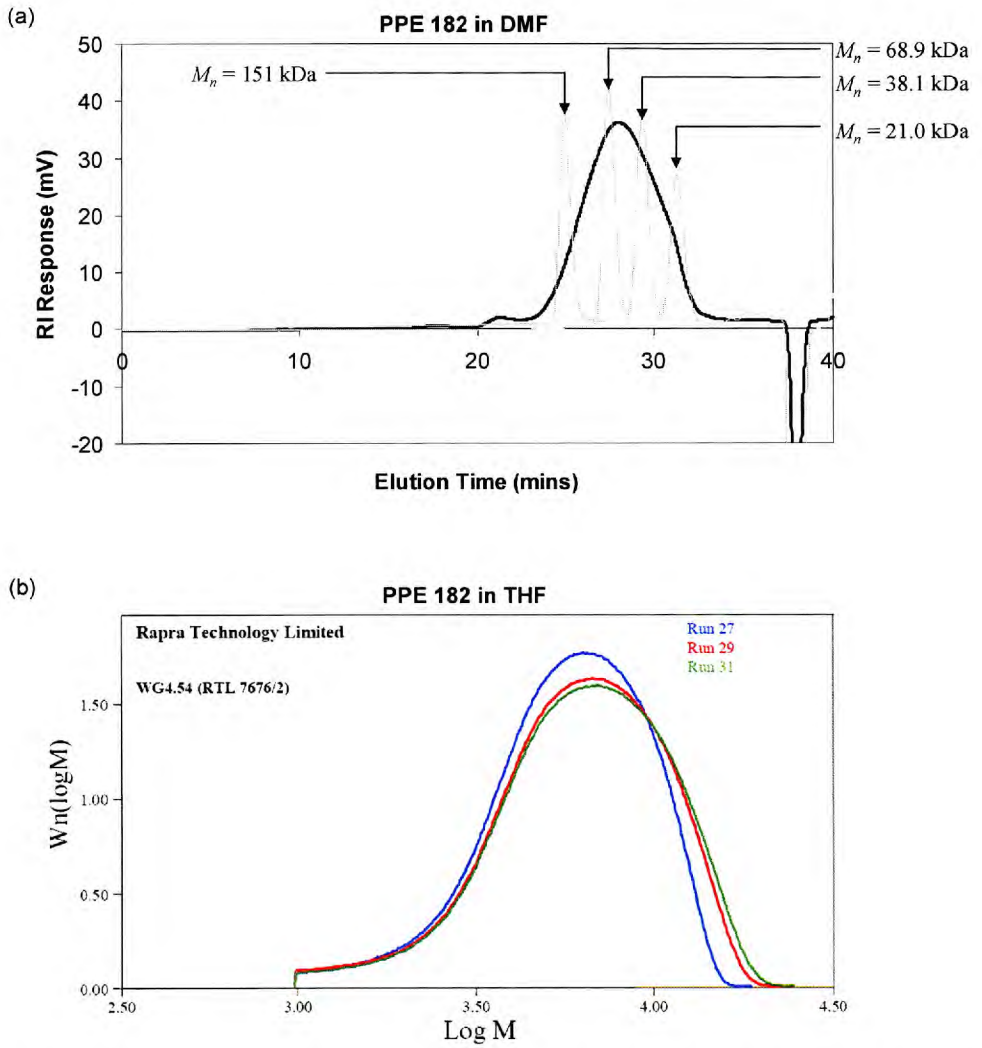

Figure 3.6 (a) GPC chromatogram for PPE **182** (DMF at 40 °C, 0.5 mL/min, RI detector); traces in light grey correspond to PS standards. (b) Molecular weight distribution curve for PPE **182** (in THF at 40 °C, 0.5 mL/min, RI detector), courtesy of Rapra Ltd; M_n = 5100 Da, M_w = 6800 Da, PDI = 1.4.

The number-average molecular weight of PPE **182** was estimated by GPC (DMF as eluant; Figure 3.6a) to be 59.8 kDa (relative to polystyrene standards) corresponding to an approximate degree of polymerisation of 147 repeat units, (the correction factor described by Bunz *et al.* reduces this to 103 repeating units).[7,8] The broad molecular weight distribution is consistent with such polycondensations,[8] but despite the apparent good solubility, some aggregation effects during the chromatography, can not be ruled out. A small sample of PPE **182** was sent to an external polymer analysis laboratory where GPC was performed in THF (the polymer displayed good solubility in the solvent). Though not the ideal solvent for this polymer, a small quantity did dissolve after prolonged heating and gave rise to the curves shown in Figure 3.6b. An appreciable amount of the polymer sample remained undissolved, even after heating and standing and this is likely to be the

higher molecular weight material, which could explain the large discrepancy between the GPC results for the THF and DMF systems.

The thermal decomposition of PPE **182** was monitored by TGA (shown in Figure 3.7). In contrast to that recorded for PPE **155**, minimal weight loss (41% in total, up to a temperature of 800 °C) was observed over the heating range, with the only significant losses occurring at between 100 – 360 °C (~ 10%) and 304 – 439 °C (~ 20%), demonstrating the increased thermal stability of this polymer compared to PPE **155**. The first of these weigh losses can be correlated with the loss of a small amount of water from the polymer sample, as confirmed by elemental analysis for this material.

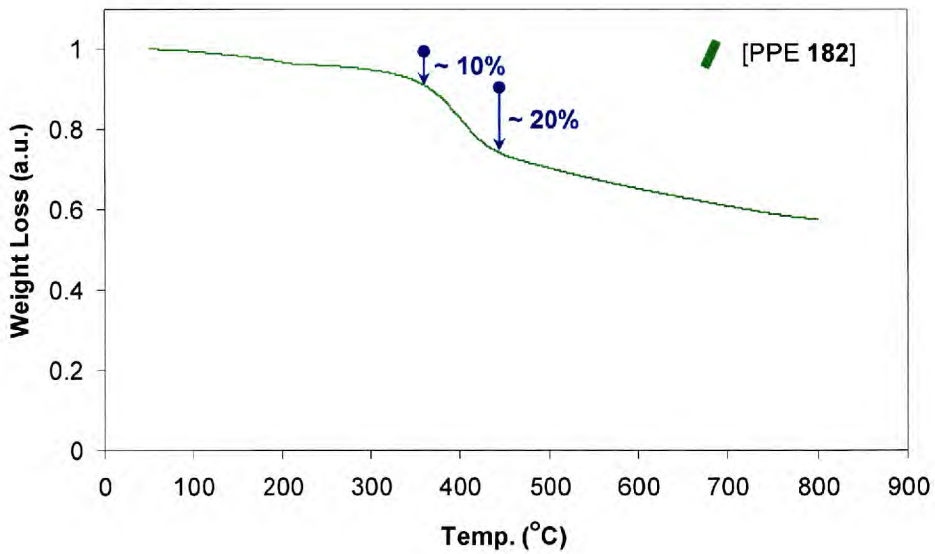

Figure 3.7 Thermogravimetric analysis (TGA) of PPE **182** (heating rate of 10 °C/min, under N_2).

The result in Figure 3.7 can be evaluated against literature examples (see section 3.1). Compared with the polymer described by Lu *et al.* (a PPE/benzothiadiazole copolymer, where a weight loss of 5% was recorded at a temperature of 321 °C)[11] and the pentiptycene-containing dialkoxy PPE first reported by Bailey and Swager (where the temperature at a weight loss of 5% was > 200 °C),[12] PPE **182** displays comparable thermal stability. In this case, a 5% weight loss corresponds to a temperature of 293 °C.

3.4 Spectroscopic investigation of the 'turn-on' effect for an isothiouronium small model analogues

In this section, the results from investigations into the fluorescent enhancement effect displayed by small model analogue PE **175** are reported.

The small model BOC-protected isothiouronium analogue PE **169** and the polymeric guanidinium analogue PPE **179** were not investigated in any quenching/un-quenching experiments as they could not be obtained in a pure form. However, despite the presence of the impurity isolated together with guanidinium small model analogue PE **178** (detailed in section 3.2), this novel material was also analysed in the same way as for PE **175** because there are no reports of guanidinium groups used as emission quenchers in an analogous way to the well documented role played by isothiouronium derivatives.

The absorption and emission spectra for PE **175** are shown in Figure 3.8 and are similar to those observed for the structurally similar dialkoxy derivative PE **154**. This was expected as changes to the peripheral functional groups would not alter the emission which emanates from the conjugated phenylene ethynylene unit.

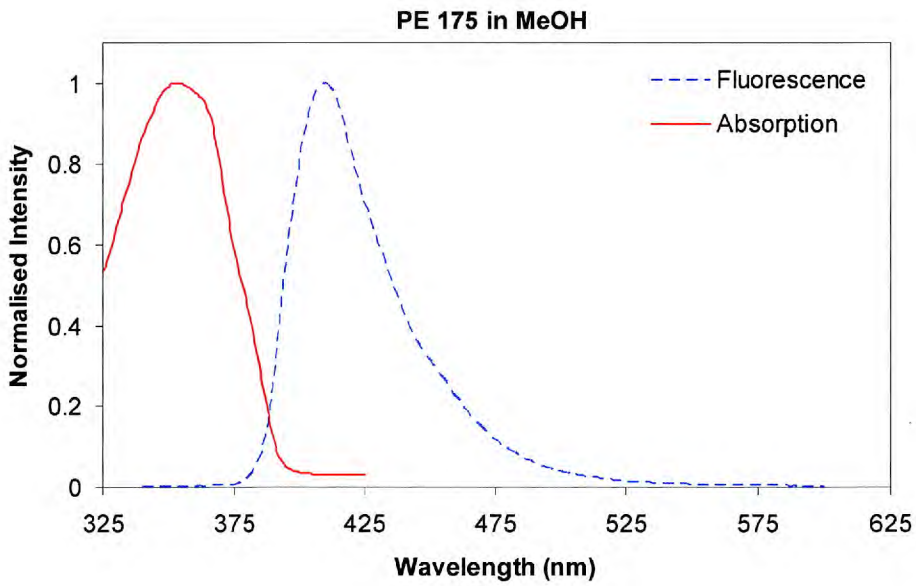

Figure 3.8 Normalised absorption and emission spectra, in methanol, of a 10 μM solution of PE **175**.

This small model analogue was highly soluble in DMSO and methanol but *not* water. The respective absorption and emission peaks are: 354 and 410 nm. The isothiouronium model

analogue PE **175** was analysed for a 'turn-on' effect. Based on similar studies it was anticipated that this material might behave as a 'turn-on' sensor – i.e. a fluorescence enhancement would be observed upon exposure of PE **175** to oxoanions such as phosphate ions. The emission spectra of a 10 μM solution of PE **175** in non-degassed methanol is shown in Figure 3.9 at increasing concentrations of potassium dihydrogen phosphate (**PDP**) as its [18-crown-6] salt.

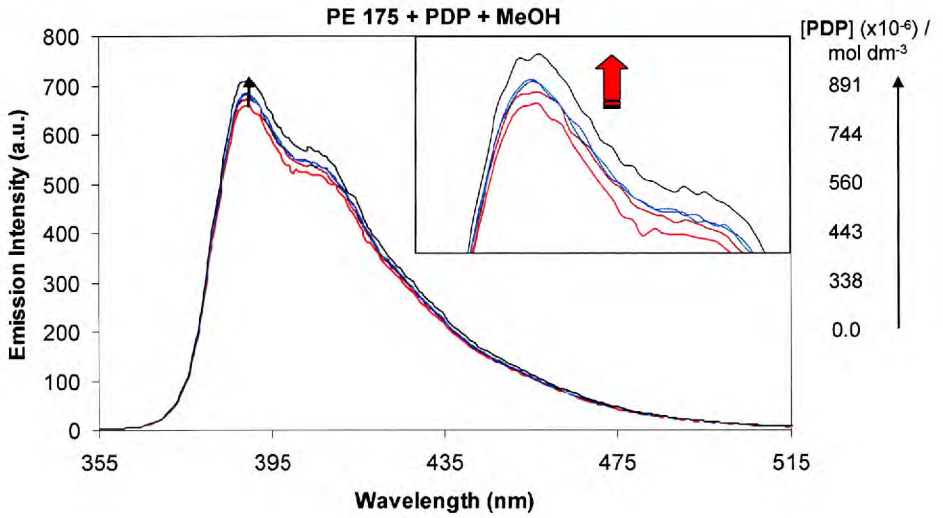

Figure 3.9 The emission spectra in non-degassed methanol of 10 μM PE **175** at increasing concentrations of potassium dihydrogen phosphate as its [18-C-6] salt ([K^+-18-C-6]) (**PDP**). The inset shows how the intensity changes with added **PDP**, though only a modest rise is observed.

A small 8% increase in the emission intensity was observed upon addition of the phosphate salt (total concentration was 0.90 mM). In the example described earlier (section 3.2), Teramae *et al.* observed an increase of ~ 400-times the initial intensity.[19] Despite the clear structural differences between the examples (Teramae *et al.* used a naphthalene unit as the fluorophore) the main change is attributed to the size of the intervening distance between the isothiouronium receptor and the PE backbone, which in our case is up to two bond-lengths longer, and contains an alkoxy linkage. These differences may be crucial and presumably disrupt the potential for efficient PET from the PE unit to the receptor and therefore recognition of anions by the isothiouronium is inefficiently reported.

Teramae *et al.* pay particular attention to this; they considered the efficiency of the PET process between, in their case, the naphthalene and isothiouronium motifs using the Rehm-Weller equation.[19] From this they reasoned that the pair act as electron donor and acceptor respectively and that the distance separating the two is of central importance in determining the emission intensity of the fluorophore. Therefore, where possible a shorter CH_2 spacer is preferable to a

longer carbon chain. To the best of our knowledge, there are no reports examining the importance of the spacer distance beyond three intervening carbons, and if heteroatoms (such as oxygen, as part of an alkoxy linkage) mitigate the PET process. In Chapter Four, this point is studied further and we report on a small model analogue that contains a recognition unit which is directly attached to the conjugated backbone.

A sample of the impure guanidinium-derived PE **178** was analysed in the same way, as it was of interest to observe what effect, if any, would be observed upon adding phosphate ions to a solution of the receptor. In methanol, this small model analogue yielded broadly similar results to those found for PE **175**; the emission from PE **178** increased by ~ 10% after addition of phosphate ions (potassium dihydrogen phosphate). Few conclusions can be drawn from this modest increase (and indeed for that measured for PE **175**) as small errors in the volumes of solutions added could lead to changes in the emission intensity recorded. Although not investigated, the impact such errors would have on the emission level could be easily checked by control experiments, though in this case we estimated that the error associated with the emission intensities to be approximately ±1%. Such dilutions (i.e. additions of small aliquots of the phosphate ion solution) would be expected to yield a decrease in emission, but importantly, the presence of polar H-bond receptor units on both small model analogues, could lead to strong self-association (giving rise to some form of aggregation, and resulting in self-quenching) that would be disrupted in the presence of anions. To clarify the differences observed, it would be necessary to investigate the impact that the size of the bridge between the receptor and PE fluorophore has on the emission intensity. This is given consideration in Chapter Four, where a PE unit directly attached to a receptor is found to be approximately twice as sensitive to analytes as compared with small model analogues like PE **175** and PE **154**.

3.5 Analysis of a neutral water-soluble PPE and PE

Though no emission quenching experiments were recorded for PE **181** and PPE **182** (as these materials were used to aid the assigning of characterisation data for this family of polymers and small model analogues and were not expected to display sensing abilities), some initial spectroscopic data was collected. As for the previously discussed PEs and PPEs, the materials are highly soluble in water and methanol (~ 30 mg/mL), and emit between 400 – 500 nm. In methanol, the respective absorption and emission peaks are: 412 and 438 nm for the polymer and 358 and 394 nm for the small model analogue. In water, the respective absorption and emission peaks are: 457 and 494 nm for the polymer and 355 and 399 nm for the small model analogue, results which are red-shifted relative to those recorded for any of the previous PEs or PPEs (summarised in Table 3.2). This result could be due *inter alia* to increased conjugation lengths in these materials, as

suggested by the molecular weight data (section 3.3) or aggregation effects that are known to red-shift absorption and emission spectra.

Table 3.2 Absorption and emission data for the novel materials PE **182** and PE **181**.[a]

Entry	Material	Solvent	Absorption λ_{max} / nm	Emission λ_{max} / nm
1	PPE **182**	H_2O	457	494
2	PE **181**	H_2O	355	399
3	PPE **182**	MeOH	412	438
4	PE **181**	MeOH	358	394

[a]All measurements were made in an aerobic environment in water or methanol.

To offset such phenomenon surfactants are often employed as de-aggregating agents, added to aqueous solutions in small (typically 0.1 – 0.3 wt.%) quantities. A more detailed treatment of the effects of surfactants in unbuffered and buffered aqueous conditions will be given in section 3.6 (where it is proposed that the surfactant is used to *promote* aggregation) but for PPE **182** the effect of Triton X-100, a oligoethylene glycol surfactant with a hydrophobic head-group, was studied (Figure 3.10). The surfactant was chosen as it has been previously reported that compared with similar commercially available surfactants, it is good at increasing the quantum yield of PPE polymers in water.[28]

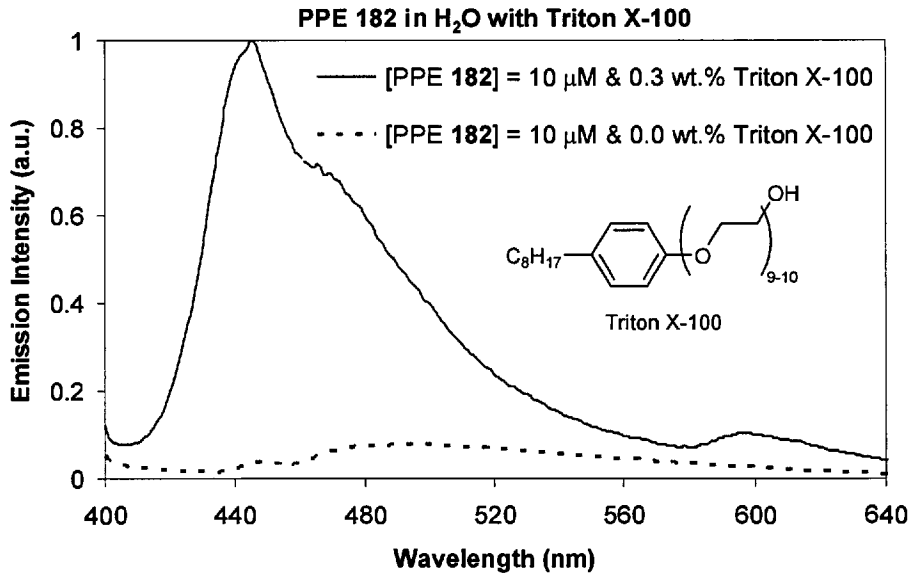

Figure 3.10 The normalised emission spectra in salt-free water for 10 μM PPE **182** in the presence (blue curve) and absence (red dashed curve) of the surfactant Triton X-100. *Inset*: Structure of Triton (full name: 4-(1,1,3,3-Tetramethylbutyl)phenyl-polyethylene glycol).

The addition of the surfactant to aqueous solutions leads to the emission intensity being significantly increased, (95% higher; Figure 3.10). This is often attributed to a reduced instance of π-π stacking (and associated self-quenching effects) but could also be explained by the polymer adopting a more rod-like shape in solution and thereby acquiring improved conformational order. In an unbuffered aqueous medium, the surfactant molecules could have two functions; first, they may serve to break-up aggregates by having preferential interactions with the polymer chains,[28] which would lead to a blue-shift in the emission properties (for PPE **182** the difference is 52 nm). This occurs as the effective conjugation length of the polymer is reduced upon interaction with the surfactant. PPE aggregates (that form as a result of π-π stacking) usually result in increased planarity of the polymer backbone and therefore increased conjugation. Alternatively the surfactant could promote the formation of aggregates, where there is improved conformational order with respect to the polymer chains. In such a regime, interpolyelectrolyte formation would result in a reduced instance of self-quenching (giving rise to an increased emission level).

By contrast, the effect of the surfactant on the polymer chains is negligible in methanol, with the presence of the surfactant resulting in no change in the emission intensity and emission maxima. Such behaviour has been previously observed for ionic PPEs where more resolved bands are observed in 'good' solvents like MeOH and THF.[28] Small model analogues such as PE **181** have a

much reduced tendency to form aggregates compared with PPEs because of their smaller dimensions and reduced interactions.

As such, the addition of surfactant to methanolic solutions of PE **181** resulted in no change in the emission spectrum of the small model analogue. In water, a modest 40% increase in the emission intensity maximum was observed (the position of the emission maximum remained the same). In summary, the effect on the emission of PE **181** and PPE **182** in water and methanol owe much to their structures; in water, PPE **182** is highly aggregated, which results in quenched, red-shifted emission. Here, the addition of surfactant is striking and results in restoration of the emission to that observed in methanol (with or without surfactant), which can be considered a good solvent for the polymer.

The emission from the small model analogue PE **181** is comparatively unaffected by the addition of surfactant and is similar in both solvents (λ_{max} differs by only 5 nm). Though these results suggest that the optimum PPE architecture should seek to avoid either aggregate formation or conformational order in which emission is relatively quenched, results to be presented in the following section suggest that for sensing purposes, aggregates may be desirable and indeed necessary in order to achieve high sensitivity.

3.6 Spectroscopic investigation of fluorescence quenching – analysis of a second generation PPE and PE in high ionic strength media

The measurements were obtained using the bis(cyclohexylammonium) salt hydrate of 4-nitrophenyl phosphate (**NPP**, **183**; Figure 3.11) as the quencher which we found to be an excellent emission quencher for PPE polymers, like other nitroaromatics (e.g. dinitrophenol).[29] It was also important to have the phosphate group in the quencher molecule for the planned phosphatase enzyme assay which is detailed in Chapter Five. **NPP** is a substrate used for the determination of acid and alkaline phosphatases.[30] In common with other electron deficient species, **NPP** is considered to induce quenching *via* an electron transfer process occurring as a result of attractive electrostatic interactions (which leads to static quenching).[6,31-33]

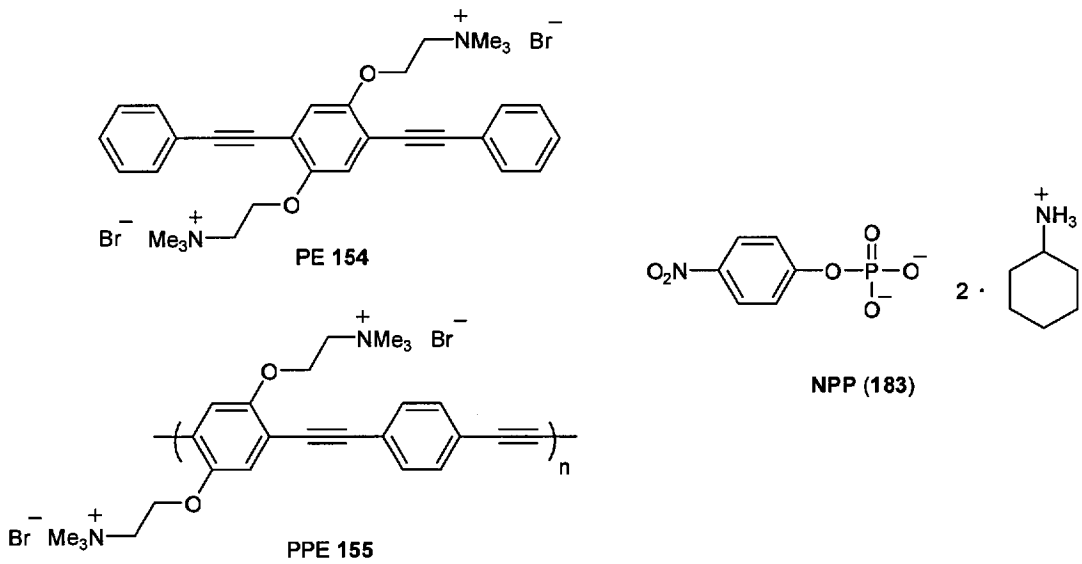

Figure 3.11 Conjugated materials used to study quenching effects in high ionic strength media and structure of the water-soluble quencher **NPP (183)**.

The absorption and emission spectra for PPE **155** and PE **154** are shown in Figure 3.12a and Figure 3.12b respectively.

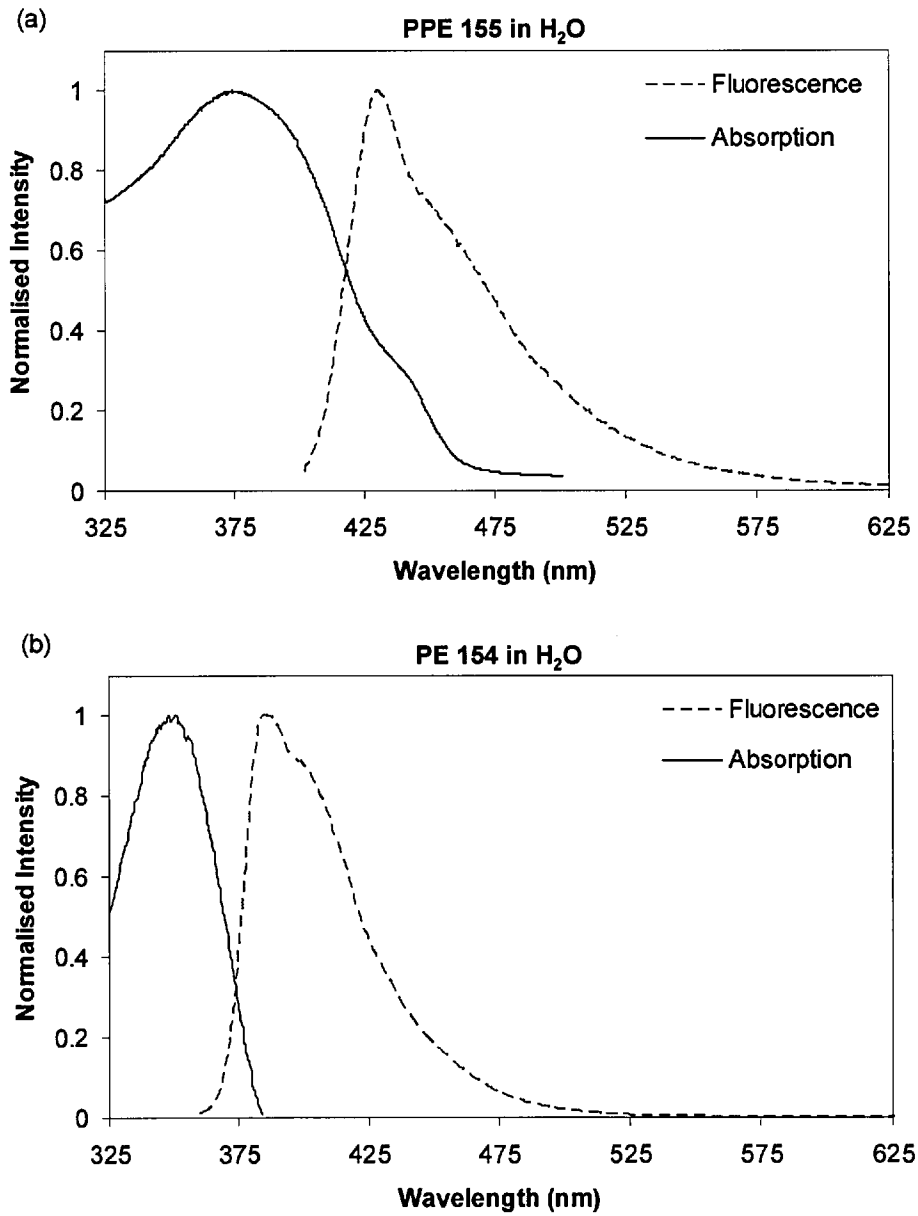

Figure 3.12 The normalised absorption and emission spectra in salt-free water for (a) 10 μM PPE **155** (excitation wavelength = 355 nm) and (b) 10 μM PE **154** (excitation wavelength = 350 nm).

In common with other similar PE and PPE derivatives, the compounds are highly soluble in DMSO, methanol, and (most importantly) water, and emit between 400 – 500 nm. The respective absorption and emission peaks are: 374 and 430 nm for the polymer and 351 and 391 nm for the small model analogue.

In order to quantify the quenching efficiencies of the polymer and small model analogue, it was necessary to devise an accurate method to measure Stern-Volmer constants. Importantly, the

technique adopted would have to ensure that any associated experimental errors were minimised and crucially, that the concentration of the sensor remained constant throughout the addition of the quencher solution.

A robust method for determining the Stern-Volmer constant has been established and is detailed in Experimental section (Chapter Seven). To establish its reliability, the technique was used to measure k_{SV} for a known system. The luminescence behaviour of $Ru(bpy)_3^{2+}$ complexes has been extensively documented and provided a good 'standard'.[34] The phenol-derived quencher 4-bromo-2,6-dimethylphenol was used to quench the emission from the metal complex, *via* a reductive mechanism. A Stern-Volmer constant of 1.8×10^3 M^{-1} was measured for this system (at pH = 11), which compares well with the reported value of 1.2×10^3 M^{-1} (measured at pH = 11.05).[34] The differences were attributed to the slight variation in pH and temperature. The quenching mechanism can occur by static or dynamic processes, or a combination of both. Unlike static quenching, for dynamic processes temperature increases lead to an enhancement in k_{SV} as there is faster diffusion and therefore more collisional quenching.[32] Additionally, the excited state of the complex is sensitive to oxygen, and we used non-degassed solutions.[34] It is likely that the small variations in the experimental conditions used here, can account for the differences between our data and that reported. A summary of the results from these standard experimental runs are shown in Chapter Seven along with the detailed experimental method and treatment of errors. From this point on, all Stern-Volmer coefficients were acquired using this technique.

The emission spectra of 5 μM PPE **155** and 5 μM PE **154** in water are shown in Figure 3.13a and Figure 3.13b respectively at increasing concentrations of **NPP**.

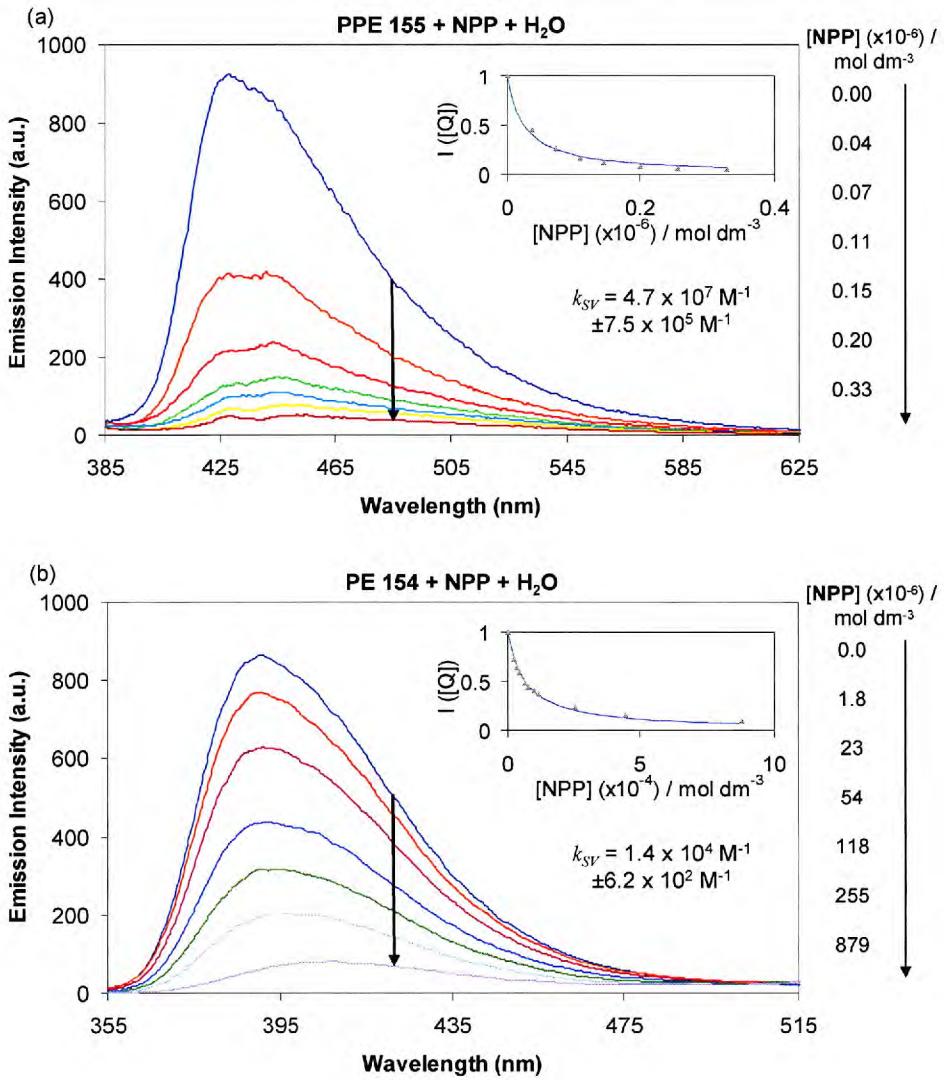

Figure 3.13 The emission spectra in salt-free water of (a) 5 μM PPE **155** and (b) 5 μM PE **154** at increasing concentrations of the quencher 4-nitrophenyl phosphate, bis(cyclohexylammonium) salt hydrate (**NPP**). The insets show Stern-Volmer plots using data extracted from the main figures. The intensities in the Stern-Volmer plots are determined from the area beneath the corresponding curves in Figure 3.13, and are normalised with respect to the measured emission intensity in the absence of **NPP**. The markers denote experimental data lines and the solid-lines indicate the optimal fit to the Stern-Volmer relation as outlined in the Experimental section. The degree of quenching is much stronger in the case of PPE **155** indicating strong amplified quenching in the polymer.

The profiles of both the PPE **155** and PE **154** emission spectra are broad and featureless at the quencher concentrations considered and are only weakly influenced by the presence of **NPP**, except at higher concentrations (> 0.20 μM) where a small red-shift in the PPE **155** emission becomes apparent. Stern-Volmer plots are shown as insets to the main diagrams, with the markers denoting experimental data points and the solid-line indicating the optimal fit to the Stern-Volmer

relation as described in the Experimental section. The difference in quenching efficiency between PPE **155** and PE **154** is striking. The Stern-Volmer coefficient of PPE **155** (4.7×10^7 M^{-1}) is approximately three thousand times higher than that of PE **154** (1.4×10^4 M^{-1}), indicative of strong "amplified quenching" intrinsic to the polymer system. The high k_{SV} value obtained for the polymer, is consistent with static rather than dynamic quenching (since dynamic quenching is a diffusion-limited process that tends to yield small Stern-Volmer coefficients, which are typically no higher than ~ 1000 M^{-1}).[32] The mechanism of amplification has been attributed to several effects including ion-pair complex formation between the polymer and quencher, the highly delocalised singlet exciton within the polymer, aggregation effects partly induced by the quencher and the ability of the polymer and quencher to undergo long-range Förster energy transfer. All of these mechanisms may play an equally vital role in quenching, though for such systems, the relative contribution of each pathway is unknown and is still under examination.[33,35]

The high Stern-Volmer coefficient of PPE **155** in water is promising but to operate effectively as a biosensor it should exhibit comparable quenching characteristics when transferred to typical biological media such as blood and urine. A variety of salts and other additives are usually present in these environments along with buffer solutions of differing pH, all of which can have a strong influence on the emission from CPs.[36] In particular, biological media have high dielectric constants, and polymer emission under such conditions is generally reduced due to hydrophobic interactions that lead to self-quenching.[28] It is important that ionic CPs should perform as well in these biological media as they do in pure water. Accordingly, in this work, we investigated the performance of PPE **155** as a biosensor for monitoring chemical processes in two standard buffer solutions, tris(hydroxymethyl) aminomethane (TRIS, 25 mM, pH = 7.5) and sodium acetate (25 mM, pH = 6.5).

In Figure 3.14, emission spectra for 5 μM PPE **155** in a 25 mM TRIS buffer at various **NPP** concentrations are shown. TRIS is a common buffer that is widely used to control pH in the physiological range (7 - 8) since it does not typically cause undesirable side reactions such as precipitation of calcium salts or inhibition of enzyme reactions. Figure 3.14a shows data for measurements undertaken in a TRIS buffer containing no added salt (NaCl), and Figure 3.14b shows data for measurements undertaken in TRIS buffer containing 150 mM NaCl, the presence of which is required by enzymes such as phosphatase for efficient operation. The Stern-Volmer plots are again shown as insets to the main diagrams.

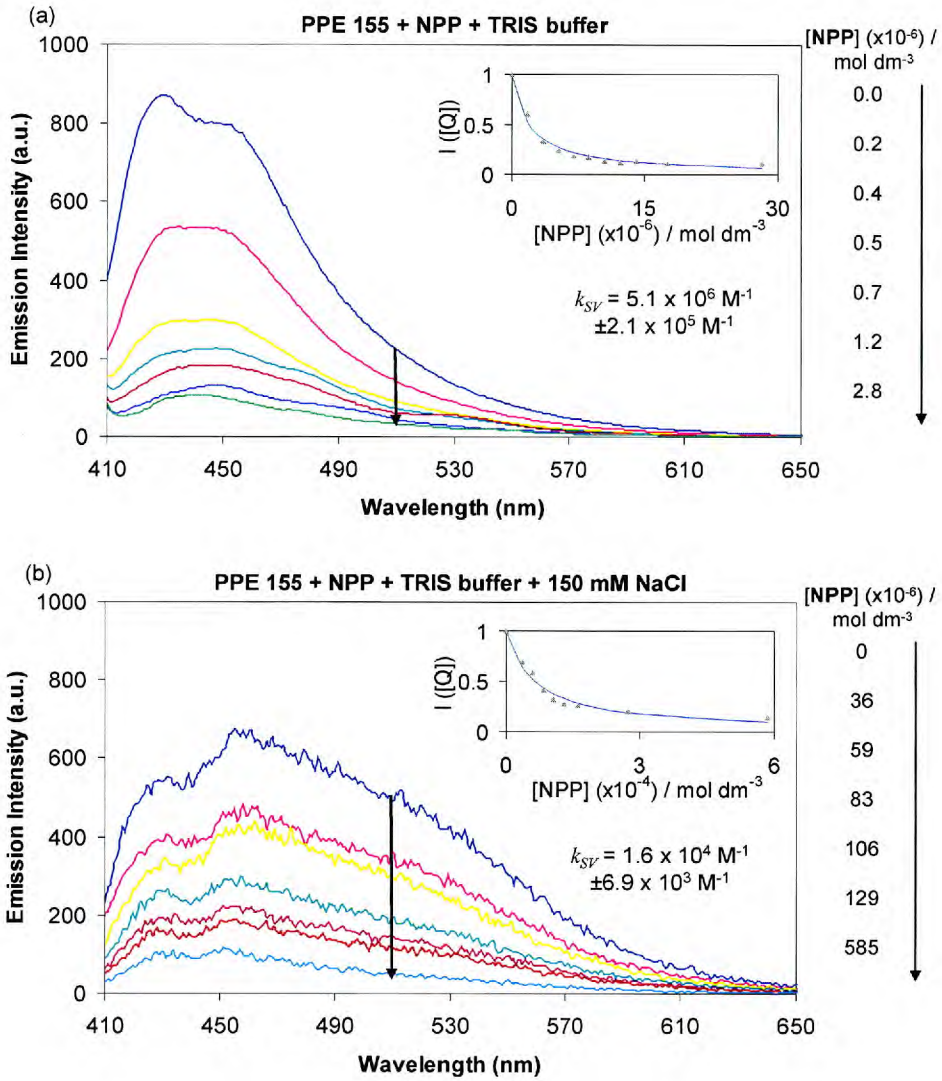

Figure 3.14 The emission spectra of PPE **155** at various concentrations of the quencher **NPP** in (a) 25 mM TRIS buffer containing no added salt and (b) 25 mM TRIS buffer containing 150 mM NaCl. The transferral of PPE **155** to the saline-buffered environments required for normal enzyme activity leads to a dramatic reduction in Stern-Volmer coefficient compared to the pure-water result shown in Figure 3.13.

The data reveals a 9-fold decrease in k_{SV} upon going from unbuffered aqueous conditions to a 25 mM TRIS buffered solution and a further 300-fold decrease on addition of the NaCl. The combined effect of the buffer and NaCl is therefore a sharp 2700-fold reduction in the Stern-Volmer coefficient relative to the value obtained in pure water.[37] A similar reduction in k_{SV} in high ionic strength media has previously been reported by Swager *et al.*,[28] rendering the materials unusable for high sensitivity detection.

To achieve high Stern-Volmer coefficients of the magnitude obtained for PPE **155** in pure water, three conditions must be satisfied: firstly, there must be a strong tendency for the polyelectrolyte to complex with the quencher; secondly, the process of electron transfer from the conjugated backbone of the polyelectrolyte to the quencher must be efficient; and, thirdly, a single quencher should be able to accept electrons from excitations on multiple conjugated segments. The sharp reduction in k_{SV} in transferring from water to the saline TRIS buffer indicates that at least one of these requirements is violated in the latter environment. The efficiency of electron transfer is determined primarily by the proximity of the quencher to the π-system of the polymer and the energy offset between their respective LUMO levels, so it is unlikely to change substantially in the presence of a background electrolyte (i.e. dissolved salt).[38] Therefore it is reasonable to conclude that the adverse influence of the ions on the Stern-Volmer coefficient is due to a reduced tendency for complexation (e.g. due to screening of the electrostatic attraction between the trimethylammonium ion and the 4-nitrophenyl phosphate ion) and/or a reduction in the ability of the quencher to harvest electrons from multiple chains.

The latter processes depend intimately on the conformation and the supramolecular structure of the dissolved polymer: a loose network of chains is desirable for achieving good interchain communication and ensuring ready access of the quencher to the polyelectrolyte binding sites, but excessive aggregation is liable to reduce the number of available binding sites for the quencher (since only those at the surface will be physically accessible to the quencher). The behaviour of conjugated polyelectrolyte chains in the presence of added salt has previously been investigated by Wang *et al.*, who used Small Angle Neutron Scattering (SANS) to investigate the conformation of poly[5-methoxy-2-(4-sulphobutoxy)-1,4-phenylvinylene] (MBL-PPV) in aqueous solution.[39] They found that the polymer chains adopt rod-like configurations in both pure (deuterated) water and in the presence of LiCl as would generally be expected for a conjugated polymer of modest length (similar PPVs commonly contain ~ 1000 repeat units per polymer chain).[40] Importantly, the SANS data for salt-free solutions revealed excess scattering at small angles (i.e. scattering features above the q^{-1} line in the scattered intensity plot). This behaviour was first explained by Ermi and Amis for the polyelectrolyte poly(*N*-methyl-2-vinylpyridinium chloride), and is due to the presence of multichain domains (aggregates) that are stable in low ionic strength media but disintegrate in the presence of excess salt.[41] Complementary light scattering studies on sodium poly(styrenesulphonate) by Sedlak[42] further revealed that the dimensions of the aggregates decrease steadily with increasing ionic strength, rather than disintegrating in an abrupt phase transition at a threshold salt concentration. The aggregation and de-aggregation of polyelectrolyte chains in solution has subsequently been studied theoretically by Ray and Manning, who used counter-ion condensation theory to obtain a simple pair-potential for two identical rod-like polyelectrolytes.[43] They demonstrated that the formation of clusters at low ionic strength and the

reduced tendency for aggregation at high ionic strength arise as natural consequences of the radial dependence of the pair potential.

As noted by Wang *et al.*, the formation of aggregates in the low ionic strength regime is advantageous for achieving high Stern-Volmer coefficients since it provides communication pathways between different chains and so allows a single bound quencher to deactivate multiple fluorophores.[39] We reasoned that, if the clusters could be chemically stabilised under high salt conditions, the usual drop in k_{SV} could be prevented. In their neutron scattering studies, Wang *et al.* also reported SANS data for mixtures of MBL-PPV and the cationic surfactant dodecyltrimethylammonium bromide (DTA), and found that aggregation of the MBL-PPV chains at low ionic strengths is enhanced in the presence of a small amount of DTA;[39] they did not report measurements in the presence of dissolved salt but we considered that a similar surfactant-based approach could be used to stabilise the PPE **155** aggregates even at high ionic strength. The affinity between DTA and the (oppositely charged) MBL-PPV chains is primarily electrostatic in origin and, due to strong screening of Coulombic attractions in high ionic strength solutions, we reasoned that it would be more effective for our purposes to use a non-ionic surfactant to stabilise the PPE **155** clusters, such as Triton X-100 or Cremophor EL (CrEL) which has been used as a formulation medium for water-insoluble drugs such as paclitaxel (Taxol).[44] Triton X-100 is commercially available, has often been used in biological buffers, and has previously been shown to promote the association of twin-tailed hydrophobically modified terpolymers *via* the formation of surfactant micelles that act as "junction points" for interpolymer network formation.[45] The networks were reported to form at surfactant concentrations far below the critical micelle concentration, with the addition of excess Triton leading to disintegration of the clusters.[46] In the context of conjugated polyelectrolytes, Triton has previously been used by Wosnick *et al.* to control aggregation in a number of structurally similar PPEs,[28] and they reported a substantial enhancement in the photoluminescence efficiency of the polyelectrolyte in the presence of Triton. We therefore considered it to be a promising surfactant for our purposes. Interestingly, Wosnick *et al.* used Triton for the opposite reason to us: in their case they wished to *prevent* aggregation of the polymer chains whereas our objective was to *promote* it.

In early studies conducted in our group, it was found that adding Triton to aqueous solutions of PPE **155** leads to a breakdown in the dimension of the polymer aggregates reducing their size from 450 nm to 300 nm (a reduction in the hydrodynamic diameter as determined by photo correlation spectroscopy, PCS).[47] Though it is difficult to predict the expected interaction of the polymer and surfactant, it is known that oppositely charged polyelectrolytes and surfactants form stable complexes (driven by Coulombic interactions and favourable entropy changes).[40] Importantly, the interactions can lead to significant differences in the conformation of the polymer.[40] For PPE **155**

and Triton favourable π-π interactions between the phenyl units of the polymer and the hydrophobic head group of the surfactant as well as other hydrophobic effects may be dominant.

As noted by Smith and McCormick, however, the role of Triton is concentration dependent; at relatively low concentrations, Triton promotes association of the polyelectrolyte chains *via* micelle junctions but, at higher concentrations, micelle bridging is disrupted and the aggregates disintegrate (the viscosity falls to a value lower than the polymer alone, indicating the presence of individual chains).[45] The surfactant concentrations corresponding to these two regimes are dependent on the hydrophobicity of the polyelectrolyte and the solvent conditions. We hoped that, by careful selection of the Triton concentration, it might be possible to form polyelectrolyte clusters that were stable even in high salt conditions.

In Figure 3.15, the emission spectra of unbuffered aqueous solutions of PPE **155** are shown for different concentrations of Triton.

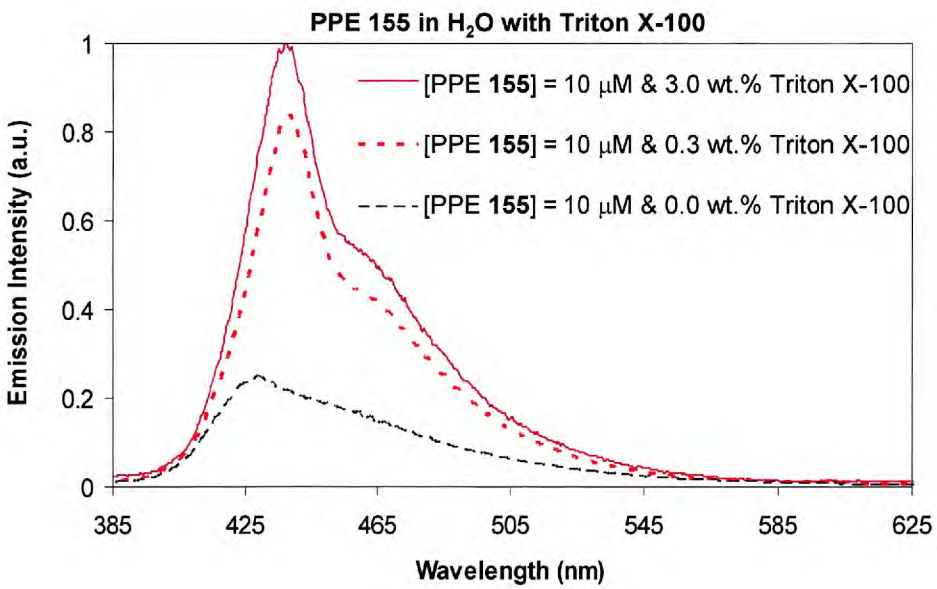

Figure 3.15 The emission spectra of PPE **155** in salt-free water in the presence of different concentrations of the non-ionic surfactant Triton X-100.

There are two important changes in the spectral characteristics on addition of the surfactant: firstly, the spectra become sharper and better resolved and, secondly, there is an enhancement in the emission intensity. It is notable that as little as 0.3 wt.% Triton X-100 (amount relative to solvent) is required to bring about these changes. The increased emission intensity and sharpening of the spectra have been widely reported and have variously been attributed to the disruption of

aggregates (which reduces interactions between the π-systems of individual chains)[28] or a reduction in the conformational disorder of the individual chains.[40,48] In the event of complete disruption of the aggregates, we would expect to observe a substantial reduction in the Stern-Volmer coefficient but experimentally, with 0.3 wt.% Triton, a comparatively small five-fold reduction in k_{SV} is observed relative to PPE **155** in pure water (see Figure 3.16a).

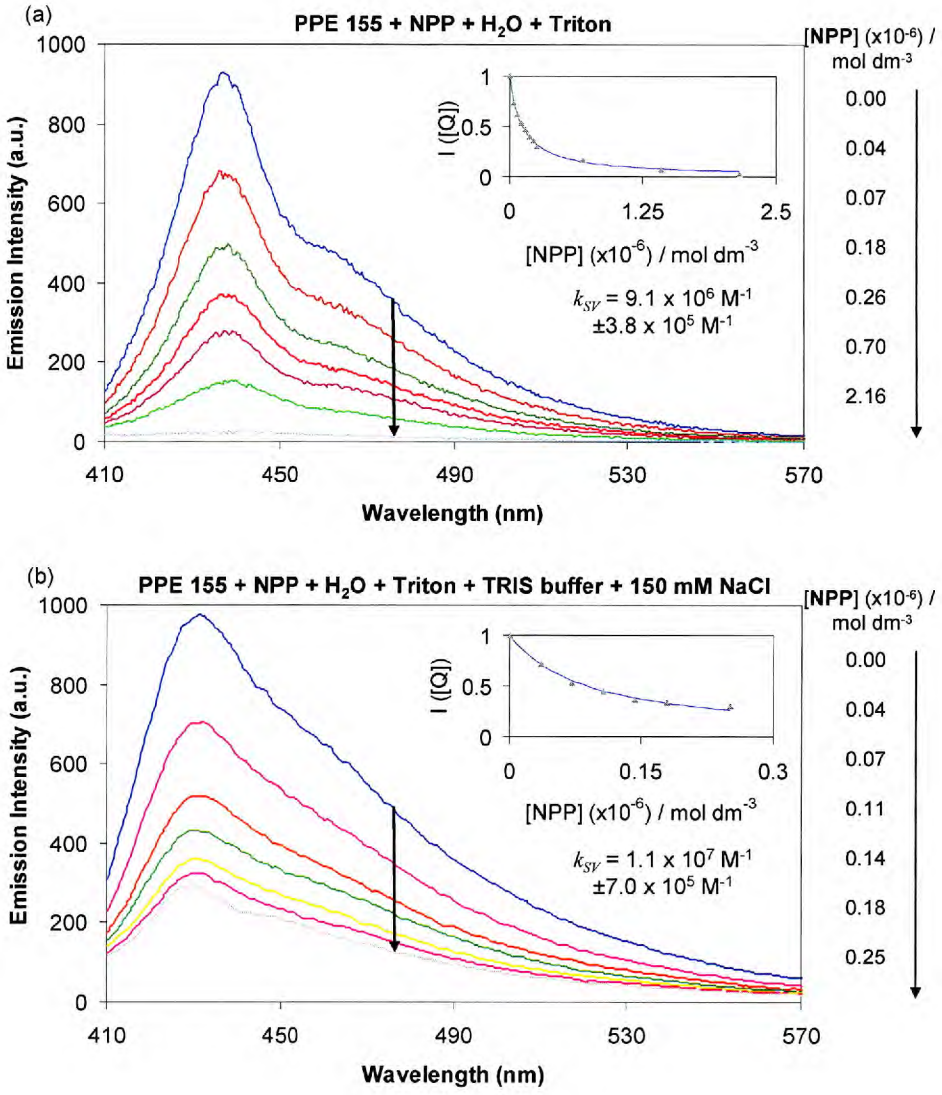

Figure 3.16 (a) The emission spectra of PPE **155** in salt-free water containing 0.3 wt.% Triton X-100 at increasing concentrations of the quencher **NPP**. (b) The emission spectra of PPE **155** in 25 mM TRIS buffer containing 150 mM NaCl and 0.3 wt.% Triton X-100 at increasing concentrations of the quencher **NPP**. The inclusion of the surfactant yields a Stern-Volmer coefficient comparable to the salt- and buffer-free case.

This suggests that changes in the conformational disorder are the primary cause of the spectral variations. The absolute value of the Stern-Volmer coefficient after addition of the surfactant is still very high (~ 10^7 M^{-1}), which indicates that, even in the presence of the surfactant, communication can still occur between multiple polyelectrolyte chains (albeit at a somewhat reduced efficiency due to interference from the surfactant). This is consistent with the neutron scattering measurements of Wang *et al.*, who found strong evidence for large polyelectrolyte/surfactant complexes comprising multiple polyelectrolyte chains.[39]

The 10^7 M^{-1} k_{SV} value obtained in the surfactant-containing salt-free water is still extremely high and we were keen to determine whether the surfactant might also preserve the high quenching efficiency in buffered high salt conditions. In Figure 3.16b we show emission spectra for PPE **155** plus 0.3 wt.% Triton in 25 mM TRIS buffer with 150 mM NaCl solution at increasing **NPP** quencher concentrations. The measured Stern-Volmer coefficient of 1.1 × 10^7 M^{-1} is much higher than for the surfactant-free case (1.6 × 10^4 M^{-1}, Figure 3.14b) and, within experimental error, is the same as for the salt-free water case shown in Figure 3.16a. It is clear that, whilst the use of Triton causes a modest five-fold reduction in the Stern-Volmer coefficient for PPE **155** relative to pure water, it prevents the catastrophic 2700-fold reduction in k_{SV} that would otherwise occur when PPE **155** is transferred to TRIS buffered saline solutions. The same general trends were observed for PPE **155** in a sodium acetate buffer, with the introduction of Triton again restoring the Stern-Volmer coefficient to levels close to the salt-free situation. The variation of the Stern-Volmer coefficient under the different conditions studied are summarised in Figure 3.17a (TRIS buffer) and Figure 3.17b (NaOAc buffer).[49]

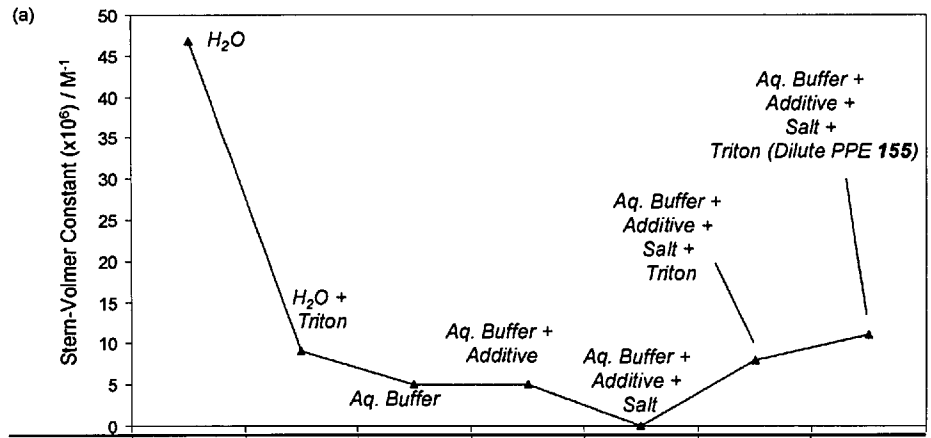

k_{SV} / M^{-1}	4.7×10^7	9.1×10^6	5.1×10^6	5.1×10^6	1.6×10^4	8.0×10^6	1.1×10^7
Buffer	×	×	25 mM TRIS	25 mM TRIS	25 mM TRIS	25 mM TRIS	25 mM TRIS
Additive	×	×	×	1 mM EDTA	1 mM EDTA	1 mM EDTA	1 mM EDTA
Salt	×	×	×	×	150 mM NaCl	150 mM NaCl	150 mM NaCl
Surfactant	×	0.3 wt.% Triton	×	×	×	0.3 wt.% Triton	0.3 wt.% Triton
[PPE **155**] / μM	5	5	5	5	5	5	1.5

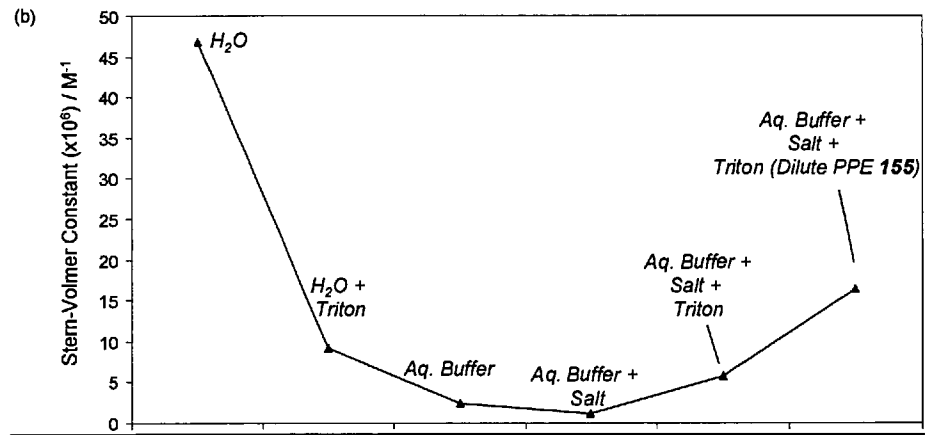

k_{SV} / M^{-1}	4.7×10^7	9.1×10^6	2.4×10^6	1.2×10^6	5.8×10^6	1.7×10^7
Buffer	×	×	25 mM NaOAc	25 mM NaOAc	25 mM NaOAc	25 mM NaOAc
Salt	×	×	×	150 mM NaCl	150 mM NaCl	150 mM NaCl
Surfactant	×	0.3 wt.% Triton	×	×	0.3 wt.% Triton	0.3 wt.% Triton
[PPE **155**] / μM	5	5	5	5	5	2.5

Figure 3.17 The dependence of the Stern-Volmer constant for PPE **155** on addition of various salts, buffers, surfactants and additives for: (a) 25 mM TRIS buffer and (b) 25 mM NaOAc buffer. The inclusion of 0.3 wt.% Triton X-100 in the buffer solutions containing 150 mM NaCl results in Stern-Volmer coefficients that are comparable to those of PPE **155** in pure water, enabling high sensitivity detection in biological media.

The remarkable restoration in both cases of k_{SV} to values comparable with the salt-free level demonstrates the importance of the surfactant in stabilising the aggregates. (The final data points in these figures show that further increases in Stern-Volmer coefficients can be achieved by further diluting the polyelectrolyte, although this obviously occurs at the expense of emission intensity).

To ensure that the results of the measurements were not specific to the particular choice of quencher molecule, measurements were also undertaken using the chemically unrelated molecule 9,10-anthraquinone-2,6-disulphonic acid disodium salt (**AQS**, **139**; which was used to quench the emission from PPE **124** in Chapter Two). These experiments yielded broadly comparable results in water and surfactant-containing solutions (Figure 3.18).

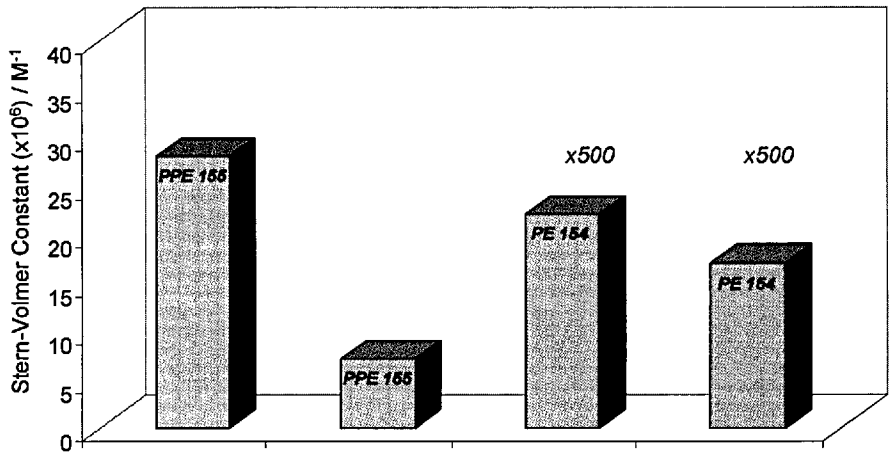

k_{SV} / M^{-1}	2.8×10^7	7.1×10^6	4.4×10^4	3.4×10^4
Solvent	H_2O	H_2O	H_2O	H_2O
Surfactant	×	0.3 wt.% Triton	×	0.3 wt.% Triton
Quencher	**AQS**	**AQS**	**AQS**	**AQS**
Sensor	PPE **155**	PPE **155**	PE **154**	PE **154**
[PPE **155**] or [PE **154**] / μM	5	5	5	5

Figure 3.18 Summary of emission quenching experiments involving PPE **155**, PE **154** and the structurally different quencher **AQS**.

The effect on the quantum efficiency of PPE **155** in different aqueous conditions is shown in Figure 3.19. As expected (and reported by Wosnick *et al.* for similar polymer systems),[28] the addition of the surfactant resulted in an increase in the QE of the polymer relative to pure water. The addition of salt (150 mM NaCl) to the pure water solution, to create a high ionic strength medium, led to a higher QE as compared with the value measured for pure water. This can be rationalised by considering that the salt screens charges along the polymer backbone, thereby minimising polymer-polymer interactions. Addition of Triton to this solution gave rise to a further

increase in the quantum yield. The addition of ions to aqueous polyelectrolyte solutions is known to induce aggregation as has recently been shown by Schanze *et al.* for the amplified quenching of an anionic PPE by Ca^{2+}.[35] However in their work, the concentration of added ions did not exceed micromolar levels. The effect of such additives is known to be concentration dependent[41] and presumably the higher salt concentration used in our studies leads to a breakdown of PPE aggregates.

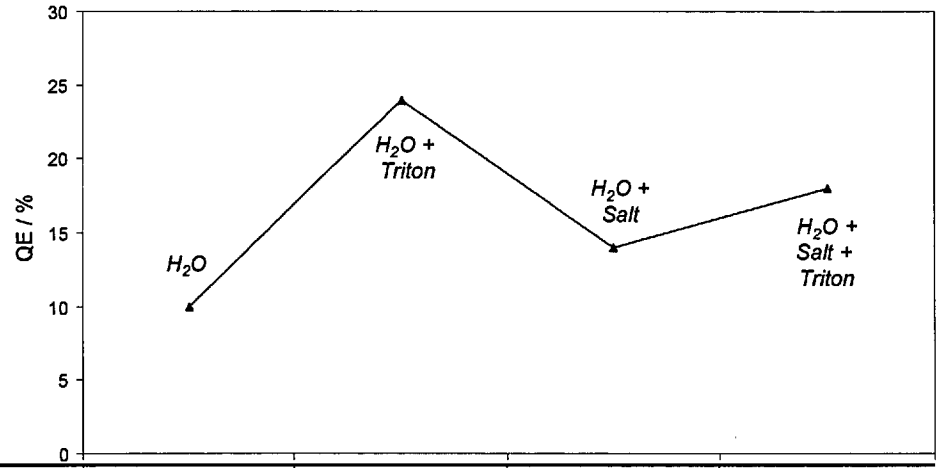

QE / %	10	24	14	18
Salt	×	×	150 mM NaCl	150 mM NaCl
Surfactant	×	0.3 wt.% Triton	×	0.3 wt.% Triton
[PPE **155**] / μM	10	10	10	10

Figure 3.19 Impact on QEs for PPE **155** upon addition of the surfactant in different aqueous milieu.

Triton X-100 has a highly beneficial effect on the quenching properties of PPE **155/NPP** in high salt buffered conditions and further investigations are now needed to determine whether similar improvements can be obtained with other surfactant/quencher/CP systems. We started evaluating the use of Triton/**NPP**/PPE **155** as a means of monitoring the kinetics of phosphatase activity and our findings are detailed in Chapter Five.

The photostability of PPE **155** was examined by irradiating an aqueous solution of the polymer (~ 5 μM) continuously for 45 minutes using typical fluorimeter settings (see Chapter Seven, Table 7.3). The impact of photobleaching was assessed by comparison of the integrated areas from the initial and final photoluminescence spectra. For an aqueous solution of the polymer, the reduction in the emission intensity over the 45 minute period was approximately 3%. The corresponding reduction in the emission intensity for a surfactant-containing aqueous solution of PPE **155** was ~ 9%. In both cases, the small photobleaching effect had a negligible impact on k_{SV}, with the

reduction being approximately within the limits of the recorded experimental error for these measurements.

3.7 Notes and references

1. M. R. Pinto, B. M. Kristal and K. S. Schanze, *Langmuir*, 2003, **19**, 6523-6533.
2. M. D'Auria and G. Mauriello, *Tetrahedron Lett.*, 1995, **36**, 4883-4884.
3. J. Clayden, N. Greeves, S. Warren and P. Wothers, *Organic Chemistry*, OUP, Oxford, 2001.
4. E. B. Merkushev, N. D. Simakhina and G. M. Koveshnikova, *Synthesis*, **1980**, 486-487.
5. Q. Zhou and T. M. Swager, *J. Am. Chem. Soc.*, 1995, **117**, 12593-12602.
6. C. Y. Tan, M. R. Pinto and K. S. Schanze, *Chem. Commun.*, **2002**, 446-447.
7. (a) H. L. Ricks, U. H. Choudry, A. R. Marshall and U. H. F. Bunz, *Macromolecules*, 2003, **36**, 1424-1425; (b) S. L. Huang and J. M. Tour, *J. Am. Chem. Soc.*, 1999, **121**, 4908-4909; (c) L. R. Jones, J. S. Schumm and J. M. Tour, *J. Org. Chem.*, 1997, **62**, 1388-1410.
8. U. H. F. Bunz, *Chem. Rev.*, 2000, **100**, 1605-1644.
9. http://www.waters.com/WatersDivision/ContentD.asp?watersit=JDRS-5LTGKK (accessed: May 2006).
10. I am grateful to Dr Emma Child (Division of Cell & Molecular Biology, Imperial College London), who analysed the sample.
11. S. L. Lu, M. J. Yang, J. Luo, Y. Cao and F. L. Bai, *Synth. Met.*, 2004, **146**, 175-180.
12. G. C. Bailey and T. M. Swager, *Macromolecules*, 2006, **39**, 2815-2818.
13. Y. Kubo, S. Ishihara, M. Tsukahara and S. Tokita, *J. Chem. Soc., Perkin Trans. 2*, 2002, **2**, 1455-1460.
14. Y. Kato, S. Nishimura and N. Teramae, *Org. Lett.*, 2002, **4**, 4407-4410.
15. J. W. Steed and J. L. Atwood, *Supramolecular Chemistry*, John Wiley & Sons, West Sussex, United Kingdom, 2000.
16. W.-S. Yeo and J.-I. Hong, *Tetrahedron Lett.*, 1998, **39**, 8137-8140.
17. See: T. Gunnlaugsson, A. P. Davis, G. M. Hussey, J. Tierney and M. Glynn, *Org. Biomol. Chem.*, 2004, **2**, 1856-1863; and references herein.
18. R. Kato, Y.-Y. Cui, S. Nishimura, T. Yokobori and N. Teramae, *Tetrahedron Lett.*, 2004, **45**, 4273-4276.
19. S. Nishizawa, Y.-Y. Cui, M. Minagawa, K. Morita, Y. Kato, S. Taniguchi, R. Kato and N. Teramae, *J. Chem. Soc., Perkin Trans. 2*, **2002**, 866-870.

20. N. B. Sankaran, S. Nishizawa, M. Watanabe, T. Uchida and N. Teramae, *J. Mater. Chem.*, 2005, **15**, 2755-2761.

21. J. K. Sorensen, M. Vestergaard, A. Kadziola, K. Kilsa and M. B. Nielsen, *Org. Lett.*, 2006, **8**, 1173-1176.

22. T. Hundertmark, A. F. Littke, S. L. Buchwald and G. F. Fu, *Org. Lett.*, 2000, **2**, 1729-1731.

23. A. S. Andersson, K. Qvortrup, E. R. Torbensen, J.-P. Mayer, J.-P. Gisselbrecht, J.-P. Boudon, M. Gross, A. Kadziola, K. Kilsa and M. B. Nielsen, *Eur. J. Org. Chem.*, 2005, 3660-3671.

24. B. Erdogan, J. N. Wilson and U. H. F. Bunz, *Macromolecules*, 2002, **35**, 7863-7864.

25. K. C. Nicolaou, J. I. Trujillo, B. Jandeleit, K. Chibale, M. Rosenfeld, B. Diefenbach, D. A. Cheresh and S. L. Goodman, *Bioorg. Med. Chem.*, 1998, **6**, 1185-1208.

26. D. A. Powell, P. D. Ramsden and R. A. Batey, *J. Org. Chem.*, 2003, **68**, 2300-2309.

27. K. Feichtinger, H. L. Sings, T. J. Baker, K. Matthews and M. Goodman, *J. Org. Chem.*, 1998, **63**, 8432-8439.

28. J. H. Wosnick, C. M. Mello and T. M. Swager, *J. Am. Chem. Soc.*, 2005, **127**, 3400-3405.

29. D. L. Wang, X. Gong, P. S. Heeger, F. Rininsland, G. C. Bazan and A. J. Heeger, *Proc. Natl. Acad. Sci. U. S. A.*, 2002, **99**, 49-53.

30. http://www.sigmaaldrich.com/Area_of_Interest/Europe_Home/UK.html (accessed: May 2006).

31. L. Chen, D. W. McBranch, H.-L. Wang, R. Helgeson, F. Wudl and D. G. Whitten, *Proc. Natl. Acad. Sci. USA*, 1999, **96**, 12287-12292.

32. J. R. Lakowicz, *Principles of Fluorescence Spectroscopy*, Plenum Press, New York, 1983.

33. C. H. Fan, S. Wang, J. W. Hong, G. C. Bazan, K. W. Plaxco and A. J. Heeger, *Proc. Natl. Acad. Sci. U. S. A.*, 2003, **100**, 6297-6301.

34. H. E. Gsponer, G. A. Arguello and G. A. Arguello, *J. Chem. Educ.*, 1997, **74**, 968-972.

35. H. Jiang, D. Zhao and K. S. Schanze, *Langmuir*, 2006, **22**, 5541-5543.

36. I.-B. Kim, A. Dunkhorst and U. H. F. Bunz, *Langmuir*, 2005, **21**, 7985-7989.

37. It is common practice in bioanalysis to add a small quantity (~ 1 mM) of the additive ethylenediamine tetraacetic acid (EDTA) to the buffer solution in order to remove, *via* complexation, metal ions that might otherwise impair enzyme activity. The addition of EDTA at this level was found to cause no noticeable change in the Stern-Volmer constant relative to the additive-free buffered solutions.

38. M. Ballauff, J. Blaul, B. Guilleaume, M. Rehahn, S. Traser, M. Wittemann and P. Wittmeyer, *Macromol. Symp.*, 1999, **211**, 1-24.

39. D. L. Wang, D. Moses, G. C. Bazan, A. J. Heeger and J. Lal, *J. Macromol. Sci. - Pure App. Chem.*, 2001, **38**, 1175-1189.

40. L. Chen, S. Xu, D. McBranch and D. Whitten, *J. Am. Chem. Soc.*, 2000, **122**, 9302-9303.

41. B. D. Ermi and E. J. Amis, *Macromolecules*, 1997, **30**, 6937-6942.

42. M. Sedlak, *J. Chem. Phys.*, 1996, **105**, 10123-10133.

43. J. Ray and G. S. Manning, *Macromolecules*, 2000, **33**, 2901-2908.

44. H. Gelderblom, J. Verweij, K. Nooter and A. Sparreboom, *Eur. J. Cancer*, 2001, **37**, 1590-1598.

45. C. L. McCormick and G. L. Smith, *Langmuir*, 2001, **17**, 1719-1725.

46. (a) F. M. Winnik and S. T. A. Regismond, *Colloids Surfaces A: Physicochem. Eng. Aspects*, 1996, **118**, 1-39; (b) P. Deo and P. Somasundaran, *Langmuir*, 2005, **21**, 3950-3956.

47. Initial findings using photo correlation spectroscopy (PCS) to study the behaviour of PPE **155** in water. Courtesy of Emma Morgan (MRes Thesis, MRes in Nanotechnology, Department of Chemistry, Imperial College London, 2006).

48. L. Chen, D. McBranch, R. Wang and D. Whitten, *Chem. Phys. Lett.*, 2000, **330**, 27-33.

49. The buffer conditions used for the sodium acetate buffer were selected because they are optimal for conducting a phosphatase enzyme assay under mildly acidic conditions.

4 Third Generation Polyelectrolytes: Synthesis and Sensing Assessments

4.1 Synthesis of third generation cationic PPEs and PEs

The last chapter related to the development of novel cationic PEs and PPEs and their emission properties in different solutions. Additionally, detailed analysis of the sensing properties of PPE **155**, in high ionic strength media, enabled us to identify the optimal conditions for sensing in such solutions. Of key importance is the use of a non-ionic surfactant, which served to improve the electronic communication between polymer chains. This allows for the high sensitivity displayed in aqueous conditions to be maintained even in the presence of various salt additives.

Hitherto, most reports on emission quenching of conjugated materials had focused on traditional (i.e. alkoxy PPVs, PPEs and PTs) polymer backbones. In these studies, subtle changes to the monomer compositions were made in attempts to 'tune' the band-gap of the final polymer and hence control the emission properties for a given application (Chapter One, section 1.5).

Though excellent progress had been made in the field, as evidenced by the development of sophisticated DNA sensors,[1] enzyme assays[2] and protein[3] and ion sensors,[4] most of these works involved simple polymer structures that were not optimised for the task. In more recent contributions, the group of Swager *et al.* revealed the synthesis of an electron-*deficient* PPE polymer that has the ability to detect electron-*rich* quenchers, thus providing a complement to existing materials. Work on metallopolymers introduced new ways of combining recognition sites directly into the polymer backbone (see Chapter One).

We too were interested in improving the applicability and sensitivity of such materials and so wanted to examine the effect of moving the recognition site – the point where quencher molecules interact with the fluorophores – closer to the conjugated unit. It was anticipated that the direct coupling of these parts of the PE/PPE would increase the efficiency of the electron/energy transfer process between the conjugated unit and quencher molecule and so result in higher Stern-Volmer constants. This idea was reinforced by Zhang *et al.* who reported that by maintaining electronic communication between the conjugated backbone and the receptor in a PPE/PT copolymer, a 2.6-fold increase in the sensitivity could be realised.[5]

Many designs for these polymers were considered (Figure 4.1), but due to the synthetic problems encountered with the isothiouroniums described in Chapter Three, we opted for guanidinium-based receptors as they afford more synthetic flexibility and can be incorporated into molecules in a variety of ways and are thus a good substitute for the isothiouronium group. Guanidiniums are

ubiquitous reocognition motifs in supramolecular chemistry and possess a variety of interesting properties.[6] The native guanidinium ion is protonated at psysiological pH ($pK_a \approx 13$) and is therefore an inherently good hydrogen bond donor.[6] This feature was first observed in naturally occurring arginine binding hosts.[6] More recently, guanidinium derivatives have been synthesised for use in a variety of anion sensors.[7] In addition to forming strong non-covalent interactions with anionic groups like phosphates and carboxylates, the guanidinium group possesses the correct geometric orientation to interact with these groups.[8] Binding constants for guanidinium-based anion sensors are typically > 10^2 M^{-1} and when a triethylbenzene scaffold was used to support three guanidinium groups in order to detect citrate, a binding constant of 7 x 10^3 M^{-1} was recorded, in pure water.[9]

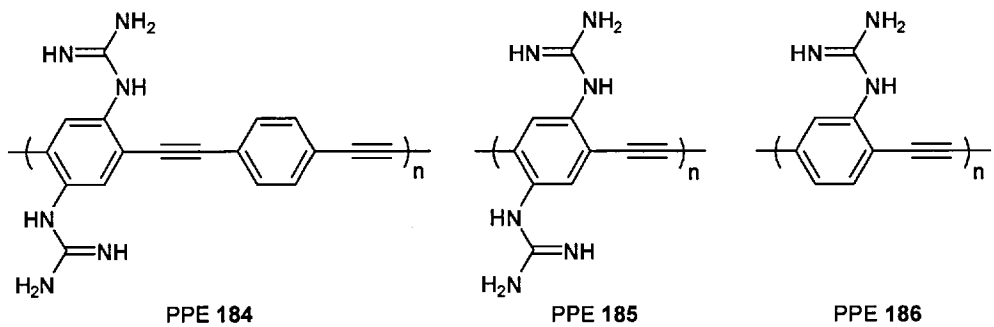

PPE **184** PPE **185** PPE **186**

Figure 4.1 Proposed third generation PPE structures.

The polymer targets shown in Figure 4.1 represent varying numbers of receptor sites and spacings, per unit length, along the polymer backbone. Our intended strategy involved the synthesis of polymers containing the recognition motifs incorporated into the polymer backbone in either of the ways described above. As we were unaware of the kind of architectures that would be best suited for sensing small molecules or biomolecules, the structures were analysed spectroscopically to judge how suitable they would be as sensors. In general, we wanted to minimise the number of functional groups along the backbone so that the approach of anions to the receptor was unhindered.

The presence of multiple guanidinium groups along the polymer backbone could lead to changes in the ability of the polymer to form complexes with DNA. The native guanidinium group has a pK_a of ~ 13 and as a result remains protonated over a wide pH range which would enable a potential sensor to operate in varied conditions and allow for the efficient formation of hydrogen bonds with the DNA bases.[6] Guanidinium-containing cationic lipids have been previously shown to undergo efficient gene transfection and such examples provide a firm basis for our overall approach to DNA recognition.[10]

4.1.1 Synthesis of a second generation guanidinium-derived PE

Reterosynthetic analysis for the structures shown in Figure 4.1 indicated that the first steps towards such polymers involved the synthesis of monomer **192**. The attempts to this molecule are shown in Scheme 4.1.

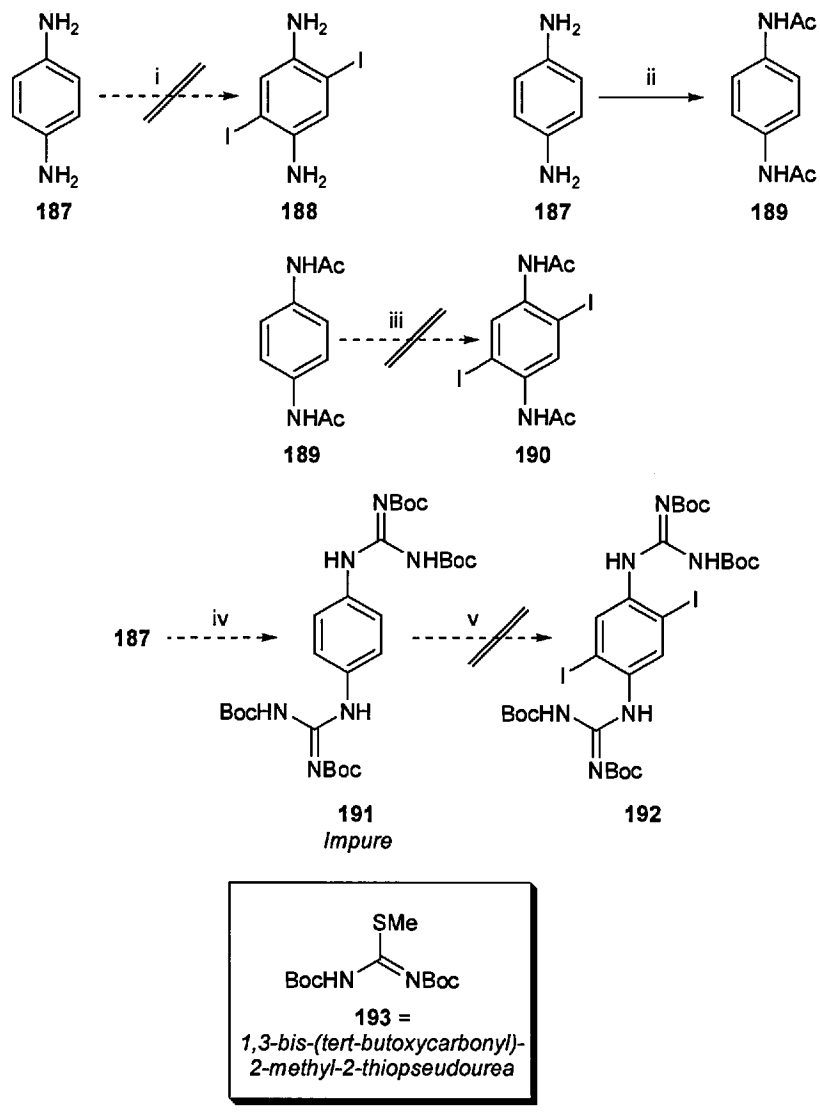

Scheme 4.1 Attempted synthesis of third generation protected guanidinium monomers. Conditions: i) 1. I_2, KIO_3, H_2SO_4, AcOH (100%), 6 h; 2. $PhI(CF_3CO_2)_2$ (**147**), I_2, CH_2Cl_2, 20 °C, 6 h; 3. ICl, NaOAc, AcOH, 80 °C, 3 h; ii) Ac_2O, NEt_3, 35 °C, 1 h, 75%; iii) 1. $PhI(CF_3CO_2)_2$ (**147**), I_2, CH_2Cl_2, 20 °C, 6 h; 2. ICl, NaOAc, AcOH, 80 °C, 6 h; iv) NEt_3, $HgCl_2$, **193**, DMF, 25 °C, 50 h, 20%; v) **147**, I_2, CH_2Cl_2, 20 °C, 8 h.

The starting point involved diamine **187** and it was envisaged that both amines on this molecule could be functionalised, after initial iodination. However, all attempts to perform this iodination led to the isolation of a dark oily residue with either no product formation evident or inseparable

mixtures (purification by column chromatography and recrystallisation were attempted). Three different methods were used;

- Initially, treatment of **187** with iodine and potassium iodate in refluxing acetic acid gave a dark solid, unidentified by ^{1}H NMR.
- Treatment of amine **187** and acetyl-protected amine **189** with the hypervalent iodine species bis(trifluoroacetoxy)iodobenzene (**147**) in CH_2Cl_2, a suitable iodinating agent for similar alkoxy derivatives,[11] also failed to give the desired products. Only iodobenzene (~ 10% from the initial amount of **147** that was added, in each case) could be extracted from the reaction mixture, an expected by-product from the reaction. The starting materials could not be detected by ^{1}H NMR.
- Iodine monochloride, another common iodinating species, was used to iodinate the protected amine **189**. Despite treating the amine for 6 hours at 80 °C (typical conditions involve heating for only 30 minutes),[12] no reaction occurred, and the starting material was reclaimed (90%). The same method was used to convert amine **187** to **188**, which again led to isolation of the starting material (~ 90%) as confirmed by ^{1}H NMR (resonance at 7.25 ppm) and MS.

Monomer **188** has been previously prepared from the dicarboxylic acid.[13] However this synthetic route, involved eight steps from commercially available starting materials.[13,14] It was believed that the difficulties that we encountered in trying to obtain gram-quantities of **188** could, in part, be due to the initial purity of diamine **187** (purity ≈ 97%). Purification of amine **187** was achieved by recrystallisation from $CHCl_3$ using activated carbon followed by hot filtration, which converted the previously dark brown solid, into light pink crystals which were of high purity (as confirmed by ^{1}H NMR; the exact purity was not determined). Unfortunately, this improvement made no difference to the outcome of the iodination, using any of the treatments discussed above. Iodination of the protected amine **189** led to similar results. To avoid such issues, the alternative route to **192** involved treatment of **187** with the electrophilic amidine species **193** (Scheme 4.1) to yield a crude sample of **191** in 20% yield. The ^{1}H NMR for this material showed the desired resonances but also indicated the presence of an aromatic impurity. This was confirmed by TLC which showed the presence of two additional spots (one with a higher R_f than the product, visible by UV irradiation). It is possible that deprotection may have occurred, which would give rise to a product with different aromatic resonances and R_f values.

The crude sample of the bis BOC-protected guanidinium entity **191** was carried forward. However, further iodination attempts on this new derivative did not yield the desired target monomer (**192**), as confirmed by ^{1}H NMR and MS, and similar purification problems arose. No further attempts

were made to investigate this reaction and at this point the iodination of aromatic amines, such as those shown Figure 4.1, was abandoned due to problems with the isolation and purification of the molecules containing the required 2,5-diiodo-1,4-diamine substitution pattern.

After all attempts to isolate pure samples of monomer **192** were exhausted a new synthetic scheme had to be found. An alternative strategy to aromatic amines had been described by Tour *et al.*[15] (Scheme 4.2a) and had the benefit of yielding both mono- and di-substituted derivatives, by further functionalisation of amine **196** (Scheme 4.2) in the following way; protection of the amine, followed by nitration, reduction and finally deprotection would lead to the desired 2,5-dibromo-1,4-diamine derivative (the bromo derivative of **188**). Due to time constraints, only the mono-substituted monomer was pursued using Tour's strategy. The first target was a small model analogue derivative of the polymer structures described in Figure 4.1. It was envisaged that by developing a successful strategy to the PE small model analogues we could establish a platform to pursue a polymer synthesis, based on the analogous structures.

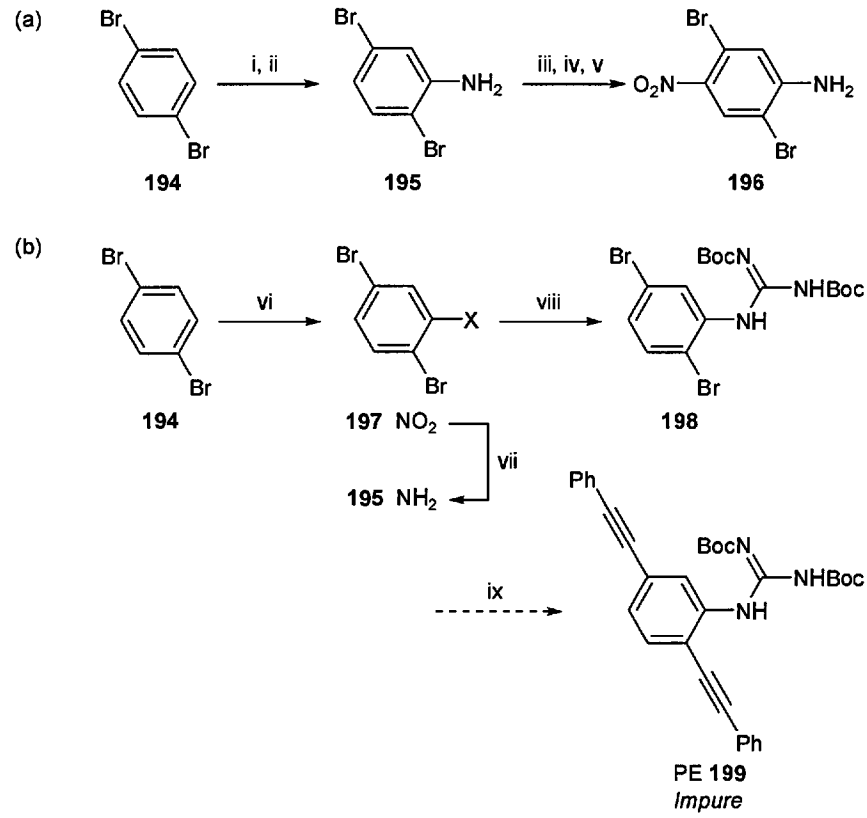

Scheme 4.2 (a) Tour's synthesis of a nitroaniline precursor (**196**).[15] Conditions: i) HNO_3, H_2SO_4, CH_2Cl_2, r. t., 1 h, 98%; ii) $SnCl_2{\cdot}H_2O$, THF, EtOH, 30 mins; iii) Ac_2O, NEt_3, 30 mins, 92% (over two steps); iv) H_2SO_4, HNO_3, -20 °C, 1 h, 63%; v) K_2CO_3, MeOH, CH_2Cl_2, 3 h, 88%. (b) Attempted synthesis of guanidinium-derived PE **199**. Conditions: vi) HNO_3, H_2SO_4, CH_2Cl_2, 25 °C, 45 mins, 65%; vii) $SnCl_2{\cdot}H_2O$, THF/EtOH, 25 °C, 22 h, 95%; viii) NEt_3, $HgCl_2$, **193**, DMF, 25 °C, 14 h, 28%; ix) phenylacetylene, $Pd(PPh_3)_4$, CuI, $^iPr_2NH$, THF, 45 °C, 26 h.

Synthetic work centred on the key monomer **198** (Scheme 4.2b) which was synthesised successfully. The coupling reaction between **198** and phenylacetylene appeared to proceed smoothly; TLC indicated the presence of two products (R_f = 0.75 and 0.45, in CH_2Cl_2/*n*-hexane, 1:1, (v/v)) which were separated by column chromatography (CH_2Cl_2/*n*-hexane, 1:1, (v/v)). The first fraction contained the starting material phenylacetylene, however ^1H NMR analysis of the second proved inconclusive; the aromatic region did not show the same coupling patterns to that expected for similar molecules (e.g. Tour *et al.* have synthesised various PE analogues for conductance tests)[15]. The resonances expected from the protected gaunidinium motif were present (~ 10.6, 11.6 and 1.5 ppm) but it was not possible to correlate them with those from the aromatic region. Additionally, integration of the BOC group resonances with those from the aromatic region gave a ratio of 0.26 instead of an expected value of 0.72 (although this could be offset by the presence of some water in the sample which has a resonance at ~ 1.5 ppm). Time constraints prevented further analysis of possible sources for impurities generated during the reaction and so

this initial attempt at cross-coupling **198** with phenylacetylene did not provide sufficiently pure samples of PE **199**.

To circumvent this, **195** was coupled directly with phenylacetylene. The reaction was monitored by TLC and two spots were detected (R_f = 0.4 and 0.2; in *n*-hexane) in the product mixture. Purification of the crude reaction mixture by column chromatography led to the first product (R_f = 0.45) being identified as the unwanted homo-coupled material **201** and the rest as starting material (Scheme 4.3).

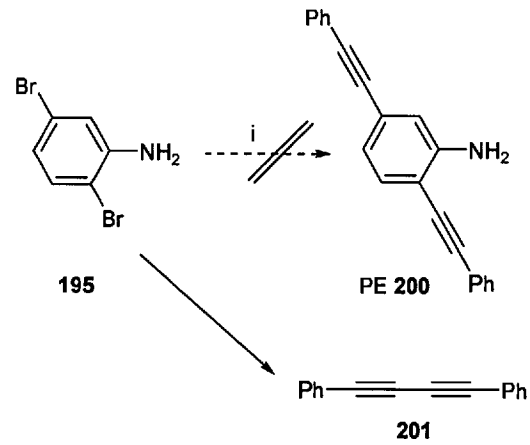

Scheme 4.3 Attempted synthesis of an amine-functionalised small model analogue PE **200**. Conditions: i) Phenylacetylene, $Pd(PPh_3)_4$, CuI, $^iPr_2NH$, THF, 20 °C, 20 h.

The possible reasons for the formation of the homo-coupled product were not considered further, but it is possible that small changes to the cross-coupling conditions may have resulted in the desired product. The conditions detailed in Scheme 4.3 were optimised for the cross-coupling of (very labile and therefore more reactive) diiodo monomers and bis-terminal alkynes. With these starting materials, a successful reaction can be achieved at room temperature. The dibromo monomer **195** and similar dibromo compounds are known to be less reactive[16] and conducting the reaction at an elevated temperature (in similar examples reactions Tour *et al.* use temperatures of 80 °C)[16] may have increased the rate of formation of the desired product PE **200**, before homo-coupling consumed the terminal alkyne, leading to unwanted **201**.

In an alternative route, the synthesis of PE **202** was achieved successfully (Scheme 4.4). The plan was to reduce the nitro small model analogue derivative (PE **202**) to the amine PE **200** with subsequent guanylation[17] expected to yield target PE **199**. Disappointingly, reduction of PE **202** with tin(II) chloride in absolute ethanol (the same conditions that were successfully employed to reduce **197** to amine **195**), gave a mixture of compounds by TLC (evidenced as a series of

luminescent spots; R_f = 0.15, 0.25 and 0.64, in *n*-hexane/CH_2Cl_2, 1:1) that proved difficult to separate. The crude mixture was recrystallised from CH_2Cl_2/*n*-hexane mixture (8:2) to yield a bright yellow powder, but the three products were still present when the solid was analysed by TLC with none of the spots corresponding to the starting material. ^{1}H NMR spectra were inconclusive, with the aromatic region displaying the same complex coupling patterns as present in PE **202**. The peak *m/z* = 293, corresponding to PE **200**, could not be confirmed by mass spectrum analysis (positive chemical ionisation with ammonia gas).

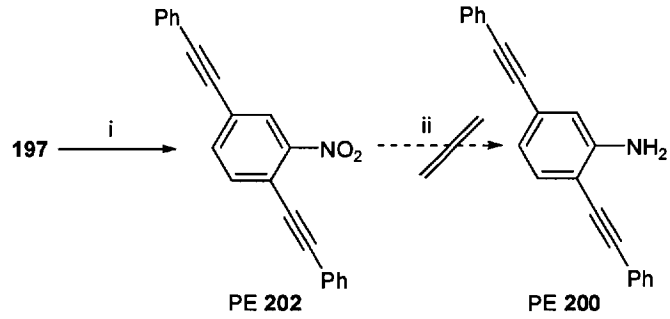

Scheme 4.4 Attempted alternative route to small model analogue PE **200**. Conditions: i) Phenylacetylene, $Pd(PPh_3)_4$, CuI, $^iPr_2NH$, THF, 45 °C, 1 h, 31%; ii) $SnCl_2 \cdot H_2O$, THF/EtOH, 70 °C, 16 h.

The difficulties associated with trying to obtain a suitable monomer that could be used to make a small model analogue and subsequently polymeric derivatives, meant that other strategies had to be sought. The setbacks encountered here, all centred on the cross-coupling procedure, which was necessary to form the PE backbone. Purification of such materials was often problematic and crude yields were moderate. To avoid such issues, we sought to invoke the palladium-catalysed step (to the PE analogues) as the last transformation, thus avoiding the previously encountered problems. In Scheme 4.5 the target is not a PE analogue but the versatile bisalkyne monomer **206** (Scheme 4.5) that can be reacted under mild conditions to form PE or PPE materials.

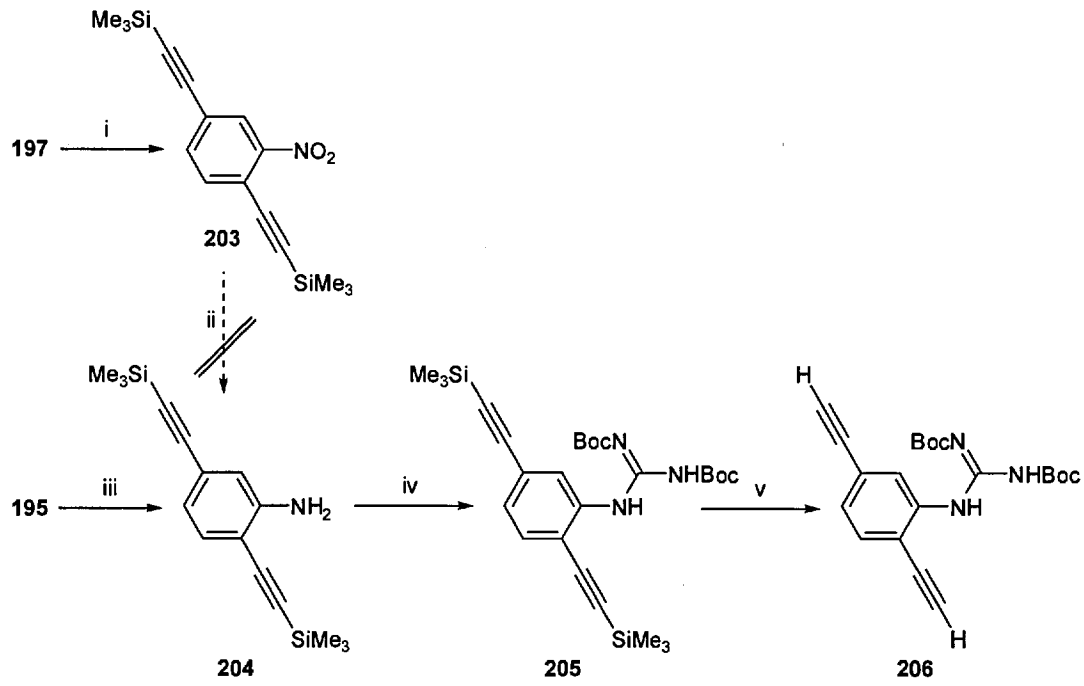

Scheme 4.5 Synthesis of key bisalkyne monomer **206**. Conditions: i) TMSA (**110**), $Pd(PPh_3)_4$, CuI, $^iPr_2NH$, THF, 45 °C, 3.5 h, 31%; ii) $SnCl_2{\cdot}H_2O$, THF/EtOH, 20 °C, 5 h; iii) TMSA (**110**), $Pd(PPh_3)_4$, CuI, $^iPr_2NH$, THF, 60 °C, 75 h, 65%; iv) NEt_3, $HgCl_2$, **193**, DMF, 25 °C, 50 h, 68%; v) K_2CO_3, MeOH/THF, 25 °C, 4 h, 71%.

The synthesis allowed access to gram quantities of bisalkyne **206**, which was then quickly employed in the synthesis of a guanidinium-derived PE small model analogue. In an initial route to **206**, the bis TMS-protected **203** was isolated by cross-coupling **197** with trimethylsilylacetylene (**110**). ^1H NMR analysis of the product was consistent with that reported in the literature. However, attempts to reduce this compound to the aniline derivative **204** failed, with several spots visible by TLC (one corresponding to the starting material).

Guanidinium functional groups are commonly incorporated into a wide range of molecules in their protected form[18] in order to aid sample handling and purification (in their protected form guanidines are less polar and basic, unlike free guanidines) and increase the compatibility of the chemistry with existing routes.[18] To incorporate the guanidinium unit into a PE analogue, amine **204** was treated with the electrophilic amidine **193** and mercury (II) chloride in DMF in accordance with literature methods,[19] which furnished guanylated **205**.[18,19] Selective deprotection of the TMS groups, to produce bisalkyne **206**, followed by cross-coupling and removal of the BOC groups (Scheme 4.6), gave PE **208** as a light-yellow crystalline solid, observed as a single luminescent spot (R_f = 0.29, Silica gel, EtOH) by TLC, and whose structure and purity were confirmed by ^1H and ^{13}C NMR and elemental analysis.

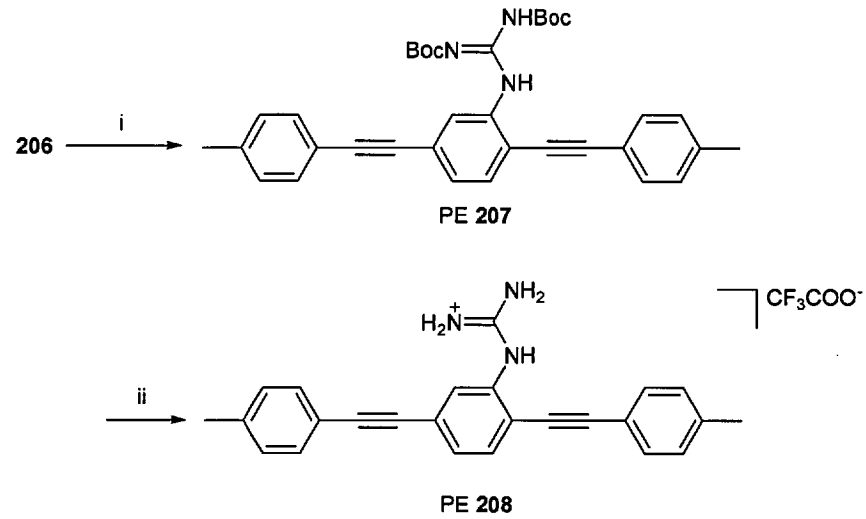

Scheme 4.6 Synthesis of small model analogues PE **207** and PE **208**. Conditions: i) $Pd(PPh_3)_4$, Cu(I)I, $^iPr_2NH$, 4-iodotoluene (**149**), THF, 25 °C, 24 h, 91%; ii) TFA in CH_2Cl_2, 25 °C, 1 h, 59%.

4.1.2 Attempted syntheses of second generation guanidinium-derived PPEs

With the small PE model analogue (PE **208**) in hand, the next stage was to synthesise the polymeric PPE version. This was accomplished using the versatile bisalkyne monomer **206** in accordance with Sonogashira conditions employed in previous PPE syntheses (see Chapter Three), to furnish the protected pre-polymer PPE **209** (Scheme 4.7). It was anticipated that the synthesis of this protected guanidinium polymer would allow for relatively easier characterisation than its deprotected variant (PPE **210**). Indeed the polymer did have good solubility in methanol and DMF and full ^1H NMR and absorption/emission data was collected. No alkyne signals were observed in the ^{13}C NMR, which in common with PPE **155** was quite noisy (presumably for similar reasons; limited solubility at the mM concentration level required for NMR), and so we were unable to check for diyne defects.

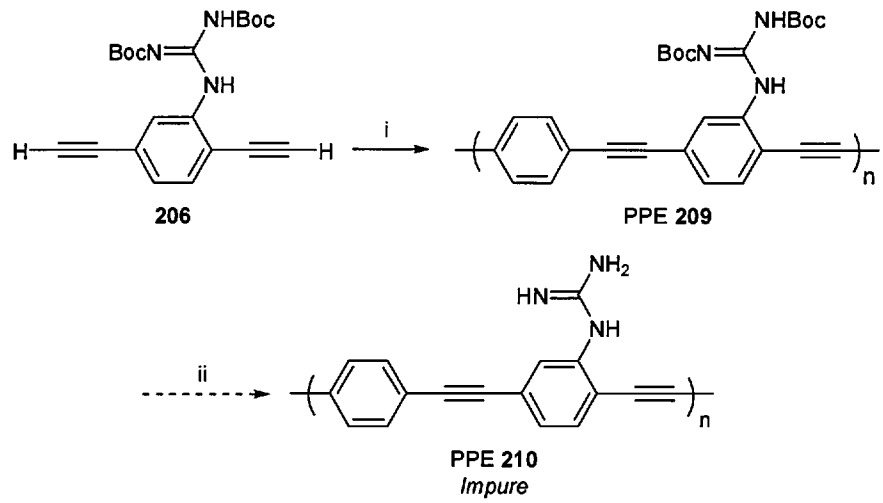

Scheme 4.7 Synthesis of third generation PPEs. Conditions: i) 1,4-Diiodobenzene (**109**), $Pd(PPh_3)_4$, CuI, $^iPr_2NH$, DMF, 50 °C, 48 h, (no yield was recorded as the polymer was stored as a stock solution in MeOH); ii) 100% TFA in CH_2Cl_2, 25 °C, 1 h.

GPC analysis was still difficult as the polymer displayed only limited solubility at the concentrations required for analysis. The protected polymer, in a solution of DMF, was heated gently (< 40 °C) for ~ 1 hour and then sonicated for 10 minutes. This resulted in a sufficient amount being dissolved which allowed the molecular weight to be determined; a value of approximately 31 kDa was calculated (GPC trace is shown in Figure 4.2).

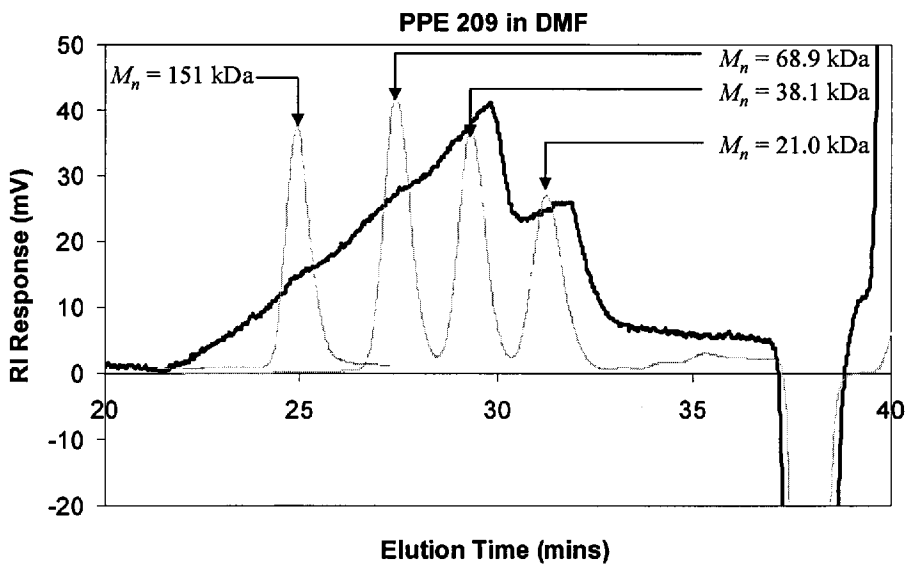

Figure 4.2 GPC chromatogram for PPE **209** (DMF at 40 °C, 0.5 mL/min, RI detector); traces in light grey correspond to PS standards.

Deprotection of PPE **209** to yield the guanidinium polymer PPE **210** appeared to occur smoothly as was backed-up by ^{1}H NMR evidence (absence of BOC group signals) but signals due to unidentified impurities were detected (e.g. a broad singlet at 5.3 ppm, in the ^{1}H NMR spectrum (in d_6-DMSO) along with signals due to diethyl ether (the deprotected polymer was precipitated by addition into diethyl ether). The polymer was placed under vacuum for six hours but the resonances due to diethyl ether still remained which suggested that the solvent may have become 'trapped' with the guanidinium group which may have been inadvertently acting as a host for this solvent. We reasoned that the broad resonance at 5.3 ppm could be attributed to the guanidinium NH protons and/or water associated with this group, as there were no broad resonances due to water in the sample (which is known to appear as a broad resonance at 3.3 ppm). Additionally, comparison of the integration of the aromatic region with the suspected NH resonances provided no further information; unexpectedly, the resonance at 5.3 ppm was approximately 30-times larger.

In an attempt to purify PPE **210** several reprecipitations were completed (all from diethyl ether, which was the most suitable solvent) along with dialysis of the crude material, but no improvement in the purity could be achieved. The crude polymer existed as a dark orange 'sticky' solid and though not pure, a stock solution (in DMSO) was prepared to assess its optical properties, which are presented in Figure 4.3 along with those of the protected precursor polymer PPE **209**.

The general method of using acidic conditions (generated by TFA) for the deprotection of BOC groups was employed at first as this was successfully used in the synthesis of the small model analogue PE **208**. However, when applied to the polymer synthesis, the precursor polymer solutions generally darkened over a short time period (~ 10 minutes) and yielded 'sticky' residues that displayed increased water solubility compared to the starting polymers, but contained impurities as determined by NMR. Mineral acids had a similar effect.

The respective absorption and emission peaks are 391 and 409 nm for PPE **209** (in MeOH) and 392 and 415 nm for deprotected version PPE **210** (in water with 0.3 wt.% Triton). The addition of the surfactant was necessary in order to record the emission spectrum of PPE **210** as in its absence there was no emission from the polymer. This is presumably due to strong self-association, leading to aggregation (though in an aqueous solution containing no surfactant, an absorption peak was visible at 394 nm). This result prompted us to consider the effects of surfactant on both PPEs (Figure 4.3).

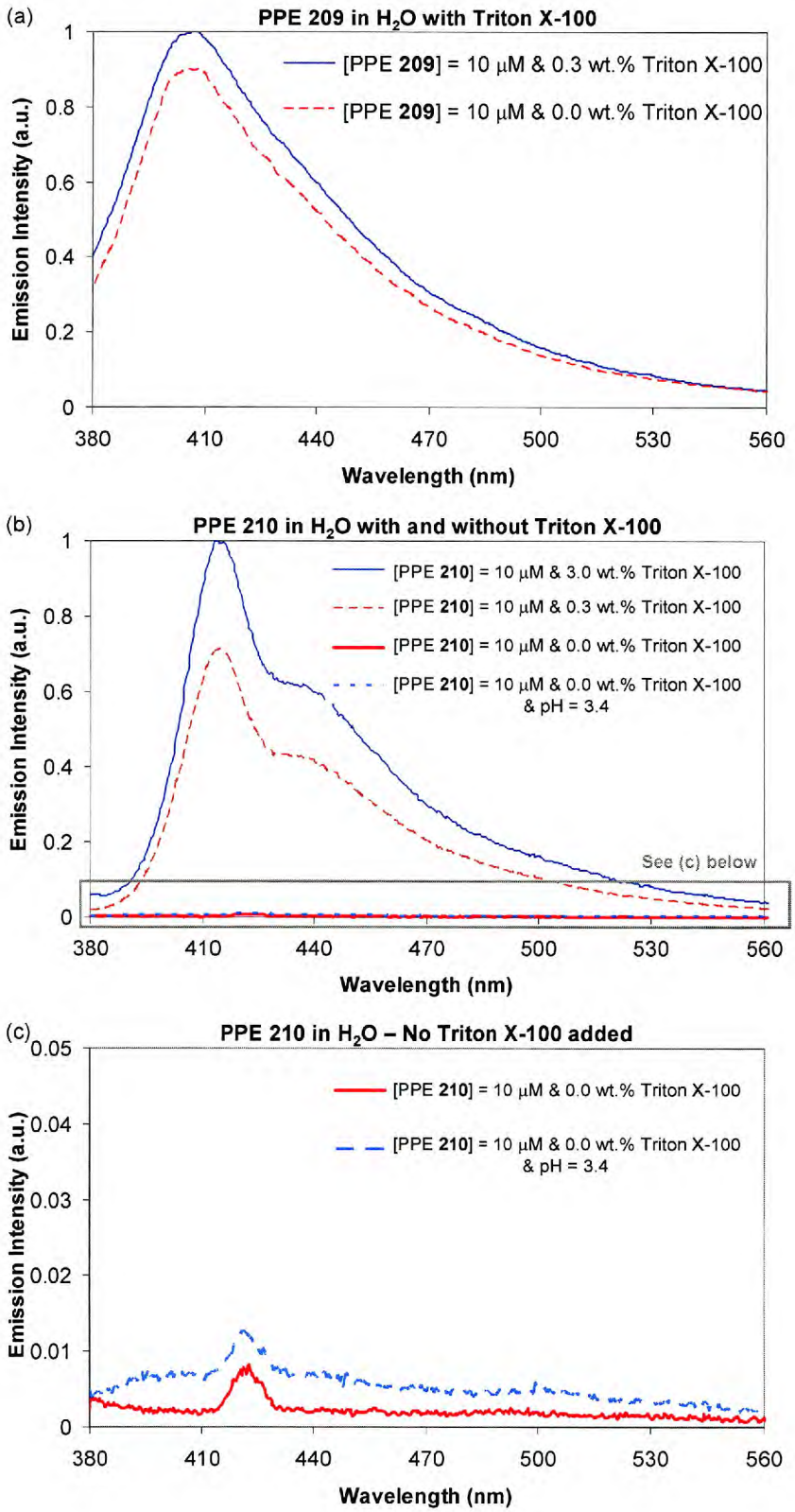

Figure 4.3 The normalised emission spectra in salt-free water and Triton-containing water for (a) 10 μM PPE **209** and (b) 10 μM PPE **210**. (c) A close-up on the emission spectra for PPE **210** in water containing no surfactant.

The emission maxima for PPEs **209** and **210** differ by small amounts (8 nm, with the addition of 0.3 wt.% Triton) in the two solvents that were used. The striking feature noticeable in Figure 4.3 is related to the variations in emission intensity depending on surfactant concentration. For the protected PPE **209**, the effect of Triton is small but when the protecting groups are removed, as for PPE **210**, the emission drops to ~ zero. The surfactant is then required to fully recover the emission from the polymer. This effect is presumably due to a lack of substitution along the PPE backbone in PPEs **209** and **210**, leading to strong π-π stacking and aggregation, which though mitigated in PPE **209** (due to the steric bulk of the BOC groups), becomes unavoidable in deprotected PPE **210**, resulting in strong self-association and self-quenching. Importantly, in this case, it is possible that the surfactant could serve in one of two ways; either, it disrupts the extent of aggregation by interfacing between the polymer chains thereby preventing self-quenching (in this case it would behave in the opposite sense to that described in Chapter Three for PPE **155**) or it alters the conformational order in the backbones of PPEs **209** and **210** leading to reduced rigidity and a lower tendency to self-associate.

The observations noted in Figure 4.3 suggested that to avoid such problems the second phenyl ring in the PPE repeating unit needed to be more heavily substituted, to prevent the polymer chains from coming into close proximity. In this regard, monomers **180** and **211** seemed suitable targets as the oligo ethylene glycol chains would minimise interaction of phenyl rings in the formed polymer whilst simultaneously ensuring water solubility, as proved in the case of PPE **182** (see Chapter Three). Copolymerisation of **180** with bisalkyne **206** led to the formation of PPE **212** as a bright yellow solid (Scheme 4.8).

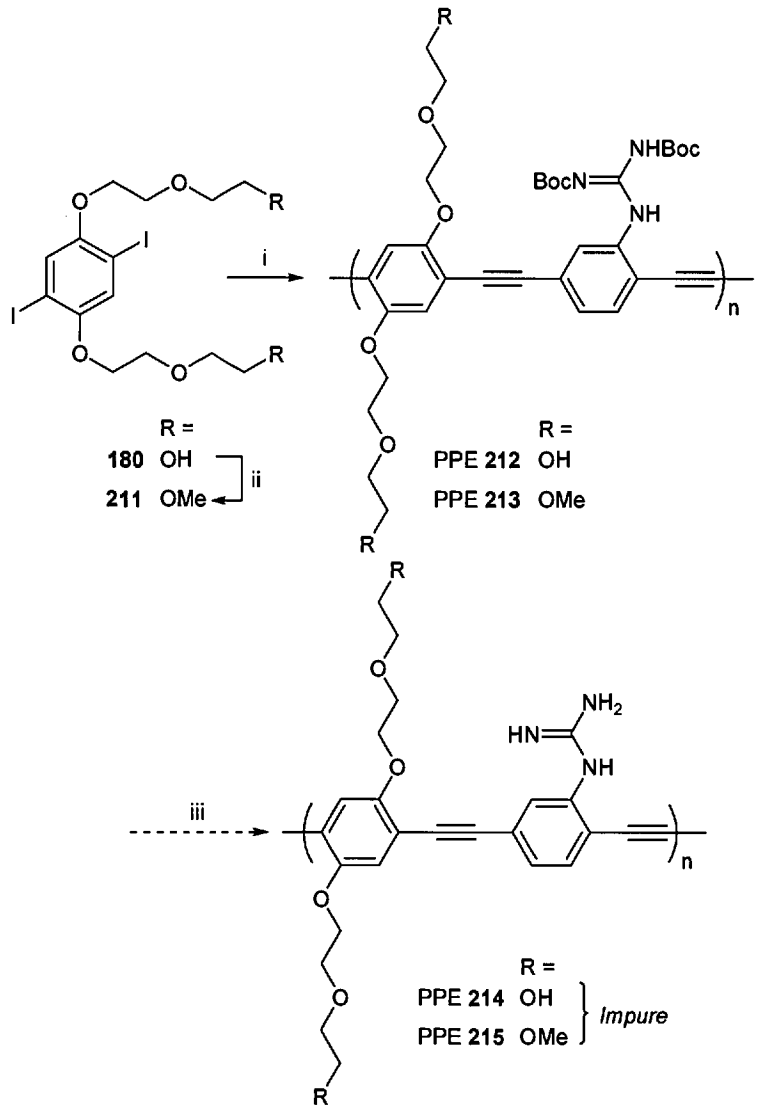

Scheme 4.8 Synthesis of PPEs **212** and **213** and attempted synthesis of PPEs **214** and **215**. Conditions: i) **206**, $Pd(PPh_3)_4$, CuI, $^iPr_2NH$, DMF, 45 °C, 24 h; ii) NaH, MeI, THF, 50 °C, 23 h, 78%; iii) TFA in CH_2Cl_2, 25 °C, 1 h.

Unfortunately, as occurred during the attempted conversion of PPE **209** to PPE **210**, the deprotection of PPEs **212** and **213** resulted in impurities being detected by ^1H NMR (acquired in d_6-DMSO for PPE **214** and d_4-MeOD for PPE **215**). The unwanted materials appeared as singlets with signals at 1.22 ppm and 1.76 ppm (for PPE **214**) and 3.20 ppm (possible singlet), 5.35 ppm (multiplet) and 10.22 (broad singlet) for PPE **215**. In common with previously described polymers (e.g. PPE **155**), PPE **214** displayed poor solubility at the concentration level required for analysis by ^{13}C NMR, and so no spectrum could be recorded. This was not a problem for PPE **215** and the ^{13}C NMR spectrum revealed the presence of several resonances (28 – 44 ppm, in d_4-MeOD) that

could not be assigned to the structure. However, possible structures for the impurity could not be postulated and due to time restrictions, the cause of the impurities was not investigated.

Attempts were made to purify the polymer by dialysis, using water. A 6 – 8 kDa molecular weight cut-off tubing was loaded with the polymers (PPE **214** and PPE **215**) dissolved in water (though the materials displayed poor solubility in this solvent; ~ 4 mg/L) and after 3 water changes the contents of the tube were lyophilised and then analysed. In both cases, there was no change in the ^{1}H NMR spectrum. This led us to conclude that a possible reason for the 'extra' resonances in the spectra could be due to the incorporation of unwanted materials into the polymer chain. The poor solubility of PPEs **212** – **215** prevented GPC spectra from being recorded, as the polymers were not sufficiently soluble in DMF.

We reasoned that subjecting PPE **212** to the acidic conditions required for the deprotection, may have led to a side reaction involving the free hydroxyl group and the carbamate unit on the BOC entity. This could lead to unwanted ring-generation or cross-linking, though in the latter case, the material would be expected to display no solubility in any solvent. PPEs **214** – **215** did show some solubility in polar solvents (DMF, H_2O; ~ 2 – 3 mg/L). The possibility of the hydroxyl group in PPE **212** undergoing reaction was reinforced when the methylated PPE **213** was subjected to the same deprotection conditions. The ^{1}H NMR spectrum for PPE **215** did not contain the two singlet resonances at ~ 1.2 ppm and ~ 1.8 ppm. Time constraints meant that the source of this impurity, formed during the deprotection with TFA, could not be fully investigated.

Several methods were attempted in order to cleanly remove the BOC protecting groups from PPEs **209**, **212** and **213** (Scheme 4.8).[20] The thermal removal of BOC groups has been successfully employed in small molecule synthesis, but treatment of PPEs with heat is generally disfavoured as this can lead to cross-linking.[21] Indeed, when this method was applied to PPE **212**, the material darkened and became insoluble in most solvents, suggesting that some cross-linking had occurred (time restraints meant that the thermal treatment of these materials under high dilution could not be attempted). The cleavage of BOC groups upon treatment with strong bases is also known.[20] This method was applied to PPE **212**, using BuLi, seemingly without success. Analysis of the formed material was not possible as it was not soluble in any of the deuterated solvents used. Our expectation was that upon deprotection of this polymer, its solubility in water would be increased due to the increased polarity associated with the guanidinium group. With all the described methods, attempts were made to monitor the reactions using IR spectroscopy, as it was envisaged that the disappearance of the BOC peaks (specifically the C=O stretch of the urethane group, which is known to appear between 1690 – 1740 cm^{-1}) would be diagnostically useful. However, the overlap of signals from the C=N group (at 1670 cm^{-1}, part of the guanidinium motif) prevented this

method from being conclusive as the intense band from this group masked other potential stretching frequencies. When TFA was employed in the deprotection, the IR technique was of no diagnostic use as the C=O stretch from TFA (at 1783 cm^{-1}) similarly blocked out other bands in this region of the IR spectrum.

The thermal decomposition of PPEs **209** and **212** was monitored by TGA and the results are shown in Figure 4.4. PPE **209** displays two weight losses; the first appears between 94 – 400 °C (a 45% weight loss) and the second is between 400 – 850 °C (a 30% weight loss). Similar analysis for PPE **212** also reveals two weight losses; the first occurred between 115 – 445 °C (a 50% weight loss), the second at 445 – 800 °C (a further 15% weight loss).

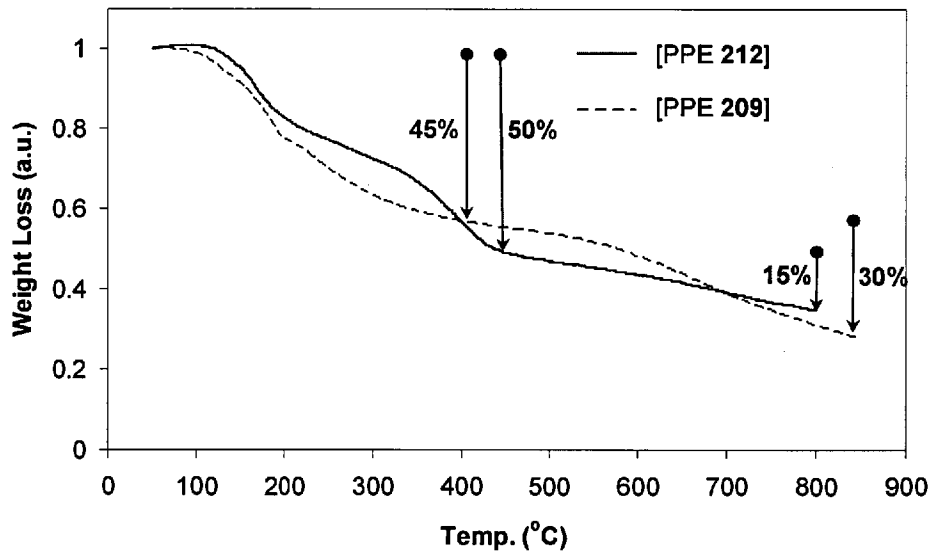

Figure 4.4 Thermogravimetric analysis (TGA) of PPEs **209** and **212** (for both analyses: a heating rate of 10 °C/min was used, under N_2).

The high thermal stability of PPEs **209** and **212** mirror the results from the thermal analysis of PPE **182** (see Chapter Three, section 3.3) where despite heating the polymer to 800 °C, the weight loss from the polymer was only 41%. The corresponding weight loss values for PPE **209** and PPE **212** are 69% and 66% respectively. As described in Chapter Three (section 3.1), TGA analyses of PPEs have been previously described and for dialkoxy-substituted PPEs, a 5% weight loss is typically observed at a temperature > 200 °C. Interestingly, for PPE **209** the 45% weight loss directly corresponds to the elimination of the BOC protecting groups from this polymer. For PPE **212**, a 30% mass loss would be expected due to elimination of the BOC groups, which may be approximately correlated with the 50% weight loss measured between 115 – 445 °C.

4.2 Spectroscopic investigation of fluorescence quenching – second generation guanidinium-derived small model analogue PE

The absorption and emission spectra for PE **208** and PE **154** in water are shown in Figure 4.5 with PE **208** showing a pronounced *blue*-shift in both spectra, relative to PE **154**.

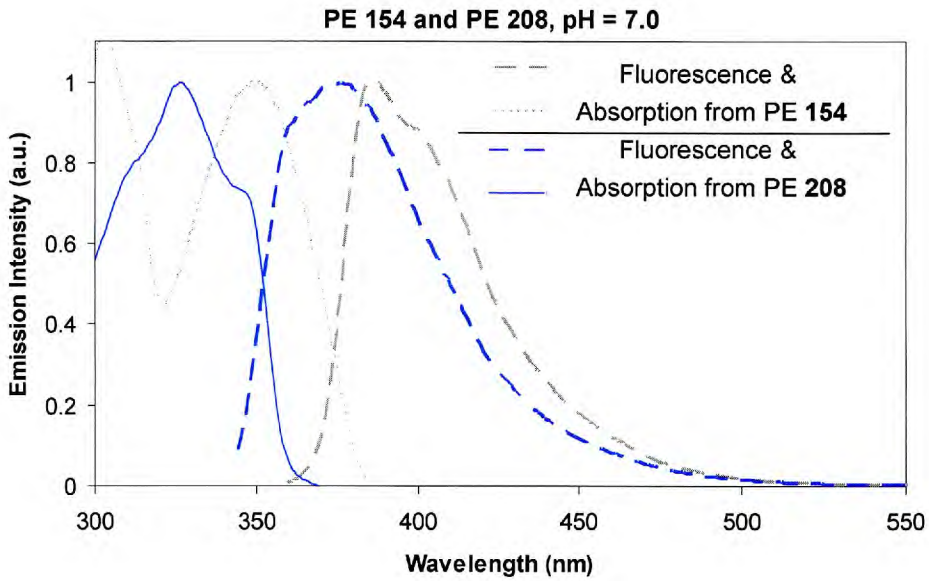

Figure 4.5 The normalised absorption and emission spectra in water for phenylene ethynylenes (PEs) **154** and **208**. PE **154**: λ_{max} (Abs.) = 351 nm, λ_{max} (Em.) = 391 nm. PE **208**: λ_{max} (Abs.) = 326 nm, λ_{max} (Em.) = 376 nm.

A comparison with structurally similar (in terms of dimensions and conjugated backbone) dialkoxy derivatives, such as PE **154**, allows for an exploratory assessment of the impact that the guanidinium motif has on the electronic properties of PE **208**. Both PE **208** and PE **154** are cationic (in water at pH = 7) but PE **208** has a single recognition unit attached directly to the conjugated backbone and PE **154** is more electron rich and may aggregate in a different mode (π-π stacking; for PE **208**, H-bonding and perhaps π-π stacking may be important). It was of interest to see whether this structural difference would lead to any changes in the sensitivity of this PE small model analogue.

As noted by Swager *et al.*,[13] amine-containing PPEs (where the amine is in direct electronic contact with the conjugated backbone) exhibit broad absorption and emission bands which tend to be red-shifted due to the electron-rich nature of the chain. Additionally their emission lack vibronic structure. The guanidinium-containing PE **208** exhibits mixed characteristics as both the absorption

and emission bands are broad (in H_2O, at pH = 7, where PE **208** is expected to be protonated), but the pronounced blue-shift suggests that the overall effect, relative to PE **154**, is reduced electron-density along the PE backbone. With a pK_a of > 12 the guanidinium group is protonated at pH = 7, in common with similar guanidinium-containing derivatives.[6,22] This would render the guanidinium motif electron-withdrawing which would also explain the blue-shifts in the absorption and emission data. This is reinforced by the ^1H NMR data where the chemical shift of the proton ortho to the guanidinium motif displays a small *downfield* shift (0.3 ppm) compared to the equivalent proton in PE **154.** The marginally larger Stokes shift for PE **208** (50 nm) relative to PE **154** (40 nm) is also consistent with this. We noted an appreciable degree of solvatochromism for PE **208**, with λ_{max} shifting from 356 nm in methanol to 376 nm in water. For PE **154** the effect was less pronounced (λ_{max} (MeOH) = 382 nm; λ_{max} (H_2O) = 391 nm). These effects were not investigated for other solvents or at different pH values.

To investigate changes in emission when PE **208** is brought into contact with electron acceptors we conducted quenching experiments using two common electron deficient quenchers: 9,10-anthraquinone-2,6-disulphonic acid disodium salt (**AQS**) and 4-nitrophenyl phosphate, bis(cyclohexylammonium) salt hydrate (**NPP**). The impact on the emission spectra of a 8 μM solution of PE **208** upon addition of **AQS** is shown in Figure 4.6 with the Stern-Volmer plots shown as insets. Emission quenching data for PE **154** is also shown.

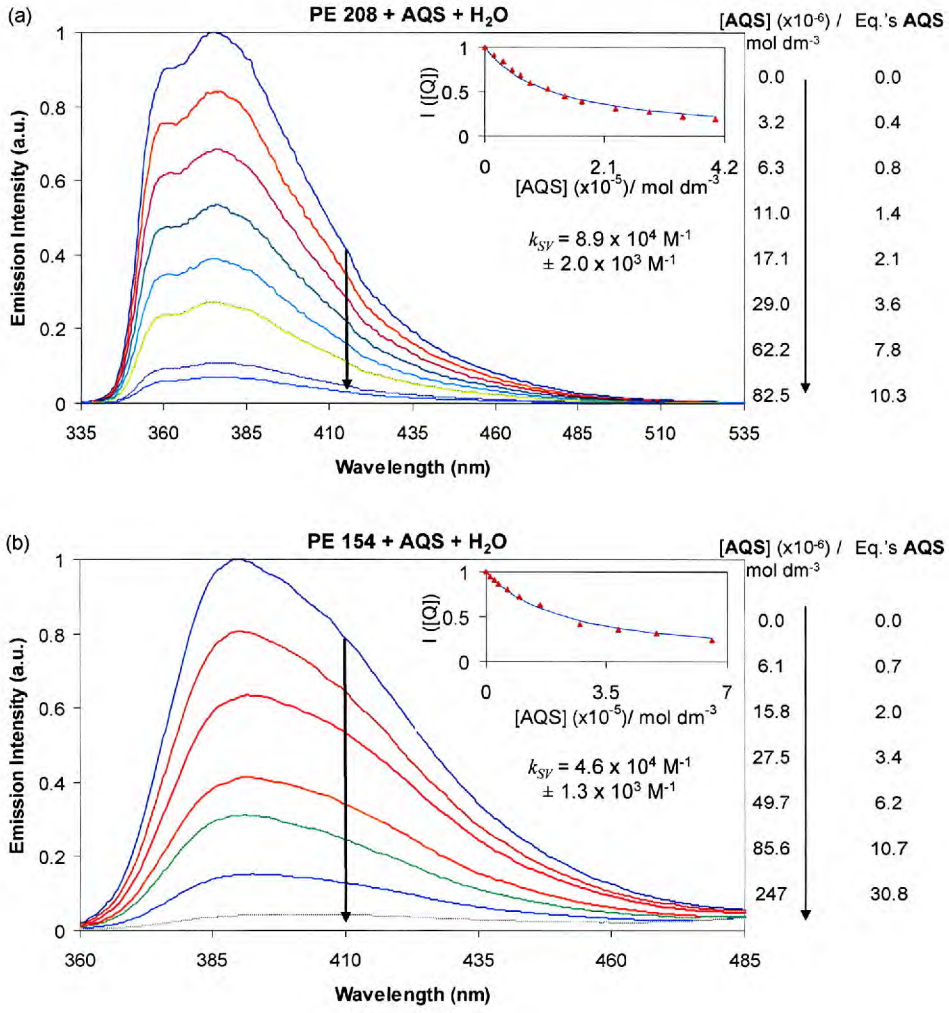

Figure 4.6 Changes in the emission spectra upon addition of the quencher **AQS** in H_2O. (a) PE **208**, and (b) PE **154**; Stern-Volmer plots are shown as insets.

Similar quenching experiments were conducted with the quencher **NPP** (Figure 4.7) and in all cases emission from the phenylene ethynylenes was quenched efficiently, with the mechanism for quenching in both cases, considered to be rapid photoinduced electron transfer (PET) through an ion-pair complex.[11,23]

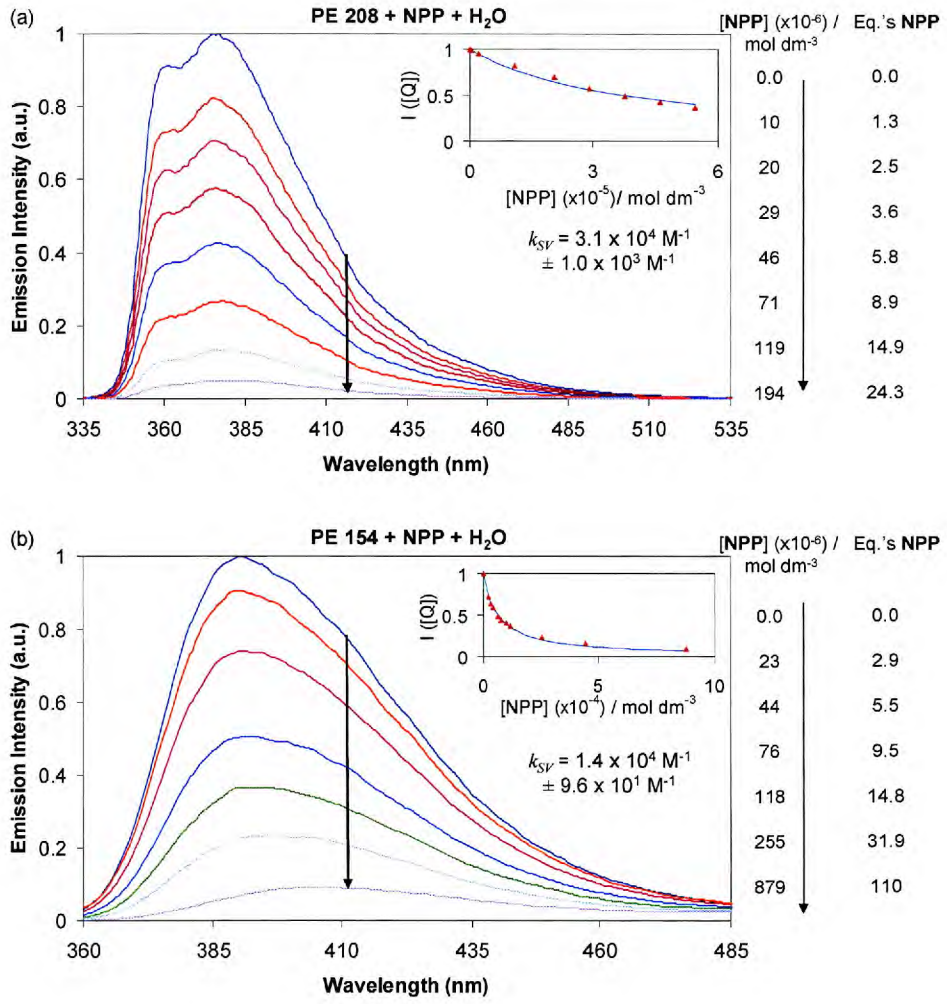

Figure 4.7 Changes in the emission spectra upon addition of the quencher **NPP** in H_2O. (a) PE **208**, and (b) PE **154**; Stern-Volmer plots are shown as insets.

Closer inspection of the quenching behaviour reveals a consistent pattern regarding the efficiency of the quenching process for the two conjugated units. For both of the quenchers used, emission quenching is more efficient for the guanidinium-containing PE **208** than for the bis-ammonium derivative PE **154**, with an approximately *two*-fold enhancement in k_{SV} observed for PE **208** over PE **154** (see Figure 4.8 for absolute numbers). This significant increase in the Stern-Volmer constant is presumably due to the proximity of the ionic recognition unit to the conjugated backbone. It is anticipated that the reduced intermolecular distance between the fluorophore and the quencher serves to facilitate the anticipated PET process and leads to a concomitant increase in k_{SV}. The Stern-Volmer values obtained for the quenching experiments with PE **208** and PE **154** are summarised in Figure 4.8.

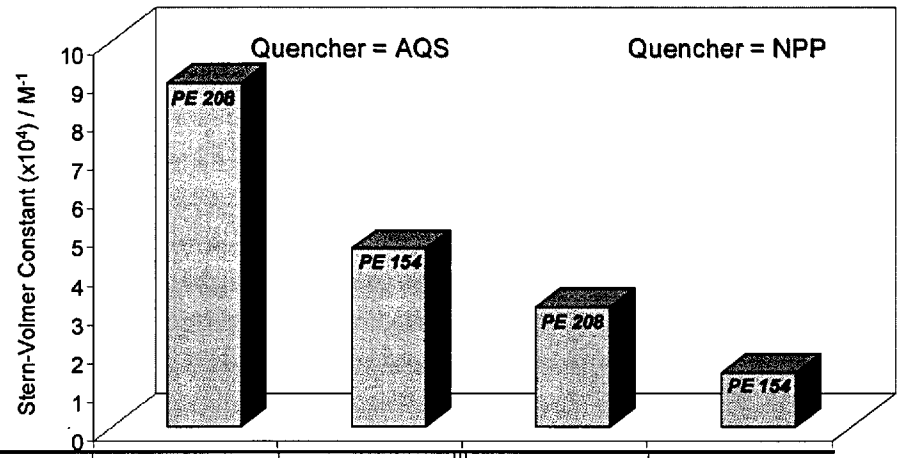

k_{sv} / M^{-1}	**8.9 x 10^4**	**4.6 x 10^4**	**3.1 x 10^4**	**1.4 x 10^4**
Error in k_{sv} / M^{-1}	2.0 x 10^3	1.3 x 10^3	1.0 x 10^3	9.6 x 10^1
Solvent	H_2O	H_2O	H_2O	H_2O
(initial pH)	pH = 6.8	pH = 6.8	pH = 6.8	pH = 6.8
Sensor	PE **208**	PE **154**	PE **208**	PE **154**
[PE **208**] or [PE **154**] / μM	8	8	8	8

Figure 4.8 Stern-Volmer constants for the emission quenching between small model analogues PE **208** and PE **154** and the quenchers **AQS** and **NPP**.

The different degree of quenching with **AQS** and **NPP** is attributed *inter alia* to the differing reduction potentials of the quenching species. Variation of the solution pH had subtle effects on the emission properties of PE **208** (due to time constraints the impact on k_{SV} could not be considered). The results are summarised in Figure 4.9. In acidic conditions (pH ~ 2.7) the emission from the analogue was almost unchanged; only a small (6%) reduction in the intensity was observed, as compared with the initial level of intensity (at pH = 6.8). At high pH levels (pH ~ 12.4) there was some broadening of the emission, possibly due to mild aggregation effects, which may have been triggered by dimerisation of PE **208**. This might occur at higher pH levels where the expected pK_a of the molecule (~ 13) would lead to more of the free base form of PE **208** being present which could then dimerise with protonated PE **208** (additionally, the formation of neutral dimers can not be ruled out). This potential pH-triggered aggregation effect could explain the broadening in the emission spectrum at elevated pH. A similar result has been observed previously for phosphonate-containing PPE polymers (PPE **42**; described in Chapter One, Scheme 1.5b).

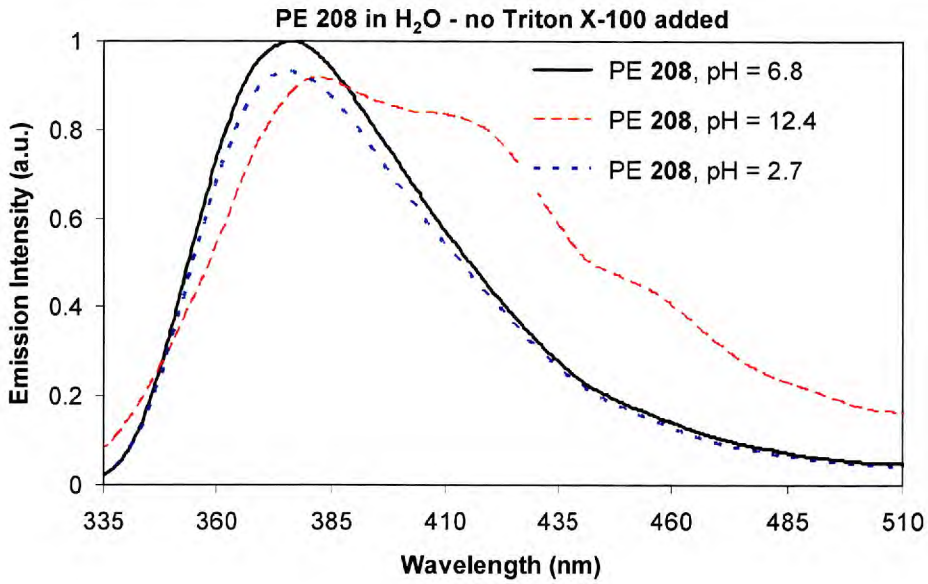

Figure 4.9 The emission spectra of PE **208** in salt-free water (containing no surfactant), at different pH levels. The pH was adjusted by addition of HCl and NaOH.

Interestingly, an in-depth study (shown in Figure 4.10) looking at possible aggregation phenomena for PE **154**, indicated that for dialkoxy small model analogues such aggregation effects had a negligible impact on either emission or k_{SV}.

Stern-Volmer constants were measured for the quenching of PE **154** by **NPP** in aqueous solutions (containing 0.3 wt.% Triton) at various concentrations of the sensor. The values differed by 1800 M^{-1} – which is only 1.6-times greater than the average expected error for such measurements (1100 M^{-1}).[24] The results are shown graphically in Figure 4.10 and suggest that solutions of structurally similar small model analogues would behave in the same way. As the solutions are of differing concentrations the amount of aggregation would also differ, a process that may be aided by the presence of the surfactant (as described in Chapter Three, section 3.6). Therefore the small change in k_{SV} over the concentration range tested suggests that aggregation effects are negligible for small dialkoxy model analogues like PE **154**, in contrast to that observed for PPE **155**. However, the subtle structural differences between PE **154** and PE **208** could result in the materials exhibiting different aggregation behaviours. This could impact the emission from PE **208** to a greater extent.

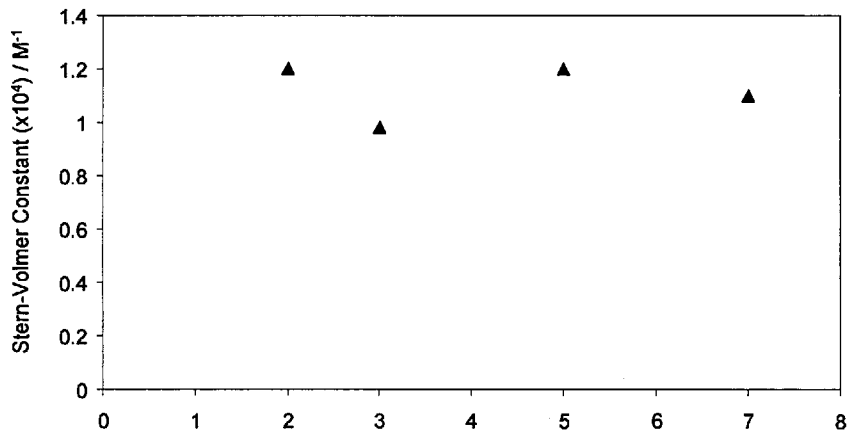

k_{sv} / M^{-1}	11500	9800	11600	10600
Surfactant	0.3 wt.% Triton	0.3 wt.% Triton	0.3 wt.% Triton	0.3 wt.% Triton
Quencher	**NPP**	**NPP**	**NPP**	**NPP**
[PE **154**] / μM	2	3	5	7

Figure 4.10 Effect of Triton X-100 on the quenching efficiency, expressed in Stern-Volmer values, for PE **154**.[25]

A MM2 simulation (Figure 4.11) of small model analogue PE **208** shows the two external phenyl rings are approximately orthogonal to the central guanidinium-derived one, as is similarly the case for PE **154**. These results are striking when compared to X-ray crystal data in other literature examples.[26] In all these cases, the π-system is almost planar across the three aromatic rings. The only exception was described by West *et al.* who noted that for their bisalkoxy PE derivative, the two terminal phenyl rings were slightly tilted with respect to the central substituted ring (as observed in the X-ray crystal structure).[27] The simulation studies were repeated with structures that lacked the receptor substituents. Using otherwise identical parameters to the previous simulation, similar results were obtained. From this we conclude that the simulation studies do not accurately reflect the true conformational molecular picture of the PE model derivatives as highlighted by crystal structures reported for numerous literature examples for similar molecules.

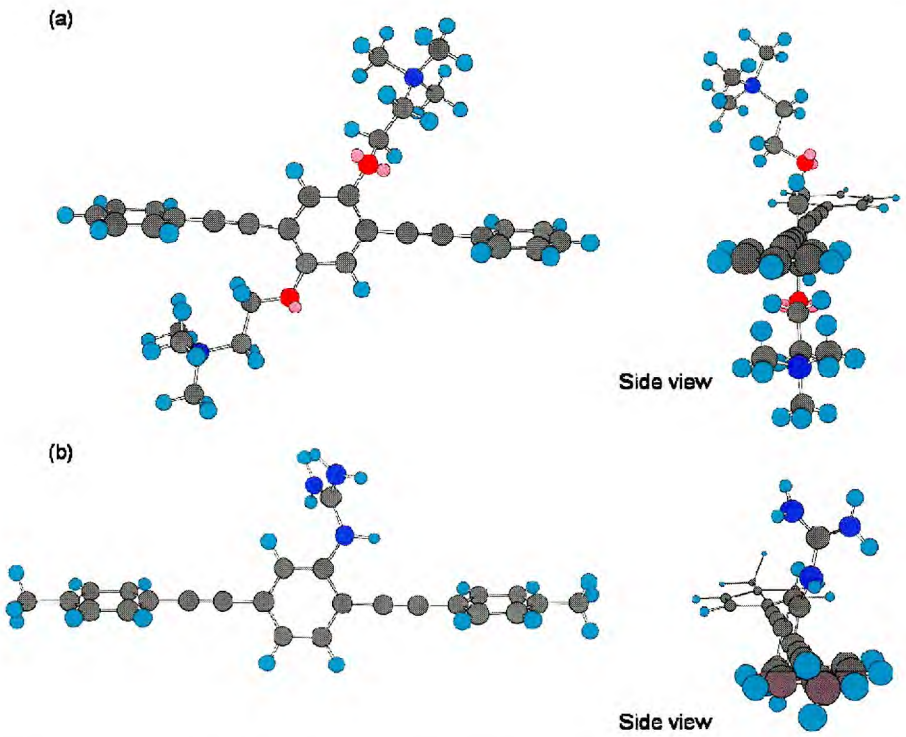

Figure 4.11 Conformations of (a) PE **154** and (b) PE **208**. Based on MM2 calculations (solvent excluded from calculations).

Overall, these findings suggest that when designing optimal PPE architectures for sensing applications, a number of requirements must be met. Maximising the number of ionic groups along a conjugated segment is important as well as considering the distance separating the ionic groups and the chromophore unit. For PE **208** the latter point may be crucial; the increased sensitivity observed for PE **208** presumably stems from the direct electronic communication of the guanidinium moiety with the PE backbone. Specific recognition groups such as guanidinium and isothiouronium units offer interesting alternatives to the commonly employed ionic water-soluble side groups and are expected to provide vastly increased selectivity when seeking to detect ions detached from electron-withdrawing moieties.

4.3 Impact on emission of small model analogues upon treatment with non-traditional quenchers

It was of interest to investigate the response of the small model analogues PE **208** and PE **154** towards simple monovalent ions and common organic anions as this would potentially broaden the scope of their use. The idea originated from the sharp responses we observed for PPE **155** towards high ionic strength conditions and in particular the presence of NaCl and buffer ions (Chapter Three, section 3.6). For this study we chose to use the commercially available disodium hydrogen

phosphate (**DHP**) and sodium acetate anions. In the first assessment, small aliquots of disodium hydrogen phosphate were added to solutions of the small model analogues and the emission monitored. Though we did not expect the presence of such ions to impart a strong quenching effect, as there is no precedent for PET processes between such moieties, any changes in the emission spectra could provide an insight into the differences between the sensors. Indeed, the addition of **DHP** to a solution of PE **208** led to approximately 80% quenching. This occurred whilst operating at similar solution concentrations as in previous experiments; the ratio (at 80% quenching) of PE **208** to **DHP** was ~ 1:13000, i.e. a very large excess of the quencher, far greater than that observed for the electron deficient quenchers, was required to get a quenching effect. Though it was not possible to fit all these data to the Stern-Volmer equation, consideration of the initial data points, corresponding to 45% quenching, could be described by this law, and yielded a k_{SV} value of 8.4 x 10^3 M^{-1}. Treatment of PE **154** in an identical fashion gave a strikingly different result; no quenching was observed. This result suggests that the sensors respond in very different ways in the presence of the phosphate anion. PE **208**, containing the guanidinium binding motif, may interact more strongly with the anion as a consequence of its recognition unit, leading to some quenching of emission. Describing a mechanism for this quenching is difficult without further experiments, though it is possible that upon binding with the anion, the guanidinium group is effectively screened and can no longer repel neighbouring PE molecules and as a result aggregation occurs (π-π stacking), leading to self-quenching. This may occur through the formation of a PE dimer, held together by the anion. It is also possible that the presence of a vast excess of anions (which would increase the ionic strength of the solution) may promote the formation of aggregates of PE **208** molecules through hydrophobic effects, a process accentuated through dimer formation. These effects would provide fertile ground for future investigations.

Sodium acetate was used in an analogous way to **DHP** in emission monitoring experiments. Exposure of PE **208** to this organic anion led to a very mild quenching effect (< 50%; the ratio of PE **208** to sodium acetate was ~ 1:35000). The Stern-Volmer equation was used to relate these data; a k_{SV} value of ~ 5 M^{-1} was recorded. This weak binding constant shows that this sensor clearly discriminates between the two anions used. As before, PE **154** showed no discernable pattern in its emission spectra upon addition of the sodium acetate anions.

In some cases, the binding of an oxoanion to a corresponding receptor can be monitored by ^{1}H NMR and an attempt was made to observe the binding of the phosphate anion diphenyl phosphate (**DPP**) with PE **208** using this technique (Figure 4.12). This phosphate was selected as it exhibited good solubility in the solvent used for NMR and was not expected to have any resonances in relevant regions of the spectrum that were being studied. By tracking the changes in chemical shifts of specific protons, usually NH resonances, binding constants can be obtained.[6] In this case,

upon addition of **DPP** to a solution of PE **208** (in d_6-DMSO), clear changes in the proton resonance due to water were observed.

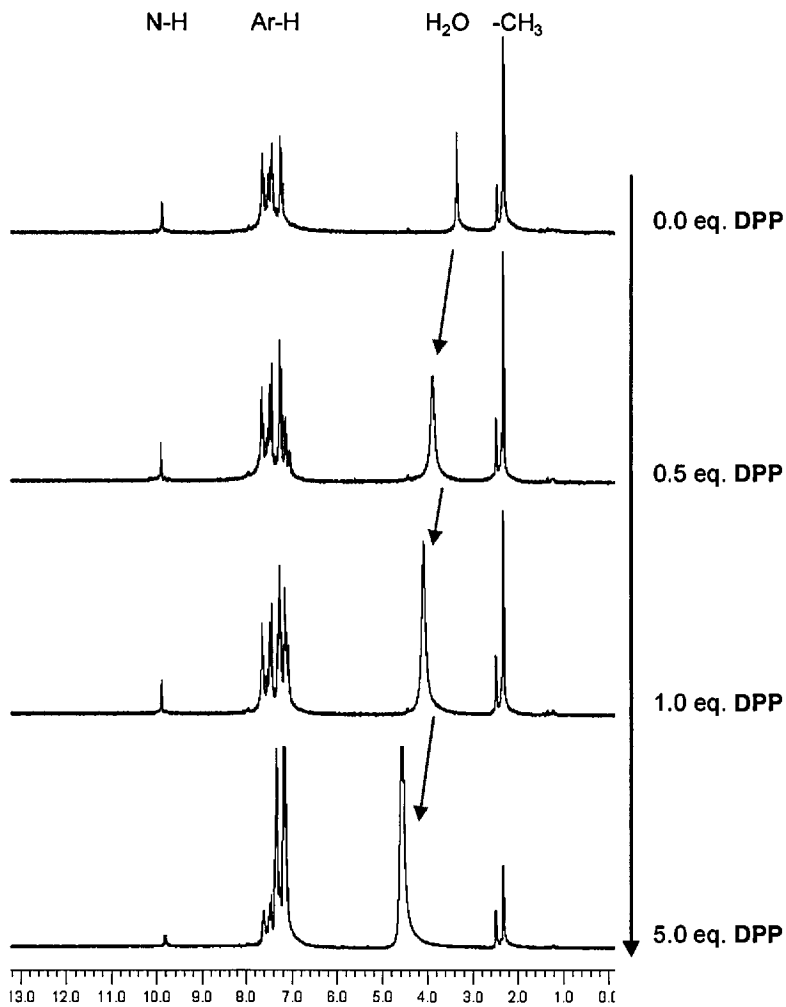

Figure 4.12 Changes in the ^{1}H NMR spectrum (d_6-DMSO, 298 K) of PE **208** upon addition of increasing amounts of the phosphate anion **DPP** (counter cation = H^+).

Only a small change in the position of the NH resonance, centred at 9.9 ppm, was observed; after the addition of 5.0 equivalents of **DPP**, this resonance had shifted downfield by 0.088 ppm. The signal due to water moved downfield by 1.2 ppm. The trend in signal shifts is different to that typically observed for similar systems.[28] Usually, changes in the thiourea resonances or -NH resonances involved in binding are observed[29] and the greatest changes occur at the early stages of the titration.[28,29] In this case, the pH of the solution may have varied during the addition of the phosphate (**DPP**) and this could impact the complexation involving PE **208**, making the titration more complex. Clearly, in a similar future experiment it would be preferable to use **DHP** in place of **DPP** which we were unable to do due to material availability and time constraints.

4.3.1 Emission quenching with PPE 210

Despite the issues regarding the purification of PPE **210**, a sample was dissolved in DMSO and a stock solution prepared, as we wanted to compare the properties of this guanidinium polymer with the dialkyl-ammonium variant PPE **155**. For PPE **210**, emission quenching studies revealed that it was a far less sensitive polymer than PPE **155**. In such experiments, it displayed k_{SV} values of 3.0 x 10^5 M^{-1} and 7.0 x 10^5 M^{-1} for **NPP** and **AQS** respectively. This compares with values as high as ~ 10^7 M^{-1} for PPE **155**. One reason for this large loss in sensitivity might be due to the presence of the surfactant that was required in order to reduce aggregation effects and obtain emission from the polymer. As has been shown in Chapter Three, the formation of aggregates is necessary in order to achieve high k_{SV} values, though certain solvent conditions can lead to a breakdown in this threshold limit. In the case of PPE **210**, no attempts were made to optimise the quantity of Triton required to generate aggregates in water. It seems reasonable to assume that the performance of this polymer could be improved if the balance between the amount of surfactant required in order to get satisfactory emission and the quantity required to allow some aggregates to remain, is met. This represents significant extra optimisation compared with PPE **155**, where the presence of the diammonium groups on each repeat unit prevented strong self-quenching, whilst allowing the free movement of photoexcitations through aggregates.

As for the small model analogues discussed before, the phosphate anion **DHP** was added to solutions of PPE **155** and PPE **210** and the impact on emission recorded. This time the diammonium-derivative PPE **155** responded more strongly towards the anion, with efficient quenching (75% reduction) expressed as a k_{SV} value of 2.1 x 10^5 M^{-1}. This contrasts with a k_{SV} value of 7.0 x 10^4 M^{-1} for PPE **210** (for a modest 45% reduction). The strong quenching observed is somewhat surprising given the nature of the 'quenching' species, but the prevalence of aggregate formation resulting in self-quenching seems likely. Both experiments were conducted in surfactant (Triton) containing water (Figure 4.13).

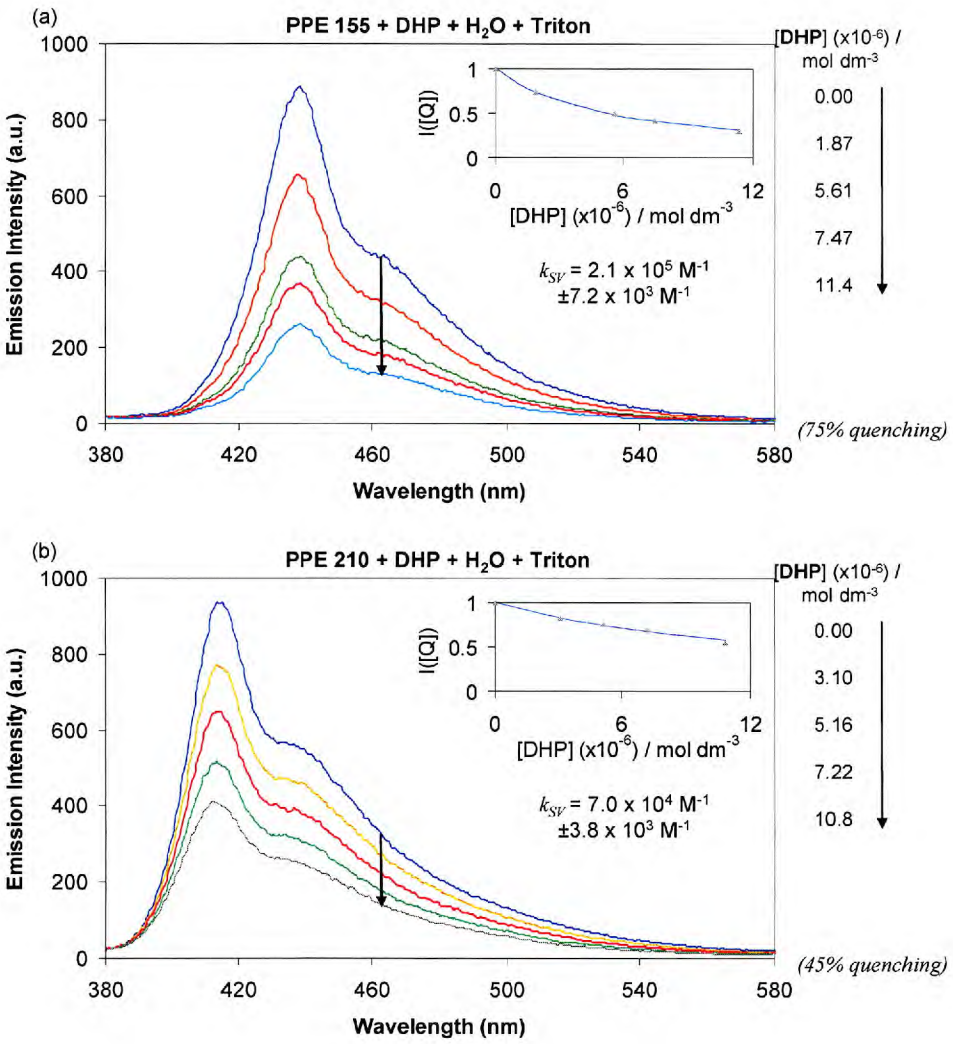

Figure 4.13 The emission spectra in salt-free water of (a) 10 μM PPE **155** and (b) 10 μM PPE **210** at increasing concentrations of **DHP**. The insets show Stern-Volmer plots using data extracted from the main figures. The degree of quenching is much stronger in the case of PPE **155**.

The emission spectra in Figure 4.13 do not display a pronounced red-shift (which is usually indicative of some degree of aggregate formation) but both absorption spectra do show subtle red-shifts upon increasing **DHP** content. This is presumably due to an increase in the conjugation length as a result of increased π-π stacking. Similar results were observed, for both polymers (PPE **155** and PPE **210**), when sodium acetate was used as the anion. The ability of these non-traditional quenchers (i.e. non-electron deficient quenchers) to behave in this way is unusual as the expected mechanism for quenching, through electron transfer to the quencher is ruled out. The results indicate that these oxoanions clearly affect the conformation of the polymer possibly through a combination of effects (similar to those described at the start of section 4.3). Further experiments are needed to probe these effects and elucidate the quenching mechanism. Monitoring the emission

lifetimes during the quenching run help identify the nature of the quenching (static or dynamic). The ability of such ions to screen the charge on these polymers is known and it seems conceivable that efficient screening of charge could lead to significant π-π stacking of the polymers (described schematically in Figure 4.14). This may occur in a cooperative way leading to strong quenching.

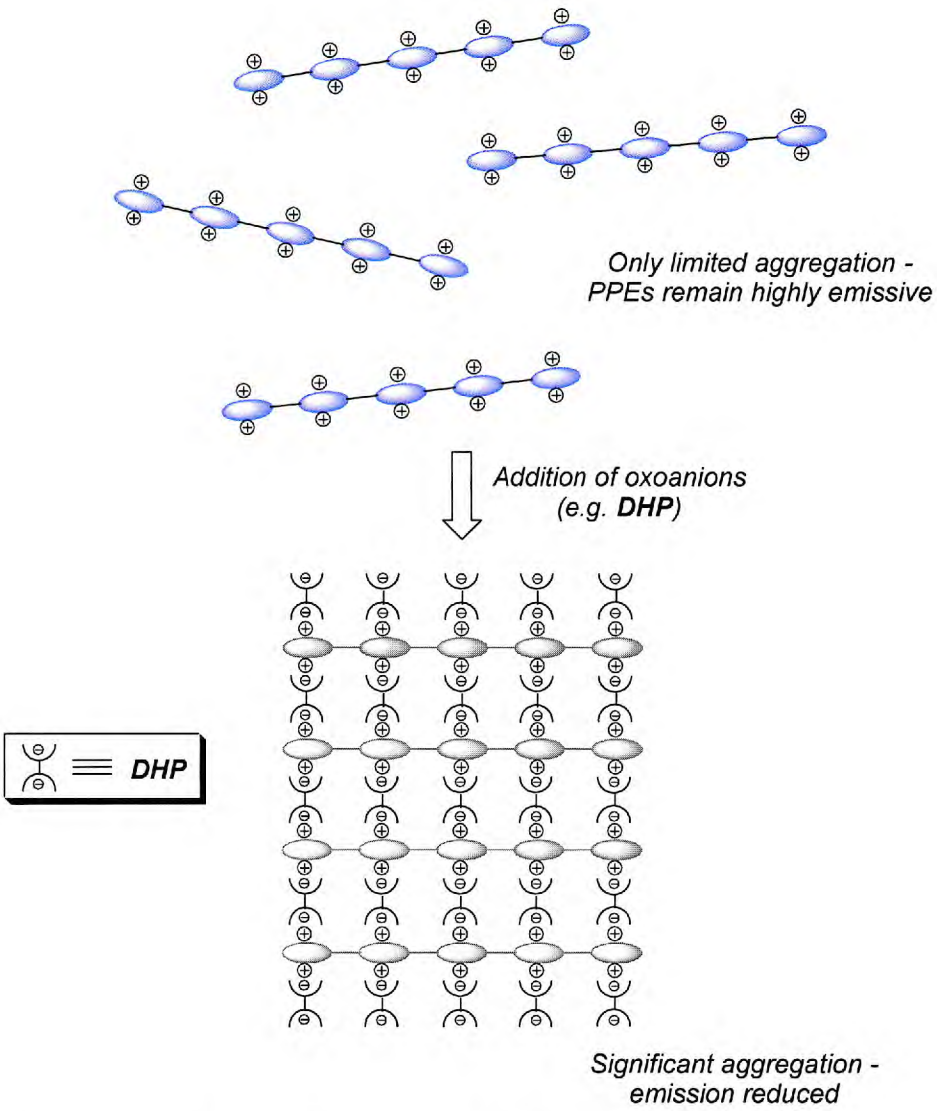

Figure 4.14 Possible effect on the CP chains (e.g. PPE **155**) upon addition of counter-ions such as NaOAc and **DHP**.

In separate experiments, CB[6] was added to aqueous solutions of PPE **155** and PPE **210**, in an effort to reduce aggregate formation (both polymers are known to be aggregated in water). CB[6], a rigid, nonadecacyclic ligand, is known to bind strongly to protonated aminoalkanes and we reasoned that it may interact/coordinate with the ammonium ions along the backbone of PPE **155** or the guanidinium motifs along PPE **210**.[30] If so, this would prevent the close association of

polymer chains and lead to increases in emission intensity (as a result of reduced self-quenching) and QEs. Unfortunately, the addition of CB[6] to a high-ionic strength solution ([NaCl] = 150 mM, at pH = 7) of the polymer had a negligible effect on the emission intensity of PPE **210** and in the case of PPE **155**, led to a small reduction (< 10%) in the emission intensity.

4.4 Notes and references

1. (a) J. W. Hong, W. L. Hemme, G. E. Keller, M. T. Rinke and G. C. Bazan, *Adv. Mater.*, 2006, **18**, 878-882; (b) F. He, Y. Tang, M. Yu, F. Feng, L. An, H. Sun, S. Wang, Y. Li, D. Zhu and G. C. Bazan, *J. Am. Chem. Soc.*, 2006, **128**, 6764-6765; (c) K. Dore, S. Dubus, H.-A. Ho, I. Levesque, M. Brunette, G. Corbeil, M. Boissinot, G. Boivin, M. G. Bergeron, D. Boudreau and M. Leclerc, *J. Am. Chem. Soc.*, 2004, **126**, 4240-4244.
2. (a) M. R. Pinto and K. S. Schanze, *Proc. Natl. Acad. Sci. USA*, 2004, **101**, 7505-7510; (b) S. Kumaraswamy, T. Bergstedt, X. Shi, F. Rininsland, S. Kushon, W. Xia, K. Ley, K. Achyuthan, D. McBranch and D. Whitten, *Proc. Natl. Acad. Sci. U. S. A.*, 2004, **101**, 7511-7515; (c) W. S. Xia, F. Rininsland, S. K. Wittenburg, X. B. Shi, K. E. Achyuthan, D. W. McBranch and D. G. Whitten, *Assay Drug Dev. Technol.*, 2004, **2**, 183-192.
3. S. J. Dwight, B. S. Gaylord, J. W. Hong and G. C. Bazan, *J. Am. Chem. Soc.*, 2004, **126**, 16850-16859.
4. F. He, Y. Tang, S. Wang, Y. Li and D. Zhu, *J. Am. Chem. Soc.*, 2005, **127**, 12343-12346.
5. Y. Zhang, C. B. Murphy and W. E. Jones Jr., *Macromolecules*, 2002, **35**, 630-636.
6. J. W. Steed and J. L. Atwood, *Supramolecular Chemistry*, Wiley, United Kingdom, 2000.
7. S. L. Wiskur, J. J. Lavigne, A. Metzger, S. L. Tobey, V. Lynch and E. V. Anslyn, *Chem. Eur. J.*, 2004, **10**, 3792-3804.
8. M. D. Best, S. L. Tobey and E. V. Anslyn, *Coord. Chem. Rev.*, 2002, **240**, 3-15.
9. A. Metzger, V. M. Lynch and E. V. Anslyn, *Angew. Chem., Int. Ed.*, 1997, **36**, 862-865.
10. J.-P. Vigneron, *Molecules*, 1999, **4**, 180-203; S. K. Sharma, A. K. Sharma, L. A. Samuelson, J. Kumar, A. C. Watterson and V. S. Parmar, *J. Macromol. Sci., Pure Appl. Chem.*, 2004, **41**, 1459–1466.
11. M. R. Pinto, B. M. Kristal and K. S. Schanze, *Langmuir*, 2003, **19**, 6523-6533.
12. D. W. Price, S. M. Dirk, F. Maya and J. M. Tour, *Tetrahedron*, 2003, **59**, 2497-2518.
13. S. W. Thomas, III and T. M. Swager, *Macromolecules*, 2005, **38**, 2716-2721.
14. Q. Zhou and T. M. Swager, *J. Am. Chem. Soc.*, 1995, **117**, 12593-12602.
15. F. Maya and J. M. Tour, *Tetrahedron*, 2004, **60**, 81-92.
16. D. V. Kosynkin and J. M. Tour, *Org. Lett.*, 2001, **3**, 993-995.

17. Definitions are as described by Powell *et al.* (D. A. Powell, P. D. Ramsden and R. A. Batey, *J. Org. Chem.*, 2003, **68**, 2300-2309): The term guanylation refers to the conversion of an amine to a guanidine. Guanidinylation involves the reaction of a nucleophilic guanidine with an electrophile to yield a highly functionalised guanidine.
18. D. A. Powell, P. D. Ramsden and R. A. Batey, *J. Org. Chem.*, 2003, **68**, 2300-2309.
19. K. C. Nicolaou, J. I. Trujillo, B. Jandeleit, K. Chibale, M. Rosenfeld, B. Diefenbach, D. A. Cheresh and S. L. Goodman, *Bioorg. Med. Chem.*, 1998, **6**, 1185-1208.
20. T. W. Greene and P. G. M. Wuts, *Protecting Groups in Organic Synthesis*, 3rd edn., Wiley-Interscience, 1999.
21. B. Erdogan, L. L. Song, J. N. Wilson, J. O. Park, M. Srinivasarao and U. H. F. Bunz, *J. Am. Chem. Soc.*, 2004, **126**, 3678-3679.
22. R. E. Marc, M. Kalloniatis and B. W. Jones, *Vision Res.*, 2005, **45**, 3454-3468.
23. C. Y. Tan, M. R. Pinto and K. S. Schanze, *Chem. Commun.*, **2002**, 446-447.
24. Based on the measurements shown in Figures 4.6 and 4.7.
25. Triton = Triton X-100 is a commercially available non-ionic surfactant that is commonly employed in bioassays and is known to act as an effective de-aggregating agent.
26. There are numerous examples of PE derivatives: (a) H. Hinrichs, A. J. Boydston, P. G. Jones, K. Hess, R. Herges, M. M. Haley and H. Hopf, *Chem. Eur. J.*, 2006, **12**, 7103-7115; (b) H. Li, D. R. Powell, R. K. Hayashi and R. West, *Macromolecules*, 1998, **31**, 52-58; (c) O. J. Dautel, G. Wantz, D. Flot, J.-P. Lere-Porte, J. J. E. Moreau, J.-P. Parneix, F. Serein Spiraua and L. Vignau, *J. Mater. Chem.*, 2005, **15**, 4446-4452; (d) C. Xuea and F.-T. Luoa, *Tetrahedron*, 2004, **60**, 6285-6294.
27. H. Li, D. R. Powell, R. K. Hayashi and R. West, *Macromolecules*, 1998, **31**, 52-58.
28. T. Gunnlaugsson, A. P. Davis, G. M. Hussey, J. Tierney and M. Glynn, *Org. Biomol. Chem.*, 2004, **2**, 1856-1863.
29. S. Nishizawa, Y.-Y. Cui, M. Minagawa, K. Morita, Y. Kato, S. Taniguchi, R. Kato and N. Teramae, *J. Chem. Soc., Perkin Trans. 2*, **2002**, 866-870.
30. K. Kim, *Chem. Soc. Rev.*, 2002, **31**, 96-107.

5 Biosensing Applications Using Second and Third Generation CPEs

In previous chapters, the synthesis, emission and quenching properties of a variety of different CPEs were described. The ability of these new materials to detect small molecule quenchers in different biologically relevant aqueous media was investigated and the importance of various additives identified. Ultimately such materials are intended to be employed in biosensing applications and in our case DNA sensing and enzyme monitoring were our main objectives, together with a more general aim to make the sensing scheme more portable and user-friendly.

In this chapter, our findings on the use of DNA bases and single-stranded materials as quenchers are detailed as well as our attempts at using cationic CPEs and their related small model analogues to detect and observe hybridisation events, monitor enzyme activity and detect small molecule quenchers in the solid state. The layout of this chapter is as follows; in sections 5.1 and 5.2, our investigations into emission quenching and hybridisation are described. The results are rationalised and possible explanations are put forward in sections 5.3 and 5.4, where our work is compared with the literature. In subsequent sections (5.5 and 5.6), an enzyme assay and our attempts at fabricating a solid state sensor are described.

5.1 Spectroscopic investigation of fluorescence quenching using tetrameric DNA strands

The ability to identify DNA or RNA strands with minimal treatment (e.g. purification or amplification) represents a challenge that has generated significant scientific interest.[1] Rapid techniques for the detection of small amounts of DNA/RNA are important for many applications including identifying genetic mutations and diseases and monitoring gene delivery and, consequently, new techniques that can identify target analytes in a highly sensitive and selective manner are eagerly sought-after.[1] Current techniques for biological molecule analysis are selective, but expensive and time-consuming (as described in Chapter One).[2-5]

The use of electronic materials, specifically conjugated polymers (CPs), is rapidly emerging as an innovative approach for the development of a new class of highly sensitive biosensor.[4] Here we describe the performance of the novel water-soluble cationic conjugated polymer PPE **155** as a sensitive probe for DNA detection. This polymer was selected as we had a thorough understanding of the factors that affected its emission and sensing properties through the extensive investigations that were detailed in Chapter Three. Additionally, this material is similar in structure to the family of cationic poly(fluorene)s that were successfully employed by Bazan *et al.* for the detection of oligonucleotides.[6] We reasoned that the high sensitivity displayed by PPE **155** (towards small

molecule quenchers) combined with the structural similarities with Bazan's polymer, would make this polymer an ideal candidate for a DNA sensor.

The sensing scheme is assumed to work, analogously to that observed for small molecule quenchers; target analytes form ion-pairs with the CPEs allowing for potentially rapid electron transfer.[2,4] Leclerc *et al.* were the first to employ CPEs (poly(thiophene)s) to detect DNA strands in solution.[7] Their strategy involved observing changes in the emission band of the polymer upon addition of probe and target DNA strands (detailed in Figure 1.17, Chapter One). Bazan *et al.* have used FRET processes with poly(fluorene)s to monitor hybridisation events (Figure 1.19 and Figure 1.20, Chapter One).[8]

As we were unsure whether changes would occur in the emission of PPE polymers upon interacting with DNA strands, a systematic study of the effects of binding was necessary. The first step involved using a single 'base-pentose-phosphate' unit as a potential quenching species to observe what effect it would have, if any, on the emission of a PPE. The selected quencher, 2'-deoxyadenosine-5'-monophosphate sodium salt, (**d-AMP**, **216**, shown in Figure 5.1), had not previously been employed for such a purpose (though the bases have been; see section 5.3). However, consideration of the reduction potentials for the four DNA bases (Table 5.1), suggests that they could operate as good emission quenchers, by readily accepting electrons. However the exact mechanism for emission quenching remains unclear (as discussed in section 5.3) as there are many examples in the literature of the bases serving to donate electrons in quenching processes and ultimately this depends on potentials of both of the species involved.

The oxidation potentials of the bases (Table 5.1) and polymer PPE **155** (estimated at +1.0 V; see section 5.3)[9] can be used to determine whether oxidation or reduction of the polymer would occur spontaneously. These data suggest that the polymer would be reduced by the DNA bases, though the resulting electrochemical potential is only weakly favourable. Indeed, the variation in the literature values of the oxidation potentials of the DNA bases, suggest that predictions based on these values may be invalid. If the emission quenching process were to operate in the reverse manner, the DNA bases would only quench the emission from the polymer efficiently if they had suitable lower lying LUMO levels. In this case, the rate of PET from PPE **155** to the quencher may be increased as the polymer/quencher complex may affect the oxidation potential of the quencher. Consequently, this would increase the free energy of PET (ΔG_{PET}) quenching.

It was anticipated that the use of **d-AMP** would provide a good benchmark for the expected results for the other bases, as it contained a base that ranked between the highest and lowest oxidation potentials listed in Table 5.1

Table 5.1 Oxidation potentials for DNA bases.

Nucleic acid base, free in solution	[a]Oxidation potential, E_0 / V
G	1.3
A	1.4
C	1.6
T	1.7

[a] as measured against the normal hydrogen electrode (NHE).[10]

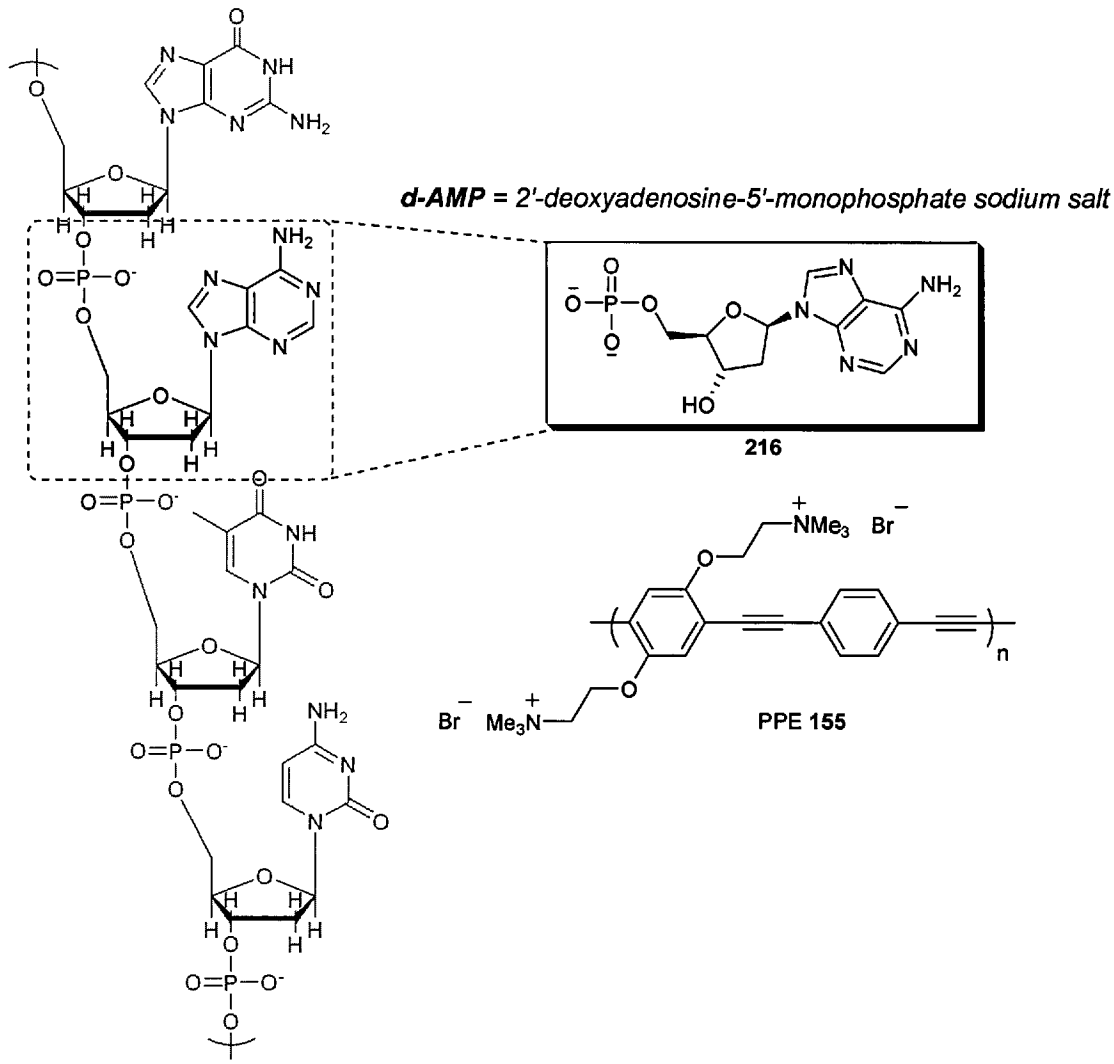

Figure 5.1 'Quencher' molecule and PPE used in the initial sensing experiment.

The emission spectra of 3 μM PPE **155** in water is shown in Figure 5.2 at increasing concentrations of **d-AMP (216)**. The emission spectra are broad and featureless at the quencher concentrations considered and are noticeably influenced by the presence of **d-AMP** at higher concentrations (>

0.20 μM) where a red-shift in the PPE **155** emission becomes apparent. The Stern-Volmer plot is shown as an inset to the main diagram, with the markers denoting experimental data points and the solid-line indicating the optimal fit to the Stern-Volmer relation.

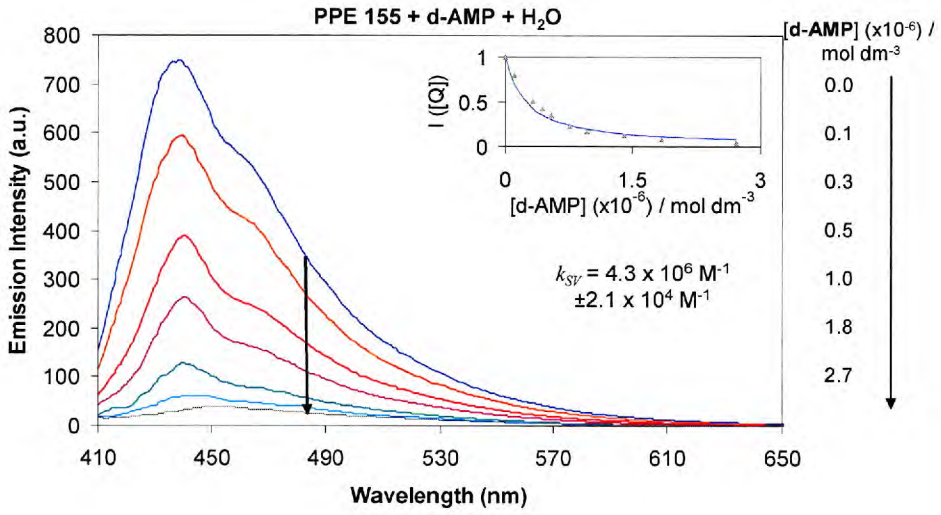

Figure 5.2 The emission spectra in salt-free water of 3 μM PPE **155** at increasing concentrations of the quencher 2'-deoxyadenosine-5'-monophosphate sodium salt (**d-AMP**, **216**). The inset shows the Stern-Volmer plot using data extracted from the main figure. The intensities in the Stern-Volmer plot are determined from the area beneath the corresponding curves in Figure 5.2, and are normalised with respect to the measured emission intensity in the absence of **d-AMP**. The markers denote experimental data lines and the solid-lines indicate the optimal fit to the Stern-Volmer relation as outlined in the Experimental section.

The quenching of emission from CPEs using individual DNA bases is hitherto unknown and so suitable direct comparisons with literature can not be made. The quenching of PPE **155** by **d-AMP** is very efficient as evidenced by the high Stern-Volmer coefficient of 4.3×10^6 M^{-1}, which suggests that single-stranded DNA could behave in a similarly way, to strongly quench emission from the polymer. To investigate this, a short, commercially available tetramer DNA sequence (*ss*-AAAA), was used as a quencher in an analogous experiment. This fragment is equivalent to four **d-AMP** units attached to each other and allowed us to compare the results with those obtained for the single 'base-pentose-phosphate' unit earlier. The results are shown in Figure 5.3.

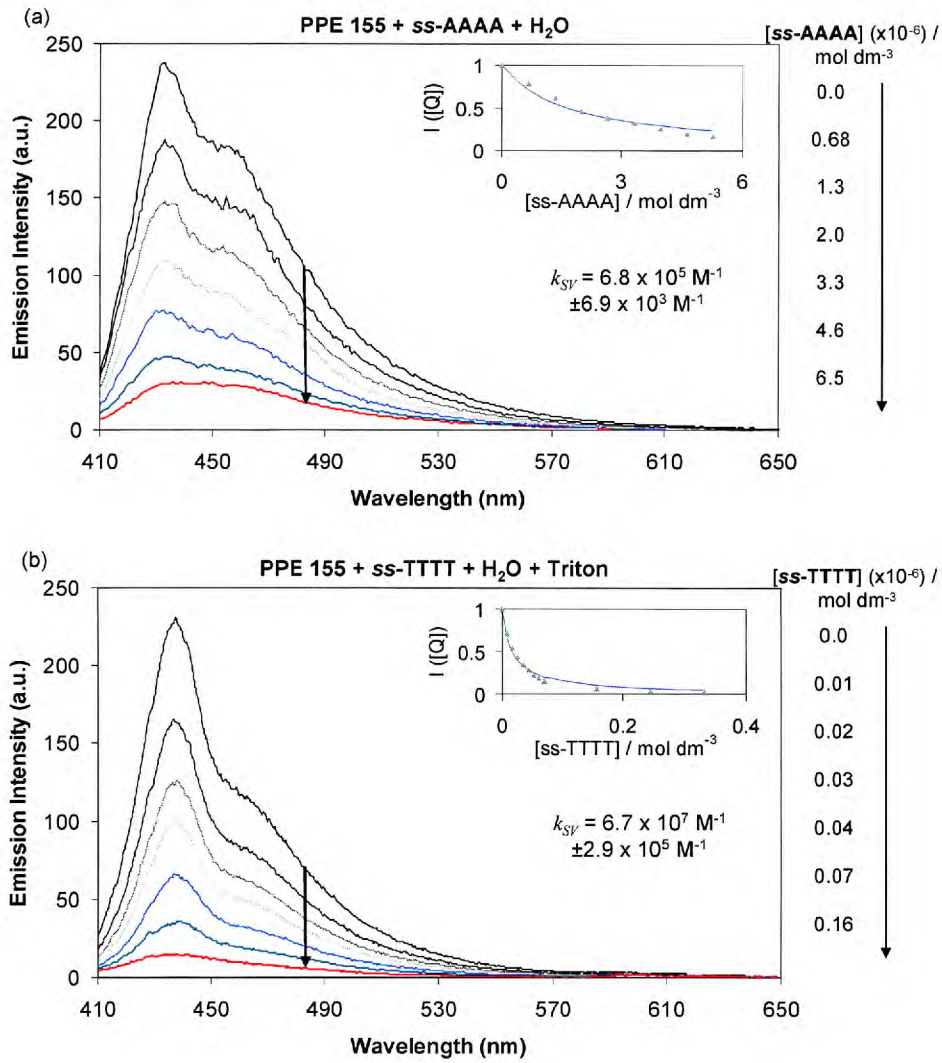

Figure 5.3 The emission spectra in salt-free water of 5 μM PPE **155** at (a) increasing concentrations of the single-stranded DNA tetramer '*ss*-AAAA' and (b) increasing concentrations of the single-stranded DNA tetramer '*ss*-TTTT'. The insets show the Stern-Volmer plots using data extracted from the main figures.

Though the quenching was not as strong as for the single base quencher **d-AMP**, a k_{SV} value 6.8 x 10^5 M^{-1} was recorded, which represents a 6.3-fold decrease relative to the single base example. A similar experiment was repeated for the complementary tetramer (*ss*-TTTT), with experimental conditions changed by the addition of 0.3 wt.% of the surfactant Triton to the aqueous solution as we wanted to explore the impact it may have on the quenching process (we assumed that *ss*-AAAA and *ss*-TTTT would be comparable in surfactant-free conditions). Interestingly, a Stern-Volmer value of 6.7 x 10^7 M^{-1} was recorded – a 99-fold increase compared to that measured for *ss*-AAAA. To rationalise this result, the impact of the surfactant and various salt additives on the emission quenching properties of PPE **155** had to be considered.

Presumably because of its increased size and multiple interactions, the complexation of the quencher *ss*-TTTT with PPE **155** is very different from that observed and described in Chapter Three where small molecule quenchers (e.g. **NPP**) were used. Traditional quenchers such as **NPP**, **AQS** and $\mathbf{MV^{2+}}$ are suspected of triggering further quenching (in addition to quenching by electron/energy transfer) by acting as a template for aggregation (thus allowing polymer self-quenching).[2] Both *ss*-AAAA and *ss*-TTTT, contain multiple negative charges along their short backbones that may allow them to bind several polymer chains at a time, mimicking the templating behaviour of small molecule quenchers. It is possible that the combined effect of the quencher and surfactant (as illustrated in Figure 5.3b) serves to further increase the conformational order in the polymer, promoting aggregation, allowing the increased movement of photexcitations, both intra- and inter-molecularly. This would raise the likelihood of excitons encountering the bound quencher, which would give rise to an increased Stern-Volmer constant. This study has considered that both *ss*-AAAA and *ss*-TTTT have an approximately equivalent ability to quench the emission from the polymer (*via* electron or energy transfer processes, *vide infra*), though time constraints meant that this could not be confirmed. As there are no other reported studies where short oligonucleotides or DNA bases have been used as emission quenchers for CPs, no comparisons with literature examples have been discussed.

5.2 Attempted detection of single-stranded DNA strands using second and third generation polyelectrolytes

5.2.1 Using PPE 155 to detect a single-stranded tetrameric DNA

Having established that both of the complementary oligonucleotides were able to induce strong quenching of PPE **155**, we wanted to study whether the hybridisation of these two strands could be 'observed' using the synthetic polymer. Although we were uncertain of the nature of the interaction between the polymer and the DNA strands, it was anticipated that any changes in emission could help to shed light on the recognition process. To test this theory, equimolar solutions of *ss*-AAAA and *ss*-TTTT were prepared in unbuffered water. The entire hybridisation experiment was conducted at 50 °C to ensure that all DNA material remained denatured, consistent with protocols reported elsewhere.[11,12]

The results from this experiment are described in Figure 5.4. After initially leaving the solution for 15 minutes to allow for temperature equilibriation, the first single strand (*ss*-AAAA) was added to the aqueous polymer solution. A further 15 minutes was allowed to enable the emission intensity to stabilise to the new value. After this period, the complementary strand *ss*-TTTT was added to the polymer solution and the emission monitored over ~ 180 minutes. The experiment was conducted

such that there were equimolar additions of the tetrameric strands. The fluorimeter was set to operate in kinetic mode to ensure that a series of measurements could be recorded over a controlled period of time. The results show that although the emission from PPE **155** was quenched (by > 95%) upon addition of *ss*-AAAA, addition of its complement resulted in a brief rise in the emission intensity (~ 25% increased), followed by a decrease to its starting level (Figure 5.4b).

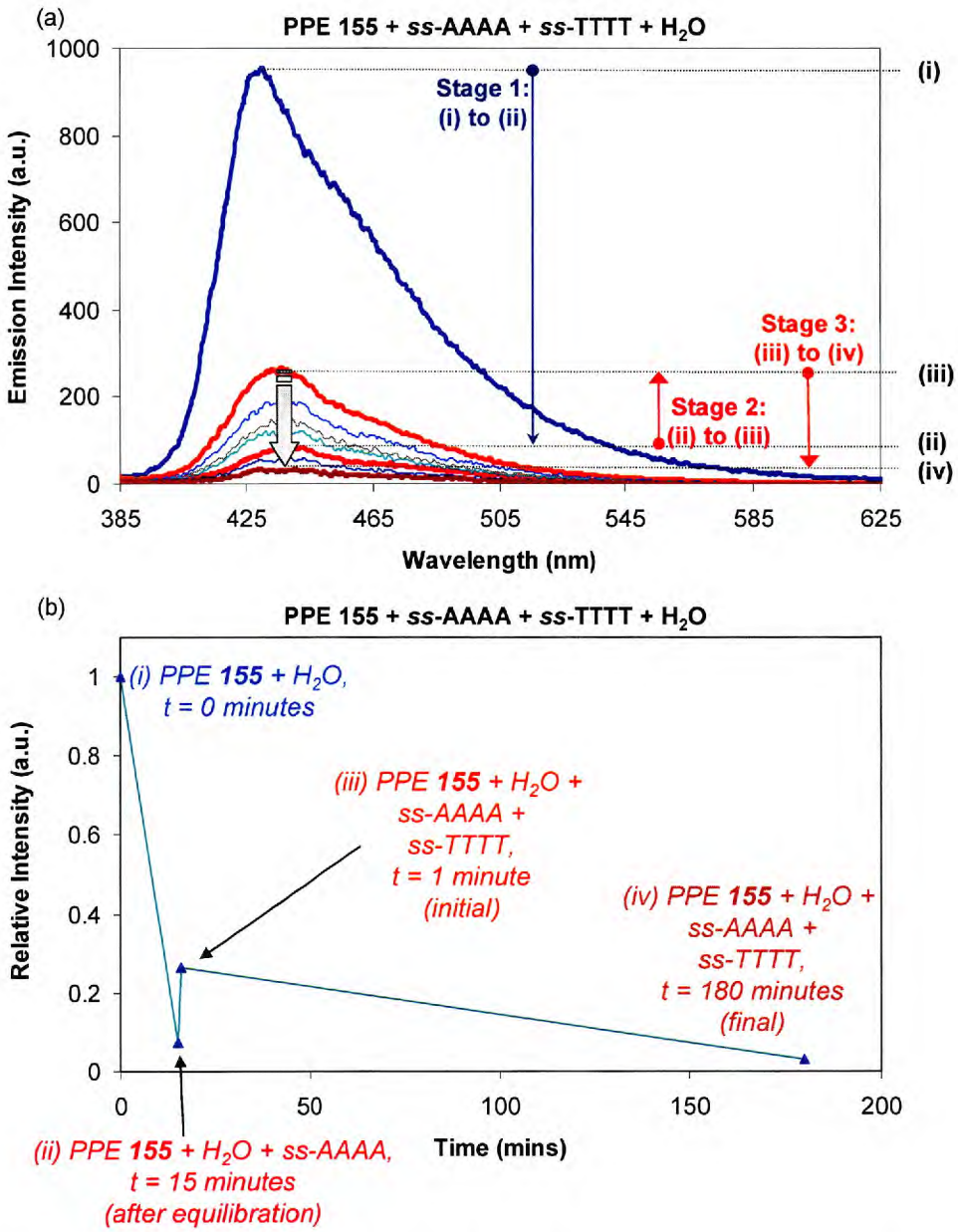

Figure 5.4 Changes in the emission from PPE **155** upon hybridisation of complementary tetrameric DNA strands. The overall result was > 95% quenching. (a) Emission spectra recorded during the different stages of the experiment: (i) Initial emission intensity, (ii) emission upon addition of *ss*-AAAA, (iii) emission after addition of *ss*-TTTT, (iv) final result after equilibration for 3 hours, (b) changes in relative emission intensity levels.

The stoichiometry of all three components (i.e. PPE **155**, *ss*-AAAA and *ss*-TTTT) after the addition of the second tetrameric strand was ~ 100:1:1 (as with all stoichiometry ratios quoted in this chapter, these values refer to repeat unit concentrations); this means that there was an equimolar amount of the single strands in a solution containing the conjugated polymer at a concentration level that was approximately 100-times higher. Importantly, to ensure that the concentration of PPE **155** remained constant throughout, the addition of both *ss*-AAAA and *ss*-TTTT were made together with appropriate amounts of the polymer (following the same protocol as used for the small molecule quenchers, detailed in Chapter Three).

On its own, it's not possible to put this result into context though the pattern of an initial decrease in emission intensity followed by a modest recovery was reproducible and does mirror results reported by Leclerc *et al.* where a conjugated PT was used to monitor the hybridisation of 20 and 50-mer oligonucleotide targets.[7] They considered the polymer backbone to undergo two significant conformational changes (see Figure 1.17, Chapter One); firstly, the addition of the polymer to the oligonucleotide probe results in a stoichiometric complex in which the polymer backbone is elongated (this 'duplex' exhibits red-shifted, reduced emission, due to the stacking of polymer chains leading to self-quenching). Then, addition of the target DNA analyte gave rise to an increase in the fluorescence signal as the polymer gains more conformational freedom by forming a helical shape, which has a lower tendency to form self-quenching aggregates.[7]

Similar arguments could be used to rationalise our data however, it may be less likely that a more rigid CP (like PPE **155**) could form a helical structure around the anionic phosphate backbone of double-stranded DNA in the same way as for the PT used by Leclerc *et al.*. In this respect, after hybridisation, the changes in the emission spectra from PPE **155** would not be expected to follow the same trend as for the more flexible PT. The results shown in Figure 5.4 confirm this; hybridisation did not lead to a recovery in the emission intensity which could be because the hybridised strands were able to quench the emission from the polymer just as efficiently as the individual strands. Alternatively, secondary effects such as induced aggregation leading to strong self-quenching may be dominant. The reasons for these observations were not investigated further.

5.2.2 Using a third generation PE small model analogue, PE 208, to detect a single-stranded tetrameric DNA

The small model analogue PE **208** was used in a comparable way to PPE **155** to monitor the hybridisation of the tetrameric DNA strands. The conjugated sensor and DNA strands were handled in an identical fashion to that described above (section 5.2.1). As observed for the hybridisation experiment involving the tetramer DNA sequences and PPE **155**, there was a steady decrease in the

emission intensity level upon addition of the first strand, *ss*-TTTT, which was followed by a further decrease upon adding an equimolar solution of the complementary strand *ss*-AAAA (Figure 5.5a and Figure 5.5b). In total there was a 15% reduction in the intensity level over an 8 hour period and the stoichiometry of PE **208**, *ss*-TTTT and *ss*-AAAA was ~ 1:0.2:0.2.

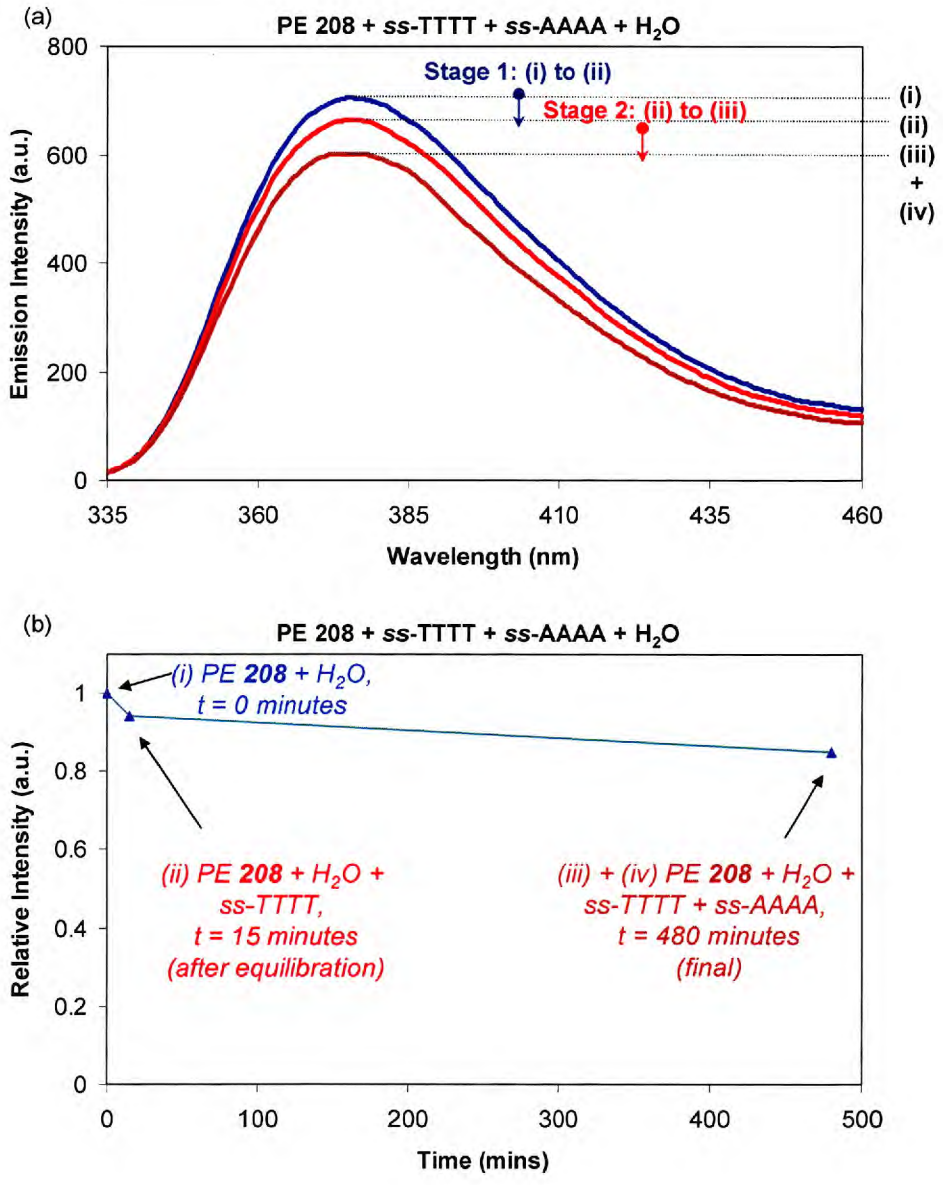

Figure 5.5 Changes in the emission from PE **208** upon hybridisation of tetrameric DNA strands. The overall result was ~ 15% quenching. (a) Emission spectra recorded during the experiment: (i) Initial emission intensity, (ii) emission upon addition of *ss*-TTTT, (iii) emission after addition of *ss*-AAAA, (iv) final result after equilibration for 8 hours, (b) changes in relative emission intensity levels.

The emission changes observed from the small model analogue PE **208** in response to the addition of the tetrameric strands is comparable to that observed for PPE **155**; in both cases a decrease in the intensity level was observed. The differences between PE **208** and PPE **155** include size (PPE **155** is ~ 9-13 repeat units,[13] whereas PE **208** is 1.5 repeat unit lengths) and recognition motif. Therefore it appears that the consistent trend in emission intensity behaviour for these conjugated materials is related to the type of 'quencher' used. The interaction of the tetrameric DNA strands and hybridised product with PE **208** and PPE **155** leads to possibly the same conformational changes in both materials and therefore comparable results overall.

5.2.3 Using PPE 155 to detect a 35 base-pair DNA single strand

The strength of binding between two complementary DNA strands to form a duplex is known to depend on the length of the single-stranded components and their nature, with longer strands resulting in stronger complex formation and alternate sequences leading to more strongly associated dimers.[14] Therefore the next set of polymer-DNA hybridisation experiments involved longer DNA strands. We wanted to use oligonucleotides that were sufficiently long to ensure strong complementary binding, whilst maintaining the ability to alter the optical response from the conjugated polymer. We opted to use strands containing 35 base-pairs as the length of these materials was between the 20 and 50-mer strands that were used in previously reported hybridisation experiments where CPs were employed.[7] Additionally these materials were readily available.[15]

As was found for the tetrameric strands, the longer strands were similarly capable of strong emission quenching, though no attempts were made to assess the exact value of k_{SV} due to time constraints (k_{SV} was estimated at ~ $10^5 - 10^6$ M^{-1}). In Figure 5.6, the results from the hybridisation of two 35-mer strands (exact sequences are detailed in the Experimental section, Chapter Seven) in the presence of PPE **155** are presented.

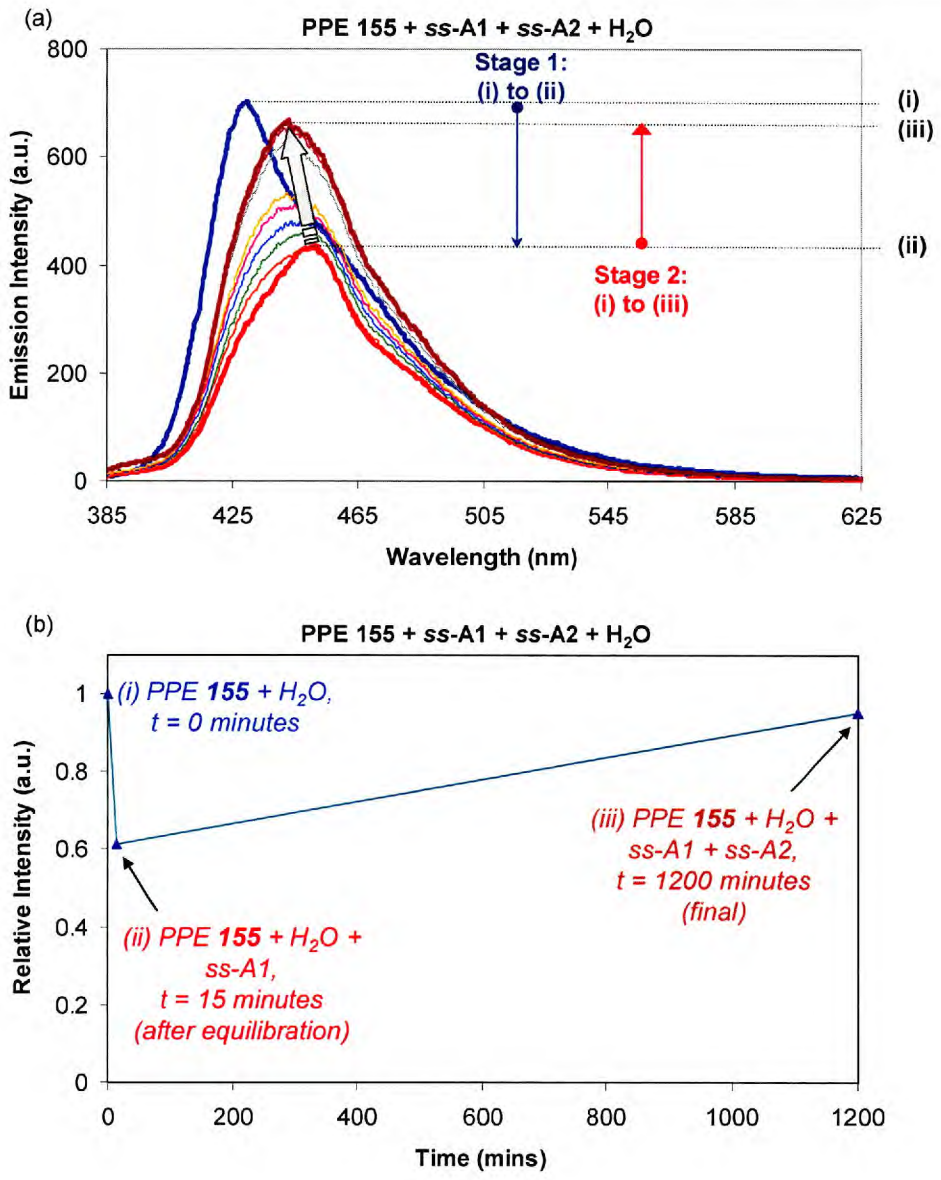

Figure 5.6 Changes in the emission from PPE **155** upon hybridisation of complementary 35-mer DNA strands. Almost complete recovery of the polymers emission was observed over a 20 hour period, in contrast to the result observed for the shorter tetramer strands. Emission spectra recorded during the experiment: (a) (i) Initial emission intensity, (ii) emission (equilibrium) after addition of *ss*-A1, (iii) emission (equilibrium) after addition of *ss*-A2, (b) changes in relative emission intensity levels.

The stoichiometry of PPE **155**, *ss*-A1 and *ss*-A2 was approximately 1:20:20. This ratio of PPE to oligonucleotide is higher than that used to detect the tetrameric strands where the polymer was present in 100-fold excess. The difference relates to the concentration of the strands that were required in order to alter the emission spectra. As described previously (5.2.1), the concentration of the polymer was kept approximately constant during the addition of the oligonucleotides.

The hybridisation experiment was conducted at 65 °C (oligonucleotides of a similar length, e.g. 20-mer *ss*-DNA strands, are known to be denatured at this temperature)[11] and equal moles of each strand were added to the polymer solution. Importantly, to ensure that secondary structures had been eliminated, the 35-mer DNA strands were heated at 94 °C for 5 minutes prior to the experiment (the T_m for both strands is estimated to be ~ 80 °C).[7,11] The initial emission curve (in blue, Figure 5.6a) is quenched by approximately 35% upon addition of the first 35-mer strand (*ss*-A1), after a 15 minute period of equilibration. It was also significantly red-shifted (22 nm), which suggests either a change in the conformational order of the conjugated backbone or self-quenching through aggregation. The amount of *ss*-A1 added was chosen such that a clear change (either an increase of decrease) in the emission spectrum could be observed. From previous experiments using the 35-mer strands, addition of the oligonucleotides at a ratio of less than 1:20:20 did not result in any spectral changes. Therefore, to observe the hybridisation process optically, the amount of *ss*-A1 was carefully adjusted and this enabled us to calculate the number of moles added which allowed for an equimolar addition of *ss*-A2 to be made.

The addition of the complementary strand (*ss*-A2) resulted in a gradual increase in emission intensity. The emission spectra were monitored overnight and after 20 hours the intensity had recovered to within 5% of the initial intensity level (Figure 5.6b), though the emission was now red-shifted, relative to the initial spectrum. The changes in the emission spectra due to the presence of the DNA strands are probably a result of a combination of effects. Firstly, it is likely that the some of the 'quenching' observed is due to π-π stacking of the polymer chains, possibly triggered by the presence of the biopolymer, which could lead to aggregation. As noted in previous sections, emission quenching by small molecule quenchers (by PET or energy transfer), generally does not result in a change in the shape of the emission spectra. The pronounced red-shift observed here therefore suggests that this is not the only mechanism at work. Moreover, the 'unquenching' effect lends weight to this argument as such an effect would not typically occur when another quenching species is added to the polymer solution. This observation can be rationalised if we consider that the DNA strands are binding with each other instead of the polymer, which is what we expect. These results are similar to those reported by Leclerc *et al.*[7,16] and may be rationalised using the same reasoning (detailed in 5.2.1).

As discussed in Chapter One (section 1.7), the increased rigidity of PPEs compared with other CPEs (like poly(thiophene)s) may be expected to preclude them from forming complexes with DNA in the same way as described by Leclerc *et al.*,[7] for the interaction of *ss*-DNA with PT structures (e.g. polymer **72**, Chapter One, section 1.6). However, the persistence length of PPEs (estimated at 15 nm; 20 PE repeat units)[17] is less than that associated with DNA (60 nm)[18] and so they do possess some flexibility which could permit them to form polyelectrolyte complexes in a

similar way to that described by Leclerc *et al.* (between polymer **72** and *ss*-DNA oligonucleotides). The changes in emission observed could then be explained in the same way (as described in section 5.2.1).

5.2.4 Use of the third generation PPE 210 to detect a single-stranded 35 base-pair DNA strand

In an analogous experiment, the single-stranded 35-mer DNA material was combined with PPE **210**, using similar conditions (in addition, Triton and 100 mM NaCl were added, *vide infra*; Figure 5.7). It was anticipated that although PPE **210** was impure (see Chapter 4) it would provide an interesting contrast to PPE **155** (e.g. PPE **210** contains a recognition unit directly attached to the polymer backbone). As it was not possible to identify the contaminants, their potential impact on the optical properties of the conjugated polymer could not be ruled out. In order to get appreciable emission from this polymer (see Chapter Four, section 4.1.2), a surfactant had to be added and in another change sodium chloride was also added as some reports declare that its inclusion may benefit hybridisation by presumably stabilising binding interactions and minimising charge repulsion along the backbone (through increased ionic strength).[7]

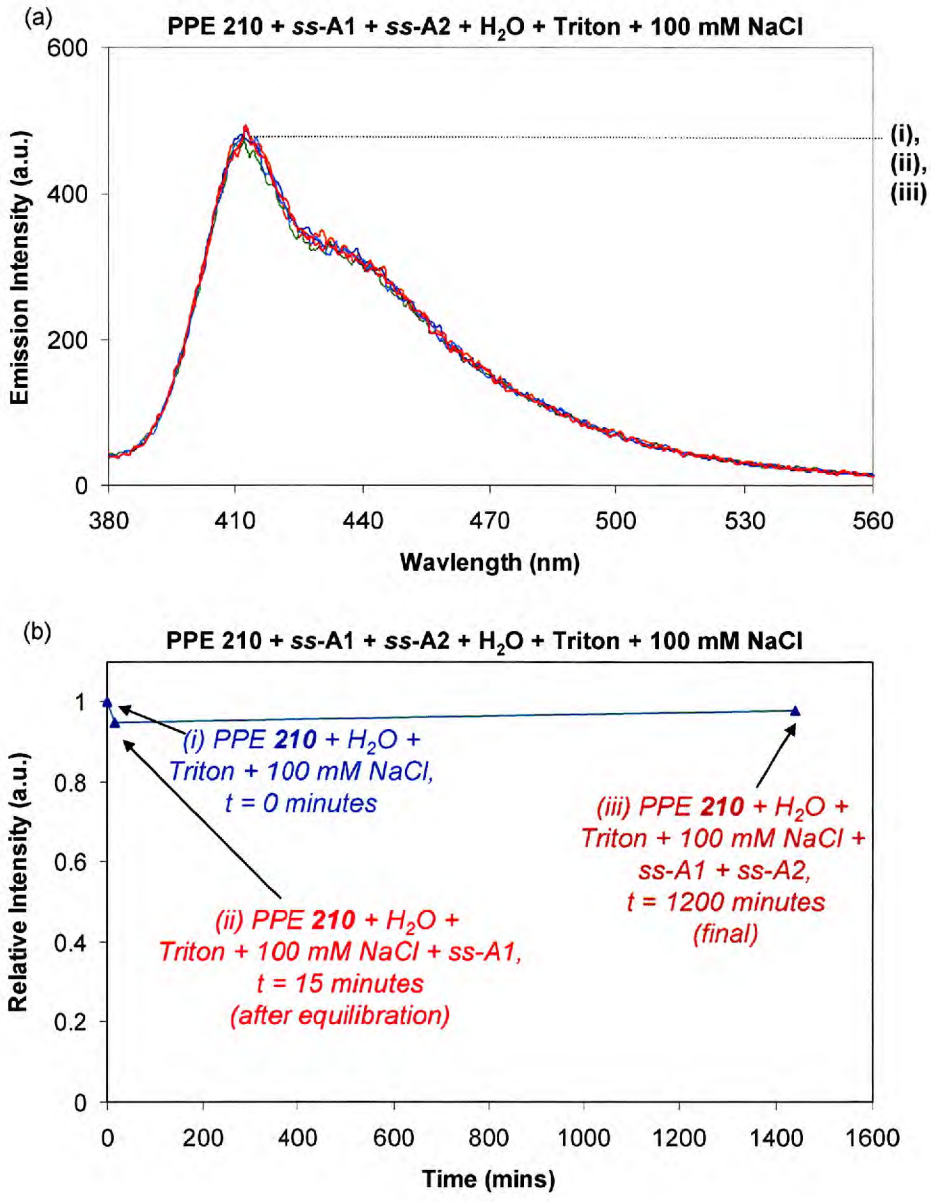

Figure 5.7 Changes in the emission from PPE **210** upon hybridisation of complementary 35-mer DNA strands. Minimal changes in the polymers emission are observed after addition of both DNA strands. (a) Emission from the polymer decreased slightly (< 5%) during the addition of *ss*-A1 (ii) and then displayed a small (< 5%) increase upon addition of *ss*-A2 (iii). (b) Changes in relative emission intensity levels.

Unlike PPE **155**, there were only minimal changes in the emission intensity of the polymer during any of the additions of the 35-mer strands. Indeed, even after 24 hours, the emission from PPE **210** remained almost identical to that observed at the start. Despite the experimental changes (addition of Triton and 100 mM NaCl to the solvent) between this experiment and the previous it is possible to speculate on the reasons for the differences in the results. The addition of the surfactant could explain why no change in the emission intensity was observed. For PPE **155**, it was suggested that

the emission changes may be attributable to aggregation effects, which would also explain the pronounced red-shift in the emission from PPE **155**. For polymer PPE **210** the surfactant may have had a different effect from that observed for PPE **155** (which contained two ammonium motifs per repeat unit). The presence of the single gaunidinium group per repeat unit along the polymer backbone in PPE **210** (the only functional group in the repeat unit) may be the reason for this. A polymer-surfactant complex[19] could disrupt the formation of conjugated polymer aggregates (formed from π-π stacking) and limit the sensitivity of the polymer.

5.2.5 Using a third generation PE small model analogue, PE 208, to detect a 35 base-pair DNA strand

In the final hybridisation experiment that was conducted, the impact of the hybridisation of two complementary 35-mer DNA strands on the emission of PE **208** was studied. The experimental conditions were again kept constant and were identical to those employed previously (in section 5.2.3).

The changes in the emission spectra upon the sequential addition of the 35-mer strands to an aqueous solution of PE **208** are shown in Figure 5.8. Unlike the results obtained for PPE **155** and PPE **210** (Figure 5.6b and Figure 5.7b), where the anticipated hybridisation of *ss*-A1 and *ss*-A2 led to a small rise in the emission, the opposite is observed for the PE **208**. In total, a 6% decrease in the emission level results upon addition of *ss*-A1 followed by *ss*-A2.

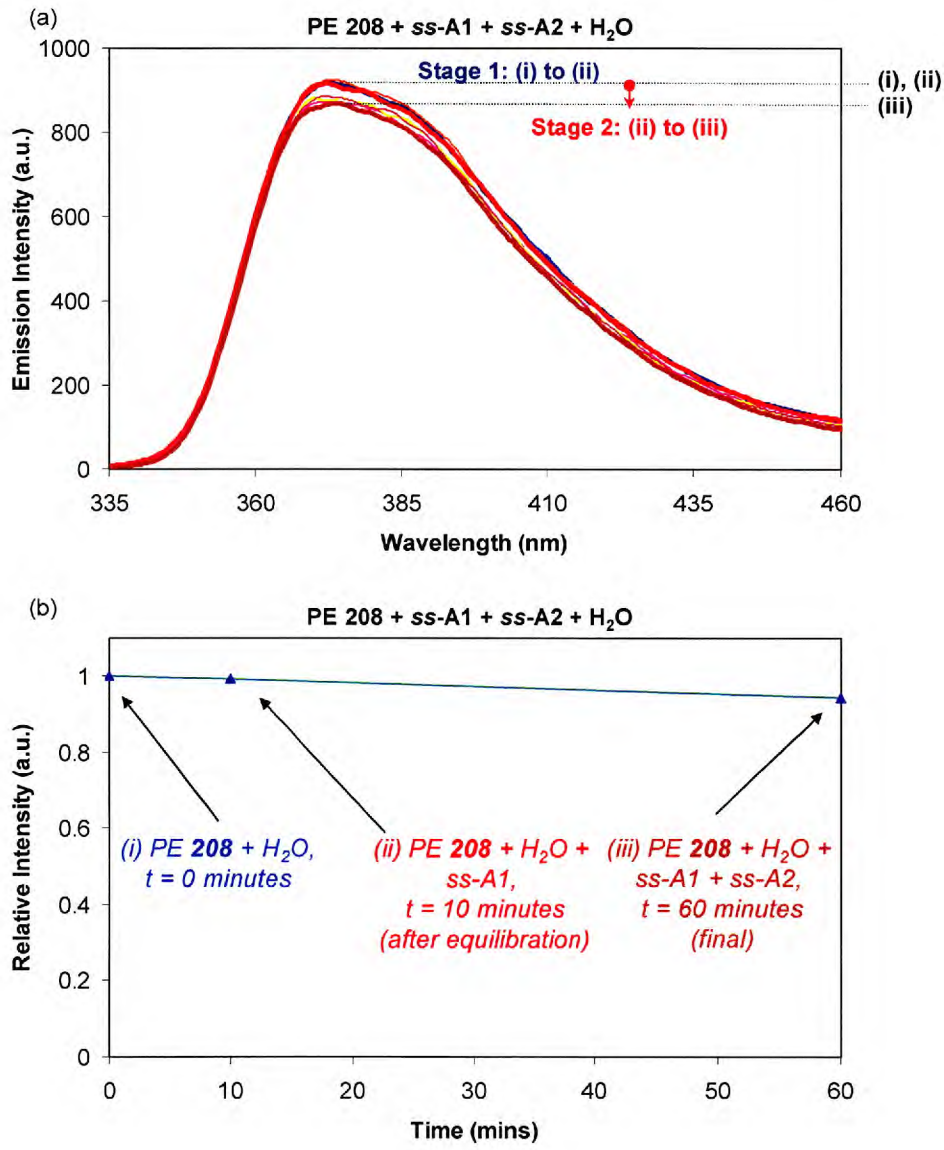

Figure 5.8 Changes in the emission from PE **208** upon hybridisation of complementary 35-mer DNA strands. A 6% decrease in the emission intensity level from the small model analogue was observed after addition of both DNA strands. (a) Emission from PE **208** (i) remained unchanged during the addition of *ss*-A1 (ii) and *ss*-A2 (iii). (b) Changes in relative emission intensity levels.

The small decrease in the emission intensity from PE **208** (Figure 5.8a) upon addition of the longer 35-mer sequence is comparable to the trend observed for the analogous experiment involving the same conjugated unit and the tetrameric strands. This finding suggests that this small model analogue interacts with the DNA strands (the tetramer and 35-mer) in a different way to PPE **155**, which could be attributed to the presence of the guanidinium motif along the backbone of PE **208**.

In summary, the following general trends have been identified:

- Upon hybridisation of the tetramer strands, the changes in the emission intensity levels from PPE **155** and PE **208** are similar; in both cases, there was an overall reduction (> 95% for PPE **155** and ~ 15% for PE **208**) in the intensity level.

- The hybridisation of the longer 35-mer strand, led to two distinct emission changes for polymers PPE **155** and PPE **210**; firstly, the emission from these polymers was reduced upon addition of the first 35-mer sequence (*ss*-A1). Then, in the presence of the complementary strand, *ss*-A2, the emission gradually recovered. The effect was more pronounced for PPE **155** where the emission increases to within 5% of the original emission intensity level.

- Interestingly, a similar analysis using the small model analogue PE **208** showed that it was unable to differentiate the hybridisation process involving short or long DNA strands. In both cases, a gradual decrease (approximately between 5 – 15%) in the emission intensity level was observed.

5.3 Possible mechanisms for emission quenching with DNA bases

There have been no reports on the use of individual DNA bases as emission quenchers for conjugated polyelectrolytes. However, there are many examples (discussed below) where the bases have been used to quench the emission from fluorescent dye molecules, but there is little consensus over the exact mechanism for this process, with both oxidation and reduction processes being suggested. Based on the evidence in the literature, the exact mechanism is highly dependent on the system studied.

The quenching of fluorescent dyes by nucleobases has been investigated. In a recent study Siedel *et al.* use the nucleobase-specific quenching of a dye, Coumarin-120, and one-electron redox potentials to probe the mechanism for quenching in aqueous solutions.[20] By considering the quenching rate constants, they found that photoinduced electron transfer (PET), proton-coupled electron transfer and hydrophobic interactions were all important factors in facilitating efficient electron transport. In aqueous media, a similar combination of factors has previously been invoked to explain such phenomena.[20,21] Comparing these outcomes to the results observed for the PPEs would be difficult due to the differences in molecular size of the dyes and PPEs and their differing reduction and oxidation potentials.[20] Moreover, differences in oxidation potentials of the DNA bases can lead to different redox outcomes; for example pyrene is quenched by all four bases (A, G,

C and T) but the mechanism of the quenching process differed; guanine was oxidised, while the rest were reduced.

The oxidation potentials for the four DNA bases (Table 5.1) confirm that guanine is the easiest to oxidise (the least positive potential indicating the base with the best electron-donating properties). Guanine is consistently recognised as the most easily oxidisable base, though the one-electron oxidation potentials for the DNA bases often vary widely. This was noted by Fukuzumi *et al.* who investigated and acquired these data in aqueous solutions at 298 K.[22] They confirmed that the guanine base (they used the 5'-monophosphate salts of guanosine, adenosine, thymidine and cytosine) has the lowest E_{ox} value (i.e. it is the best electron-donating base), though all four bases differ by less than 0.19 V. These results were confirmed when the G, A and T bases were employed as quenchers for the emissive $Ru(bpy)_3^{3+}$ complex, a one-electron oxidant.[22] It is not possible to quantify the effect that a 0.19 V difference in oxidation potentials between the bases would have on a quenching process involving PPEs, without conducting individual emission quenching experiments. The difference may lead to a change in the nature of the redox process (e.g. from a reduction to oxidation process, or *vice versa*), however this may not impact the overall value of k_{SV}.

The occurrence of PET processes involving DNA bases (with electron transfer from the base) has also been shown using laser flash photolysis (LFP), where electron transfer from GMP (guanosine 5'-monophosphate) to the triplet excited state of pyrene was observed (manifested as an absorption band at 420 nm in a transient absorption, (TA) spectrum).[22,23] Numerous reports detailing the use of photooxidants in DNA transport studies have highlighted the importance of oxidative damage in DNA.[24] Indeed, bound photooxidants are known to induce damage at remote guanine sites.[24]

It is quite possible that DNA-induced aggregation effects may be responsible for some of the quenching but in light of the literature examples discussed (*vide supra*) it remains a possibility that electron transfer from the bases to the CPE could occur, resulting in emission quenching through the formation a negative polaron.

The inverse process, of *electron transfer to DNA*, has also received attention. Ito and Rokita looked at the movement of excess electrons in DNA.[25] They found that by use of a suitable donor and acceptor embedded within a given DNA sequence, electron transfer could be observed (in their case *via* a decomposition process, as observed by polyacrylamide gel electrophoresis). Based on the oxidation potentials listed in Table 5.1, the bases most likely to accommodate the additional charge would be C and T, though protonation of the radical anion of C ($C^{-\bullet}$) leads to a radical species that competes during electron migration. The ability of DNA to absorb charge is also recognised by Dekker *et al.* who used current-voltage curves based on electrical transport

measurements to confirm that DNA (10.4 nm in length; double-stranded poly(G) and poly(C) DNA molecules) can be considered as a large-bandgap semiconductor, exactly the type of material that could be used to absorb electrons from electron donors, although this would depend on suitable matching of its HOMO and LUMO energy levels with that of the quencher.[26]

This idea has been reinforced by Bazan *et al.* who synthesised a series of water-soluble oligofluorenes and examined their interactions with single and double-stranded oligonucleotides.[27] They found that the emission from the oligofluorene was quenched by approximately 50% in the presence of a 20-mer single-stranded DNA fragment, with no change in the position of the emission or absorption spectra. From this they concluded that the observed quenching can be attributed to self-quenching (with the *ss*-DNA molecule acting as a template for aggregation of the oligofluorene units, as is seen with small molecule quenchers[2]) or photoinduced charge transfer to the DNA bases.[27,28] This result allows for an interesting comparison with the findings detailed in section 5.2 where a 35-mer single-stranded DNA fragment quenched the emission from PPE **155** by 35%. In that case, we too speculated that the quenching could be attributed to self-quenching effects or PET processes. Indeed, in recent work, Schanze *et al.* were able to measure the oxidation potential for the anionic polymer PPE **41** (+1.0 V vs. SCE);[9] their result suggests that the PPEs are better electron-donors than any of the DNA bases and could quite easily donate electrons to oligonucleotides. At higher oligonucleotide concentrations, self-quenching of the synthetic polymer through aggregation is possible,[7] and photoinduced charge transfer to the DNA bases may also be important.

In unrelated work, Swager *et al.* have commented on the mechanism for quenching between electron-rich PPE polymers and electron-deficient quenchers, as detailed in previous chapters.[29] The exquisite efficiency of the process is linked to the favourable ionisation potential (IP) of the polymer relative to the quencher.[29,30] In this regard, dialkoxy-PPEs like PPE **155**, have low IPs relative to electron-deficient variants, as has been recently reported.[29] This is intuitive based on arguments concerning electron-donating abilities and concomitant effects on varying band-gap levels (e.g. the electron-rich nature of alkoxy PPEs is evidenced by upfield shifts in their ^{1}H NMR spectra). For these reasons, such polymers are expected to show a limited response, if any, to emission quenchers that are electron-rich, such as indoles and phenols, as the reduction of such materials is inherently disfavoured.[29] The difference in ionisation potential between two structurally comparable pentiptycene-containing PPEs – one with alkoxy groups (and therefore electron-rich; PPE **217**), the other with perfluoroalkyl groups (electron poor; PPE **218**) has been estimated by Swager *et al.* to be 0.79 eV (Figure 5.9).[29] Interestingly, this difference led to an 18.3-fold decrease in the sensitivity (measured as a Stern-Volmer value) of the electron-rich PPE towards the electron-rich quencher indole.

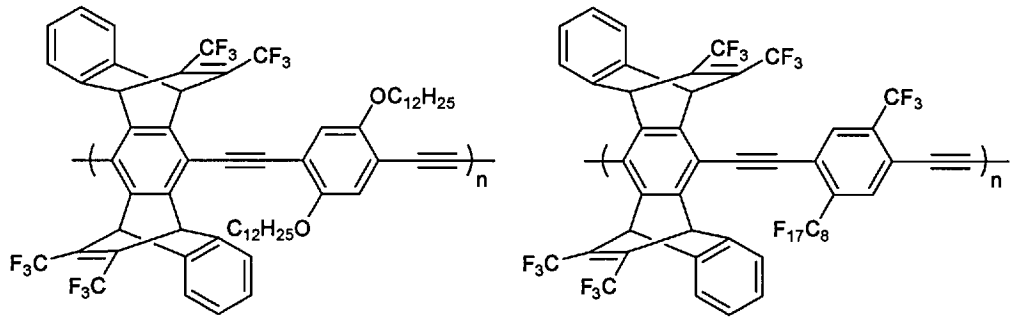

PPE **217**

Ionisation potential (eV) = 5.96

k_{SV} = 1.4 M^{-1} (quencher = indole)

PPE **218**

Ionisation potential (eV) = 6.75

k_{SV} = 25.6 M^{-1} (quencher = indole)

Figure 5.9 High ionisation potential PPEs for use in the detection of electron-rich quenchers.[29]

In order to achieve responses from PPEs towards electron-rich quenchers, subtle clues as to the type of structures required are provided by the Swager group (Figure 5.9). Using PPEs designed with perfluoroalkyl chains – thus rendering the polymers electron-deficient – they showed that the high-ionisation potential, wide band-gap materials were able to respond to electron-rich quenchers.[29] Such a result would suggest that in order to detect the highly oxidisable DNA bases, good excited-state oxidants (electron acceptors), such as the new PPEs described by Swager, may be best suited.

However our results show that dialkoxy-PPE materials exhibit strong quenching towards the DNA bases, as observed in Figure 5.2 and Figure 5.3. Inspection of these emission spectra does not reveal any pronounced red-shift at the quencher concentrations studied (at the μM concentration level, the decrease in emission intensity was > 90%). Absorption spectra would need to be recorded at the same time as the emission spectra to shed more light on this behaviour; red-shifts in both measurements would provide further evidence that, in part, aggregation was a key mechanism for quenching. Alternatively, a blue-shift in the absorption spectra could point to more complex behaviour where the conformational order of the PPE backbone is more important and aggregation effects are of reduced significance. In this case, the DNA base quencher may not serve as a template for aggregation of the polymer chains, but may lead to a polymer-quencher interaction that results in reduced conjugation along the polymer backbone (possibly by the introduction of 'kinks' in the chain). Such measurements were not recorded simultaneously due to time constraints, but would provide a good starting point for future studies.

5.4 Examining the interactions between cationic CPEs and DNA

Due to the large expansion in the field of non-viral gene delivery systems,[31] there have been many studies into the structural ordering of DNA polyplexes.[32,33] The types of polycation trialled as potential gene-delivery systems (e.g. poly(ethylene oxide)-*g*-poly(L-lysine) and poly(ethylene glycol)-*g*-polyethylenimine) are based on synthetic polymers with flexible chains and short persistence lengths and so direct comparisons with conjugated polymers can not be made.[32,34] However, as a guide to synthetic polymer/biopolymer interactions, such works are useful; DeRouchey *et al.* used synchrotron small-angle X-ray scattering (SAXS) to probe the internal structure of polyplexes and found that they exist as condensed macromolecular phases.[32] Specifically for *ds*-DNA, they considered the polycation to wrap around the rigid DNA backbone (persistence length 50 nm).[32] In general PPEs, considered as 'rigid-rods', do have flexibility above their persistence length (which defines the stiffness of a polymer;[35] for PPEs this value corresponds to about 15 nm or 20 PE repeat units)[36] but are more rigid than the typical polymers used in gene-delivery applications. For this reason, it is unlikely that they would wrap around DNA strands in quite the same way, although tight interactions leading to self-quenching are likely. Additionally, Bazan *et al.* noted that, in charge unit terms, *ss*-DNA was a more effective quencher than *ds*-DNA, which is probably due to increased flexibility in the *ss*-DNA structure and/or increased hydrophobic interactions, as differences between hydrophobic surfaces of single and double-stranded DNA are known.[27,37]

Probing the interactions between water-soluble cationic polyelectrolytes and anionic biopolymers such as DNA is difficult as the formed polyelectrolyte complexes are sensitive to the solvent conditions. Light scattering techniques may help in distinguishing aggregates from duplexes (assuming that the polymer concentrations are high enough) as well as observation of the optical properties upon thermal treatment. As has been noted by Kabanov *et al.*, complex formation can also be monitored by gel electrophoresis and their group was the first to use synthetic polycationic molecules for the recognition of tertiary DNA structure.[37] Using this method, the progress of DNA in the gel is modulated by the presence of the cationic polymer, a process dependent on the N/P ratio. Additionally, DNA melting analysis (the DNA melting temperature increases upon complexation with cationic polymers)[37] can provide useful information on polymer/DNA complexation.

In our hybridisation experiments, no isosbestic points were observed in the emission spectra upon addition of the *ss*-DNA suggesting that only a single conformational structure exists throughout the titration, though it is difficult to quantify the effect that DNA-induced aggregation has on the conformation of the synthetic polymer.[5]

A useful recent study to monitor the conformational changes of a water-soluble polymer, is provided by Dai *et al.* who looked at the aggregation behaviour of amphiphilic poly(L-lysine *iso*-phthalamide) polymers endowed with low-levels of cyanine dyes.[34] The incorporation of the dye molecules along the polymer backbone allowed them to observe changes in the polymer conformation as the solution pH was varied using steady-state fluorescence spectroscopy. They noted an overall decrease in the emission from the polymer upon acidifying (beyond a critical pH of 4.5) the solution which was attributed to a collapse of the polymer into a globular structure ('hypercoil') leading to strong self-quenching.[34] Further evidence for this model came from dynamic light scattering (DLS) measurements which showed that at low concentrations, a high degree of aggregation can occur.[34] The findings of such studies provide useful indicators for the types of techniques that can be used to examine the conformational structure of water-soluble polymers. Though Dai *et al.* used non-conjugated polymers for their work, correlating changes in the emission from a CPE with lifetime studies and DLS measurements would enable a greater understanding of the behaviour of CPEs.

5.5 Monitoring of phosphatase enzyme activity using a second generation polyelectrolyte

There is considerable interest in the use of water-soluble ionic CPs as sensors for monitoring enzymatic activity in biological media such as blood, urine and saliva.[38] The ability of enzymes to function is dependent on maintaining an appropriate three dimensional conformation, and enzymatic activity is therefore highly sensitive to the chemical and physical environment. In this context, the efficacy of a biosensor is determined primarily by its ability to operate effectively at (or close to) the optimal enzymatic conditions, i.e. its ability to function in a buffered solution of appropriate temperature, pH and ionic strength.[39] Several groups have investigated the effects of pH and ionic strength on the emission properties of ionic CPs.[40,41] They found extremely high k_{SV} values for many ionic CPs in unbuffered water solutions, but reported sharp reductions in Stern-Volmer coefficients when the polyelectrolytes were transferred to buffered solutions and other high ionic strength media. This behaviour prevents the materials from being used as high sensitivity biosensors and, in this work, we aimed to develop new material systems and strategies that would preserve the high quenching efficiencies of ionic CPs even when transferred to archetypal biological media.

Enzymes represent an attractive target for analysis as they are of importance in a variety of biochemical processes. In particular, kinases and phosphatases are a vitally important class of enzymes as they regulate cellular activity. To this end, assays that can accurately monitor such enzymes would help shed light on their behaviour. Phosphatase is an enzyme that removes phosphate groups from molecules and is present in the human body. We wanted to design a

phosphatase assay using the second generation PPE **155**, in combination with the quencher **NPP**. The choice of quencher was critical to the design of the assay; it had to contain the phosphate functional group that would be recognised by the phosphatase enzyme and be an efficient emission quencher for conjugated polymers. In this regard **NPP**, which is a substrate for the phosphatase enzyme, was an ideal choice for a quencher molecule, as it met these criteria. The use of PPE **155** in combination with **NPP** allowed us to have a good platform for understanding the assay as the underlying features that affect the quenching efficiency had already been identified (as detailed in Chapter Three). The working principle for the assay is shown in Figure 5.10.

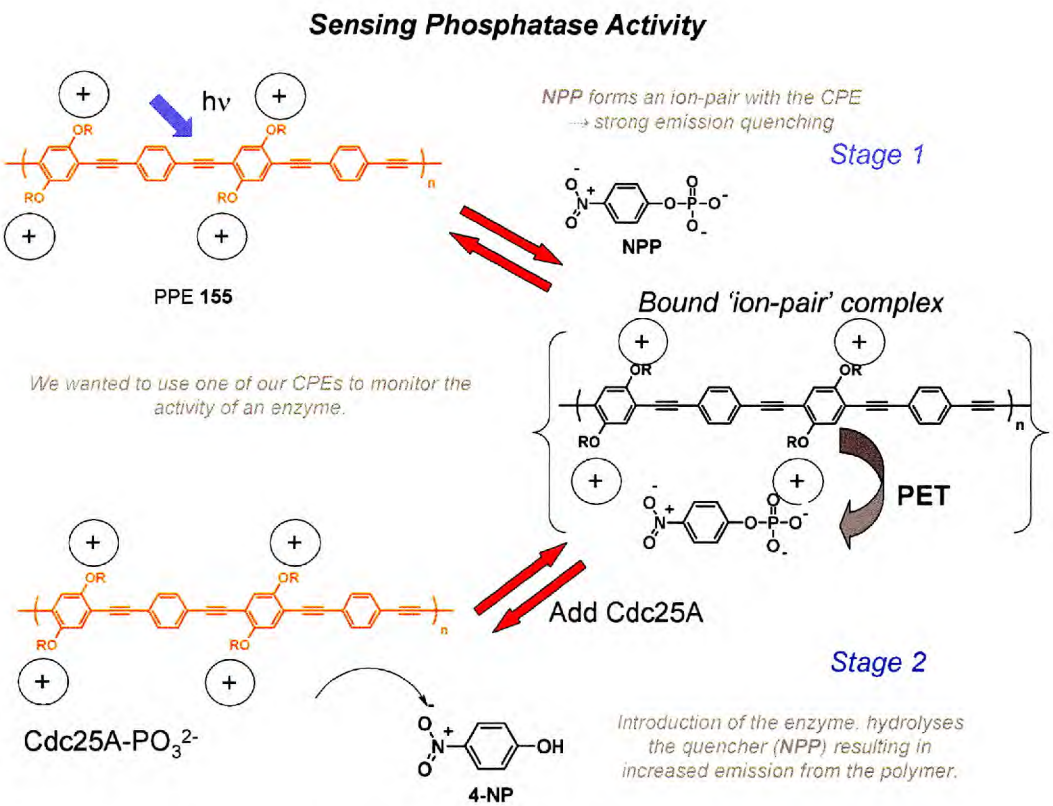

Figure 5.10 Working principle for a conjugated polymer-based enzyme assay.

As detailed in Chapter Three, the initial quenching (Stage 1 in Figure 5.10) was optimised and values for the Stern-Volmer constant determined in a variety of conditions. One of the key features of the system was to balance the optimal conditions for achieving high k_{SV} values, with those optimal for phosphatase activity. This optimisation of the sensitivity of the polymer ensured that a minimum amount of quencher could be used. For the enzyme measurements detailed herein, we decided to omit the surfactant from the solution for these measurements as the initial emphasis centred on obtaining emission recovery (Stage 2, Figure 5.10). Once this had been established, we

intended to use the surfactant additive to increase the sensitivity of the polymer in the quenching stage of the assay, and check the performance of the enzyme in its presence.

In the first experiment, a TRIS buffer solution, at pH = 7.5 – 8.0, containing 150 mM NaCl and importantly *no Triton*, was analysed to determine the Stern-Volmer constant (Figure 5.11a); relatively efficient quenching was observed (k_{SV} = 1.6 x 10^4 M^{-1}) which was three orders-of-magnitude lower than the best result (~ 10^7 M^{-1}, obtained for PPE **155** and **NPP** in an aqueous solution containing Triton) but still more efficient that the quenching of emission from the small model analogue PE **154** using **NPP** (where a k_{SV} of 1.4 x 10^4 M^{-1} was recorded). Upon addition of the phosphatase enzyme (denoted as Cdc25A, in Figure 5.11)[42] a modest 19% recovery in the emission intensity was observed (Figure 5.11b). The changes in the emission intensity levels during these three distinct phases are summarised in Figure 5.11c.

The entire assay was conducted at 35 – 38 °C which is known to be a temperature at which phosphatases operate optimally (the activity of free phosphatase is approximately 100% at this temperature).[43] A period of 10 minutes was allowed to elapse after the addition of the quencher to the cuvette to ensure that the solution could reach thermal equilibrium (checked by taking the initial and final temperatures). This time delay also allowed the emission spectrum from the polymer to stabilise to its final position (indicated in red in Figure 5.11b, stage ii). Importantly, the addition of the phosphatase enzyme was adjusted such that the following two criteria were met;

(i) the addition of Cdc25A should not cause a quenching effect – the emission from the PPE should remain constant

(ii) the addition of the enzyme must be able to convert all of the NPP substrate.

To ensure that these two conditions were met, a series of experiments were conducted where different aliquots of the phosphatase were added to PPE solutions prepared in an identical fashion to that used in the actual assay. Solutions containing the quencher **NPP** were also analysed, using UV spectroscopy (*vide infra*), to check if any of the substrate existed after the addition of Cdc25A. In these studies, after only 10 minutes, a single peak in the absorption spectrum at 405 nm could be observed which is due to the production of *p*-nitrophenol (**4-NP**). This indicated that the substrate had been completely consumed. The results from these experiments allowed us to optimise the volume of the enzyme that was added to the cuvette during the assay.

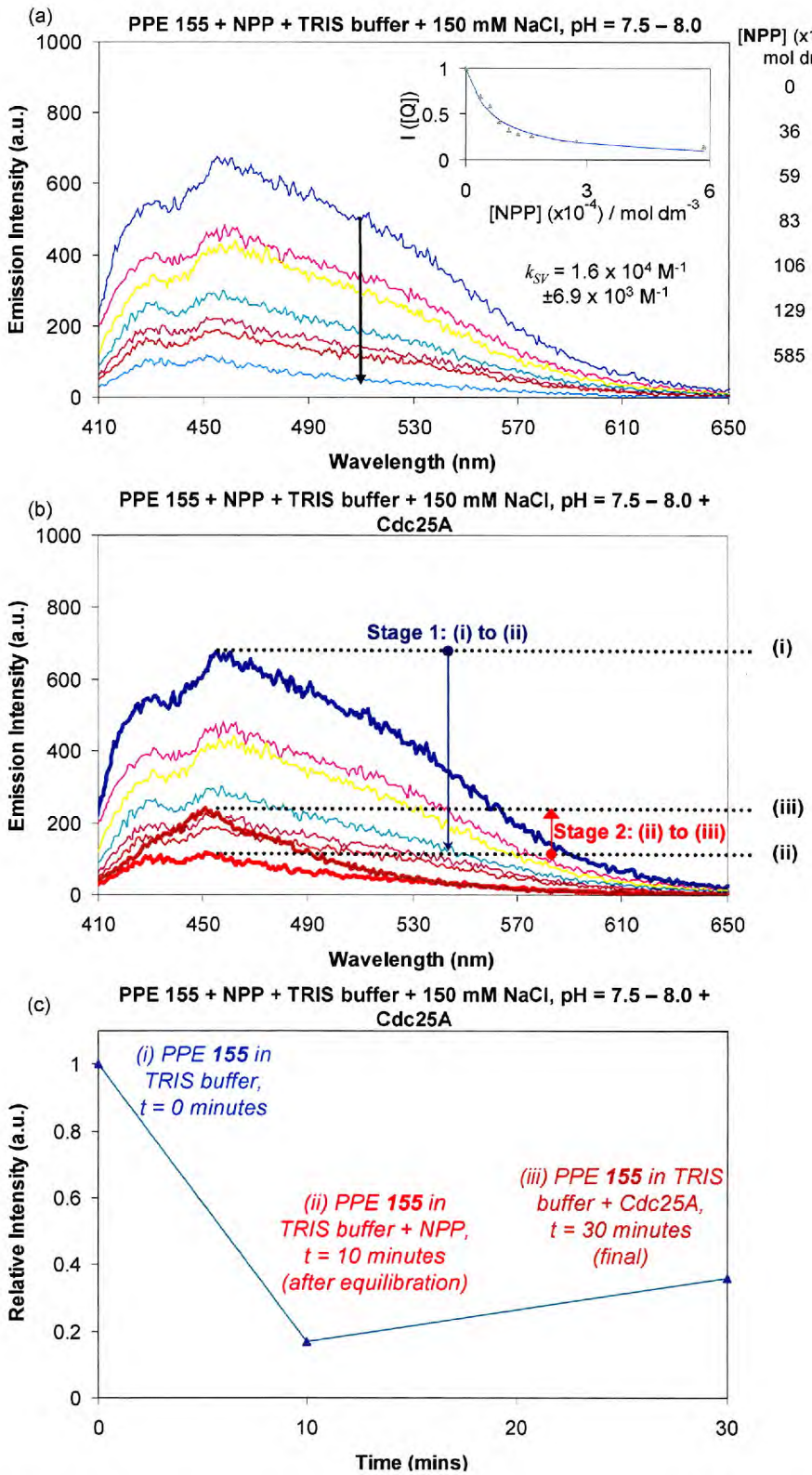

Figure 5.11 The emission spectra of PPE **155** at increasing concentrations of the quencher **NPP** in (a) 25 mM TRIS buffer containing no added salt and (b) the emission spectra upon addition of an aliquot of the phosphatase enzyme (Cdc25A). (i) Initial emission intensity, (ii) emission after quenching by **NPP**, (iii) recovered emission level. (c) Changes in relative emission intensity levels.

Clearly the assay needed to be improved if it were to be employed in the field, with the main optimisation required for the second stage, where the rise in emission intensity was limited. A variety of aqueous conditions were used to determine the optimal conditions for the initial quenching (Stage 1); all of these results are shown in Figure 3.17a and Figure 3.17b (Chapter Three). Briefly, the solvent conditions that led to the most efficient quenching consisted of a sodium acetate buffer (25 mM), with added sodium chloride (150 mM) and 0.3 wt.% Triton. This resulted in a Stern-Volmer constant of the order 10^7 M^{-1} which was comparable to the highest values that we recorded in any buffer used. To the best of our knowledge, there are no instances in the literature where Stern-Volmer constants of this magnitude have been reported in aqueous milieu *of such high ionic strength.*

The solvent conditions were also known to be suitable for the phosphatase enzyme that we sought to use, as confirmed by comparison to previous examples (were the activity of phosphatase was monitored)[43] and reference literature.[44] However, when attempting to recover the emission from the polymer, by addition of the enzyme, our results were broadly comparable with the finding in Figure 5.11 above – in general emission recovery was limited (< 10%). This outcome forced us to evaluate the nature of the quencher under the chosen solvent conditions and in particular the pK_a value of the chosen phosphate group (being part of the quencher structure). Presumably, for the assay to work as described in Figure 5.10, the phenolate formed after reaction of the enzyme, would have to be protonated to ensure that it did not serve to quench the emission from the polymer. To assess 4-nitrophenol (**4-NP**) in this respect, an emission quenching experiment with PPE **155** and **4-NP** was conducted (Figure 5.12).

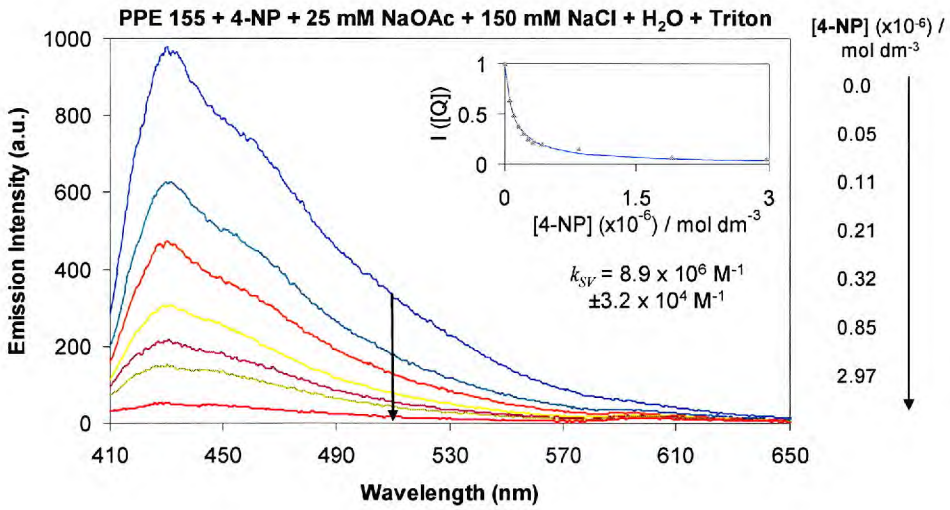

Figure 5.12 The emission spectra of PPE **155** in 25 mM sodium acetate buffer containing 150 mM NaCl and 0.3 wt.% Triton X-100 at increasing concentrations of the quencher **4-NP** (4-nitrophenol). The new phenol quencher strongly reduces the emission from the polymer, with a Stern-Volmer constant of 8.9 x 10^6 M^{-1}, which is comparable to **NPP**.

The emission spectra of 10 μM PPE **155** in the optimised solvent conditions is shown in Figure 5.12 at increasing concentrations of **4-NP**. As is seen in the figure, this work has illustrated the fortuitous discovery of a new quencher (**4-NP**) for PPE **155**, which proves to be very effective at reducing the emission from this cationic CPE.[45] In the selected aqueous conditions, the Stern-Volmer constant is almost indistinguishable from that of its derivative **NPP**, which is unsurprising as presumably the modification of **NPP** by the enzyme (to form **4-NP**) does not significantly affect the electron-accepting ability of the quencher, an idea supported by these results.

The overall effect of this finding conclusively proves that in the selected buffer conditions, the phenolate ion that was generated can quench the emission from the polymer as efficiently as its precursor and so conditions ensuring the protonation of this ion are required. By reducing the pH of the buffer to 2.90, it was quickly established that the yellow colour (associated with the phenolate ion) of a solution of **4-NP** could be eliminated. Satisfyingly, repetition of the quenching experiment with PPE **155** and **NPP**, at pH = 2.90 (but otherwise identical buffer conditions as described in Figure 5.12), yielded a similar k_{SV} value (1.2 x 10^6 M^{-1}). At this stage conditions that satisfied two important requirements for the enzyme assay, as described in Figure 5.10, were met: (i) The initial quenching with the phosphate quencher **NPP** was optimised and strong – k_{SV} values of 10^6 – 10^7 M^{-1} were routinely recorded. (ii) Conditions that ensured that the phenolate ion (formed by action of the enzyme on **NPP**) remained protonated throughout the assay had been identified. The final issue that remained concerned the operational 'window' for the enzyme. This

is illustrated in Figure 5.13 below, where the activity of the enzyme used is plotted against solution pH.[43]

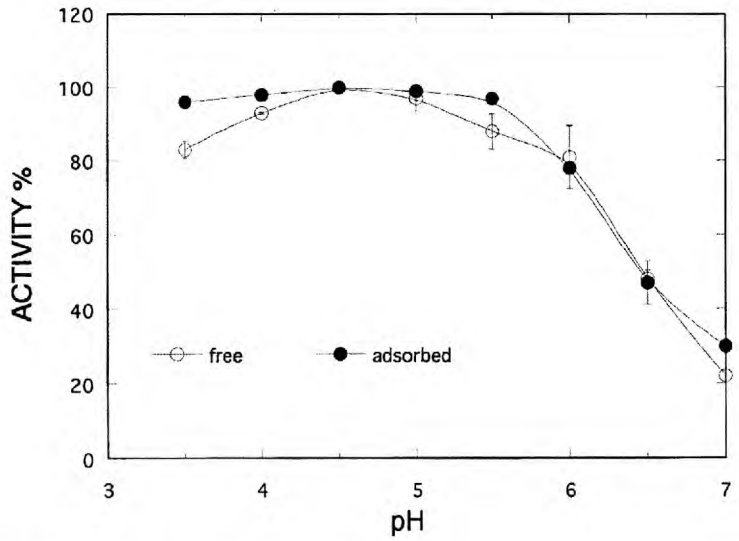

Figure 5.13 Activity profile of the phosphatase enzyme free in solution and adsorbed onto a silica surface. Reproduced from '*Kinetic properties and stability of potato acid phosphatase immobilized on Ca-polygalacturonate*' by Marzadori *et al.*.[43]

At pH = 3.50, the free phosphatase has an activity of ~ 80%. No activity is quoted for pH values below 3.50 but from the curvature of the graph, extrapolation suggests that the activity of the enzyme would diminish gradually. Importantly, it is likely that there would be sufficient activity from the enzyme at pH = 2.90 for the assay to succeed. To assess whether this is the case, the activity of the phosphatase was tracked by observing the accumulation of *p*-nitrophenol.

An absorption experiment was conducted where a TRIS buffered aqueous solution (at pH = 2.90) of **NPP** was treated with the enzyme. After 5 minutes, an excess of NaOH was added (to deprotonate the *p*-nitrophenol, forming the phenolate) which gave rise to a bright yellow colour originating from the phenolate ion. Encouraged by this, the enzyme assay in the presence of PPE **155** was attempted again using the new conditions (Figure 5.14).

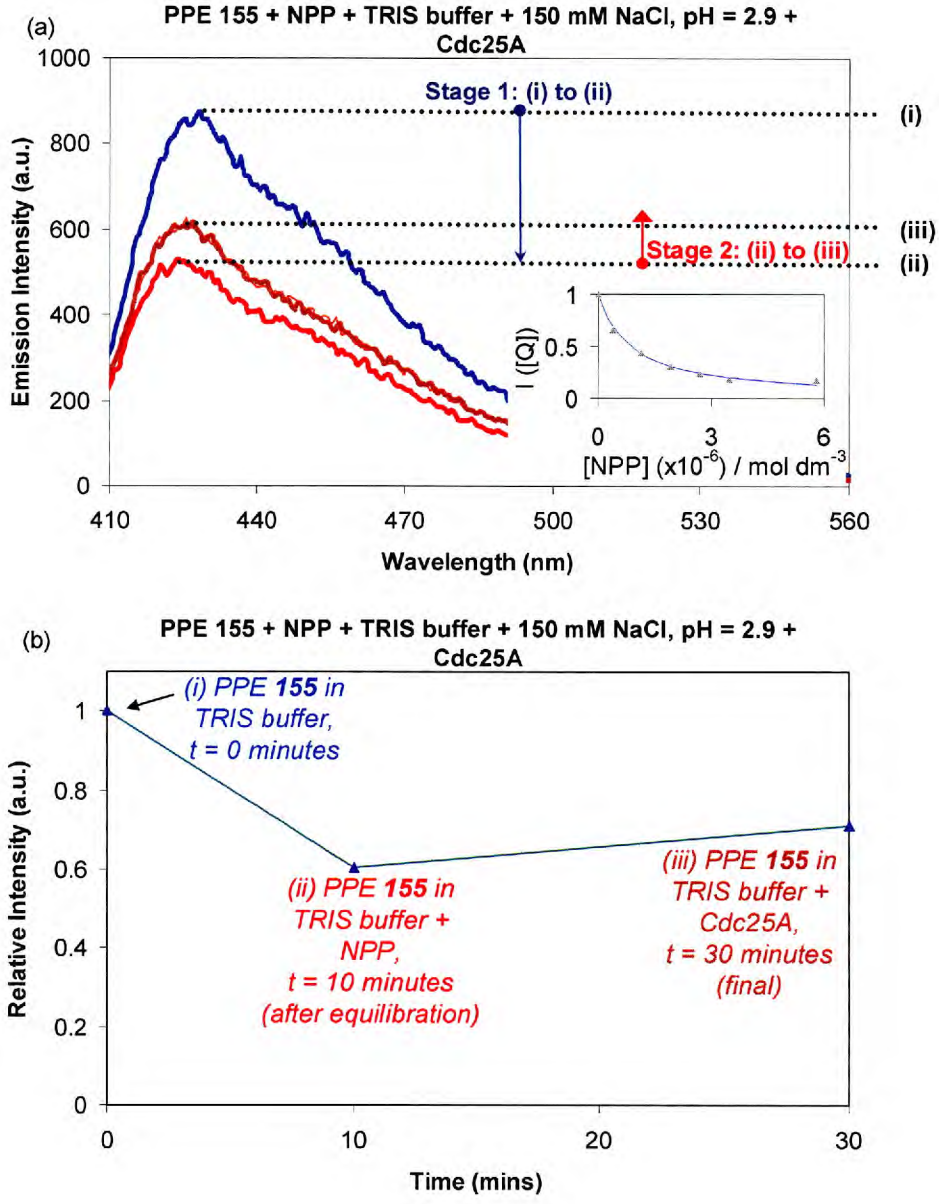

Figure 5.14 Results from the optimised phosphatase assay; (a) (i) the emission spectrum of PPE **155**; (ii) effect of the quencher and (iii) the phosphatase on the emission properties of the polymer. The inset shows the Stern-Volmer plot for this process (k_{SV} = 1.2 x 10^6 M^{-1}). (b) Changes in relative emission intensity levels: (i) Initial emission intensity, (ii) emission after quenching by **NPP**, (iii) recovered emission level. The assay was optimised by adjusting the solution pH (= 2.90) to ensure protonation of the product from the enzyme reaction.

Under the optimised conditions a modest emission recovery of 11% was observed from the point when the quencher was added. There are many factors that could explain why the modified conditions used in the assay failed to produce a better result. It is possible that the conformational order of the polymer in solution is altered in a way that 'traps' the quencher within the vicinity of

the backbone. The change in solution pH may also have influenced the emission properties of the polymer. There was insufficient time to investigate these issues, though clearly such factors would provide a starting point for further studies in the future.

5.6 Fabrication of a solid state sensor

The fabrication of a solid state sensor remains a formidable challenge as the existence of orbital coupling, which necessarily leads to self-quenching, is prevalent.[46] The quenching mechanism operates in addition to the usual electron transfer process (which proceeds through a polymer/quencher complex) and complicates an already difficult picture. Furthermore, aggregation effects, which are known to occur in solution upon addition of quencher species,[2] may also be a factor in the solid state though, the polymer chains would be expected to be more rigidly fixed thereby mitigating this effect.

The widespread applicability for this mode of quenching has been amply demonstrated by several elegant examples in the literature.[47] These results have demonstrated that conjugated polymers have a remarkable ability to enhance emission quenching effects. This innate sensitivity is attributed to the nature of the singlet excited state – the exciton – which samples the entire conjugated network. Thus, upon binding a quencher molecule, the emission from a CP is rapidly quenched as excitations that are distant on a fluorophore are quickly transferred to the quencher.

So far, the vast body of work on the use of such materials for sensing has concentrated on solution state studies. To broaden this scope and allow for the wider applicability of such technologies in, for example, instant medical diagnostic applications, it is necessary to develop solid state methodologies which avoid the use of complex assays with multiple handling steps and potentially multiple solutions. Whitten *et al.* have already shown how poly(phenylene ethynylene) (PPE) polymers coated on microspheres can be used as a sensitive platform for the detection of oligomeric DNA strands in a 'turn-on' assay that utilises a PNA capture ligand.[48]

However, transferring the emission quenching concept to a solid state sensor design has proved more problematic as issues regarding polymer-polymer interactions become more important.[40] This has led to ever-increasing complexity being introduced into the polymer design in attempts to reduce interchain interactions which have a negative impact on the emission intensity and quantum yield.[49]

Despite these issues, the case for fabricating conjugated polymers in the solid state is compelling; exciton motion would be expected to occur in three-dimensions thereby extending the potential

range of sites that it could sample during its lifetime. In a recent report, Swager summarised the rationale;[50] in solution the exciton will travel along isolated polymer chains in a random fashion sampling receptors that were previously visited, along with new ones. This occurs in a haphazard fashion as the exciton embarks on a random-walk process which means that for much of the time it is essentially limited in its ability to sample new receptor sites. To avoid this, two- and three-dimensional constructs would increase the efficiency of the random-walk of the exciton and maximise the sampling ability (*via* nearest neighbour hopping) of the exciton during its lifetime. This is an important point as emphasised by Kleimen and Schanze, who noted that the random walk mechanism is inherently time-dependent.[51] They used an anionic PPE in solution to model exciton hopping and observed that fast excitation hopping is the crucial and dominant quenching mechanism (static quenching) for their system.[51]

In this study, we demonstrate that structurally undemanding PPEs can be used as sensors in the solid state, though sensitivity levels are moderate as the polymer structure has yet to be optimised for this particular sensing format. The ability of a poly(phenylene ethynylene) conjugated polyelectrolyte to detect a small molecule quencher in the solid state was assessed by coating the polymer onto a plastic-backed, non-fluorescent, silica-gel TLC plate. The efficiency of the emission quenching process was quantified by noting the resulting loss of emission with increasing quencher concentration, in accordance with the Stern-Volmer relationship. The emission quenching induced by the addition of the analyte was quantified in the usual way.

To obtain a thin film of the polymer, a plastic-backed TLC plate was immersed into an aqueous solution containing PPE **155** (~ 1 mM in repeat units). After 15 minutes, the plate was removed from the solution and then dried under a gentle stream of nitrogen. The plate was then rinsed with water (to remove the excess PPE **155** from the surface, which failed to coat the surface) and dried under nitrogen. The experimental set-up for measuring the performance of the polymers coated onto the TLC plates is shown in Figure 5.15, along with the structures of PPE **155** and the emission quencher **NPP**. As it is important to ensure that there was no leaching of the polymer from the TLC plate during the course of the experiments, the newly-coated plate, following the coating and washing procedure (described in the Experimental section, Chapter Seven), was placed in the aqueous solution in the cuvette (as shown in Figure 5.15a) and the solution left to stand for 30 minutes. After this time, the plate was removed and the emission spectrum recorded. Satisfyingly, no emission could be detected from the aqueous solution and therefore this confirmed that no leaching of the conjugated polymer from the TLC plate had occurred.

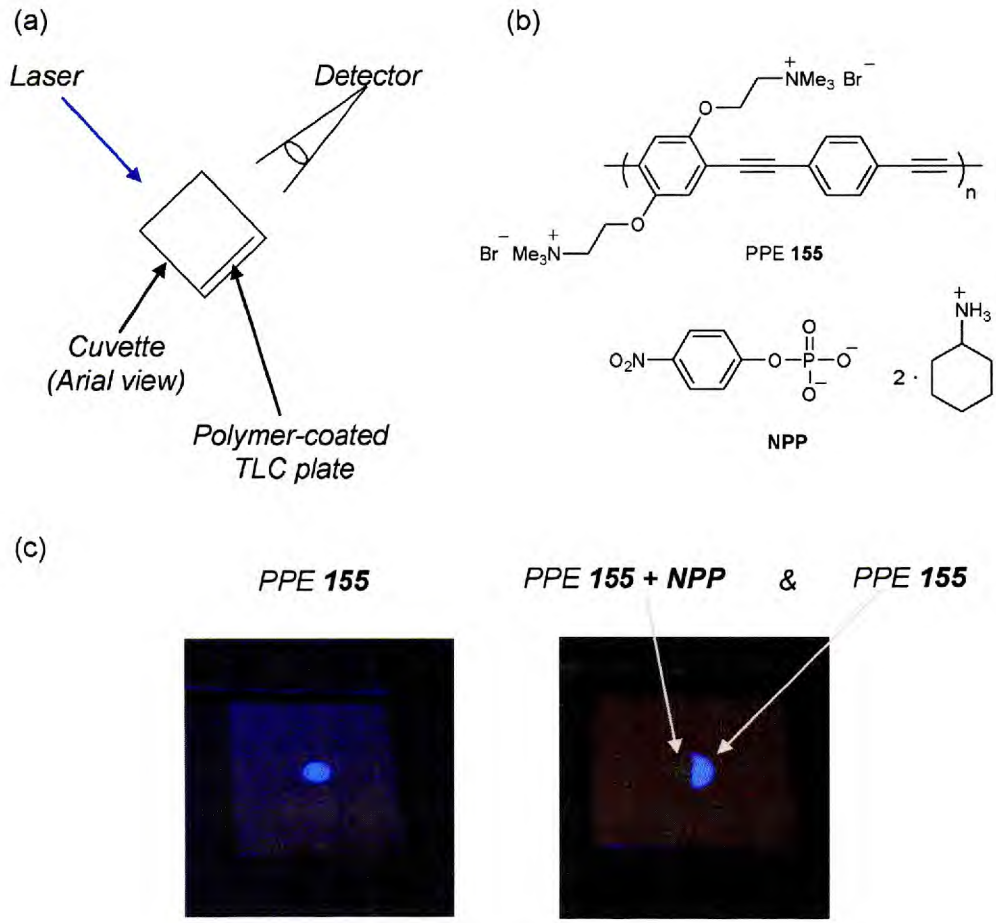

Figure 5.15 (a) Cuvette set-up for thin film sensing in water, of PPE **155** coated onto a plastic-backed TLC plate, (b) the structures of the polymer and quencher used, (c) images of the quenching process as conducted on plastic-backed TLC plates.

To investigate the ability of PPE **155** to detect the small molecule quencher **NPP**, the sensing strip was set-up as shown in the diagram (Figure 5.15a) and small known amounts of **NPP** were added to the cuvette, whilst examining the emission intensity using photoluminescence spectroscopy. The loss of fluorescence upon increasing the quencher concentration was correlated with the Stern-Volmer equation[52] which allowed us to quantify the efficiency of the quenching process. The Stern-Volmer plot is shown in Figure 5.16 (k_{SV} = 5.5 x 10^3 M^{-1}) along with emission spectra for this series of quenching experiments. The Stern-Volmer constant is 8500-times lower than that measured for the analogous solution based experiment. This significant reduction reflects the difficulties in obtaining the combination of good exciton transport and correct conformational order, factors that were identified as being important to enable high k_{SV} values to be obtained in the solution state (Chapter Three).

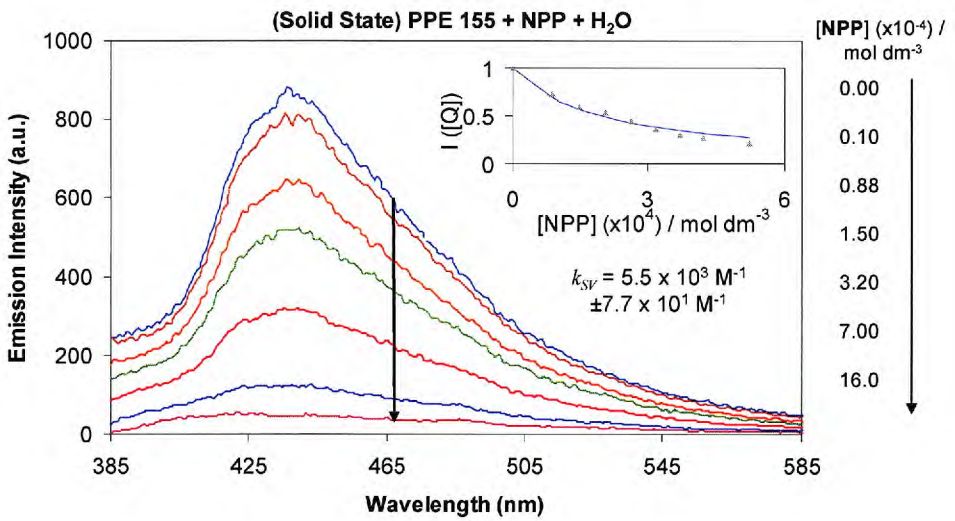

Figure 5.16 The emission spectra a thin film of PPE **155** coated onto a plastic-backed TLC plate at increasing concentrations of the quencher **NPP**. The inset shows the Stern-Volmer plot using data extracted from the main figure. The intensities in the Stern-Volmer plots are determined from the area beneath the corresponding curves in Figure 5.16, and are normalised with respect to the measured emission intensity in the absence of **NPP**. The markers denote experimental data lines and the solid-lines indicate the optimal fit to the Stern-Volmer relation.

The effect of coating PPE **155** onto a TLC plate led to a significant change in the overall shape of the emission profile. In solution based experiments, the emission spectra are much sharper (and display some vibronic structure), and are *blue*-shifted relative to the solid state emission which is relatively broad and featureless, characteristic of limited emission from a partially quenched state. Importantly, in order for us to observe any significant emission using our sensing strips, the polymer had to be coated onto the silica surface[53] from a PPE solution of relatively high concentration (~ 1 mM in repeat units). This may be because there was insufficient absorption from the coated polymer at the more dilute concentrations. This highlights several important points:

- Aggregation of polymer chains remains one of the main obstacles to developing solid state sensors based on conjugated polymers. Specifically, the development of non-aggregating PPEs has been investigated by many groups and the strategy adopted involves developing suitable co-monomers that permit three-dimensional excitonic motion, without the drawback of having aggregates and self-quenching effects, often prevalent in such materials.[54]
- An additional issue concerns the detection geometry (Figure 5.15a) which may have limited the amount of light entering the detector. Changes in the emission are therefore

detected partially indirectly from the solution and not directly from the surface of the polymer-coated TLC plate.

- It has been previously noted[2] during solution-based quenching experiments, that increasing the polymer concentration can be detrimental for the efficiency of the quenching process as measured by the Stern-Volmer constant.

The impact of these factors can help explain the results we observed for the solid state quenching experiments. In order to obtain a measurable signal, we coated the plates from a polymer stock solution at a moderately high concentration (~ 1 mM). As a result, the amount of polymer deposited onto the silica surface was approximately 1000 times higher (assuming the entire polymer sample on the plate is emissive) than that usually used for conducting such sensing measurements in solution. In solution based studies it has been previously reported that a 10-fold increase in the sensor concentration (1 μM to 10 μM) can lead to an order-of-magnitude decrease in the measured k_{SV} value.[2]

Clearly, the concept of concentration can not be directly applied to the solid state, but the 8500-fold decrease in the size of the Stern-Volmer constant reported here is consistent with the previous concentration-dependent finding. Additionally, the structure of PPE **155** was not optimised to achieve a balance between efficient exciton motion and minimal self-quenching. As a result, coating **NPP** onto the silica surface in this manner probably resulted in inefficient exciton motion.

To address these issues, and in order to exert some control over the alignment of the conjugated polymer chains in the solid state, we decided to explore the effect of the addition of a surfactant. The non-ionic surfactant Triton X-100, has been previously used by other groups to improve the quantum efficiency of conjugated polymers in aqueous solutions, by preventing the close alignment of polymer chains and thus self-quenching.[40,55] In our experimental scheme, we envisaged that the addition of a surfactant to the solution of PPE **155** used for coating, would perhaps lead to an increased distance between neighbouring chains when coated on to the silica surface. To test this idea, we repeated the above quenching experiments changing only the solution that were used to coat the TLC plates. In the only change, 5 wt.% of the surfactant (~ 30-fold excess), was added to the polymer solution.

Figure 5.17 shows the Stern-Volmer plot for the quenching of PPE **155** coated from a surfactant-containing solution by **NPP**. A Stern-Volmer constant of 5.6×10^3 M^{-1} was obtained; given the margin of error associated with these measurements, this value is essentially the same as that recorded in the previous experiment.

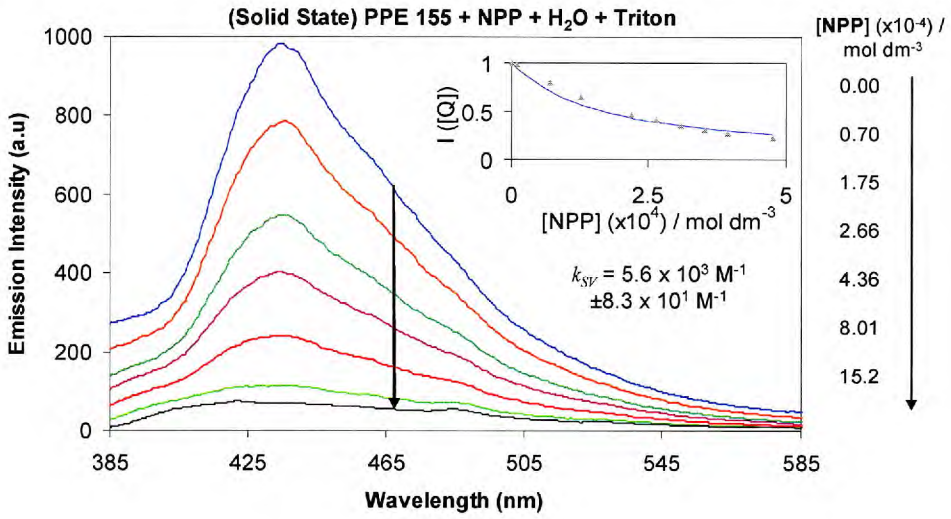

Figure 5.17 The emission spectra in water of PPE **155** coated onto plastic-backed TLC plates at various concentrations of the quencher **NPP**. The inset shows the Stern-Volmer plot using data extracted from the main figure and treated as before.

Therefore the addition of the surfactant had a negligible effect in terms of improving the overall efficiency of the sensing process, though clearly further experiments would be necessary in order to determine whether high concentrations would have a beneficial effect. The surfactant led to a small blue-shift in the emission intensity (2 nm) which is approximately five-times smaller than the typical red-shifts in the solution state emission spectra that were measured for PPE **155** in water. These changes highlight the limited action of the surfactant in affecting both the conformational order of the polymer and the disruption of aggregates in the solid state.

It was assumed that the surface coverage on the silica TLC plates was uniform for each quenching experiment, though surface analysis would need to be conducted to confirm this. However, this initial finding does suggest that surfactants, or indeed miscible matrix polymers (that serve as scaffolds that prevent strong self-quenching whilst allowing the facile movement of photoexcitations) can be useful when creating solid state structures from aqueous solutions of conjugated polymers. When spin-coating thin films this contribution could, in some circumstances, negate the need for complex synthetic modifications of the polymer in order to reduce excessive π-π stacking in the solid state. Thin films made by spin-coating onto glass slides, would also allow for an estimate of the film coverage. For example, previous reports with water-soluble cationic PPP systems,[56] suggest that the film coverage is approximately equal to that expected for a single monolayer of the polymer (2.4×10^{-10} mol cm^{-2}).[56]

5.7 Notes and references

1. L. Chen, D. W. McBranch, H.-L. Wang, R. Helgeson, F. Wudl and D. G. Whitten, *Proc. Natl. Acad. Sci. USA*, 1999, **96**, 12287-12292.
2. C. Y. Tan, M. R. Pinto and K. S. Schanze, *Chem. Commun.*, **2002**, 446-447.
3. L. Chen, D. W. McBranch, H.-L. Wang, R. Helgeson, F. Wudl and D. G. Whitten, *Proc. Natl. Acad. Sci. U. S. A.*, 1999, **96**, 12287-12292.
4. Q.-H. Xu, S. Wang, D. Korystov, A. Mikhailovsky and G. C. Bazan, *Proc. Natl. Acad. Sci. U. S. A.*, 2005, **102**, 530-535.
5. J. W. Hong, W. L. Hemme, G. E. Keller, M. T. Rinke and G. C. Bazan, *Adv. Mater.*, 2006, **18**, 878-882.
6. B. Liu and G. C. Bazan, *Chem. Mat.*, 2004, **16**, 4467-4476.
7. K. Dore, S. Dubus, H.-A. Ho, I. Levesque, M. Brunette, G. Corbeil, M. Boissinot, G. Boivin, M. G. Bergeron, D. Boudreau and M. Leclerc, *J. Am. Chem. Soc.*, 2004, **126**, 4240-4244.
8. B. Liu and G. C. Bazan, *Proc. Natl. Acad. Sci. U. S. A.*, 2005, **102**, 589-593.
9. (a) A. M. Funston, E. E. Silverman, J. R. Miller and K. S. Schanze, *J. Phys. Chem. B*, 2004, **108**, 1544-1555; (b) J. K. Mwaura, M. R. Pinto, D. Witker, N. Ananthakrishnan, K. S. Schanze and J. R. Reynolds, *Langmuir*, 2005, **21**, 10119-10126.
10. (a) S. Delaney and J. K. Barton, *J. Org. Chem.*, 2003, **68**, 6475-6483; (b) S. Steenken and S. V. Jovanovic, *J. Am. Chem. Soc.*, 1997, **119**, 617-618.
11. H. A. Ho, K. Dore, M. Boissinot, M. G. Bergeron, R. M. Tanguay, D. Boudreau and M. Leclerc, *J. Am. Chem. Soc.*, 2005, **127**, 12673-12676.
12. In these reported hybridisation experiments, the oligonuleotides used were < 100 b.p's.
13. See Chapter Three for a further discussion on the molecular weight of PPE **155**.
14. P. E. Nielsen, *Peptide Nucleic Acids: Protocols and Applications*, Garland Science, 2004.
15. Kindly donated by Dr David Mann, Department of Biochemistry, Imperial College London, UK.
16. (a) H.-A. Ho, M. Bera-Aberem and M. Leclerc, *Chem. Eur. J.*, 2005, **11**, 1718-1724; (b) H.-A. Ho, M. Boissinot, M. G. Bergeron, G. Corbeil, K. Dore, D. Boudreau and M. Leclerc, *ACS Symp. Ser.*, 2005, **888**, 359-367.
17. See Chapter One (section 1.7).
18. M. R. Pinto and K. S. Schanze, *Synthesis*, **2002**, 1293-1309.
19. L. Chen, S. Xu, D. McBranch and D. Whitten, *J. Am. Chem. Soc.*, 2000, **122**, 9302-9303.
20. C. A. M. Seidel, A. Schulz and H. M. Sauer, *J. Phys. Chem.*, 1996, **100**, 5541-5553.
21. (a) J.-P. Lecomte, A. Kirsch-De Mesmaeker, J. M. Kelly, A. B. Tossi and H. Gorner, *Photochem. Photobiol.*, 1992, **55**, 681-689; (b) S. J. Atherton and A. Harriman, *J. Am.*

Chem. Soc., 1993, **115**, 1816-1822; (c) S. Steenkan, *Free Rad. Res. Commun.*, 1992, **16**, 349-379; (d) L. P. Candeias and S. Steenkan, *J. Am. Chem. Soc.*, 1992, **114**, 699-704; (e) L. P. Candeias, P. Wolf, P. O'Neill and S. Steenkan, *J. Phys. Chem.*, 1992, **96**, 10302-10307; (f) D. J. Deeble, M. N. Schuchmann, S. Steenkan and C. von Sonntag, *J. Phys. Chem.*, 1990, **94**, 8186-8192; (g) L. Michaelis, *Chem. Rev.*, 1935, **16**, 243-286; (h) L. Michaelis and M. P. Schubert, *Chem. Rev.*, 1938, **22**, 437-470; (i) Z. R. Grabowski and W. Rubaszewska, *J. Chem. Soc., Faraday Trans. 1*, 1977, **73**, 11-28.

22. S. Fukuzumi, H. Miyao, K. Ohkubo and T. Suenobu, *J. Phys. Chem.*, 2005, **109**, 3285-3294.
23. K. Kobayashi and S. Tagawa, *J. Am. Chem. Soc.*, 2003, **125**, 10213-10218.
24. E. M. Boon and J. K. Barton, *Curr. Opin. Struct. Biol.*, 2002, **12**, 320-329.
25. T. Ito and S. E. Rokita, *Angew. Chem., Int. Ed.*, 2004, **43**, 1839-1842.
26. D. Porath, A. Bezryadin, S. de Vries and C. Dekker, *Nature*, 2000, **403**, 635-638.
27. S. Wang, B. Liu, B. S. Gaylord and G. C. Bazan, *Adv. Funct. Mater.*, 2003, **13**, 463-467.
28. J. P. Knemeyer, N. Marme and M. Sauer, *Anal. Chem.*, 2000, **72**, 3717-3724.
29. Y. Kim, J. E. Whitten and T. M. Swager, *J. Am. Chem. Soc.*, 2005, **127**, 12122-12130.
30. S. W. Thomas, III, J. P. Amara, R. E. Bjork and T. M. Swager, *Chem. Commun.*, **2005**, 4572-4574.
31. A. V. Kabanov, P. Felgner and L. W. Seymour, eds., *Self-Assembling Complexes for Gene Delivery. From Laboratory to Clinical Trial*, John-Wiley, Chichester, 1998.
32. J. DeRouchey, R. R. Netz and J. O. Radler, *Eur. Phys. J. E*, 2005, **16**, 17-28.
33. T. Bronich, A. V. Kabanov and L. A. Marky, *J. Phys. Chem. B*, 2001, **105**, 6042-6050.
34. X. Dai, M. E. Eccleston, Z. Yue, N. K. H. Slater and C. F. Kaminski, *Polymer*, 2006, **47**, 2689-2698.
35. H.-G. Elias, *Macromolecules*, John Wiley & Sons Canada, Ltd., 2005.
36. U. H. F. Bunz, *Chem. Rev.*, 2000, **100**, 1605-1644.
37. T. K. Bronich, H. K. Nguyen, A. Eisenberg and A. V. Kabanov, *J. Am. Chem. Soc.*, 2000, **122**, 8339-8343.
38. (a) M. R. Pinto and K. S. Schanze, *Proc. Natl. Acad. Sci. USA*, 2004, **101**, 7505-7510; (b) N. DiCesare, M. R. Pinto, K. S. Schanze and J. R. Lakowicz, *Langmuir*, 2002, **18**, 7785-7787.
39. (a) M. Gerard, A. Chaubey and B. D. Malhotra, *Biosens. Bioelectron.*, 2002, **17**, 345-359; (b) B. Wang, W. Yang and H. Fang, *Chem. Commun.*, **2003**, 792-793.
40. J. H. Wosnick, C. M. Mello and T. M. Swager, *J. Am. Chem. Soc.*, 2005, **127**, 3400-3405.
41. (a) M. R. Pinto, B. M. Kristal and K. S. Schanze, *Langmuir*, 2003, **19**, 6523-6533; (b) Q.-L. Fan, Y. Zhou, X.-M. Lu, X.-Y. Hou and W. Huang, *Macromolecules*, 2005, **38**, 2927-2936.

42. Kindly donated by Dr David Mann, Department of Biochemistry, Imperial College London, UK.

43. C. Marzadori, C. Gessa and S. Ciurli, *Biol. Fertil. Soils*, 1998, **27**, 97-103.

44. A useful reference source for information on suitable buffers, including advice on preparation see: http://www.sigmaaldrich.com/Area_of_Interest/Biochemicals/Buffer_Explorer.html

45. **4-NP** has been used previously to quench the emission from a glucose-functionalised PPE (I.-B. Kim, B. Erdogan, J. N. Wilson and U. H. F. Bunz, *Chem. Eur. J.*, 2004, **10**, 6247-6254).

46. D. Zhao and T. M. Swager, *Macromolecules*, 2005, **38**, 9377-9384.

47. Y. Liu, S. J. Jiang and K. S. Schanze, *Chem. Commun.*, **2003**, 650-651.

48. (a) S. Kumaraswamy, T. S. Bergstedt, X. B. Shi, F. Rininsland, S. A. Kushon, W. S. Xia, K. D. Ley, K. E. Achyuthan, D. W. McBranch and D. G. Whitten, *Proc. Natl. Acad. Sci. U. S. A.*, 2004, **101**, 7511-7515; (b) D. G. Whitten, S. A. Kushon, K. Bradford, V. Marin, C. Suhrada, B. A. Armitage and D. W. McBranch, *Langmuir*, 2003, **19**, 6456-6464.

49. H.-h. Yu, A. E. Pullen, M. G. Bueschel and T. M. Swager, *Angew. Chem., Int. Ed.*, 2004, **43**, 3700-3703.

50. J. Zheng and T. M. Swager, *Adv. Polym. Sci.*, 2005, **177**, 151-179.

51. J. G. Muller, E. Atas, C. Tan, K. S. Schanze and V. Kleiman, *J. Am. Chem. Soc.*, 2006, **128**, 4007-4016.

52. J. R. Lakowicz, *Principles of Fluorescence Spectroscopy*, Plenum Press, New York, 1983.

53. No attempts were made to analyse the silica surface used.

54. D. W. Lee and T. M. Swager, *Synlett*, **2004**, 149-154.

55. J. J. Lavigne, D. L. Broughton, J. N. Wilson, B. Erdogan and U. H. F. Bunz, *Macromolecules*, 2003, **36**, 7409-7412.

56. B. S. Harrison, M. B. Ramey, J. R. Reynolds and K. S. Schanze, *J. Am. Chem. Soc.*, 2000, **122**, 8561-8562.

6 Conclusions and Perspectives

6.1 Conclusions

The investigations presented in this thesis centred on the optimisation of polyelectrolyte biosensors and sought to provide a systematic study of the quenching mechanisms in these systems with a view to maximising Stern-Volmer coefficients. These optimised systems were then employed in the detection of oligomeric DNA strands and in an enzyme assay.

To accomplish this, a variety of organic and water-soluble conjugated polymers and shorter small model analogues were synthesised. Analysis of the first generation polymers revealed the importance of conjugation length; their sensitivity, as evaluated by measuring Stern-Volmer coefficients, suggested that they were comparable with polymers described in the literature ($k_{SV} \approx 10^6$ M^{-1}),[1] with the modest differences attributed to variations in the effective conjugation lengths, between our polymers and those reported.

In order to achieve improved performance as sensors, a detailed study of the Sonogashira-Hagihara polymerisation was undertaken with neutral bis(cetyloxy)-PPEs. This revealed that the best conditions, evaluated by considering molecular weights using NMR and GPC data, involved long reaction times (minimum of 48 hours), a vigorously anaerobic environment, freshly prepared/bought catalysts and importantly good solubility of all monomers. The use of these measures allowed a degree of polymerisation, of approximately 30, to be routinely recorded for the synthesis of the neutral polymers.

Armed with this knowledge, a series of second generation materials were synthesised including a potentially phosphate-selective isothiouronium-containing small model analogue. The new materials were based on previously reported ion sensors which could discriminate between phosphate and carboxylate ions. In similar previous work reported by Teramae *et al.*, where naphthalene-functionalised isothiouronium-based receptors were studied, a 4-fold increase in the emission intensity was recorded. This was ascribed to a suppression of the PET process that occurred between the donor fluorophore and acceptor isothiouronium motif.[2] Although we had no direct evidence to suggest that our new small model analogues would behave in a similar manner, initial results allowed us to speculate on possible reasons for this.

Early experiments showed no clear optical response from these materials upon treatment with target oxoanions (e.g. only a ~ 10% rise in the emission was observed when an excess of 90:1 of phosphate ions to sensor PE **175** was used). This was attributed to the relatively large distance

between the recognition unit and fluorophore (4 bond lengths), which prevented potential photoinduced charge transfer between the fluorophore and the isothiouronium motif. This is consistent with previous findings where efficient PET has been reported when the distance separating the fluorophore and isothiouronium units is reduced.[2,3]

The novel cationic polymer PPE **155** and its small model analogue (PE **154**) were synthesised. Compared with previously reported PPEs, the new materials contained a shorter bridge between the conjugated backbone and the recognition unit (that also serves as a water-solubilising motif) which we envisaged would lead to an improvement in the emission quenching efficiency.

The Stern-Volmer coefficient for the polymer (with **NPP**) was found to be approximately 3000 times higher than that of the small model analogue (4.7×10^7 M^{-1} versus 1.4×10^4 M^{-1}), indicating strong amplified quenching. This is in common with a number of structurally similar materials, where the amplified quenching effect has been demonstrated. The origin of this effect is expected to arise from the highly delocalised singlet excited state present in PPEs coupled with ion-pairing. The combination of these effects enhances the effective quenching radius of the quencher.[4]

The high Stern-Volmer coefficient of the polymer, however, was found to reduce dramatically under the high ionic strength conditions typically encountered in biological assays – a widely reported effect that renders the polymer unusable for high sensitivity detection in such environments.[5,6] This reduction in k_{SV} is attributable to the dissolution of polyelectrolyte aggregates under high salt conditions, which prevents excitons from communicating with multiple chains. This is based on a number of key observations that are supported by various experimental data. We assume that in pure water PPE **155** is fully aggregated. This supposition has been suggested by others and we consider that this idea is of central importance in allowing interchain interactions, through face-to-face π-stacking, which gives rise to a number of effects. For example, the facile movement of excitons in such aggregates increases the sphere-of-action of a quencher molecule. In addition, such aggregated structures were found to have lower quantum efficiencies compared with de-aggregated polymer chains (which are formed by the addition of a surfactant, like Triton, to a solution of the polymer in pure water). Finally, PPE **155** displayed broad emission spectra in pure water, which is consistent with polymer aggregation.

The non-ionic surfactant Triton X-100 had previously been used to induce association of (non-conjugated) polyelectrolyte chains in low ionic strength solutions; we anticipated it would have a similar effect in high ionic strength solutions, and hence might offer a potential means of preventing the catastrophic loss in k_{SV}. The addition of Triton to pure water solutions of the polyelectrolyte was found to have a slightly detrimental effect on the Stern-Volmer coefficient,

leading to a five-fold reduction compared to the surfactant-free case (k_{SV} = 9.1 × 10^6 M^{-1}). This reduction is consistent with a reduced ability of excitons to migrate between multiple polyelectrolyte chains in the polyelectrolyte/surfactant complexes. This result is in agreement with previously reported literature data, and can be rationalised by considering that the effect of the surfactant on the polymer chains in *pure water* could be to reduce interchain interactions, serving as a de-aggregating agent, *in this medium*. Importantly, however, a similar k_{SV} value of 1.1 × 10^7 M^{-1} was also obtained for PPE **155**/Triton in 25 mM TRIS buffer containing 150 mM NaCl. This compares with only 1.6 × 10^4 M^{-1} in the absence of Triton. This key finding contradicts previous reports where the addition of the surfactant Triton (to buffered aqueous solutions) has resulted in further reductions in the Stern-Volmer constant.[6] In this case, the differences between our analysis and the literature example include the nature of the conjugated polyelectrolyte (ours was cationic, the literature example involved an carboxylic acid-functionalised polymer) and the ionic strength of the solutions (we used a 25 mM buffered solution containing 150 mM of NaCl; in the reported example a 50 mM Tris buffer was used with 150 mM NaCl).[6] These differences suggest that the role of the surfactant depends on the specific conjugated polyelectrolyte and solvent conditions (our data indicates that its impact on the Stern-Volmer constant is dependent on the ionic strength of the solution). These assumptions are backed-up by quantum efficiency data for the polymer both in pure water and a high-ionic strength solution. Upon transferring PPE **155** from the former to the latter medium, a small rise in the quantum efficiency is noted, which suggests that the polymer is in a reduced aggregation state. The presence of Triton therefore prevents the substantial reduction in Stern-Volmer coefficient that usually occurs when a conjugated polyelectrolyte is used in buffered conditions.

This study represents the first thorough analysis of the impact of realistic buffer conditions on the emission quenching properties of a typical class of PPE polymer. Moreover, the ability to maintain high Stern-Volmer constants in high ionic strength conditions extends the applicability of ionic conjugated polymers to high sensitivity detection in biological media, greatly enhancing their versatility as biological sensors.

In order to enhance the emission quenching effect, the synthesis of third generation materials involved a key difference in the sensor design, with the recognition unit coupled directly to the conjugated backbone. These new materials are the first examples where receptor units are directly appended to the conjugated PE and PPE backbone. The anticipated enhanced electronic communication resulted in approximately a doubling in the Stern-Volmer values for the new PE small model analogue PE **208** as compared with a structurally related alkoxy variant (PE **154**). This important finding indicates the importance of minimising the distance between the receptor unit

and conjugated backbone which, presumably, allows for increased rates of PET between the fluorophore and quencher.

The use of the novel second and third generation materials for biosensor applications was investigated. The individual bases and shorter oligonucleotides (tetramers) were efficient emission quenchers ($k_{SV} = 10^5 - 10^7$ M^{-1}). Initial DNA hybridisation assays with 35-mer strands, revealed an optical response that resembled that reported by Leclerc *et al.*; initially, the emission from PPE **155** was quenched upon addition of the first 35 base-pair strand, but addition of the complementary strand resulted in almost complete recovery in the emission intensity level from the polymer (to within ~ 5%). From this, we concluded that the interaction of PPE **155** with the single-stranded probe and target DNA strands, was similar to that described by Leclerc *et al.*[7] despite the differences in persistence lengths of the polymers (15 nm for PPEs compared with approximately 6 nm for poly(thiophene)s).[8] Clearly further measurements are needed to verify this claim (see Future Work section) but these initial results are intuitive, especially when considered in light of our quenching studies involving the single-base moieties, where the bases were found to be efficient emission quenchers.

An assay involving the application of PPE **155** for the real-time monitoring of the activity of a phosphatase enzyme was designed. In the first stage, efficient quenching of the emission from the polymer was observed which was followed by a modest (19%) 'turn-on' effect in the presence of the enzyme. The small recovery in the emission intensity was attributed to the strong quenching effect of 4-nitrophenol (**4-NP**), a by-product formed by the action of the phosphatase on **NPP**. However, despite amending the assay conditions to account for this unintended quenching effect, no improvement in the emission recovery could be obtained. We suspected that new solvent conditions (specifically the increased acidity, pH = 2.90) may have altered the conformation of the polymer leading to self-quenching effects.

Finally, emission quenching experiments on the solid state have been performed and the efficiency of the quenching measured (k_{SV} ~ 5000 M^{-1}). These values are at least a 1000 times lower than those commonly recorded for solution based systems and for Langmuir-Blodgett (LB) monolayers[9] but demonstrate that such materials can be used in a more user-friendly format, allowing for such sensors to be employed in instant medical diagnostic work.

6.2 Perspectives and future work

The exquisite sensitivity of conjugated polymers and small model analogues can be harnessed to provide a platform for a new generation of biosensors. A glimpse of potential future applications

has been provided in works by Leclerc *et al.*,[7] and currently such materials are already being exploited as explosive detectors in commercial devices.[10]

6.2.1 Solution state emission quenching

However, more research is required in order to better our understanding of the fundamental processes regarding emission quenching, particularly in biological media. As we found, the sensing response from CPEs can be greatly diminished in high-ionic strength conditions but can be recovered by the addition of surfactants. It would be beneficial to know what impact such aqueous conditions have on the polymer conformation, with a view to optimising the structure of the side chains (e.g. by introducing some of the structural features present in surfactants like Triton). To investigate these ideas light scattering techniques may help.

Additionally, building selectivity into such devices is central to fabricating a successful biosensor. In this regard, these polymers have been used as 'optical-only' units with a secondary sensing element being employed. Though satisfactory, this approach neglects the potential for CPEs to be all encompassing units – our findings on guanidinium-oligo(phenyleneethynylene)s show that when in direct electronic communication with the conjugated backbone, greater increases in sensitivities can be realised (though we could not prove this effect for the polymeric versions). Our studies have shown that CPE materials such as PPE **155** can be used to interrogate biological systems. An important future experiment would involve the detection of multiple and single base-pair mismatches along an oligonucleotide sequence, in a similar experiment to that described in Chapter Five, for a 35-mer complementary strand. Presumably the rate of formation of a complex between a CPE and oligonucleotides containing different mismatches would vary, which would allow one to track the progress of the hybridisation process by monitoring the changing emission spectra with time.

A strategy to broaden the scope of functionalised PPEs could involve the use of 'click chemistry'.[11] In principle, this would allow a wide variety of recognition moieties to be appended to the polymer backbone. The added advantage of this technique centres on the nature of the formed product, which would maintain the electronic communication between both entities, through the formation of an aromatic triazole unit (e.g. if an alkyne were combined with an azide-containing monomer). In preliminary studies we proved that the formation of an azide variant of monomer **140** was straightforward, although ideally the azide functional group would need to be attached to the aromatic ring such that the electronic communication between the receptor motif and conjugated backbone could be maintained.

Another avenue worth pursuing involves the translation of the solution state work into a format that is generally applicable for biological analysis. The use of conjugated polymers for sensing is ideally set-up for detection in 'on-chip' applications.[12] Micro- and nanofluidic systems could potentially extend the detection limits for these systems and would allow for greater control to be exercised over the quenching process, by allowing for the easy addition of reagents. Additionally, any problems with photobleaching are mitigated as chip-based systems use a continuous flow of the polymer solution, thereby maintaining a constant emission level.

6.2.2 Solid state sensing

One of the biggest problems concerns the accommodation of analytes in a sufficiently porous structure. Swager *et al.* opted to synthesise PPEs containing the sterically demanding pentiptycene units that effectively isolate PPE chains, thus preventing self-quenching effects.[13] They also have the additional benefit of providing 'free-volume' allowing for facile analyte diffusion, all without compromising exciton motion.[13]

In our initial investigations we sought to avoid complex synthetic manipulations in favour of an approach based on the use of a surfactant. In pure aqueous solution, surfactants are known to moderate polymer-polymer interactions and so it was envisaged that they may have a similar effect in the solid state, though our initial results failed to verify this.

Clearly, more work on the impact of surfactants is necessary. In particular, the use of thin films as the sensing platform would increase the consistency of film preparation. Thin films made by spin-coating surfactant-containing polymer solutions, would allow for a systematic study of the impact of such additives. Moreover, coating a pre-arranged open porous network with the selected polymer sensor may provide a better way of avoiding self-quenching interactions without complex polymer architectures.

6.2.3 Materials for biosensing

The initial application of CPEs, in particular polycations, for biosensing requires further optimisation. The promising enzyme assay may suffer from a poorly designed quencher, as it was observed that the action of the phosphatase generates a molecule that retains the ability to induce strong quenching in the polymer. To circumvent this, an alternative quenching species is needed that does not remain electron deficient after dephosphorylation by the enzyme. One idea involves increasing the length of the tether between the electron-deficient aromatic unit and the phosphate unit, such that after the enzyme reaction, the generation of an aromatic phenol is avoided.

Optimising the DNA sensing applications for CPEs requires more work on understanding the nature of the interactions. With the 35-mer strands used in the initial hybridisation events, control experiments, involving non-complementary strands, are necessary to confirm the optical response. Additionally, single strands containing single, double and possibly further mismatches would need to be analysed, in a bid to observe differences that would allow one to distinguish between the anomalies in the target material.

Cationic conjugated polymers and small model analogues can also be explored as fluorescent markers. Current available techniques for monitoring transfection events for gene delivery systems consist mainly of chemical treatments. Polymers like PPE **155**, being highly emissive and water-soluble, could be ideal candidates for such applications for use in sequencing, detection and sensing.

6.3 Notes and references

1. J. Zheng and T. M. Swager, *Adv. Polym. Sci.*, 2005, **177**, 151-179.
2. S. Nishizawa, Y.-Y. Cui, M. Minagawa, K. Morita, Y. Kato, S. Taniguchi, R. Kato and N. Teramae, *J. Chem. Soc., Perkin Trans. 2*, **2002**, 866-870.
3. N. B. Sankaran, S. Nishizawa, M. Watanabe, T. Uchida and N. Teramae, *J. Mater. Chem.*, 2005, **15**, 2755-2761.
4. (a) L. Chen, D. W. McBranch, H.-L. Wang, R. Helgeson, F. Wudl and D. G. Whitten, *Proc. Natl. Acad. Sci. USA*, 1999, **96**, 12287-12292; (b) M. R. Pinto, B. M. Kristal and K. S. Schanze, *Langmuir*, 2003, **19**, 6523-6533; (c) D. L. Wang, J. Wang, D. Moses, G. C. Bazan and A. J. Heeger, *Langmuir*, 2001, **17**, 1262-1266; (d) J. Wang, D. L. Wang, E. K. Miller, D. Moses, G. C. Bazan and A. J. Heeger, *Macromolecules*, 2000, **33**, 5153-5158; (e) C. Y. Tan, E. Atas, J. G. Muller, M. R. Pinto, V. D. Kleiman and K. S. Schanze, *J. Am. Chem. Soc.*, 2004, **126**, 13685-13694.
5. M. R. Pinto and K. S. Schanze, *Proc. Natl. Acad. Sci. USA*, 2004, **101**, 7505-7510.
6. J. H. Wosnick, C. M. Mello and T. M. Swager, *J. Am. Chem. Soc.*, 2005, **127**, 3400-3405.
7. K. Dore, S. Dubus, H.-A. Ho, I. Levesque, M. Brunette, G. Corbeil, M. Boissinot, G. Boivin, M. G. Bergeron, D. Boudreau and M. Leclerc, *J. Am. Chem. Soc.*, 2004, **126**, 4240-4244.
8. U. H. F. Bunz, *Chem. Rev.*, 2000, **100**, 1605-1644.
9. G. D. Joly, L. Geiger, S. E. Kooi and T. M. Swager, *Private Communication*, 2006.

10. These systems are commercially known as Fido sensors, sold by Nomadics Inc. in Stillwater, OK, USA.
11. H. C. Kolb, M. G. Finn and K. B. Sharpless, *Angew. Chem., Int. Ed.*, 2001, **40**, 2004-2021.
12. J. H. Moon, R. Deans, E. Krueger and L. F. Hancock, *Chem. Commun.*, **2003**, 104-105.
13. D. Zhao and T. M. Swager, *Macromolecules*, 2005, **38**, 9377-9384.

7 Experimental Section

7.1 General

Unless indicated otherwise, all reactions requiring anhydrous conditions were performed using oven-dried glassware and conducted under a nitrogen (99.998%) or argon (99.998%) atmosphere and starting materials were obtained from commercial suppliers (Sigma-Aldrich Chemical Company, Lancaster Synthesis, Avocado, Fisher Scientific, Strem Chemicals) and were used without further purification (Strem: $Pd(PPh_3)_4$, 99.9+%-Pd. Sigma-Aldrich: CuI, 99.999%; diisopropylamine, purified by redistillation, 99.95%; 1,3-propanesultone, ≥ 99%; 4,4′-dipyridyl hydrate, **DPy**, 98%; 9,10-Anthraquinone-2,6-disulphonic acid disodium salt, **AQS**, ≥ 98%; 1,1′-dimethyl-4,4′-bipyridinium dichloride hydrate, $\mathbf{MV^{2+}}$, 98%; *N,N′*–di-(*tert*-butoxycarbonyl)thiourea, 97%; 1,3-bis(*tert*-butoxycarbonyl)guanidine, 98%; 1,3-bis(*tert*-butoxycarbonyl)-2-methyl-2-thiopseudourea, 98%; 4-Nitrophenyl phosphate, bis(cyclohexylammonium) salt hydrate, **NPP**, 97%. Lancaster Synthesis: bis(trifluoroacetoxy)iodo]benzene, 97%). All reaction temperatures recorded indicate the temperature of the bath in contact with the reaction vessel. Anhydrous solvents were prepared in accordance with known protocols; tetrahydrofuran was distilled from sodium/benzophenone. Methanol was distilled from $CaSO_4$ and acetone from potassium carbonate. Diethyl ether was distilled from K/Na/Ph_2CO. Methylene chloride and acetonitrile were distilled from phosphorus pentoxide. Toluene was distilled from sodium/benzophenone. All other solvents were purchased from the Sigma-Aldrich Chemical Company and used as received (ACS grade or GPR grade).

All intermediates were purified by column chromatography using Kieselgel BDH F_{254} 30-70 μm grade silica gel. Solvents used were ACS grade or GPR grade. Routine monitoring of reactions was performed using analytical thin layer chromatography on pre-coated silica gel $F_{254/366}$ Merck Kieselgel 60 Å aluminium or glass-backed plates and visualised by the quenching of UV fluorescence ($\lambda_{ex.}$ = 254 nm) or one of the following visualisation reagents: anisaldehyde, permanganate, iodine vapour or cerium ammonium molybdate (CAM).

^{1}H-NMR and ^{13}C-NMR spectra were recorded on a Jeol GSX 270 MHz (270 MHz and 67.5 MHz), a Bruker Avance 400 MHz instrument running with a dual resonance BBO probe with z-gradients (400 MHz and 100.6 MHz) or a Bruker 500 MHz instrument running with a dual resonance BBO probe with z-gradients (500 MHz and 125.8 MHz). All NMR chemical shifts were referenced to residual solvent resonances or to $SiMe_4$ as an internal standard, unless otherwise indicated. Chemical shifts are expressed in parts per million, (ppm, δ) downfield from tetramethylsilane (TMS). Coupling constants are quoted in Hz. Splitting patterns are designated as s, singlet; d,

doublet; dd, doublet of doublets; t, triplet; q, quartet; sep, septet; m, multiplet; br, broad. Two-dimensional spectra were recorded on the Bruker Avance 400 MHz instrument.

Infrared spectra were recorded on a Perkin-Elmer Spectrum RX FT-IR spectrometer. Spectra were analysed as thin films between KBr or CaF disks. The values obtained are quoted in wavenumbers (cm^{-1}).

Mass spectra and HRMS were recorded under CI^+, EI or FAB^+ conditions on a Micromass Platform II or a Micromass AUTOSPEC-Q instrument, at the Imperial College Department of Chemistry Mass Spectrometry Service facility. Matrix assisted laser desorption ionisation time of flight (MALDI-tof) mass spectra measurements were performed on a Bruker Reflex IV spectrometer. The instrument was equipped with a nitrogen laser (λ = 337 nm), detector (high mass, HMASS^{TM}) and the applied voltage was varied using the method of pulse ion extraction (PIE^{TM}), up to 20 kV in reflection mode. For sample preparation see Chapter Two (section 2.3.2). Elemental analyses were determined by the University of North London Analytical Service. Melting points were obtained using a GallenKamp melting point apparatus and are uncorrected. TGA analyses were conducted on thermogravimetric analyser (Perkin-Elmer) at Imperial College.

Ultraviolet-visible (UV-vis) measurements were conducted on a Perkin-Elmer Lambda 25 UV-vis spectrometer. Fluorescence measurements were conducted on either a Varian Cary-Eclipse Fluorescence Spectrometer with a xenon lamp as a light source or a SPEX Fluoromax-3 Spectrofluorimeter or a Perkin-Elmer LS 50B Luminescence Spectrometer. Both absorption and emission spectra were measured in quartz cuvettes (10 mm x 10 mm x 45 mm, path length = 10 mm); solutions were thoroughly degassed with argon (where stated) prior to use. Unless otherwise stated, all experiments were conducted at 25 °C (± 0.5 °C). Emission quenching techniques are described in section 7.3. A list of the materials used for the absorption and emission measurements along with those used to make the buffer solutions are listed in Table 7.1.

Table 7.1 Chemicals used in the preparation of solutions for photophysical analysis

Chemical	Supplier	Purity	CAS
Water	Fisher	(deionised)	7732-18-5
Methanol	Sigma	≥ 99.5%	67-56-1
Trizma® base (Tris(hydroxymethyl)aminomethane)	Sigma	≥ 99.9%	77-86-1
Trizma® hydrochloride (Tris(hydroxymethyl)aminomethane hydrochloride)	Sigma	≥ 99.9%	1185-53-1
Sodium acetate	Sigma	≥ 99.5%	127-09-3
Triton X-100	Sigma	grade = SigmaUltra	9002-93-1
Phosphatase, acid from potato	Sigma	-	9001-77-8

Fluorescence lifetime measurements were acquired on a Hamamatsu ~ 60 ps, ~ 409 nm diode laser, a chromex 250 spectrograph imaging system and a Hamamatsu C4334-01 streak camera. This system was under the control of HPD-TA32 software (High Performance Digital Temporal Analyser). Quantum efficiency (QE) measurements were measured relative to the standard reference of quinine bisulphate (ϕ_f = 0.546, in 1N H_2SO_4), which has an emission range of 400 – 600 nm.[1,2] The calculation of the QEs of the polymers required the measurement of absorption and emission spectra, (recorded on the instruments described above) consistent with Equation 9 (Chapter Two, section 2.1.4). Fluorescence spectra were corrected for variations in the lamp efficiency using correction curves generated on the instrument. The absorbance for these fluorescence measurements was limited to ~ 0.05 (to minimise inner filter effects). Corrections for refractive indices were obtained from reference sources[2] and the techniques used are described in Fery-Forgues and Lavabre.[3]

The pH of solutions was determined using a pH metre (HI-98105) supplied from Hanna Instruments (http://www.hannainst.co.uk). The pocket pH metre was calibrated using standard buffer sachets supplied from Sigma.

Dialysis membrane tubing (6 – 8 kDa MWCO) was purchased from Fisher Scientific (catalogue number: 132655) and was made from regenerated natural cellulose. To prepare for use, the membrane was soaked in deionised water for 2.5 hours and then rinsed with more deionised water.

Washing procedure for NaH:

NaH was placed in an oven-dried round bottomed flask and argon was flushed though the system for 10 minutes. THF was then added and the suspension stirred for 5 minutes and allowed to stand for 25 minutes. The oily residue was then decanted off under argon and the above procedure repeated once more. This provided fresh samples of NaH that were then rapidly employed in subsequent reactions.

7.1.1 Gel permeation chromatography (GPC)

GPC at Imperial College London

Sample concentrations were ~ 4-5 mg/mL and the prepared polymer solutions were left overnight to aid dissolution, when possible, before being filtered through a 0.45 μm and 0.2 μm membrane pore filter (Whatman Puradisk 13 mm syringe filters, PTFE membrane). GPC analyses were performed on:

(i) A Waters Alliance GPC V2000 separation module equipped with three detectors; viscosity, UV and a Wyatt Technology Mini-DAWN light scattering detector (an 18-angle detector with a 30 mW gallium-arsenide 690 nm laser light source). Alliance GPC 2000 series software was used to process data. The system ran with H_2O (containing $NaNO_3$ (0.2 M) and NaN_3 (0.04%)) or DMAc as the eluant at 30 °C. A guard column (TSK GMPW) and two analytical columns (TSK GMPWXL) were used, as supplied from Tosoh Bioscience LLC (pore size: 100 – 1000 Å). The system was calibrated against polyethylene glycol or polystyrene standards (Polymer Laboratories).

(ii) A triple-detector Viscotek TriSEC model 302 system, running at 1.0 mL/min (nominal), equipped with a three detectors (refractive index, viscosity and 90° light scattering), in combination with TriSEC version 3 software. The system ran with THF as the eluant at 30 °C, with mixed-bed TSK gel columns (7.5 mm x 300 mm; pore size: 100 – 1000 Å, Tosoh Corporation) and was calibrated against polystyrene standards.[4]

(iii) A Polymer Laboratories PL-GPC 50 Integrated System, running at between 0.5 and 1.0 mL/min (nominal), at 40 °C, equipped with two detectors (refractive index and viscosity) using DMF as the eluant and PLgel guard and two PL gel 5

μm MIXED-D columns (supplied by Polymer Laboratories) and calibrated using polystyrene standards. The data was collected and analysed using Cirrus GPC Offline/Online software, version 2.0 (2003).

UK GPC Service, at Rapra Technology Ltd.

Sample concentrations were ~ 1 – 2 mg/mL and the prepared polymer solutions were left overnight to aid dissolution before being filtered through a 0.2 μm membrane. GPC analyses were performed on a Viscotek system with PL gel guard and 2 mixed bed-D, 30 cm, 5 μm coloumns and the system was equipped with a refractive index (with differential pressure and light scattering) detector. Chloroform was used as the eluant at a flow rate of 1.0 mL/min (nominal), at 30 °C.

7.1.2 Determination of the molecular weight of PPE 155 by SDS gel electrophoresis[5]

A small (10 mg) sample of PPE **155** was dissolved in 10 μL of H_2O and then vortexed and heated for 5 minutes at 65 °C. The sample was then vortexed again and then spun for 1 minute at 14000 rpm. The supernatant (a yellow colour) was transferred to a new tube and 10 μL 2x SDS PAGE buffer was added. The sample was spun again for 1 minute and the supernatant loaded onto the gel. Much of the polymer appeared to be insoluble. This insoluble material was collected and 20 μL 2x SDS PAGE buffer was added and the resulting mixture vortexed and this was also loaded on the gel. A 15% tricine gel run at 100 V, at 4 °C (to prevent overheating) was used over a period of 2 hours. The gels were comprised of the following (2 gels):

Resolving gel:
6.7 mL 3M TRIS HCl pH = 8.5; 10.1 mL 30% acrylamide; 2.0 mL glycerol; 200 μL 10% SDS; 1 mL dd H_2O; APS and temed to polymerise.

Stacking gel:
3.8 mL 3 M TRIS HCl pH = 8.5; 1.3 mL 30% acrylamide; 375 mL 10% SDS; 4.6 mL dd H_2O; APS and temed to polymerise.

For the lower tank buffer: 0.2 M TRIS HCl pH = 8.9
The upper tank buffer: 0.1 M TRIS HCl, 0.1 M tricine, 0.1% SDS

Once the gels were finished they were visulised using a UV transilluminator and then the gels were stained with coomassie blue.

7.2 Syntheses

[ref] molecule has been previously described in the literature.

7.2.1 2,5-Diiodo-1,4-dimethoxybenzene (**114**).[6]

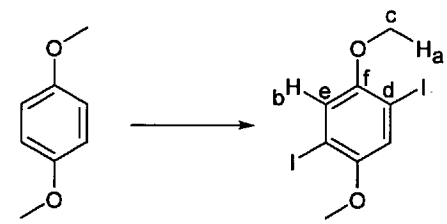

113 **114**

114 was prepared using a previously described procedure; characterisation data correspond to literature values.[6]

114: (4.27 g, 52%), a white crystalline solid, m.p. 170 – 171 °C (Lit. 171 °C);[6] IR (Film) ν_{max}/cm^{-1} 743 (Ar CH def.), 1062 (CO str.), 1215 (CO str.), 1378 (CH def.), 1460 (CH def.), 2856 (CH str.), 2927 (CH str.); δ_H (270 MHz, $CDCl_3$) 3.81 (6H, s, H_a), 7.17 (2H, s, H_b); δ_C (67.5 MHz, $CDCl_3$) 57.3 (C_c), 85.5 (C_d), 121.7 (C_e), 153.4 (C_f); *m/z* (CI, NH_3) 390 (10%, $[M+H]^+$); HRMS (CI, NH_3) Found: $[M]^+$, 389.8611. $C_8H_8I_2O_2$ requires: $[M]^+$, 389.9569.

7.2.2 2,5-Diiodo-1,4-hydroquinone (**108**).[6]

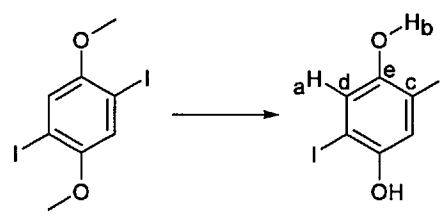

114 **108**

108 was prepared using a previously described procedure; characterisation data correspond to literature values.[6]

108: (2.49 g, 77%), as beige needle-shaped crystals; R_f = 0.5 (THF:*n*-Hexane, 1:1, v/v); m.p 193 – 194 °C (Lit. 195 – 197 °C);[6] IR (Film) ν_{max}/cm^{-1} 873 (Ar CH def.), 1048 (CO str.), 1190 (CO str.), 1377 (CH def.), 1462 (CH def.), 2857 (CH str.), 3434 (OH str.); δ_H (270 MHz, d_6-acetone) 7.27 (2H, s, H_a), 8.78 (2H, s, H_b); δ_C (100.6 MHz, d_6-acetone) 84.3 (C_c), 125.0 (C_d), 151.7 (C_e); *m/z* (CI,

NH_3) 362 (100%, $[M+H]^+$); HRMS (CI, NH_3) Found: $[M]^+$, 361.8314. $C_6H_4I_2O_2$ requires: $[M]^+$, 361.9037.

7.2.3 2,5-Diiodo-1,4-bis(propyloxy sulphonate)benzene (**115**).[7]

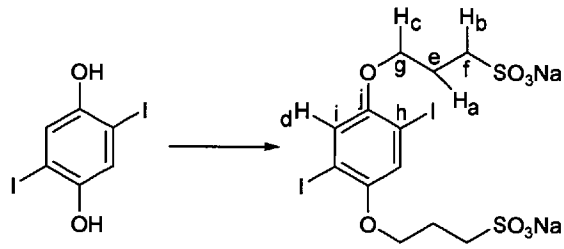

108 **115**

115 was prepared using a previously described procedure; characterisation data correspond to literature values.[7]

115: (1.34 g, 37%), a white powder; IR (Film) ν_{max}/cm^{-1} 629 (C-I str.), 849 (Ar CH def.), 1060 (C-O str.), 1205 (C-O str.), 1482 (CH def.), 1623 (S=O str.), 2868 (CH str.); δ_H (270 MHz, d_6-DMSO) 2.00 (4H, m, H_a), 2.60 (4H, m, H_b), 4.03 (4H, t, $^3J_{H\text{-}H}$ = 6.3 Hz, H_c), 7.29 (2H, s, H_d); δ_C (67.5 MHz, d_6-DMSO) 25.9 (C_e), 48.6 (C_f), 69.5 (C_g), 87.5 (C_h), 122.9 (C_i), 152.8 (C_j).

7.2.4 PPE **41**.[7]

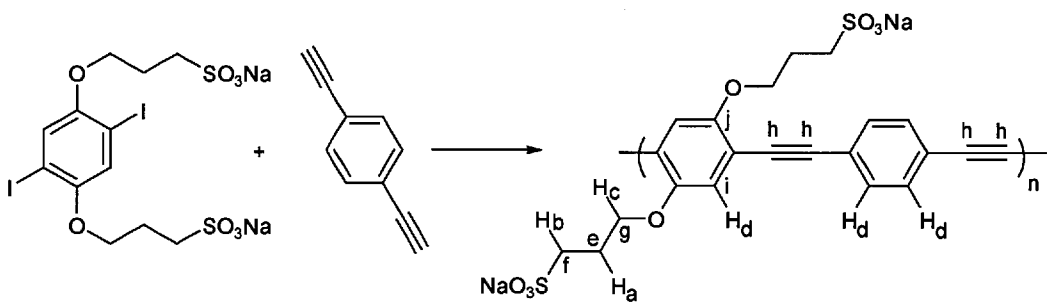

115 **106** **PPE 41**

2,5-Diiodo-1,4-bis(propyloxy sulphonate)benzene (**115**, 1.01 g, 1.55 mmol) and 1,4-diethynylbenzene (**106**, 0.201 g, 1.59 mmol) were dissolved in a mixture of H_2O (20 mL) and DMF (20 mL) at 60 °C in a Schlenk flask with a gentle flow of argon and with magnetic stirring. The resulting clear solution was deoxygenated by three cycles of vacuum-argon cycling. Another solution comprised of $Pd(PPh_3)_4$ (50 mg, 43 μmol) and CuI (10 mg, 53 μmol) in a mixture of diisopropylamine (10 mL) and DMF (10 mL) was likewise deoxygenated (three cycles of vacuum-argon cycling) and was subsequently added to the former solution by means of a cannula. The final

mixture was again deoxygenated by vacuum-argon cycling and was then warmed to 50 – 55 °C and stirred under a positive pressure of argon for 40 hours. The resulting solution was viscous, brown in colour and exhibited an intense blue fluorescence when illuminated with a near-UV lamp. The solution was cooled and then slowly added to 1 L of a MeOH/acetone/Et_2O mixture (10:40:50, v/v/v). The polymer precipitated as greenish fibres. It was redissolved in 200 mL of H_2O/MeOH (70:30, v/v) treated with 0.100 g of Na_2S, and then the solution was filtered through quantitative filter paper, followed by a 10 – 20 μm fritted glass filter, and finally through a 0.8 μm nylon membrane. The polymer was precipitated by addition to a 800 mL volume of MeOH/acetone/Et_2O (10:40:50, v/v/v). The polymer was dissolved in H_2O/MeOH and reprecipitated from THF three more times. Finally, the polymer was dissolved in 150 mL of H_2O, 0.050 g of NaCN was added, and the resulting solution was dialysed against distilled H_2O using a 6 – 8 kD MWCO cellulose membrane, over three days (six H_2O changes). The polymer was then precipitated from THF, filtered and dried under vacuum to give PPE **41** (0.682 g, 85%) as a light yellow powder; GPC (DMAc), PS standards): $M_n \approx 2500$; IR (Film) ν_{max}/cm^{-1} 723 (Ar CH def.), 1049 (CO str.), 1169 (CO str.), 1377 (CH def.), 1461 (CH def.), 1623 (S=O str.), 2859 (CH str.), 2940 (CH str.); δ_H (270 MHz, d_6-DMSO, 298 K) 2.04 – 2.07 (4H, m, H_a), 2.49 – 2.69 (4H, m, H_b), 3.87 – 4.30 (4H, m, H_c), 7.07 – 7.58 (6H, m, H_d); δ_C (100.6 MHz, d_6-DMSO, 298 K) 25.3 (C_e), 48.0 (C_f), 68.9 (C_g), 86.9 (C_h), 122.4 (C_i), 152.3 (C_j). Absorbance λ_{max} (in MeOH): 374 nm; emission λ_{max} (in MeOH): 435 nm.

7.2.5 Palladium tetrakis(triphenylphosphine), $[Pd(PPh_3)_4]$.[8]

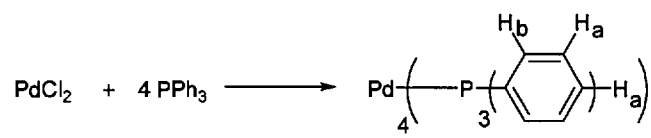

A mixture of palladium dichloride (0.500 g, 2.82 mmol), triphenylphosphine (3.84 g, 14.7 mmol) and 60 mL of freshly distilled DMSO was placed in a 250 mL 2-necked flask equipped with a magnetic stirrer bar and the system was then flushed with nitrogen with provision made for pressure relief through a paraffin oil bubbler. The resulting mixture was then heated with vigorous stirring until the solution became completely homogeneous (140 °C). The bath was then taken away and the solution rapidly stirred for another 15 minutes. At this point hydrazine hydrate (0.933 g, 18.6 mmol) was added dropwise over a period of 5 minutes. A vigorous reaction took place with the evolution of nitrogen. The dark red solution was then allowed to cool to room temperature unaided and then cannula filtered. The yellow solid was recrystallised from hot MeOH (40 mL), filtered and washed successively with cold MeOH (2 x 10 mL) and Et_2O (2 x 10 mL). The product was dried by blowing a slow stream of nitrogen over it for 14 hours, to afford pure $Pd(PPh_3)_4$

(2.58 g, 80%) as a bright yellow solid. The catalyst was then stored under nitrogen in the freezer and away from sources of light; δ_H (270 MHz, $CDCl_3$) 7.28 – 7.57 (36H, m, H_a), 7.62 – 7.85 (24H, m, H_b); δ_P (100.6 MHz, $CDCl_3$) 8.3, 24.0, 28.3, 29.8, 33.7.

7.2.6 Purification of Cu(I)I.[9]

Cuprous Iodide was purified by continuous extraction (14 hours) with tetrahydrofuran in a soxhlet apparatus. The purified material was stored away from light, in an argon atmosphere, and was light-grey in colour.

7.2.7 1,4-Bis-(3-bromopropoxy)-2,5-diiodobenzene (122).

Method 1 – adapted from Swager et al.[6]

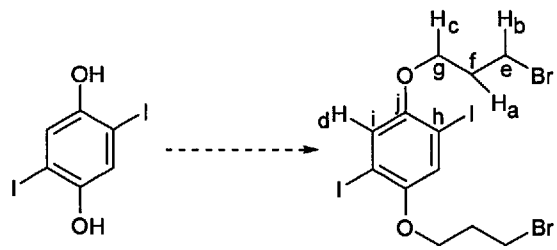

108 **122** *Impure*

A flask was charged with 1,3-dibromopropane (1.10 mL, 11.1 mmol), potassium carbonate (7.92 g, 55.8 mmol), and acetone (100 mL). Then, 2,5-diiodhydroquinone (**108**, 2.00 g, 5.53 mmol) was dissolved in acetone (30 mL) and drawn into a 50 mL syringe and the solution added dropwise over 96 hours to the solution held at 70 °C. The reaction was monitored by TLC and when it was deemed complete (96 hours) the turbid mixture was cooled to room temperature the solvent removed. The solids were partitioned between H_2O and $CHCl_3$. The organic layer was washed with 10% saturated aqueous KOH (30 mL), H_2O (30 mL) and saturated aqueous NaCl solution (30 mL). The organic layer was dried over Na_2SO_4, filtered and concentrated. The resulting golden oil was placed under vacuum, resulting in the oil solidifying and the solid was recrystallised from Et_2O to yield crude **122** (1.31 g, 40%) as a white powder; IR (Film) ν_{max}/cm^{-1} 761 (Ar CH def.), 1021 (CO str.), 1215 (CO str.), 1378 (CH def.), 1455 (CH def.), 2855 (CH str.), 2930 (CH str.); δ_H (270 MHz, $CDCl_3$) 2.32 (4H, q, $^3J_{H\text{-}H}$ = 6.0 Hz, H_a), 3.67 (4H, t, $^3J_{H\text{-}H}$ = 6.4 Hz, H_b), 4.07 (4H, t, $^3J_{H\text{-}H}$ = 4.7 Hz, H_c), 7.20 (2H, s, H_d); δ_C (100.6 MHz, $CDCl_3$) 30.1 (C_e), 32.3 (C_f), 67.6 (C_g), 86.4 (C_h), 123.0 (C_i), 152.7 (C_j); *m/z* (CI, NH_3) 604 (85%, $[M+H]^+$), 622 (65%, $[M+NH_4]^+$); HRMS (CI, NH_3) Found: $[M]^+$, 603.7428. $C_{12}H_{14}Br_2I_2O_2$ requires: $[M]^+$, 603.8553.

The material was not isolated cleanly. Possible structures and sources of impurities are discussed in Chapter Two, section 2.2.

7.2.8 1,4-Bis-(3-bromopropoxy)-2,5-diiodobenzene (**122**).

Method 2 – adapted from Whiteside et al.[10]

A solution of 2,5-diiodhydroquinone (**108**, 0.400 g, 1.11 mmol), 1,3-dibromopropane (0.34 mL, 3.3 mmol), K_2CO_3 (0.693 g, 5.01 mmol) and acetone (10 mL) were stirred at reflux for 24 hours during which time the reaction was deemed complete by TLC; R_f = 0.75 (*n*-pentane:EtOAc, 2:1, v/v). K_2CO_3 was removed by filtration through celite (1 cm depth, 4 cm diameter in a sinter funnel) and the solvent was removed on the rotary evaporator. The resulting brown solid was taken up in CH_2Cl_2 (50 mL) and washed with H_2O (3 x 30 mL), 3 M NaOH (3 x 30 mL), 3 M HCl (3 x 30 mL) and brine (3 x 30 mL) and dried over $MgSO_4$. The solvent was removed *in vacuo* to yield a brown solid that was recrystallised from EtOAc and *n*-hexane (1:1, v/v) to yield crude **122** (0.463 g, 69%) as white crystals. Spectral analysis was identical to previous (above; Method 1 – Swager *et al.*). Possible structures and sources of impurities are discussed in Chapter Two, section 2.2.

7.2.9 1,4-Bis-(3-(trimethylammonium)propoxy)-2,5-diiodobenzene (**123**).

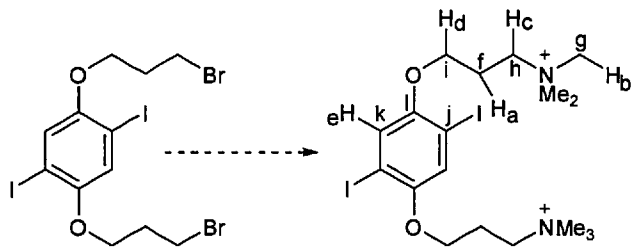

122
Impure

123
Impure

1,4-Bis-(3-bromopropoxy)-2,5-diiodobenzene, **122**, (2.00 g, 3.34 mmol) was suspended in 45% trimethylamine in H_2O (45 mL), EtOH (65 mL) and acetone (65 mL). The suspension was heated to 130 °C. At 95 °C the suspension clarified and refluxing commenced shortly afterwards. The reaction was heated for a total of 18 hours. The pale-yellow solution was then concentrated on the rotary evaporator to yield a solid, which was recrystallised from EtOH/Et_2O (1:1, v/v) to give crude **123** (1.91 g, 79%) as a fine white powder; IR (Film) ν_{max}/cm^{-1} 937 (Ar CH def.), 1058 (CO def.), 1210 (CN str.), 1377 (CH def.), 1462 (CH def.), 2851 (CH str.); δ_H (270 MHz, d_4-MeOD) 2.30 – 2.36 (4H, m, H_a), 3.22 (18H, s, H_b), 3.61 – 3.67 (4H, m, H_c), 4.08 – 4.13 (4H, m, H_d), 7.38 (2H, s, H_e); δ_C (100.6 MHz, d_4-MeOD) 24.5 (C_f), 53.9 (C_g), 65.8 (C_h), 68.2 (C_i), 87.3 (C_j), 124.4

(C_k), 154.3 (C_l); *m/z* (FAB, +ve) 642 (50%, $[M\text{-}Br^-]^+$); HRMS (FAB, +ve) Found: $[M\text{-}Br^-]^+$; 642.9725. $C_{18}H_{32}BrI_2N_2O_2$ requires: $[M\text{-}Br^-]$, 642.1713.

The molecule was not isolated cleanly. Unassigned signals: δ_H (270 MHz, d_4-MeOD) 4.40 – 4.50 (br m), 4.15 – 4.25 (m), 7.35 (s). See Chapter Two, section 2.2 for further details.

7.2.10 PPE **124**.

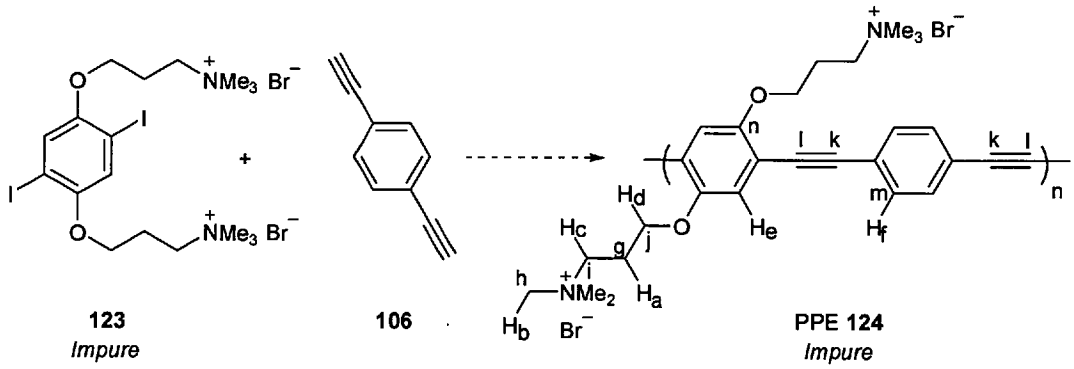

123 *Impure* **106** PPE **124** *Impure*

1,4-Bis-(3-(trimethylammonium)propoxy)-2,5-diiodobenzene (**123**, 1.25 g, 1.73 mmol) and 1,4-diethynylbenzene (**106**, 0.193 g, 1.52 mmol) were dissolved in a mixture of H_2O (20 mL) and DMF (20 mL) at 50 °C in a Schlenk flask with a gentle flow of argon and with magnetic stirring. The resulting clear solution was deoxygenated by three cycles of vacuum-argon cycling. Another solution comprised of $Pd(PPh_3)_4$ (52 mg, 45 μmol) and Cu(I)I (10 mg, 45 μmol) in a mixture of diisopropylamine (10 mL) and DMF (10 mL) was likewise deoxygenated (three cycles of vacuum-argon cycling) and was subsequently added to the former solution by means of a cannula. The final mixture was again deoxygenated by vacuum-argon cycling and was then warmed to 50 – 55 °C and stirred under a positive pressure of argon for 48 hours. The resulting solution was viscous, brown in colour and exhibited an intense blue fluorescence when illuminated with a near-UV lamp. The solution was cooled and then slowly added to 1 L of a MeOH/acetone/Et_2O mixture (10:40:50, v/v/v). The polymer precipitated as yellow fibres. It was redissolved in 200 mL of H_2O/MeOH (70:30, v/v) treated with 0.100 g of Na_2S, and then the solution was filtered through quantitative filter paper, followed by a 10 – 20 μm fritted glass filter, and finally through a 0.8 μm nylon membrane. The polymer was precipitated by addition to 800 mL of MeOH/acetone/Et_2O (10:40:50, v/v/v). The polymer was dissolved in H_2O/MeOH and reprecipitated from THF twice more. Finally, the polymer was dissolved in 150 mL of H_2O, 0.050 g of NaCN was added, and the resulting solution was dialysed against distilled H_2O using a 6 – 8 kD MWCO cellulose membrane, over two days (two H_2O changes). The polymer was then precipitated from acetone, filtered and dried in a vacuum oven to give crude PPE **124** (0.463 g, 45%) as a light yellow-tan solid; IR (Film) ν_{max}/cm^{-1} 722 (Ar CH def.), 1155 (CO str.), 1305 (CN str.), 1377 (CH def.), 1454 (CH def.), 2847

(CH str.); δ_H (270 MHz, d_4-MeOD, 298 K) 2.22 – 2.44 (4H, m, H_a), 3.14 – 3.23 (18H, m, H_b), 3.58 – 3.67 (4H, m, H_c), 4.16 – 4.24 (4H, m, H_d), 7.12 – 7.30 (2H, m, H_e), 7.40 – 7.62 (4H, m, H_f); δ_C (125.8 MHz, D_2O, 363 K) 26.6 (C_g), 56.8 (C_h), 67.9 (C_i), 70.6 (C_j), 91.1 (C_k), 98.8 (C_l), 135.1 (C_m), 156.5 (C_n). Due to the limited solubility of this polymer only a partial ^{13}C NMR has been obtained. Absorbance λ_{max} (in unbuffered H_2O): 400 nm; emission λ_{max} (in unbuffered H_2O): 468 nm.

The polymer was not isolated cleanly. Unassigned signals: δ_H (270 MHz, d_4-MeOD, 298K) 4.37 – 4.55 (br m). See Chapter Two, section 2.2 for further details.

7.2.11 1,4-Bis-(3-bromopropoxy)benzene (**132**).[10]

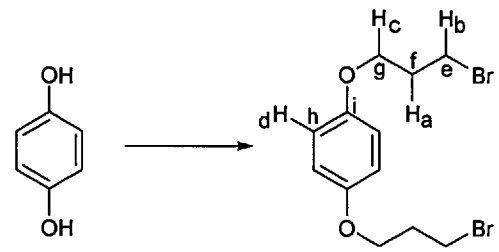

131 **132**

132 was prepared using a previously described procedure; characterisation data correspond to literature values.[10]

132: (6.73 g, 21%) as white crystals, m.p. 69 – 71 °C (Lit. 68 – 69 °C);[76] IR (Film) ν_{max}/cm^{-1} 821 (Ar CH def.), 1032 (CO def.), 1233 (CO str.), 1377 (CH def.), 1461 (CH def.), 2855 (CH str.), 2925 (CH str.); δ_H (270 MHz, $CDCl_3$) 2.28 (4H, q, $^3J_{H\text{-}H}$ = 6.1 Hz, H_a), 3.59 (4H, t, $^3J_{H\text{-}H}$ = 6.4 Hz, H_b), 4.04 (4H, t, $^3J_{H\text{-}H}$ = 5.8 Hz, H_c), 6.83 (4H, s, H_d); δ_C (100.6 MHz, $CDCl_3$) 30.1 (C_e), 32.5 (C_f), 66.1 (C_g), 116.6 (C_h), 153.1 (C_i); *m/z* (CI, NH_3) 370 (100%, $[M+NH_4]^+$), 352 (15%, $[M]^+$); HRMS (CI, NH_3) Found: $[M+NH_4]^+$, 370.9878. $C_{12}H_{20}Br_2NO_2$ requires: $[M+NH_4]^+$, 370.1002.

7.2.12 1,4-Bis-(3-bromopropoxy)-2,5-diiodobenzene (**122**).[6]

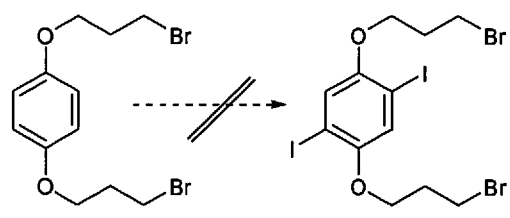

132 **122**

1,4-Bis-(3-bromopropoxy)benzene (**132**, 0.500 g, 1.42 mmol) was added to a mixture of glacial AcOH (10 mL), H_2SO_4 (12 M, 1.0 mL), H_2O (2.0 mL), KIO_3 (0.150 g, 0.710 mmol) and I_2 (0.379 g, 1.49 mmol). The mixture was slowly heated to reflux. After 6 hours the reaction was cooled to room temperature and H_2O (20 mL) was added to the cooled mixture (25 °C) and then the whole mixture was cooled in an ice/H_2O bath. A dark brown solid was isolated (25 mg), which was unidentified by ^1H NMR. It is believed that the starting material decomposed under the reaction conditions used – see section 2.2 (Chapter Two for further details).

7.2.13 1,4-Bis-(3-(trimethylammonium)propoxy)benzene (**134**).

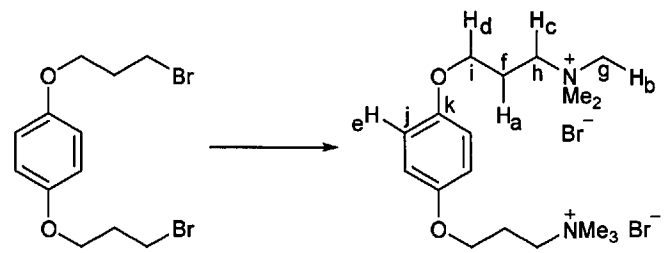

132 **134**

1,4-Bis-(3-bromopropoxy)benzene (**132**, 0.752 g, 2.14 mmol) was suspended in 45% trimethylamine in H_2O (10 mL), EtOH (10 mL) and acetone (15 mL). The suspension was heated to 130 °C. At 95 °C the suspension clarified and refluxing commenced shortly afterwards. The reaction was heated for a total of 18 hours. The solution was concentrated on the rotary evaporator to yield a solid, which was recrystallised from EtOH/Et_2O (1:1) to give **134** (0.764 g, 76%) as a white crystalline solid; IR (Film) ν_{max}/cm^{-1} 825 (Ar CH def.), 1060 (CO def.), 1226 (CN str.), 1378 (CH def.), 1466 (CH def.), 2852 (CH str.); δ_H (270 MHz, d_4-MeOD) 2.27 (4H, t, $^3J_{H\text{-}H}$ = 5.4 Hz, H_a), 3.20 (18H, s, H_b), 3.59 (4H, t, $^3J_{H\text{-}H}$ = 8.4 Hz, H_c), 4.06 (4H, t, $^3J_{H\text{-}H}$ = 5.7 Hz, H_d), 6.90 (4H, s, H_e); δ_C (100.6 MHz, d_4-MeOD) 24.5 (C_f), 53.8 (C_g), 65.6 (C_h), 66.3 (C_i), 116.7 (C_j), 154.5 (C_k); *m/z* (FAB, +ve) 389 (20%, $[M\text{-}Br^-]^+$); HRMS (FAB, +ve) Found: $[M\text{-}Br^-]^+$, 389.1816. $C_{18}H_{34}BrN_2O_2$ requires: $[M\text{-}Br^-]$, 389.1798.

7.2.14 1,4-Bis-(3-(trimethylammonium)propoxy)-2,5-diiodobenzene (**123**).

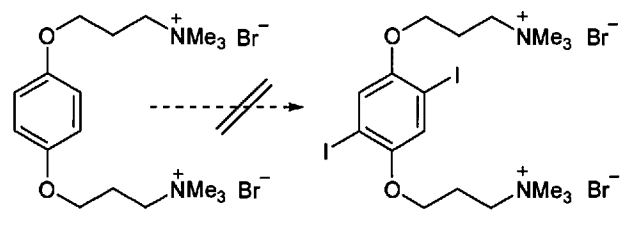

134 **123**

1,4-Bis-(3-(trimethylammonium)propoxy)benzene (**134**, 0.10 g, 0.21 mmol) was added to a mixture of glacial AcOH (10 mL), H_2SO_4 (12 M, 1.0 mL), H_2O (2.0 mL), KIO_3 (0.0228 g, 0.106 mmol) and I_2 (0.0565 g, 223 mmol). The mixture was slowly heated to reflux. After 6 hours the reaction was cooled to room temperature and H_2O (20 mL) was added to the cooled mixture (25 °C) and then the whole mixture was cooled in an ice/H_2O bath. A black solid was isolated (~ 11 mg), which was unidentified by ^1H NMR. It is believed that the starting material decomposed under the reaction conditions used – see section 2.2, Chapter Two for further details.

7.2.15 1,4-Bis-(3-iodopropoxy)-2,5-diiodobenzene (**133**).

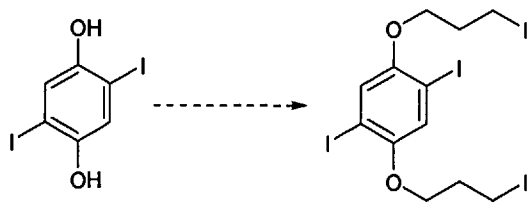

108 **133**
Impure

A solution of 2,5-diiodhydroquinone (**108**, 0.500 g, 1.38 mmol), 1,3-diiodopropane (0.48 mL, 4.1 mmol), K_2CO_3 (0.86 g, 6.2 mmol) and acetone (20 mL) were stirred at reflux for 24 hours during which time the reaction was deemed complete by TLC; R_f = 0.70 (100% CH_2Cl_2). K_2CO_3 was removed by filtration through celite (1 cm depth, 4 cm diameter in a sinter funnel) and the solvent was removed on the rotary evaporator. The resulting brown solid was taken up in CH_2Cl_2 (50 mL) and washed with H_2O (3 x 30 mL), 3 M NaOH (3 x 30 mL), 3 M HCl (3 x 30 mL) and brine (3 x 30 mL) and dried over $MgSO_4$. The solvent was removed *in vacuo* to yield a brown solid that was recrystallised from EtOAc and *n*-hexane (1:1, v/v) to yield crude **133** (0.611 g, 63%) as an off-white solid. ^1H NMR analysis indicated the presence of an impurity (δ_H (270 MHz, $CDCl_3$) 4.1 ppm), that could not be separated; this is discussed in Chapter Two, section 2.2.

7.2.16 Dibromomethyltriphenylphosphonium bromide (**136**).[11]

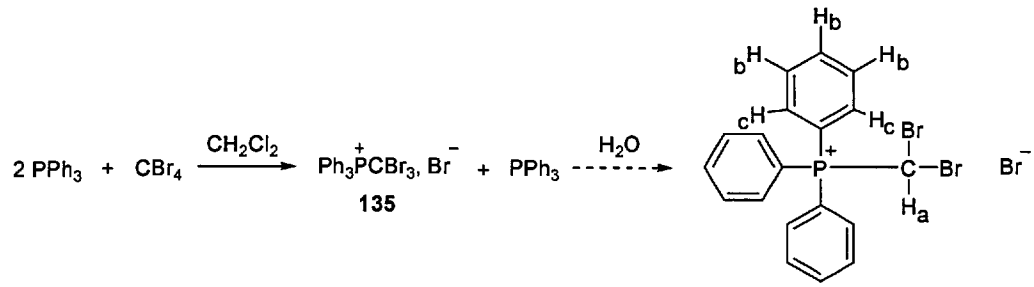

136
Impure

Carbon tetrabromide [N.B. CBr_4 must be a colourless solid; used as purchased from Sigma, purity = 99%] (8.6 g, 26 mmol) was added to a solution of triphenylphosphine (6.8 g, 26 mmol) in MeCN (35 mL). The solution was stirred for 15 minutes at room temperature. H_2O (5 mL) was added to this resulting red-coloured mixture. After 15 minutes of vigorous stirring, the aqueous layer was separated with CH_2Cl_2. The organic layer was dried and evaporated at reduced pressure to yield a syrup. The salt was precipitated by addition of MeCN (5 mL). The yellow powder obtained was filtered, dried under vacuum and recrystallised from dry MeCN. The solution was filtered hot to give crude dibromomethyltriphenylphosphonium bromide (**136**, 8.12 g, 61%), as a yellow solid; δ_H (270 MHz, $CDCl_3$) 5.28 (1H, s, H_a), 7.67 – 7.84 (9H, m, H_b), 8.11 – 8.19 (6H, m, H_c). *The material was not isolated cleanly.* Unassigned signals: δ_H (270 MHz, $CDCl_3$) 10.29 (d, $^3J_{H\text{-}H}$ = 2.5 Hz). See Chapter Two, section 2.2 for further details.

7.2.17 1,4-Diethynylbenzene (**106**).[12]

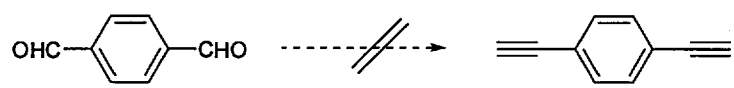

111 **106**

Under an argon atmosphere, **136** (2.06 g, 4.00 mmol) and *t*-BuOK (1.0 M in THF; 3.80 mL, 3.80 mmol) were dissolved in THF (15 mL). The solution was stirred for a few minutes, and the aldehyde **111** (0.268 g, 2 mmol) was then added. After 10 minutes, *t*-BuOK (1.0 M in THF; 10 mL, 10 mmol) was added at room temperature. The solution was quenched with saturated brine (30 mL) and extracted twice with Et_2O (30 mL). The organic layers were dried over Na_2SO_4 and concentrated. *After the work-up, there was no evidence for the formation of the alkyne, as confirmed by the absence of resonances in the expected region (~ 3.1 ppm).*

7.2.18 1,4-Bis-(1,1,1-(trichloromethyl)benzene methanol 4-methylbenzenesulphonate) (**137**).

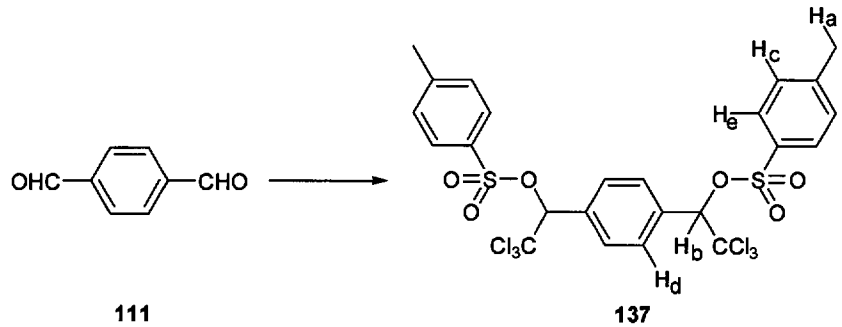

111 **137**

To a mixture of terthaldehyde (**111**, 2.00 g, 14.9 mmol) and $CHCl_3$ (4.77 mL, 59.6 mmol) was added dropwise under nitrogen, 1 equivalent of DBU (4.46 mL, 29.8 mmol). The reaction was stirred for 3 hours and cooled to 0 °C and a solution of *p*-toluenesulphonyl chloride (6.82 g, 35.8 mmol) and triethylamine (2.2 mL, 30 mmol) in $CHCl_3$ (30 mL) was added dropwise. After 12 hours the reaction was diluted with Et_2O (50 mL) and washed with saturated NH_4Cl (3 x 30 mL). The organic phase was dried over Na_2SO_4, filtered and evaporated to give a light-brown solid that was purified by recrystallisation from H_2O twice to give **137** (4.50 g, 45%) as a tan-brown solid; full characterisation was not obtained as this route was not used to make bisalkyne **106** – see Chapter Two, section 2.2 for details. δ_H (270 MHz, $CDCl_3$) 2.33 (6H, s, H_a), 6.02 – 6.04 (2H, d, $^3J_{H\text{-}H}$ = 6.2 Hz, H_b), 7.18 – 7.22 (4H, m, H_c), 7.40 – 7.43 (4H, d, $^3J_{H\text{-}H}$ = 6.9 Hz, H_d), 7.54 – 7.61 (4H, dd, $^3J_{H\text{-}H}$ = 10.1, 8.4 Hz, H_e).

7.2.19 1,4-Diethynylbenzene (**106**).[13]

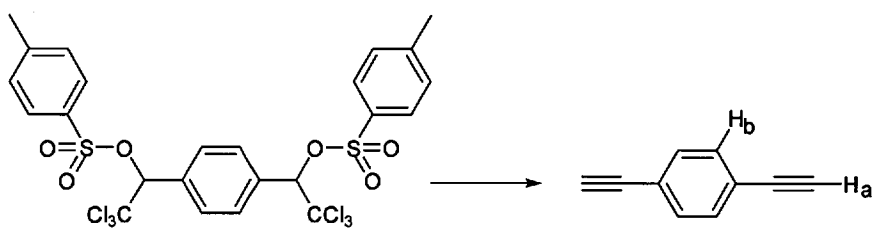

137 **106**

To a stirred solution of **137** (1.50 g, 2.20 mmol) in THF (25 mL) at -10 °C was added methyllithium (6.20 mL of 1.6 M solution in Et_2O, 9.91 mmol) dropwise. The solution was warmed to 0 °C over 1 hour. The reaction was quenched with saturated ammonium chloride and diluted with *n*-hexane, and the layers were separated. The aqueous phase was extracted with *n*-hexane (3 x 50 mL). The combined organic extracts were washed with brine and dried over anhydrous $MgSO_4$ and filtered. Evaporation of the resulting orange solution afforded an orange

solid which was purified by chromatography (R_f = 0.7, *n*-pentane:EtOAc, 1:1, v/v) to give **106** (40.4 mg, 4.9%) as a pale yellow crystalline solid; full characterisation was not obtained as this route was not used to make bisalkyne **106** – see Chapter Two, section 2.2 for details. δ_H (270 MHz, $CDCl_3$) 3.16 (2H, s, H_a), 7.43 (4H, s, H_b).

7.2.20 1,4-Bis-trimethylsilanylethynyl-benzene (**138**).[14]

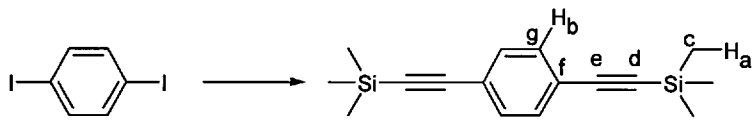

109 **138**

1,4-Diiodobenzene (**109**, 3.01 g, 9.09 mmol) was coupled with TMSA (2.83 mL, 20.0 mmol) following the usual Pd/Cu protocol using $Pd(PPh_3)_4$ (0.114 g, 0.090 mmol), copper(I) iodide (40 mg, 0.19 mmol), THF (25 mL) and diisopropylamine (5.10 mL, 36.4 mmol). The reaction was stirred at room temperature for 1.5 hours. Column chromatography (silica gel, using *n*-hexane as eluant) afforded the desired product, which was purified by recrystallisation from MeOH twice to give **138** (1.8 g, 73%) as colourless needle-shaped crystals; m.p. 120 – 121 °C (Lit. 122 – 125 °C);[14] δ_H (270 MHz, $CDCl_3$) 0.25 (18H, s, H_a), 7.38 (4H, s, H_b); δ_C (100.6 MHz, $CDCl_3$) 0.28 (C_c), 96.4 (C_d), 104.7 (C_e), 123.3 (C_f), 131.9 (C_g); *m/z* (CI, NH_3) 271 (100%, $[M+H]^+$); HRMS (CI, NH_3) Found: $[M+H]^+$, 271.1341. $C_{16}H_{23}Si_2$ requires: $[M+H]^+$, 271.5248.

7.2.21 1,4-Diethynylbenzene (**106**).[14]

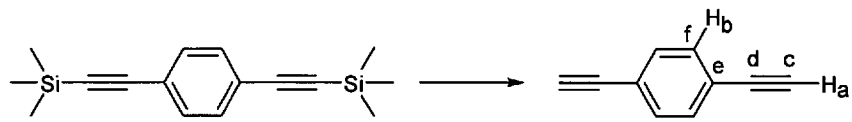

138 **106**

The TMS-protected alkyne (**138**, 3.15 g, 11.6 mmol) and 6 equivalents of K_2CO_3 (9.66 g, 69.9 mmol) were dissolved in MeOH (90 mL) and CH_2Cl_2 (90 mL). The reaction vessel was sealed with a rubber septum and then filled with nitrogen. The reaction was allowed to go to completion (3.5 hours, by TLC) at which time it was quenched with a saturated solution of NaCl (50 mL). The layers were separated and the aqueous layer was extracted with CH_2Cl_2 (3 x 40 mL). The combined organic layers were dried over $MgSO_4$ and the solution was then filtered and concentrated on the rotary evaporator, to give **106** (1.41 g, 96%) which was purified by recrystallisation using MeOH to yield colourless needle-shaped crystals; R_f = 0.79 (*n*-

hexane:EtOAc, 3:1, v/v); δ_H (270 MHz, $CDCl_3$) 3.16 (2H, s, H_a), 7.43 (4H, s, H_b); δ_C (100.6 MHz, $CDCl_3$) 78.0 (C_c), 82.0 (C_d), 121.6 (C_e), 131.0 (C_f); *m/z* (CI, NH_3) 126 (100%, $[M]^+$), 144 (65%, $[M+NH_4]^+$; HRMS (CI, NH_3) Found: $[M+NH_4]^+$, 144.0816. $C_{10}H_{10}N$ requires: $[M+NH_4]^+$, 144.1926. Anal. Calcd. for $C_{10}H_6$: C, 95.21; H, 4.79. Found: C, 95.29; H, 4.68.

7.2.22 PPE **143**.

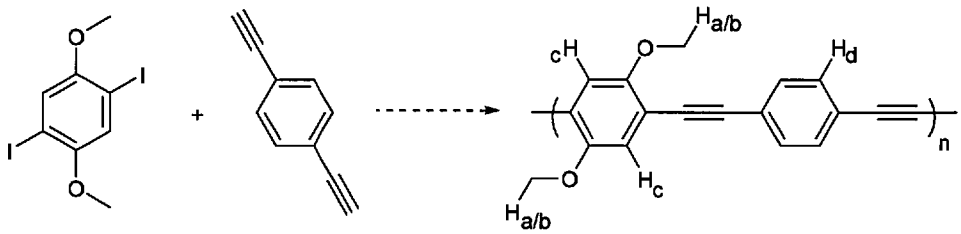

114 **106** PPE **143**

A degassed solution of tetrakis-(triphenylphosphine)palladium(0), $Pd(PPh_3)_4$, (70 mg, 0.060 mmol) and copper(I) iodide (11 mg, 0.060 mmol) in a mixture of DMF/diisopropylamine (20 mL, 1:1, v/v) was added, *via* cannula, to a degassed solution of **114** (0.750 g, 1.92 mmol) and 1,4-diethynylbenzene (**106**, 0.266 g, 2.11 mmol) in DMF (20 mL) contained in a Schlenk flask under argon. The resulting deep yellow (with blue fluorescence) solution was stirred at 50 °C for 24 hours. The viscous solution was poured into Et_2O (500 mL), which induced the polymer to precipitate. The light yellow polymer fibres formed were isolated by filtration and subsequently redissolved in THF (~ 20 mL) and precipitated again through addition of Et_2O (500 mL). This reprecipitation procedure was repeated twice more, yielding crude PPE **143** (1.09 g) as a light yellow powder. δ_H (400 MHz, $CDCl_3$) 3.80 (~ 3H, s, H_a), 3.81 (~ 3H, s, H_b), 6.87 – 6.96 (~ 2H, m, H_c), 7.36 – 7.65 (~ 4H, m, H_d).

The polymer was not isolated cleanly. Unassigned signals: δ_H (400 MHz, $CDCl_3$) 3.51 (sep), 3.85 (s), 7.95 (s), 8.28 (br s). See Chapter Two, section 2.3.1 for further details.

7.2.23 PPE **144**.

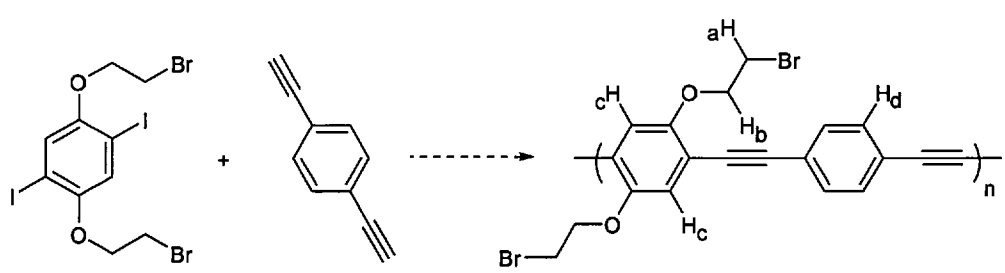

140 **106** PPE **144**

A degassed solution of tetrakis-(triphenylphosphine)palladium(0), $Pd(PPh_3)_4$, (70 mg, 0.060 mmol) and copper(I) iodide (11 mg, 0.060 mmol) in a mixture of DMF/diisopropylamine (20 mL, 1:1, v/v) was added, *via* cannula, to a degassed solution of **140** (1.15 g, 2.00 mmol) and 1,4-diethynylbenzene (**106**, 0.250 g, 2.00 mmol) in DMF (20 mL) contained in a Schlenk flask under argon. The resulting deep yellow (with blue fluorescence) solution was stirred at 50 °C for 24 hours. The viscous solution was poured into MeOH (500 mL), which induced the polymer to precipitate. The light yellow polymer fibres formed were isolated by filtration and subsequently redissolved in acetone (10 mL) and precipitated again by addition of MeOH (500 mL). This reprecipitation procedure was repeated twice more, to yield crude PPE **144** (0.607 g) as a light yellow powder. δ_H (270 MHz, $CDCl_3$) 3.65 – 3.73 (~ 4H, m, H_a), 4.23 – 4.39 (~ 4H, m, H_b), 6.91 – 7.06 (~ 2H, m, H_c), 7.29 – 7.61 (~ 4H, m, H_d).

The polymer was not isolated cleanly. Unassigned signals: δ_H (270 MHz, $CDCl_3$) 4.23 – 4.39 (m). See Chapter Two, section 2.3.1 for further details.

7.2.24 1,4-Didecyloxybenzene (141).[15,16]

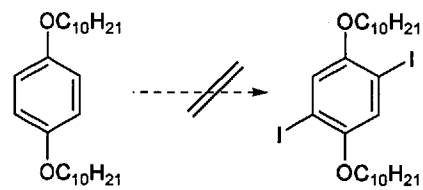

145 **141**

A mixture of **145** (1.00 g, 2.56 mmol), [bis(trifluoroacetoxy)iodo]benzene (**148**, 1.24 g, 2.88 mmol), and I_2 (0.681 g, 2.68 mmol) in CH_2Cl_2 (50 mL) was stirred at room temperature for 4 hours at which point the reaction mixture was then diluted with *n*-pentane (60 mL) and cooled in an ice/H_2O bath. As no precipitate formed, the solvents were removed *in vacuo*, to reveal a dark red/black residue. Suitable solvents for chromatography could not be identified – the following were tried; Et_2O, *n*-hexane, *n*-pentane, acetone, CH_2Cl_2. ^1H NMR analysis of the crude material was not consistent with the expected structure (discussed further in Chapter Two, section 2.3.2). TLC (*n*-hexane:Et_2O, 1:1, v/v) confirmed the presence of the starting material with at least two other unidentified products (R_f = 0.78 (starting material), 0.70, 0.65).

7.2.25 1,4-Bis(*n*-hexadecyloxy)benzene (**146**).[15,16]

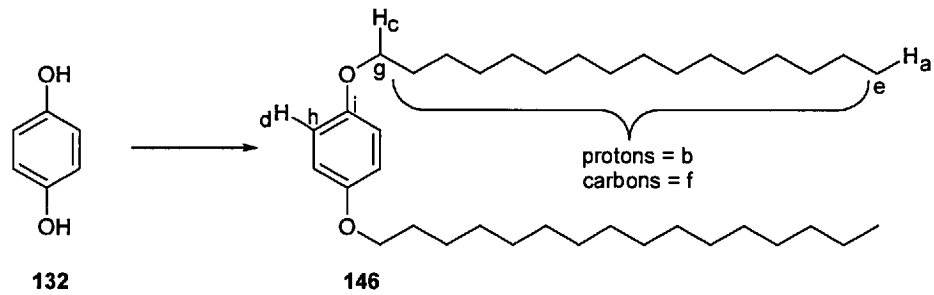

132 **146**

146 was prepared using a previously described procedure; characterisation data correspond to literature values.[15,16]

146: (24.0 g, 66%), a white solid, m.p. 87 – 88 °C (Lit. 86 – 87 °C);[16] IR (Film) ν_{max}/cm^{-1} 721 (Ar CH def.), 1293 (CO str.), 1446, 1377 (CH def.), 2950, 2842 (CH str.); δ_H (400 MHz, $CDCl_3$) 0.90 (6H, t, $^3J_{H\text{-}H}$ = 7.0 Hz, H_a), 1.30 (48H, m, H_b), 1.50 (4H, m, H_b), 1.75 (4H, q, $^3J_{H\text{-}H}$ = 8.0 Hz, H_b), 3.90 (4H, t, $^3J_{H\text{-}H}$ = 6.6 Hz, H_c), 6.80 (4H, s, H_d); δ_C (100.6 MHz, $CDCl_3$) 14.1 (C_e), 22.7, 26.0, 29.4, 29.6, 29.7, 31.9 (C_f), 70.0 (C_g), 115.4 (C_h), 153.2 (C_i); *m/z* (CI, NH_3) 558 (75%, $[M]^+$), 576 (100%, $[M+NH_4]^+$); HRMS (CI, NH_3) Found: $[M+NH_4]^+$, 576.5724, $C_{38}H_{74}NO_2$ requires: $[M+NH_4]^+$, 576.9991; Anal. Calcd. for $C_{38}H_{70}O_2$: C, 81.65; H, 12.62. Found: C, 81.54; H, 12.74.

7.2.26 2,5-Diiodo-1,4-bis(*n*-hexadecyloxy)benzene (**142**).[15]

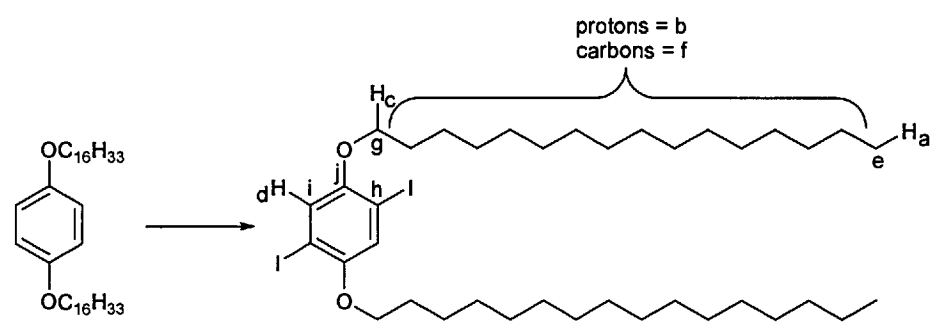

146 **142**

A mixture of 1,4-bis(*n*-hexadecyloxy)benzene (**146**, 2.50 g, 4.48 mmol), [bis(trifluoroacetoxy)iodo]benzene (**147**, 2.31 g, 5.37 mmol) and I_2 (1.25 g, 4.92 mmol) in CH_2Cl_2 (100 mL) was stirred at room temperature for 24 hours. The reaction mixture was then diluted with MeOH (60 mL) and cooled in an ice/H_2O bath, which promoted the crystallisation of the product. Light pink crystals of the product were obtained after vacuum filtration. The product was washed with cold MeOH (40 mL) which furnished pure 2,5-diiodo-1,4-bis(*n*-hexadecyloxy)benzene (**142**,

1.61 g, 44%) as a light pink solid, m.p. 79 – 81 °C (Lit. 76 – 77 °C);[15] IR (Film) ν_{max}/cm^{-1} 719 (Ar CH def.), 1216 (CO str.), 1377, 1461 (CH def.), 2855, 2927 (CH str.); δ_H (400 MHz, $CDCl_3$) 0.88 (6H, t, $^3J_{H\text{-}H}$ = 6.8 Hz, H_a), 1.20 – 1.40 (44H, m, H_b), 1.47 – 1.54 (8H, m, H_b), 1.77 – 1.83 (4H, m, H_b), 3.92 (4H, t, $^3J_{H\text{-}H}$ = 6.4 Hz, H_c), 7.17 (2H, s, H_d); δ_C (100.6 MHz, $CDCl_3$) 14.1 (C_e), 22.7, 26.0, 29.2, 29.3, 29.4, 29.6, 29.7, 30.9, 31.9 (C_f), 70.4 (C_g), 86.3 (C_h), 122.8 (C_i), 152.8 (C_j); *m/z* (CI, NH_3) 684 (28%, $[M\text{-}I]^+$), 810 (55%, $[M]^+$); HRMS (CI, NH_3) Found: $[M]^+$, 810.3303, $C_{38}H_{68}I_2O_2$ requires: $[M]^+$, 810.3309; Anal. Calcd. for $C_{38}H_{68}I_2O_2$: C, 56.29; H, 8.45. Found: C, 56.38; H, 8.52.

7.2.27 PPE **150**.

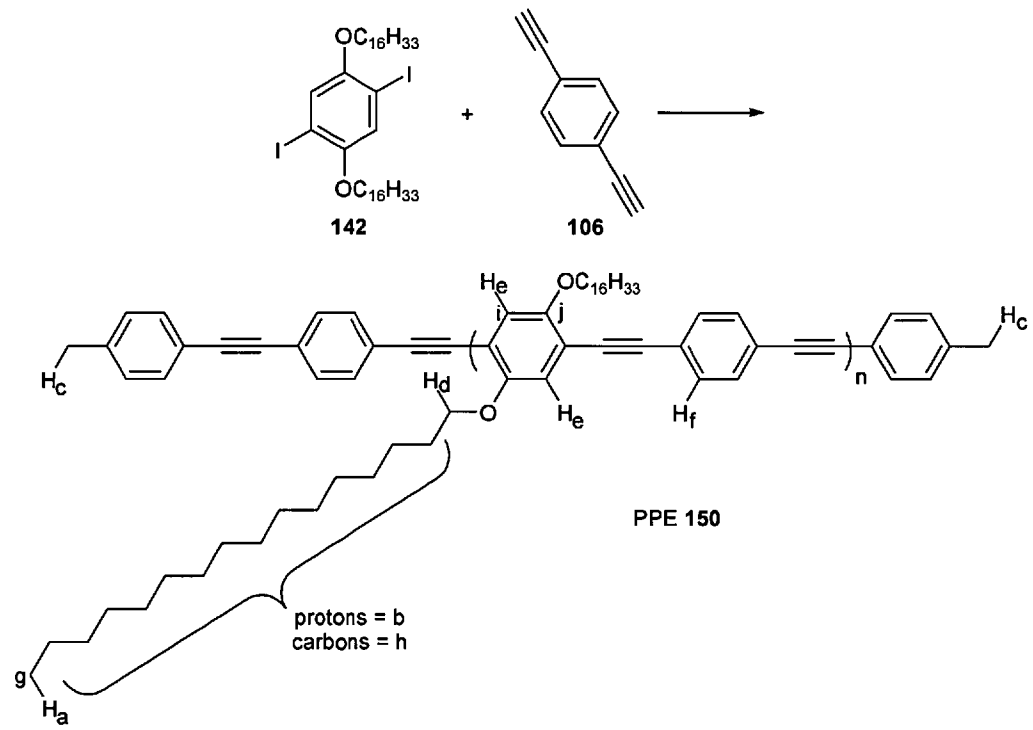

A Schlenk flask was oven-dried and then cooled to room temperature. The diiodo monomer 2,5-diiodo-1,4-bis(*n*-hexadecyloxy)benzene (**142**, 0.219 g, 0.271 mmol), 1,4-diethynylbenzene (**106**, 36 mg, 0.29 mmol), 4-iodotoluene (**149**, 12 mg, 0.060 mmol), tetrakistripehnylphosphine palladium (0) ($Pd(PPh_3)_4$, 25 mg, 0.022 mmol) and Cu(I)I (25 mg, 0.13 mmol) were added to the flask followed by distilled and degassed toluene (6 mL) and diisopropylamine (6 mL). The flask was closed under an argon atmosphere and the resulting mixture stirred at 55 °C for 70 hours. The reaction solution was then allowed to cool to room temperature and then poured cool MeOH (400 mL) which induced the precipitation of polymer PPE **150** (re-precipitation was repeated twice; a representative yield is ~ 90%; a specific yield could not be determined due to storage conditions – see Chapter Two, section 2.3.2, for details) as a light yellow solid which was stored as a solution in

toluene; note that the polymer cannot be redissolved after it has been recovered as a dry solid film by evaporation from a solution of a good solvent (e.g., $CHCl_3$, CH_2Cl_2 or toluene). Thus, the material was stored as a stock solution in MeOH that was kept in the dark. To obtain NMR spectra in a deuterated solvent it was necessary to recover the polymer from the non-deuterated solvent as follows; a methanolic solution of the polymer was isolated by centrifugation and decanting. The resulting precipitate was then redissolved in the deuterated solvent for NMR analysis. Nevertheless, even using this procedure, it was not possible to obtain samples that were entirely free of non-deuterated solvent, and consequently some of the resonances in the NMR spectrum are partially obscured by resonances arising from the residual solvent (toluene signals were visible, at < 5% between 7.0 – 7.5 ppm). The partially-dried polymer samples were bright yellow solids; M_n (^{1}H NMR) = 20.8 kDa (30 PE repeat units; see Chapter Two, section 2.3.2, for details); IR (Film) ν_{max} (CaF_2 pellet)/cm^{-1} 1215 (CO str.), 1377, 1462 (CH def.), 2853, 2922 (CH str.); δ_H (400 MHz, $CDCl_3$) 0.87 (6H, m, H_a), 1.25 – 1.38 (44H, m, H_b), 1.54 (8H, br m, H_b), 1.86 (4H, br m, H_b), 2.38 (6H (end group), br s, H_c), 4.04 (4H, br m, H_d), 7.01 (2H, br s, H_e), 7.50 (4H, br s, H_f); δ_C (100.6 MHz, $CDCl_3$) 14.1 (C_g), 22.7, 26.1, 29.4, 29.7, 31.9 (C_h), 131.5 (C_i), 153.7 (C_j). Absorbance λ_{max} (in THF, 0 wt.% Triton): 418 nm; emission λ_{max} (in THF, 0 wt.% Triton): 445 nm.

7.2.28 1,4-Bis(2-bromoethoxy)benzene (**152**).[17]

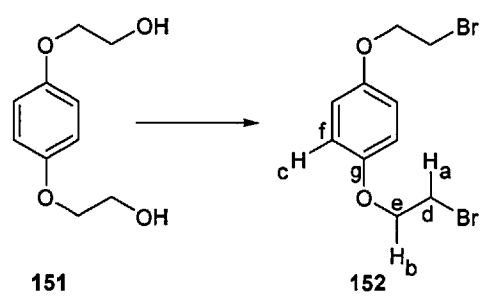

151 **152**

152 was prepared using a previously described procedure; characterisation data correspond to literature values.[17]

152: (14.7 g, 89%) as white needle-shaped crystals; R_f = 0.54 (*n*-hexane:EtOAc, 5:1, v/v); m.p. 113 – 114 °C (Lit. 112 – 114 °C);[17] IR (Film) ν_{max}/cm^{-1} 730 (Ar CH def.), 1231 (CO str.), 1461, 1377 (CH def.), 2924, 2854 (CH str.); δ_H (400 MHz, $CDCl_3$) 3.54 (4H, t, $^3J_{H\text{-}H}$ = 6.3 Hz, H_a), 4.18 (4H, t, $^3J_{H\text{-}H}$ = 6.3 Hz, H_b), 6.80 (2H, s, H_c); δ_C (100.6 MHz, $CDCl_3$) 29.3 (C_d), 68.8 (C_e), 116.1 (C_f), 152.9 (C_g); *m/z* (CI, NH_3) 322 (51%, $[M+H\ (^{79}Br_2)]^+$), 324 (100%, $[M+H]^+$, (^{79}Br, ^{81}Br)), 326 (47%, $[M+H\ (^{81}Br_2)]^+$); HRMS (CI, NH_3) Found: $[M(^{81}Br_2)]^+$, 325.9163. $C_{10}H_{10}{}^{81}Br_2O_2$ requires: $[M(^{81}Br_2)]^+$, 326.2036. Found: $[M(^{81}Br^{79}Br)]^+$, 323.9184. $C_{10}H_{10}{}^{81}Br^{79}BrO_2$ requires:

$[M(^{81}Br^{79}Br)]^+$, 324.2036. Found: $[M(^{79}Br_2)]^+$, 321.9204. $C_{10}H_{10}{}^{79}Br_2O_2$ requires: $[M(^{79}Br_2)]^+$, 322.2036.

7.2.29 2,5-Diiodo-1,4-bis(2-bromoethoxy)benzene (**140**).[17]

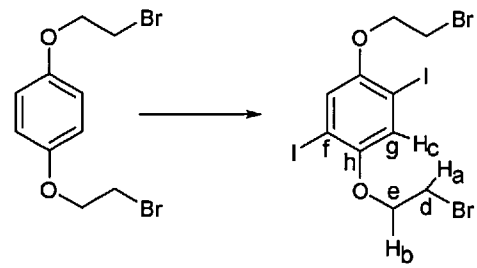

152 **140**

140 was prepared using a previously described procedure; characterisation data correspond to literature values.[17]

140: (10.36 g, 84%) as white needle-shaped crystals; R_f = 0.63 (*n*-hexane:EtOAc, 8:1, v/v); m. p. 140 – 143 °C (Lit. 140 – 142 °C);[17] IR (Film) ν_{max}/cm^{-1} 722 (Ar CH def.), 1218 (CO str.), 1461, 1377 (CH def.), 2952, 2859 (CH str.); δ_H (400 MHz, $CDCl_3$) 3.59 (4H, t, $^3J_{H\text{-}H}$ = 6.4 Hz, H_a), 4.20 (4H, t, $^3J_{H\text{-}H}$ = 6.3 Hz, H_b), 7.15 (2H, s, H_c); δ_C (100.6 MHz, $CDCl_3$) 28.5 (C_d), 70.4 (C_e), 86.7 (C_f), 124.0 (C_g), 153.8 (C_h); *m/z* (CI, NH_3) 574 (51%, $[M+H(^{79}Br_2)]^+$), 576 (100%, $[M+H]^+$, (^{79}Br, ^{81}Br) 100%), 578 (50%, $[M+H(^{81}Br_2)]^+$); HRMS (CI, NH_3) Found: $[M(^{81}Br_2)]^+$, 577.7096. $C_{10}H_{10}{}^{81}Br_2I_2O_2$ requires: $[M(^{81}Br_2)]^+$, 577.9968. Found: $[M(^{81}Br^{79}Br)]^+$, 575.7117. $C_{10}H_{10}{}^{81}Br^{79}BrI_2O_2$ requires: $[M(^{81}Br^{79}Br)]^+$, 575.9968. Found: $[M(^{79}Br_2)]^+$, 573.7137. $C_{10}H_{10}{}^{79}Br_2I_2O_2$ requires: $[M(^{79}Br_2)]^+$, 573.9968.

7.2.30 1,4-Bis-(3-(trimethylammonium)ethoxy)benzene (**153**).

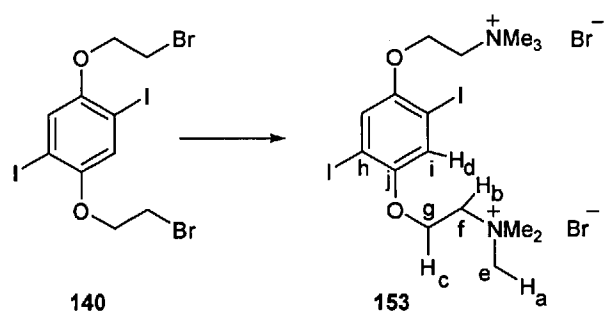

140 **153**

2,5-Diiodo-1,4-bis(2-bromoethoxy)benzene (**140**, 5.33 g, 7.66 mmol) was suspended in 45% trimethylamine in H_2O (50 mL), EtOH (40 mL) and acetone (40 mL). The suspension was heated

to 130 °C at which point the suspension clarified giving a pale yellow homogeneous solution which was refluxed for a total of 18 hours. The solution was concentrated on the rotary evaporator to yield a solid, which was recrystallised from EtOH/Et_2O (1:1, v/v) to give **153** (5.54 g, 64%) as a white crystalline solid; R_f = 0.16 (100% EtOH, on neutral Alumina plates); m.p. 289 – 291 °C; IR (Film) ν_{max}/cm^{-1} 722 (Ar CH def.), 1198 (CO str.), 1305 (CN str.), 1461, 1377 (CH def.), 2922, 2853 (CH str.); δ_H (400 MHz, d_6-DMSO) 3.24 (18H, s, H_a), 3.84 (4H, m, H_b), 4.49 (4H, m, H_c), 7.50 (2H, s, H_d); δ_C (100.6 MHz, d_6-DMSO) 53.3 (C_e), 63.3 (C_f), 64.0, (C_g), 86.3 (C_h), 122.5 (C_i), 151.9 (C_j); *m/z* (FAB, +ve) 613 (45%, $[M - {}^{81}Br^-]^+$), 615 (43%, $[M - {}^{79}Br^-]^+$); HRMS (FAB, +ve) Found: $[M - H - {}^{79}Br^-]^+$, 614.9403. $C_{16}H_{33}{}^{81}BrI_2N_2O_2$ requires: $[M - H - {}^{79}Br^-]^+$, 614.0944; Found: $[M - H - {}^{81}Br^-]^+$, 612.9424. $C_{16}H_{33}{}^{79}BrI_2N_2O_2$ requires: $[M - H - {}^{81}Br^-]^+$, 612.0964; Anal. Calcd. for $C_{16}H_{28}Br_2I_2N_2O_2$: C, 27.69; H, 4.07; N, 4.04. Found: C, 27.74; H, 3.98; N, 4.03.

7.2.31 2,5-Bis-(phenylethynyl)-1,4-bis(2-trimethylammonium ethoxy)benzene, bromide salt (PE **154**).

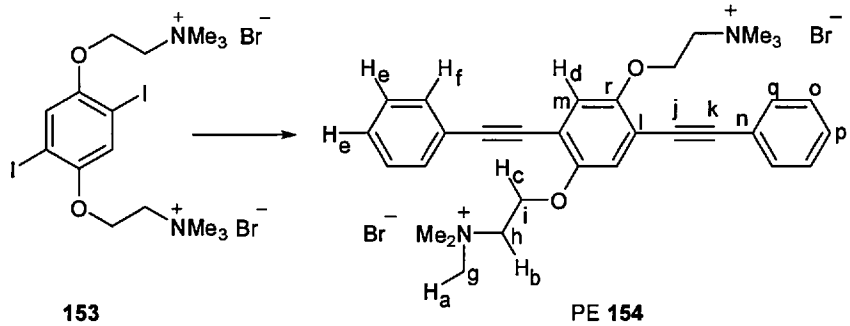

153 PE **154**

A mixture of 1,4-bis-(3-(trimethylammonium)ethoxy)benzene (**153**, 0.700 g, 1.00 mmol), phenylacetylene (0.360 mL, 3.32 mmol), tetrakis-(triphenylphosphine) palladium(0), $Pd(PPh_3)_4$, (104 mg, 90.0 μmol), copper (I) iodide (17 mg, 90 μmol) and diisopropylamine (5 mL) in a MeOH/H_2O mixture (40 mL, 4:1, v/v), was refluxed for 24 hours under argon with stirring. After this time, the yellow-green reaction mixture was then filtered through a short pad of celite (1 cm depth, 4 cm diameter in a sinter funnel), the solvents removed under reduced pressure, and the remaining solid was crystallised from MeOH, to furnish PE **154** (0.753 g, 75%) as a white crystalline solid; R_f = 0.36 (100% EtOH, on neutral Alumina plates); m.p. 303 – 305 °C; IR (Film) ν_{max}/cm^{-1} 722 (Ar CH def.), 1212 (CO str.), 1461, 1377 (CH def.), 1594 (C=N str.), 2959, 2860 (CH str.); δ_H (400 MHz, d_6-DMSO) 3.25 (18H, br s, H_a), 3.86-3.88 (4H, m, H_b), 4.59 (4H, m, H_c), 7.38 (2H, s, H_d), 7.46-7.47 (6H, m, H_e), 7.53-7.55 (4H, m, H_f); δ_C (100.6 MHz, d_6-DMSO) 53.2 (C_g), 62.8 (C_h), 63.9 (C_i), 85.5 (C_j), 95.0 (C_k), 112.8 (C_l), 116.7 (C_m), 121.9 (C_n), 128.8 (C_o), 128.9 (C_p), 131.1 (C_q), 152.1 (C_r); *m/z* (FAB, +ve) 467 (70%, $[M-Br_2-Me]^+$); Anal. Calcd. for

$C_{32}H_{38}Br_2N_2O_2 \cdot 6H_2O$: C, 51.21; H, 6.71; N, 3.73. Found: C, 51.21; H, 5.65; N, 3.74. Absorbance λ_{max} (in unbuffered H_2O): 351 nm; emission λ_{max} (in unbuffered H_2O): 391 nm.

7.2.32 PPE **155**.

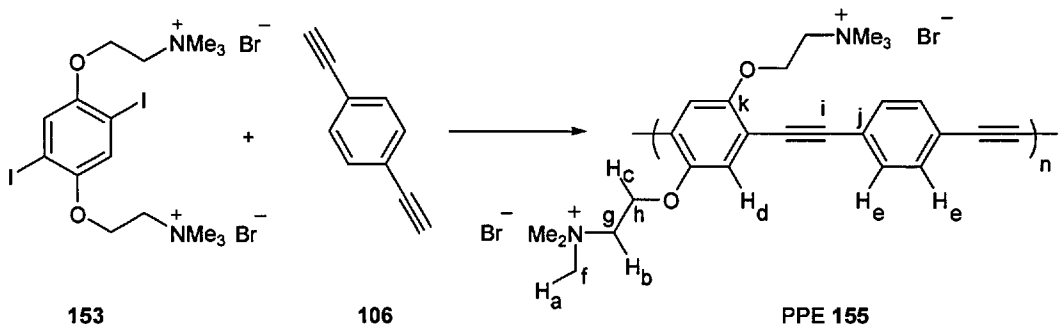

153 **106** **PPE 155**

1,4-Bis-(3-(trimethylammonium)ethoxy)benzene (**153**, 1.10 g, 1.59 mmol) and 1,4-diethynylbenzene (**106**, 0.211 g, 1.67 mmol) were dissolved in a mixture of H_2O and DMF (16 mL, 1:1, v/v) at 50 °C in an argon-purged Schlenk flask with magnetic stirring. The resulting clear solution was deoxygenated by three cycles of the freeze-pump-thaw technique. The catalysts – consisting of tetrakis-(triphenylphosphine) palladium(0), $Pd(PPh_3)_4$, (55 mg, 48 μmol) and copper (I) iodide (9.0 mg, 48 μmol) in a mixture of diisopropylamine and DMF (10 mL, 1:1, v/v) – were deoxygenated as described above and quickly added to the former solution by means of a cannula. The final mixture was deoxygenated using three freeze-pump-thaw cycles and was then warmed to 50 °C and stirred under a positive pressure of argon for 30 hours. The resulting solution was viscous and bright yellow in colour and exhibited an intense blue fluorescence when illuminated with a near-UV lamp (excitation wavelength at 254 nm). The solution was cooled to room temperature and then slowly added to a cold (~ 0 °C) solution of MeOH (200 mL) which prompted the precipitation of the polymer as a yellow fibre-like material. The product was re-dissolved in H_2O (15 mL), treated with Na_2S (0.100 g, 1.28 mmol), and then the solution was filtered through quantitative filter paper, followed by a 10 – 20 μm fritted glass filter, and finally through a 0.8 μm nylon membrane. The polymer was dissolved in H_2O and reprecipitated into MeOH twice more to give PPE **155** (0.637 g, 71%) as a light yellow solid; GPC (DMF, PS Standards): M_n = 7500 Da, (see Chapter Three, section 3.1 for detail); IR (Film) ν_{max}/cm^{-1} 722 (Ar CH def.), 1155 (CO str.), 1461, 1377 (CH def.), 2924, 2854 (CH str.); δ_H (400 MHz, d_6-DMSO) 3.25 (18H, br s, H_a), 3.82 – 3.85 (4H, m, H_b), 4.49 – 4.61 (4H, m, H_c), 7.31 – 7.36 (6H, m, H_d + H_e). Due to the limited solubility of the polymer only a partial ^{13}C NMR spectrum was acquired; δ_C (100.6 MHz, d_6-DMSO) 53.3 (C_f), 63.3 (C_g), 64.0 (C_h), 86.4 (C_i), 122.5 (C_j), 151.9 (C_k). Anal. Calcd. for $C_{26}H_{32}Br_2N_2O_2 \cdot 23H_2O$: C, 31.91; H, 8.03; N, 2.86. Found: C, 31.72; H, 4.41; N, 3.70. Absorbance

λ_{max} (in unbuffered H_2O): 374 nm; emission λ_{max} (in unbuffered H_2O): 430 nm. DSC showed decomposition.

7.2.33 2,5-Diiodo-1,4-bis((*N,N'*-dimethylisothiouronium)ethoxy)benzene bromide (**159**).

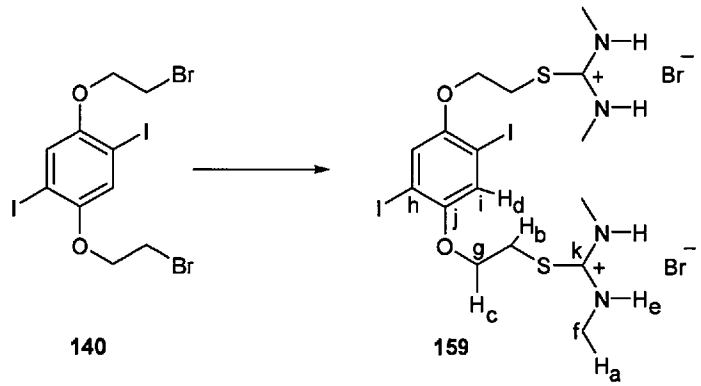

2,5-Diiodo-1,4-bis(2-bromoethoxy)benzene (**140**, 5.00 g, 8.72 mmol) was added to a stirred solution of 1,3-dimethylthiourea (**170**, 22.7 g, 218 mmol) in a mixture of dry MeOH (70 mL) and dry MeCN (70 mL) under a nitrogen atmosphere. The reaction solution was stirred for 24 hours at 80 °C and then the solvent was concentrated to about 10% of the original volume. MeCN (100 mL) was added and the solid that precipitated was collected at the pump. The white flaky material was recrystallised from H_2O to yield **159** (5.41 g, 79%) as a shiny white material, m.p. 250 – 251 °C; IR (Film) ν_{max}/cm^{-1} 723 (Ar CH def.), 1211 (CO str.), 1460, 1378 (CH def.), 1622 (C=N str.), 2921, 2855 (CH str.), 3423 (NH str.); δ_H (270 MHz, d_6-DMSO) 2.93 – 3.00 (12H, m, H_a), 3.63 – 3.67 (4H, m, H_b), 4.24 – 4.28 (4H, m, H_c), 7.38 (2H, s, H_d), 9.15 (4H, br s, H_e); δ_C (100.6 MHz, d_6-DMSO) 30.7 – 31.0 (C_f), 67.6 (C_g), 86.8 (C_h), 122.8 (C_i), 151.9 (C_j), 166.4 (C_k); *m/z* (FAB, +ve) 703 (30%, $[M-^{81}Br^-]^+$), 705 (30%, $[M-^{79}Br^-]^+$); HRMS (FAB, +ve) Found: $[M-H-^{79}Br^-]^+$, 704.8750. $C_{16}H_{25}{}^{81}BrI_2N_4O_2S_2$ requires: $[M-H-^{79}Br^-]^+$, 704.3700. Found: $[M-H-^{81}Br^-]^+$, 702.8770. $C_{16}H_{25}{}^{79}BrI_2N_4O_2S_2$ requires: $[M-H-^{81}Br^-]^+$, 702.3700; Anal. Calcd. for $C_{16}H_{26}Br_2I_2N_4O_2S_2$: C, 24.51; H, 3.34; N, 7.14. Found: C, 24.50; H, 3.41; N, 6.98.

7.2.34 2,5-Bis-(phenylethynyl)-1,4-bis(2-(*N,N'*-dimethylisothiouronium) ethoxy)benzene, bromide salt (PE **162**).

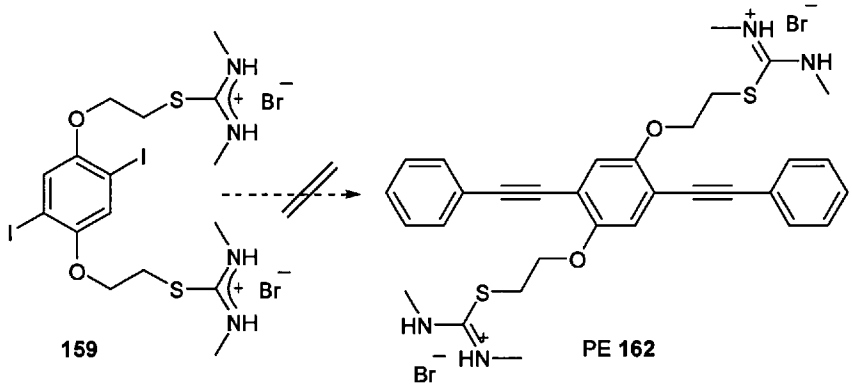

A solution of **159** (0.600 g, 0.78 mmol), phenylacetylene (0.281 mL, 2.56 mmol), tetrakis-(triphenylphosphine) palladium(0) (90 mg, 78 μmol), copper-(I) iodide (15 mg, 79 μmol), and diisopropylamine (5 mL) in DMF (50 mL), was stirred for 67 hours under argon at 20 °C. Evaporation of the solvents *in vacuo* gave a dark residue. Addition of MeOH (~ 10 mL) to this residue led to the formation of a turbid solution after heating and a brown oil then separated. The oil was filtered off and the remaining solvent allowed to cool, revealing a yellow precipitate (213 mg). *Analysis of the oil and yellow precipitate by NMR was inconclusive – both remained unidentified.* Unassigned signals: δ_H (270 MHz, d_6-DMSO) 1.19 – 1.21 (m), 1.46 (br m), 2.20 (br m), 2.73 (s), 4.05 – 4.12 (m). These data were also recovered when different solvents were used (MeOH, MeOH/H_2O (7:3, v/v), DMSO) at different temperatures (20 – 100 °C) and over different time periods (20 – 67 h). See section 3.2 Chapter Three, for further details.

7.2.35 2,5-Diiodo-1,4-bis((*N,N'*-dimethylisothiourea)ethoxy)benzene (**161**).

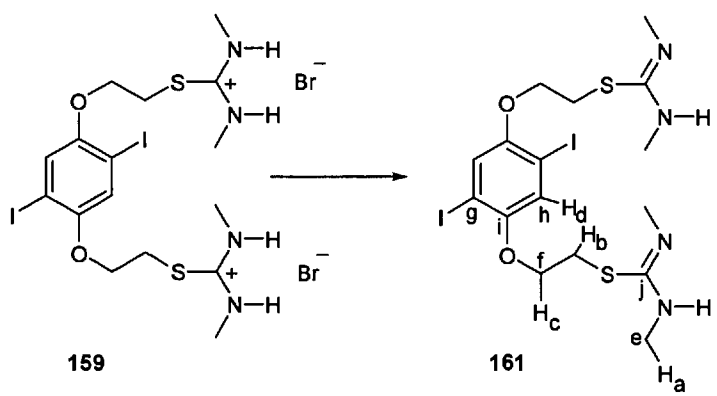

2,5-Diiodo-1,4-bis((*N,N'*-dimethylisothiouronium)ethoxy)benzene bromide, **159**, (2.60 g, 3.32 mmol) was dissolved in hot H_2O (95 °C, 400 mL). To the vigorously stirred solution was added 2.0 M NaOH (3.5 mL) which resulted in the formation of **161** (1.46 g, 71%) as an off-white precipitate which was filtered under vacuum, m.p. 140 – 141 °C; IR (Film) ν_{max}/cm^{-1} 853 (Ar CH def.), 1212 (CO str.), 1458, 1378 (CH def.), 1612 (C=N str.), 2922, 2853 (CH str.), 3232 (NH str.); δ_H (270 MHz, $CDCl_3$) 2.80 – 3.09 (12H, br s, H_a), 3.28 (4H, t, $^3J_{H\text{-}H}$ = 6.2 Hz, H_b), 4.14 (4H, t, $^3J_{H\text{-}H}$ = 6.2 Hz, H_c), 7.28 (2H, s, H_d); δ_C (100.6 MHz, $CDCl_3$) 31.7 (C_e), 70.2 (C_f), 86.3 (C_g), 123.7 (C_h), 152.8 (C_i), 172.5 (C_j); *m/z* (CI, NH_3) 519 (35%, $[M\text{-}SC(NMe)(NHMe)]^+$); Anal. Calcd. for $C_{16}H_{24}I_2N_4O_2S_2$: C, 30.88; H, 3.89; N, 9.00. Found: C, 31.05; H, 3.61; N, 8.74.

7.2.36 2,5-Bis-(phenylethynyl)-1,4-bis(2-(*N,N'*-dimethylisothiouronium) ethoxy)benzene, bromide salt (PE **163**).

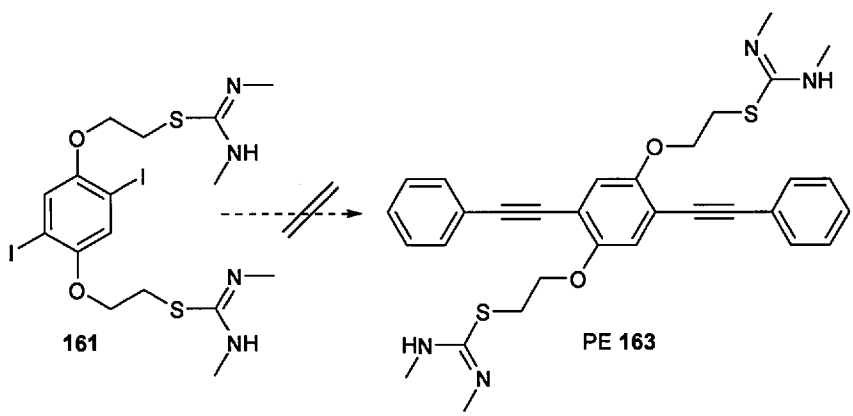

A solution of **161** (0.121 g, 0.194 mmol), phenylacetylene (0.071 mL, 0.65 mmol), tetrakis-(triphenylphosphine) palladium(0) (45 mg, 39 μmol), copper-(I) iodide (8.0 mg, 42 μmol), and diisopropylamine (2 mL) in DMSO (10 mL), was stirred for 65 hours under argon at 30 °C. Evaporation of the solvents *in vacuo* gave a dark yellow residue. *Analysis of the residue by ^1H NMR indicated that the desired molecule was not present – the residue remained unidentified.* Unassigned signals: δ_H (270 MHz, d_6-DMSO) 7.25 – 7.80 (Ar-*H*, br m). See Chapter Three, section 3.2 for further details.

7.2.37 2,5-Diiodo-1,4-bis((*N,N'*-dimethylisothiouronium)ethoxy)benzene tetraphenyl borate (**160**).

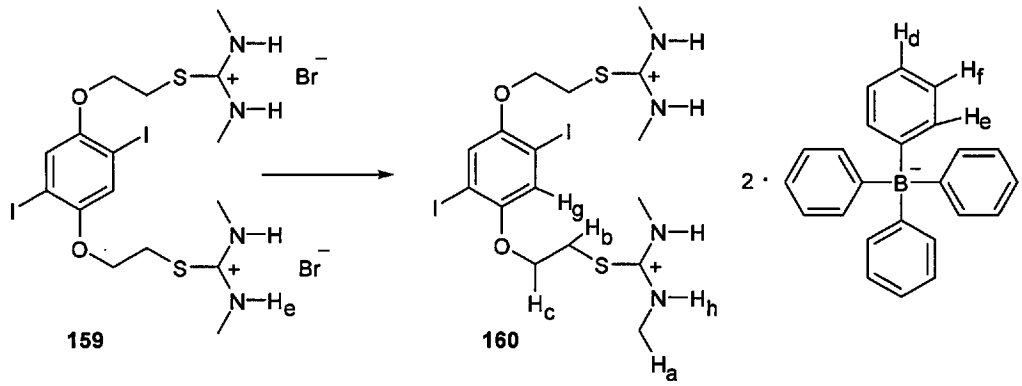

2,5-Diiodo-1,4-bis((*N,N'*-dimethylisothiouronium)ethoxy)benzene bromide (**159**, 2.60 g, 3.32 mmol) was dissolved in MeOH (200 mL) at 80 °C and the solution filtered through a pad of celite (1 cm depth, 4 cm diameter in a sinter funnel). To the filtrate was added tetraphenyl borate (an excess, ~ 5 g) which resulted in the formation of **160** (2.58 g, 62%) as a white precipitate which was recrystallised from acetone/H_2O (9:1, v/v), m.p. 211 – 212 °C; IR (Film) ν_{max}/cm^{-1} 740, 712 (Ar CH def.), 1294 (CO str.), 1462, 1378 (CH def.), 1622, 1538 (C=N str.), 2923, 2855 (CH str.), 3231 (NH str.); δ_H (270 MHz, $CDCl_3$) 2.91 – 3.00 (12H, br m, H_a), 3.59 – 3.63 (4H, br m, H_b), 4.24 – 4.28 (4H, br m, H_c), 6.79 – 6.81 (8H, m, H_d), 6.90 – 6.95 (16H, m, H_e), 6.95 – 7.18 (16H, m, H_f), 7.42 (2H, s, H_g), 9.08 (4H, br s, H_h); *m/z* (FAB, +ve) 623 (70%, $[M\text{-}2(BPh_4)]^+$), 943 (50%, $[M\text{-}(BPh_4)]^+$); HRMS (FAB, +ve) Found: $[M]^+$, 943.1271, $C_{40}H_{46}{}^{11}BI_2N_4O_2S_2$ requires: M, 943.5677.

7.2.38 2,5-Bis-(phenylethynyl)-1,4-bis(2-(*N,N'*-dimethylisothiouronium) ethoxy)benzene, tetraphenyl borate salt (PE **164**).

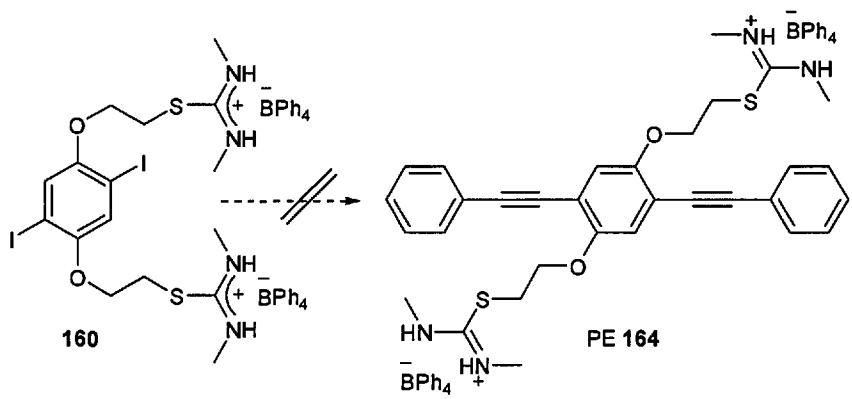

A solution of **160** (0.450 g, 0.356 mmol), phenylacetylene (0.130 mL, 1.18 mmol), tetrakis-(triphenylphosphine) palladium(0) (80 mg, 69 μmol), copper-(I) iodide (14 mg, 74 μmol), and diisopropylamine (5 mL) in DMF (20 mL), was stirred for 30 hours under argon at 20 °C. Evaporation of the solvents *in vacuo* gave a dark residue (~100 mg). Column chromatography (acetone and 10%, NH_3 in H_2O) was used to separate the two fractions that were observed by TLC (R_f = 0.80, 0.11, 100% CH_2Cl_2). *Analysis of both fractions by ^1H NMR was inconclusive.* Unassigned signals: δ_H (270 MHz, $CDCl_3$) 0.85 – 1.39 (m), 1.41 – 2.17 (m), 2.50 (br s), 2.90 – 3.88 (br m), 6.70 – 7.70 (m), 7.95 (s). See Chapter Three, section 3.2 for further details.

7.2.39 2,5-Diiodo-1,4-bis(*N,N'*-di-(*tert*-butoxycarbonyl)-1,3-dimethyl-2-thiourea ethoxy)benzene (**168**).

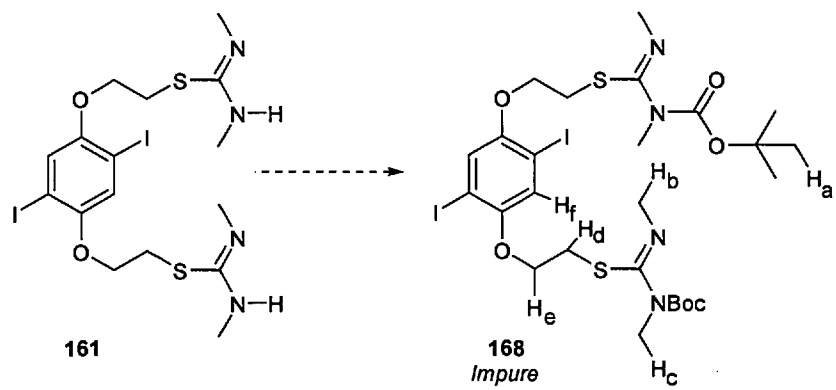

To a cooled solution (ice/H_2O bath) of **161** (0.500 g, 0.803 mmol) in dry THF (40 mL) under argon, was added NaH (0.309 g, 12.9 mmol, 60% in mineral oil). After 5 minutes, the ice bath was removed and the reaction was stirred 10 minutes at room temperature. Then, the reaction mixture was cooled to 0 °C and di-*tert*-butyldicarbonate (1.05 g, 4.82 mmol) was added. After 30 minutes, the ice bath was removed and the reaction mixture was stirred for another 19 hours at room temperature. The reaction was carefully quenched by the dropwise addition of a saturated $NaHCO_3$ solution (60 mL). The mixture was poured into H_2O (200 mL) and the aqueous layer was extracted with EtOAc (3 x 60 mL). The combined organic phases were washed with brine, dried over $MgSO_4$, filtered and the solvent removed under reduced pressure to give crude **168** as an impure off-white precipitate. Purification of **168** was attempted by flash column chromatography (silica gel, 100% $CHCl_3$); two bands were visible during the column however they coalesced as they travelled down the column (2 bands, R_f = 0.20 + 0.23); A light yellow solid (0.35 g) was isolated; δ_H (270 MHz, $CDCl_3$) 1.43 – 1.46 (18H, br s, H_a), 2.97 (6H, s, H_b), 3.14 (6H, s, H_c), 3.18 – 3.28 (4H, m, H_d), 4.09 – 4.18 (4H, m, H_e), 7.36 (2H, s, H_f).

The material was not isolated cleanly. Unassigned signals: δ_H (270 MHz, $CDCl_3$) 4.09 (m), 7.18 (s). See Chapter Three, section 3.2 for further details.

7.2.40 2,5-Bis-(phenylethynyl)-1,4-bis(*N,N'*-di-(*tert*-butoxycarbonyl)-1,3-dimethyl-2-thiourea ethoxy)benzene (PE **169**).

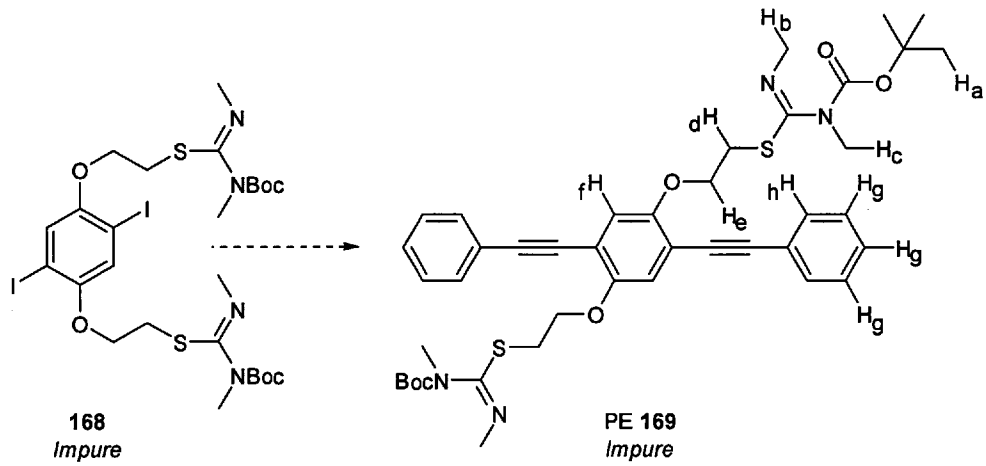

A solution of **168** (0.288 g, 0.350 mmol), phenylacetylene (0.154 mL, 1.40 mmol), tetrakis-(triphenylphosphine) palladium(0), $Pd(PPh_3)_4$, (80 mg, 69 μmol), copper-(I) iodide (13 mg, 68 μmol), and diisopropylamine (2 mL) in toluene (10 mL), was stirred for 20 hours under argon with stirring at 20 °C. The reaction mixture was then filtered through a glass sinter funnel, the solvents removed *in vacuo* and the remaining solid was recrystallised from *n*-hexane, to give crude PE **169** (0.091 g) as a brown-beige solid. R_f = 0.09, 0.40, 0.80 (100% *n*-hexane); δ_H (400 MHz, $CDCl_3$) 1.49 (18H, s, H_a), 2.97 (6H, s, H_b), 3.14 (6H, s, H_c), 3.30 – 3.32 (4H, m, H_d), 4.23 – 4.28 (4H, m, H_e), 7.23 (2H, s, H_f), 7.34 – 7.35 (6H, m, H_g), 7.54 – 7.56 (4H, m, H_h).

The material was not isolated cleanly. Unassigned signals: δ_H (400 MHz, $CDCl_3$) 3.09 (s), 3.20 (s), 3.27 (m), 4.22 (m). See Chapter Three, section 3.2 for further details.

7.2.41 *N,N'*-Di-(*tert*-butoxycarbonyl)-1,3-dimethyl-2-thiourea (**171**).

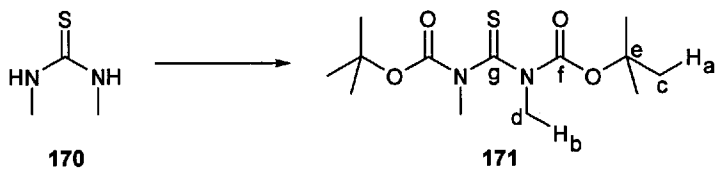

To a cooled (ice/H_2O bath) solution of 1,3-dimethyl-2-thiourea (**170**, 1.00 g, 9.60 mmol) in dry THF (70 mL) under argon, was added NaH (1.70 g, 72.0 mmol, 60% in mineral oil). After 5 minutes, the ice/H_2O bath was removed and the reaction was stirred for 10 minutes at room temperature. Then, the reaction mixture was cooled to 0 °C and di-*tert*-butyldicarbonate (4.60 g, 21.1 mmol) was added. After 30 minutes, the ice bath was removed and the reaction mixture was

stirred for another 19 hours at room temperature. The reaction was quenched carefully, drop-by-drop, with a saturated $NaHCO_3$ solution (60 mL). The mixture was poured into H_2O (200 mL) and the aqueous layer was extracted with EtOAc (3 x 60 mL). The combined organic phases were washed with brine, dried over $MgSO_4$, filtered and the solvent removed under reduced pressure. The resultant yellow-orange residue was purified by flash column chromatography (silica gel, 100% CH_2Cl_2) to give the protected thiourea **171** (2.09 g, 72%) as a light yellow oil, R_f = 0.65 (silica gel, 100% CH_2Cl_2); IR (Film) ν_{max}/cm^{-1} 1134, 1279, 1326 (CS str.), 1460 (CH def.), 1726 (C=O str.), 2935, 2979 (CH str.); δ_H (270 MHz, $CDCl_3$) 1.45 (18H, s, H_a), 3.46 (6H, s, H_b); δ_C (100.6 MHz, $CDCl_3$) 27.9 (C_c), 39.5 (C_d), 83.3 (C_e), 151.1 (C_f), 191.2 (C_g); *m/z* (CI, NH_3) 304 (65%, $[M]^+$), 305 (100%, $[M+H]^+$); HRMS (CI, NH_3) Found: $[M+H]^+$, 305.1527, $C_{13}H_{25}N_2O_4S$ requires: $[M+H]^+$, 305.4136.

7.2.42 2,5-Diiodo-1,4-bis(*N,N'*-di-(*tert*-butoxycarbonyl)-1,3-dimethyl-2-thiouronium ethoxy)benzene, bromide salt (**172**).

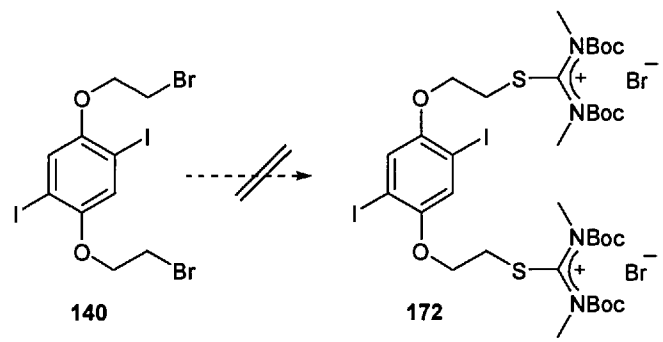

140 **172**

2,5-Diiodo-1,4-bis(2-bromoethoxy)benzene (**140**, 0.100 g, 0.174 mmol) was added to a stirred solution of **171** (0.530 g, 1.74 mmol) in dry MeCN (20 mL) under a nitrogen atmosphere. The reaction solution was stirred for 48 hours at 85 °C and then the solvent was concentrated to about 10% of the original volume. MeCN (10 mL) was added and the solid that precipitated was collected at the pump. *There was > 95% recovery of starting material, with no evidence for the desired target by ^1H NMR.*

7.2.43 2,5-Diiodo-1,4-bis(*N,N'*-bis-*tert*-butoxycarbonylthiourea ethoxy)benzene (**174**).

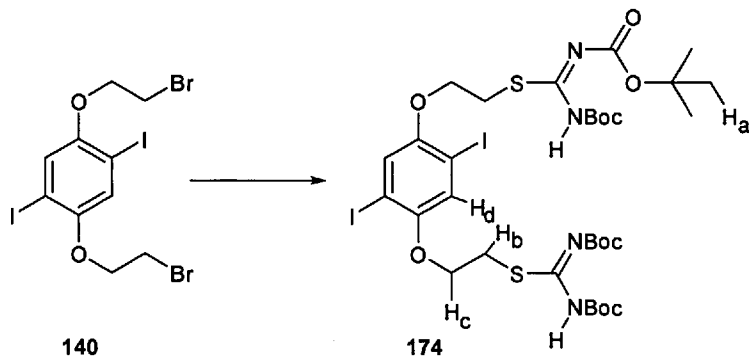

To a cooled (ice/H_2O bath) solution of **173** (0.276 g, 0.999 mmol) in dry THF (20 mL) under argon, was added NaH (0.350 g, 14.6 mmol, 60% in mineral oil). After 5 minutes, the ice//H_2O bath was removed and the reaction was stirred for 10 minutes at room temperature. Then, the reaction mixture was cooled to 0 °C and **140** (0.251 g, 0.436 mmol) was added. After 30 minutes, the ice bath was removed and the reaction mixture was stirred for another 19 hours at room temperature before being carefully quenched by the dropwise addition of a saturated $NaHCO_3$ solution (60 mL). The mixture was poured into CH_2Cl_2 (40 mL) and the aqueous layer was extracted with CH_2Cl_2 (3 x 30 mL). The combined organic phases were washed with brine, dried over $MgSO_4$, filtered and the solvent removed under reduced pressure to give **174** (0.404 g, 96%) as an off-white solid; δ_H (400 MHz, $CDCl_3$) 1.52 (36H, s, H_a), 3.65 (4H, t, $^3J_{H\text{-}H}$ = 6.3 Hz, H_b), 4.27 (4H, t, $^3J_{H\text{-}H}$ = 6.3 Hz, H_c), 7.22 (2H, s, H_d).

7.2.44 2,5-Bis-(phenylethynyl)-1,4-bis(2-(*N,N'*-dimethylisothiouronium) ethoxy)benzene, bromide salt (PE **175**).

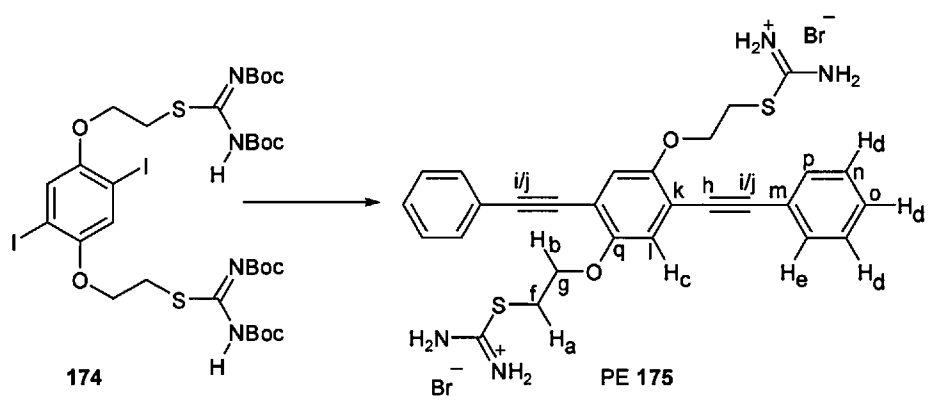

A solution of **174** (0.193 g, 0.200 mmol), phenylacetylene (0.10 mL, 0.80 mmol), tetrakis-(triphenylphosphine) palladium(0) (63 mg, 90 μmol), copper-(I) iodide (10 mg, 90 μmol), and

diisopropylamine (5 mL) in toluene (5 mL), was stirred for 20 hours under argon at 20 °C. The crude product was recrystallised from EtOH and after filtration gave PE **175** (93 mg, 69%) as a white crystalline solid; δ_H (270 MHz, $CDCl_3$) 3.69 (4H, t, $^3J_{H\text{-}H}$ = 6.4 Hz, H_a), 4.37 (4H, t, $^3J_{H\text{-}H}$ = 6.4 Hz, H_b), 7.04 (2H, s, H_c), 7.34 – 7.36 (6H, m, H_d), 7.54 – 7.57 (4H, m, H_e); δ_C (100.6 MHz, $CDCl_3$) 28.9 (C_f), 69.8 (C_g), 85.0 (C_h), 95.7 (C_i), 97.3 (C_j), 114.9 (C_k), 118.4 (C_l), 123.1 (C_m), 128.4 (C_n), 128.6 (C_o), 131.7 (C_p), 153.3 (C_q). Absorbance λ_{max} (in $CHCl_3$, 0 wt.% Triton): 354 nm; emission λ_{max} (in $CHCl_3$, 0 wt.% Triton): 410 nm.

7.2.45 2,5-Diiodo-1,4-bis(1,3-bis(*tert*-butoxycarbonyl)guanidine ethoxy)benzene (**177**).

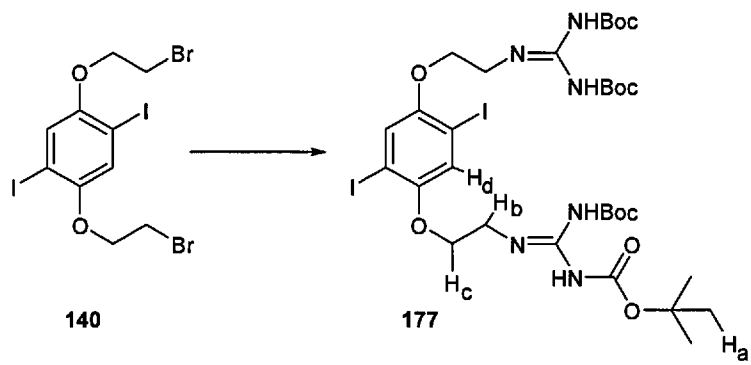

NaH (0.350 g, 14.6 mmol, 60% dispersion in mineral oil) was added in small portions to a suspension of **176** (0.518 g, 2.00 mmol) in anhydrous THF (20 mL) at -45 °C under an argon atmosphere. After the addition was complete, the mixture was allowed to stir for 1 hour at -45 °C. Then, 2,5-diiodo-1,4-bis(2-bromoethoxy)benzene, **140**, (0.500 g, 0.868 mmol) was added, and the mixture was allowed to warm to room temperature and stir overnight (18 hours). The solvent was evaporated *in vacuo*, and the residue was dissolved in a mixture of CH_2Cl_2 (50 mL) and $NaHCO_3$ (25 mL). The phases were separated and the aqueous layer was extracted with CH_2Cl_2 (2 x 50 mL). The extracts were combined, washed with 1 N HCl and H_2O, and dried over $MgSO_4$. Filtration and evaporation of the solvent, gave **177** (0.75 g, 93%) as a white crystalline solid; δ_H (400 MHz, $CDCl_3$) 1.51 (36H, s, H_a), 3.65 (4H, t, $^3J_{H\text{-}H}$ = 6.4 Hz, H_b), 4.26 (4H, t, $^3J_{H\text{-}H}$ = 6.4 Hz, H_c), 7.22 (2H, s, H_d).

7.2.46 2,5-Bis-(phenylethynyl)-1,4-bis(2-(1,3-bis(*tert*-butoxycarbonyl)guanidine) ethoxy)benzene (PE **178**).

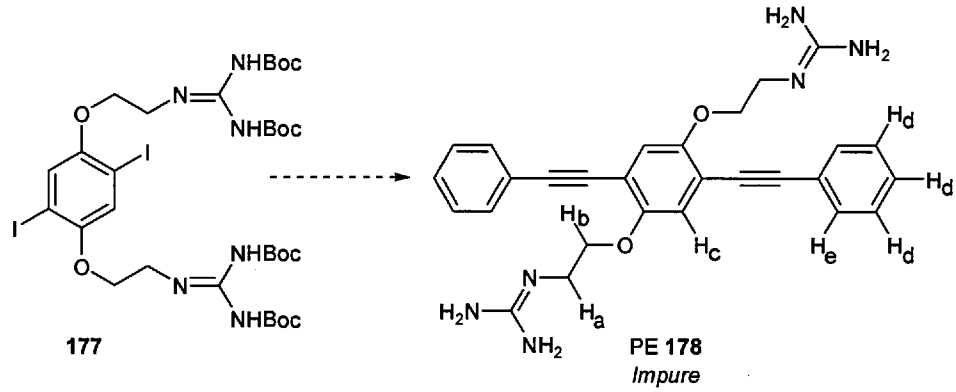

A solution of **177** (0.300 g, 0.322 mmol), phenylacetylene (0.121 mL, 1.10 mmol), tetrakis-(triphenylphosphine) palladium(0) (63 mg, 55 μmol), copper-(I) iodide (10 mg, 53 μmol) and diisopropylamine (5 mL) in DMF (5 mL) was stirred for 20 hours under argon. The crude product was tritiated using EtOH and after filtration gave crude PE **178** (30 mg) as a light-yellow solid. δ_H (270 MHz, $CDCl_3$) 3.68 – 3.72 (4H, m, H_a), 4.34 – 4.39 (4H, m, H_b), 7.04 (2H, s, H_c), 7.32 – 7.38 (6H, m, H_d), 7.52 – 7.58 (4H, m, H_e).

The material was not isolated cleanly. Unassigned signals: δ_H (270 MHz, $CDCl_3$) 3.48 (m), 4.37 (m), 7.04 (s). See Chapter Three, section 3.2 for further details.

7.2.47 PPE **179**.

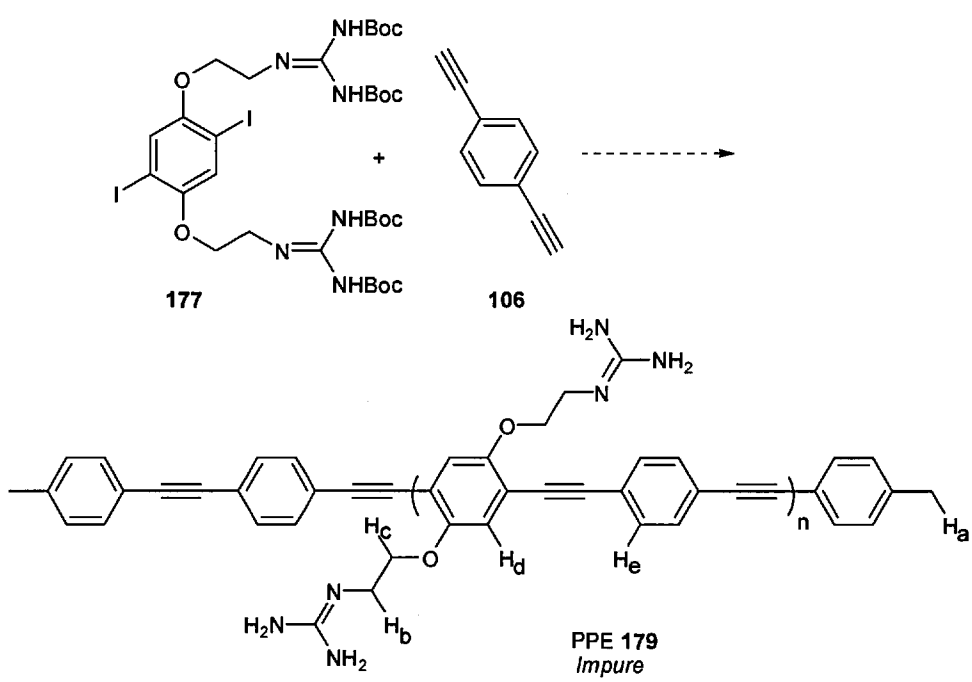

A solution of monomer **177** (0.300 g, 0.322 mmol), 1,4-diethynylbenzene (**106**, 43 mg, 0.38 mmol) and 4-iodotoluene (**149**, 14 mg, 0.064 mmol) were dissolved in DMF (8 mL) at 50 °C in an argon-purged Schlenk flask with magnetic stirring. The resulting clear solution was deoxygenated by three cycles of the freeze-pump-thaw technique. The catalysts – consisting of tetrakis-(triphenylphosphine) palladium(0), $Pd(PPh_3)_4$, (35 mg, 30 μmol) and copper (I) iodide (35 mg, 180 μmol) in a mixture of diisopropylamine and DMF (12 mL, 1:1, v/v) – were deoxygenated as described above and quickly added to the former solution by means of a cannula. The final mixture was deoxygenated again by three cycles of the freeze-pump-thaw technique and was then warmed to 50 °C and stirred under a positive pressure of argon for 90 hours. The resulting solution was viscous and bright yellow in colour and exhibited an intense blue fluorescence when illuminated with a near-UV lamp (excitation wavelength at 254 nm). The solution was cooled to room temperature and then slowly added to a cold (~ 0 °C) solution of THF (800 mL) which prompted the precipitation of the polymer as yellow fibres. The product was re-dissolved in H_2O (50 mL) and then the solution was filtered through quantitative filter paper. The polymer was dissolved in H_2O and reprecipitated into THF once more to give crude PPE **179** as a light yellow solid; δ_H (400 MHz, $CDCl_3$) 2.38 (6H, s, H_a), 3.06 – 3.09 (4H, m, H_b), 3.96 – 3.99 (4H, m, H_c), 7.02 – 7.06 (2H, m, H_d), 7.48 – 7.54 (4H, m, H_e).

This material was not isolated cleanly. Unassigned signals: δ_H (400 MHz, $CDCl_3$) ~1.05 (br m), 2.88 – 2.98 (br m), 4.19 (br m), 4.33 (br m). See Chapter Three, section 3.2 for further details.

7.2.48 1,4-Bis[2-(2-hydroxyethoxy)ethoxy]-2,5-diiodobenzene (**180**).[6,18]

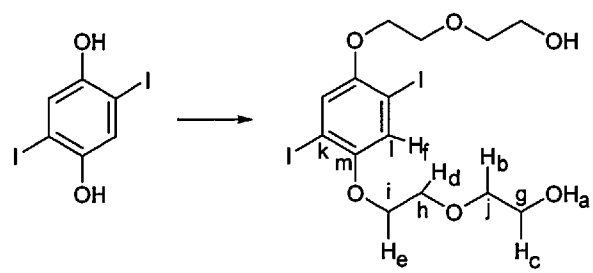

108 **180**

A solution of 1,4-dihydroxy-2,5-diiodobenzene (**108**, 6.50 g, 18.0 mmol) in dry DMF (15 mL) was added over 30 minutes to a stirred suspension of K_2CO_3 (20.0 g, 144 mmol) in dry DMF (40 mL) under nitrogen. After an additional 30 minutes, a solution of 2-(2-chloroethoxy)ethanol (7.6 g, 72 mmol) was added dropwise over 10 minutes, and the temperature was raised to 75 °C. The resulting mixture was heated and stirred under argon. The reaction was followed by TLC (*n*-hexane/EtOAc, 1:1, v/v) and was deemed complete after 6 days. After cooling to room temperature, the reaction mixture was filtered and the residue was washed with DMF (20 mL). The

solvent was removed *in vacuo* and the residue was partitioned between CH_2Cl_2 (50 mL) and brine (25 mL). The pH was adjusted to ~ 2 with 0.1 M HCl, and the aqueous phase was washed with CH_2Cl_2 (2 x 50 mL). The combined organic solutions were washed with H_2O (20 mL), dried ($MgSO_4$), and concentrated *in vacuo*. Recrystallisation of the residue from CH_2Cl_2/*n*-pentane (8:1, v/v) afforded the *title molecule* **180** (5.79 g, 60%) as a light pink solid; R_f = 0.48 (100% EtOAc); m.p. 106 – 107 °C (Lit. 104 – 105.5 °C);[6] IR (Film) ν_{max} (CaF_2 pellet)/cm^{-1} 1118 (C-O str.), 1378, 1460 (CH def.), 2856, 2926 (CH str.), 3546 (OH str.); δ_H (400 MHz, $CDCl_3$) 1.93 (2H, br s, H_a), 3.70 – 3.72 (4H, m, H_b), 3.76 – 3.78 (4H, m, H_c), 3.88 – 3.90 (4H, m, H_d), 4.11 – 4.13 (4H, m, H_e), 7.24 (2H, s, H_f); δ_C (100.6 MHz, $CDCl_3$) 61.8 (C_g), 69.5 (C_h), 70.1 (C_i), 72.6 (C_j), 86.4 (C_k), 123.5 (C_l), 153.1 (C_m); *m/z* (CI, NH_3) 556 (100%, $[M+NH_4]^+$). HRMS (CI, NH_3) Found: $[M+NH_4]^+$, 555.9687. $C_{14}H_{24}I_2NO_6$ requires: 555.9688. Anal. Calcd. for $C_{14}H_{20}I_2O_6$: C, 31.25; H, 3.75. Found: C, 31.18; H, 3.70.

7.2.49 2,5-Bis-(phenylethynyl)-1,4-bis(2-(2-hydroxyethoxy)ethoxy ethoxy)benzene (PE **181**).

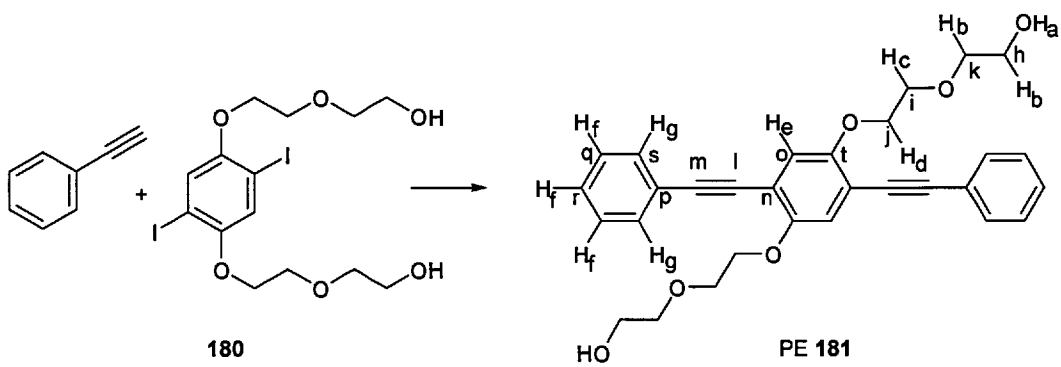

To a solution of **180** (0.600 g, 1.12 mmol), tetrakis (triphenylphosphine) palladium(0) (122 mg, 106 μmol), copper-(I) iodide (20.0 mg, 105 mmol) and diisopropylamine (10 mL) in THF (10 mL) was added phenylacetylene (0.39 mL, 3.52 mmol) dropwise over 5 minutes. The resulting mixture was stirred at room temperature under argon for 44 hours, by which time the reaction was deemed complete by TLC. The solvents were removed *in vacuo* and the crude material was purified *via* recrystallisation from *n*-hexane/EtOAc (1:2, v/v) and MeOH/H_2O (9:1, v/v) to give the *title molecule* PE **181** (0.451g, 83%) as an off-white crystalline solid; R_f = 0.21 (*n*-hexane:EtOAc, 1:2, v/v); m.p. = 104 – 105 °C; IR (Film) ν_{max} (CaF_2 pellet)/cm^{-1} 1221 (C-O str.), 1376, 1460 (CH def.), 2360 (C≡C), 2853, 2923 (CH str.), 3424 (O-H str.); δ_H (400 MHz, $CDCl_3$) 1.64 (2H, br s, H_a), 3.71 – 3.75 (8H, m, H_b), 3.92 – 3.95 (4H, m, H_c), 4.22 – 4.24 (4H, m, H_d), 7.06 (2H, s, H_e), 7.34 – 7.38 (6H, m, H_f), 7.53 – 7.56 (4H, m, H_g); δ_C (100.6 MHz, $CDCl_3$) 61.9 (C_h), 69.6 (C_i), 69.6 (C_j), 72.8 (C_k), 85.5 (C_l), 95.2 (C_m), 114.4 (C_n), 117.7 (C_o), 123.1 (C_p), 128.4 (C_q), 128.5 (C_r), 131.6 (C_s), 153.6 (C_t); *m/z* (CI, NH_3) 487 (75%, $[M+H]^+$), 504 (100%, $[M+NH_4]^+$); HRMS (CI, NH_3) Found:

$[M+NH_4]^+$, 504.2359. $C_{30}H_{34}NO_6$ requires: 504.5935; Anal. Calcd. for $C_{30}H_{30}O_6$: C, 74.06; H, 6.21. Found: C, 73.98; H, 6.19. Absorbance λ_{max} (in unbuffered H_2O, 0 wt.% Triton): 355 nm; emission λ_{max} (in unbuffered H_2O, 0 wt.% Triton): 399 nm; absorbance λ_{max} (in unbuffered H_2O, 0.3 wt.% Triton): 365 nm; emission λ_{max} (in unbuffered H_2O, 0.3 wt.% Triton): 398 nm; absorbance λ_{max} (in MeOH, 0 wt.% Triton): 358 nm; emission λ_{max} (in MeOH, 0 wt.% Triton): 394 nm; absorbance λ_{max} (in MeOH, 0.3 wt.% Triton): 358 nm; emission λ_{max} (in MeOH, 0.3 wt.% Triton): 394 nm.

7.2.50 PPE **182**.

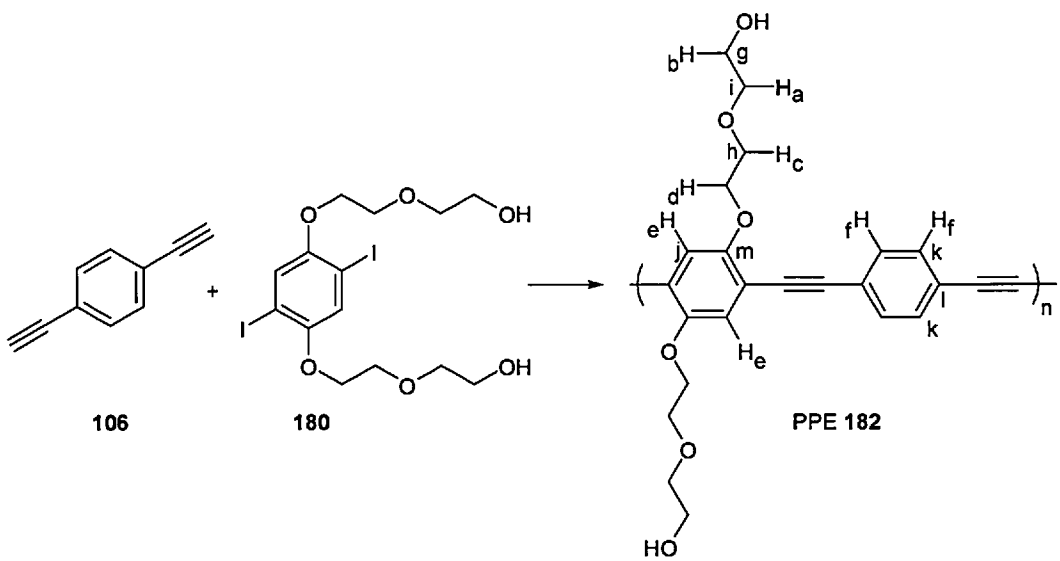

To a solution of DMF (12 mL) and diisopropylamine (6 mL) was added 1,4-diethynylbenzene (**106**, 50 mg, 0.40 mmol) and **180** (0.203 g, 0.377 mmol). The Schlenk flask was fitted tightly with a rubber septum, and the solution was deoxygenated by applying the freeze-pump-thaw technique consecutively over three iterations. After backfilling with argon, to this solution was added $Pd(PPh_3)_4$ (25 mg, 22 μmol) and Cu(I)I (25 mg, 130 μmol). The resulting suspension was deoxygenated again by applying the freeze-pump-thaw technique consecutively over three iterations. A voluminous precipitate, believed to be alkylammonium iodide, formed in less than five minutes. The solution was heated at 45 °C for 26 hours with stirring in the dark. After this time, a second batch of the catalyst and co-catalyst was added (same amounts as before) and the solution deoxygenated again and stirred at 45 °C for a further 8 hours before the cooled reaction mixture was poured into MeOH (400 mL) which prompted the precipitation of the polymer as a yellow fibre-like material which was then filtered and redissolved in a small volume (< 4 mL) of DMF. The precipitation and redissolution process was repeated once more to give PPE **182** (0.135 g, 87%) as a light yellow solid; GPC (DMF, PS Standards): M_n = 59.8 kDa, (see Chapter Three,

section 3.3 for detail); IR (Film) on CaF_2 disc ν_{max}/cm^{-1} 1377, 1461 (CH def.), 2205 (C≡C), 2855, 2923, (CH str.), 3427 (OH Str.); δ_H (400 MHz, d_6-DMSO) 3.54 – 3.58 (4H, br m, H_a), 3.70 – 3.97 (4H, br m, H_b), 4.09 – 4.39 (4H, br m, H_c), 4.92 – 4.77 (4H, br m, H_d), 7.14 – 7.32 (2H, br s, H_e), 7.44 – 7.67 (4H, br m, H_f); δ_C (100.6 MHz, d_6-DMSO) 60.3 (C_g), 68.9 (C_h), 72.7, (C_i), 116.7 (C_j), 131.5 (C_k), 132.7 (C_l), 153.1 (C_m). Anal. Calcd. for $C_{24}H_{26}O_6 \cdot 2H_2O$: C, 64.56; H, 6.77. Found: C, 64.57; H, 6.02. Due to the limited solubility of the polymer only a partial ^{13}C NMR spectrum was acquired. Absorbance λ_{max} (in unbuffered H_2O, 0 wt.% Triton): 462 nm; emission λ_{max} (in unbuffered H_2O, 0 wt.% Triton): 497 nm; absorbance λ_{max} (in unbuffered H_2O, 0.3 wt.% Triton): could not be determined under these conditions. Emission λ_{max} (in unbuffered H_2O, 0 wt.% Triton): 445 nm; absorbance λ_{max} (in MeOH, 0 wt.% Triton): could not be determined under these conditions. Emission λ_{max} (MeOH, 0 wt.% Triton): 438 nm; absorbance λ_{max} (in MeOH, 0.3 wt.% Triton): 411 nm; emission λ_{max} (in MeOH, 0 wt.% Triton): 438 nm; DSC showed decomposition.

7.2.51 2,5-diiodophenylenediamine (188).[6,17,19]

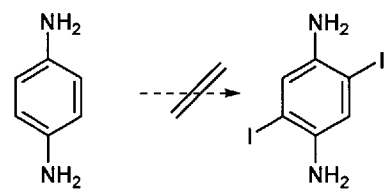

187 **188**

Method 1

p-Phenylenediamine (**187**, 0.500 g, 4.62 mmol) was added to a mixture of glacial AcOH (20 mL), H_2SO_4 (12 M, 0.33 mL), H_2O (1 mL), KIO_3 (0.50 g, 2.31 mmol) and I_2 (1.23 g, 4.85 mmol). The mixture was slowly heated to reflux. After 6 hours, the reaction was cooled to room temperature and H_2O (100 mL) was added to the cooled mixture (25 °C) and then the whole mixture was cooled in an ice/H_2O bath. Dark crystals were collected, washed with H_2O (15 mL) and dried under vacuum. The dark crystals were then dissolved in $CHCl_3$ and heated at 75 °C with activated carbon (10.0 mg) for 10 minutes followed by hot filtration. The filtrate was cooled and a dark brown/black solid was isolated. *^1H NMR was inconclusive.*

Unassigned signals: δ_H (270 MHz, $CDCl_3$) 1.24 – 1.70 (m), 3.10 – 3.25 (m). See Chapter Four, section 4.1.1 for further details.

Method 2

A mixture of *p*-phenylenediamine (**187**, 0.500 g, 4.62 mmol), [bis(trifluoroacetoxy)iodo]benzene (**147**, 2.24 g, 5.20 mmol) and I_2 (1.23 g, 4.85 mmol) in CH_2Cl_2 (100 mL) was stirred at room temperature for 18 hours. The reaction mixture was then concentrated and CH_2Cl_2 and H_2O (30 mL of each) were added. $NaHSO_3$ was added and the excess filtered off. The two phases were separated and the organic layer was dried and concentrated *in vacuo*. *^1H NMR confirmed the formation of iodobenzene as a by-product, but was otherwise inconclusive.*
Unassigned signals: δ_H (270 MHz, d_6-DMSO) 3.15 (br m), 4.01 – 4.32 (br m), 9.91 (br m). See Chapter Four, section 4.1.1 for further details.

Method 3

To a solution of **187** (0.50 g, 4.6 mmol) in AcOH (15 mL) was added NaOAc (0.82 g, 9.9 mmol). To this solution was added ICl (1.6 g, 9.9 mmol) in AcOH (10 mL) and the reaction mixture heated at 80 °C for 3 hours. *^1H NMR data indicated the presence of the starting material only (reclaimed in ~ 90% yield).*

7.2.52 1,4-Acetanilide (**189**).[19]

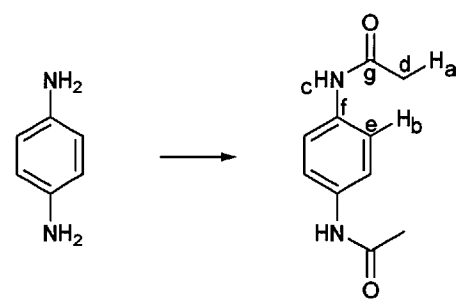

187 **189**

p-Phenylenediamine (**187**, 1.00 g, 9.25 mmol) was added to Ac_2O (3.5 mL) and the solution stirred for 10 minutes. Triethylamine (1.5 mL) was added and the resulting solution heated at 35 °C for 1 hour. The afforded white liquid was washed with 50% aqueous MeOH (100 mL) and extracted with Et_2O (50 mL). The volume of solvent was reduced *in vacuo* to reveal **189** (1.34 g, 75%) as a white solid; IR (Film) ν_{max} (CaF_2 pellet)/cm^{-1} 1369, 1462 (CH def.), 1516 (benzene ring), 1569 (amide), 1662 (amide), 2855, 2921 (CH str.), 3079 (secondary amide band), 3169 (secondary amide band), 3297 (secondary amide band); δ_H (400 MHz, d_6-DMSO) 2.00 (6H, s, H_a), 7.47 (4H, s, H_b), 9.82 (2H, s, H_c); δ_C (100.6 MHz, d_6-DMSO) 23.7 (C_d), 119.2 (C_e), 134.5 (C_f), 167.8 (C_g);

m/z (CI, NH_3) 193 (15%, $[M+H]^+$), 210 (100%, $[M+NH_4]^+$). HRMS (CI, NH_3) Found: $[M+NH_4]^+$, 210.1240. $C_{10}H_{16}N_3O_2$ requires: $[M+NH_4]^+$, 210.2524.

7.2.53 2,5-Diiodo-1,4-acetanilide (**190**).

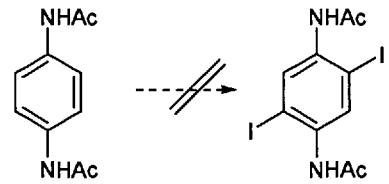

189 **190**

Method 1

A mixture of **189** (0.300 g, 1.56 mmol), [bis(trifluoroacetoxy)iodo]benzene (**147**, 0.758 g, 1.76 mmol) and I_2 (0.416 g, 1.64 mmol) in CH_2Cl_2 (100 mL) was stirred at room temperature for 18 hours. The reaction mixture was then concentrated (~10 mL) and *n*-pentane (30 mL) was added. No precipitate formed and all of the solvent was then removed *in vacuo* and the solid analysed by ^{1}H NMR. *^{1}H NMR data was inconclusive.*
Unassigned signals: δ_H (400 MHz, $CDCl_3$) 2.18 – 2.24 (br m), 2.71 (m), 7.21 (s). See Chapter Four, section 4.1.1 for further details.

Method 2

189 (0.393 g, 2.04 mmol) was added to a 100 mL round bottom flask and to this was added NaOAc (0.369 g, 4.50 mmol) and AcOH (30 mL). A solution of ICl (0.731 g, 4.50 mmol) in AcOH (10 mL) was added and the reaction mixture heated at 80 °C for 6 hours. Analysis of the reaction mixture by TLC (R_f = 0.24, 100% EtOAc) indicated that no reaction had occurred. *^{1}H NMR data indicated the presence of the starting material only (reclaimed in 90% yield).*

7.2.54 1,4-Bis(1,3-bis(*tert*-butoxycarbonyl)guanidine)benzene (**191**).

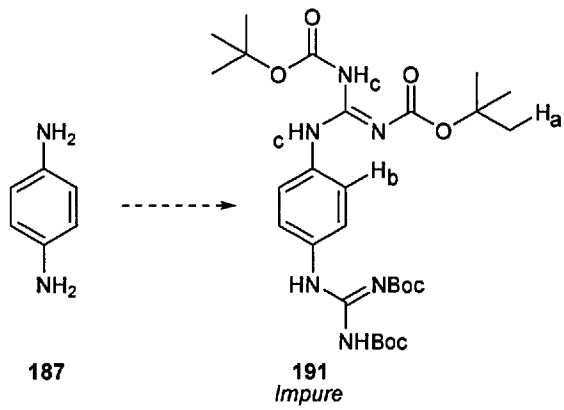

To a solution of *p*-phenylenediamine (**187**, 0.400 g, 3.70 mmol) in THF (30 mL) was added 1,3-bis-(*tert*-butoxycarbonyl)-2-methyl-2-thiopseudourea (**193**, 2.68 g, 9.25 mmol), triethylamine (2.06 mL, 14.8 mmol) and mercury(II) dichloride (2.31 g, 8.51 mmol) at room temperature. After 4 hours, the reaction mixture was diluted with EtOAc (15 mL) and filtered over a short path of celite (0.5 cm depth, 4 cm diameter in a sinter funnel). The filtrate was successively washed with H_2O (2 x 20 mL), brine (20 mL) and dried over $MgSO_4$. After filtration and evaporation of the solvent *in vacuo* crude **191** (0.41 g, 20%) was isolated as a pale yellow solid. R_f = 0.85, 0.70, 0.25 (*n*-hexane:THF, 1:1, v/v); δ_H (270 MHz, $CDCl_3$) 1.39 – 1.61 (~ 36H, m, H_a), 7.55 (~ 4H, s, H_b), 10.3 (~ 4H, br s, H_c).

The molecule was not isolated cleanly. Unassigned signals: δ_H (270 MHz, $CDCl_3$) 2.37 (s), 7.28 – 7.36 (br m), 11.6 (s). See Chapter Four, section 4.1.1 for further details.

7.2.55 2,5-Diiodo-1,4-Bis(1,3-bis(*tert*-butoxycarbonyl)guanidine)benzene (**192**).

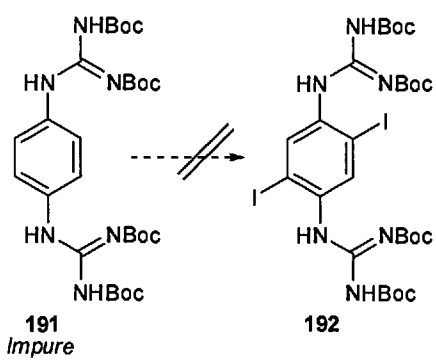

A mixture of **191** (0.150 g, 0.253 mmol), [bis(trifluoroacetoxy)iodo]benzene (**147**, 0.122 g, 0.284 mmol) and I_2 (67 mg, 0.27 mmol) in CH_2Cl_2 (10 mL) was stirred at room temperature for 8 hours. The reaction mixture was then concentrated *in vacuo* and analysis by TLC (R_f = 0.85, *n*-

hexane:EtOAc, 2:1, v/v) indicated that no reaction had occurred. *^{1}H NMR data indicated the presence of the starting material only.*

7.2.56 2,5-Dibromonitrobenzene (197).[20]

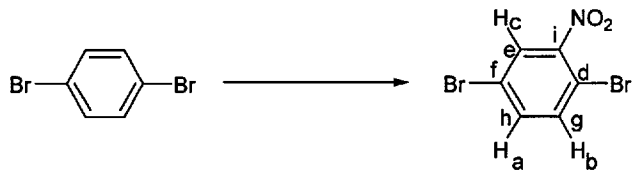

194 197

[Nitration of aromatics can lead to polynitrated compounds that are explosive and therefore blast-protection was used throughout this process, as a precaution]

197 was prepared using a previously described procedure; characterisation data correspond to literature values.[20]

197: (15.6 g, 65%) as light yellow crystals; R_f = 0.63 (silica gel, *n*-hexane/EtOAc, 3:1, v/v); m.p. 87 – 89 °C (Lit. m.p. 83.5 – 84.5 °C);[20,21] δ_H (400 MHz, $CDCl_3$) 7.54 – 7.65 (2H, m, H_a + H_b), 7.98 (1H, d, $^4J_{H\text{-}H}$ = 2.2 Hz, H_c); δ_C (100.6 MHz, $CDCl_3$) 113.2 (C_d), 121.5 (C_e), 123.9 (C_f), 128.5 (C_g), 136.2 (C_h), 150.3 (C_i); *m/z* (CI, NH_3) 298 (100%, $[M+NH_4]^+$); HRMS (CI, NH_3) Found: $[M+NH_4]^+$, 298.8854. $C_6H_7Br_2N_2O_2$ requires: $[M+NH_4]^+$, 298.9400; Anal. Calcd. for $C_6H_3Br_2NO_2$: C, 25.65; H, 1.08; N, 4.99. Found: C, 25.77; H, 1.01; N, 4.95.

7.2.57 2,5-Dibromoaniline (195).[22]

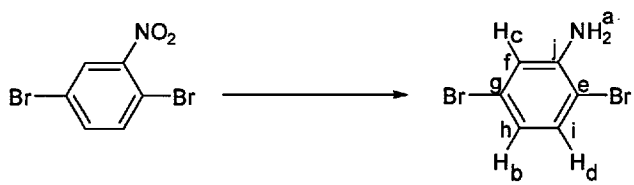

197 195

195 was prepared using a previously described procedure; characterisation data correspond to literature values.[22]

195: (3.40 g, 95%), a white crystalline solid; R_f = 0.72 (silica gel, *n*-hexane/EtOAc, 3:1, v/v); m.p. 56 – 58 °C (Lit. m.p. 54.5 – 55 °C);[21] δ_H (400 MHz, $CDCl_3$) 3.77 – 4.53 (2H, br s, H_a), 6.73 (1H, dd, $J_{H\text{-}H}$ = 8.5, 2.2 Hz, H_b), 6.90 (1H, d, $^4J_{H\text{-}H}$ = 2.2 Hz, H_c), 7.23 – 7.25 (1H, m, H_d); δ_C (100.6 MHz, $CDCl_3$) 107.7 (C_e), 118.1 (C_f), 121.7 (C_g), 122.1 (C_h), 133.6 (C_i), 145.3 (C_j); *m/z* (CI, NH_3)

251 (65%, $[M+H]^+$). HRMS (CI, NH_3) Found: $[M]^+$, 250.8768. $C_6H_5Br_2N$ requires: $[M]^+$, 250.9186; Anal. Calcd. for $C_6H_5Br_2N$: C, 28.72; H, 2.01; N, 5.58. Found: C, 28.83; H, 1.98; N, 5.50.

7.2.58 2,5-Dibromo(1,3-bis(*tert*-butoxycarbonyl)guanidine) (**198**).

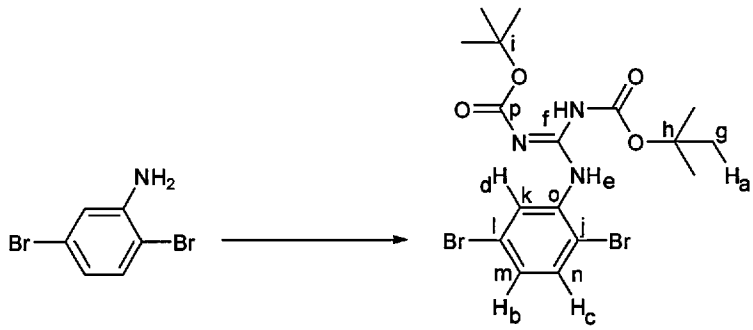

195 **198**

To a solution of **195** (0.250 g, 1.00 mmol) in THF (25 mL) was added 1,3-bis-(*tert*-butoxycarbonyl)-2-methyl-2-thiopseudourea (**193**, 0.376 g, 1.30 mmol), triethylamine (0.21 mL) and mercury(II) dichloride (0.350 g, 1.30 mmol) at room temperature. After 14 hours, the reaction mixture was diluted with EtOAc (20 mL) and filtered over a short path of celite (0.5 cm depth, 4 cm diameter in a sinter funnel). The filtrate was successively washed with H_2O (2 x 20 mL), brine (20 mL) and dried over $MgSO_4$. After filtration and evaporation of the solvent under reduced pressure the crude molecule was purified by flash column chromatography to give **198** (0.138 g, 28%) as a colourless solid, R_f= 0.60 (silica gel, EtOAc/*n*-hexane, 1:6, v/v); m.p 129 – 131 °C; IR (Film) ν_{max} (CaF_2 pellet)/cm^{-1} 1378, 1460 (CH def.), 1640 (C=N str.), 2855, 2922, (CH str.); δ_H (400 MHz, $CDCl_3$) 1.54 (18H, m, H_a), 7.11 (1H, dd, $^3J_{H\text{-}H}$= 2.3, 8.5 Hz, H_b), 7.39 (1H, d, $^3J_{H\text{-}H}$ = 8.5 Hz, H_c), 8.57 (1H, s, H_d), 10.6 (1H, br s, H_e), 11.6 (1H, br s, H_f); δ_C (100.6 MHz, $CDCl_3$) 28.1 (C_g), 80.1 (C_h), 84.1 (C_i), 114.1 (C_j), 121.3 (C_k), 127.8 (C_l), 128.6 (C_m), 133.4 (C_n), 136.7 (C_o), 153.3 (C_p); *m/z* (CI, NH_3) 494 (100%, $[M+H]^+$); HRMS (CI, NH_3) Found: $[M+H]^+$, 494.0113. $C_{17}H_{24}Br_2N_3O_4$ requires: $[M+H]^+$, 494.0134.

7.2.59 2-(1,3-bis(*tert*-butoxycarbonyl)guanidine)-1,4-bis-phenylethynyl-benzene (PE **199**).

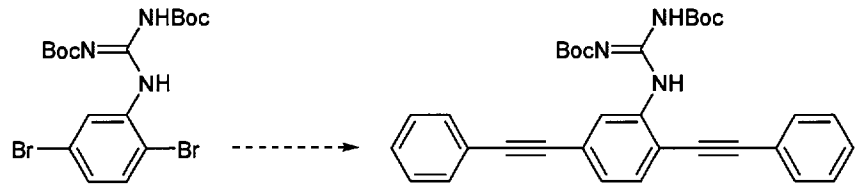

198 PE **199** *Impure*

A solution of **198** (0.100 g, 0.200 mmol), phenylacetylene (0.074 mL, 0.67 mmol), tetrakis-(triphenylphosphine) palladium(0) (10 mg, 9 μmol), copper-(I) iodide (10 mg, 53 μmol) and diisopropylamine (2 mL) in THF (10 mL), was stirred for 26 hours under argon at 45 °C. The solvents were removed under reduced pressure, and the remaining solid purified by column chromatography (R_f = 0.23, 0.45, CH_2Cl_2/*n*-hexane, 1:1, v/v); *two fractions were collected (combined yield: 0.101 g) and by ^1H NMR it was not possible to confirm the structure of the target molecule.*

Unassigned signals: δ_H (400 MHz, $CDCl_3$) 6.86 – 8.73 Ar-H. See Chapter Four, section 4.1.1 for further details.

7.2.60 2-Aniline-1,4-bis-phenylethynyl-benzene (PE **200**).

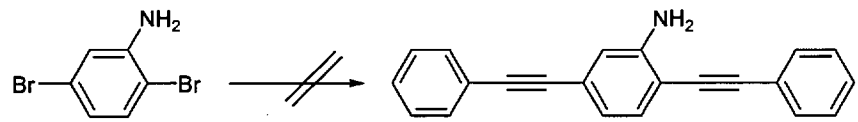

195 PE **200** *Impure*

A solution of **195** (1.50 g, 5.98 mmol), phenylacetylene (1.97 mL, 17.9 mmol), tetrakis-(triphenylphosphine) palladium(0) (69 mg, 60 μmol), copper-(I) iodide (11 mg, 58 μmol) and diisopropylamine (2 mL) in THF (10 mL), was stirred for 20 hours under argon at 20 °C. The solvents were removed under reduced pressure, and the remaining solid purified by column chromatography (100% *n*-hexane); *two fractions were collected. The first (0.152 g) was identified as the unwanted homocoupled product of phenylacetylene (R_f = 0.40, 100% n-hexane) and the second (R_f = 0.20, 100% n-hexane) as the starting material **195** (1.12 g).*

Unassigned signals (second fraction): δ_H (270 MHz, $CDCl_3$) 6.59 – 7.84 Ar-H. See Chapter Four, section 4.1.1 for further details.

7.2.61 2-Nitro-1,4-bis-phenylethynyl-benzene (PE **202**).[23]

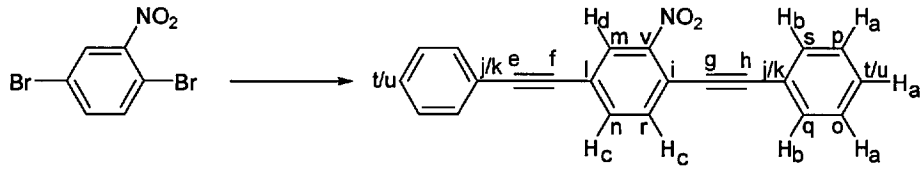

A solution of 2,5-dibromonitrobenzene (**197**, 1.00 g, 3.56 mmol), bis(triphenylphosphine) palladium(II) dichloride (50 mg, 0.071 mmol), copper(I) iodide (27 mg, 0.14 mmol), THF (40 mL), diisopropylamine (5 mL) and phenylacetylene (0.86 mL, 7.8 mmol) was stirred for 1 hour under argon at 45 °C. After cooling to room temperature, the mixture was flushed through a silica plug (*n*-hexane/CH_2Cl_2, 2:1, v/v) followed by recrystallisation from 95% EtOH afforded the desired product PE **202** (0.36 g, 31%) as yellow needle-shaped; δ_H (400 MHz, $CDCl_3$) 7.37 – 7.41 (6H, m, H_a), 7.55 – 7.62 (4H, m, H_b), 7.67 – 7.72 (2H, m, H_c), 8.22 (1H, m, H_d); δ_C (100.6 MHz, $CDCl_3$) 84.8 (C_e), 86.8 (C_f), 93.6 (C_g), 98.8 (C_h), 118.1 (C_i), 122.2 (C_j), 122.3 (C_k), 124.1 (C_l), 127.5 (C_m), 128.4 (C_n), 128.5 (C_o), 129.1 (C_p), 129.4 (C_q), 131.7 (C_r), 132.1 (C_s), 134.5 (C_t), 135.2 (C_u), 149.5 (C_v).

7.2.62 2-Aniline-1,4-bis-phenylethynyl-benzene (PE **200**).

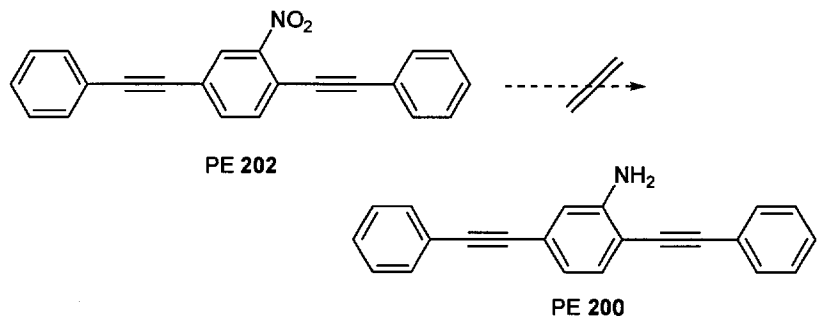

PE **202** (2.88 g, 8.90 mmol) was dissolved in EtOH (50 mL) and to this solution was added tin(II) chloride dihydrate (10.0 g, 44.5 mmol) in small portions, avoiding an excessive increase in the temperature. The resulting pale-yellow solution was stirred at 70 °C for 16 hours at which time the starting material disappeared by TLC. The turbid solution was poured onto 20 g of ice and the pH made slightly basic by addition of solid $NaHCO_3$ (~ 5 g) before the solution was extracted with EtOAc (3 x 50 mL). The organic phases were combined and washed with brine (3 x 30 mL) and the combined organic extracts dried over $MgSO_4$. Evaporation of the solvent gave an unidentified material (1.31 g) as a white crystalline solid. *^1H NMR was inconclusive; TLC, R_f = 0.15, 0.25, 0.64 (n-hexane/CH_2Cl_2, 1:1, v/v).*

Unassigned signals: δ_H (270 MHz, $CDCl_3$) 6.84 – 8.65 Ar-H. See Chapter Four, section 4.1.1 for further details.

7.2.63 2-Nitro-1,4-bis-trimethylsilanylethynyl-benzene (**203**).[23]

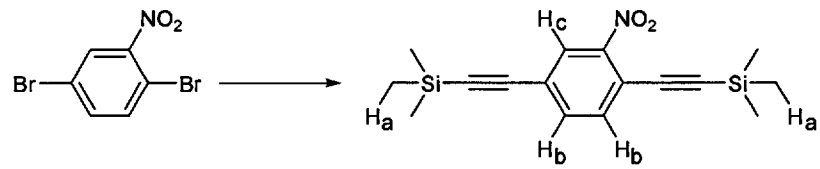

197 **203**

203 was prepared using a previously described procedure; characterisation data correspond to literature values.[23]

203: (1.02 g, 41%), a light-yellow solid; δ_H (270 MHz, $CDCl_3$) 0.15 – 0.29 (18H, m, H_a), 7.56 (2H, br s, H_b), 8.05 (1H, br s, H_c). *The crude material was directly employed in the following reaction.*

7.2.64 2,5-Bis-trimethylsilylethynyl-aniline (**204**).[24]

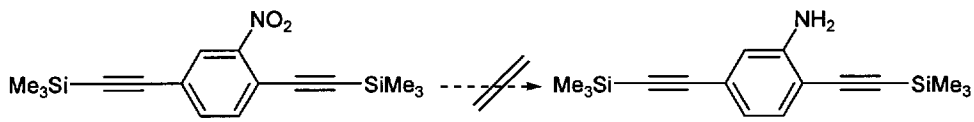

203 **204**

203 (1.02 g, 3.23 mmol) was dissolved in EtOH (30 mL) and THF (20 mL) and to this solution was added tin(II) chloride dihydrate (3.65 g, 16.1 mmol) in small portions, avoiding an excessive increase in the temperature. The resulting pale-yellow solution was stirred at 20 °C for 5 hours at which time the starting material disappeared by TLC. The turbid solution was then treated with 50% aqueous KOH to dissolve tin compounds. The phases were then separated. The aqueous phase was then extracted with Et_2O (3 x 30 mL) and then discarded. The extracts were combined with the organic phase, washed with brine (3 x 30 mL), dried over $MgSO_4$ and evaporated *in vacuo* which gave a dark orange residue, unidentified by NMR. *^1H NMR was inconclusive.* See Chapter Four, section 4.1.1 for further details.

7.2.65 2,5-Bis-trimethylsilylethynyl-aniline (**204**).[25]

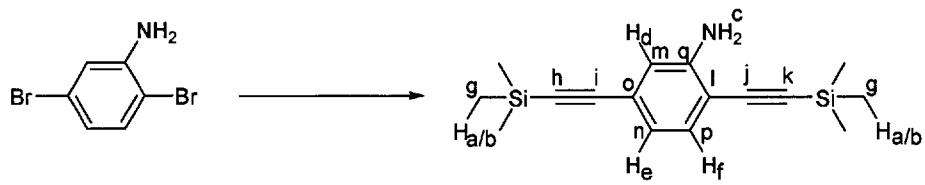

195 **204**

204 was prepared using a previously described procedure; characterisation data correspond to literature values.[25]

204: (3.75 g, 66%), a pale-yellow crystalline material; R_f = 0.83 (silica gel, *n*-hexane/EtOAc, 3:1, v/v); m.p. 121 – 123 °C (Lit. m.p. 121 °C);[26] IR (Film) ν_{max} (CaF_2 pellet)/cm^{-1} 1377, 1462 (CH def.), 1612 (NH bending), 2145 (C≡C), 2858, (CH str.), 3387, 3485 (unsymmetrical and symmetrical NH str.); δ_H (400 MHz, $CDCl_3$) 0.23 (9H, br s, H_a), 0.26 (9H, br s, H_b), 3.91 – 4.47 (2H, br s, H_c), 6.75 – 6.78 (1H, m, H_d), 6.79 – 6.80 (1H, m, H_e), 7.21 (1H, d, $^3J_{H\text{-}H}$ = 7.9 Hz, H_f); δ_C (100.6 MHz, $CDCl_3$) -0.08 (C_g), -0.06 (C_g), 95.2 (C_h), 101.3 (C_i), 101.5 (C_j), 105.0 (C_k), 108.2 (C_l), 117.2 (C_m), 121.5 (C_n), 124.1 (C_o), 132.0 (C_p), 147.8 (C_q); *m/z* (CI, NH_3) 286 (100%, $[M+H]^+$); HRMS (CI, NH_3) Found: $[M+H]^+$, 286.1447. $C_{16}H_{24}NSi_2$ requires: $[M+H]^+$, 286.5394.

7.2.66 2,5-Bis-trimethylsilyl-4-(*N,N'*-bis(*tert*-butyloxycarbonyl)-*N''*-guanidine)benzene (**205**).

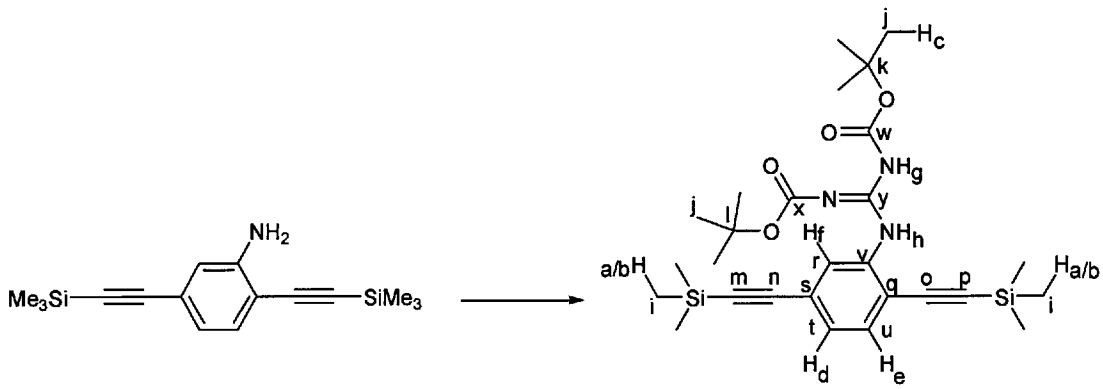

204 **205**

To a solution of **204** (3.75 g, 13.1 mmol) in DMF (10 mL) was added 1,3-bis-(*tert* butoxycarbonyl)-2-methyl-2-thiopseudourea (**193**, 4.19 g, 14.4 mmol), triethylamine (3.7 mL, 26.5 mmol) and mercury(II) dichloride (3.92 g, 14.4 mmol) under argon and at 25 °C. The resulting mixture was stirred and after 50 hours, the reaction mixture was diluted with EtOAc and filtered over a short path of celite (1.5 cm depth, 4 cm diameter in a sinter funnel). The filtrate was successively washed with H_2O (2 x 20 mL), brine (1 x 20 mL) and dried over $MgSO_4$. After

filtration and evaporation of the solvent under reduced pressure the crude molecule was purified by tritiation using MeOH to give **205** (4.70 g, 68%) as a white crystalline solid; R_f = 0.71 (silica gel, *n*-hexane/EtOAc, 5:1, v/v); m.p. 147 – 149 °C; IR (Film) ν_{max} (CaF_2 pellet)/cm^{-1} 1370, 1464 (CH def.), 1572 (C=O amide str.), 1644 (NH bending), 1727 (C=O amide str.), 2147 (C≡C), 2855, 2923 (CH str.); δ_H (400 MHz, $CDCl_3$) 0.23 (9H, br s, H_a), 0.29 (9H, br s, H_b), 1.52 – 1.54 (18H, m, H_c), 7.09 (1H, dd, $J_{H\text{-}H}$ = 8.0, 1.5 Hz, H_d), 7.34 (1H, d, $^3J_{H\text{-}H}$ = 8.0 Hz, H_e), 8.76 (1H, br s, H_f), 10.77 (1H, br s, H_g), 11.62 (1H, br s, H_h); δ_C (100.6 MHz, $CDCl_3$) -0.18 (C_i), -0.15 (C_i), 28.1 (C_j), 28.2 (C_j), 79.7 (C_k), 83.4 (C_l), 96.0 (C_m), 99.6 (C_n), 103.8 (C_o), 105.1 (C_p), 114.2 (C_q), 124.0 (C_r), 125.8 (C_s), 126.8 (C_t), 132.1 (C_u), 139.0 (C_v), 152.5 (C_w), 153.2 (C_x), 163.2 (C_y); *m/z* (CI, NH_3) 328 (20%, $[M - (1 \times BOC\ group)]^+$), 428 (40%, $[M - (2 \times BOC\ groups)]^+$), 528 (100%, $[M+H]^+$); HRMS (CI, NH_3) Found: $[M+H]^+$, 528.2714. $C_{27}H_{42}N_3O_4Si_2$ requires: $[M+H]^+$, 528.8110; Anal. Calcd. for $C_{27}H_{42}N_3O_4Si_2$: C, 61.44; H, 7.83; N, 7.96. Found: C, 61.37; H, 7.93; N, 8.07.

7.2.67 2,5-Diethynyl-4-(*N,N'*-bis(*tert*-butyloxycarbonyl)-*N''*-guanidine)benzene (**206**).

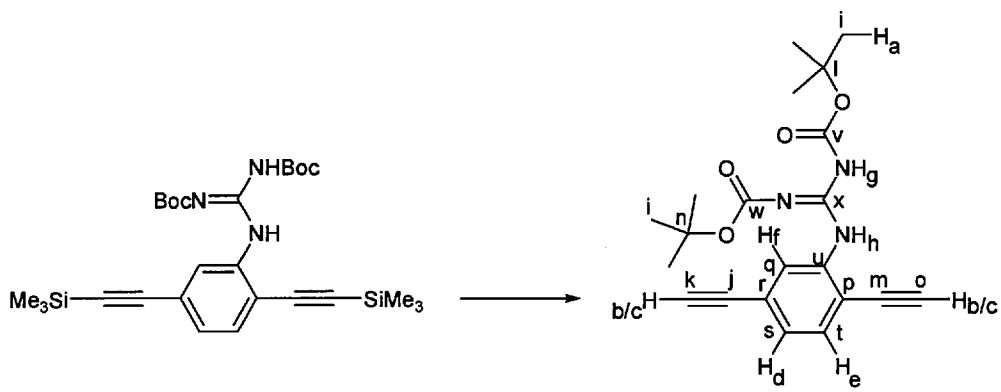

205 **206**

To a solution of **205** (4.00 g, 7.60 mmol) in MeOH (15 mL) and THF (30 mL) was added K_2CO_3 (1.10 g, 7.96 mmol). The reaction mixture was stirred for 4 hours at 25 °C and then quenched with saturated NH_4Cl (15 mL) and diluted with EtOAc (30 mL). The organic layer was washed with H_2O (2 x 15 mL), dried over $MgSO_4$ and the solvent was removed *in vacuo*. The residue was purified by tritiation from MeOH (20 mL) to afford the bisalkyne **206** (2.06 g, 71%) as a white crystalline solid; R_f = 0.77 (silica gel, *n*-hexane/EtOAc, 3:1, v/v); m.p. 160 – 161 °C; IR (Film) ν_{max} (CaF_2 pellet)/cm^{-1} 1377, 1461 (CH def.), 1574 (C=O amide str.), 1615 (C=N str.), 1722 (C=O amide str.), 2106 (C≡C), 2850, 2922 (CH str.); δ_H (400 MHz, $CDCl_3$) 1.52 – 1.53 (18H, m, H_a), 3.15 (1H, s, H_b), 3.55 (1H, s, H_c), 7.15 (1H, dd, $J_{H\text{-}H}$ = 8.0, 1.5 Hz, H_d), 7.38 (1H, d, $^3J_{H\text{-}H}$ = 8.0 Hz, H_e), 8.62 (1H, s, H_f), 10.86 (1H, br s, H_g), 11.6 (1H, br s, H_h); δ_C (100.6 MHz, $CDCl_3$) 28.0 (C_i), 28.1 (C_i), 78.7 (C_j), 78.9 (C_k), 80.0 (C_l), 83.3 (C_m), 83.6 (C_n), 86.1 (C_o), 113.8 (C_p), 123.4 (C_q),

125.9 (C_r), 127.4 (C_s), 132.0 (C_t), 139.5 (C_u), 152.3 (C_v), 153.3 (C_w), 163.8 (C_x); *m/z* (CI, NH_3) 184 (100%, [M – (1 x BOC group)]$^+$), 278 (80%, [M – (2 x BOC group)]$^+$), 384 (100%, [M+H]$^+$); HRMS (CI, NH_3) Found: [M+H]$^+$, 384.1917. $C_{21}H_{26}N_3O_4$ requires: [M+H]$^+$, 384.4488; Anal. Calcd. for $C_{21}H_{25}N_3O_4$: C, 65.78; H, 6.57; N, 10.96. Found: C, 65.68; H, 6.67; N, 11.00.

7.2.68 2,5-Bis-(4-methylphenylethynyl)-4-(*N,N'*-bis(*tert*-butyloxycarbonyl)-*N''*-guanidine)benzene, (PE **205**).

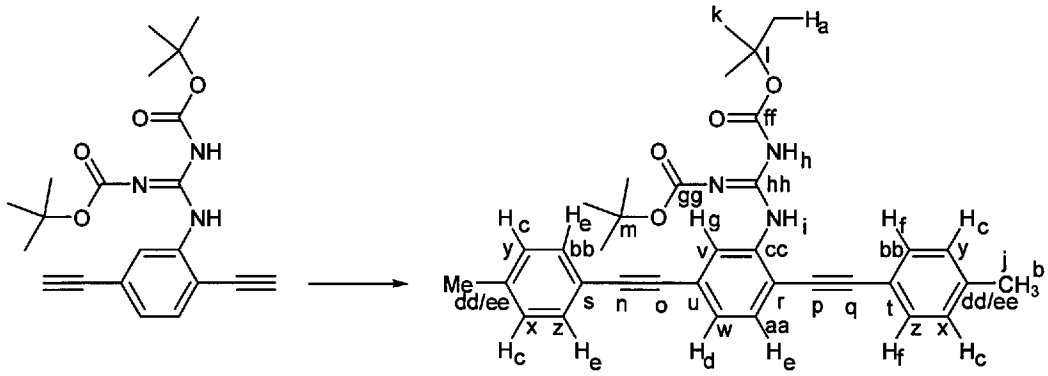

206 **PE 207**

A solution of **206** (600 mg, 1.56 mmol), 4-iodotoulene (**149**, 1.02 g, 4.69 mmol), tetrakis (triphenylphosphine) palladium(0) (0.180 g, 156 μmol), copper (I) iodide (30 mg, 160 μmol), and 5 mL of diisopropylamine in 5 mL of THF was stirred under argon at 25 °C for 24 hours, by which time the reaction was deemed complete by TLC. The solvents were removed *in vacuo* and the crude material was purified by *two* recrystallisations from MeCN (~ 5 mL) to give PE **207** (806 mg, 91%) as a light-yellow crystalline solid; R_f = 0.83 (silica gel, *n*-hexane/EtOAc, 3:1, v/v); m.p. 163 – 165 °C; IR (Film) ν_{max} (CaF_2 pellet)/cm^{-1} 1377, 1461 (CH def.), 1568 (C=O amide str.), 1640 (C=N str.), 1727 (C=O amide str.), 2853, 2924 (CH str.); δ_H (400 MHz, $CDCl_3$) 1.54 (18H, br s, H_a), 2.37 (6H, s, H_b), 7.12 – 7.17 (4H, m, H_c), 7.20 – 7.23 (1H, m, H_d), 7.41 – 7.46 (3H, m, H_e), 7.59 – 7.62 (2H, m, H_f), 8.75 (1H, s, H_g), 11.1 (1H, br s, H_h), 11.7 (1H, br s, H_i); δ_C (100.6 MHz, $CDCl_3$) 21.6 (C_j), 28.1 (C_k), 79.9 (C_l), 83.6 (C_m), 84.1 (C_n), 89.1 (C_o), 91.2 (C_p), 98.1 (C_q), 114.4 (C_r), 119.7 (C_s), 120.1 (C_t), 124.0 (C_u), 125.1 (C_v), 127.0 (C_w), 128.9 (C_x), 129.1 (C_y), 131.5 (C_z), 131.7 (C_{aa}), 131.8 (C_{bb}), 138.4 (C_{cc}), 138.5 (C_{dd}), 138.8 (C_{ee}), 152.8 (C_{ff}), 153.2 (C_{gg}), 163.1 (C_{hh}); *m/z* (CI, NH_3) 564 (55%, [M+H]$^+$), 363 (100%, [M – (2 x BOC groups)]$^+$); HRMS (CI, NH_3) Found: [M+H]$^+$, 564.2862. $C_{35}H_{38}N_3O_4$ requires: [M+H]$^+$, 564.2863; Anal. Calcd. for $C_{35}H_{37}N_3O_4$: C, 74.58; H, 6.62; N, 7.45. Found: C, 74.54; H, 6.72; N, 7.38. Absorbance λ_{max} (in MeOH, 0 wt.% Triton): 327 nm; emission λ_{max} (in MeOH, 0 wt.% Triton): 360 nm; absorbance λ_{max} (in MeOH, 0.3 wt.% Triton): 327 nm; emission λ_{max} (in MeOH, 0.3 wt.% Triton): 360 nm.

7.2.69 2,5-Bis-(4-methylphenylethynyl)-4-(guanidinium)benzene, trifluoroacetate salt (PE **208**).

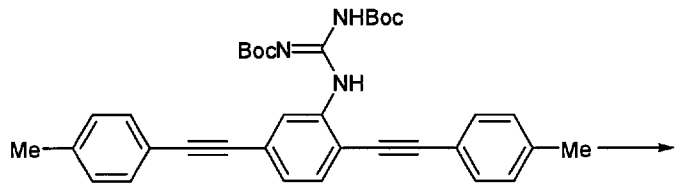

PE **207**

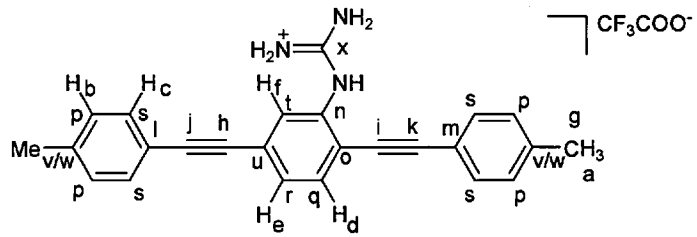

PE **208**

To a solution of PE **207** (40 mg, 71 μmol) in CH_2Cl_2 (3.5 mL), trifluoroacetic acid (3.5 mL) was added dropwise. The reaction mixture was stirred at 25 °C for 1 hour. The solvents were removed *in vacuo* and the crude material was purified by recrystallisation from *n*-hexane/CH_2Cl_2 (1:1, v/v, ~ 3 mL) to give PE **208** (20 mg, 59%) as a light-yellow crystalline solid; R_f = 0.29 (silica gel, 100% EtOH); m.p. 218 – 221 °C (decomp.); IR (Film) ν_{max} (CaF_2 pellet)/cm^{-1} 1377, 1462 (CH def.), 1664 (C=N str.), 1700 (C=O str.), 2858, 2936 (CH str.), 3470 (O-H str.); δ_H (400 MHz, d_4-MeOD) 2.37 (6H, s, H_a), 7.21 – 7.23 (4H, m, H_b), 7.41 – 7.45 (4H, m, H_c), 7.51 – 7.52 (1H, m, H_d), 7.53 – 7.56 (1H, m, H_e), 7.63 – 7.65 (1H, m, H_f); δ_C (100.6 MHz, d_4-MeOD) 21.5 (C_g), 85.0 (C_h), 88.2 (C_i), 93.5 (C_j), 98.1 (C_k), 120.7 (C_l), 120.8 (C_m), 123.3 (C_n), 126.2 (C_o), 130.4 (C_p), 131.6 (C_q), 132.4 (C_r), 132.6 (C_s), 134.3 (C_t), 137.0 (C_u), 140.6 (C_v), 140.9 (C_w), 158.4 (C_x); *m/z* (CI, NH_3) 364 (20%, $[M+H]^+$); HRMS (CI, NH_3) Found: $[M+H]^+$, 364.1816. $C_{25}H_{22}N_3$ requires: $[M+H]^+$, 364.4617; Anal. Calcd. for $C_{25}H_{22}N_3 \cdot C_2F_3O_2^- \cdot H_2O$: C, 65.45; H, 4.88; N, 8.48. Found: C, 65.96; H, 4.12; N, 8.26. Absorbance λ_{max} (in unbuffered H_2O, 0 wt.% Triton): 326 nm; emission λ_{max} (in unbuffered H_2O, 0 wt.% Triton): 376 nm; absorbance λ_{max} (in unbuffered H_2O, 0.3 wt.% Triton): 333 nm; emission λ_{max} (in unbuffered H_2O, 0.3 wt.% Triton): 365 nm; absorbance λ_{max} (in MeOH, 0 wt.% Triton): 326 nm; emission λ_{max} (in MeOH, 0 wt.% Triton): 356 nm; absorbance λ_{max} (in MeOH, 0.3 wt.% Triton): 326 nm; emission λ_{max} (in MeOH, 0.3 wt.% Triton): 357 nm.

7.2.70 PPE **209**.

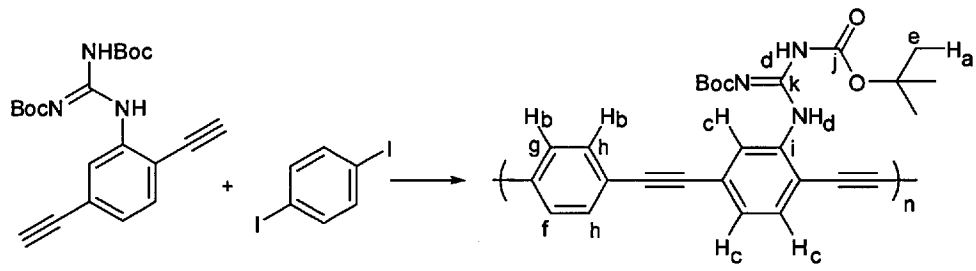

206 **109** **PPE 209**

To a solution of DMF and diisopropylamine (1:1, v/v, 6 mL each) were added 1,4-diiodobenzene (**109**, 0.204 g, 0.618 mmol) and bisalkyne **206** (0.250 g, 0.652 mmol) and 4-iodotoluene (**149**, 16 mg, 0.073 mmol). The Schlenk flask was fitted tightly with a rubber septum, and the solution was deoxygenated by applying the freeze-pump-thaw technique consecutively over three iterations. After backfilling with argon, to this solution was added $Pd(PPh_3)_4$ (72 mg, 0.062 mmol) and CuI (12 mg, 0.062 mmol). The resulting suspension was deoxygenated again by applying the freeze-pump-thaw technique consecutively over three iterations. A voluminous precipitate, believed to be alkylammonium iodide, formed in less than five minutes. The solution was heated at 45 °C for 48 hours with stirring in the dark. After this time, a second batch of the catalyst and co-catalyst was added (same amounts as before), and the solution deoxygenated again for a further 8 hours before the cooled reaction mixture was poured into MeOH to precipitate the polymer, which was then filtered (but not allowed to dry completely) and redissolved in a small volume (< 5 mL) of DMF. The precipitation and redissolution process was repeated once more. Note that the polymer cannot be redissolved after it has been recovered as a dry solid film by evaporation from a solution of a good solvent (e.g., $CHCl_3$ or CH_2Cl_2). Thus, the material was stored as a stock solution in MeOH that was kept in the dark (a specific yield could not be determined due to storage conditions). To obtain NMR spectra in a deuterated solvent it was necessary to recover the polymer from the non-deuterated solvent as follows; the MeOH solution of the polymer was isolated by centrifugation and decanting. The resulting precipitate was then redissolved in the deuterated solvent for NMR analysis. Nevertheless, even using this procedure, it was not possible to obtain samples that were entirely free of non-deuterated solvent, and consequently some of the resonances in the NMR spectrum are partially obscured by resonances arising from the residual solvent. The partially-dried polymer samples were bright yellow solids; IR (Film) ν_{max} (CaF_2 pellet)/cm^{-1} 1412, 1450 (CH def.), 1669 (C=N str.), 2525 (C≡C), 2833, 2945 (CH str.), 3337 (O-H str., from methanolic solution); δ_H (400 MHz, $CDCl_3$) 1.55 (18H, br s, H_a), 7.40 – 7.57 (4H, m, H_b), 7.63 – 7.76 (3H, m, H_c), 8.65 – 8.86 (1H, m, H_d), 10.85 – 10.96 (1H, m, H_d), 11.73 (1H, br s, H_d), 12.68 (1H, br s, H_d); δ_C (100.6 MHz, $CDCl_3$) 28.1 (C_e), 128.4 (C_f), 129.6, (C_g), 132.0 (C_h), 134.3 (C_i), 153.2 (C_j), 162.5

(C_k). Anal. Calcd. for $C_{27}H_{27}N_3O_4 \cdot 3H_2O$: C, 63.39; H, 6.50; N, 8.21 Found: C, 63.38; H, 4.61; N, 8.00. Due to the limited solubility of the polymer only a partial ^{13}C NMR spectrum was acquired. Absorbance λ_{max} (in MeOH, 0 wt.% Triton): 391 nm; emission λ_{max} (in MeOH, 0 wt.% Triton): 409 nm.

7.2.71 PPE **210**.

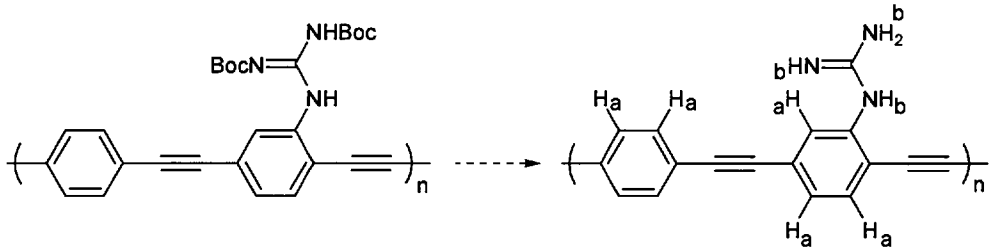

PPE **209** PPE **210**
Impure

To a solution of PPE **209** (~ 20 mg) in CH_2Cl_2 (3.5 mL), trifluoroacetic acid (3.5 mL) was added dropwise. The reaction mixture was stirred at 25 °C for 6 hours. The solvents were removed under reduced pressure to give crude PPE **210** as a deep-orange solid (10 mg); IR (Film) ν_{max} (CaF_2 pellet)/cm^{-1} 1408, 1437 (CH def.), 1665 (C=N str.), 2332 (C≡C), 2913, 2996 (CH str.), 3477 (NH str.); δ_H (400 MHz, d_6-DMSO) 1.06 (t, Et_2O), 3.35 (q, Et_2O), 5.28 (br s, unidentified, possible NH), 7.33 – 7.93 (br m, H_a), 9.81 – 10.05 (br m, H_b). The limited solubility of the polymer prevented a ^{13}C NMR spectrum from being acquired. Absorbance λ_{max} (in unbuffered H_2O, 0 wt.% Triton): 397 nm; emission λ_{max} (in unbuffered H_2O, 0 wt.% Triton): could not be determined under these conditions; absorbance λ_{max} (in unbuffered H_2O, 0.3 wt.% Triton): 392 nm; emission λ_{max} (in unbuffered H_2O, 0.3 wt.% Triton): 415 nm.

The polymer was not isolated cleanly. See Chapter Four, section 4.1.2 for further details.

7.2.72 PPE **212**.

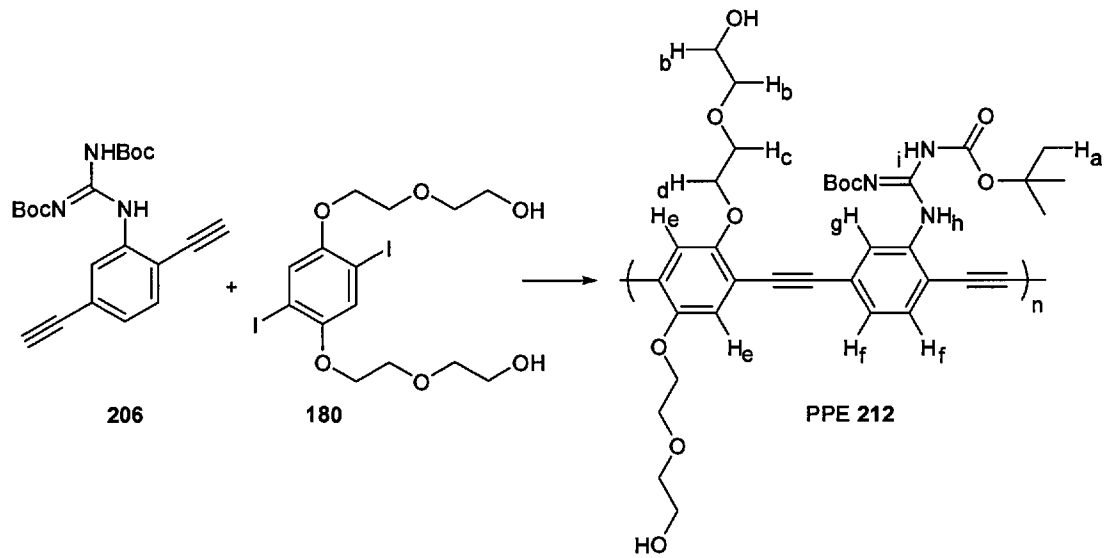

To a solution of toluene and diisopropylamine (12 mL; 6 mL each) was added **206** (0.120 g, 0.313 mmol) and **180** (0.160 g, 0.299 mmol). The Schlenk flask was fitted tightly with a rubber septum, and the solution was deoxygenated by applying the freeze-pump-thaw technique consecutively over three iterations. After backfilling with argon, to this solution was added $Pd(PPh_3)_4$ (30 mg, 26 μmol) and CuI (30 mg, 160 μmol). The resulting suspension was deoxygenated again by applying the freeze-pump-thaw technique consecutively over three iterations. A voluminous precipitate, believed to be alkylammonium iodide, formed in less than five minutes. The solution was heated at 45 °C for 24 hours with stirring in the dark. After this time, a second batch of the catalyst and co-catalyst was added (same amounts as before), and the solution deoxygenated as before and stirred at 45 °C for a further 8 hours before the cooled reaction mixture was poured into MeOH to precipitate the polymer, which was then filtered (but not allowed to dry completely) and redissolved in a small volume (< 2 mL) of DMF. The precipitation and dissolution process was repeated once more. Note that the polymer cannot be redissolved after it has been recovered as a dry solid film by evaporation from a solution of a good solvent (e.g., $CHCl_3$ or CH_2Cl_2). Thus, the material was stored as a stock solution in MeOH that was kept in the dark (a specific yield could not be determined due to storage conditions). To obtain NMR spectra in a deuterated solvent it was necessary to recover the polymer from the non-deuterated solvent as follows; the MeOH solution of the polymer was isolated by centrifugation and decanting. The resulting precipitate was then redissolved in the deuterated solvent for NMR analysis. Nevertheless, even using this procedure, it was not possible to obtain samples that were entirely free of non-deuterated solvent and consequently some of the resonances in the NMR spectrum are partially obscured by resonances arising from the residual solvent. The partially-dried polymer samples were bright yellow solids;

IR (Film) on CaF_2 disc ν_{max}/cm^{-1} 1288 (CO str.), 1637 (C=O str.), 2890, 2958 (CH str.), 3305, (OH str.); δ_H (400 MHz, $CDCl_3$) 1.50 – 1.55 (18H, br m, H_a), 3.69 – 3.78 (8H, br m, H_b), 3.89 – 3.95 (4H, br m, H_c), 4.21 (4H, br m, H_d), 6.98 – 7.07 (2H, m, H_e), 7.44 – 7.70 (2H, m, H_f), 8.60 – 8.65 (1H, m, H_g), 10.9 (1H, br m, H_h), 11.7 (1H, br m, H_i). The limited solubility of the polymer prevented a ^{13}C NMR spectrum from being acquired. Anal. Calcd. for $C_{35}H_{43}N_3O_{10}$: C, 63.14; H, 6.51; N, 6.31 Found: C, 63.03; H, 6.60; N, 6.23. Absorbance λ_{max} (in MeOH, 0 wt.% Triton): 422 nm; emission λ_{max} (in MeOH, 0 wt.% Triton): 447 nm; absorbance λ_{max} (in MeOH, 0.3 wt.% Triton): 426 nm; emission λ_{max} (in MeOH, 0.3 wt.% Triton): 447 nm.

7.2.73 1,4-Bis[2-(2-methylethoxy)ethoxy]-2,5-diiodobenzene (**211**).[18,27]

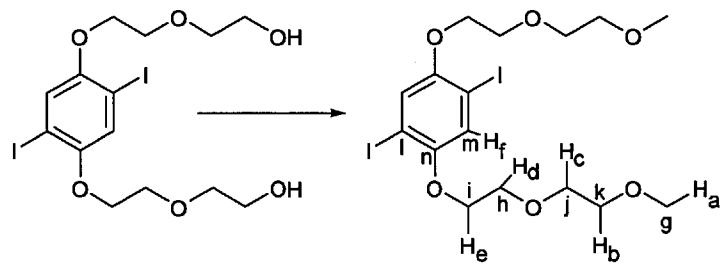

180 **211**

A solution of 1,4-bis(2-(2-hydroxyethoxy)ethoxy)benzene (**180**, 2.00 g, 3.71 mmol) in dry THF (5 mL) was added over 15 minutes to a stirred suspension of NaH (0.600 g, 14.9 mmol, 60% in mineral oil, was previously washed with dry THF; see section 7.1) in dry THF (20 mL) under argon. After 1 hour a solution of MeI (0.950 mL, 14.9 mmol) was added over 10 minutes. The reaction mixture was then heated to 50 °C for 23 hours and then cooled to room temperature. Excess NaH was quenched by the addition of H_2O (1 mL) dropwise and then the solvent was removed *in vacuo* and the remaining residue was partitioned between CH_2Cl_2 (20 mL) and H_2O (20 mL). The organic phase was washed with ammonium chloride (2 x 20 mL) and brine (2 x 20 mL), dried over $MgSO_4$ and then concentrated *in vacuo*. The crude material was recrystallised from MeOH/H_2O (9:1, v/v) to give the *title molecule* **211** (1.64 g, 78%) as a white crystalline material; R_f = 0.74 (100% EtOAc); m.p. 84 – 86 °C; IR (Film) ν_{max} (CaF_2 pellet)/cm^{-1} 2856, 2935 (CH str.), 1377, 1464 (CH def.), 1129, 1210 (C-O str.); δ_H (400 MHz, $CDCl_3$) 3.39 (6H, s, H_a), 3.56 – 3.58 (4H, m, H_b), 3.75 – 3.77 (4H, m, H_c), 3.86 – 3.88 (4H, m, H_d), 4.09 – 4.11 (4H, m, H_e), 7.23 (2H, s, H_f); δ_C (100.6 MHz, $CDCl_3$) 59.1 (C_g), 69.6 (C_h), 70.3 (C_i), 71.1 (C_j), 72.0 (C_k), 86.3 (C_l), 123.4 (C_m), 153.1 (C_n); *m/z* (CI, NH_3) 584 (100%, $[M+NH_4]^+$); HRMS (CI, NH_3) Found: $[M+NH_4]^+$, 584.0006. $C_{16}H_{28}I_2NO_6$ requires: $[M+NH_4]^+$, 584.0001; Anal. Calcd. for $C_{16}H_{24}I_2O_6$: C, 33.94; H, 4.27. Found: C, 34.08; H, 4.27.

7.2.74 PPE **214**.

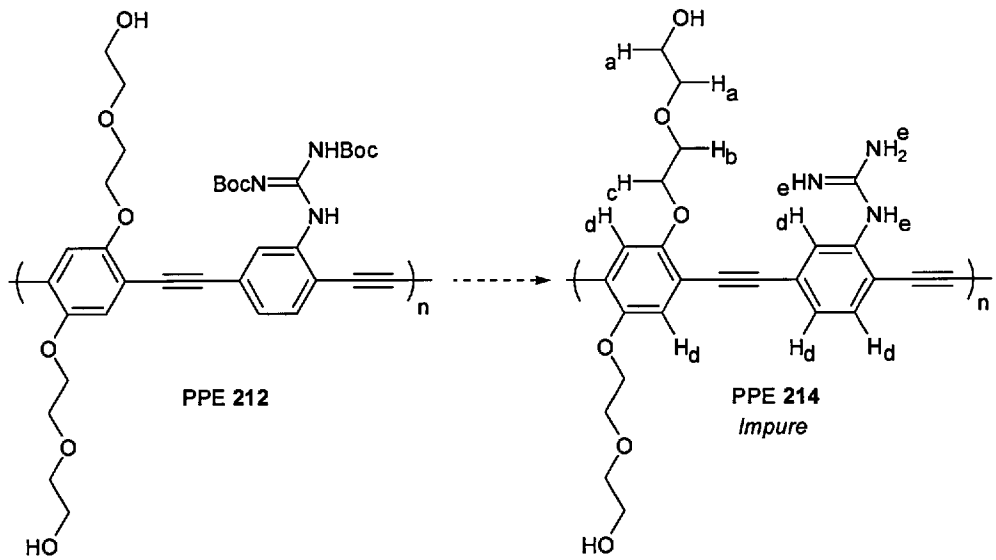

To a solution of PPE **212** (~ 20 mg) in CH_2Cl_2 (4 mL), trifluoroacetic acid (4 mL) was added dropwise at 25 °C. The reaction mixture was stirred at 25 °C for 20 minutes. The solvents were removed *in vacuo* to give crude PPE **214** as a dark-orange residue (8 mg); IR (Film) on CaF_2 disc ν_{max}/cm^{-1} 1670 (CN/CO str.), 2128, 2254 (C≡C), 3433, (NH str.); δ_H (400 MHz, d_6-DMSO) 1.22 (unidentified), 1.73 – 1.76 (m, unidentified), 3.79 – 3.95 (8H, br m, H_a), 4.16 – 4.28 (4H, br m, H_b), 4.42 – 4.58 (4H, br m, H_c), 6.17 – 7.80 (>9H, br m, H_d + H_e). The limited solubility of the polymer prevented a ^{13}C NMR spectrum from being acquired. Emission λ_{max} (in MeOH, 0 wt.% Triton): 439 nm; emission λ_{max} (in MeOH, 0.3 wt.% Triton): 440 nm.

The polymer was not isolated cleanly. See Chapter Four, section 4.1.2 for further details.

7.2.75 PPE 213.

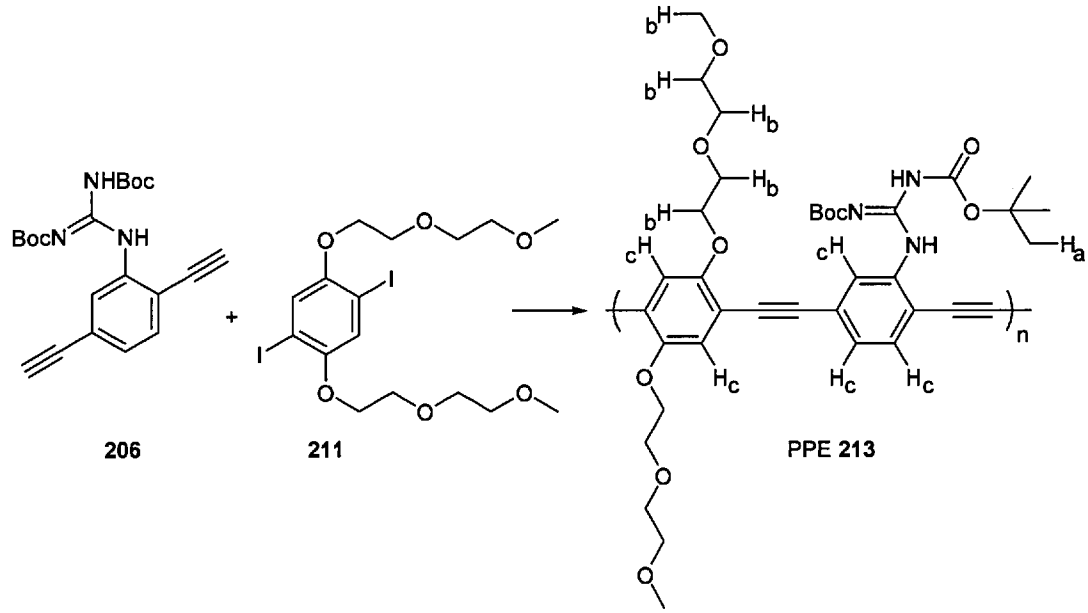

To a solution of DMF (6 mL) and diisopropylamine (6 mL) was added **206** (0.100 g, 0.261 mmol) and monomer **211** (0.141 g, 0.249 mmol). The Schlenk flask was fitted tightly with a rubber septum, and the solution was deoxygenated by applying the freeze-pump-thaw technique consecutively over three iterations. After backfilling with argon, to this solution was added $Pd(PPh_3)_4$ (30 mg, 26 μmol) and CuI (30 mg, 160 μmol). The resulting suspension was deoxygenated again by applying the freeze-pump-thaw technique consecutively over three iterations. A voluminous precipitate, believed to be alkylammonium iodide, formed in less than five minutes. The solution was heated at 45 °C for 22 hours with stirring in the dark. After this time, a second batch of the catalyst and co-catalyst was added (same amounts as before) and the solution deoxygenated as before and stirred at 45 °C for a further 8 hours before the cooled reaction mixture was poured into MeOH to precipitate the polymer, which was then filtered (but not allowed to dry completely) and redissolved in a small volume (< 5 mL) of DMF. The precipitation and dissolution process was repeated once more. Note that the polymer cannot be redissolved after it has been recovered as a dry solid film by evaporation from a solution of a good solvent (e.g., $CHCl_3$ or CH_2Cl_2). Thus, the material was stored as a stock solution in MeOH that was kept in the dark (a specific yield could not be determined due to storage conditions). To obtain NMR spectra in a deuterated solvent it was necessary to recover the polymer from the non-deuterated solvent as follows; the MeOH solution of the polymer was isolated by centrifugation and decanting. The resulting precipitate was then redissolved in the deuterated solvent for NMR analysis. Nevertheless, even using this procedure, it was not possible to obtain samples that were entirely free of non-deuterated solvent, and consequently some of the resonances in the NMR

spectrum are partially obscured by resonances arising from the residual solvent. The partially-dried polymer samples were yellow-orange solids; IR (Film) ν_{max} (CaF_2 pellet)/cm^{-1} 1279 (CO str.), 1377, 1461 (CH def.), 1628 (C=N str.), 2203 (C≡C), 2854, 2924 (CH str.); δ_H (400 MHz, d_6-DMSO) 1.56 (18H, br s, H_a), 3.36 – 4.21 (16H, m, H_b), 7.37 – 7.70 (5H, br m, H_c). The limited solubility of the polymer prevented a ^{13}C NMR spectrum from being acquired. Absorbance λ_{max} (in MeOH, 0 wt.% Triton): 434 nm; emission λ_{max} (in MeOH, 0 wt.% Triton): 445 nm; absorbance λ_{max} (in MeOH, 0.3 wt.% Triton): 430 nm; emission λ_{max} (in MeOH, 0.3 wt.% Triton): 445 nm.

7.2.76 PPE **215**.

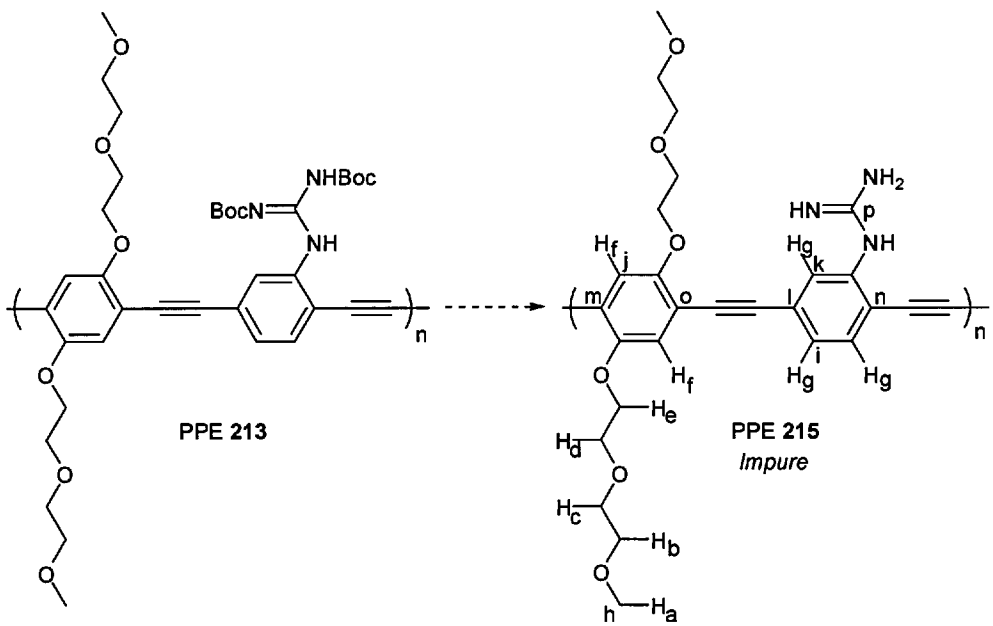

To a solution of PPE **213** (~ 20 mg) in CH_2Cl_2 (4 mL), trifluoroacetic acid (2 mL) was added dropwise at 25 °C. The reaction mixture was stirred at 25 °C for 1 hour. The solvents were removed *in vacuo* to give crude PPE **215** (7 mg) a light yellow residue. IR (Film) ν_{max} (CaF_2 pellet)/cm^{-1} 1179 (CO str.), 1365, 1460 (CH def.), 1726 (C=O str.), 1779 (C=O), 2863, 2974 (CH str.), 3503 (NH str.), 3578 (NH); δ_H (400 MHz, d_4-MeOD) 3.20 – 3.22 (10H, br m, H_a + H_b), 3.74 – 3.77 (4H, br m, H_c), 4.18 (4H, br m, H_d), 4.51 (4H, br m, H_e), 5.32 – 5.38 (m, unidentified), 8.87 (2H, br s, H_f), 9.43 – 9.63 (3H, br m, H_g), 10.23 (br m, unidentified); δ_C (100.6 MHz, d_4-MeOD) 55.7 (C_h), 134.3 (C_i), 137.4 (C_j), 138.1 (C_k), 138.2 (C_l), 140.8 (C_m), 140.9 (C_n), 141.5 (C_o), 160.8 (C_p). Emission λ_{max} (in unbuffered H_2O, 0 wt.% Triton): 440 nm; emission λ_{max} (in unbuffered H_2O, 0.3 wt.% Triton): 439 nm; emission λ_{max} (in MeOH, 0 wt.% Triton): 439 nm; emission λ_{max} (in MeOH, 0.3 wt.% Triton): 440 nm.

The polymer was not isolated cleanly. See Chapter Four, section 4.1.2 for further details.

7.3 Emission quenching experiments

7.3.1 General procedure for the measurement of Stern-Volmer constants.

The Stern-Volmer coefficients were determined using the following technique: N_S moles of the sensor (e.g. PPE **155** or PE **154**) were dissolved into a volume V of solvent which was then divided into two smaller solutions A and B, each of volume $½V$. The quencher (dissolved in a small amount of the same solvent) was then added dropwise to solution B, and the volume of quencher solution required to achieve full quenching (> 95%) was determined. The same amount again of quencher solution was added to solution B, resulting in a final solution that contained exactly twice the number N_Q of moles required for full quenching of solution B alone (and therefore the appropriate amount for full quenching of the combined solutions A and B). This (double) volume of quencher solution is denoted ΔV. An identical volume ΔV of pure solvent was then added to solution A so that solutions A and B both had the total same volume $V' = ½V + \Delta V$ after the addition of solvent and quencher solution respectively. Importantly, since solutions A and B contain equal concentrations of sensor (PPE **155** or PE **154**), dropwise addition of B to A does not alter the sensor concentration. Solution A was then transferred to a cuvette and, using an appropriate excitation wavelength, its fluorescence intensity I_0 was measured. Small controlled volumes (V_Q) of solution B were added to solution A using a μL-resolution syringe and, after each addition of B, the fluorescence intensity $I([Q])$ was measured. This process was repeated until all of solution B had been added to solution A. If n is defined as the number of droplets of B added to A, then the quencher concentration $[Q]$ is related to n by the relation:

$$[Q] = \frac{nV_Q N_Q}{V'(nV_Q + V')}$$

Equation 11

The Stern-Volmer coefficient may be determined from Equation 5 (Chapter One, section 1.3) using least-squares optimisation. It is common in the literature to use a linearised approach, in which k_{SV} is determined as the best-fit slope obtained from a plot of $I_0/I[Q]$ versus $[Q]$. This approach, however, does not take into account the existence of measurement errors in both the abscissa $[Q]$ and the ordinate $I[Q]$, and accordingly its use results in biased estimates of k_{SV}.[28] In this work, we therefore use a total least squares procedure wherein the optimal value of k_{SV} is obtained by minimising the summation:

$$S = \sum_i \left[\frac{(x_i^* - x_i)^2}{\sigma_{xi}^2} + \frac{(y_i^* - y_i)^2}{\sigma_{yi}^2} \right]$$

Equation 12

where x_i and y_i represent the ordinate and abscissa of the individual experimental data points, x_i^* and y_i^* represent the optimal estimators of x_i and y_i, and σ_{xi} and σ_{yi} represent the measurement errors, which were conservatively estimated at 20% and 5% respectively. The estimators x_i^* and y_i^* are constrained by the Stern-Volmer relation $y_i^* = y_i^0/(1+k_{SV}x_i^*)$. The determination of the confidence intervals for k_{SV} is problematic since closed analytical expressions are not generally available for non-linear regression.[28] We therefore used a numerical 'bootstrap' procedure to evaluate the sensitivity of the k_{SV} to random fluctuations in the experimental data.[29] The errors reported in the discussion and figures in this report correspond to 95% confidence intervals for k_{SV}. Full experimental details of the procedure we use to determine the Stern-Volmer coefficients and associated confidence intervals will be described in a separate paper.[30] A summary of the findings for a standard system are shown in Table 7.2.

Table 7.2 Summary of $Ru(bpy)_3^{2+}$ luminescence quenching by 4-Br-2,6-DMP.

pH	k_{SV} / M^{-1} (Reported)[31]	k_{SV} / M^{-1} (Measured)[a] (non-linear fit)	k_{SV} / M^{-1} (Measured)[a] (linear fit)
11.05	1180	1838 (451 nm)	1788 (451 nm)
11.05	1180	1750 (491 nm)	1888 (491 nm)

[a]Our experiments were conducted at 24-25 °C. The reported results were measured at 22 ±2 °C.[31]

In addition to using two excitation wavelengths to excite the metal complex, the extracted data was fitted using both linear and non-linear methods. All the techniques were in agreement with each other and validated the quenching protocol used. The results were similar to those reported in the literature procedure followed with slight deviations attributed to small differences in the pH of the buffer solution used.[31,32]

7.4 General procedure for the hybridisation experiments

All experiments were conducted in spectrometric grade water, containing either no added salts or 100 mM NaCl with added surfactant (Triton X-100). All DNA material was stored at -20 °C. Stock solutions of the tetrameric sequences were suspended in spectrometric grade water and were used

as received from Sigma-Aldrich (Purification: desalt). To ensure that the strands were dissociated, the solutions were kept above 12 °C prior to experiments and hybridisation experiments with the tetrameric strands were conducted at 50 °C. Due to the small size of these oligonucleotides, Sigma-Aldrich were unable to verify the purity by quality control. Instead, they provided an estimate of the 'Desalt' purity (for longer strands of approximately 20 base-pairs) of 80%. For these experiments, the polymer concentration was held at 10 μM and ~ 0.25 nmoles of each tetramer was used in the annealing procedure.

The longer sequences (35-mer strands) were used as kindly provided by Dr David Mann (Biochemistry, Imperial College London). They were treated at 94 °C for ~ 5 minutes to remove any secondary structure that they may have possessed and the hybridisation experiments were conducted at 65 °C.[33,34]

The sequences for the 35-mer strands used in the hybridisation assay are given below (all are written 5' to 3'):

S1068A1	35mer	ATGAAACAATGCTGGCGCCTCGAGAAAAGATTTTC
S1068A2	35mer	GAAAATCTTTTCTCGAGGCGCCAGCATTGTTTCAT

(Materials used for results presented in Chapter Five)

S1035A1	35mer	GATGCTCCTCCACTGGCGCCCTATCCATTTGTAAG
S1035A2	35mer	CTTACAAATGGATAGGGCGCCAGTGGAGGAGCATC

(Used in previous experiments)

To determine the concentration of these solutions, the method described by Sigma-Proligo was followed[35] which allowed us to ensure that exact stoichiometric amounts of each strand were added for the annealing procedure and to prevent signal artefacts. The concentration of the DNA stock solutions were typically ~ 1000 μg/mL. These solutions were adjusted such that the addition of an A1 and A2 strand led to a solution concentration of 10 μM for each (which corresponds to an approximately equimolar solution). The starting polymer solution was also of this concentration.

The polymer solutions (10 μM, with a volume of 2.5 mL), in glass cuvettes, were placed in the heated fluorimeter and allowed to equilibrate for 10 minutes. The 35-mer DNA analytes were denatured for 5 minutes at 94 °C prior to their addition into the sample quartz cell, to avoid secondary structures and the resulting signal artefacts as reported previously.[33] An aliquot of known concentration of the *ss*-DNA material was then added and the resulting complex allowed to reach thermal equilibrium for a period of 15 minutes. This was followed by addition of the

complementary strand, at the same concentration. Throughout this time, emission spectra were collected with the fluorimeter set in kinetic mode. Spectra were recorded at 1 minute intervals, with settings similar to those used in the emission quenching experiments and stated in Table 7.3.

7.5 Monitoring enzyme activity

All measurements were conducted on a Perkin-Elmer LS 50B Luminescence Spectrometer. All data was processed using FLWinLab Molecular Spectroscopy software and for the enzyme assay, emission spectra were collected with the software in kinetic mode.

All solutions were prepared by using spectrophotometric grade water. Buffer solutions were prepared with reagent-grade materials (Sigma-Aldrich). Concentrated aqueous solutions of the polymers were diluted with appropriate buffers to a final concentration. Stock solutions of the enzymes were prepared immediately before their use in the assays. The enzyme solutions were maintained at ~ 0 °C before use, and they were used within 3 hours of preparation. All enzyme assays were conducted at 35 – 38 °C. Assay solutions were prepared by placing 2.5 mL of the PPE polymer solution into a silica glass cuvette (10 mm x 10 mm x 45 mm) with a path length of 1 cm. The initial emission intensity was recorded after the solution was allowed to equilibrate. Addition of a known amount of the quencher (phosphate substrate, **NPP**), as determined by prior quenching experiments, was then added, with the combined solution again allowed to thermally equilibrate for a further 10 minutes. The new emission spectrum was recorded and then an aliquot (previously adjusted such that no quenching is observed) of the phosphatase enzyme was then added to the polymer solution and with the fluorimeter set in kinetic mode, emission spectra were recorded every 20 seconds. Typical fluorimeter settings are given below (Table 7.3).

Table 7.3 Typical fluorimeter settings (in kinetic mode) for enzyme assays.

Parameters	**For Polymer PPE 155**
Excitation slit (nm)	2.5
Emission slit (nm)	8
Excitation wavelength (nm)	315
Range (nm)	325 – 590
*Scan speed (nm/min)	300
Delay (s)	60

*related to the integration time

7.6 Prototype solid state biosensor

Emission spectra were measured in quartz cuvettes (10 mm x 10 mm x 45 mm, path length = 10 mm), with solutions being thoroughly degassed with argon prior to use. The TLC plates were used as received from the Eastman Kodak Company, Rochester New York, USA (they were the only type of non-fluorescent TLC plates available to us at the time). The cationic polymer (PPE **155**) used for the prototype sensor was coated onto plastic-backed non-fluorescent silica gel TLC plates, by submerging the plate, cut to size, into a solution of the polymer at ~ 1.0 mM concentration (in repeat units) for 10 minutes. The plates were then dried under a gentle stream of nitrogen and rinsed with deionised water (5 mL) three times to ensure that there was no unbound residual polymer on the surface. This was checked by recording the emission spectrum of the solutions used to rinse the plates. See Chapter Five (section 5.6) for further details.

7.7 Notes and references

1. (a) W. H. Melhuish, *J. Phys. Chem.*, 1961, **65**, 229; (b) S. R. Meech and D. Phillips, *J. Photochem.*, 1983, **23**, 193; S. Dhami, A. J. DeMello, G. Rumbles, S. M. Bishop, D. Phillips and A. Beeby, *Photochem. Photobiol.*, 1995, **61**, 341.
2. D. F. Eaton, *Pure & Appl. Chem.*, 1988, **60**, 1107-1114.
3. S. Fery-Forgues and D. Lavabre, *J. Chem. Ed.*, 1999, **76**, 1260-1264.
4. S. P. Gretton-Watson, E. Alpay, J. H. G. Steinke and J. S. Higgins, *Ind. Eng. Chem. Res.*, 2005, **44**, 8682-8693.
5. I am grateful to Dr Emma Child (Division of Cell & Molecular Biology, Imperial College London), who analysed the sample.
6. Q. Zhou and T. M. Swager, *J. Am. Chem. Soc.*, 1995, **117**, 12593-12602.
7. C. Y. Tan, M. R. Pinto and K. S. Schanze, *Chem. Commun.*, **2002**, 446-447.
8. D. R. Coulson, *Inorg. Syn.*, 1990, **28**, 107-109.
9. L. M. Harwood, C. J. Moody and J. Percy, *Experimental Organic Chemistry, 2nd edition*, Oxford, 1998.
10. M. S. Whiteside, D. Kurrasch-Orbaugh, D. Marona-Lewicka, D. E. Nichols and A. Monte, *Bioorg. Med. Chem.*, 2002, **100**, 3301.
11. F. Dolhem, C. Lievre and G. Demailly, *Tetrahedron Lett.*, 2002, **43**, 1847-1849.
12. P. Michel, D. Gennet and A. Rassat, *Tetrahedron Lett.*, 1999, **40**, 8575-8578.
13. Z. Wang, S. Campagna, K. Yang, G. Xu, M. E. Pierce, J. M. Fortunak, P. N. Confalone, *J. Org. Chem.*, 2000, **65**, 1889-1891.

14. D. W. Price, S. M. Dirk, F. Maya and J. M. Tour, *Tetrahedron*, 2003, **59**, 2497-2518.
15. T. M. Swager, C. J. Gil and M. S. Wrighton, *J. Phys. Chem. A*, 1995, **99**, 4886-4893.
16. M. Kidowaki, M. Moriyama, M. Wada and N. Tamaoki, *J. Phys. Chem. B*, 2003, **107**, 12057-12061.
17. M. R. Pinto, B. M. Kristal and K. S. Schanze, *Langmuir*, 2003, **19**, 6523-6533.
18. P. L. Anelli, P. R. Ashton, R. Ballardini, V. Balzani, M. Delgado, M. T. Gandolfi, T. T. Goodnow, A. E. Kaifer, D. Philp, M. Pietraszkiewicz, L. Prodi, M. V. Reddington, A. M. Z. Slawin, N. Spencer, J. F. Stoddart, C. Vicent and D. J. Williams, *J. Am. Chem. Soc.*, 1992, **114**, 193-218.
19. F. Maya and J. M. Tour, *Tetrahedron*, 2004, **60**, 81-92.
20. F. Maya and J. M. Tour, *Tetrahedron*, 2004, **60**, 81-92.
21. J. J. S. Lamba and J. M. Tour, *J. Am. Chem. Soc.*, 1994, **116**, 11723-11736.
22. F. D. Bellamy and K. Ou, *Tetrahedron Lett.*, 1984, **25**, 839-842.
23. D. W. Price, S. M. Dirk, F. Maya and J. M. Tour, *Tetrahedron*, 2003, **59**, 2497-2518.
24. D. V. Kosynkin and J. M. Tour, *Org. Lett.*, 2001, **3**, 993-995.
25. T. Pautzsch, L. Blankenburg and E. Klemm, *J. Polym. Sci. Part A: Polym. Chem.*, 2004, **42**, 722-723.
26. L. Blankenburg and E. Klemm, *Designed Monomers and Polymers*, 2003, **6**, 57-65.
27. K. Koishi, T. Ikeda, K. Kondo, T. Sakaguchi, K. Kamada, K. Tawa and K. Ohta, *Macromol. Chem. Phys.*, 2000, **201**, 525–532.
28. M. Lybanon, *Am. J. Phys.*, 1984, **52**, 22-26.
29. K. Baumann, *Process Control and Quality*, 1997, **10**, 75-112.
30. W. N. George, J. H. G. Steinke and J. C. deMello, *Manuscript in preparation.*
31. H. E. Gsponer, G. A. Arguello and G. A. Arguello, *J. Chem. Educ.*, 1997, **74**, 968-972.
32. W. Tsuzuki, A. Ue, A. Nagao and K. Akasaka, *Analyst*, 2002, **127**, 669-673.
33. K. Dore, S. Dubus, H.-A. Ho, I. Levesque, M. Brunette, G. Corbeil, M. Boissinot, G. Boivin, M. G. Bergeron, D. Boudreau and M. Leclerc, *J. Am. Chem. Soc.*, 2004, **126**, 4240-4244.
34. H. A. Ho, K. Dore, M. Boissinot, M. G. Bergeron, R. M. Tanguay, D. Boudreau and M. Leclerc, *J. Am. Chem. Soc.*, 2005, **127**, 12673-12676.
35. http://www.proligo.com/pro_primprobes/PP_08-8_UVAbsorbance.html (accessed: 2005)